The Influence of Fire on the Design of Polymer Composite Pipes and Panels for Offshore Structures

Volume 1 of 2

David W Dewhurst

Telford Research Institute
Department of Civil and Environmental Engineering
University of Salford, Salford, UK

Submitted in Partial Fulfilment for the Degree of
Doctor of Philosophy, April 1997

TABLE OF CONTENTS

PAGE

VOLUME 1

VOLUME 2

ACKNOWLEDGEMENT

The author wishes to express his sincere thanks to Professor J M Davies for his supervision, guidance and encouragement throughout the period of study, also for the review of this thesis.

Sincere thanks are due to Mr D C O'Leary for his supervision after the authors period of active research with The University of Salford, and also to Dr J B McNicholas for his helpful advice and support.

Also the author wishes to express his thanks to those members of the technical staff of the Department of Civil Engineering and Construction for their assistance in the preparation of experimental work.

DECLARATION

None of the material contained in this thesis has been submitted in support of an application for another degree or qualification of this or any other university or institution of learning.

David W Dewhurst

March 1997

ABSTRACT

Stainless and other high quality steels are used extensively in the topside construction of oil rigs. Steel is heavy, expensive and even the special grades are prone to corrosion in the aggressive marine environment. New materials are needed which are lighter, more cost effective and free from corrosion related problems. Glass fibre reinforced plastics (GRP) have the required properties but their performance in fire conditions is not known.

Fire is a very real and possibly catastrophic threat. Before specifying the use of GRP components it is essential to quantify their reaction to fire. Panels and pipes to be used in fire risk areas were the components of interest, and the objectives of the research, based on experimental testing, were as follows:

1) To evaluate GRP laminates for use as structural panel skins, noting their structural and fire performance.

2) To develop incombustible, low cost cores for sandwich panels.

3) To produce sandwich panel design proposals which satisfy specified fire exposure requirements.

4) To assess the fire performance of empty and dry, stagnant water filled and flowing water filled polymer composite pipes with or without fire protection.

5) To use finite difference modelling as part of the design process for fire exposed pipes and panels. Factors of water content for hygroscopic cores and the ablation mechanism of fire exposed GRP were taken account of.

6) To assess the validity of the standard furnace fire resistance test with respect to combustible materials, and with respect to the reproducibility of results between different furnace arrangements.

CHAPTER 1 - INTRODUCTION

1.1 General Introduction

From the discovery of fire man has attempted to both use it and control it. Unexpected and uncontrolled fire is possibly the most common destructive force known to man, from its harm to life and economic impact. In modern engineering, design of a structure against fire onslaught is of paramount importance, demanding increasing attention as fire risk and isolation of the structure increases. Possibly one of the most severe cases for fire design is for the offshore environment where fires although infrequent can have catastrophic effects due to their intensity and the isolation of the offshore construction.

There are two basic manners in which fires can be fought: active and passive. Active fire fighting is commonly provided by automatic detection (smoke detectors and heat sensors), water sprinklers, deluges and sprays, and the use of fire suppressive foam and gas. Although active systems are designed for all known eventualities they are insufficient on their own for protection of life and structure in large scale fires offshore. In addition to active measures passive fire protection is now being increasingly used to minimise the consequences of a fire. Passive protection is either achieved by the design of the structure itself, or by a cladding, coating or free standing system that is designed to impede the spread of the fire, saving both the structure, and life within the fire

environment. The choice between active and passive systems (or their combination), will be influenced by the protection philosophy, the anticipated fire and duration, the equipment and structure requiring protection, and the time required for evacuation. Since structural engineering is concerned predominantly with passive fire protection this thesis does not consider active fire protection. This thesis concentrates on fibre reinforced plastics, state of the art fire barrier materials and construction methods (predominantly sandwich technology) for use in fire situations.

1.2 Types of Fire Hazard.

As fuels have become more sophisticated and powerful, and as demand for production has increased, the risk of a fire being out of control has escalated. The offshore oil industry is one which has inherent risks due to the nature of the work and the isolation of the locations. These coupled with the unpredictability of offshore weather can, in a fire situation, lead to a disaster.

At 11.30 pm July 6 1988, a blast occurred at Occidental Petroleum (Caledonia) Ltd's Piper Alpha production platform in the North Sea, 120 miles northeast of Aberdeen[1,2,3]. The following fire was still burning 17 hours later and flames which soared to 700ft at the peak of the fire could be seen for 25 miles. This disaster brought about the death of over 160 workers aboard the platform and many others were injured from burns, smoke inhalation and broken bones from jumping into the sea. Following this tragedy was a 13 month inquiry into the

reason for the explosions and a series of detailed recommendations were given in the report compiled by Lord Cullen. This whole disaster could possibly be the worst death toll in the history of offshore platforms and lessons must be learned from it. The philosophy of having temporary safe refuges (TSR's) is one step towards ensuring this scale of disaster does not happen again. The TSR's are to be capable of withstanding a severe (hydrocarbon) fire insult, usually for a minimum of two hours. The Cullen report also placed the onus on offshore operators to ensure safety, rather than just requiring regulatory compliance. The major outcome of the Cullen report, however, was a retreat from prescriptive design towards performance based design. This change in design ideology gives more flexibility in the choice of materials which can be used, and again places more onus on the operators to ensure correct and safe design.

There are an infinite different number of fire scenarios due to fire being dependent not only on heat source and materials but on all external conditions also. Fire, however, can be grouped into many broad bands. A few which may occur in offshore/petrochemical environment[4] are as follows:

1) Cloud Fire - Transient fire resulting from the ignition of a cloud of gas and not subject to a significant flame acceleration via the effects of containment or turbulence.

2) FireBall - Rapid turbulent combustion of fuel as an expanding usually rising ball of flame. It is more intense than a cloud fire and can be comparable to an explosion.

3) BLEVE - (**B**oiling **L**iquid **E**xpanding **V**apour **E**xplosion) results from the

sudden failure of a vessel containing a pressurised liquid at a temperature well above its normal (atmospheric) boiling point.

4) Pool Fire - A turbulent diffusion fire burning above an upward facing horizontal pool of vaporising fuel under conditions where the fuel vapour or gas has zero or very little initial momentum. A boiling pool fire in difficult to control; it may accompany a jet fire where liquid rains out of the jet.

5) Running Fire - A fire from a burning liquid fuel which flows by gravity over surfaces.

6) Jet or Spray Fire - A turbulent diffusion flame resulting from the combustion of a fuel continuously released with some significant momentum in a particular direction.

7) Blow-Out - A form of jet fire resulting from a well blow-out.

The potential durations, temperatures and intensities of these different types of fires are given below in table 1.1

FIRE TYPE	Duration	Temperature °C	Heat Flux KW/m²
Blow-out	Months	1000-1700	100-1000
Fireball/BLEVE	Seconds	1000-1400	113-1200
Pool Fire	Hours	1100-1200	150-220
Running Fire	Hours	800	-
Jet/Spray Fire	Hours	900-1500	80-1550

Table 1.1 - Potential durations, temperatures and heat fluxes for different fire types.
(From BRE Client report for Department of Energy[9])

1.3 Existing Panel Structures and their Features.

The first large scale development of sandwich materials dates back to the second world war where the need for stiff light materials for aircraft construction[5] was first realised. In building construction the use of sandwich panels can be dated back to 1939 where steel skins separated by springs were used to provide a light, rigid structure for Le Maison du Peuple at Clichy, France.

Structural sandwich panels consist of two stiff, strong, relatively thin faces and a thick layer of a much lighter, weaker material for a core. The faces can be flat, lightly profiled, deep profiled or any combination of these. The faces of the panel are normally made of steel, aluminium or fibre reinforced polymers whereas the cores may consist of polymeric foams or honeycomb patterns of paper or light metal alloys. More recently fire resistant cores have been developed involving ceramics or non-combustible particulate composites. These cores tend to be much heavier than the foams and honeycombs. However, they are stronger materials. Figure 1.3.1 overleaf shows some typical forms of sandwich panels used in construction today.

Sandwich panels are now found in most areas of construction in one form or another. Following are a few of their advantages:

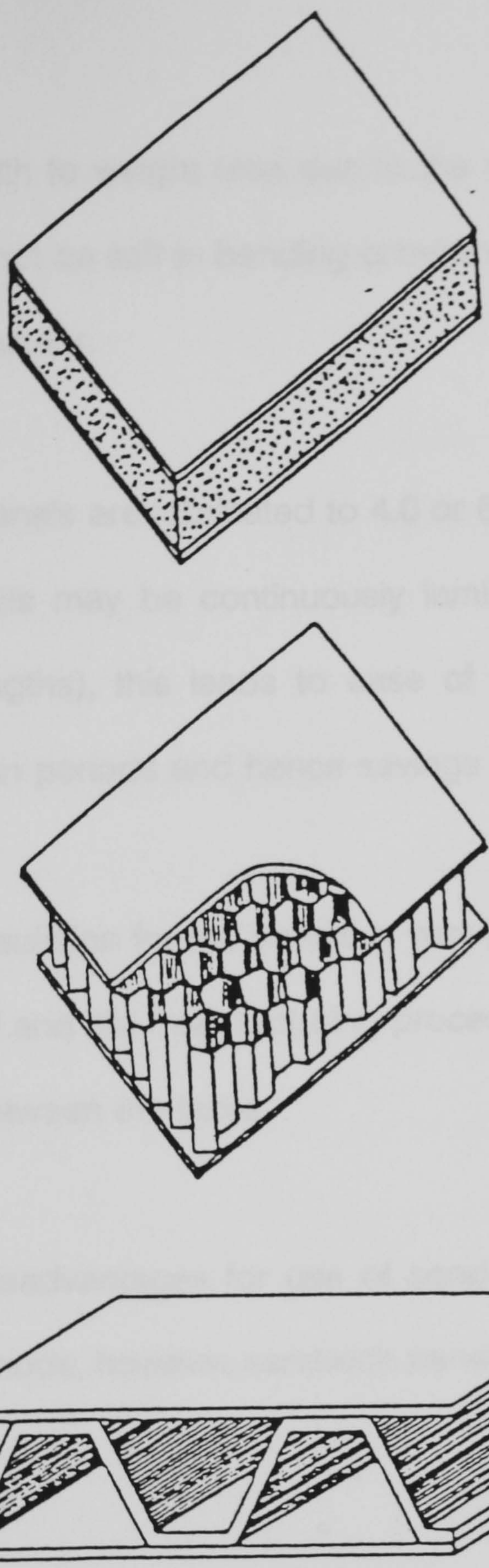

Figure 1.3.1 - Sandwich Panels with (a) rigid foam core (b) honeycomb core (c) corrugated core (d) profiled faces

- High strength to weight ratio due to the use of low density core. The core need not be stiff in bending providing that it is significantly strong and stiff in shear.

- Typically panels are fabricated to 4.0 or 6.0m lengths off site (although some panels may be continuously laminated and supplied at much greater lengths), this leads to ease of installation, providing shorter construction periods and hence savings on site expenses.

- Thermal insulation for the panels is very good where low density cores are utilised and the manufacturing process means there are no thermal bridges between the faces.

There are few disadvantages for use of sandwich materials over traditional construction methods, however, sandwich panels do have some less desirable properties:

- Panels utilising foamed polymeric cores generally fail to meet specified fire resistance criteria both in terms of insulation and structural stability.

- The high thermal resistance of core materials used can lead to substantial thermal loading in direct sunlight due to the differential expansion of the faces. This can be designed for, and is usually limited by using light colours for external faces.

- Foamed polymers may experience a degree of creep under sustained loading over long periods of time.

- Traditional foaming agents (eg. CFC's) have had a significant effect on ozone depletion. Environmentally friendly alternatives are however being developed, and brought into use.

So far the panel structures described have been typically for on-shore use, offshore panels are usually of a much different construction. Externally exposed panels on offshore oil rigs usually have demanding requirements for strength and stiffness together with fire resistance. Typical offshore panels in current use are deeply profiled stainless steel sheeting insulated by multiple layers of ceramic or mineral wool. Figure 1.3.2 shows a typical cross section through a fire resistant panel.

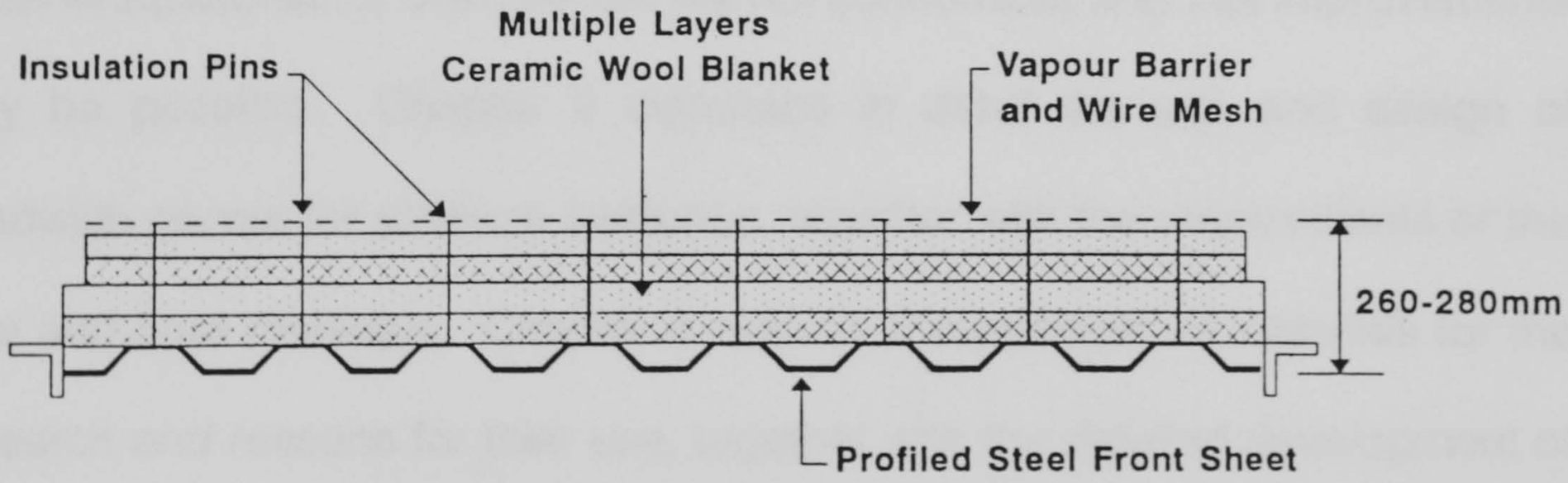

Figure 1.3.2 Typical Offsore Wind Loaded Panel

This method of construction has several disadvantages:

- Even using stainless steel, aggressive marine conditions cause corrosion and deterioration of the panel.

- Panel structures tend to be heavy, typical external offshore panels may be in the order of 40kg/m^3. In a situation where topside weight must be counterbalanced (one tonne above water requires an additional three tonnes below water level) the need for keeping topside weight to a minimum is evident.

- The panel constructions used, by their very nature, are very thick. Thicknesses of 250mm and over are not uncommon, and this takes up a lot of room where space may be extremely valuable.

All the above information would lead to the decision that the current designs of panel structures for offshore use are not economical, and that improvements may be possible. Chapter 2 discusses in detail the use and design of sandwich panels for offshore platforms, together with the requirements of the face and core materials. Chapter 3 outlines the selection of materials for the research and reasons for their use, together with the detailed development of new and novel core materials. Chapter 3 also demonstrates the optimisation of sandwich panel designs together with an investigation into an apparently superior structural solution, the stringer panel.

1.4 Existing Pipe Systems and their Features.

The pipe systems considered in this thesis are typically those of the deluge systems on offshore structures which are designed to be operated automatically in the event of a fire-related emergency. With existing technology, the pipe systems will typically consist of a ring main at low level filled with stagnant water from which vertical riser pipes will convey water to the sprinkler heads in the event of a fire. These riser pipes are normally dry (though they are tested at regular intervals). The whole pipe system would typically be steel based, and this has major disadvantages over other materials:

As mentioned before, steel including stainless steel can be corroded in aggressive marine conditions. This has related problems as well, not just to performance of pipes, but the effect it can have on blocking sprinkler heads or causing valves to seize.

Steel piping (in particular stainless steel) is very expensive and also heavy. This coupled with the obvious need to replace it at regular intervals due to corrosion shows it not to be the most economical solution.

Where the fire water system is not running as is expected (i.e. if the valves or sprinklers are not working properly) high steam over-pressures may be developed in fires where the piping contains static water. These over-pressures may develop to a stage where they reach the pressure rating of the pipe

causing it to fail. Failure in this manner is potentially explosive, and may result in a great deal of damage in the surrounding area. This could cause not only damage to the structure through the failure of the pipe, but also damage to the structure and possibly loss of life from failure to contain or suppress the fire attack. An example of the destructive potential of an exploding water filled vessel can be seen from the Building Research Establishment tests on water heater explosions[6]. In this investigation a water heater was allowed to overheat to the point at which it exploded to simulate a blocked piping or pressure relief system. The explosion not only destroyed the water heater, but also the majority of the building which it was contained in. This demonstration is a good example of the catastrophic failure that a water-steam explosion can have.

1.5 Polymer Composites and their Advantages.

Polymer composites or fibre reinforced plastics (FRP's) can consist of one or more out of many alternative types of fibres held in a polymer matrix. Fibres are generally glass, however, carbon and aramid fibres are used where special material properties are required. The polymer matrix is generally one of the following five resins - polyester, vinyl ester, epoxy, phenolic or modified acrylic (Modar). The reinforcing fibres, which in their unimpregnated form are only capable of carrying tensile loads, contribute the majority of the tensile, flexural and shear stiffness and strength of the composite. Incorporation of fibres converts a brittle resin into a tough, fatigue-resistant composite. Chapter 3 contains more information on GRP, its manufacture and properties.

The use of glass fibre reinforced plastics offshore has many advantages over conventional steel:

The potential weight savings for various pipe dimensions between glass fibre reinforced plastic (GRP) and high molybdenum steel varies between 50 and 70% for large and small diameters respectively[7]. General weight reductions for other applications such as tanks and cable tray ladders can be as high as 50-60%.

GRP has an inherent corrosion and environmental resistance which leads to an increased life expectancy over steel solutions. GRP can be susceptible to

attack from ultra violet light and water absorption along the fibres however this can be effectively prevented by using a resin rich surface layer, and liner.

GRP is a much lower cost material to work with than steel. There is no need for on-site welding and hence it is easy to install. The weight saving topside reduces the ballast required below the water line of the rig. The corrosion resistance means that the expected life is longer than steel, and hence means fewer work days are lost during replacement of components.

There is one major disadvantage of GRP when compared to other materials, its flammability. Furthermore, there are many variations possible in the manufacture of GRP, not just the resin and reinforcement types, but the volume fraction of the resin, angle of winding in pipes etc. These many variables add to the general lack of knowledge and confidence about the performance of GRP in fire.

The use of polymer composite pipes and panels in fire will be investigated in depth with respect to the philosophy behind the materials use, as well as the actual performance in standard fire test conditions. Chapter 4 investigates FRP panels and sandwich panels in fire and discusses the applicability of the testing conditions adopted to real fire scenarios. Chapter 5 discusses the use of FRP pipes in fire conditions, together with development work at increasing the fire endurance of the pipes when in the critical empty and dry condition.

1.6 Polymer Composites in Fire

As mentioned previously, fibre reinforced plastics degrade in fire and may also be flammable. The following text is written with regard to the use of the major resin systems - modified acryllic, phenolic, polyester, vinyl ester and epoxy in pipe and panel applications offshore. There has been a great deal of interest in the use of GRP pipe systems offshore and a lot of testing has been carried out in this field over the last ten years. The pipe area of GRP fire research will be covered in detail in chapter 5.

All of the above resins contain carbon and hydrogen, and therefore all the resins will burn. It is difficult to comment on the flammability of resins in general as each resin will have different characteristics dependant on what form the resin takes and what additives it contains. There is conflicting evidence with regard to smoke production and smoke toxicity of burning GRP pipes, however with regard to offshore use it is thought that smoke toxicity arising as a consequence of burning GRP components would not be important compared to the smoke production of a hydrocarbon fire.

Phenolic resins are well known for their high temperature resistance and low smoke production. They yield high amounts of char during pyrolysis and are very stable in temperatures up to 300°C. Decomposition commences at approximately 300°C and from 300-600°C mainly gaseous components are emitted accompanied by relatively small shrinkage. Above 600°C, the

shrinkage is high, the density increases and the permeability markedly decreases[8]. Water is one of the degradation products (in the form of steam) and in situations where porosity is low, sufficient pressure can build up for this to cause violent delamination of the samples.

Polyester resins are the most common form of resin used in GRP production, and by far the most important. The resin decomposes rapidly at a relatively low temperature when compared to phenolic resin (approximately 200-250°C). Polyester resins are inherently flammable and the use of additives and fillers to combat this problem will be discussed briefly in chapter 4. Vinyl ester resins are found to perform very similarly to polyester resins in fire tests though having superior mechanical properties.

Epoxy resins are used sparingly in GRP production as they are 2-3 times more expensive than polyester. They exhibit superior mechanical properties to polyesters in many cases, however, they may need to be cured at elevated temperatures. In fire they exhibit many similar properties to polyesters, but have the added advantage of being more stable when heated. The main disadvantage of epoxy resins when compared to polyesters is their much higher heat release rate.

Modified acryllic resins have a major advantage over the other resin systems, that being their very low viscosity. The low viscosity allows the resin to be used in a very heavily filled state whilst maintaining good workability.

1.7 Fire Testing and Current Limitations.

For the purpose of classification of fire performance, materials and components are considered in terms of their "reaction to fire" and their "resistance to fire". This thesis is primarily considered with the latter.

Currently the standard method of fire resistance testing of materials and elements of construction is the furnace test. Many alternative test methods have been used in the testing of structures and in particular pipes, usually in order to produce test conditions considered to be more representative of real fires, but without standardisation of test methods there is difficulty in analysis of test results and comparison of fire performance. Some of these alternative tests will be discussed later in this section.

There are two main time-temperature regimes which are used for furnace testing, the hydrocarbon curve (eg. Mobil, DoE) and the cellulosic curve (BS476, SOLAS, ASTM E-119). Variations do exist between the different heating regimes and, in the tests carried out by the author, all furnace testing was performed to either BS476 part 20[10] or to the DoE interim hydrocarbon curve[9]. Both of these time-temperature curves are governed by numerical equations as follows:

DoE hydrocarbon curve:-

$$T = 1100\ [1 - 0.325\exp(-0.1667t) - 0.204\exp(-1.417t) - 0.471\exp(-15.833t)]$$

The BS476 part 20 curve:-

$$T - T_o = 345\ \log_{10}(8t + 1)$$

Where: T_o = Initial room temperature
t = Time (minutes)

For testing, samples of materials are either mounted to the furnace (eg panel elements) or placed within the furnace (eg pipe loops, columns etc). The temperature within the furnace is measured via bare wire or sheathed thermocouples arranged symmetrically within the furnace. The positioning of the thermocouples is such that the hot junction is maintained at 100mm from the nearest point of the specimen. The temperature within the furnace is deemed to be the average of all four thermocouples at any specific time. Failure of the samples is deemed to have occurred when one or more of the following criteria has occurred:

1) **Stability** failure is deemed to have occurred when the unloaded specimen under test collapses, or if deflections are beyond acceptable limits. For load bearing specimens more stringent conditions are applied.

2) **Integrity** failure is deemed to have occurred when a crack appears in the material through which flames or hot gasses may pass to light a cotton wool pad held near the cold face, or if a fully developed crack exists.

3) **Insulation** failure is deemed to have occurred when the temperature on the unexposed face increases on average by more than 140°C or if the temperature at any single point increases more than 180°C above ambient t_o. This form of failure generally limits the materials and assemblies considered in this thesis.

Figure 1.6.1 shows a comparison of the hydrocarbon and BS476 cellulosic curves. The hydrocarbon curve, although not reaching as high a temperature as the cellulosic curve, does demand a very rapid increase in furnace temperature and as such imposes a severe thermal shock to the materials under test. The hydrocarbon curve reaches a temperature of 1100°C in approximately twenty minutes where as the cellulosic curve takes three hours to reach this same temperature.

There are discrepancies between these testing conditions and the ones which may be experienced in real fire situations. It has been reported that a large scale pool fire reached temperatures of 1200°C after only two or three minutes, with a full temperature range of 1000-1270°C[11]. Hence it must be accepted that fire testing will not necessarily give reliable results of how a material will perform in real fire situations, rather it is a way of testing for an acceptable level of

performance, and for comparing different materials.

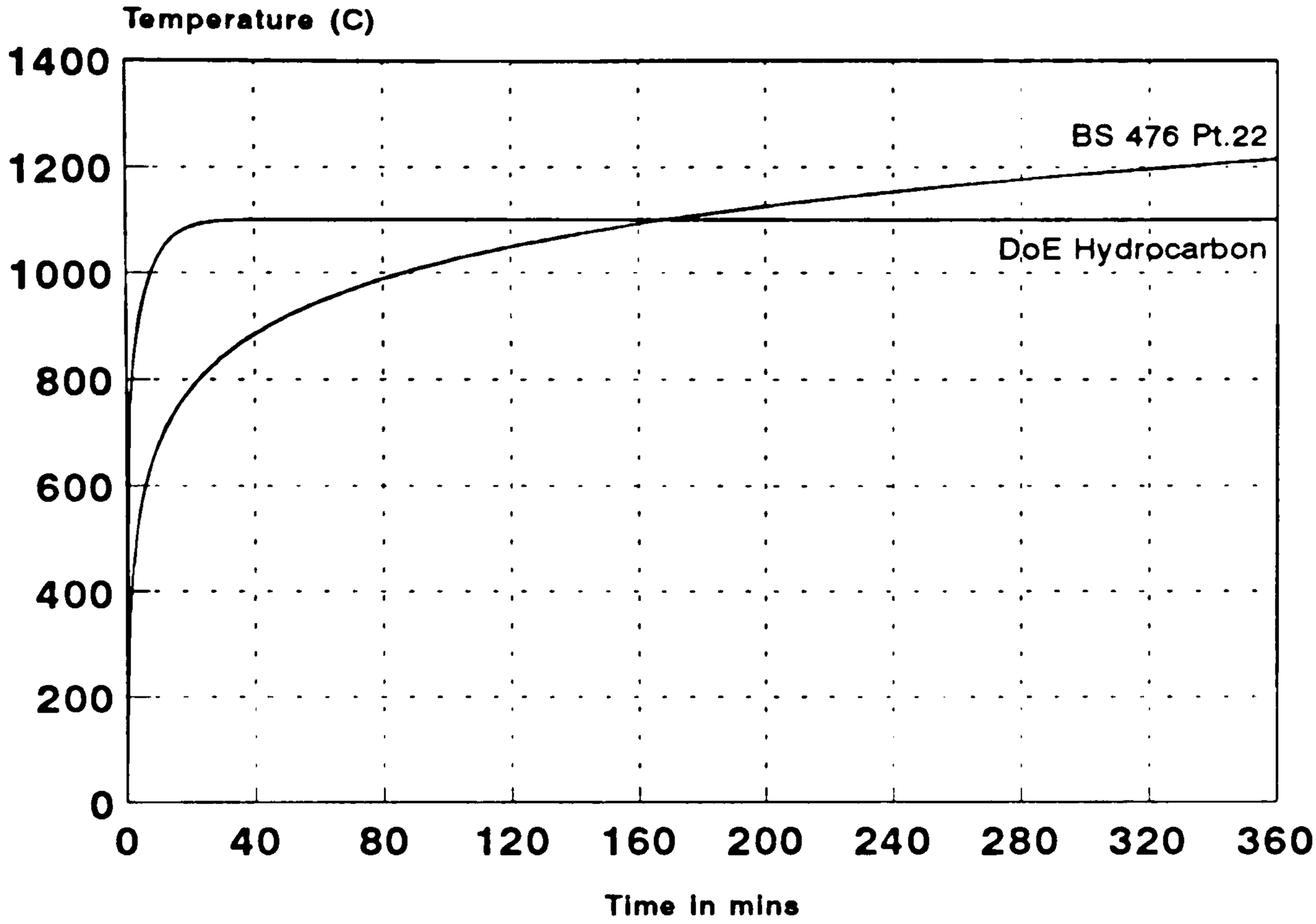

Figure 1.6.1 - Comparison of DoE Simulated Hydrocarbon Fire Test Curve and BS 476 Simulated Cellulosic Fire Test Curve

Furnace testing to British Standard conditions may well not be the best method of testing for fire resistance, particularly where the material under test is inherently flammable. The control of temperature within the furnace may not alone be sufficient where other factors such as heat flux and oxygen content within the furnace can have a large effect on the failure time of the tested sample. During a furnace panel test, the oxygen content may be at very low levels, some tests have reported just 4%[12] and, in these conditions, it is likely that the material under test will pyrolyse rather than burn. Under these conditions the sample experiences a general heat uptake from the furnace rather than a heat release while burning. It is thought that factors such as

furnace lining material and condition, fuel type, control type, number of burners and locations, orientation of the test piece will all have an effect on the fire endurance test results of materials. These factors will be discussed in much greater detail in chapter 6.

Alternative test methods for fire endurance testing are many and varied, however a few of the common ones are as follows:

Jet fire (large scale):

Jet fires typically consist of large reservoirs of stored natural gas or propane released under great pressure through a small diameter nozzle. Gas release rates can be anywhere between 1 and 20kg per second and the nozzle diameter is normally in the 20-75mm diameter range. Resulting flames can be anywhere up to 50m long, in many cases the first 5-20m of the flame is unburned gas, and the majority of the flame may be downstream of the target. Typical heat fluxes can be in the 100-300kW/m^2 range. Temperatures at the target are in the 1200-1400°C typically, with corresponding flame velocities of 50-60m/s[13].

Jet fire (reduced scale):

The reduced scale jet fire testing procedure is aimed at reproducing the

essential conditions (temperature and flame velocity) of large scale tests at laboratory scale. Many of the tests have used premixed combustion and high velocity gas burners, which lead to much more severe conditions than those associated with large scale diffusion flames. Fluxes of up to 1500kW/m² have been measured during tests, and the relevance of these tests must be questioned. The small scale jet fire as developed at SINTEF NBL (Norwegian Fire Research Laboratory, Trondheim) is more representative of actual conditions in diffusion jet fires. Typical characterisation work[14,15] for the SINTEF test shows temperatures of 1250°C, total heat flux of approximately 320kW/m² and flame velocities in the 45-60m/s range. The SINTEF test is not strictly representative of the large scale jet fire tests due to the method of testing. In a large scale jet fire the majority of heat available to the test specimen is in the form of back radiation from the downstream section of the flame. Hence, the points of maximum erosion/ablation, and maximum heating are in different locations on the sample. In the SINTEF test, due to its nature, the flame plume is generally on the upstream side of the sample, and hence the positions of maximum heating, and maximum erosion are much closer to each other on the sample surface.

Pool fire (full scale):

The pool fire test is normally carried out on either a full scale construction, or an element of one. The test fuel could be one of many, however in known test data[11] the fuel was kerosene. As its name suggests, the fuel source lies in a pool around the tested structure and is kept replenished via underground supply pipes. As mentioned previously rapid increase in temperature may be observed with temperatures over 1200°C after only 2 or 3 minutes. Total heat flux during the test referenced was typically 200-350kW/m^2 . Pool fires are greatly influenced by prevailing weather conditions, and as such temperatures and total heat fluxes observed during tests may vary. This of course will also be true if different fuel types are used.

Propane multiburner test (or sandbed diffusion burner):

This test method is generally used for fire testing water filled pipes or fire protected pipes. Flame velocities and heat flux tend to be low. In the case of the multiburner test[16] the flame control is based not on temperature, but maintaining a total heat flux of 113.6kW/m^2 (+/- 10%) 12.5 +/- 1cm above the centreline of the burner array which corresponds to the lowest point of the test specimen. The sandbed diffusion burner method[17] appears to be less controlled, and average

temperatures at the lowest point of the samples was in the 800-850°C range in known tests. Samples were mounted 350mm above the diffusion burner, and the temperature on the upper surface of the pipes may well have been higher than the figures reported due to back radiation from the flame.

As mentioned previously, furnace testing cannot be expected to be representative of some of these conditions (especially jet fires and pool fires), however it does give a common ground for materials to be assessed on and also a standard testing procedure. There are an infinite different number of test scenarios which could be adopted, many of those which have been used are likely to have been to assess a material or structure in a specific type of fire insult. The problem with non standard test methods is in the comparison of test results with those tested in furnace conditions.

Recently a modification of the hydrocarbon curve has been adopted in some test procedures, using what is known as the "simulated deluge ramp". As its name suggests, the reason for this adaptation is to simulate the cooling effect of the sprinkler/deluge system coming into operation during the progression of the fire. In these tests the control curve for the furnace normally follows the hydrocarbon curve for a specified period of time (usually five minutes) after which it is reduced to a constant temperature (usually 870°C). This again indicates the desire to represent real life fire situations in test arrangements. However the applicability of test results to what may be expected in real fires

cannot be commented on without defining the fire situation to be replicated. It is doubtful however that performance in test situations will mirror real fire performance.

These alternative test methods have been studied, and where possible, results obtained from other sources testing to these methods have been reviewed, and used to provide a "feel" for a materials performance in fire. Within this thesis however the standard furnace based fire resistance testing has been adopted, in particular furnace testing to simulated hydrocarbon fire conditions.

1.8 Numerical Modelling and the need for Reproducible Furnace Characteristics.

In both the onshore and offshore construction industries it is common to develop structural panels with specified fire resistance requirements. The most widespread method for development of these panels is on the basis of past experience, together with indicative and full scale furnace tests. A typical development process would start with small scale tests to determine material properties, indicative fire tests on basic panel elements, indicative fire tests on jointed panel elements and finally end with full size furnace testing. As can be seen, this method is both lengthy and correspondingly costly. Numerical modelling could ease the burden of need for testing dramatically as it can be used as a tool to predict the performance of a panel in a fire test. For this numerical prediction to be made, accurate test data is required about the thermal properties of the materials concerned.

As mentioned previously, furnace testing provides a common ground for the comparison of materials in fire situations. However a recent study of three different furnaces[18] concluded that different test furnaces had differing degrees of thermal severity during the test runs. The reason behind this is the non-standard design of fire test furnaces throughout Europe. Variations exist not just in the lining materials, but also in dimension, burner locations, fuel types etc. Numerical modelling, if it is to be an effective tool, needs "standard" test data for input. In the absence of non-standardised testing methods it is

essential that there are numerical data on the effect that the variations in test methods will have on fire test results. Cooke[18] forecast that to standardise approved test furnaces in Europe may cost in the region of £50 million and hence there is no clear incentive for the laboratories to perform this work. Furnace characterisation is covered in chapter 6, where the effects of furnace variables on heating rates of calibration rods and standard test pieces are investigated in greater detail.

Cone calorimeter data may be of great use in the numerical modelling as it is a standard test apparatus which has international standards and requirements. It is unlikely that cone calorimeter results alone will yield sufficient data for modelling for fire performance, however, coupled with knowledge of the effects of furnace variations on fire resistance tests it could provide accurate data sets for numerical predictions.

Accurate data sets for numerical modelling can aid successful forecasting of fire test performance. Figure 1.7.1 overleaf shows the results of an actual fire test carried out on a sandwich panel consisting of 6mm GRP faces with a 60mm Vermiculux core. The core in this case is hygroscopic, and the faces pyrolyse during the test (and hence burn away leaving only a glass tissue). Both of these factors make the numerical analysis increasingly difficult. The predicted result shows how accurate and useful numerical analysis can be when applied to fire testing. The use of numerical modelling as a design tool is considered in detail in chapter 4 for panels, and chapter 5 for the case of FRP pipes.

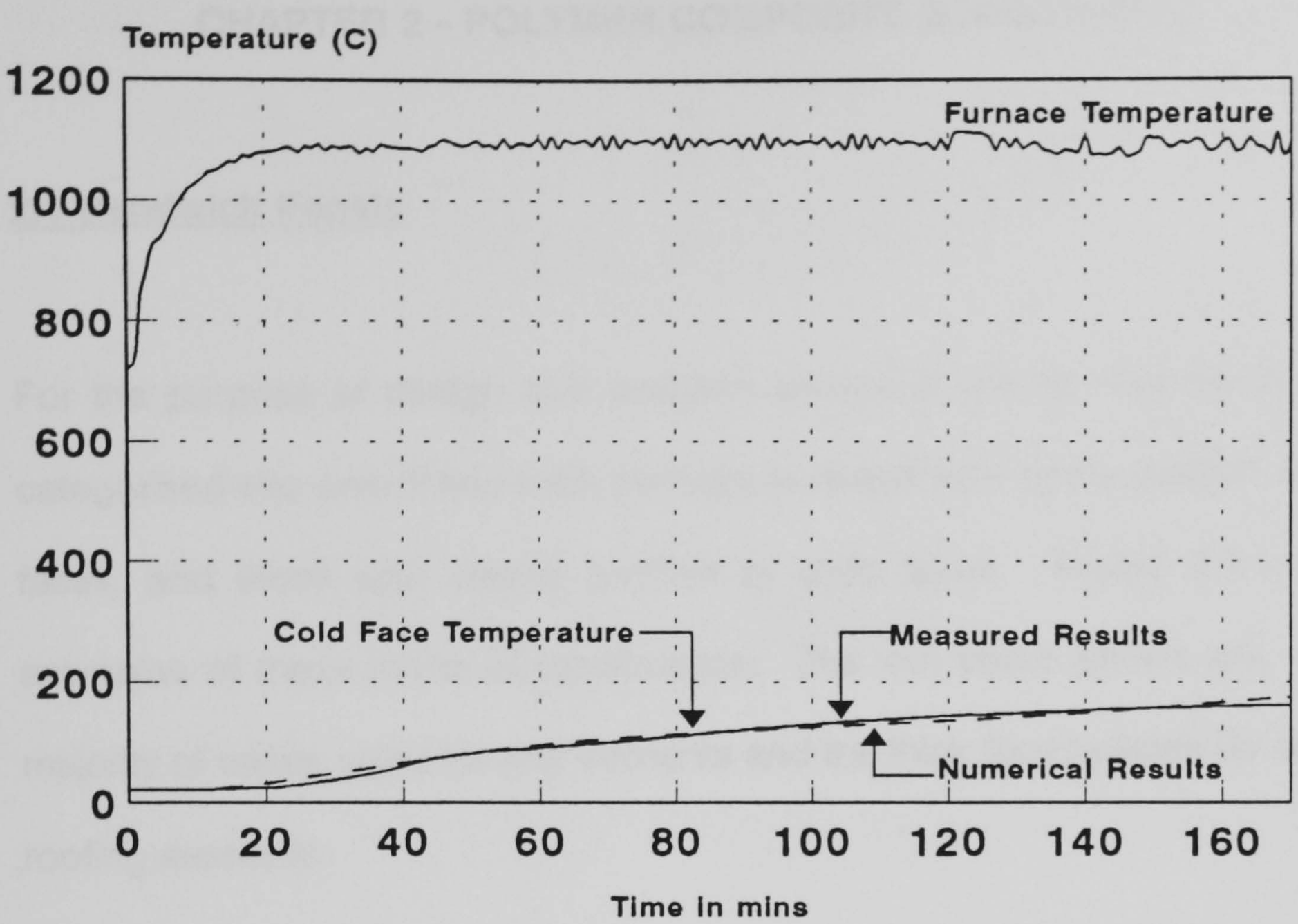

Figure 1.7.1 - 60mm Vermiculux with two GRP skins
Hydrocarbon Fire Test
Test results and Numerical Model

CHAPTER 2 - POLYMER COMPOSITE STRUCTURES

2.1 Sandwich Panels

For the purpose of design and analysis, sandwich panels may be broadly categorised into one of two main formations, those with lightly profiled or thin faces, and those with deeply profiled or thick faces. Figure 2.1.1 gives examples of these forms of construction. The thin faced panels are, in the majority of cases, used for wall elements and the thick faced panels for wall or roofing elements.

Sandwich panels consisting of two relatively thin metallic faces and a foamed polymer core have been finding increasing use as the cladding of buildings over the last 25+ years. In an offshore environment it is unlikely that they will satisfy the structural performance requirements, and almost certainly not satisfy the fire requirements. To this end there has been increasing research into the use of non-polymer based panel cores and GRP faces with a view to their use in fire situations.

There are several classes of fire resistant panels, most common in offshore situations are those denoted A60, H60 and H120. The letter of the panel A or H refers to the fire environment for which it is suitable, A represents cellulosic fire conditions, H represents hydrocarbon fire conditions, and the number represents the required fire resistance time in minutes. In addition to fire

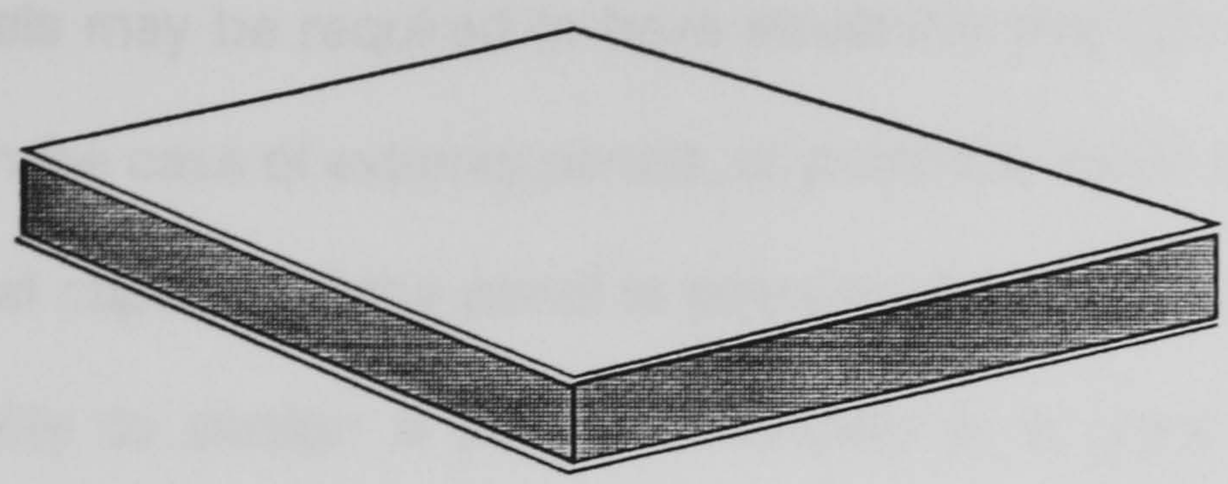

a) Panels with thin flat or lightly profiled faces

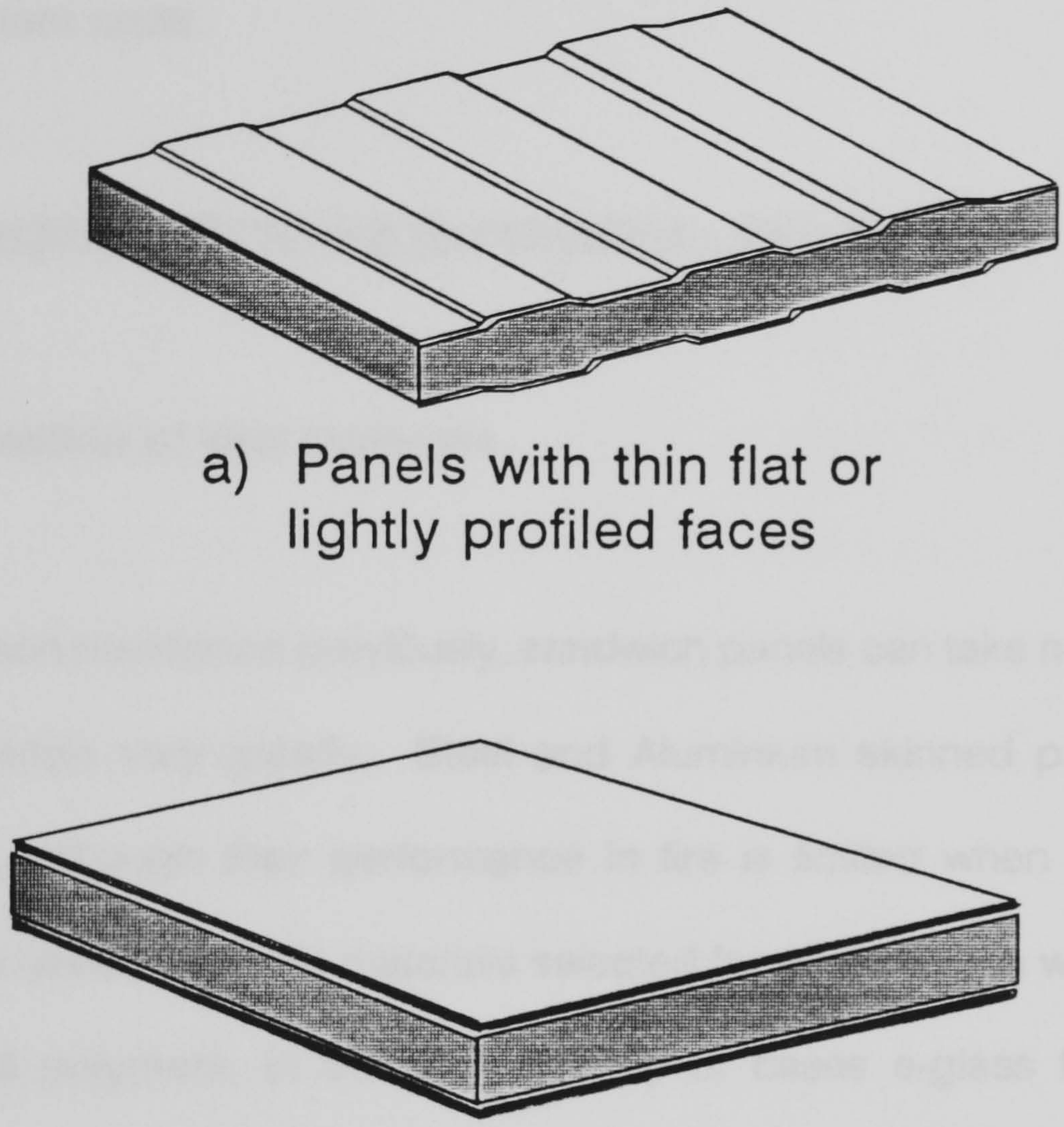

b) Panels with thick flat or heavily profiled faces

Figure 2.1.1 Typical Forms of Sandwich Panels

ratings, panels may be required to have structural strength to resist offshore wind loads in the case of external panels, or point/line loads for internal panels. The structural capacity of the panel is essential if it is to perform its function, and the ability to design a panel numerically is a great aid to reducing development costs.

2.2 Materials for Sandwich Construction - Skin Materials

2.2.1 Selection of skin materials

As has been mentioned previously, sandwich panels can take many forms, and skin materials vary greatly. Steel and Aluminium skinned panels are quite common, although their performance in fire is limited when foamed plastic cores are used. The skin materials selected for the research work are all fibre reinforced polymers, in the vast majority of cases e-glass fibre reinforced polyester. The combination of glass fibre and polyester resin was selected due to its common use, and price considerations.

There are many different resins which can be used in the production of GRP, being broadly grouped under the headings of polyesters, vinylesters, epoxies or phenolics. In addition to these, certain hybrid resins may be available such as polyester-polyurethane which may exhibit greatly enhanced properties over either of the parent ingredients. Epoxy resins are renowned for their superior strengths to polyesters, however they do carry a cost premium, as do phenolic

resins which are noted for their temperature stability and low smoke index in fire. As with resins there is a great variety of available reinforcing fibres. Glass is one of the most common, but for more mechanically demanding elements, aramid or carbon fibres may be used.

2.2.2 Requirements of the skin

The requirements of the skin material have been briefly described in the previous sections. The main requirement of the skins in a structural sandwich panel is to resist bending moments in conjunction with the core maintaining them at the required distance apart. It would be a misconception to presume that the skins of an FRP faced sandwich panel must provide a degree of fire resistance as this is not necessarily the case, however, they must not substantially add to the fire load when in a fire situation, nor provide a substantial increase to the toxicity of the burning products. The primary fire barrier of an FRP faced panel is usually the core material. Other requirements of the skins are that they must be reasonably light weight, must be easily fabricated and easily installed in the form of the completed panel.

In addition to the above, to prove financially viable, the panel faces must be corrosion resistant, giving an increased life expectancy over mild and stainless steel alternatives and reduced maintenance and hence reduced cost during its lifetime. To this end fibre reinforced plastics appear to be an obvious material for use, however, the inherent flammability of the resin matrices, and lack of

design standards have brought about a lack of confidence in, and a lack of enthusiasm for their use. Overall, there appears to be little understanding about how these materials perform structurally, both in the short and long term, and in fire situations. To begin to understand the structural performance of the materials it is probably easiest first to investigate their macrostructure and possible failure mechanisms.

2.2.3 Macrostructure of FRP

Reinforcing fibres may carry only tensile loads when in their unimpregnated form. However, they provide the majority of the tensile, flexural and shear strength and stiffness to a laminate when combined with a suitable resin. Incorporation of fibres (which act as microscopic crack arrestors) converts what may be a brittle resin into a tough fatigue resistant composite. GRP being a fibrous composite is inherently much stiffer and stronger than its constituents in bulk form[19]. This is due to the near perfect structure of fibres, and hence fewer defects than would be expected in a bulk material. Fibres in general are characterised by very high length to diameter ratios.

The strength of GRP laminates cannot be readily predicted from the properties of its constituents and as such must be evaluated with reference to test data[20]. Properties which may be required for the design of GRP are tensile, compressive and flexural strengths and stiffness, together with in plane and

inter laminar shear properties.

GRP may experience a decrease in strength when exposed to water[21], the rate of which depends on the resin matrix, laminate composition and quality, thickness, curing conditions and curing agents. This may be allowed for in the design of the structure by the use of a small material safety factor if desired, although as will be shown later, the faces of the panel are rarely the critical element. The effect of 5-10 years submersion in water may reduced the structural properties of GRP by more than 10%[22].

2.2.4 Failure mechanisms of FRP

The tensile failure mode of FRP is governed by microscopic defects distributed randomly along the length of the fibre from the manufacturing process. Failure occurs at the most severe defect, transferring load to others, then progressively to the next severe defect until all fibres fail. More complex failure mechanisms may be evident where unidirectional fibres are used. Here, if the strain to failure of the resin is lower than the strain to failure of the fibres then resin cracking will occur prior to fibre fracture (except where the fibre volume is very low). Failure due to fibre fracture generally results in an irregular failure surface where fibre pull out may be apparent. If the fibres have been degraded in some manner then a smooth failure surface may occur where the pull out force required is greater than the fibre strength.

Failure of a unidirectional fibre reinforced plastic laminate under tensile load across the line of fibres occurs by fibre debonding and matrix cracking. The failure load is normally less than that of the unreinforced matrix.

Where cross ply or fabric reinforced laminates are used, the failure mode is likely to be intermediate between the longitudinal and transverse strength of unidirectional fibres outlined previously. As such, the expected strength of the laminate will lie between the two also.

Under compression, failure is most likely to occur via microscopic buckling of individual fibres which act as cylindrical beams and columns in an elastic foundation of surrounding matrix. Buckling may be extensional (out-of-phase) at low shear stresses or of shear form (in-phase) leading to the formation of 'kink bands' which are commonly seen in the compressive failure of laminates. With high rigidity fibres (i.e large diameter hollow and/or high modulus) shear failure of the matrix may precede fibre instability.

The compressive strength of GRP is strongly influenced by imperfect fibre straightness, fibre continuity, deficient fibre/matrix adhesion and voids (particularly at the fibre-resin interface).

Fibre reinforced laminates, particularly filament wound cylinders may be more susceptible to fatigue failure under compressive than under tensile loads. It has been found that an increase in fibre contents results in an improvement of

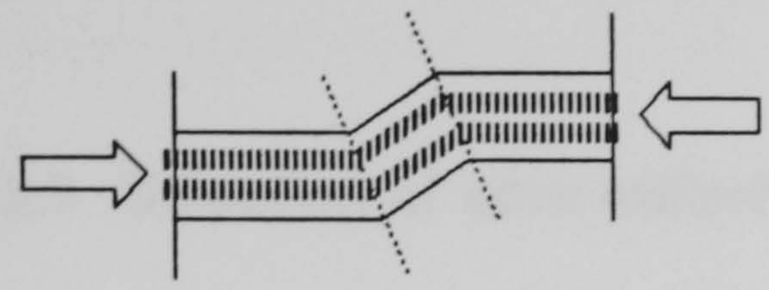

Buckling form of compressive failure

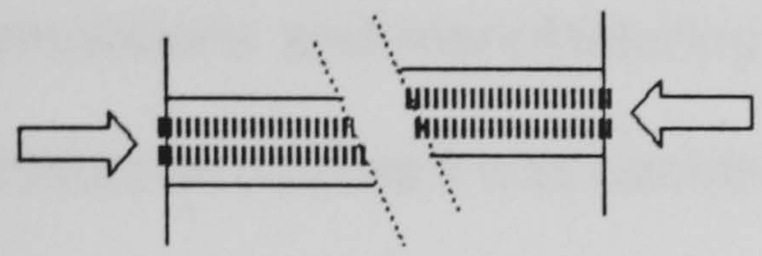

Shear form of compressive failure

fatigue strength.

Below 20% of the short term ultimate strength fatigue failure is unlikely to occur[21,22]. The fatigue failure mechanism begins with local debonding between fibres and resins, followed by numerous microcracks along fibre-resin interphases. Tensile failure of single fibre will then occur, and finally a microscopic crack will develop and propagate to failure. Below 20% of the short term ultimate stress creep under load will also not cause problems.

2.3 Materials for Sandwich Construction - Core Materials

2.3.1 Selection of core materials

There are several core materials in current use incorporating many different formulations and manufacturing methods. As this research is based around offshore structures it was decided to select a few available core materials which may show sufficient fire resistance, and also to develop a new material which may be used in severe fire situations. The requirements for the new material were that it must provided adequate structural and fire performance whilst remaining easy to manufacture and incorporate low cost constituents. The new material development will be presented fully in chapter 3. The predominant materials selected for investigation within this research were the fire resistant core materials as produced by Cape Boards Limited, namely Vermiculux (two different formulations), and Newtherm. In addition to these, phenolic foam of nominal density 150kg/m^3 by Permali was also investigated. It was felt by the author that investigation of other foamed polymer core materials such as polystyrene and polyurethane was not required in the investigation due to their relatively poor fire performance. The materials selected were seen as being the state-of-the-art available materials at the time of research.

Fibrous core materials such as stack bonded mineral and ceramic fibres were not investigated in the authors research. The research was predominantly to deal with core materials available for use with fibre reinforced polymer faces.

The difficulty in working with these fibrous materials negated the possibility of including them within the research. However, ceramic fibre was included within the work used as a core material for the structural stringer panel investigation. In this case it was used as a non-structural core of low density and high thermal resistance and was used in the form of a pressed blanket. Stack bonded fibrous cores are manufactured from parallel bonded fibres which are pressed with the inclusion of a resin binding agent, cut to lengths (100mm for example for a 100mm thick core) and then bonded between the panel faces. Thus a series of sections are used "on end" for the core construction.

2.3.2 Requirements of a core material

The main structural requirement of a sandwich panel core is to maintain integrity and support the faces at the required distance apart whilst carrying the shear between the two faces. The core should be relatively stiff in shear however it need not have excessive compressive strength as long as it can carry the design load without crushing at supports or points of load. Another requirement of the core is that it should be sufficiently strong to stabilise the faces and resist compression or shear buckling. The resistance to buckling is also effected by the bonding method between the core and the faces.

The core should have a certain integral amount of toughness to absorb shock loads and dynamic stresses as well as the ability to recover and ensure reliable functioning of the component over its designed lifespan. It is a requirement

also that the core and skins are chosen to complement each other. For instance if the skin requires a high curing temperature then a core must be chosen which will withstand that temperature. This point of choosing a core and skins to compliment each other is essential in continuous production processes. However, where core and skins are manufactured separately and then bonded together it becomes less of a problem as long as a suitable glue or resin is chosen that will not attack the face or core.

One important requirement of the core material, particularly for offshore use, is fire resistance. The core may act as the primary fire barrier in panels which require a high degree of fire resistance. To this end it must resist the passage of heat through it at the same time as maintaining structural stability and integrity. These factors are very important in the case of GRP faced sandwich panels as due to the nature of the faces it is likely that they will burn and disintegrate as the fire progresses, and may even fall off. The fire requirements of a panel and core will be presented in greater detail in chapter 4.

2.3.3 Failure Mechanisms of the Core

Structural failure mechanisms of core materials depend on the nature of the materials used. With cores of low compressive strength crushing at supports or points of load may be a likely failure mechanism. If the loaded face is flat or only lightly profiled the point or line load is resisted predominantly by the core. It is also possible that the crushing load may interact with bending forces which

are also present hence reducing the bending resistance of the sandwich section.

Apart from the local influences of load, i.e. near points of support etc, the only other significant stresses within the core of a sandwich panel are the shear stresses necessary to obtain composite action. These shear stresses within the core although not being uniform are close enough to be treated as such. Providing that the shear strength of the core, and the bond strength of the core material with the faces are known, the shear capacity of the sandwich section can be designed for as shown later in this chapter.

In practice, with GRP faced panels and substantial fire resistant cores, the design limitation will often be one of allowable deflection. This is due to the relatively low elastic modulus of fibre reinforced plastics (when compared to steel), and reasonably high shear strength of fire resistant cores which tend to be substantial and relatively dense materials when compared to thermoplastic foams.

2.4 Determination of Design Parameters for Sandwich Materials

Material design parameters are generally obtained through the testing to failure of small samples in compression, flexure and shear. Several samples cut from a single original, or from several mother samples may be used in these tests to provide a reliable average of the materials performance and also to give information on the standard deviation of structural properties to provide a reasonable safety factor.

The following sections give information on the testing methods adopted within the research to obtain the mechanical properties of core and face materials required for designing panels.

2.4.1 Compression test

This test is used to determine the compressive strength and corresponding relative deformation of a material.

Specimens of 50 x 50 x 50mm thick of the core are tested between two flat hardened steel plates in a universal testing machine or compression machine. This size of sample adopted for the research is not always adopted in standard compression tests. A sample size of 100 x 100 x 100mm thick is also frequently used and referred to in national and international standards. It was decided that a standard strain of 2% per minute should be adopted for all

materials up to a maximum strain of 10%. The compressive stress at failure of the sample can be calculated as:

$$\sigma_{cr} = \frac{P_{max}}{A}$$

and the elastic modulus can be determined from the load-deflection curves produced during the test on an autographic recorder.

Typical cube compression traces are shown in figure 2.4.1 for varying materials. The oscillating curve for the phenolic foam is due to the build up of stress and crushing of layers of cells rather than the whole sample at once.

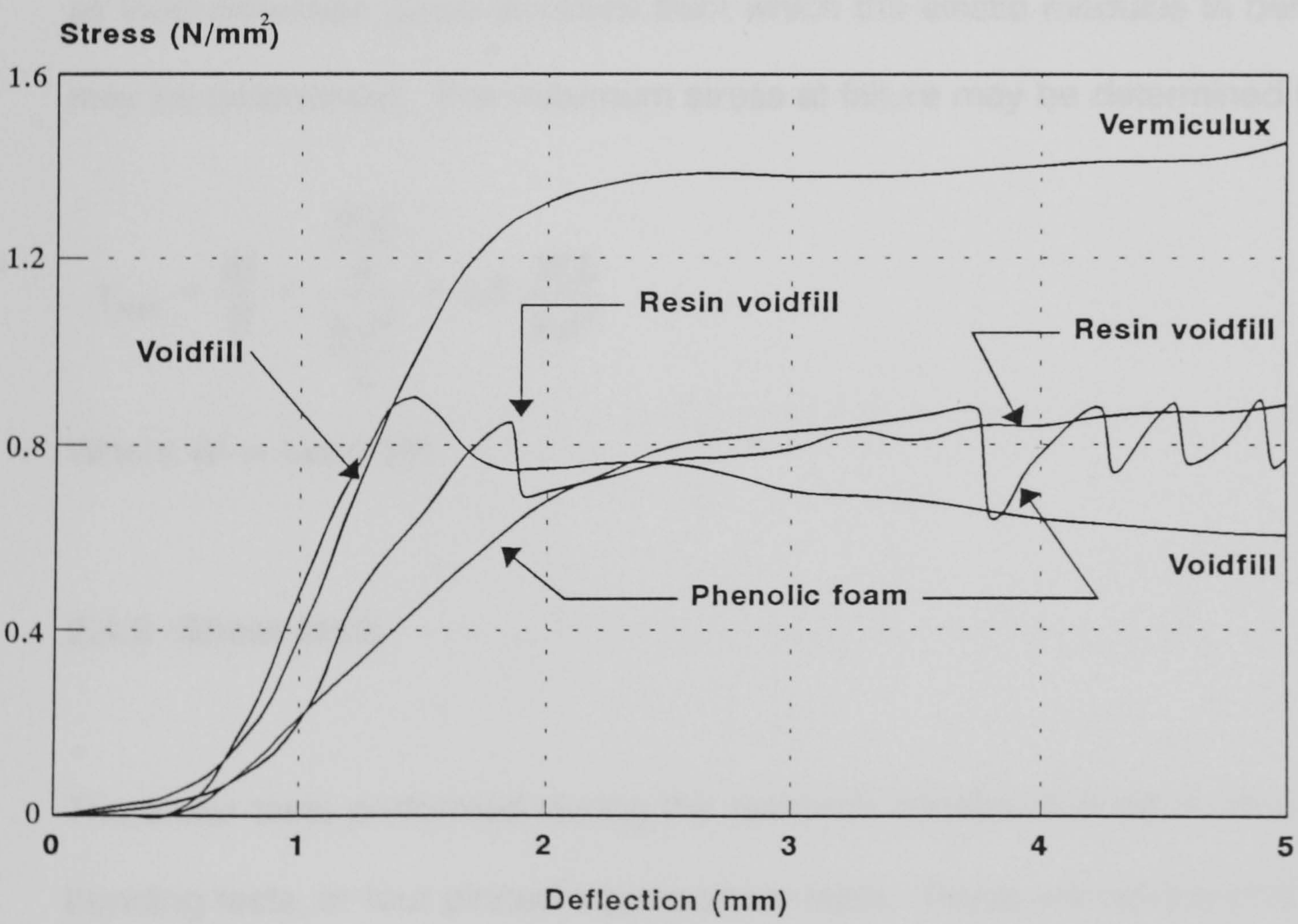

Figure 2.4.1 Typical Cube Compression Traces for Different Core Materials.

2.4.2 Flexural test

These tests were performed on a simple support frame, loading the samples at midspan via a load hanger and spreader plate. The test is not effective for determining whether a sandwich sample would fail in shear or bending (cracks progressing from the tension surface), however, it does provide a 'feel' for the materials bending characteristics.

Load was applied in steps of 0.2, 0.5, 1.0 or 2.0kg during the test depending on the strength of the sample and the deflection was measured using a dial gauge with a gauge step of 0.01mm. The results were then plotted to provide as load-deflection curve to failure from which the elastic modulus in bending may be determined. The maximum stress at failure may be determined from:

$$\tau_{max} = \frac{M}{Z} = \frac{\frac{W.L}{4}}{\frac{b.d^2}{6}} = 1.5\ \frac{W.L}{b.d^2}$$

Where W = Load (N)

2.4.3 Shear tests

The shear tests performed during the research consisted of either four point bending tests, or four pinned square shear tests. These are not the only tests available to determine the shear modulus and shear strength of materials. However, they are the preferred manner of determination of material properties.

Lapped shear tests may be performed to determine shear parameters, but they appear to be unduly pessimistic when used to determine design values[23]. Davies[23] summarises the findings of Basu[24] when investigating the effect of test method on derived shear properties.

The four pinned square shear test (as shown in figure 2.4.2) is designed to induce pure shear into a sample with thick metal faces glued to its edges. The sample is then loaded in compression along its edges via two small bars between the joining points of the steel faces at two opposite corners. The load-deflection characteristics are recorded on an autographic recorder. The core shear properties can be found from the following equations:

$$\tau = \frac{P}{a.c.\sqrt{2}}$$

$$\gamma = \frac{2.\delta}{a.\sqrt{2}}$$

Where

a/2 = the distance between opposite diagonals of the sample
P = the load at which the sample fails
δ = the relative deflection at which the sample fails

The shear modulus can be found from the slope of the load deflection curve.

Four point bending tests were performed on samples of core material sandwiched between thin steel faces of known dimensions. The test span of these samples was 600mm, the core width 25mm, and the core depth generally 50mm. Load was applied via loose weights and a load hanger, in connection

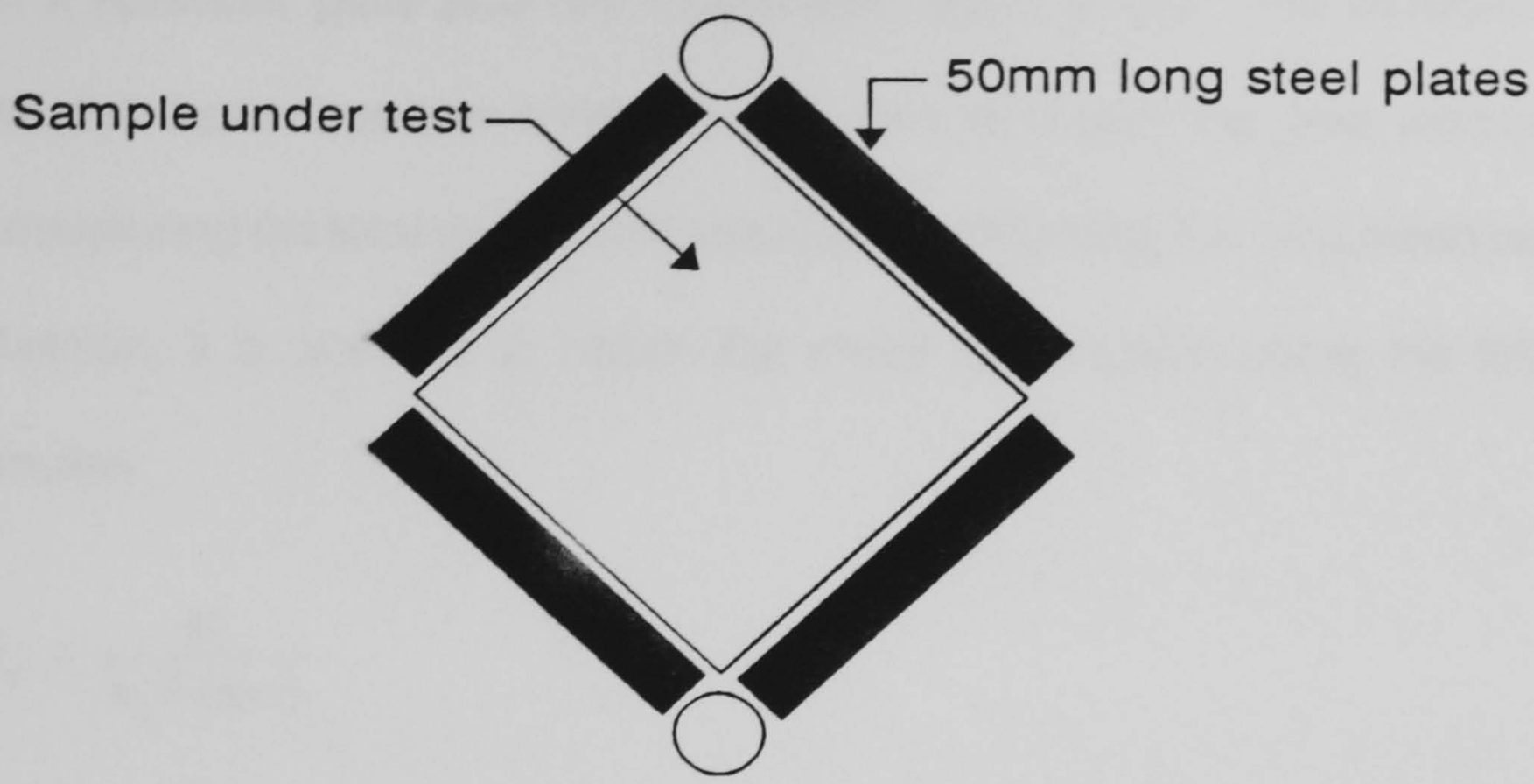

Figure 2.4.2 - Four pinned square shear test arrangement

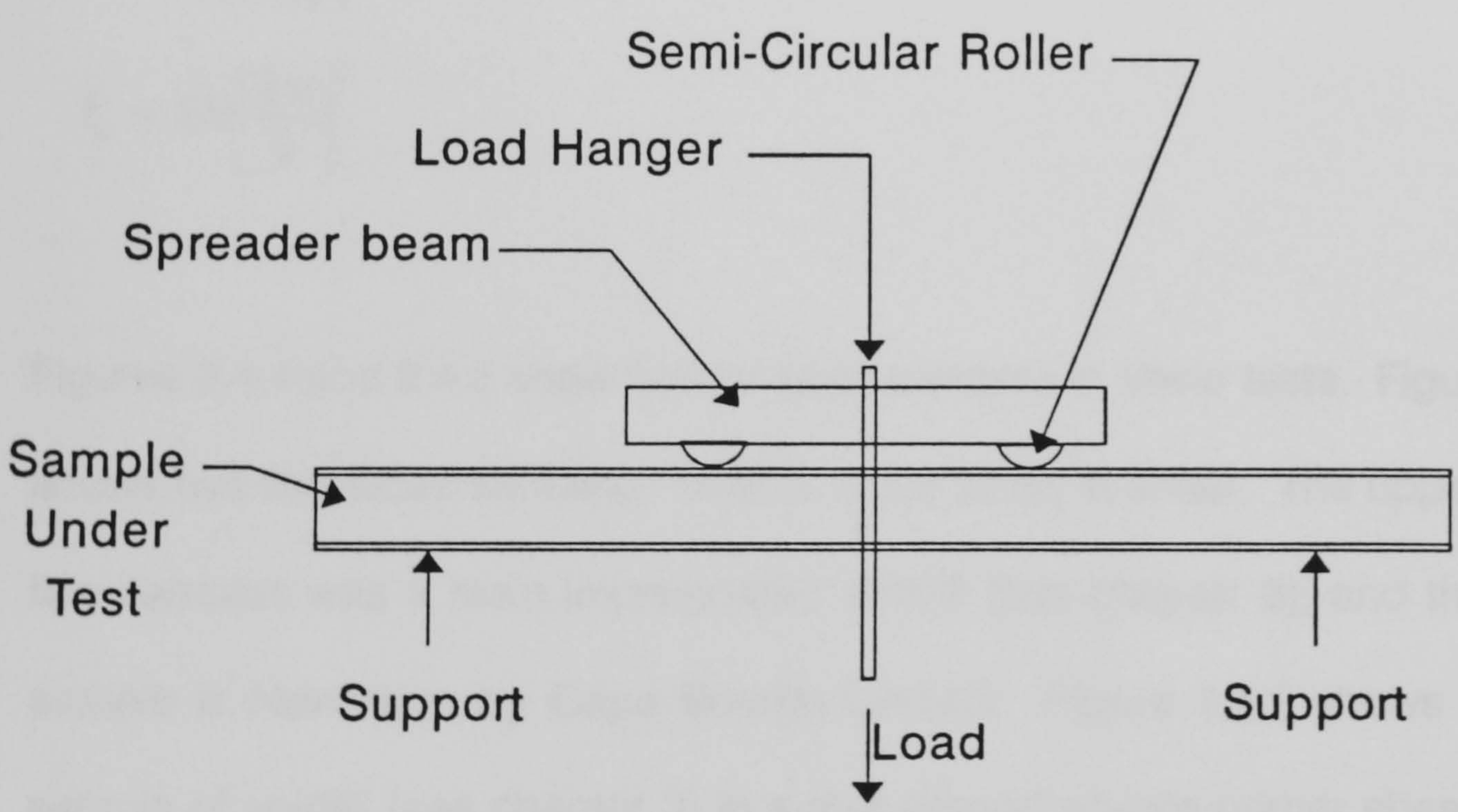

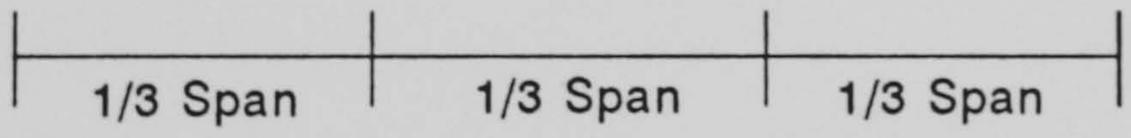

Figure 2.4.3 - The Four Point Bending Test

with a spreader plate and two rollers (see figure 2.4.3). The deflection of a sandwich beam has two components, shear and bending (see section 2.5). By measuring the total central deflection and subtracting the calculated bending deflection, it is possible to obtain the shear deformation using the following formulae:

$$G_c = \frac{M}{\delta_s . b.(h+t)}$$

$$\tau = \frac{Q}{b(h+t)}$$

where:

$$\delta_s = \delta_t - \delta_b$$

$$\delta_b = \frac{Ml^2}{9.39E_sI_s}$$

$$I_s = 2bt\left[\frac{h+t}{2}\right]^2$$

Figures 2.4.4 and 2.4.5 show typical failed samples in shear tests. Figure 2.4.4 shows two thin faces sandwich beams which failed in shear. The upper of the two samples was a resin impregnated voidfill (see chapter 3), and the lower sample is Newtherm by Cape Boards Limited. Figure 2.4.5 shows a failed sample of voidfill (see chapter 3) in a four pinned square corner shear test.

2.4.4 Tensile tests

Direct tensile tests were performed on face material formulations in order to deduce the failure stress in direct tension, and also to find the elastic modulus.

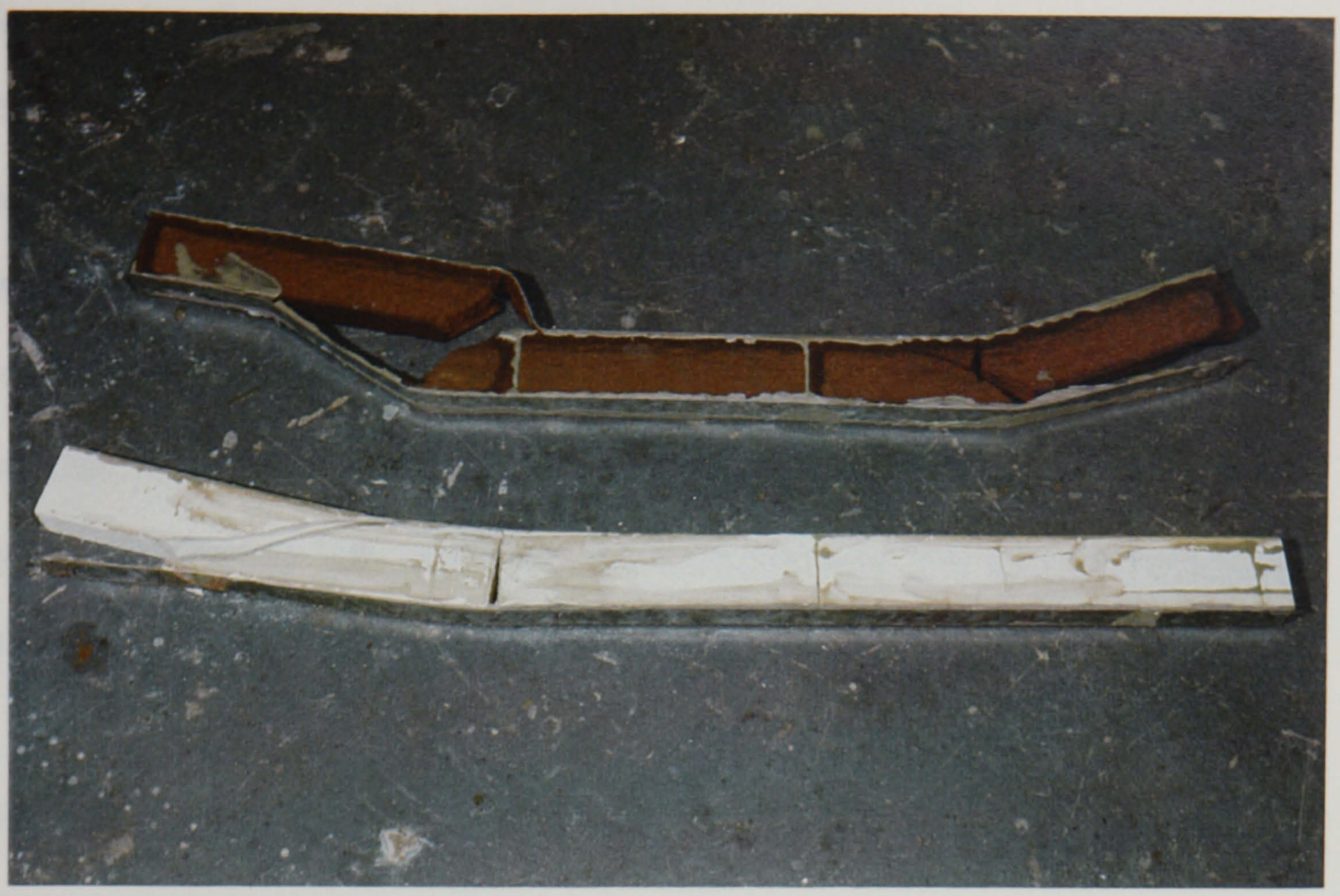

Figure 2.4.4 - Thin faced sandwich beams after testing
(top) Resin impregnated Voidfill, (btm) Newtherm

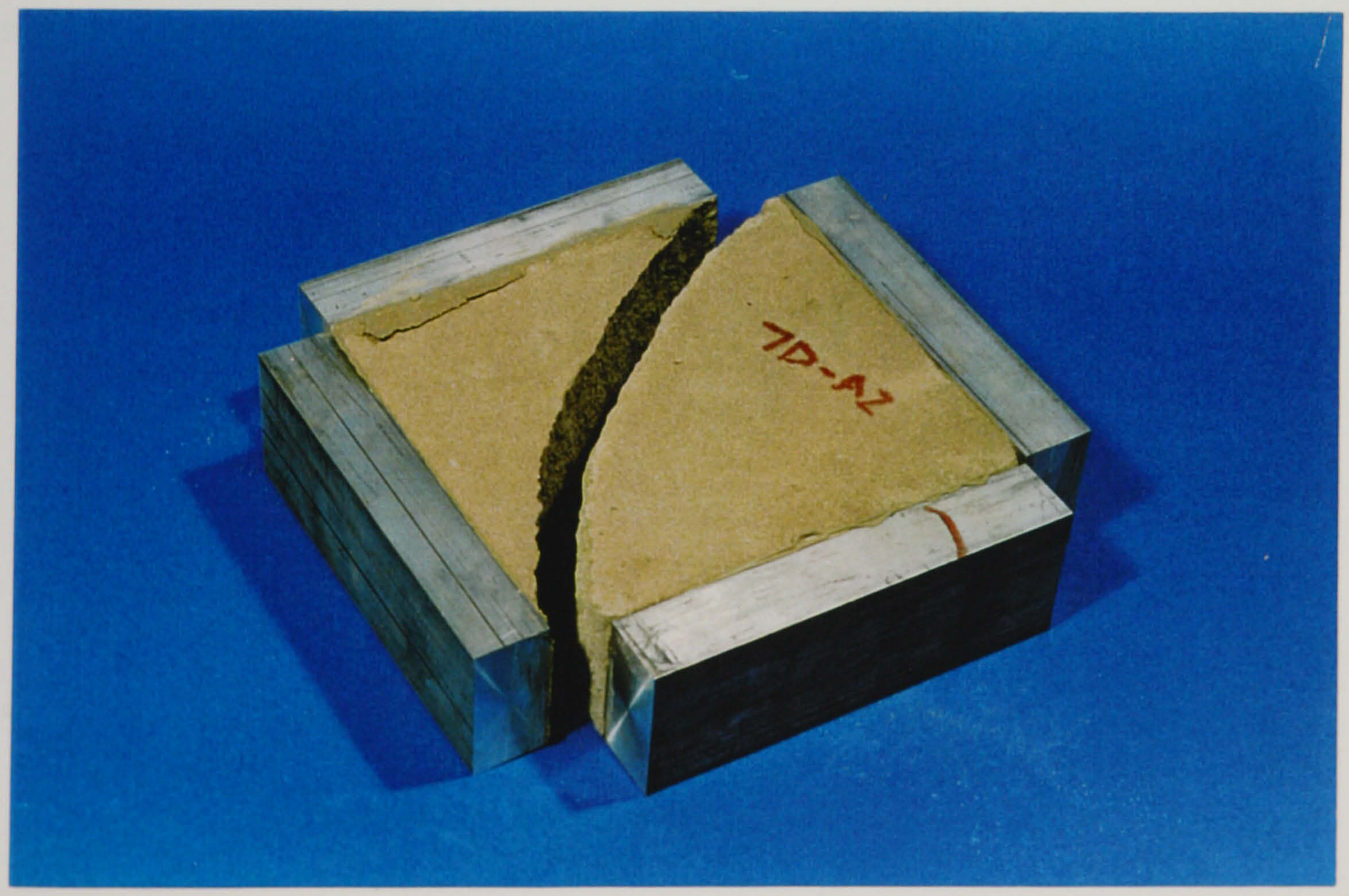

Figure 2.4.5 - Voidfill 7D after four pinned square shear test

Samples for direct tensile testing were cut on a bench saw to a "dog-bone" shape as prescribed in BS 2782[25]. These samples were then mounted in the jaws of a universal testing machine, and load was gradually applied to the point where there was no slip between the sample and the jaws. The load was then released and an extensometer was mounted within the gauge length of the sample. The load-deflection characteristics were recorded at 0.5kN intervals until approximately 75% of the expected failure load. The extensometer was removed, and the sample was then loaded to failure.

This relatively simple test method provides results from which the tensile failure stress and elastic modulus can easily be calculated. Stress being force divided by area, and the elastic modulus being stress divided by strain (determined from the extensometer).

2.5 Principles of Sandwich Construction

As has been mentioned previously, a typical sandwich panel consists of two relatively thin, stiff and strong faces with a thicker layer of a much weaker core material. The main requirement of the core material is to maintain the faces at a constant distance apart and to be reasonably stiff in shear. The faces act to carry in plane compressive and tensile loads hence resisting bending deflection whilst contributing no shear resistance to the section and having little or no bending strength individually. The core conversely being a much weaker material is considered only to carry shear deflection loads and not contribute to bending resistance. The design of panels is complicated in the case of thick faced panels where the faces of the panel will have a significant bending strength of their own. Below is a list of general assumptions for the design of thin faced sandwich panels.

1) The faces and the core are both linearly elastic.

2) There is adequate adhesion between the core and the faces.

3) The shear stress distribution through the depth of the core is constant.

4) Deflections are small in relation to span.

5) The core is too weak to provide significant flexural rigidity to the panel.

6) There is no deformation of the core in a direction perpendicular to the core.

Following are the solutions from Allens theory[26] for the design and analysis of sandwich panels with thin faces under a single central point load and also fora uniformly distributed load. The solutions are based upon ordinary beam theory.

The general displacement equation which is derived contains two terms, the first as given below represents the ordinary bending deflection and the second is the additional displacement caused by shear strain of the core. The final solution is as follows:

$$\delta = \frac{W L^3}{48 D} + \frac{W L}{4 A G}$$

Where:

W = Load (N)
L = Span (mm)
D = E_f.(b.t.d^2)/2 (N/mm^2)
A = b.d^2/c (mm^2)
G = Shear modulus of core (N/mm^2)

Similarly, for a simply supported beam with an imposed uniformly distributed load q, the total central deflection is:

$$\delta = \frac{5 q L^4}{384 D} + \frac{q L^2}{8 A G}$$

As can be seen, the solutions are relatively simple and easy to use, but highly accurate provided that the assumptions are correct. These solutions,however, only describe the load deflection characteristics of the sandwich beam. The shear stress in the core, τ, can be calculated as described in section 2.4.3 and

allowing for an appropriate safety factor the panel may be assessed for shear capacity. Wrinkling of the compression face is another factor which should be considered for thin faced sandwich panels. The stress, usually at the point of maximum bending, at which wrinkling of the compression face will occur is generally calculated as:

$$\sigma_{wr} = K_1 \sqrt[3]{G_c E_c E_f}$$

Where

G_c = Shear modulus of the core
E_c = Elastic modulus of the core (average of tensile and compressive moduli)
E_f = Elastic Modulus of the face
K_1 = Semi-empirical factor to take account of imperfections. Generally taken as 0.65 from European recommendations.

In the case of analysis of a sandwich beam with thick faces, the process is much more involved, and the solution a great deal more complex. Thick faced sandwich panels have been analyzed by many people, but by far the neatest and most comprehensive is that presented by Stamm and Witte[27], and Davies[28]. The solution for a simply supported single span beam with point load at a variable along its length is presented here together with a description of how this is to be modified for four point bending.

The behaviour of thick faces refers to the situation where the local bending rigidity of the facings contributes significantly to the overall sandwich stiffness. The contribution of the thick face has two separate components (See Figs. 2.5.1(a) and 2.5.1(b).)

From the figures 2.5.1(a) and 2.5.1(b), the Stamm and Witte theory is as follows, in which a derivative with respect to x is denoted by a prime (′).

The relationship between stress resultants and deformations are:

$$M_1 = - B_1 W'' \; , \; M_2 = - B_2 W'' \; , \; M_3 = B_S \, (\gamma' - W'' + \theta) \qquad (2.5.1)$$

Where B_s = Bending stiffness of sandwich part of construction

$$Q_1 = - B_1 W''' \; , \; Q_2 = - B_2 W''' \; , \; Q_s = A \; G_{eff} \; \gamma \qquad (2.5.2)$$

As stress resultants in the two faces are proportional to the same deformations, it is convenient to treat them together.

$$M_D = M_1 + M_2 \; ; \; M = M_D + M_s$$
$$Q_D = Q_1 + Q_2 \; ; \; Q = Q_D + Q_s$$
$$B_D = B_1 + B_2 \; ; \; B = B_D + B_s$$

From equations (2.5.1), (2.5.2) and the above convenient combinations the following differential equations can be formed;

$$AG_{eff} - B''_{DW} = Q \qquad (2.5.3)$$

$$B_s \, (\gamma' + \theta) - BW''' = M \qquad (2.5.3)$$

Eliminating γ and noting that Q' = -q a fourth order differential equation in terms of W is obtained:

$$W^{IV} - \left(\frac{\lambda}{L}\right)^2 W'' = \left(\frac{\lambda}{L}\right)^2 \frac{M}{B} + \left(\frac{1+\alpha}{\alpha}\right) \frac{q}{B} - \left(\frac{\lambda}{L}\right)^2 \frac{\theta}{1+\alpha} \qquad (2.5.4)$$

where L is the total span of the panel and;

$$\alpha = \frac{B_o}{B_s} \; ; \; \beta = \frac{B_s}{AG_{eff} L^2} \; ; \; \lambda^2 = \frac{1+\alpha}{\alpha \beta} \qquad (2.5.5)$$

Similarly, eliminating W from equations (2.5.3)

$$\gamma'' - \frac{\lambda^2}{L}\gamma = -\frac{1}{B}\beta\lambda^2 Q \qquad (2.5.6)$$

The equations in this form are particularly useful when the distribution of bending moment M and shear force Q are known, i.e. in statically determinate systems. For such cases, the general solutions of equations (2.5.4) and (2.5.6) are:-

$$W = C_1\cosh\frac{\lambda x}{L} + C_2\sinh\frac{\lambda x}{L} + C_3 + C_4 x + W_p \qquad (2.5.7)$$

$$\gamma = D_1\cosh\frac{\lambda x}{L} + D_2\sinh\frac{\lambda x}{L} + \gamma_p \qquad (2.5.7)$$

Where W_p and γ_p are particular integrals which depend on the loading case, etc. As these solutions must also satisfy (2.5.3) it can be shown that:

$$D_1 = (1+\alpha)\frac{\lambda}{L}C_2 \quad ; \quad D_2 = (1+\alpha)\frac{\lambda}{L}C_1 \qquad (2.5.8)$$

Hence the number of constants of integration reduces to four, and these can be readily obtained from boundary conditions, e.g for a simply supported beam;

$$W(o) = 0 \; ; \; W''(o) = 0 \; ; \; W(L) = 0 \; ; \; W''(L) = 0 \qquad (2.5.9)$$

Stamm and Witte give three specific solutions to the previous equations for simply supported panels subjected to:

1) Uniformly distributed load

2) Single point load within the span

3) Uniform temperature difference between the faces

and from combinations of the above three solutions more complex loading cases can be considered. Following is a solution for the simply supported panel with a single point load case. The principle of superposition can be used to find Stamm and Witte solutions for the four point bending case (see later) that the sandwich panel developments were tested to.

Simply supported panel with point load, P

Consider the simply supported panel as shown in figure 2.5.2(c), if the point load P is applied at a position x = e, ie $\xi = e/L = \epsilon$ the bending moment and shear force are given by;

$$M = \frac{P}{L}(L-e)x - P\langle x-e\rangle^{o} \qquad (2.5.10)$$

$$Q = \frac{P}{L}(L-e) - P\langle x-e\rangle^{o} \qquad (2.5.10)$$

where $\{...\}^{\circ}$ is the McCawley convention and denotes that the bracketed value is set to zero when the contents are negative.

The Particular integrals in equation (2.5.7) are now,

$$W_p = \frac{P}{6BL}[-(L-e)x^3+L\{x-e\}^3]-\frac{PL}{B\lambda^2}\left[(L-e)x+\frac{L}{\alpha}\left(x-e-\frac{\sinh\lambda(x-e)/L}{\lambda/L}\right)\{x-e\}^o\right]$$

$$\gamma_p = \frac{\beta PL}{B}\left[L-e-L\left(1-\cosh\frac{\lambda(x-e)}{L}\right)\{x-e\}^o\right] \qquad (2.5.11)$$

Giving index value 1 valid for $0\le\xi\le\epsilon$ and 2 for $\epsilon\le\xi\le1$

$$W_1 = \frac{PL^3}{B}\left(\frac{1}{6}(1-\varepsilon)\xi(2\varepsilon-\varepsilon^2-\xi^2) + \frac{1}{\alpha\lambda^2}(1-\varepsilon)\xi - \frac{1}{\alpha\lambda^3}\frac{\sinh\lambda(1-e)}{\sinh\lambda}\sinh\lambda\xi\right)$$

$$W_2 = \frac{PL^3}{B}\left(\frac{1}{6}\varepsilon(1-\xi)(-\varepsilon^2+2\xi-\xi^2) + \frac{1}{\alpha\lambda^2}e(1-\xi) - \frac{1}{\alpha\lambda^3}\frac{\sinh\lambda e}{\sinh\lambda}\sinh\lambda(1-\xi)\right)$$

$$\gamma_1 = \frac{PL^2}{B}\beta\left(1-\varepsilon+\frac{\sinh\lambda(1-\varepsilon)}{\sinh\lambda}\cosh\lambda\xi\right)$$

$$\gamma_2 = \frac{PL^2}{B}\beta\left(-\varepsilon+\frac{\sinh\lambda\varepsilon}{\sinh\lambda}\cosh\lambda(1-\xi)\right)$$

$$M_{s_1} = PL\frac{1}{1+\alpha}\left((1-\varepsilon)\xi - \frac{\sinh\lambda(1-\varepsilon)}{\lambda\sinh\lambda}\sinh\lambda\xi\right)$$

$$M_{s_2} = PL\frac{1}{1+\alpha}\left(\varepsilon(1-\xi) - \frac{\sinh\lambda\varepsilon}{\lambda\sinh\lambda}\sinh\lambda(1-\xi)\right)$$

$$M_{D_1} = PL\frac{\alpha}{1+\alpha}\left((1-\varepsilon)\xi - \frac{\sinh\lambda(1-\varepsilon)}{\alpha\lambda\sinh\lambda}\sinh\lambda\xi\right)$$

$$M_{D_2} = PL\frac{\alpha}{1+\alpha}\left(\varepsilon(1-\xi) + \frac{\sinh\lambda\varepsilon}{\alpha\lambda\sinh\lambda}\sinh\lambda(1-\xi)\right)$$

$$Q_{s_1} = P\frac{1}{1+\alpha}\left(1-\varepsilon-\frac{\sinh\lambda(1-\varepsilon)}{\sinh\lambda}\cosh\lambda\xi\right)$$

$$Q_{s_2} = P\frac{1}{1+\alpha}\left(-\varepsilon+\frac{\sinh\lambda\varepsilon}{\sinh\lambda}\cosh\lambda(1-\xi)\right)$$

$$Q_{D_1} = P\frac{\alpha}{1+\alpha}\left(1-\varepsilon+\frac{\sinh\lambda(1-\varepsilon)}{\alpha\sinh\lambda}\cosh\lambda\xi\right)$$

$$Q_{D_2} = P\frac{\alpha}{1+\alpha}\left(-\varepsilon-\frac{\sinh\lambda\varepsilon}{\alpha\sinh\lambda}\cosh\lambda(1-\xi)\right)$$

As the solution outlined above is for a general point load anywhere within the span, it follows from the consideration of superposition that for a four point loaded member the solutions for loads P_1 and P_2 at respective eccentricities e_1 and e_2 can be added together for the overall solution as shown in fig. 2.5.1(d).

References 27 and 28 also give Stamm and Wittes solutions for thick faced sandwich panels subjected to a uniformly distributed load. This solution in particular has been programmed into a MathCad environment to allow simple investigation into the relative effects and the degree of effect on the structural performance of a panel when changing face and core material properties, and also panel element thicknesses. Appendix B contains the MathCad model, and an example calculation deriving core shear stress, compression and tensile stresses in the upper and lower faces respectively, and the deflection of the sandwich. It can be seen in this example that calculating the stresses and deflections at steps along the length of the panel is easy to achieve.

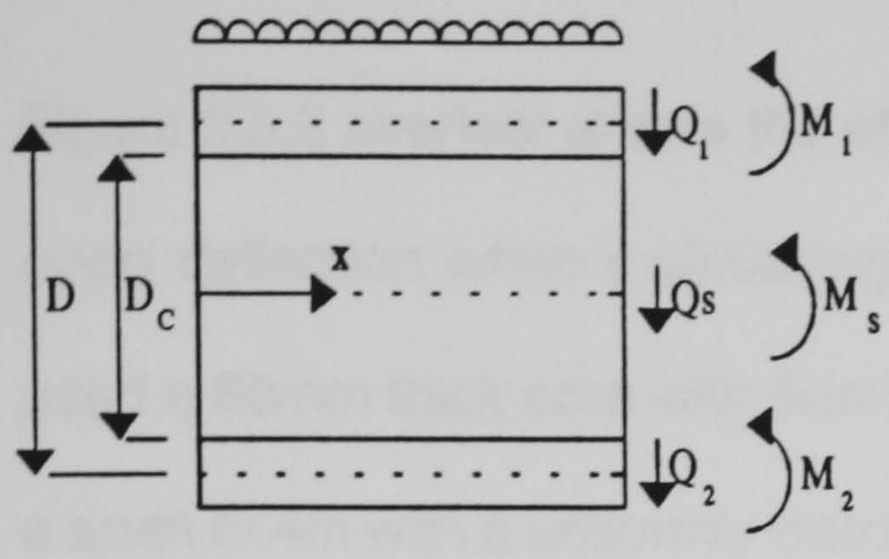

2.5.1(a) Stress Resultants

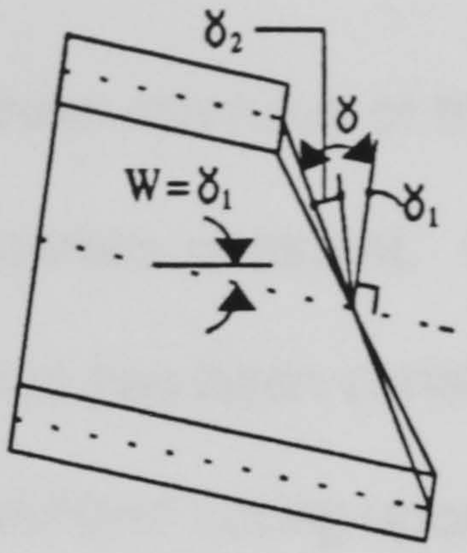

2.5.1(b) Deformation Element

Force and Deformation in a Typical Sandwich Element

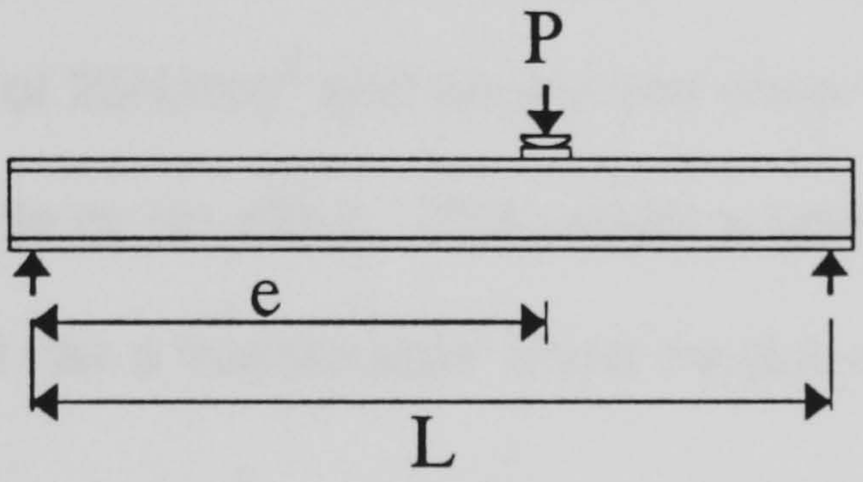

2.5.1(c) Simply Supported Beam with Transverse Load

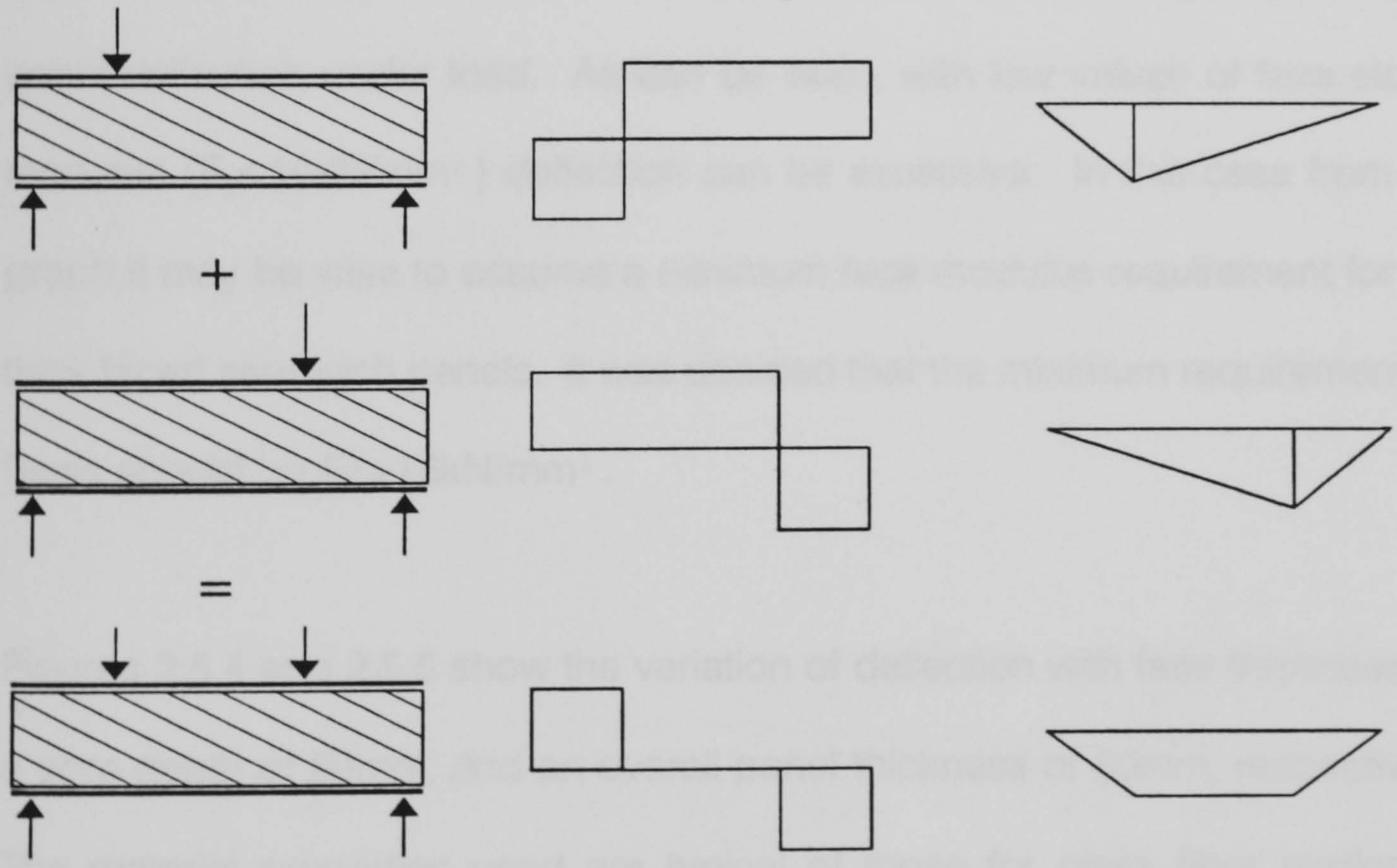

2.5.1(d) Diagramatic Representaion of 4-point Loading

Figure 2.5.2 overleaf shows the effect that the shear modulus of the core has upon deflection when maintaining all other properties constant. In the case used a 60mm thick core with 5mm thick GRP faces has been considered, and a span of 4m with a uniformly distributed load of $2kN/m^2$ acting upon the panel. These values of span and load are typical requirements for structural panels offshore. As can be seen, at low values of shear modulus ($1\text{-}15N/mm^2$) the value of shear modulus has a significant effect on the deflection of the panel, however at values of $25N/mm^2$ and above, the shear modulus of the core can be seen to have little or no effect. This would suggest that providing that the panel core material has a "reasonable" shear modulus then this is a non-critical material property.

Figure 2.5.3 shows the effect of the elastic modulus of the face material on panel deflection under load. As can be seen, with low values of face elastic modulus ($E_f<10kN/mm^2$) deflection can be excessive. In this case from the graph it may be wise to assume a minimum face modulus requirement for the thick faced sandwich panels. It was decided that the minimum requirement for faces should be $Ef>15kN/mm^2$.

Figures 2.5.4 and 2.5.5 show the variation of deflection with face thickness for a core depth of 60mm, and an overall panel thickness of 80mm, respectively. The material properties used are typical of those for glass fibre reinforced polyester resin faces and a Vermiculux I (Cape Boards Ltd) core. From these it can be seen that using a 60mm thick core, with the properties assumed, a

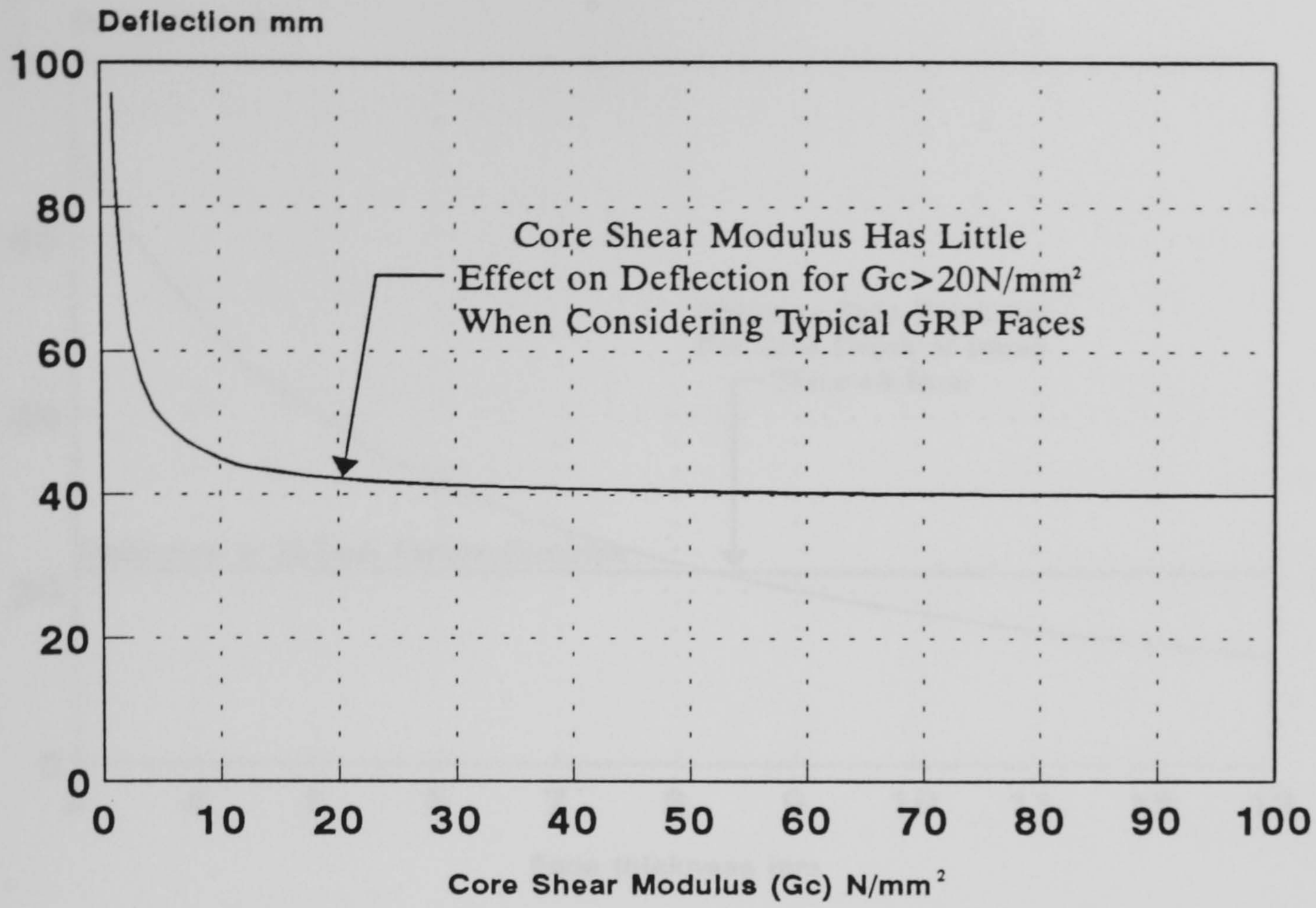

Figure 2.5.2 - Stamm and Witte Solutions
For Variation of Deflection with Core Shear Modulus
Span=4m, Tf=5mm, Ef=16kN/mm², Tc=60mm, Qo=2kN/m²

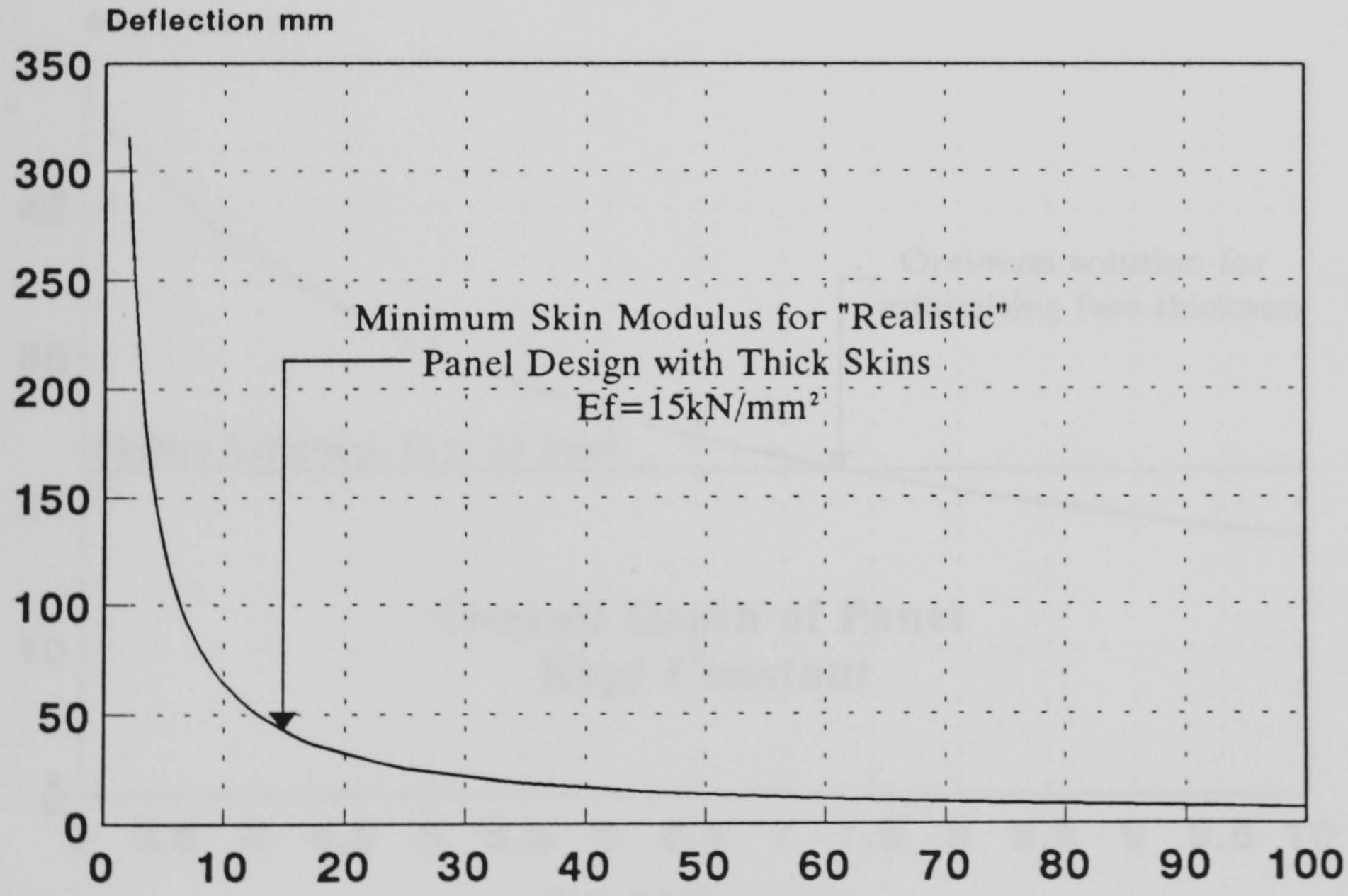

Figure 2.5.3 - Stamm and Witte Solutions for
Variation of Deflection with Skins Youngs Modulus
Span=4m, Tf=5mm, Gc=95N/mm², Tc=60mm, Qo=2kN/mm²

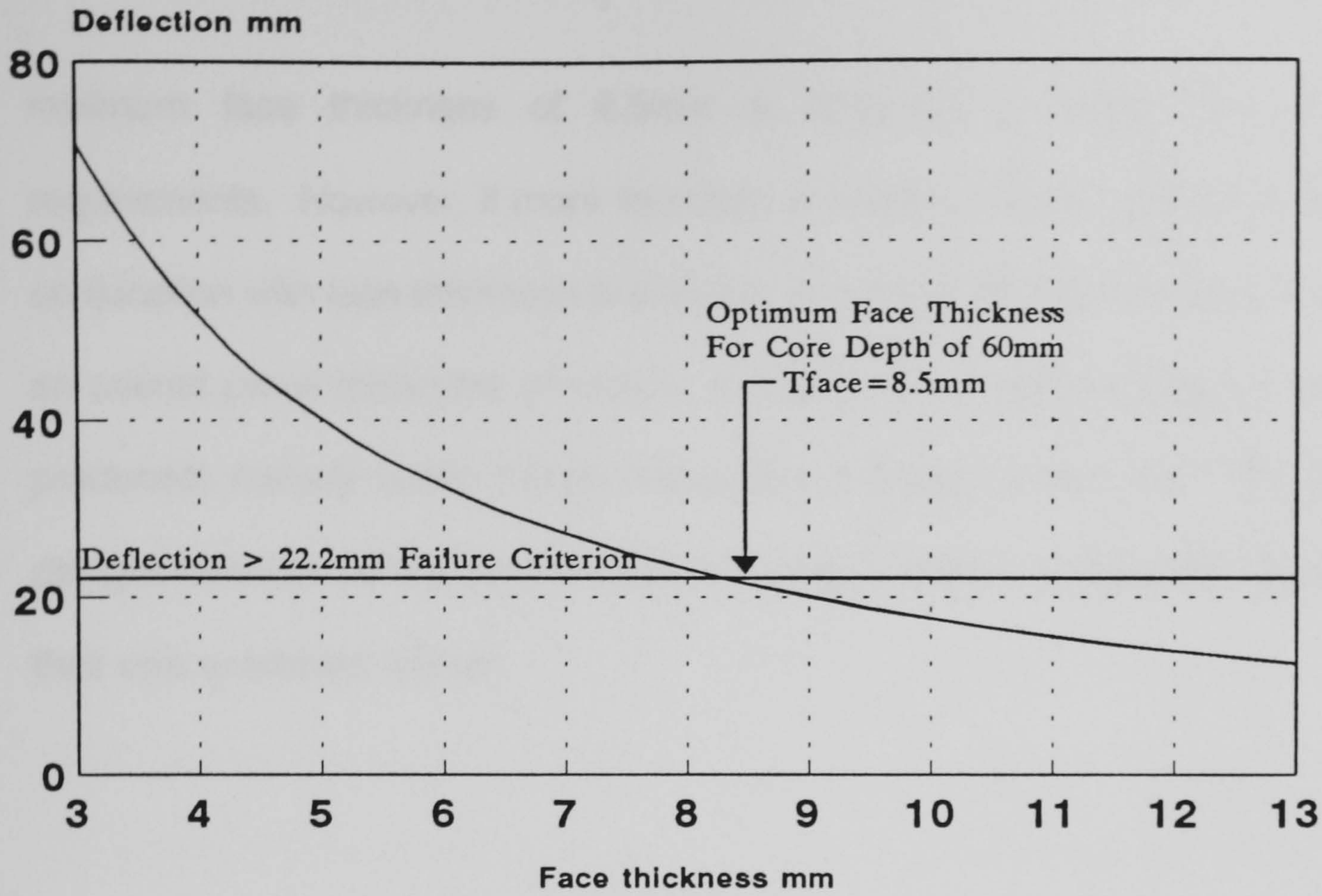

Figure 2.5.4 - Stamm and Witte Solutions for Variation of Deflection with Face Thickness (Contant Core Depth)
Span=4m, Ef=16kN/mm², Gc=95N/mm², C=60mm, Qo=2kN/m²

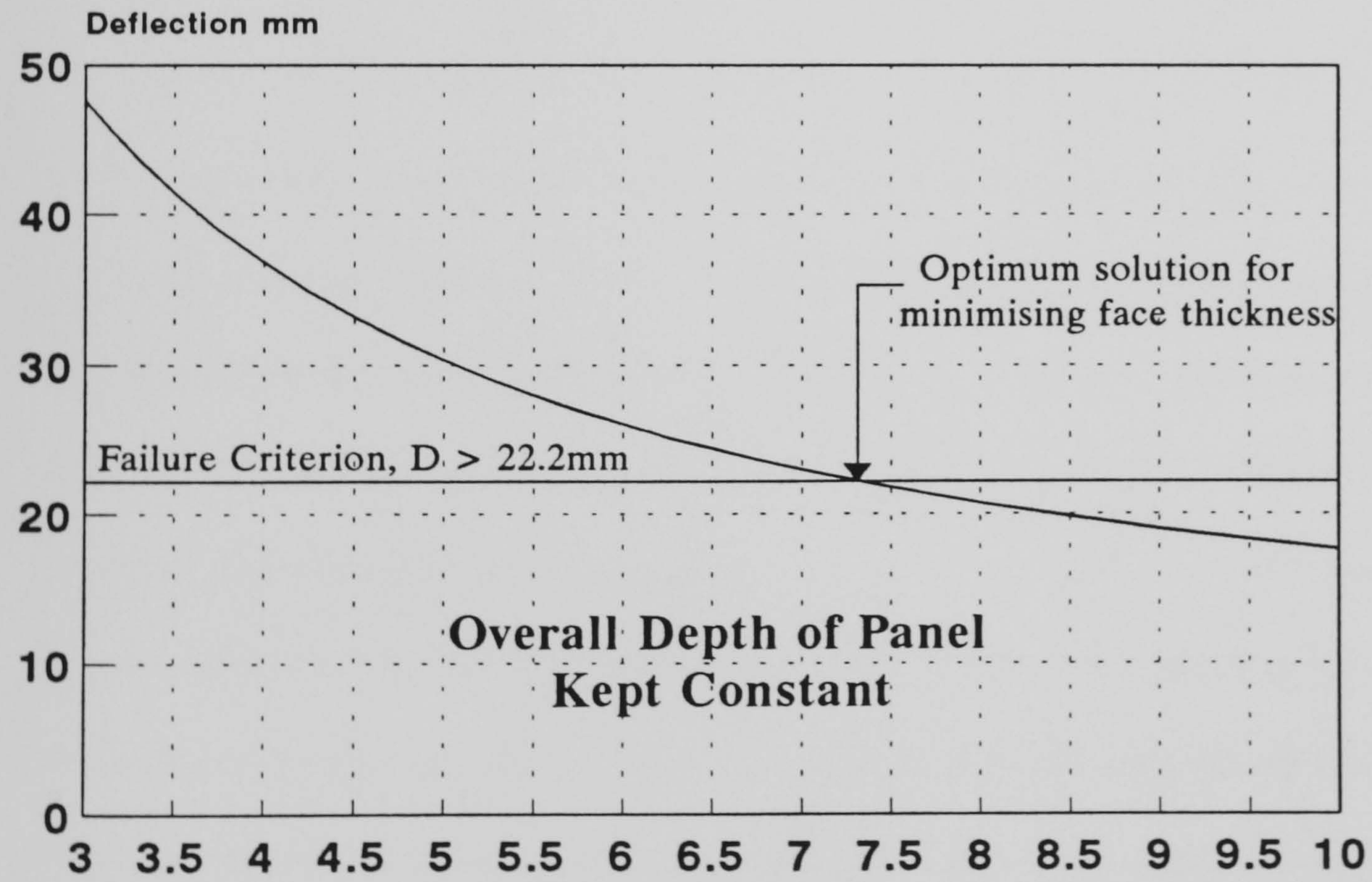

Figure 2.5.5 - Stamm and Witte Solutions for Variation of Deflection with Face Thickness
Span=4m, Ef=16kN/mm²,Gc=95N/mm², Qo=2kN/m²,Panel Depth=80mm

minimum face thickness of 8.5mm is required to satisfy the design requirements. However, if more freedom of variation of the core thickness in conjunction with face thickness is allowed, and constraining the design only to an overall panel thickness of 80mm, a slightly more efficient design can be produced, namely using 7.5mm faces and a 65mm thick core. The panel designs considered are commented on further in section 3.5 and the validity of their use examined further.

2.6 Pipe systems and their fire protection

2.6.1 Selection of materials

Material selection for FRP pipes is similar to that for FRP panels and there are a variety of resin systems which are suitable and also many fibres which can be used. It is less likely in FRP pipe manufacture that the more sophisticated aramid and carbon fibres would be required due to the method of manufacture. As generally low resin contents would be used for filament wound pipes it can be economical to use epoxy resins as opposed to the cheaper polyester resins in order to utilise their higher mechanical strengths and better temperature stability.

FRP pipes are generally wound onto a spinning mandrel at a prescribed angle, the most common being +/- 45°. Firstly a gel coat is applied to the mandrel and allowed to part cure, several strands of fibres are then wound onto the gel coat after passing them through a resin bath. The speed of rotation of the mandrel and transverse speed of the winding arm will determine the winding angle, and the tension in the filament will help to determine resin fraction. This method of manufacture produces a very high quality product where the resin fraction may be very low indeed compared to other fibre systems, and very high wall tensile strengths may be achieved. This method of manufacture (and the low resin content) makes the selection of the more expensive epoxy and phenolic resins a viable choice.

The resin matrix in FRP pipes will degrade when exposed to fire, and in certain fire scenarios additional fire resistance may be require in addition to that which is afforded by the pipe wall alone. This can be achieved by increasing the pipe wall thickness (i.e. including a sacrificial layer) or by using insulating materials or intumescents. Insulating materials commonly used include phenolic foam and ceramic fibres, however, these increase the cost of the pipe system significantly, and also make pre-fabrication and erection more difficult. Intumescent materials are ones which expand to many times their original thickness when exposed to fire. They form a stable char layer which insulates the polymer matrix from the fire, and are particularly effective when a fine mesh is incorporated to help hold the char in place once formed. Intumescent paints and coatings again add significantly to the cost of a pipe system.

2.6.2 The effect of winding angle for FRP pipes[29]

Filament winding has two predominant features. Firstly the reinforcement is a unidirectional fibrous material of either filament, roving or tape form. Secondly the reinforcement is continuously wound onto a spinning mandrel and impregnated with resin either before or during the winding process.

The choice of winding angle is predominantly a structural one. Approximate design can be made of a filament wound pipe by using netting analysis. This, however, is only an approximate design as it does not consider the influence of the resin matrix on strength. If the following cylinder is considered:

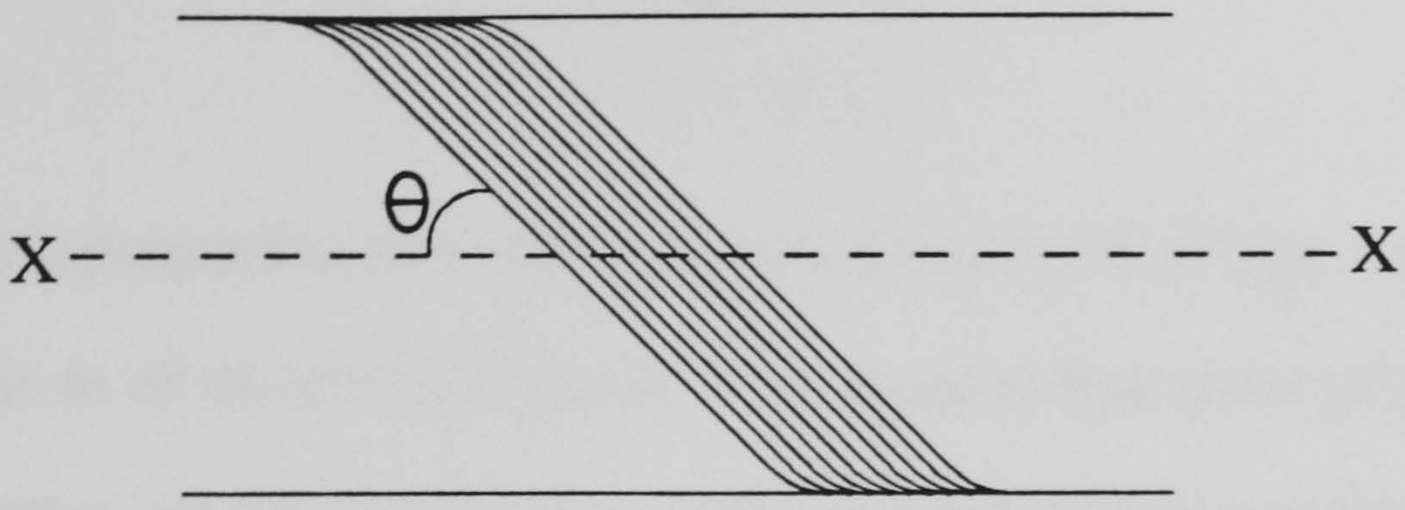

The number of filaments crossing the line x-x diminishes as sinθ diminishes, and hence the girth component of force from each fibre varies directly with sinθ.

Hence it can be shown that the **Girth Strength is proportional to $\sin^2\theta$**

It can also be shown that the **Longitudinal strength is proportional to $\cos^2\theta$**

For equal strength in both the longitudinal and girth directions:

$$\frac{\sin^2\theta}{\cos^2\theta} = 1 = \tan^2\theta$$

$$\therefore\theta = 45°$$

Similarly if the section is required to be twice as strong in the longitudinal direction than in the girth direction:

$$\frac{\sin^2\theta}{\cos^2\theta} = 2$$

$$\therefore \tan\theta = \sqrt{2}$$

$$\theta = 54.74°$$

The elastic properties of a balanced cylindrical structure (i.e. +/-45°) are such that strain in all directions is equal. This ensures that none of the windings in any direction will become over stressed and fail until overall failure of the wall. The strength of an FRP pipe can be calculated as follows:

$$GirthStrength = \frac{\sin^2\theta.t}{T}.P$$

$$LongitudinalStrength = \frac{\cos^2\theta.t}{T}.P$$

Where:

t=thickness of the windings at angle θ

T=overall wall thickness

P=tensile strength of the unidirectional windings.

It has been shown in the previous sections that the structural design procedures for GRP sandwich panels and filament wound pipes are readily available, and reasonably easy to perform. These structural design procedures, however, consider only the short term structural properties. The full design of FRP elements and composites should also take account of factors such as weathering and long term mechanical properties, fatigue, and creep. These factors have not been considered within this thesis as they are relative to the

materials used and the manufacturing techniques employed. They will thus vary for all different composite formulations.

A brief investigation into the requirements for a new sandwich panel core material has been presented. This analysis showed the effect that the mechanical material properties, both of the faces and of the core, have upon the deflection characteristics of a thick faced sandwich panel. The development of new core materials with respect to mechanical properties is presented in detail in chapter 3 together with an investigation into what would appear to be a more efficient panel design - the structural stringer panel. Also presented in detail in chapter 3 is a discussion of the validity of using sandwich panels with thick FRP faces as a cost effective replacement for the deep profiled steel panels which are commonly used. The optimisation of sandwich panel and structural stringer panel design, for weight considerations, is also included in chapter 3.

Chapters 4 and 5 show fire test results for panels and pipes respectively, together with numerical modelling and prediction of the thermal response of core materials, FRP laminates, sandwich panels and FRP pipes when exposed to standard fire resistance test conditions.

CHAPTER 3 - TEST PANELS, MATERIAL SELECTION AND DEVELOPMENT

3.1 Introduction

The following sections describe in detail the use of fibre reinforced composites, state-of-the-art fire resistant core materials, and the development of a new core material within the authors research.

The research, development and results presented within this chapter are with respect to structural properties alone. At each stage of the development work the fire performance was also investigated. The fire performance of different materials and panel formations are presented in chapter 4, and an investigation into the fire performance of GRP pipes is presented in chapter 5.

Details of the materials used for the research are given at the beginning of section 3.2 for GRP laminates, and in section 3.3 for the development of new fire resistant core materials. Section 3.4 gives a detailed description of the development of new core materials with respect to their structural properties, and section 3.5 investigates the validity of pure sandwich panel solutions as a cost effective replacement for the traditional steel and ceramic/mineral fibre solution. Section 3.5 also details the investigation into what would appear to be a superior structural solution to the sandwich panel for composite materials, the structural stringer panel.

The emphasis behind the majority of the research was to investigate and develop *cost effective* solutions for use in locations where fire may be a hazard. Cost effective solutions in the authors research was taken to mean ones which would have superior performance to the traditional steel-fibre panels with respect to life span, weight and cost whilst providing similar fire and structural performance.

It has been described previously how GRP products can be cost effective as their increased life span can offset the higher material costs. Savings due to reduced installation costs can also be significant. Where GRP is used as a material in its own right, for instance in the deluge pipe system, substantial weight savings can be achieved, however this may not be true for fire resistant panels. The weight considerations for fire resistant GRP faced sandwich panels are also commented on in section 3.5.

3.2 Fibre reinforced composites.

For the purpose of the research programme, it was decided that two different resins should be used for the manufacture of samples, one a polyester resin, the other a phenolic resin. The manufacture of panels using these two resins differed in that the polyester resin required the addition of a catalyst before curing would commence, and that the resin was cured at room temperature (indeed the curing process is exothermic). The phenolic,however,was a resol (the resin as delivered contained all the components required to cure it) and all that was required to cure the resin was elevated temperature.

3.2.1 Polyester resins

Polyester resins were among the first synthetic resins to be developed in the plastics industry. Their first occurrence can be traced back to the late 1840's however the first published work on their discovery and chemistry was by Vorlander[30] in 1894 following the development of an unsaturated polyester resin.

The commercial development of unsaturated polyester resins began in the United States in 1941, but until 1946 all polyester resin were hot curing resins. In 1946 it was found that use of a promoter would enable curing at room temperature. The ability to cold cure resins has been common from the late 1940's to the present date.

Unsaturated polyester resins typically consist of the ester dissolved in a monomer which provides cross-linking units to unite the ester chains three dimensionally. The most common monomer in use is styrene. The two components co-react or copolymerize when a catalyst is added. For styrene/ester mixtures catalysts are generally organic peroxides.

Most resins are manufactured in the pre-accelerated form. This eliminates the risk of the violent reactions which may occur when an accelerator and catalyst are directly combined.

The initial heat distortion temperature of isopthalic polyester resins could be as low as 95°C[20]. However, the heat distortion temperature of a polyester-glass laminate will be well in excess of this, and also integrity may be maintained to temperatures well in excess of the heat distortion temperature. The actual ignition temperatures of polyester resin based GRP are typically in excess of 350°C for flash ignition, and in excess of 450°C for self ignition[20]. The onset of thermal degradation of the resin and release of volatiles occur at temperatures much lower than those for flash ignition or self ignition.

3.2.2 Phenolic resins

Phenolic resins are produced by the reaction of phenols with aldehydes, the simplest representatives of these compounds, phenol and formaldehyde, are by far the most important. Heat curing (progressive or finite polymerisation) is

by far the most important process for phenolic resols. It generally occurs at temperatures of 100-200°C and is distinguished by the cross linking of mainly linear chains with the occurrence of gelation at some intermediate stage in the reaction. The gelling of the resol corresponds to the formation of an infinite network in which cross linked polymer molecules are transformed into macroscopic molecules.

PF (phenol-formaldehyde) resins are known to be quite temperature resistant materials which yield a high amount of char during pyrolysis. The thermal degradation process of PF resins is conveniently segmented into three stages[8] indicated by weight loss and volume change.

In the first stage up to 300°C the polymer resin remains virtually intact. The quantity of gaseous products released is relatively low (1-2%). The gaseous releases consist mainly of water and unreacted monomers, phenol and formaldehyde, which were trapped during the curing process.

Decomposition commences at approximately 300°C. From 300-600°C mainly gaseous components are emitted. The reaction rate reaches a maximum within this period. In this second stage, water, carbon monoxide, carbon dioxide, methane, toluene, phenol, cresols and xylenes are released. Random chain scission occurs in this temperature range,however,no de-polymerisation occurs and shrinkage is relatively low. The porosity of the resin will increase, with a corresponding decrease in density.

In the third stage above 600°C similar compounds are released as during the previous stage with slight chemical changes. The main characteristic in this stage is high shrinkage with a considerable permeability change and a corresponding density increase.

The thermophysical properties of phenolic resins within their serviceability limiting temperature range has been investigated by Taylor and Mottram[31]. They investigated a composite of silica fibres arranged to provide an orthogonal 3D reinforcement within a phenolic matrix. In addition to this the properties of phenolic resins alone were investigated at differing heating rates between 0.5 and 20K/min.

Figure 3.2.1 shows Taylor and Mottram's results from thermal expansion experiments up to 210°C for four samples taken from different locations and orientations within a mother sample. The actual values are not of great importance to this report, however, the apparent expansion-contraction-expansion cycle is a point of interest. In all samples there is a contraction above 93°C until above 130°C where the sample begins to expand again. The rates of thermal expansion are similar for all orientations, however the actual degree of expansion/contraction seems to be highly orientation dependant.

The heating of resin samples in the range of room temperature to 200°C were accompanied by weight losses of 3-6.5%, and length decreases of 1-1.5%. Further weight or dimensional changes were experienced if the specimen was

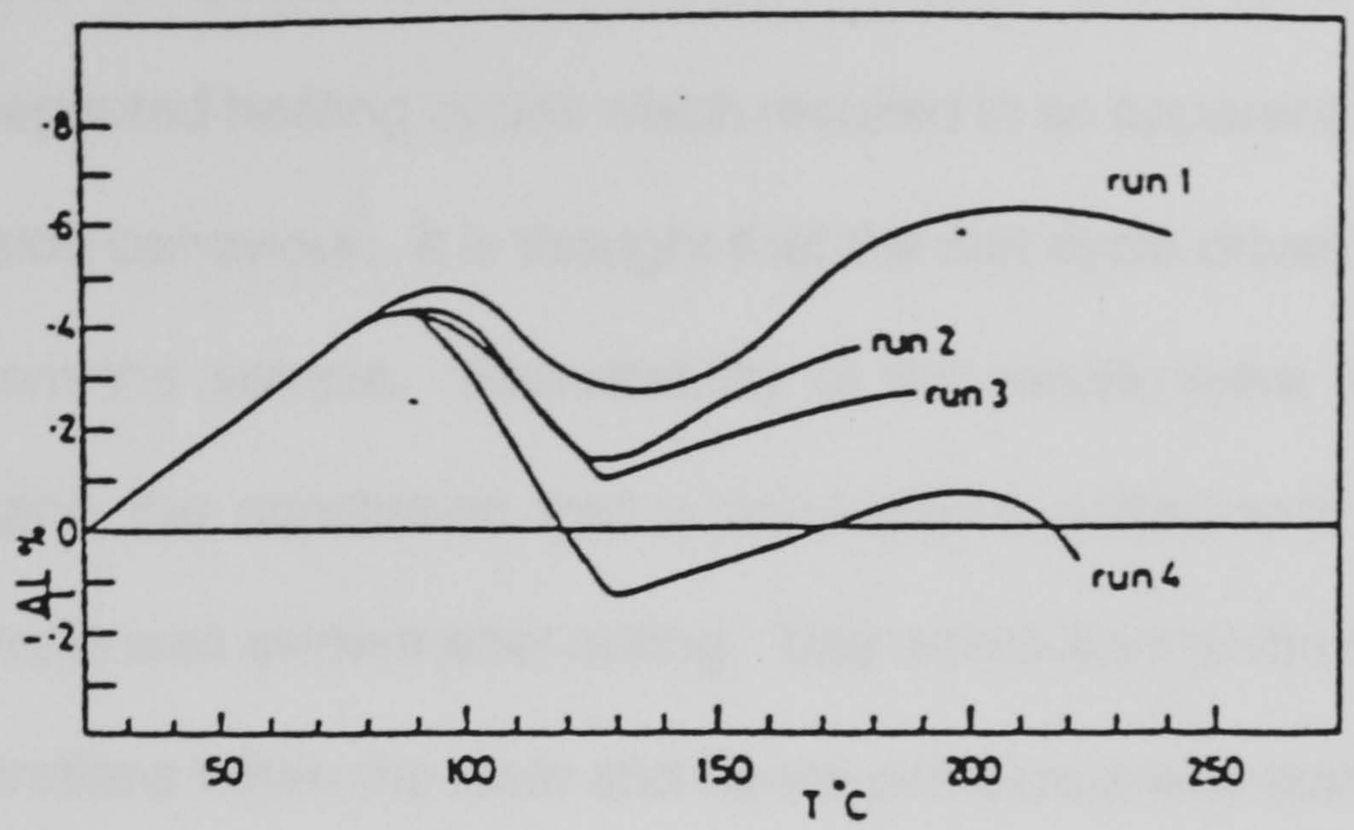

Figure 3.2.1 - Thermal expansion of various specimens of phenolic resin at heating rates of 0.5K min^{-1}

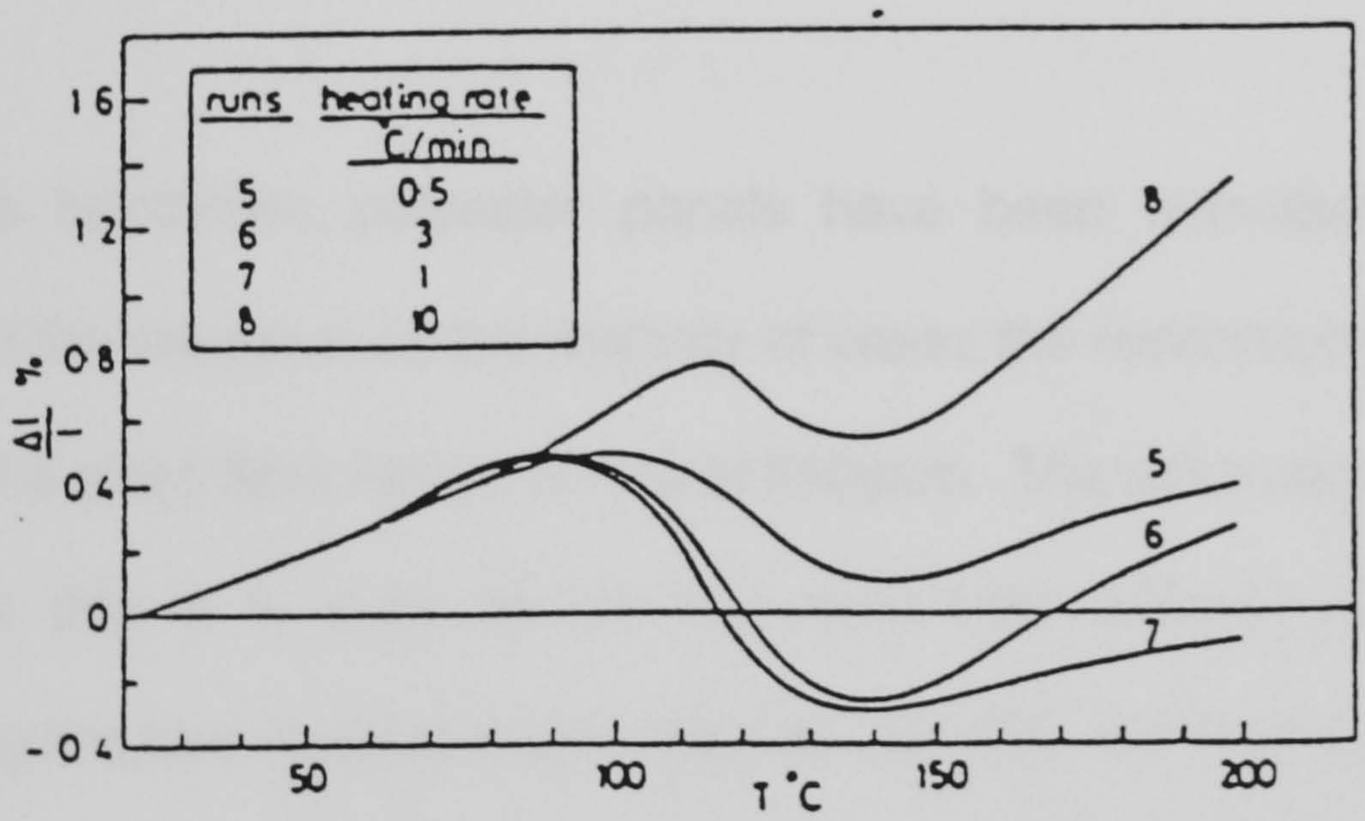

Figure 3.2.2 - Thermal expansion of phenolic resin specimens at different heating rates. 5 - 0.5K min^{-1}, 6 - 3.0K min^{-1}, 7 - 1.0K min^{-1}, 8 - 10K min^{-1}

heated to higher temperatures or if the thermal cycles were repeated. Figure 3.2.2 shows repeated heating cycles which resulted in an apparent stabilisation of the expansion behaviour. It is thought that the first cycle drives off volatiles and water from the sample. Repeatability of the results were found to be difficult, bringing the conclusion that a non-uniform entrapment of volatiles within the sample was evident after curing. This would lead to the formation of local concentrations within the resin and hence produce a very complex stress field. This would explain many of the problems found with phenolic resin impregnation of a cement based composite as described in chapter 3.4.3.1

3.2.3 Reinforcements for fibre reinforced composites - Panels

Many fibre reinforced polyester panels have been manufactured for the purpose of the research, in the majority of cases the reinforcement has taken the form of a glass fibre woven roving at 600gsm. The advantage of using this material is that it is seen to be the most cost effective solution when considering fire (see chapter 4 for comparisons of fire performance when using different reinforcement fibres). The panel faces were hand laid by brushing resin onto the woven roving and rolling with a washer or grooved roller. This method was found to be very satisfactory in terms of mechanical performance of the laminates. Table 3.1[7] following shows a summary of typical short term tensile properties of GRP and other commonly used materials offshore.

Material	Mat.	Woven	Fabric	Cont.	Alumin. AlMg 2.5	High Mo Steel and Stainless Steel	Cu/Ni 90/10
Fibre Orientation	Random	Bidir.	Bidir.	Unidir			
Fibre Content(%)	20-40	45-60	50-70	50-90			
Tensile Strength N/mm^2	60-170	210-350	260-500	430-1730	170-300	450-650	300-380
Tensile Modulus kN/mm^2	6-12	12-21	16-30	22-62	70	210	130

Table 3.1 Tensile Properties of GRP and commonly used materials (E-glass fibres for fibre reinforced composites)

In addition to woven roving alone, laminates were manufactured using differing thicknesses of resin wetted ceramic fibre blanket within the laminate up to the exclusion of glass fibre altogether. These materials have been referred to as GRP, GCRP and CRP. GCRP is followed by two figures, the first being the number of layers of woven roving, and the second the thickness of uncompressed ceramic wool encompassed in the resin matrix. Table 3.2 gives the percentage by weight of the constituents of the samples, and table 3.3 the averaged tensile properties of all samples tested.

Sample	Density kg/m^3	Glass %	Resin %	Ceramic Wool %
GRP	1806.8	66.8	33.2	-
CRP	1258.1	-	66.6	33.4
GCRP (6+25)	1553.3	30.4	26.6	43.0
GCRP (10+3)	1813.2	57.2	36.7	6.1

Table 3.2 Material Proportions by Weight for GRP, CRP and GCRP

Sample	Tensile σ_{cr} N/mm² Warp	Weft	Tensile E_t N/mm² Warp	Weft
GRP	312.3		18590.4	
CRP	24.55		757.4	
GCRP (6+25)	161.1	131.4	9367.5	7990.5
GCRP (10+3)	272.7	273.2	18098.2	

Table 3.3 Material Properties of GRP, CRP and GCRP

The ceramic wool for the GCRP (6+25) laminates was at the centre of the panel and had 3 layers of woven roving either side of it. For the GCRP (10+3) the ceramic wool position was biased towards to foreseen hot face of the laminate (when considering fire testing). The GCRP (10+3) sample was (from hot face to cold face) 2 layers of woven roving, 3mm original thickness ceramic blanket, 8 layers of woven roving.

The use of ceramic wool within the laminate has great advantages with respect to fire resistance as will be discussed in greater depth in chapter 4. It can be seen from the averaged tensile properties above that the inclusion of a thin layer of ceramic wool to the exclusion of 2 layers of woven roving does not sacrifice a great deal of strength and its effect on the tensile modulus is barely distinguishable. This is a significant effect when considering possible designs for fire resistant panels as discussed later in this chapter. Where a large thickness of ceramic wool is included within the laminate to the exclusion of 6 layers of glass fibre the structural properties are significantly decreased and hence this would limit the materials use to less demanding structural

applications. CRP has little structural strength as it contained no glass fibre, and the ceramic wool used was of parallel bonded form, and hence had very little tensile strength. However, as an additional layer which has no structural requirements it may be of great use.

The following photographs (figure 3.2.3 and 3.2.4) show typical failed samples from the tensile tests. As can be seen in all the samples, the failure path through the impregnated ceramic wool is smooth as fibre strength is lower than the matrix resin, and where the glass fibres have failed the failure surface is irregular.

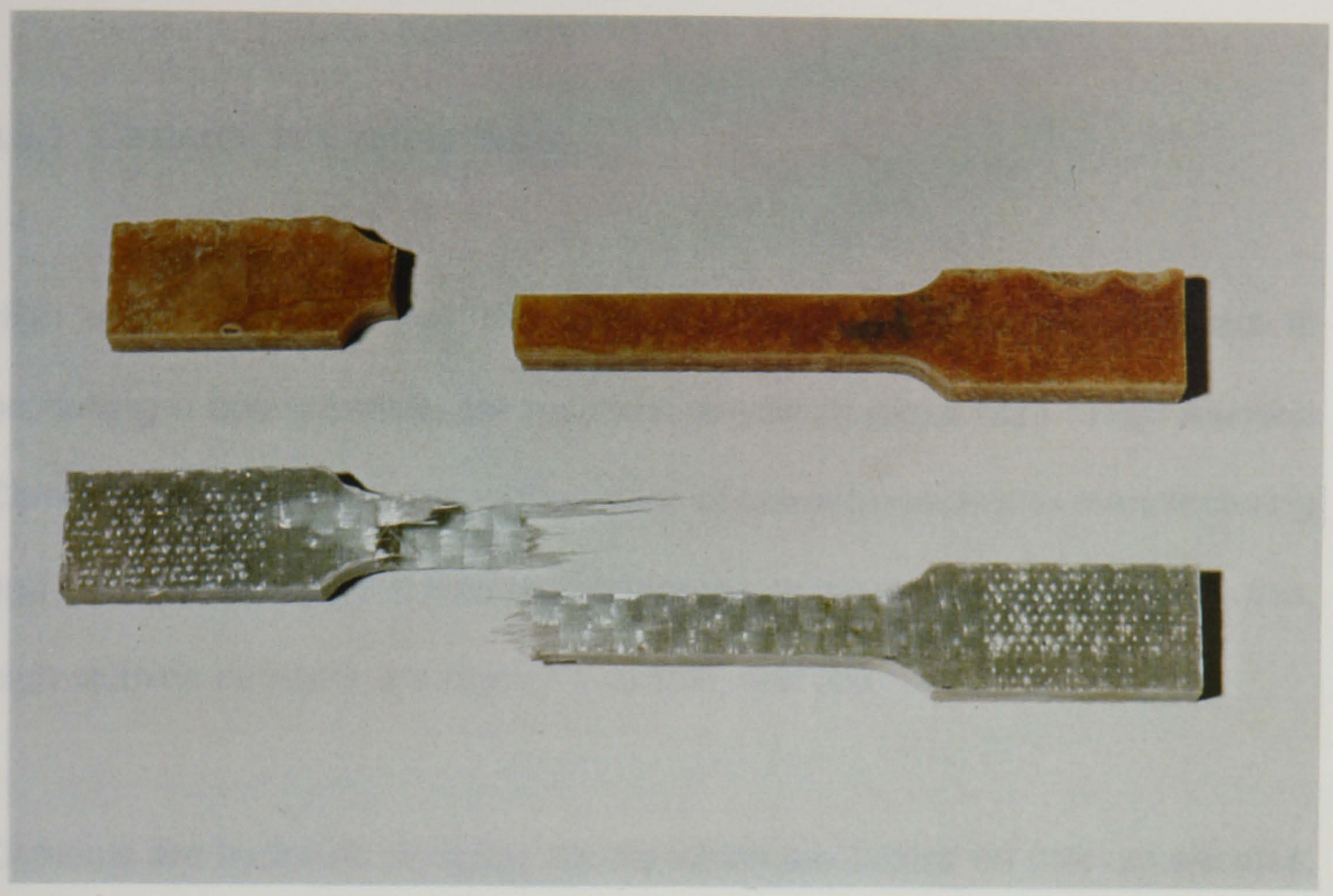

Figure 3.2.3 - Tensile specimens of CRP, top, and GCRP(6+25), bottom

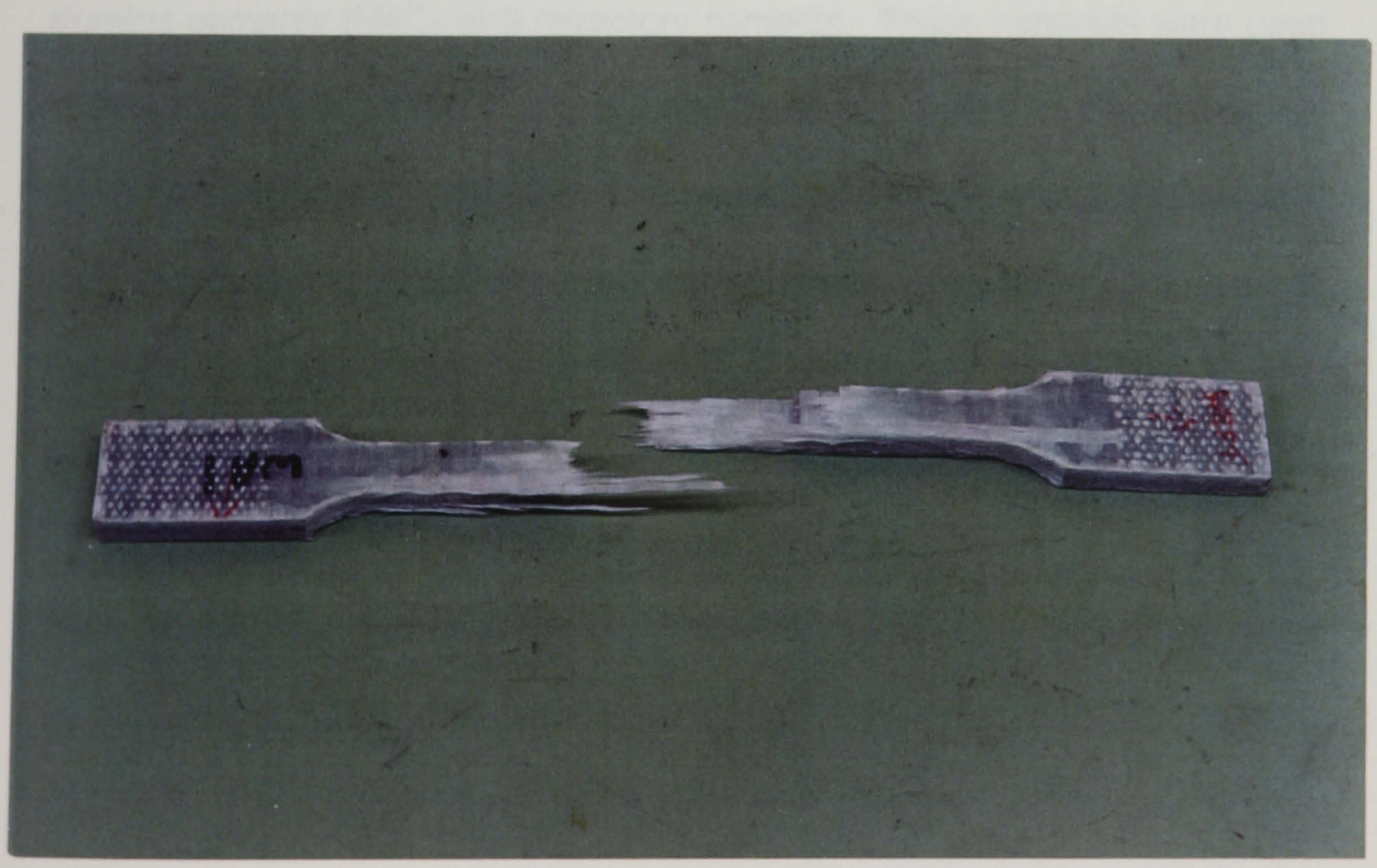

Figure 3.2.4 - Tensile specimen of GCRP(10+3)

3.3 Materials used for the Development of New Panel Cores

3.3.1 Cements and refractories.

High alumina cement was the main material investigated with respect to producing a cost effective, fire resistant, sandwich panel core. High Alumina Cements were selected due to their ease of use with respect to manufacturing and curing methods, and their high temperature resistance. In addition to this, high alumina cements are readily available, and are reasonably cheap.

Cements are hydraulic bonding agents which are based on calcium silicates, such as ordinary portland cement (OPC), or calcium aluminates such as high alumina cements (HAC) and refractory cements. These materials were used in the research for medium density panel cores, i.e. acting as the primary fire barrier of a sandwich panel with FRP faces. Due to this it was decided that high alumina cements and refractory cements would be used in preference to ordinary portland cement due to their higher temperature stability and melting points.

High alumina cements[32] are rapid hardening although setting times are comparable to OPC, and are better suited to heat resistant or refractory situations. The strength developed is a function of the heat liberated during the hydration of the calcium aluminates, the surrounding environment and time. For concretes of small cross section, keeping cool (≈20°C) during hardening

can encourage very high strengths to be achieved at early ages. With time, strength can decrease from this level before climbing again to its final level. The level of strength of the finished material composite is greatly influenced by the nature of the aggregates, for instance calcerous aggregates give the highest mechanical strengths.

Refractory cements have particularly high alumina contents (>50%) and are characterised by their pale colours and very high operating temperatures (>1300°C). The cement composite formed will have gained the majority of its final strength after five days, however, the strength of the material may be increased from "drying" at 110°C as during heating more hydration may occur and a strong C_3AH_6/AH_3 structure can develop.

Givan et al.[33] studied the effects of curing temperature upon the strength of a refractory concrete after curing, after drying at 110°C, and after firing at 1100°C. Their results shown in figure 3.3.1 show that curing temperatures have a pronounced effect on the strength especially after drying or firing. George[34] also found an influence of curing temperatures on mechanical properties of dried and fired cements, however, he found a beneficial effect in strength of high purity cements up to 54°C. Despite these results, the effect of curing temperature upon strength is still not established. Kula at al.[35] found that fondu pastes showed similar strengths after firing to 300-500°C regardless of curing conditions.

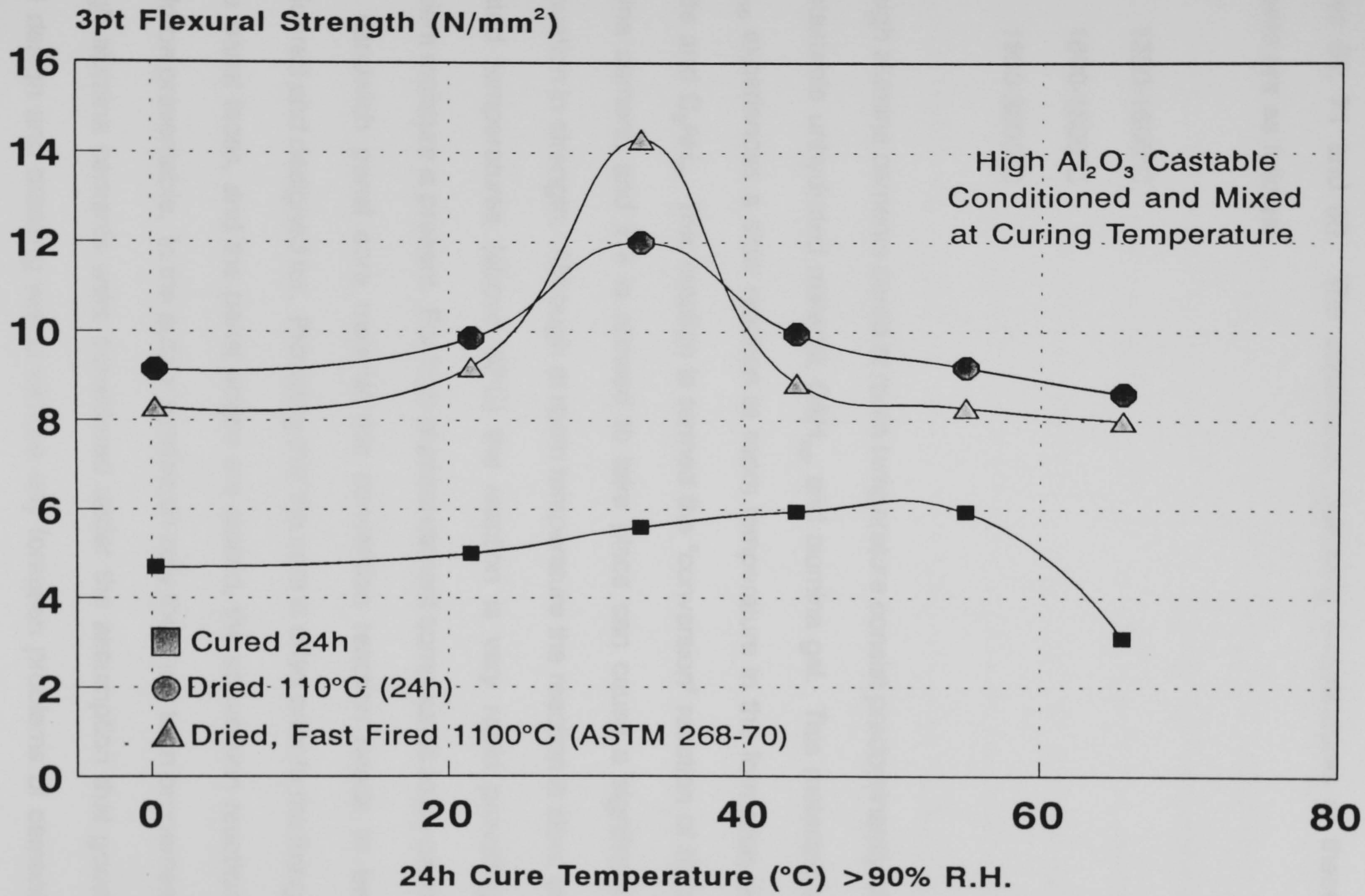

Figure 3.3.1 - Flexural Strength of Tabular Alumina
High Purity Cement Castable (ASTM C268)

Three different refractory cements were selected for the research programme in addition to a standard high alumina cement. These will be referred to as grades 51, 71 and 80. The continuous operating temperatures of these cements are as follows:

51: 1350-1600°C

71: 1600-1800°C

80: 1800-2000°C

Set high alumina cements cured at room temperature consist predominantly of a metastable unhydrated material, CAH_{10}, and alumina gel. This metastable CAH_{10} experiences a slow reaction at room temperature in the formation of gibbite and C_3AH_6. This reaction is termed the "conversion" reaction of high alumina cement, and if it is allowed to take place can cause a significant diminuation in strength. Although at room temperature the reaction is slow, at elevated temperatures (above 80°C) the reaction is very rapid providing sufficient moisture is present. For high alumina cement compounds to be used as a sandwich panel core material this conversion reaction needs to be considered and designed for. Providing that the core is dried prior to the fixing of the panel faces, and the panel edges are sealed, the conversion reaction should be preventable. In the author's research only the short term properties of high alumina cements were considered under the assumption that good panel design and detailing would remove any foreseen problems of cement conversion and its associated loss in strength.

3.3.2 Ball and china clays

Ball and china clays[36] consist of three principal materials, those being kaolinite, a micaceous material and quartz. Clays are generally in fine powder form in their raw state, and these must be moulded and the fired to high temperatures to produce a strong and rigid state. The firing process incorporates several phase changes together with a loss of weight, and shrinkage. At approximately 400°C kaolin dehydroxylates to form an amorphous stage known as metakaolin. At about 450°C the micaceous mineral also dehydroxylates to form an amorphous stage. At approximately 950°C the amorphous stages begin to re-crystallise to give a spinel structure which may ultimately re-crystallise at temperatures between 1100 and 1350°C as a mixture of mullite and an amorphous glassy stage. The true melting temperatures of ball clays is unlikely to occur at temperatures below 1600°C and many may remain unmelted at 1700°C.

Clays would be particularly suited to panel core materials due their pre-firing, and hence temperature stability. The relatively high thermal conductivity however, may lead to difficulty with respect to insulation. The use of lightweight expanded and exfoliated aggregates leads to better heat resisting composites but forming satisfactory samples is difficult to due shrinkage and distortion during the firing cycle.

3.3.3 Perlite[37,38]

Perlite is a naturally occurring siliceous volcanic rock. The distinguishing feature which sets perlite apart from other naturally occurring volcanic glasses is that when heated to a suitable point in its softening range (>870°C) it expands to between four and twenty times its original volume.

The expansion is due to between two and six percent combined water in the crude perlite rock. When heated to a high temperature the combined water vaporises producing a significant pressure and the crude rock pops in a similar manner to popcorn. The vaporised water creates bubbles which account for perlites' physical properties. Chemically, perlite is a complicated alumino-silicate and under normal conditions is inert with a neutral pH. It contains no organic matter and has a moisture content below five percent. Perlite is insoluble in water and relatively un-reactive in alkaline environments, it is also stable in most strong mineral acids.

Perlite when expanded has a bulk density usually in the range of 40-140kg/m^3. In fire conditions it can begin to soften and change phase at temperatures above 890°C, and has a fusion point at 1280-1350°C. Perlite has a fragile structure, and retention of volume is a prime consideration where mechanical mixing is used with binding agents.

3.3.4 Vermiculite[39]

Vermiculite is a member of the phyllosilicate group of materials and resembles mica in appearance. It is mined from open cast mines by drilling and blasting the host rock, the vermiculite is then separated from the host rock by a combination of crushing and air separation.

Vermiculite, as Perlite, has the ability to expand to many times its original volume upon heating - a property known as exfoliation. This is obtained by passing the vermiculite through a controlled furnace environment. Vermiculite is incombustible and insoluble in either water or organic solvents. In fire conditions it is stable up to temperatures in excess of 1300°C, this is combined with a low thermal conductivity of 0.062-0.065W/m°C.

Exfoliated vermiculite is normally used in conjunction with hydraulic binding agents eg cement/sodium and calcium silicates, from which the strength of the finished product is derived. One downfall of vermiculite is that mechanical mixing is detrimental to the retention of volume of the material, a problem which is particularly aggravated by the abrasiveness of other mix components.

3.4 Development of Core Materials for Panel Construction

3.4.1 Existing and newly developed fire resistant sandwich panel cores.

For the purpose of developing a new sandwich panel core with good fire resistance it was decided first to investigate some materials currently available. Three main materials were chosen, those being Vermiculux and Newtherm, both by Cape boards limited, and a phenolic foam (≈150kg/m^3) by Permali of Gloucester.

Vermiculux was investigated in two formulations, both are based on calcium silicate and vermiculite, and will be referred to as Vermiculux I and II. Vermiculux I had a dried density of approximately 475kg/m^3 and Vermiculux II 520kg/m^3. Newtherm is of similar composition with a dried density of approximately 270kg/m^3. It was found from testing that both these core materials exhibited excellent structural and fire performance and decided that, if it were to be competitive, the new material developed should show similar performance but at a reduced cost. The cost of Vermiculux is quite high at approximately fifty pounds per square metre at 50/60mm thick. Newtherm offers a cost saving on this but is still relatively expensive.

Phenolic foam offers excellent structural properties at the low density of 150kg/m^3. However, its fire performance is limited. Phenolic foam pyrolyses in fire, during which it is prone to high shrinkage and hence cracking and integrity

failure. The structural properties of these materials investigated will be presented in the same tables as the properties of the newly developed materials.

3.4.2 The development of cost effective cores with good fire resistance.

The aims of the core material development were to produce a cheap, easily made core which was capable of carrying the loads required in an offshore fire panel whilst providing a suitable fire resistance. This section will describe the material development and investigation with respect to structural properties.

A typical external wind loaded panel for offshore use would be required to support a load of $2kN/m^2$, have a span of 4m and a limiting deflection of span/240. Vermiculux is in current use as a fire panel with GRP skins, and as such it was decided that its structural properties should be used as target figures. The main constituents chosen for the core materials were high alumina and refractory cements, perlite and vermiculite, and phenolic resin. The use of cements and lightweight aggregate gave very reasonable forecast costs and it was decided to use these where possible.

Initial investigations into the manufacture of a cement-perlite composite revealed that a density of less than $300kg/m^3$ (using high alumina cement and pack 3 perlite) would not produce a material of sufficient strength/integrity. A nominal density of approximately $320kg/m^3$ was chosen as a target figure, and mix

designs were manufactured to investigate the variation of compressive strength with aggregate-cement ratio. The aggregate-cement ratio was varied within the bounds of 0.35 and 1.23 and the effect on compressive strength is shown in figure 3.4.1. The effect these variations in aggregate-cement ratio had on elastic modulus are shown in figure 3.4.2. As can be seen, there is a reasonably well defined plateau in strength for an aggregate/cement ratio of 1.2 or greater. Fire tests were performed to cellulosic conditions for each of these mixes, and figure 3.4.3 shows the variation of fire resistance (insulation failure) with aggregate-cement ratio. It can be seen in this case that there is a well defined peak performance at an aggregate-cement ratio of approximately 0.5.

Comparing the data for structural behaviour with the fire resistance data it was decided that a reasonable compromise would be obtained by using an aggregate-cement ratio of 0.9. This would still give near optimum mechanical properties, whilst still maintaining adequate fire resistance.

This optimum mix is referred to as Voidfill 7D. Further improvements in mechanical properties were obtained from reducing the mechanical mixing time (and hence aiding volume retention of the relatively fragile perlite particles), and oven drying at 110°C to promote final formation of the hydraulic bonds. Further development of the material was performed with consideration not only of the structural properties, but also of the fire resistance (see chapter 4).

Voidfill 7D was formed as a wet mix of perlite, high alumina cement, and water.

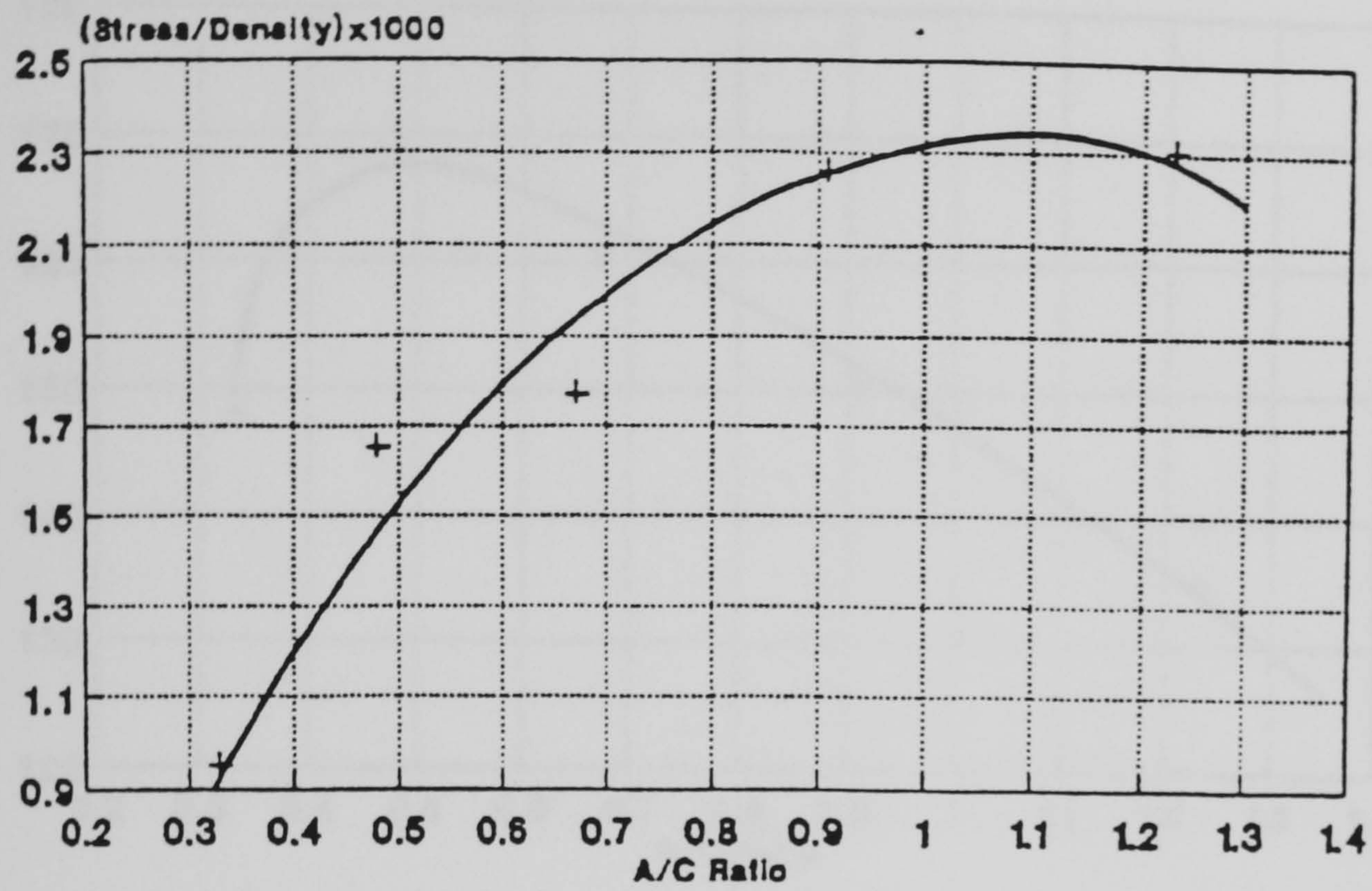

Figure 3.4.1 - Strength/density ratio as a function of the aggregate/cement ratio

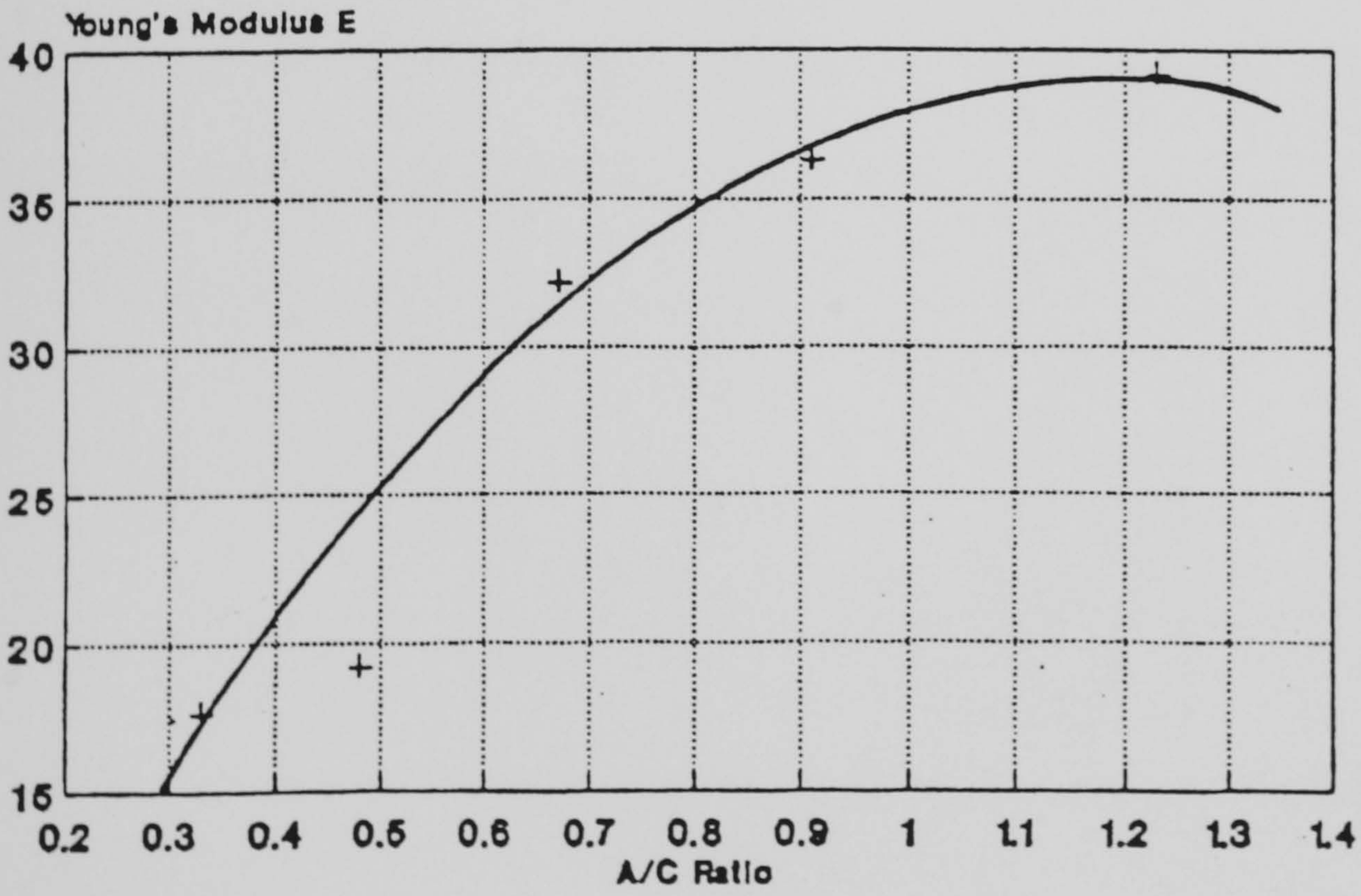

Figure 3.4.2 - Compression modulus as a function of the aggregate/cement ratio

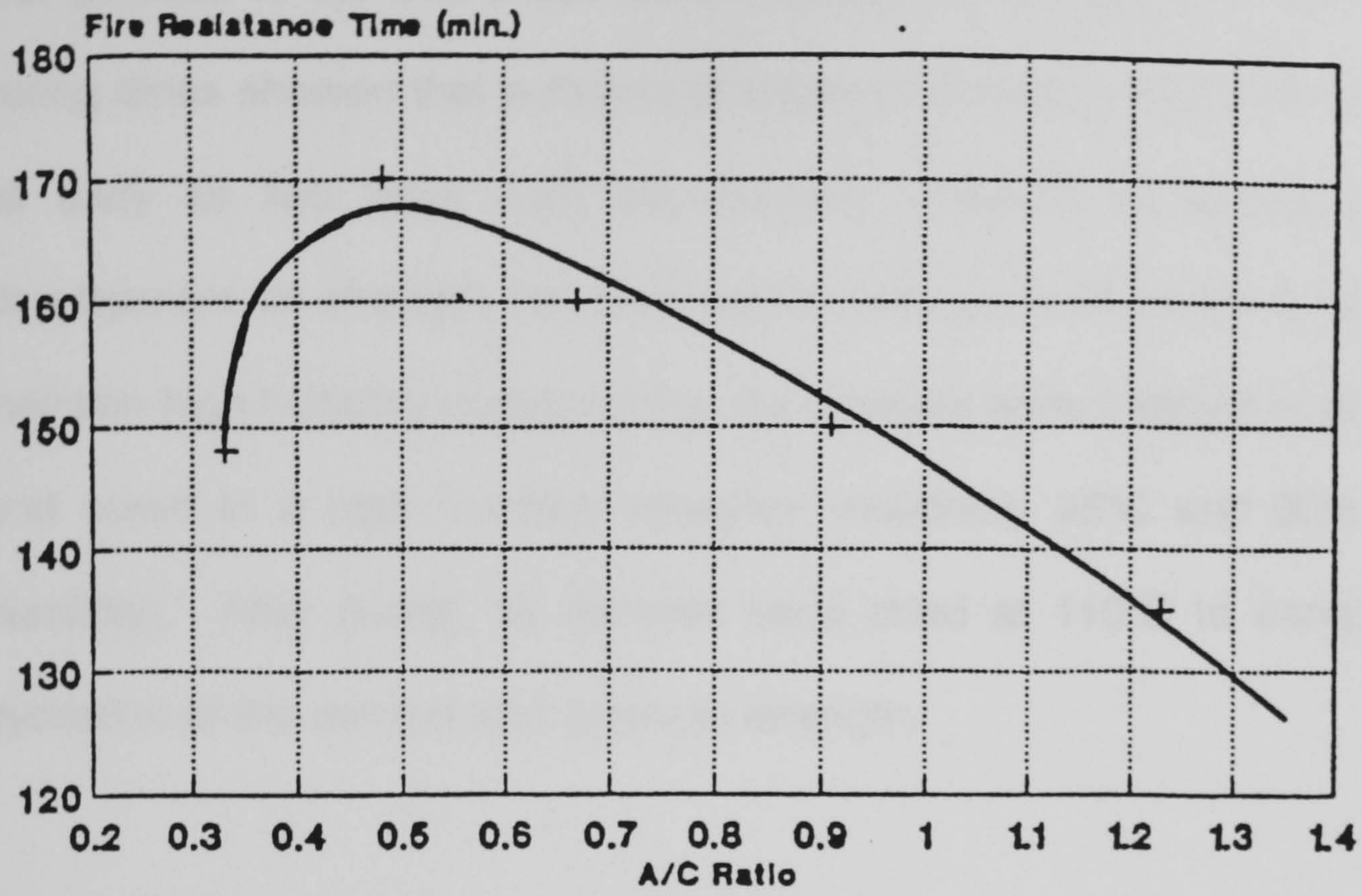

Figure 3.4.3 - Cellulosic fire resistance time as a function of the aggregate cement ratio

After mechanical mixing, the mix was transferred to a rigid aluminium mould and pressed to the final shape before curing. Investigation on the effect of curing times showed that sufficient strength for handling could be developed as early as two days from manufacture, however, to ensure near full development of strength the cure period was decided to be 5 days. To maintain high humidity during curing, the samples were bagged in polythene, and cured in a high humidity chamber (notionally 25°C and 90% relative humidity). After curing, all samples were dried at 110°C to complete the hydration of the cement and promote strength.

The first stage of the voidfill development was to determine whether the structural performance could be improved by reducing the water content of the mix. For this purpose the density, perlite and cement contents were kept constant, and several mixes were produced whilst reducing the water content. Mix proportions for the samples are given overleaf in table 3.4a and the structural testing results are given in table 3.4b.

Sample	Perlite (g)	Cement (g)	Water (g)
7D	729	594	954
7DW1	729	594	854
7DW2	729	594	754
7DW2	729	594	654

Table 3.4a Mix proportions of Reduced Water Mixes (Mix proportions are for slab of 300x300x50mm)

Mix No.	Density (kg/m^3)	E (N/mm^2) Compression	Failure Stress (N/mm^2)	E (N/mm^2) Bending	Failure Stress (N/mm^2)
7D	320	58.0	0.860	400.0	0.400
7DW1	318	49.13	0.818	337.5	0.410
7DW2	316	58.07	0.813	426.0	0.475
7DW2	313	52.53	0.782	287.8	0.428

Table 3.4b Structural Properties of Reduced Water Mixes

From this is can be seen that there is little or no advantage in reducing the water content of the mix. The structural properties of Vermiculux I and II are given below in table 3.5 together with those for the phenolic foam investigated.

Mix No.	Density (kg/m^3)	E (N/mm^2) Compression	Failure Stress (N/mm^2)	E (N/mm^2) Bending	Failure Stress (N/mm^2)
Vermiculux I	468.0	58.44	1.183	615	1.26
Vermiculux II	519.5	62.91	1.058	776	1.75
Newtherm	261.5	37.09	1.106	381	0.67
Phen. Foam	154.0	24.61	0.82	54.69	1.00

Table 3.5 Structural Properties of Core Materials

From comparison of the structural properties of voidfill and those of the materials commonly used it can be seen that although it has sufficient compressive strength it is relatively weak in flexure. In order that like could be compared with like the mix proportions of voidfill were kept constant, and the density increased to 520kg/m^3. This as could be expected improved the structural properties dramatically, however, forming the sample at this density was difficult. The force required to press one 300x300x50mm sample was 5.2kN. As can be seen, this would soon become preventative where large samples were required. It was decided to amend the mix proportions, increasing the cement-aggregate ratio to 1.39 from 0.81 in order to increase density. This mix proportion was used with mix 10 at a target density of 475kg/m^3, which again gave a noticeable improvement in structural properties.

Table 3.6 below gives a summary of the structural performance of samples 7D-520 and 10 compared to the original 7D.

Sample	Density kg/m^3	E_c N/mm^2	σ_{cr} N/mm^2	E_b N/mm^2	τ_{ult} N/mm^2
7D	320	58	0.86	400	0.400
10	473	127	1.55	422	0.618
7D-520	511	136	1.62	451	0.582

Table 3.6 - Structural properties of Core Materials 7D, 10 and 7D-520

As mentioned in chapter 2, it is essential to know the core shear properties in order to design a panel. Vermiculux (both formations), phenolic foam and newly developed materials were tested in shear to find the ultimate shear strength and also the shear modulus. Table 3.7 below lists the shear properties of several core materials.

Sample	Density kg/m^3	Shear Modulus G_c (N/mm^2)	Shear Strength σ_{cr} (N/mm^2)
Vermiculux I	468	95.3	0.23
Vermiculux II	519	193.8	>0.21
Newtherm	262	50.2	0.12
Voidfill 7D	320	23	0.11
Phenolic Foam	154	8.2	0.21

Table 3.7 Shear Properties of Core Materials

As can be seen from the above table, the Voidfill 7D mix, although being the weakest of the materials in terms of shear strength still has sufficient strength for use as a panel core, and its shear stiffness is sufficient to avoid the problems of large deflections forecast for panels with core materials of shear modulus less than 20 N/mm^2. It was decided that any further development of the material which increased mechanical properties in general (i.e. greater compressive or tensile strength or modulus) would also have a similar effect on shear properties, and as such the simpler compression and flexural tests could be used as a guide to structural performance in the material development.

As flexural strength was seen to be the weak point of the material (and hence a possible source of handling difficulties during manufacture) several possible methods of improving flexural strength were investigated.

Samples L1 and L2 were made using 7DW1 cores and very high cement to aggregate ratio (L1 agg/cem=1:3, L2 agg/cem/fibre=1:8.6:0.3) faces of 5mm and 2mm thick respectively. In addition to this, the L2 faces were reinforced with 12mm long chopped strand glass fibres. Sample L1 failed during the drying stage of the curing process. It is thought that this may be due to large differential stresses from the core and face heating at different rates. Sample L2 suffered similar problems,however,there were sufficient undamaged samples to test. The test results for L2 were poor, and the multi-layer idea was discarded due to its inherent manufacturing difficulties.

The next stage was to investigate the use of fibre reinforcements for the voidfill material. Samples F1, F2 and F3 were cores with chopped strand glass fibres included at the mixing stage. F1 and F2 included fibres which were 12mm long, and F3 included fibres at 25mm long. It was found that the inclusion of glass fibres through the thickness of the core did not improve its structural performance, but did in fact reduce it significantly. Upon inspection of the samples after curing and drying it could be seen that the inclusion of glass fibres had an aerating effect on the voidfill, and the composite appeared to shrink away from the glass fibres after pressing the sample. It is thought that this could have been due to the low water content of the sample, and the high

affinity glass has for water.

Fibre reinforcement was also used in the form of mesh within the depth of the core. Sample FM incorporated a light nylon mesh approximately 5mm from each face (pressed) and sample 7DW2-M incorporated a light aluminium mesh of approximately 17.5mm^2 cross sectional area (per 50mm width), again, 5mm from each face (pressed). The results for sample FM were disappointing, and a slight decrease in strength was observed from that expected of the core material alone. It was observed during the test, and post test inspection that the mesh had pulled through the relatively weak core. Sample 7DW2-M showed a remarkable increase in strength over that expected of the core material alone at only nominal increase in density. It was decided,however,that the formation process would be too complex to make this a viable alternative.

Some samples were autoclaved as an attempt to promote high strengths in a short period of time as can be achieved with calcium silicate and ordinary portland cement. Samples of 7DW1, 7DW2, F3 and 10 were autoclaved in a 12 hour cycle reaching a maximum of 200°C in a saturated atmosphere of approximately 200lb/in^2. These samples are denoted by the suffix a/clave. Sample F3 did not reach sufficient strength for testing to be carried out, and in general the structural strength of these samples was poor. It is thought that this is due to accelerating the well documented deterioration in strength of high alumina cement with moisture and heat with time[40]. Appendix A contains further information regarding the curing, and firing of high alumina cements.

Table 3.8 gives a summary of the flexural properties of the material mixes as described previously. All values are averaged over a minimum of three tests.

Sample	Density kg/m^3	E_b N/mm^2	τ_{ult} N/mm^2
7D	320	400.0	0.400
L2	465	166.7	0.327
F1	248	*	*
F2	271	94	0.154
F3	297	133.2	0.129
FM	311	235.4	0.350
7DW2-M	335	436.0	1.590
7DW1 a/clave	330	126.1	0.129
7DW2 a/clave	315	124.7	0.158
F3 a/clave	288	*	*
10 a/clave	440	157.9	0.213

* = Sample failed at first load increment - little or no mechanical strength.

Table 3.8 - Mechanical Properties of Developed Core Materials

At this stage in the research it was decided that mix 7D was to be adopted for comparisons with the state-of-the-art materials such as Vermiculux and Newtherm. Modified mixing techniques had provided substantial improvements in the structural strength of Voidfill 7D, and mechanical properties of the material were foreseen as being sufficient for use as a fire resistant structural sandwich panel core. Mix 7DW2, however, was noted as showing slight improvements in flexural strength when compared to 7D. In terms of structural properties of the core, and referring to previous numerical analysis of the

factors effecting deflection characteristics of GRP faced sandwich panels, it can be seen that mix 7D is a viable alternative to Vermiculux. Voidfill 7D has a lower shear modulus and lower shear strength than Vermiculux of either formulation. However, assuming that the allowable deflection would be the governing factor in the GRP faced sandwich panel design, Voidfill 7D cored panels should show similar performance to Vermiculux cored panels due to the foreseen negligible effect of core shear modulus when above 20N/mm^2.

3.4.3 Use of additives to improve Voidfill mechanical performance

In order to further improve the mechanical performance of the Voidfill mixes it was decided to investigate the effect of including a latex admixture, and also phenolic resin within the core material. Two methods of inclusion of the resin were investigated, namely, impregnation of a previously cured and dried Voidfill slab, and also premixing of the resin with the wet Voidfill mix prior to forming the sample. The latex additive was included within the material at the mixing stage of the core material. The inclusion of phenolic resin or latex within the Voidfill mass was in attempt to further improve the structural properties of Voidfill, particularly with respect to handling of the core material. It was envisaged that inclusion of the phenolic resin would in effect produce a heavily filled phenolic foam. Sections 3.4.3.1 and 3.4.3.2 detail the research performed on phenolic resin impregnation, and phenolic resin premixing respectively, and section 3.4.3.3 details the inclusion of latex within the Voidfill mix.

3.4.3.1 The impregnation of Voidfill with phenolic resin.

For the purpose of impregnating a Voidfill sample with a phenolic resin, it was decided to use a methylated spirits based resol of approximately 55% solids. The initial stages of the research were performed by soaking a weighed Voidfill sample in excess resol, however, in this way it was difficult to control the volume of solids entering the sample. Subsequent impregnations were calculated by curing and drying the Voidfill slab at 110°C to constant mass. The sample was then weighed and the amount of resol required was determined as a fraction of the dried Voidfill mass.

i.e. for a sample of 1440g, if a 20% impregnation were required then this would be calculated for a 55% solids solution as follows:

Mass of resol required = 1440 * 20% / 55% = 523.6g

This volume of phenolic resol was then let down with further solvent to a volume capable of soaking the full voidfill mass, and then cured in an electric oven in a well ventilated room. There was a large drawback with a methylated spirits based resin, that being the fire hazard, and other side effects such as unpleasant smell and effects of alcohol vapour. Due to this it was decided to try a different resol, and this will be discussed in chapter 3.5.3.2. Table 3.9 gives a summary of the structural performance of resin impregnated voidfill.

The curing method adopted for the meths based resin was a gradual rise in

temperature to 60°C which was maintained for 4 hours followed by a gradual rise in temperature to 120-130°C which was then maintained for 24 hours to achieve the primary cure. During this whole process methylated spirits vapours were leaving the sample and this was a major concern. It was decided that a programmable electric kiln would be used in close proximity to a powerful extractor fan to minimise the fire hazard.

		Compression		Bending(3pt)		Corner shear	
Sample	Dens Kg/m^3	E c N/mm^2	σ cr N/mm^2	E b N/mm^2	τ ult N/mm^2	G c N/mm^2	τ ult N/mm^2
7D	310	58	0.86	400	0.40	23	0.11
20 (M)	365	65	0.90	1300	1.16	18	0.31
20 (M)	370	65	0.88	4206	0.30	33	0.21
27 (M)	406	85	1.27	-	-	38	0.39
40 (M)	455	-	-	2108	1.29	-	-
60 (M)	476	-	-	1814	1.51	-	-
70 (M)	528	-	-	2514	2.11	-	-
90 (M)	604	97	8.90	3180	2.79	50	1.50

Table 3.9 Structural performance of resin impregnated voidfill

After the initial cure the sample was very gradually cooled and then quickly reheated to 145°C for the final stage of the curing process to maximise the cross linking of the resin. This temperature was maintained for a minimum of two hours after which the sample was gradually cooled again.

The careful cooling of the impregnated voidfill was necessary as very large differential stresses were formed when the resin cooled and hence shrank (see

chapter 3.2.2 for explanation). In general the migration of solvent to evaporate from the faces together with the curing expansion and post cure shrinkage acted to concentrate the resin at the faces of the material and leave the mid-plane with less resin. Several samples failed due to fast cooling, in one case a 300x300x50mm sample failed both along its neutral axis and in the plane perpendicular to that, rendering it useless. As phenolic resol is an expensive material (≈£1200 per tonne) wastage on a large scale would be very costly. This anomaly, however, did act to produce a quasi sandwich panel which would improve handleability.

The impregnation of voidfill with phenolic resin did produce excellent improvements in structural performance, at a nominal 90% impregnation improvements in failure loads due to compression, flexure and shear were 1085%, 581% and 1364% respectively when compared to the original 7D mix. The use of phenolic resin in conjunction with voidfill, however, did lead to a severe loss in fire performance as shown in chapter 4.

3.4.3.2 Phenolic resol premixing for Voidfill

The second type of resol investigated was a water based phenolic. Due to the solubility of the resol in water it was decided to add the resin to Voidfill mix at the manufacturing stage. It was envisaged that impregnation of a cured and dried Voidfill slab with this resol would produce similar results to those obtained for the impregnation of Voidfill with the meths based resol. It was found from

preliminary trials that the phenolic resol had a detrimental effect on the strength of the cement-aggregate bond. It was assumed that this was due to the resols interference in the formation of the cements hydraulic bonds in a similar manner to starch. It was decided that the cement content of the sample should be reduced due to this and be replaced by the same mass of phenolic resin solids.

The initial investigation into resin premixing was to decide on the most suitable curing method. The methods investigated ranged from curing at elevated temperature immediately after pressing to curing in polythene bags for five days prior to curing at elevated temperature. In reality there was little difference in the strengths achieved using either method, and a method of curing, bagged, at room temperature for 24 hours prior to curing at 120°C was adopted. This method appeared to give marginally better results than other methods.

Table 3.10 shows the structural test results for resol premixing. As can be seen the inclusion of phenolic resol by premixing had a lesser effect on the strength of the voidfill than was evident from impregnation. A progression of steps were taken to find a viable mix proportion for similar or better structural properties than voidfill 7D. In each case, all variables were kept constant other than the one being investigated. The results of the structural tests for resin premixing show that the developed materials were not sufficiently stronger than voidfill 7D to warrant the considerable increase in cost from the volume of resin required.

Sample	Density kg/m^3	E_c N/mm$_2$	σ_{cr} N/mm^2
20 (W)	311	18.3	0.25
27 (W)	326	43.1	0.85
42 (W)	357	57.2	1.05
50 (W)	393	41.1	0.86
53 (W)	450	54.4	1.06

Table 3.10 Compressive strengths of resin premixed voidfill

Several particulate composites were produced without the inclusion of cement. These samples consisted of perlite, vermiculite and phenolic resin alone. Structural testing of these samples showed that sufficient structural properties could be developed at reasonable density. In fire, as the resin pyrolyses and shrinks, it is likely that the majority if not all of the structural capacity would be lost. As such the material may not be suitable for fire situations as its integrity would not be sufficient.

3.4.3.3 The admixing of latex with Voidfill

The use of a latex admixture within the Voidfill mix was in attempt to improve the flexural (and hence handling) properties of the Voidfill. It was envisaged that the use of an admixture would not excessively increase the sample density, or reduce fire performance, due to the small volume used. The latex used was specifically designed for use in concrete repair work and was a styrene-butadene copolymer latex. The recommended dosage of the latex was 10 litres per 50kg of cement and with a specific gravity of 1.01 this set the ratio at

approximately 20% of the mass of cement. Table 3.11 shows the structural properties of the two main mixes used, the improvement in flexural strength can be seen to be quite substantial. Sample 7D-Latex was a mix of 7D proportions (see section 3.4.2) with an inclusion of 20% mass of cement Febond SBR Latex admixture. Sample 7D2-Latex was a mix of 7DW2 proportions with 20% mass of cement Febond SBR latex admixture.

Sample	Density kg/m^3	E_c N/mm^2	σ_{cr} N/mm^2	E_b N/mm^2	τ_{ult} N/mm^2
7D-Latex	321.6	61.2	0.92	278.4	0.60
7D2-Latex	324.8	64.2	0.95	256.6	0.59
7D	320.0	58.0	0.86	400.0	0.40

Table 3.11 Structural properties of voidfill with latex admixture

The advantages of using a latex admixture are that the pressed finish of the Voidfill was much finer, and less friable. When cutting the samples the cut surfaces were much smoother. In addition to this the latex admixture is claimed to give improved freeze-thaw resistance, better workability, greater water and water borne salt resistance. The greater water resistance provided by using the latex admixture would be advantageous with respect to preventing moisture development within the core which could promote the conversion reaction of the high alumina cement. All the above points are of importance in a marine environment, however, they must be considered against the increased cost of the voidfill material. As the amount of latex admixture used within the sample is relatively small, it may be economically viable to include a latex admixture

within the Voidfill mix where improved flexural properties or water resistance are required.

3.4.4 The use of refractory cements for Voidfill.

Limited experimentation with Voidfill incorporating refractory cements was undertaken to investigate the possible improvements in strength with higher purity-higher alumina cements. Several test panels were made using the standard high alumina cement and grades 51, 71, and 80 as mentioned previously. The refractory cements are better suited for high temperature applications than standard high alumina cement, and will exhibit less shrinkage during fire testing with higher alumina content. Structural testing of the refractory cements showed a remarkable decrease in failure stress with increasing alumina content. Table 3.12 shows a summary of the structural test results.

Sample	Density kg/m^3	E_c N/mm^2	σ_{cr} N/mm^2	E_b N/mm^2	τ_{ult} N/mm^2
7D	320	58.0	0.86	400.0	0.40
7D-51	319	69.8	0.94	266.4	0.48
7D-71	313	58.3	0.69	260.7	0.33
7D-80	293	34.6	0.35	116.3	0.18
7D-51-SBR	345	67.9	1.33	391.1	0.66

Table 3.12 Compressive and flexural strength of refractory voidfill

The use of higher alumina content cements does carry with it a cost premium,

and as can be seen from table 3.12 above there is no benefit in their use with the exception of Secar 51 cement. Secar 51 is only slightly more expensive than the standard grade Alumina cement, and as such could be adopted as a standard material for the manufacture of Voidfill for little extra cost. The use of a latex admixture with the grade 51 cement was investigated briefly, and is shown in table 3.12 as 7D-51-SBR. It can be seen that the use of the latex admixture with the higher alumina cement gives significant improvements in mechanical properties. The mechanical properties of 7D-51-SBR are comparable with those of the higher density samples 7D-520 and mix 10 whilst not unduly increasing the density of the core. This is highly beneficial where weight of the panel is of primary concern.

3.5 Summary of New Core Materials Development

An extensive research program has been performed by the author into the development of structural fire resistant core materials for use with GRP faces in sandwich panels. Several suitable materials have been developed for use as a GRP faced sandwich panel core material suitable for offshore loading requirements.

The standard mix, Voidfill 7D, has been shown to have reasonable mechanical properties. Section 3.6 contains theoretical calculations and sandwich panel designs for offshore loading cases using a Voidfill 7D core and thick GRP faces.

The use of glass fibre within the Voidfill mix had a detrimental effect on its strength as did the inclusion of a light nylon mesh approximately 5mm from the faces of the pressed core. The inclusion of a light aluminium mesh within the Voidfill core was found to improve the flexural strength of the material significantly. The use of an aluminum mesh within the core material,however, was discarded due to foreseen difficulties in manufacture.

The effect of increasing density on mechanical properties was investigated in two ways. Pressing the standard Voidfill 7D mix proportions to a higher density showed distinct improvements in mechanical properties, however, a greater effect was found by increasing the cement-aggregate ratio as well as pressing

to a higher density. These materials (Voidfill 7D-520 and Voidfill 10) would be suited to demanding structural applications, however, were not adopted as standard materials in the core and panel development due to increased cost.

Multi-layer core construction was considered in the core development work. However, the large differential stresses developed (in particular during the drying stage) caused several samples to fail during manufacture. This multi-layer construction was discarded as being impractical.

The inclusion of phenolic resin within the core material was investigated in two ways, namely, resin impregnation and resin premixing. Resin impregnation was shown to have substantial effects on the structural strength of the Voidfill mix. Concentration of the resol solids at the faces of the samples during curing posed some manufacturing difficulties by the formation of complex stress fields within the samples. However, at a nominal inclusion of 90% by weight phenolic resin solids by impregnation the failure loads due to compression, flexure and shear were increased by 1085%, 581% and 1364% respectively. The inclusion of phenolic resin within the Voidfill core material did have a detrimental effect on fire performance (see chapter 4). As such, the use of these core materials would have to be limited to situations where fire load may not be a primary concern and high mechanical strengths are required.

The inclusion of phenolic resin by premixing gave disappointing results with respect to mechanical strength. The inclusion of phenolic resin prior to the

curing of the Voidfill sample caused an inhibition in the formation of the cements hydraulic bonds, thus inhibiting strength development. To develop mechanical properties comparable to those of Voidfill 7D without phenolic resin a resin inclusion of 40% mass of voidfill solids was required. This development was soon discarded due to the increased cost of the core material for little or no improvement in core mechanical properties.

Further improvements in the mechanical properties of the Voidfill core material were obtained by using a higher alumina content cement, and also by including a latex admixture at the time of mixing. Core materials made with cements of significantly higher alumina content gave disappointing mechanical properties. However, using Secar 51 cement to replace the standard high alumina cement did give improved mechanical properties. This was further improved by the copolymer latex additive to give nominal increases of 54% and 65% in compressive and flexural failure strengths respectively at an increase in density of less than 8%.

The fire resistance of the various formulations of Voidfill are discussed in greater detail in chapter 4.

3.6 Test panels - Design and Manufacture

As the primary purpose of the research described in this thesis was to further the understanding of fibre reinforced composites in fire, it was decided to adopt a relatively simple design case to represent the structural and fire requirements of an offshore panel. The requirements were as follows:

1) Structural	Span 4.0 metres, wind loading 2.0 kN/m^2 and limiting deflection of span/180 for sandwich panels. Stringer panels were limited to span/240 in order to reduce stress on the smaller bond line.
2) Fire rating	H120 (120 minutes in hydrocarbon fire)

The weight of a fire-protected steel panel which meets these criteria is $48kg/m^3$ with a steel skin thickness of 2.5mm and an overall thickness of 266mm.

Several pure sandwich panel solutions, of glass reinforced polyester faces and a Vermiculux II core, were examined to find the optimum solution for both structural and fire terms. A numerical model using the finite-difference technique (as described in chapter 4) was used to predict the fire resistance to simulated hydrocarbon conditions after the individual components and panel configurations had been tested to build a database of material properties. The structural optimisation was performed using a MathCad based solution of Stamm and Wittes theory. The failure criteria for the panels designed were an

average rise of 140°C of the cold face of the panel, a deflection exceeding span/180 at mid-span or a core shear stress greater than 66% of its ultimate shear strength.

The structural properties of the faces were typical short term properties of GRP produced in an industrial process, incorporating woven roving. The structural properties of the cores were taken to be those found in laboratory experiments as described earlier in the chapter. A sandwich panel of Vermiculux core and GRP faces would hence have the following material properties:

GRP Faces:

Tensile properties. $\sigma_{ult}=300N/mm^2$ $E_t=16.0kN/mm^2$

Vermiculux II core:

Flexural properties. $\tau_{ult}=1.75N/mm^2$ $E_t=776kN/mm^2$

Shear properties. $\tau_{max}>0.21N/mm^2$ $G_c=193.8kN/mm^2$

It was decided in the first analysis to assume that a core of 60mm Vermiculux would be used in conjunction with GRP faces of various thicknesses. The faces thickness was varied in the models from 4 to 10mm thick in 1mm steps. It was also necessary to assume a moisture content for the Vermiculux core and a density. After carefully drying samples in an electric oven, the average density was found to be $503kg/m^3$ and the moisture content was 11.26% (calculated from the change in mass during fire testing).

Using the finite difference model (as described in chapter 4) to predict the fire response of the panel designs, and Stamm and Wittes theory for predicting the structural performance of the panel designs, the following results, shown in table 3.13, were obtained:

60mm Vermiculux Core				
Skin Thickness (mm)	Maximum Deflection (mm)	Core Shear Stress (N/mm^2)	Insulation Failure (mins)	Pass or Fail?
4.00	51.01	0.062	155.0	F
5.00	39.66	0.061	166.0	F
6.00	32.08	0.060	177.0	F
7.00	26.70	0.059	190.0	F
8.00	22.69	0.058	203.0	F
9.00	19.60	0.057	217.0	P
10.00	17.14	0.056	233.0	P

Table 3.13 Results of Structural and Heat Transfer Analysis.

Figure 3.6.1 following shows the numerical predictions of cold face temperature with time of the panels when exposed to a simulated hydrocarbon fire test. The furnace temperature curve has not been shown to accentuate the differences between the cold face temperature curves.

From the structural calculations it can be seen that the critical design consideration is deflection. This is almost always the case for sandwich panels with face materials of low tensile modulus. Knowing that the core had not failed under laboratory test conditions at a shear stress of $0.21N/mm^2$, the limiting core shear should be $0.14N/mm^2$ (66%) and, as can be seen from above the factor of safety with respect to core shear is approximately 2.5 for the two

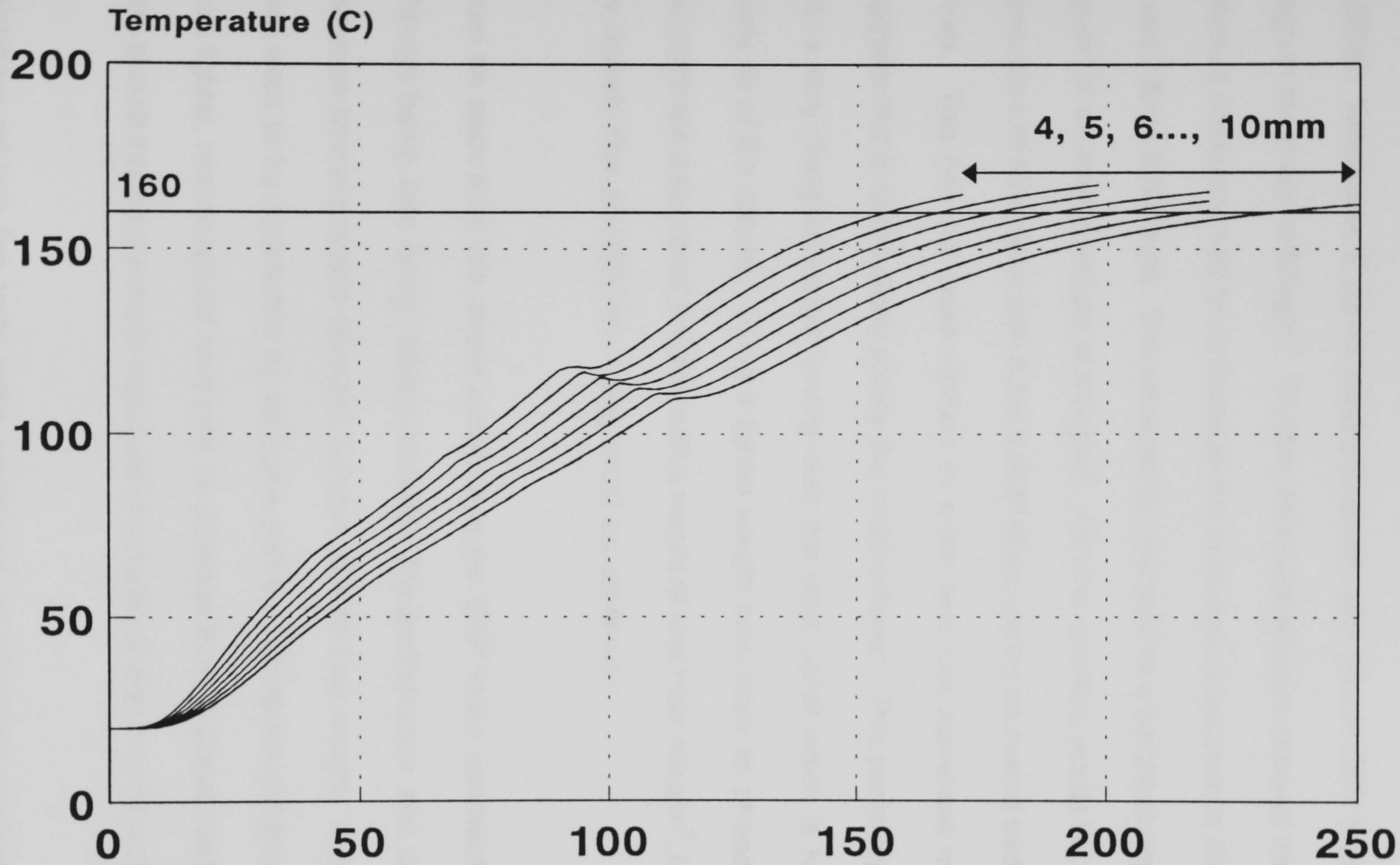

Figure 3.6.1 - Predicted Cold Face Response to Simulated Hydrocarbon Furnace Test (Face Thicknesses 4mm - 10mm)

panels which satisfied the design criteria.

A 60mm Vermiculux II cored sandwich panel with 10mm GRP faces would weigh in the order of 67kg/m^2. Further structural analysis showed that a near optimum solution would be to increase the thickness of the core to 65mm and to use 7.5mm GRP faces. This arrangement represents a weight saving of over 6kg/m^2 at an overall weight of 61kg/m^2. Another solution would be to use a 60mm core of Newtherm with 8.5mm GRP skins, giving an overall thickness of 77mm. This has not been verified in a fire test, but numerical modelling suggests that it would easily satisfy the H120 criterion. This panel represents only a very marginal weight saving over the steel panel which is known to satisfy all of the criteria. Using a lighter weight core such as phenolic foam could provide a structural solution with a weight of less than 40kg/m^2, however, it is unlikely that an H120 fire rating could be achieved.

It can be seen from the above results that the GRP faced sandwich panels although being less bulky, having excellent fire performance and corrosion resistance become a less attractive solution due to their weight. If the panel faces were to be connected by stringers and fire resistance enhanced by a much lighter, non-structural core infill, (a common form of panel manufacture in the aircraft industry) a much improved structural solution may be achieved[41].

Preliminary ad-hoc fire tests were performed on structural stringer panels consisting of steel channels, GRP faces and Voidfill or Vermiculux cores. The

first test, STRING 1, incorporated a steel stringer channel section. 0.5mm thick 40mm deep with 25mm webs and 10mm stiffeners. This channel was insulated from the faces with 5mm Vermiculux strips, and was filled with a high density Voidfill material (≈420kg/m^3, mix 10). The panel faces were GRP (12 layers woven roving glass, Crystic 489 polyester resin, catalyst M) at approximately 5.3mm thick, screwed to the steel stringer. The low density panel fill was again a Voidfill material at approximately 190kg/m^3. The overall panel weight would be in the region of 32kg/m^2 at an overall depth of 61mm.

The second test, STRING 2, again incorporated a steel stringer however it was not insulated from the faces. The stringer was again a channel 0.5mm thick but had a depth of 60mm, 25mm webs and 10mm stiffeners. The channel was filled with a Vermiculux II core which was cemented in place with a ball clay - sodium silicate mix. The panel faces were GCRP (2+3mm+8) again made with Crystic 489 polyester resin at an average thickness of 5.6mm and screwed to the steel stringer. The panel fill material was Voidfill 7D (≈320kg/m^3) made with standard high alumina cement and approximately 62.5mm thick. The whole panel was cemented together with a ball clay - sodium silicate mix and had an overall weight of approximately 47.5kg/m^2 .

Figures 3.6.2(a) and 3.6.2(b) overleaf show cross sections through STRING 1 and STRING 2.

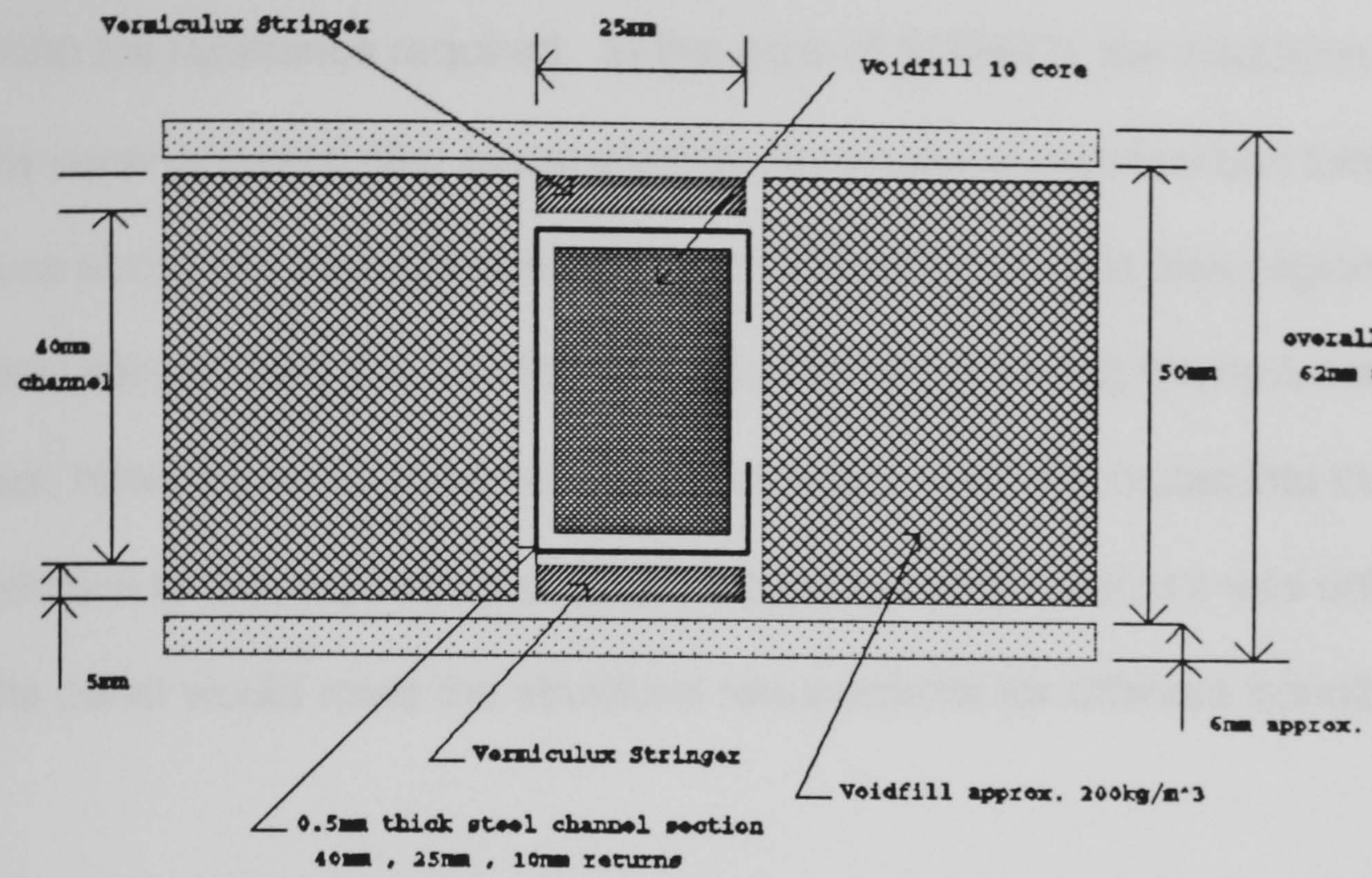

Figure 3.6.2(a) - STRING 1

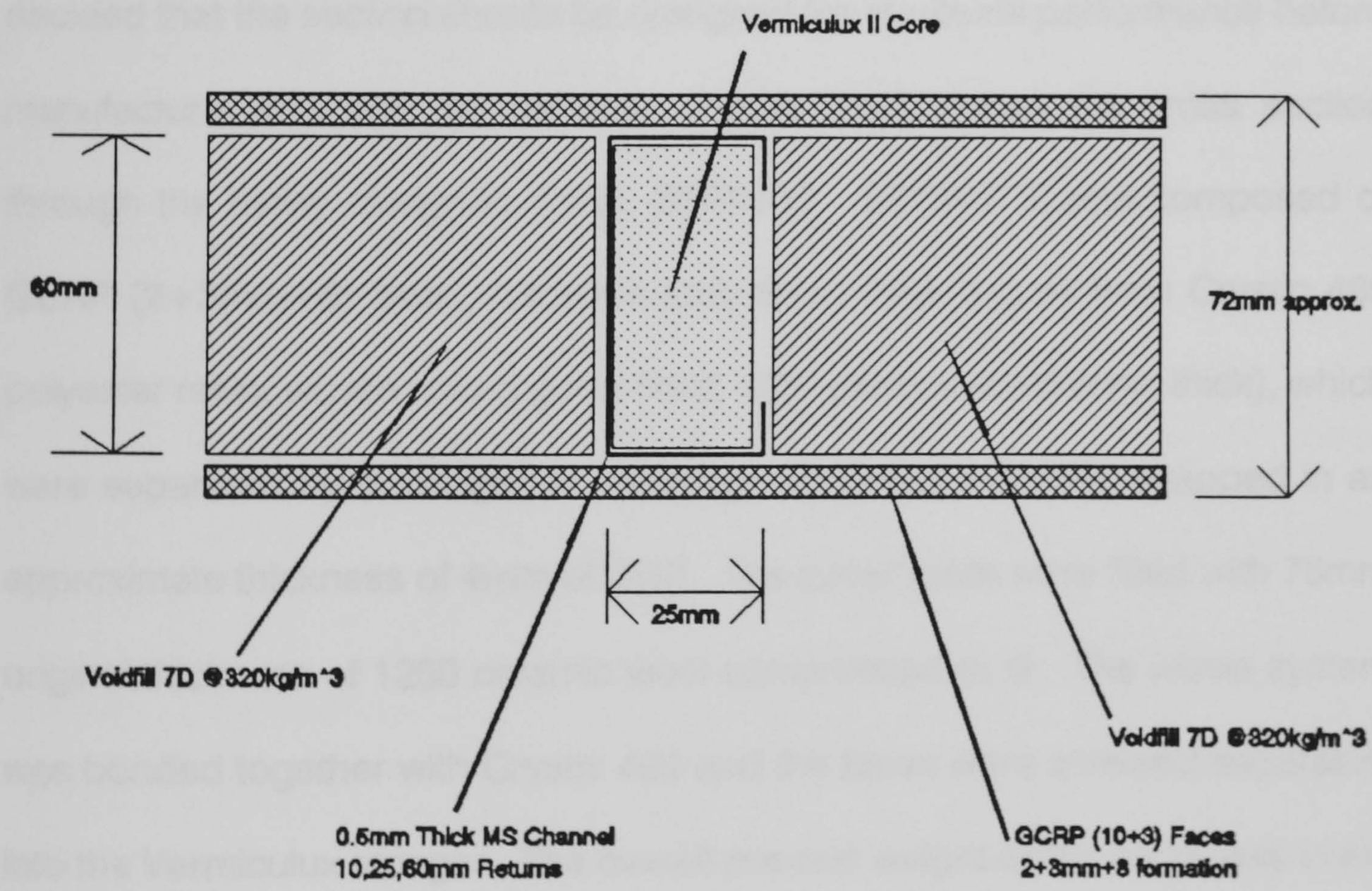

Figure 3.6.2(b) - STRING 2

The fire testing of these panels showed that neither were able to provide the H120 fire resistance required. In the case of STRING1 the insulation failure of the panel occurred after approximately 60 minutes of hydrocarbon testing in the area above the steel channel. Again in STRING2 the cold face region over the steel stringer was the location of insulation failure during the hydrocarbon fire test, however, in this case failure did not occur until 90 minutes into the test. In addition to this, equivalent section calculations showed that it was unlikely that the panel would meet the structural requirements for offshore conditions.

It was decided that stringer type panels may meet the design requirements if the stringer were to be constructed from GRP rather than steel (and hence reducing the heat conduction through that section of the panel). It was also decided that the section should be designed for structural performance before manufacture (see later for details). Figure 3.6.3 shows the cross section through the newly designed panel, STRING3. STRING 3, was composed of GCRP (2+3mm+8) faces, approximately 6mm thick (made from Crystic 489 polyester resin, woven roving glass fibre, 1250 ceramic wool 3mm thick), which were separated by a stringer of Vermiculux II 50mm x 50mm, wrapped in an approximate thickness of 4mm of GRP. The panel voids were filled with 75mm original thickness of 1250 ceramic wool compressed to fit. The whole system was bonded together with Crystic 489 and the faces were screwed separately into the Vermiculux stringer. The overall pre-test weight of the panel was in the order of 38.5kg/m^2 with an overall depth of ≈70mm.

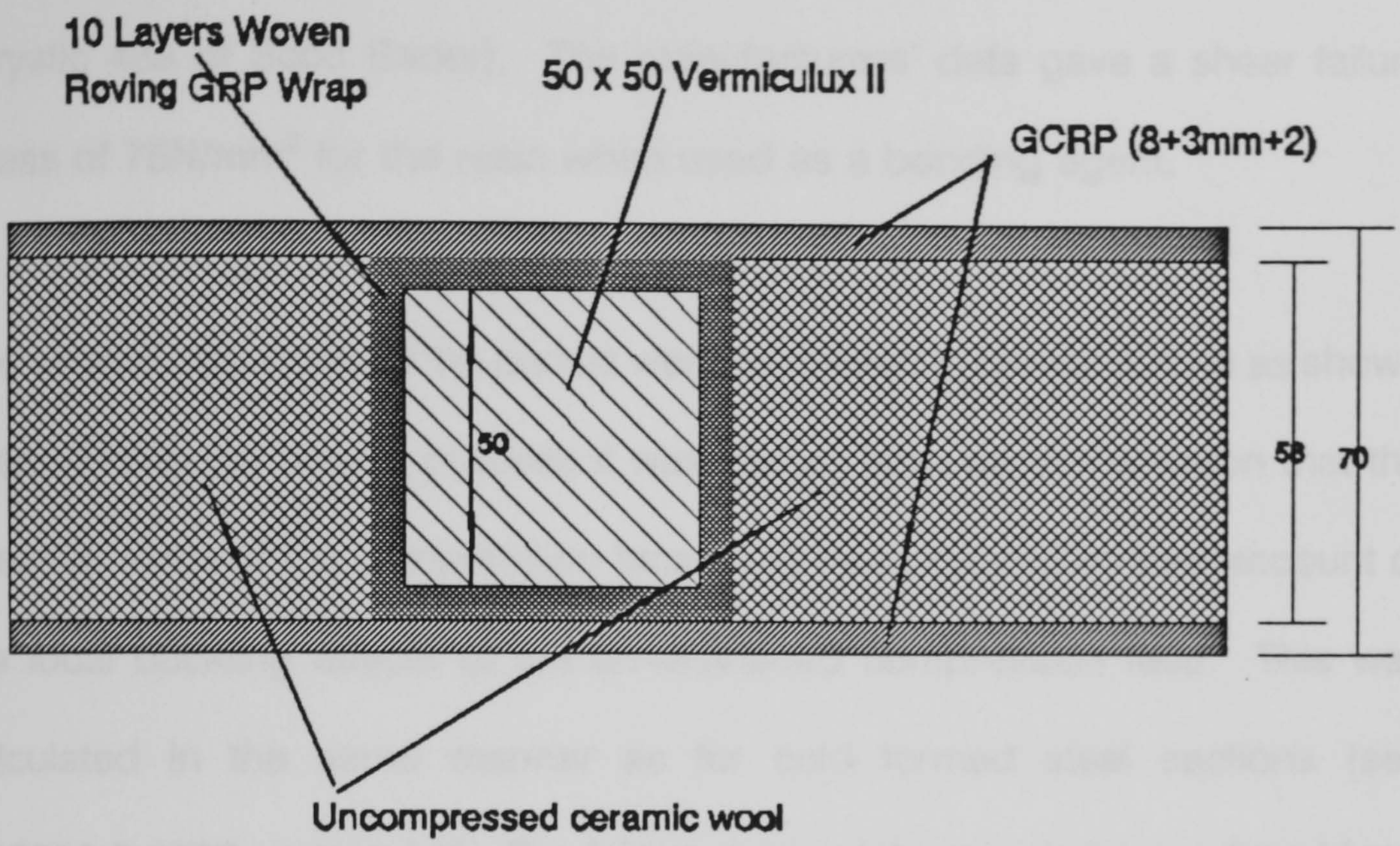

Figure 3.6.3 - STRING 3

In a hydrocarbon fire test, STRING3 did not fail in insulation prior to termination of the test at 135 minutes. Hence it could easily achieve the H120 fire requirement. It was still realised however that this particular panel arrangement was not the optimum solution.

At this point reduced scale stringer panels of 38mm overall depth were constructed using an open C section for a stringer. Typical samples were 1000mm long and were tested in four point bending over an 800mm span. The thickness of the GRP on the stringers was slightly less than that of the faces due to the method of manufacture. The GRP wrap was hand laid up over a Vermiculux former, and a waxed rigid mould was then forced over the assembly and left in place for 24 hours for the resin to cure. After curing the panel was bonded together with the same resin as used to form the GRP components.

The GRP was formed from woven roving e-glass of 600gsm and polyester resin (Crystic 489 of Scott Bader). The manufacturers' data gave a shear failure stress of 75N/mm^2 for the resin when used as a bonding agent.

The section properties of the panels were calculated in tabular format as shown later. Within the design process it was shown from experimentation that the effective width of the compression face must be calculated to take account of the local buckling effects of the un-restrained compression face. This was calculated in the same manner as for cold formed steel sections (see BS5950:5:1987 section 4.3). The failure stress of the panel was predicted from the failure stress of the bond connecting the stringers to the compression face. Test results showed that although it was necessary to consider the effective width of the compression face in stress calculations, it was prudent to consider the compression face as being fully effective for deflection calculations.

The material properties of the GRP used for the scale model were assumed to be the same as for hand laid laminates tested previously. These were as follows:

E_t = 18.59kN/mm^2 $\quad\quad$ σ_{ult} = 312.5N/mm^2

In order to calculate the section properties of the panel it was first necessary to measure the dimensions of the stringers and faces accurately. Figure 3.6.4 following shows the dimensions of the stringers. The faces were each 250mm

wide and 2.9mm average thickness.

The first step in the design process was to find the effective width of the unrestrained compression face:

Span = 780mm
Assuming Poissons ratio for GRP to be 0.3
The unrestrained face width = 250-60 = 190mm
Also assuming the compressive capacity of the GRP is 85% of its tensile strength:

$$P_{cr} = \frac{\pi^2.E}{12(1-\nu^2)}.k.\left(\frac{t}{b}\right)^2$$

$$P_{cr} = \frac{\pi^2.18590}{12(1-0.3^2)}.4.\left(\frac{2.9}{190}\right)^2$$

$$P_{cr} = \underline{15.657}$$

$$\frac{F_c}{P_{cr}} = \frac{0.85x312.5}{15.657} = 16.965$$

$$\therefore B_{eff} = 190.\left[1+14((16.965)^{\frac{1}{2}} - 0.35)^4\right]^{-0.2}$$

$$B_{eff} = 60 + 38.77 = 98.77mm$$

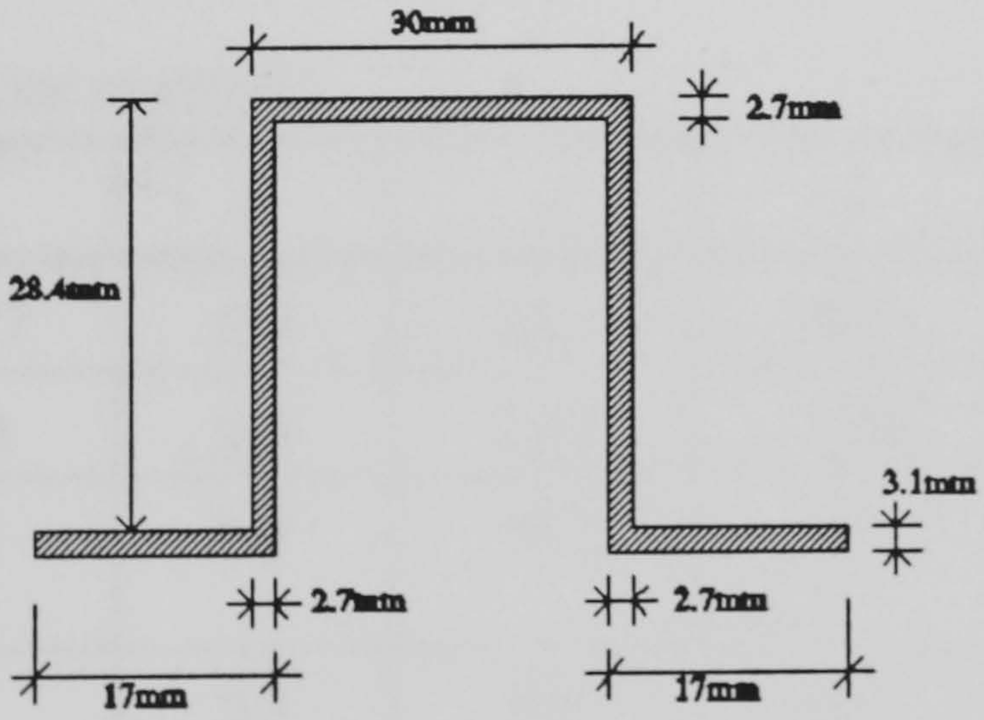

Figure 3.6.4 Dimensions of GRP stringers

The neutral axis of the effective section is next to be calculated by taking moment areas about the base line of the section:

$$\bar{y} = \frac{\Sigma\ Ay}{\Sigma\ A}$$

$$\bar{y} = \frac{(2.9x98.77x35.85)+(2x30x2.7x33.05)+(4x25.7x2.7x18.85)+(4x17x3.1x4.45)+(2.9x250x1.45)}{(2.9x98.77)+(2x30x2.7)+(4x25.7x2.7)+(4x17.3x3.1)+(2.9x250)}$$

$$\therefore\ \bar{y} = 13.75mm$$

The deflection of the beam/panel is governed by the following equation for four point bending (two point loading)

$$\delta = \left[\frac{23\left(\frac{W}{2}\right)l^3}{648\ E\ I}\right]$$

Where:

W/2 = Point load in kN
E = Youngs modulus of material
I = Second moment of area of sample
L = Span = 780mm

Therefore the only requirement to design the panel with respect to load-deflection is to calculate the second moment of area. The easiest form of doing this is the tabular method:

Element	b	d	y	A	Ay^2	I_G
C Face	98.77	2.9	22.1	286.4	139896.7	200.7
T Face	250	2.9	12.3	725	109685.3	508.1
C Flange (2)	30	2.7	19.3	81	30171.7	49.2
T Flange (4)	17	3.1	9.3	52.7	4558.0	42.2
Webs (4)	2.7	25.7	5.1	69.39	1804.8	3819.3

Where:

y = Distance from element centroid to neutral axis
I_G = Elements own second moment of area (= $bd^3/12$)

Now, the second moment of the section is given by:

$$I_{NA} = I_G + A\overline{y^2}$$

$$\therefore I_{NA} = 200.7+508.1+(2x49.2)+(4x42.2)+(4x3819.3)+139896.7$$
$$+109685.3+(2x30171.7)+(4x4558.0)+(4x1804.8)$$
$$=351629.8mm^4$$

Hence, if we know that the glue bond has a failure strength of 75 N/mm² , the bending moment is given by M=Wl/6, and the eccentricity of the bond from the neutral axis is 20.65mm we can calculate the load required to fail the bond as follows:

$$W = \frac{75 \ x \ 6 \ x \ 351629.8}{780 \ x \ 20.65}$$

Therefore the theoretical failure load is **9.82 kN**

Similar calculations as previously can show that for the compression face fully effective, the neutral axis of the section is 18.3mm from the lower surface of the tension face, and also that $I_{NA} = 521746mm^4$

Now, substituting this and other known values into the deflection equation we get:

$$\delta = \left[\frac{23 \ x \left(\frac{1000}{2}\right) x \ 780^3}{648 \ x \ 18590 \ x \ 521746}\right]$$

Giving: $\delta = 0.806$ **mm/kN**

Comparing theoretical value with experimental ones:-

Deflection: $\delta_{theory} = 0.806$ mm/kN $\delta_{experiment} = 0.783$ mm/kN

Failure load: $W_{theory} = 9.82$ kN $W_{experiment} = 8.92$ kN

The experimental failure mode observed was one of debonding between the tension surface of the stringers and the tension face.

Figures 3.6.5a and 3.6.5b show comparisons between the predicted and actual results, and also show the predicted deflection if the compression face were assumed partially effective. As can be seen, for deflection purposes if the effective width of the compression face is considered, this significantly under estimates the stiffness of the stringer panel. When assuming the compression face is fully effective a good correlation between experimental and theoretical results can be seen.

Figure 3.6.6a shows a similar comparison produced from Stamm and Witte's theory for thick faced sandwich panels. In this case the panel under test is a 60mm deep Voidfill 7D Core with 6mm thick GRP Faces. This comparison of theoretical and experimental results highlights the difficulties which can be encountered where design methods encompass assumptions that the core is antiplane ($\sigma_x = \sigma_y = \tau_{xy} = 0$), and homogenous. These two conditions are difficult to comply with in small batch mixes of particulate composites. This is, however, not a fault of the theory which is an effective design tool when considering foamed plastics etc, but rather this is a failing of the quality control of the laboratory scale manufacture of the 7D core. It is envisaged that in a manufacturing process these problems would not arise, and the panels may be designed with a high degree of accuracy. Figure 3.6.6b also shows a comparison of Stamm and Wittes theoretical results with experimental results.

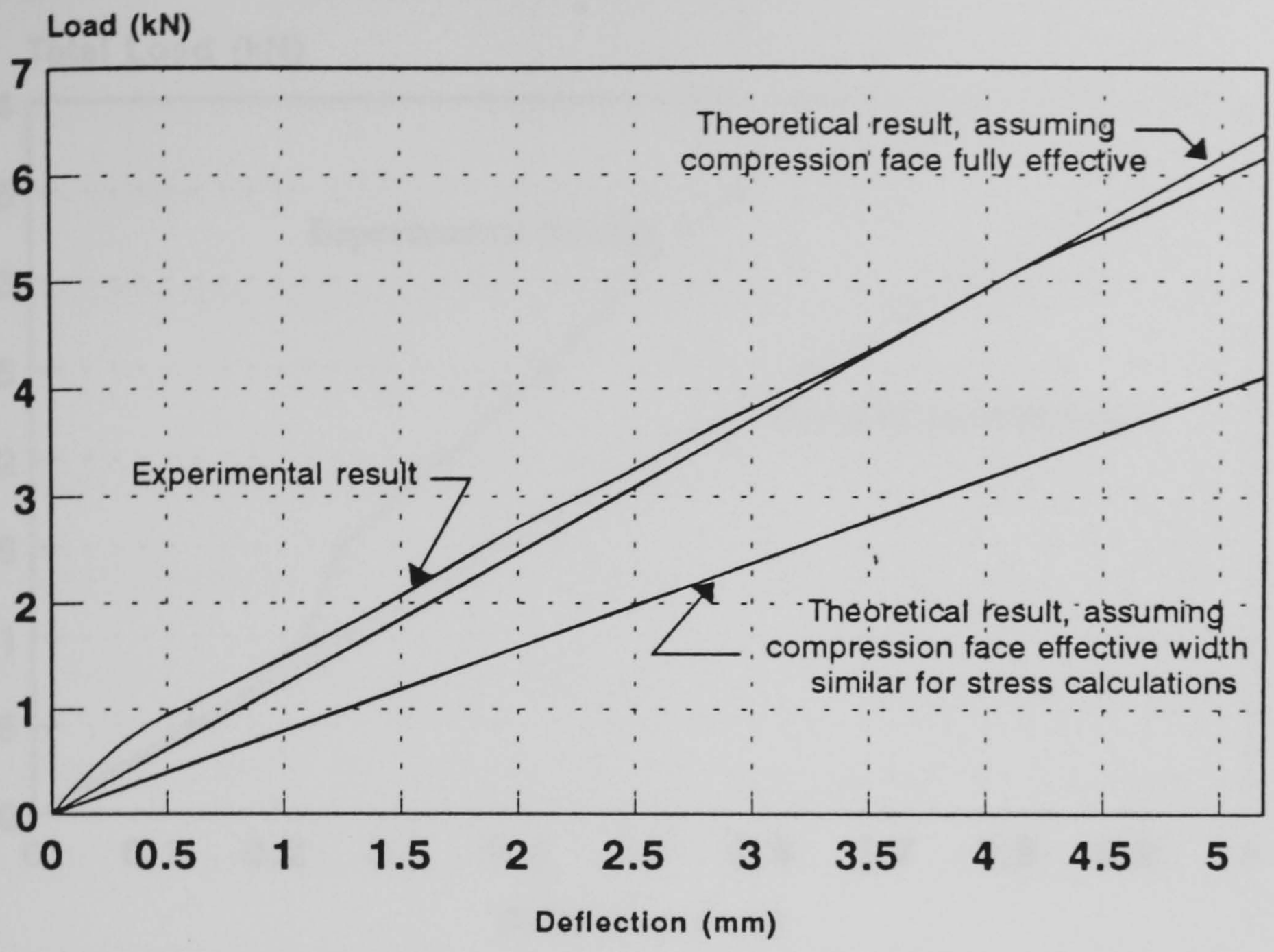

Figure 3.6.5(a) Four point load results for STRING 4
Comparison of theoretical and experimental results
SALFORD UNIVERSITY 17-06-94

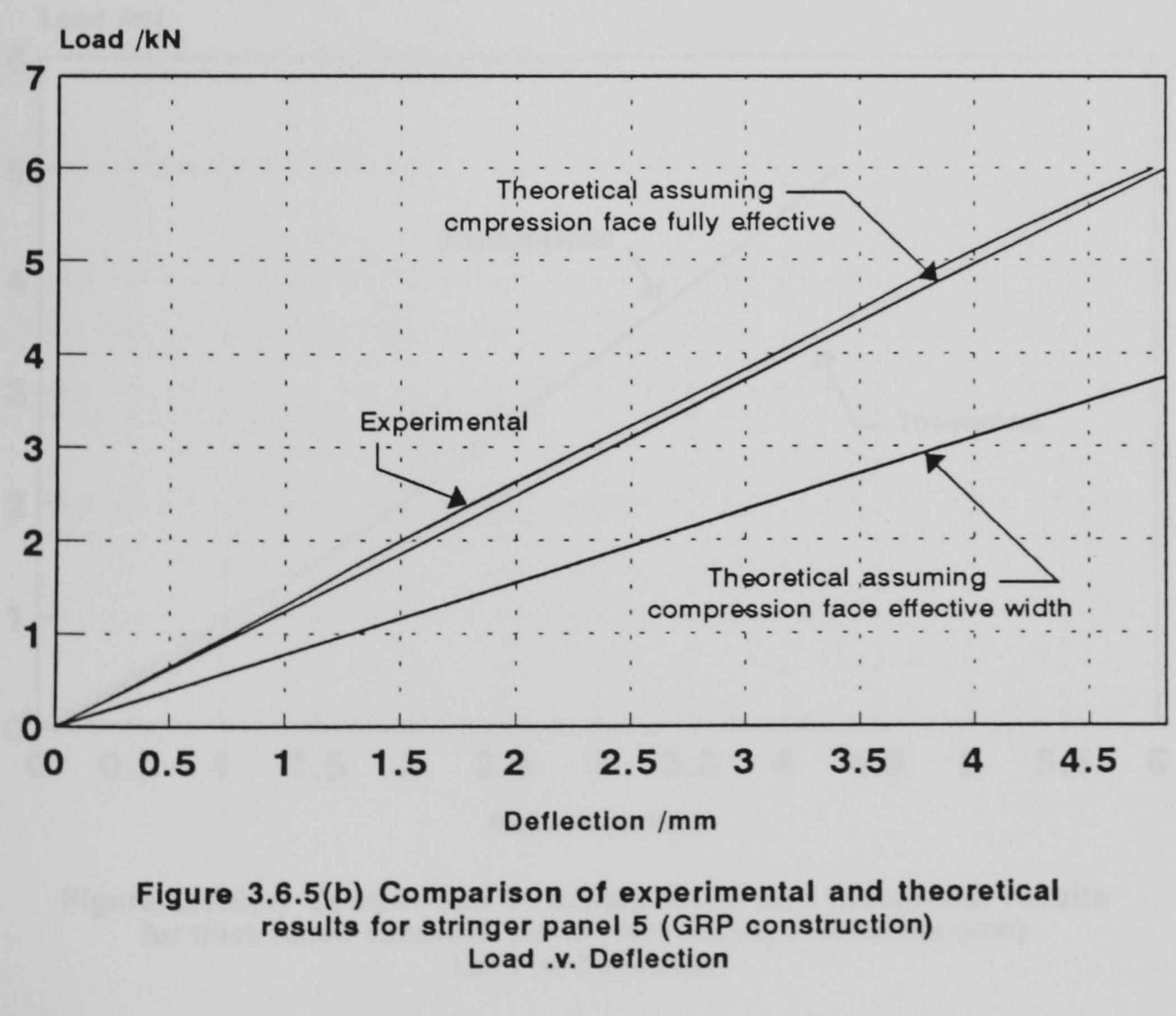

Figure 3.6.5(b) Comparison of experimental and theoretical results for stringer panel 5 (GRP construction)
Load .v. Deflection

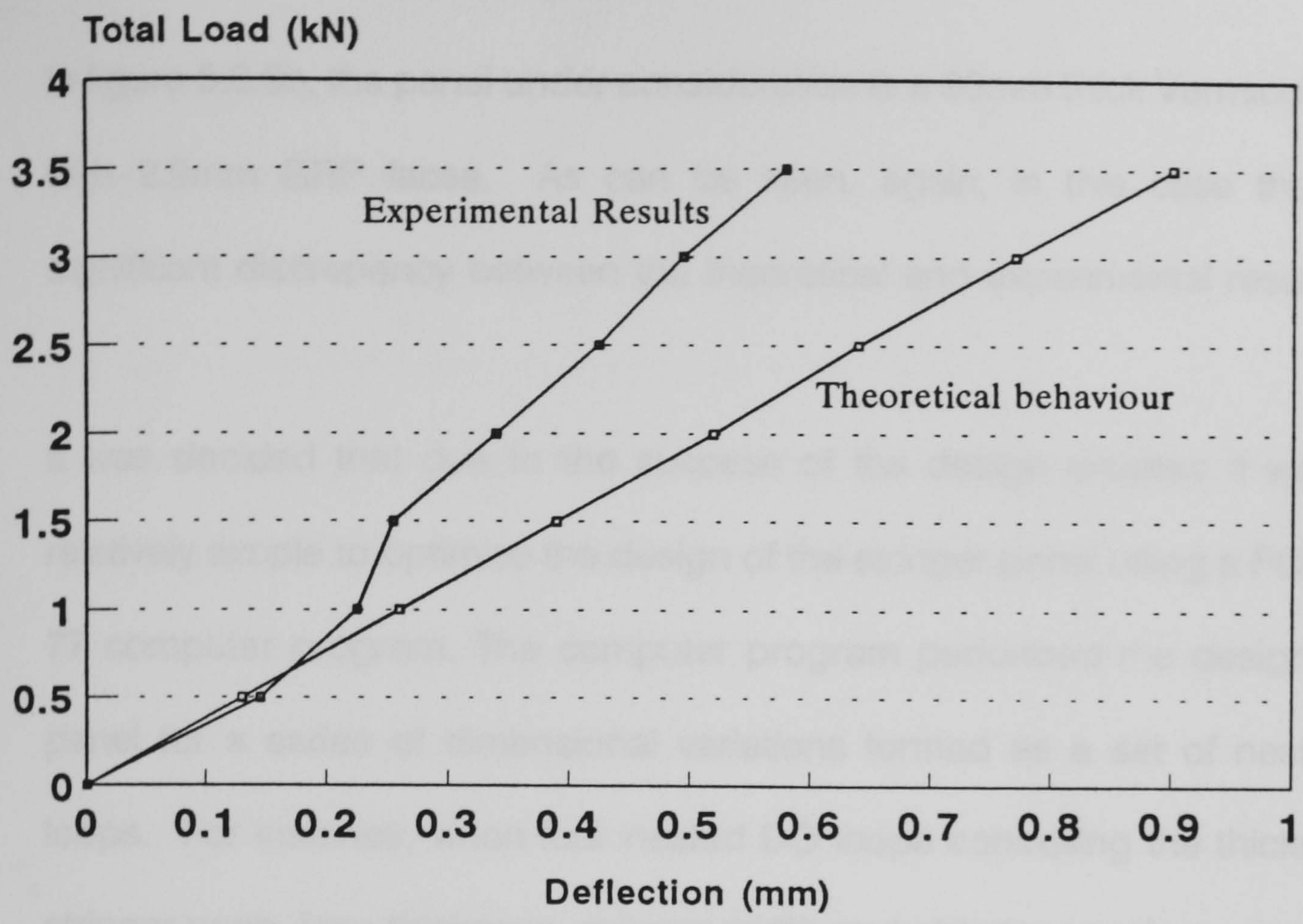

Figure 3.6.6(a) - Comparison of Experimental 4 point bending test results with Stamm and Witte Theoretical results

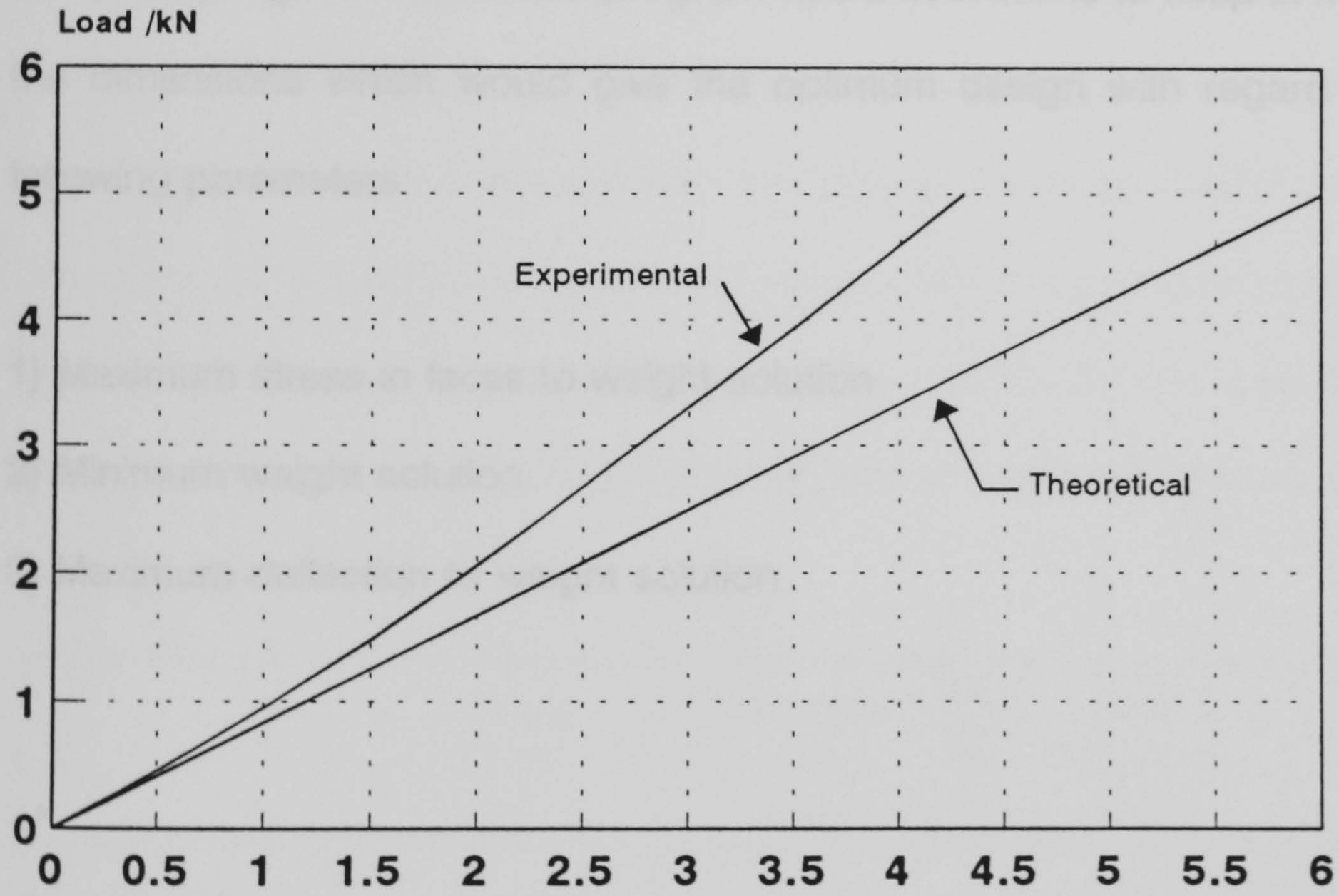

Figure 3.6.6(b) Comparison of experimental and theoretical results for thick faced sandwich panel (GRP faces, Vermiculux core) Load .v. Deflection

In figure 3.6.6b, the panel under consideration is a 30mm thick Vermiculux core with 2.9mm GRP faces. As can be seen, again, in this case there is a significant discrepancy between the theoretical and experimental results.

It was decided that due to the success of the design process it would be relatively simple to optimise the design of the stringer panel using a FORTRAN 77 computer program. The computer program performed the design of the panel for a series of dimensional variations formed as a set of nested DO loops. For instance, when four nested DO loops controlling the thickness of stringer wrap, face thickness, stringer width and stringer spacing were used it was possible to perform many thousands of panel designs in one run of the computer program. Within the program was a subroutine to keep in memory the dimensions which would give the optimum design with regard to the following parameters:

1) Maximum stress in faces to weight solution

2) Minimum weight solution

3) Maximum deflection to weight solution

Within the program, all solutions which did not fulfil all of the following eligibility criteria were discarded:

A) Maximum GRP compressive stress < 220N/mm^2

B) Maximum GRP tensile stress < 250N/mm^2

C) Maximum deflection < 16.7mm (span/240)

D) Maximum panel weight < 40kg/m^3

The limit of deflection to span/240 was to provide a safety factor with regard to the deflection as neither material safety factors nor load factors had been included within the design. However, the load assumed of 2kN/m^2 was seen as being a conservative estimate for offshore non-loadbearing panels. As with the GRP sandwich panel calculations deflection was foreseen as being the main design criterion due to the relatively low Youngs modulus of GRP materials. The computer program was run several times, each time giving more scope for variation of the variables mentioned previously. Tables 3.14 to 3.19 show the optimised stringer panel designs with regards to the required parameters of performance (1) to (3)

	Stringer Width (mm)	Stringer Wrap (mm)	Face Thickness (mm)	Stringer Spacing (mm)
Range	25 - 50	2 - 10	2 - 10	200 - 500
Optimal -1	25	9	4	500
Optimal -2	50	10	2	440
Optimal -3	35	10	2	370

Table 3.14 - Optimised stringer panel, practical panel 1.

Compressive Stress (N/mm^2)	Tensile Stress (N/mm^2)	Loaded Deflection (mm)	Panel Weight (kg/m^2)
38.924	15.816	16.673	31.422
32.763	20.269	16.589	29.155
32.701	20.678	16.698	29.172

Table 3.15 - Calculated results for practical panel 1.

	Stringer Width (mm)	Stringer Wrap (mm)	Face Thickness (mm)	Stringer Spacing (mm)
Range	10 - 50	2 - 10	2 - 10	60 - 500
Optimal -1	10	10	4	490
Optimal -2	10	2	4	100
Optimal -3	25	10	2	370

Table 3.16 - Optimised stringer panel, practical panel 2.

Compressive Stress (N/mm^2)	Tensile Stress (N/mm^2)	Loaded Deflection (mm)	Panel Weight (kg/m^2)
39.892	16.069	16.608	31.060
26.242	17.591	16.365	28.853
32.701	20.678	16.698	29.172

Table 3.17 - Calculated results for practical panel 2.

	Stringer Width (mm)	Stringer Wrap (mm)	Face Thickness (mm)	Stringer Spacing (mm)
Range	10 - 50	0.5 - 10	0.5 - 10	50 - 500
Optimal -1	10	10	4	494
Optimal -2	10	0.5	4	69
Optimal -3	10	0.5	4	69

Table 3.18 - Optimised stringer panel, rigorous panel 3.

Compressive Stress (N/mm^2)	Tensile Stress (N/mm^2)	Loaded Deflection (mm)	Panel Weight (kg/m^2)
40.165	16.097	16.697	31.013
23.439	19.008	16.654	26.447
23.439	19.008	16.654	26.447

Table 3.19 - Calculated results for rigorous panel 3.

With each progression in the above tables the computer program was allowed more scope for variation within the dimensional variables. The range of variables which could be used increased, as well as the magnitude of each variable change being reduced. The final "rigorous" design run considered almost 6.5 million possible panel designs.

As can be seen from the results, there is little benefit in weight terms from allowing the analysis routine more scope to vary the dimensions of the stringers and faces. Taking a realistic solution (i.e one not requiring a GRP layer of less than 2mm) it can be seen that the predicted weight is in the order of $30kg/m^2$ which represents a weight saving of approximately 40% on the typical steel panel to satisfy the same criteria. As the panels have effectively been designed for unfactored live load deflection it is prudent to consider the stress at the stringer-face bond line. Assuming a safety factor of 1.5 the maximum allowable bond line stress would be $50N/mm^2$. Comparing this with the design results in tables 3.14 to 3.19 it can be seen that the maximum extreme fibre stress is less than $21N/mm^2$ and hence there is a large margin of safety over failure of the stringer-face bond line (stress at the bond line is less than stress at the

extreme fibre).

The design of the panel did not take into account the encapsulation of a 3.5mm layer of ceramic blanket within the faces. It has been assumed that this would not contribute significantly to the structural performance of the panel. However, the increase in weight has been allowed for in the calculation.

3.7 Summary of Panel Design Optimisation

Investigation into the structural performance of both GRP faced sandwich panels, and structural stringer panels has shown that effective panel design techniques are readily available. In the case of GRP (thick) faced sandwich panels Stamm and Witte's theory has been used to compare theoretical load-deflection predictions with those obtained experimentally. The design technique would at first appear to be unsatisfactory. However, the differences between theoretical behaviour and experimental results may be attributed to the difficulty in obtaining homogenous, antiplane cores in small batch mixes. It is thought that these problems would not arise if larger batch mixes and industrial manufacturing processes were employed in the production of the core material.

The design of structural stringer panels has been performed in a manner similar to that which would be used for built-up steel sections. The design method has been shown to be highly accurate where the compression face is assumed to be fully effective for deflection calculations, and partially effective for stress

calculations. The design method has been verified against experimental testing and good agreement has been found between theoretical and experimental results.

The calculations and investigations in chapters 2.5 and 3.6 show that although GRP faced structural sandwich panels are still an attractive solution for fire risk areas in terms of their corrosion resistance and ease of installation they become less so due to their weight. It has been shown that in the case of GRP faced Vermiculux II cored sandwich panels the optimum design to satisfy the design requirements would be 80mm thick (compared to 266mm thick for steel solution) and 61kg/m^2 (compared to 48kg/m^2 for the conventional steel solution). The sandwich panel, although representing a space saving due to it's reduced thickness when compared to the steel solution, may not be a cost effective replacement for the traditional deep profiled steel panel.

The structural stringer panel appears to represent a much more efficient panel design. It has similar properties to the GRP faced sandwich panel in its inherent corrosion resistance and foreseen ease of installation, and is a more attractive solution due to its reduced weight. However, manufacturing costs of the structural stringer panel have not been considered and these will almost certainly be higher than for a simple sandwich panel. Preliminary trials and predictive calculations have shown that the stringer panel may represent a weight saving of up to 40% with respect to the conventional steel solution, and over 50% with respect to the GRP faced sandwich panel solution. Trials have

also shown that the stringer panel is capable of withstanding a two hour hydrocarbon fire resistance test without failing (see chapter 4).

Chapter 4, following, discusses the fire performance of GRP panels, and GRP faced sandwich panels, and also shows the fire test results for the GRP based structural stringer panel development. Chapter 4 also contains an outline of the factors which need to be considered in the numerical modelling and prediction of fire resistance tests and shows the finite difference equations used in the modelling work.

CHAPTER 4 - FRP PANELS IN FIRE SITUATIONS

4.1 Test Methodologies

4.1.1 Furnace Based Testing

Within the panel development and fire testing, two furnace control regimes have been selected for use as discussed in chapter 1. These are the BS476 cellulosic curve and the DoE/NPD hydrocarbon curve. The two control curves are used as the basis for assessing the performance of a material with respect to different fire conditions. For an offshore installation, the cellulosic curve may be used to test materials which may be used in the accommodation areas (and subject to normal household type fires). The simulated hydrocarbon curve, however, would be used to test materials and structures for use in processing areas, temporary safe refuges and escape routes. The failure criterion for the fire testing of panels are insulation, stability and integrity as described in chapter 1. The requirements for achieving a fire rating are as follows:

A60 - **Cellulosic rating** - Shall prevent flames and smoke from advancing through the partition for a minimum of **one** hour. Average temperature on the unexposed wall surface must not exceed 140°C above initial temperature within the first **60** minutes of testing.

H60 - **Hydrocarbon rating** - Shall prevent flames and smoke from advancing through the partition for a minimum of **two** hours. Average temperature on the unexposed wall surface must not exceed 140°C above initial temperature within the first **60** minutes of testing.

H120 - **Hydrocarbon rating** - Shall prevent flames and smoke from advancing through the partition for a minimum of **two** hours. Average temperature on the unexposed wall surface must not exceed 140°C above initial temperature within the first **120** minutes of testing.

The research was performed using one of two available furnaces, both fired by premixed natural gas burners and controlled by similar computer programs. The first furnace, the Phase I furnace, has an active volume of approximately 1.0x1.0x1.0m and is fired by two 3 therm burners. The furnace is lined with fire brick (a mixture of fire clay and crushed fire clay brick to stabilise shrinkage) to approximately 150mm thick with a backing of ceramic wool. The second furnace, the Phase II furnace, has an active volume of 1.5x1.5x1.5m and is fired by a single lateral 15 therm burner. The furnace is lined with 250mm thick stack bonded ceramic wool.

Indicative panel tests were performed on samples which were mounted to the front of the furnaces as shown in figures 4.1.1 and 4.1.2. The phase 1 furnace

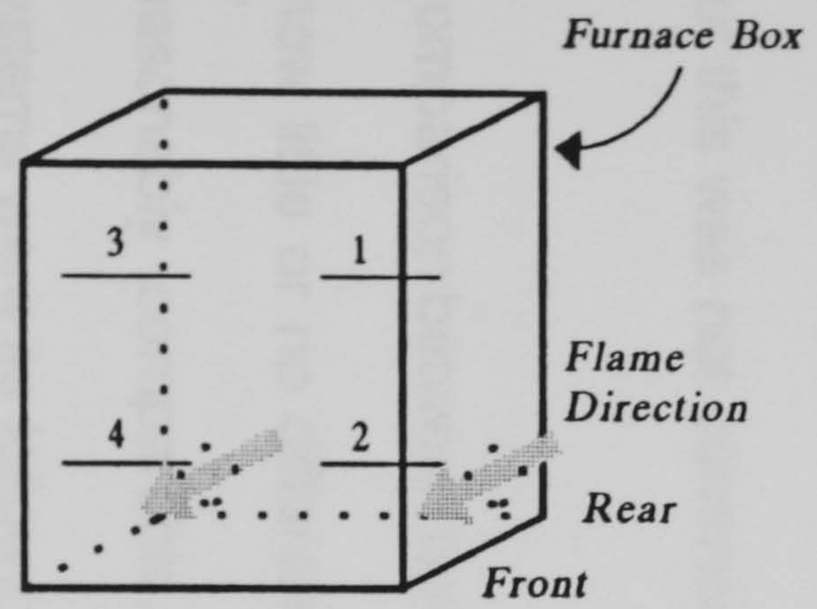

Control Thermocouples

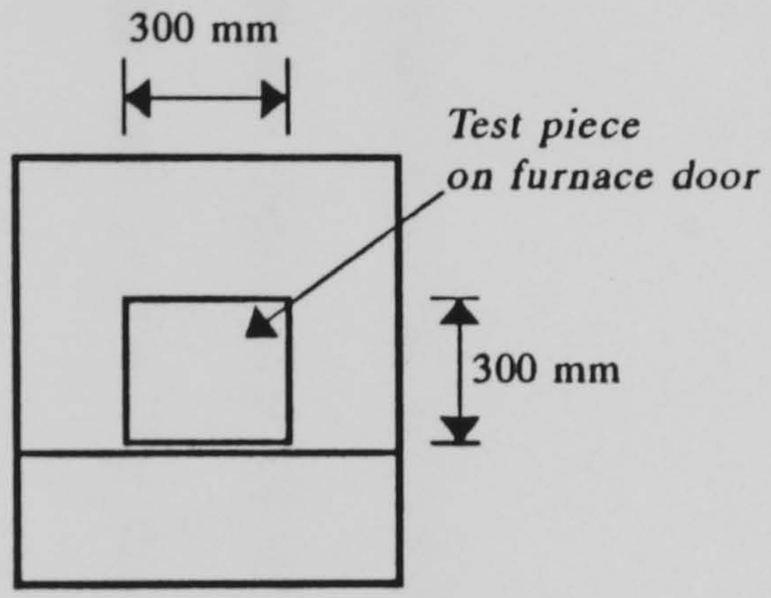

Arrangement of test piece
on furnace door

Figure 4.1.1 Assembly of test piece and Furnace arrangement

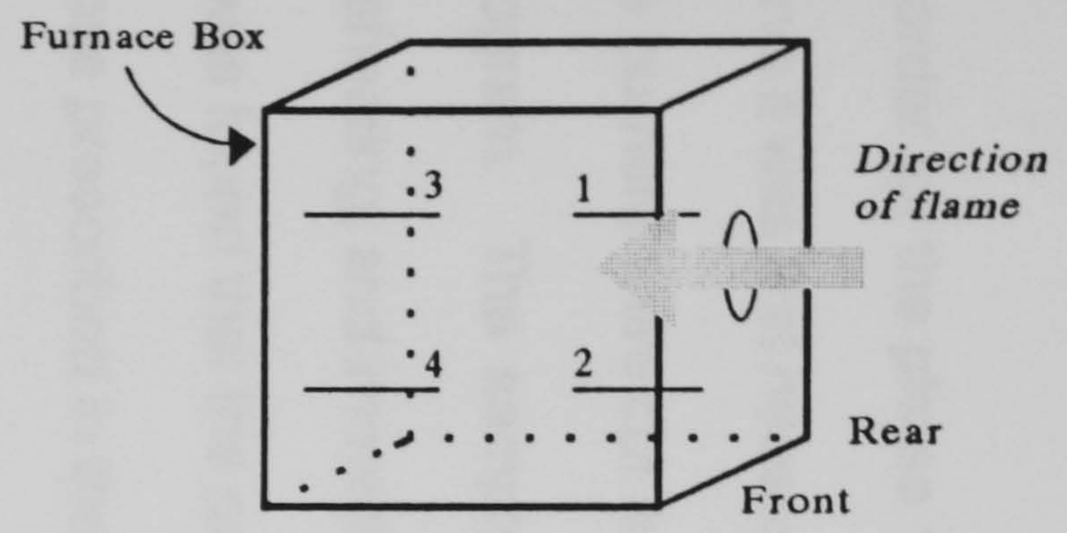

Control Thermocouples

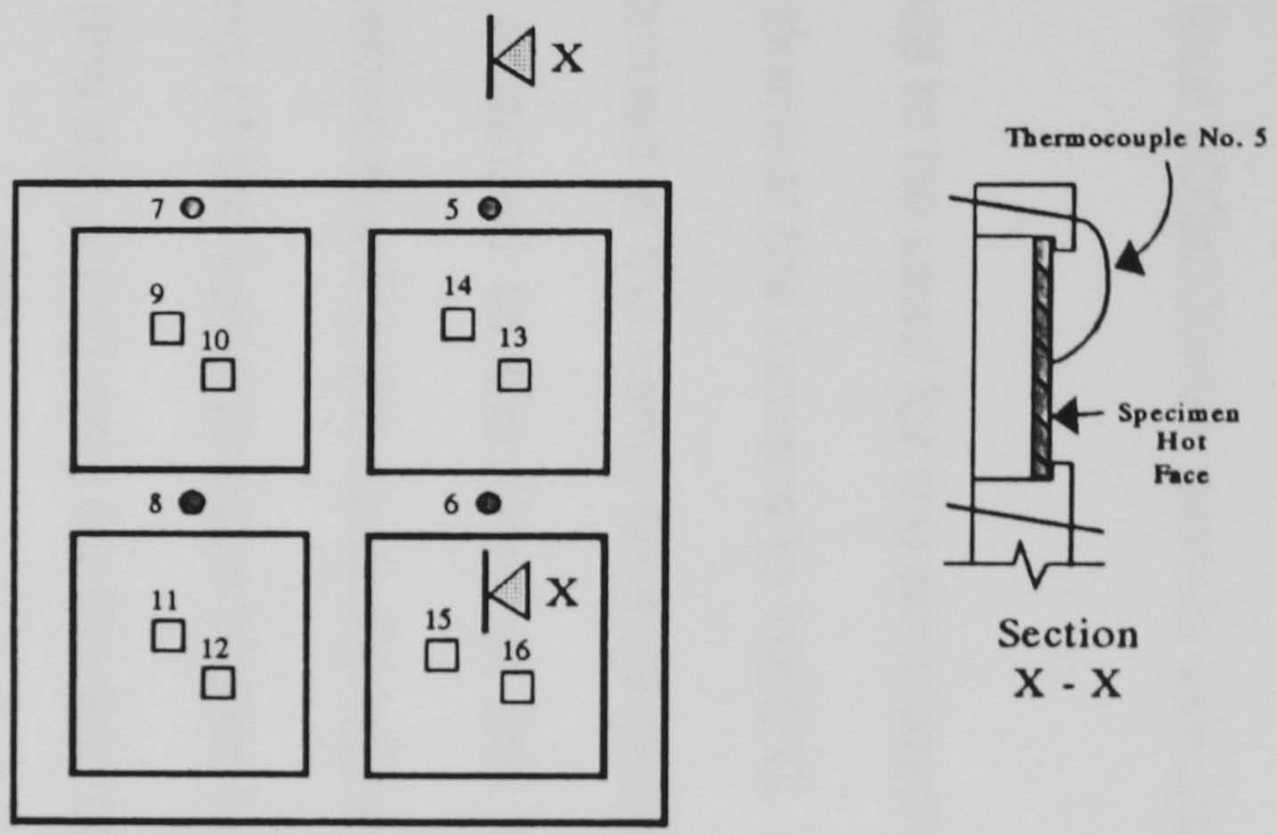

Hot face and cold face Thermocouples

Figure 4.1.2 Thermocouple layout for furnace and specimens

was only capable of testing one sample per test run, and the phase 2 furnace was capable of testing up to four 300x300mm panels simultaneously.

In order for the phase 1 furnace to be used for the simulated hydrocarbon fire curve it was first necessary to preheat the furnace to 1000°C. After preheating, the burners were cut and re-primed at the same time as re-starting the control program. The sample was mounted to the front of the furnace after the preheating, and immediately before starting the control program data collection. It was found that the preheating of the furnace gave higher temperatures than those prescribed in the code (the set point) only for the first 30 seconds. After this the furnace had cooled to the prescribed temperature and the furnace temperature followed the set point accurately.

The failure criterion for the fire tests performed was generally one of insulation failure as described in chapter 1. In certain cases, for instance occasional tests performed on phenolic foam, integrity failure occurred prior to insulation failure, but this was not common.

Comparison between tests performed on similar materials with the two furnaces show little or no difference in results. Accuracy of furnace control was also reasonably comparable. Typical test errors for the computer controlled systems were as follows:

1m^3 (phase 1) furnace

* BS476 Pt 20 Cellulosic Test

T_{10} ±4.5%
T_{30} ±3.0%
$T_{>60}$ ±1.5%

* Hydrocarbon Test (Furnace preheated to 1000°C)

T_{10} ±2.0%
T_{30} ±0.5%
$T_{>60}$ ±0.5%

3.5m^3 (phase 2) furnace

* BS476 Pt 20 Cellulosic Test

T_{10} ±3.5%
T_{30} ±2.0%
$T_{>60}$ ±1.5%

* Hydrocarbon Test

T_{10} ±3.0%
T_{30} ±2.0%
$T_{>60}$ ±1.0%

4.1.2 Cone calorimetry

A cone calorimeter is a standardised piece of equipment which has been designed specifically to measure properties of combustible materials such as the effective heat of combustion, heat release rate, mass loss rate, ignitability, and smoke and soot production. The "standard" cone is built to the requirements of ISO5660:1993[42] (BS476:Part 15:1993), and consists of the

following essential components:

a) A cone shaped radiant electric heater capable of producing irradiances of up to 100kW/m² at the surface of the sample. The temperature of the cone heater is maintained by a controller which can control the element temperature to within +/- 2°C.

b) A load cell of accuracy 0.1g to measure the mass loss rate of the sample. The load cell should be able to accommodate a wide variety of samples, and have a tare facility to compensate for the mass of the sample holder.

c) Specimen holders of standard design.

d) Exhaust gas system with flow measuring instrumentation.

e) Electrical spark igniter.

f) Gas sampling apparatus consisting of a ring sampler in the exhaust duct, a cold trap, desiccant and CO_2 removal.

g) A paramagnetic type Oxygen analyzer with a range of 0-25%.

h) A heat flux meter with which to calibrate the heater.

i) A calibration burner connected to a supply of methane of at least 99.5% purity.

j) A data logging system of minimum stated accuracy.

In addition to the above, the cone calorimeter used during the research also had:

k) A 0.5mW helium-neon laser and twin photodiodes (one reference, and one for measurements) for smoke obscuration measurements.

l) An infra red absorption analyzer for measurement of carbon monoxide and carbon dioxide production.

The basic operating principle of the cone calorimeter is that for organic materials the net heat of combustion is proportional to the amount of oxygen required for combustion. This relationship for organic materials is that approximately 13.1×10^3kj of heat are released per kg of oxygen consumed.

The heat release from a material and also the rate of heat release are important factors when considering a material for use in a fire hazard area. For a material to be suitable for fire protection not only should it satisfy integrity, stability and insulation requirements, but it should also not significantly add to the fire load.

Figures 4.1.3 and 4.1.4 following show views of the major components of a cone calorimeter, and also the some of the critical dimensions used in a "standard" cone calorimeter design.

The test principle is that the cone calorimeter is calibrated for the measurement of oxygen depletion, and carbon monoxide and carbon dioxide production on every day of testing for that day's atmospheric conditions. The load cell is calibrated and tared for the mass of the sample holder without sample, and then is assembled with the sample in place. The mass of the samples are double checked by weighing the samples accurately on scales, and comparing with the tared load of the assembled sample holder and sample. This assembled test piece is then placed away from the cone heater. Following that the cone heater is set to supply a particular incident heat flux to the sample. This is done by means of accurately controlling the temperature of the cone heater while measuring the heat flux supplied at sample surface level with a flux meter. Heat fluxes within the range of 0-100kW/m^2 can be produced by the cone heater.

When the incident flux is at the correct level, the flux meter is removed, and a final automatic calibration by the cone calorimeter is performed. The sample is then placed on the load cell, a spark igniter is placed over the sample to encourage combustion of volatiles, and data collection commences. Post test, a report is generated in graphical form with a summary sheet of material burning properties. Appendix C contains reports for polyester resin (Crystic

489PA) resin with woven roving glass fibre reinforcement at incident fluxes of 35, 50, 75 and 100kW/m^2 as examples of the information derived from the test. These polyester resin GRP samples were manufactured by the author using the materials adopted as standard within the authors research.

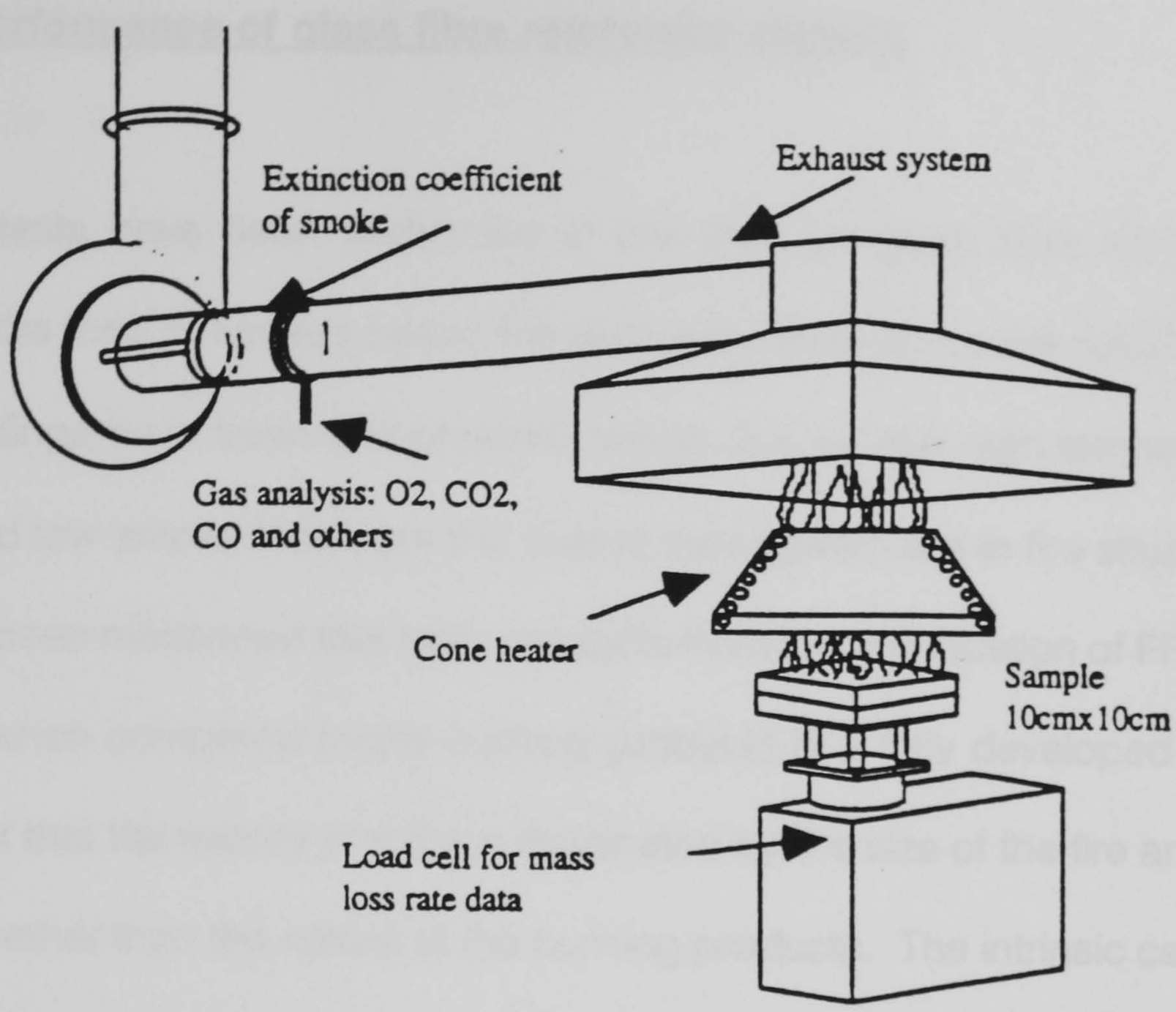

Figure 4.1.3 - Major Components of a Cone Calorimeter

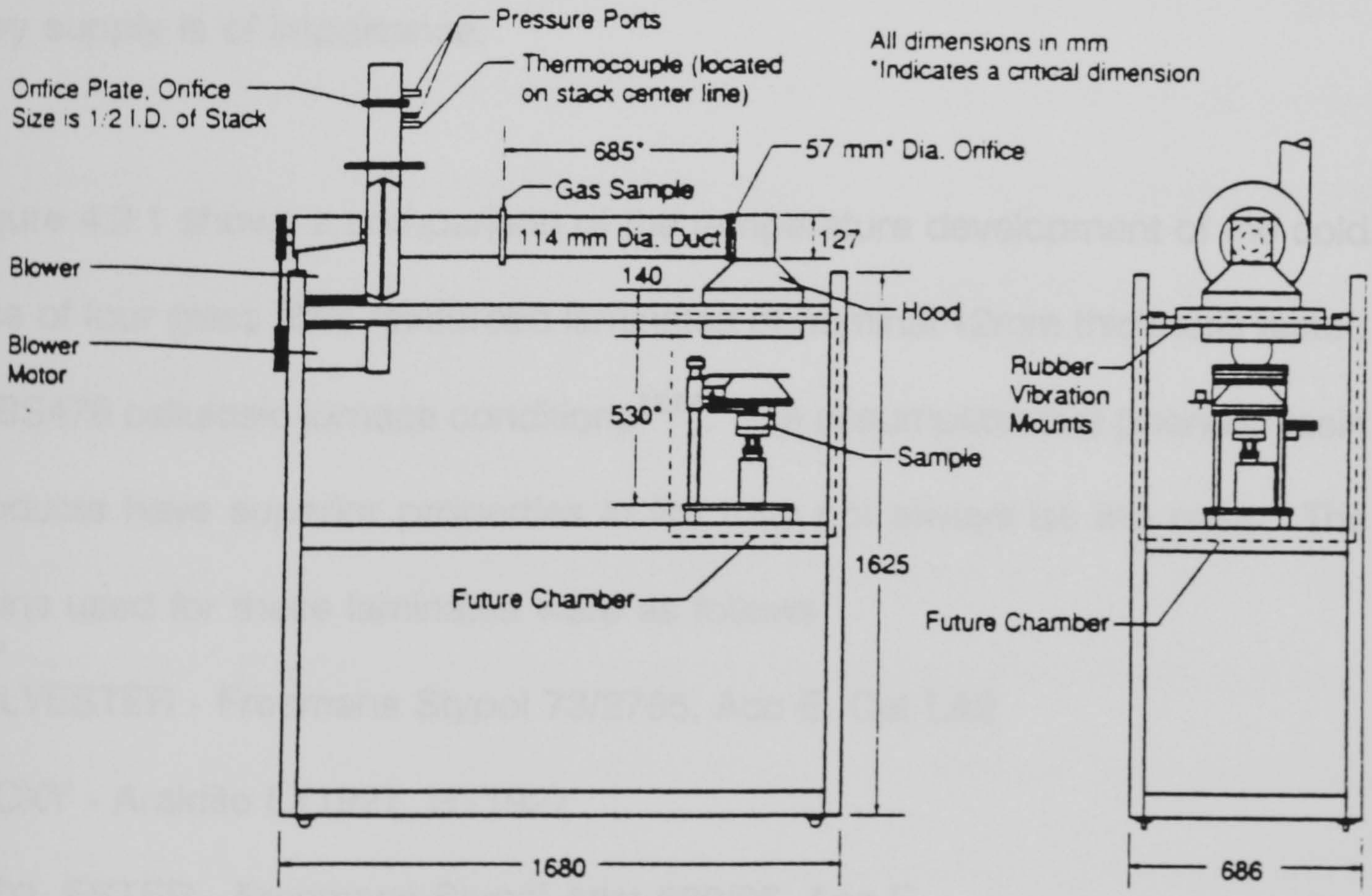

Figure 4.1.4 - Some Critical Dimensions of a Cone Calorimeter

4.2 Fire performance of glass fibre reinforced plastics

Many fire tests have been performed in the past on glass fibre reinforced plastics in the form of furnace based fire resistance tests and cone calorimetry. Typical findings have been that phenolic resins due to their high temperature stability and low smoke index are the overall best performers in fire situations. It has also been mentioned that toxic products from the combustion of FRP are negligible when compared to the burning products of a fully developed fire[12]. It is thought that the toxicity of a fire is dominated by the size of the fire and the ventilation rather than the nature of the burning products. The intrinsic carbon, hydrogen, oxygen nature of the resins gave good toxic potency test results showing that release of toxic and irritant gases was not a major issue, however, the degree to which the materials are involved in a fire, and hence the fire load they supply is of importance.

Figure 4.2.1 shows a comparison of the temperature development of the cold face of four glass fibre reinforced laminates of nominal 12mm thickness tested to BS476 cellulosic furnace conditions[12,64]. The assumption that phenolic resin products have superior properties in fire may not always be the case. The resins used for these laminates were as follows:

POLYESTER - Freemans Stypol 73/2785, Acc E, Cat LA2

EPOXY - Araldite LY1927, HY1927

VINYL ESTER - Freemans Stypol Atlat 580/05, Acc E

PHENOLIC - BP Cellobond J2018/L, Phencat 10

Table 4.1 Below summarises the insulation and integrity failure times[12] of the laminates as tested:

Resin Type	Insulation Failure Minutes	Integrity Failure Minutes
Polyester	38	182
Epoxy	25	194
Vinyl Ester	24	175
Phenolic	35	108

Table 4.1 Fire Performance of GRP Panels

It is note worthy that phenolic resin laminates have a tendency to delaminate violently in fire conditions. The degradation products (one of which is water) can get trapped in between the laminates (as the porosity decreases dramatically with temperature) and significant overpressures can be produced. The release of these overpressures tends to take the form of violent delaminations as the glass-resin layers are separated. This phenomenon is one which must be considered carefully should phenolic based FRP be selected for a fire risk area.

As can be seen from figure 4.2.1 and table 4.1, although phenolic resins have higher ignition temperatures, lower heat release during combustion, and have lower smoke emissions than other resins, they may not be the best performers with regards to heat transfer and integrity characteristics. Of the four resins tested the phenolic performed worst in terms of time to integrity failure, and

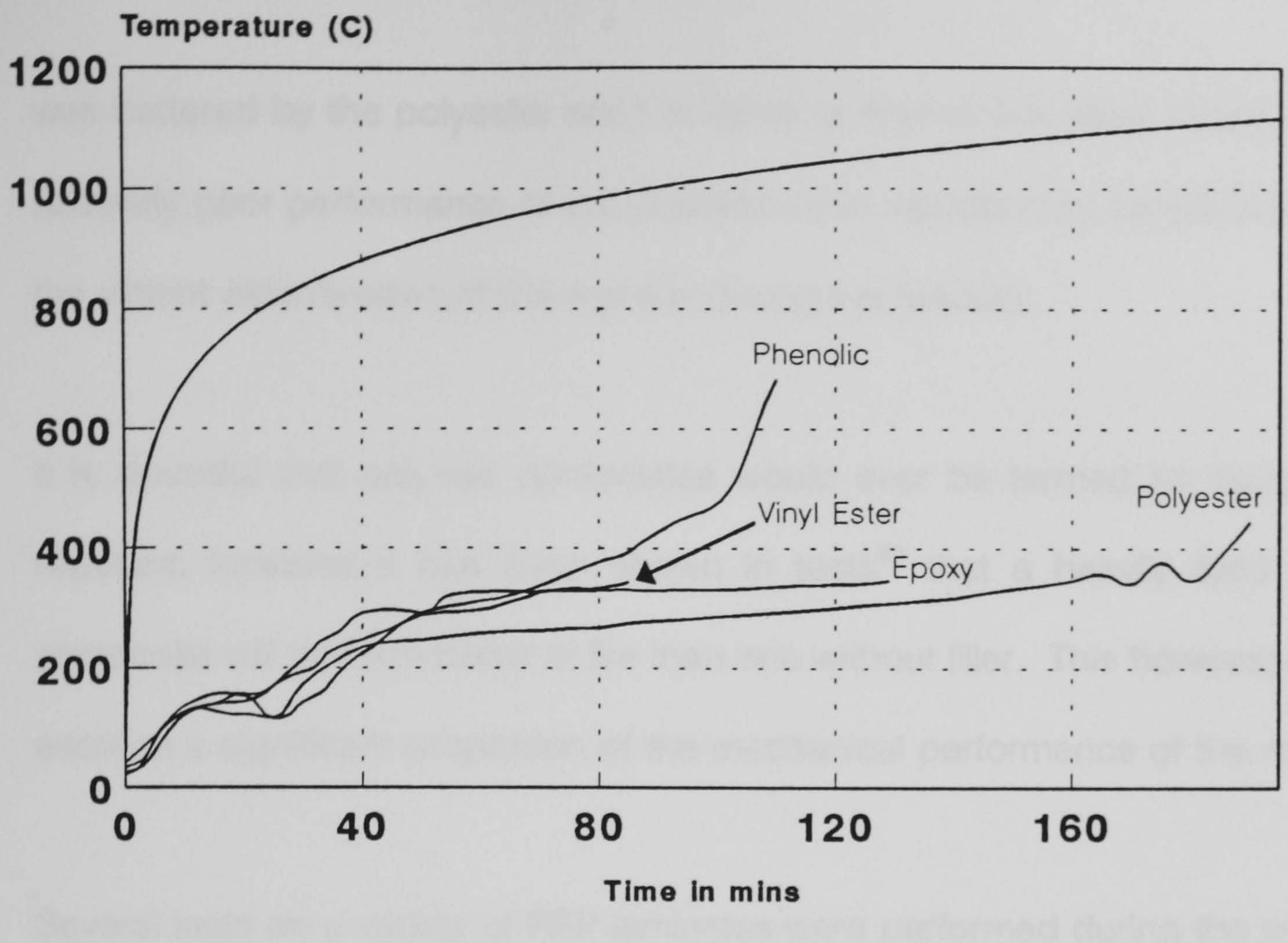

Figure 4.2.1 - Comparison of Cold Face Temperature Development of Glass Fibre Reinforced Plastics, 12mm thick Tested to BS476 pt 20 Cellulosic Conditions

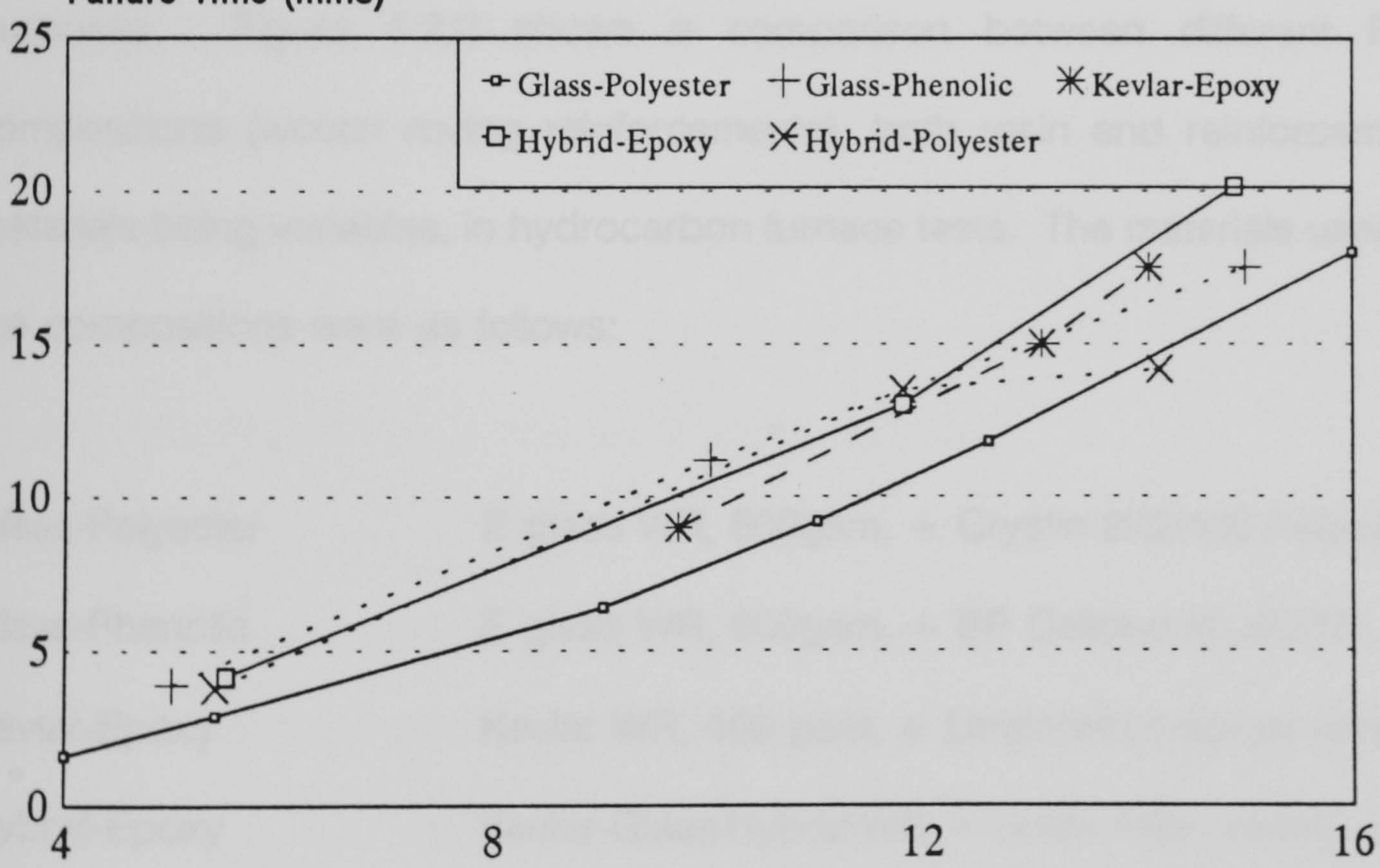

Figure 4.2.2 - Comparison of Insulation Failure Times for GRP Panels Tested to DoE Hydrocarbon Curve Woven Roving Laminates

was bettered by the polyester resin in terms of time to insulation failure. This relatively poor performance of the phenolic resin sample may be attributed to the violent delamination of the sample during the fire test.

It is doubtful that polymer composites would ever be termed as being fire resistant, however, it has been shown in tests[43] that a heavily filled resin composite will perform better in fire than one without filler. This however does sacrifice a significant proportion of the mechanical performance of the resin.

Several tests on a variety of FRP laminates were performed during the period of research. These furnace fire tests were carried out to determine the fire behaviour of the laminates, and to gather data for numerical modelling purposes. Figure 4.2.2 shows a comparison between different FRP compositions (woven roving reinforcements), both resin and reinforcement materials being variables, in hydrocarbon furnace tests. The materials used in the compositions were as follows:

Glass-Polyester	E glass WR, 600gsm, + Crystic 272/489 Polyester
Glass-Phenolic	E glass WR, 600gsm, + BP Cellobond J2027L
Kevlar-Epoxy	Kevlar WR, 460 gsm, + Unidentified epoxy resin
Hybrid-Epoxy	Kevlar-Glass Hybrid WR, + Unidentified epoxy resin
Hybrid-Polyester	Kevlar-Glass Hybrid WR, + Crystic 272/489 Polyester

As can be seen for the majority of tests the composition of the laminate has

little effect on its fire performance, with the notable exception of the polyester resin/e-glass fibre laminates. The assumptions initially made from the cellulosic fire test results that the fire performance would be superior to other resins appears to be incorrect. Comparing glass-polyester hydrocarbon fire test results with glass-phenolic results shows that in the range of thicknesses from 5mm to 15mm the phenolic laminates outperforms polyester laminates by 8 to 37 percent (in terms of insulation failure time) depending on the laminate thickness.

If this effect is compared in conjunction with results from cone calorimeter testing (see section 4.3) it can be seen that this result may be explained. The heat release rate (and hence the rate of degradation) of polyester resin is heavily influenced by the applied heat flux. Thus, at the lower incident flux levels of the cellulosic fire test the polyester resin would expected to perform significantly better than to the hydrocarbon fire test. The rate of degradation of phenolic resin laminates under fire conditions is also dependent on the incident heat flux, however, to a much lesser degree.

Thus the hydrocarbon tests on polymer reinforced composites show that polyester-glass formulations do not provide the best fire performance as suggested from cellulosic testing. Reasons for this, other than the rate of degradation of the resin, may be the char formation of the resin, and the stability of the char. Phenolic resin has been noted as producing a dense, highly stable char[8] in fire conditions, and as such this produces an insulating

layer. The char formed by polyester resin may be able to withstand the gradual increase in temperature (and lower incident heat fluxes) of a cellulosic fire test, however, it may be more easily broken down and eroded in hydrocarbon conditions than that of the more dense phenolic char. This coupled with the expected higher thermal conductivity of the phenolic resin char, the damage to the phenolic resin laminate through explosive delamination, and the rates of resin decomposition, could explain these unexpected test results.

It should not be forgotten,however,that the fibre reinforced polymer materials considered here are predominantly being investigated for their use as panel faces. Experimental work carried out investigated the effect of using the FRP as a panel face with respect to the rate of decomposition (mass loss) when compared to that which would occur when used as a laminate in its own right. The material selected for investigation was woven roving e-glass fibre with Crystic 489PA polyester resin.

Preliminary investigations into the hand laying of glass fibre reinforced polyester showed that a glass percentage by mass of over 60% could be expected. There would obviously be some variation in the actual figures however a composition of almost 68% glass by weight was found to be an average over several samples.

Preliminary studies indicated that after 45 minutes testing to hydrocarbon conditions a 6mm polyester GRP laminate would have failed or be near to

failing in integrity, the majority of the resin being lost within the first 20 minutes of the test. It was therefore decided to choose a maximum exposure of 45 minutes for mass loss investigations, with test periods of 2.5, 5, 10, 15, 30 and 45 minutes being the incremental exposure periods selected for the laminates. Due to the manner in which the testing was carried out (i.e. the sample was clamped to the face of the furnace) an unburnt perimeter of approximately 20mm remained after the exposure period where the sample had been in contact with the furnace door, and hence insulated from the hot furnace gases. On a notional panel size of 350x350mm this represented a sample area of 21.6 percent of the original, and assuming a resin content of 31 percent (this notional figure was chosen as it was the most common percentage for different specimens) it represented 6.7 percent of the total resin content of the panel. Hence for total combustion of the resin in the exposed area of the panel (including erosion of the char formed during the combustion process) a mass loss of approximately 24.3% would be expected with respect to the total mass of the original sample. Table 4.2 shows the mass loss of GRP alone and GRP with a phenolic foam backing when exposed to hydrocarbon fire conditions. In the table the results have been normalised (assuming a linear relationship between mass loss and percentage resin of the sample) for a resin content of 32%, and also for a fully exposed sample (i.e. removing the effect of the unburnt perimeter).

Exposure Time (mins)	Mass Loss % GRP Alone	Mass Loss % GRP + Phenolic Foam Backing Layer
2.5	10.1	14.2
5.0	14.7	17.4
10.0	21.2	22.7
15.0	26.4	27.9
30.0	28.4	29.3

Table 4.2 Comparison of Mass Loss Rates of Polyester-Glass GRP With and Without Phenolic Foam Backing Layer in Hydrocarbon Fire Resistance Test

As can be seen, the overall effect of an insulating backing layer is to marginally increase the initial rate of mass loss, however, after 30 minutes exposure there is little difference in mass loss as the majority of the resin has burned away. The marginal increase in decomposition rate can be attributed to the inability of the test piece to lose heat from the unexposed surface of the GRP where a backing layer is included in the test.

4.3 Cone Calorimeter Testing of GRP Laminates

For the purpose of cone calorimeter testing it was decided to predominantly investigate one GRP material only, this consisted of 12 layers of woven roving e-glass at 600gsm, and Crystic 489PA polyester resin. Polyester laminates were tested at incident fluxes of 35, 50, 75 and 100kW/m² on the cone calorimeter. It should be noted that cone calorimeter testing differs from furnace based fire resistance testing in the fact that there is excess oxygen available to the flaming surface of the sample, and also that there is no positive pressure to the hot face of the specimen. It can be seen when comparing cone calorimeter tests (appendix C) with furnace fire resistance tests that the mass loss rate during the cone calorimeter test is much higher than for the furnace test. This increased mass loss (increased rate of resin consumption) is partially due to the excess oxygen available. If considered fully, the flaming sample during a cone calorimeter test would also have a negative pressure at the sample surface, and hence the flames would encourage volatile release rather than suppress it. These factors together explain the much higher mass loss rate for cone calorimeter testing. Under an incident flux of 100kW/m² during a cone calorimeter test a polyester-glass sample reached a mass loss of 27.7% after approximately 7 minutes of testing. In a furnace based fire resistance test this same mass loss would take approximately 15 minutes (with comparable cold face conditions).

The peak heat release rate observed for any cone calorimeter test on the

material combination of e-glass fibre with Crystic 489 resin was 308kW/m² when tested at an incident flux of 100kW/m² . The average heat release rate for samples tested within the range of 35-100kW/m² ranged from 88 to 209kW/m^2. This illustrates the sensitivity of the rate of resin decomposition to the incident heat flux as discussed in section 4.2.

A useful flammability index is the Extinction Sensitivity Index (ESI)[12] which may be obtained by plotting average heat release rate against the applied flux. Interpolation back to zero gives the nominal heat release rate with no flux which is termed the ESI. A negative ESI suggests that a material will stop burning once the heat source is removed. The scatter of results (as GRP is non-homogenous) from the cone calorimeter testing of the e-glass/Crystic 489 resin made this procedure difficult to do. However, plotting a line of best fit through the results suggests that this material combination does not have a negative ESI, and this is reinforced by the experiences with the material during furnace testing. The samples when tested on the furnace continued to burn after removal from the heat source, and had to be extinguished with a carbon dioxide extinguisher. It has been shown in previous research[12] that the thickness of the samples being tested is a critical dimension with respect to the ESI and rapid extinguishment of flaming samples. It was shown in this research that when much thicker panels are used a negative ESI can be obtained for even the highly flammable resins. The recommendations were that panels of less than 10mm thickness should be avoided. The samples used in the authors cone calorimetry testing were all 6mm thick, and this could explain the

positive ESI and flaming after furnace test conclusion.

The Thermal Sensitivity Index (TSI)[12] is obtained from the same graph as the used for finding the ESI. The TSI is defined as the slope of the plotted line of average heat release rate against applied flux. A TSI of greater than one (as shown by the material tested in the authors research) implies that the heat release from the combustion flames back to the sample is more than the heat loss elsewhere. This means that thermal feedback to the specimen from its own combustion products increases the rate of burning, and implies that the material will propagate a fire when heat is applied. Again, the TSI is sensitive to physical dimensions, and may dictate a minimum panel thickness for safe use in fire situations.

Although the contribution to the fire can be considered in terms of a materials ESI and TSI it should be remembered that in a large scale fire the total heat contribution of the materials used is more important than their burning characteristics. If a "real" fire situation is considered, the nature of the fire is dependent on ventilation (and hence available oxygen), the size of the fire enclosure, and the fire source. A point of consideration is that in a fully developed offshore fire, the heat contribution of the materials used for panel faces may be insignificant when compared to the fire source (such as pool fires or jet fires).

The effective increase in the rate of thermal degradation with increasing incident

heat flux is a factor which should be carefully considered when using fibre reinforced plastics in situations where fire may be a hazard. It may be prudent in certain situations that a GRP thicknesses of no less than 10mm is used in order to reduce the likelihood of flame propagation due to the burning properties of the laminate. Within the authors research the GRP laminates used for panel faces have all been approximately 6mm thick. It has been shown in chapter 3 that, structurally, the minimum face thickness required for a sandwich panel consisting of GRP skins and a Vermiculux core is of the order of 8mm. The use of 8 or 10mm thick skins was not seen as necessary during the authors research as it was assumed that the fire resistance of the sandwich panels under test was predominantly due to the core material.

Cone calorimetry has shown that the use of thicker (>10mm) GRP skins is beneficial in terms of flammability and minimising fire propagation[12]. The use of thicker GRP skins would also be beneficial in terms of heat transfer through the sandwich panel. The increased overall thickness of the panel would obviously be advantageous with respect to heat transfer. In addition to this benefit it should be noted that the thermal degradation of the resins is generally highly endothermic. The endothermic nature of the resins, and hence the heat energy absorbed during the resin degradation process, is an important factor which limits the heat transfer through the laminates and produces a slow burning mechanism. This effect is discussed further in section 4.5.1.

4.4 Fire Testing of Core Materials

The core materials under investigation were fire tested as described in section 4.1.1. For core materials which were likely to contain free water, (i.e Voidfill, Vermiculux, and Newtherm) samples were dried prior to fire testing. The drying process consisted of oven drying at 110°C to constant mass, followed by a 24 hour period at room temperature and humidity. The drying time taken to reach constant mass was dependant on original moisture content of the material, and the type of material. The 24 hour period at room conditions allowed the fire test specimens to "relax" slightly and absorb some degree of moisture from the atmosphere. This drying process was considered to be the worst case scenario for the samples which could be expected in their use offshore.

Unless mentioned otherwise, the standard thickness of the fire test samples was 50mm for the sandwich panel core materials. The nominal face area was 300x300mm of which approximately 250x250mm was exposed to the furnace conditions.

The fire testing performed during the authors research was to either the cellulosic or hydrocarbon curve. The reason for the testing conditions fell into one of several broad categories:

1) Cellulosic fire testing of the core material alone for determination of the core materials fire performance, and also for derivation of heat transfer

coefficients for numerical modelling.

2) Hydrocarbon fire testing of the core material alone for determination of the core materials fire performance, and also for derivation of heat transfer coefficients for numerical modelling.

3) Cellulosic fire testing of steel faced sandwich panels (A60 rating required) for accommodation modules.

4) Hydrocarbon fire testing of steel faced sandwich panels (H60 rating required) for accommodation modules and processing areas.

5) Hydrocarbon fire testing of GRP faced sandwich panels (H120 rating required) for processing areas, escape routes and temporary safe refuges.

4.4.1 Fire testing of core materials - no faces

Furnace fire resistance tests were performed on core materials to both the BS476 cellulosic curve, and the DoE Hydrocarbon curve. In all cases the tests results given in this chapter were for tests performed on the Phase I furnace as described at the beginning of this chapter.

The sample sizes tested were generally 300x300mm with an area of

250x250mm exposed to the hot furnace gases. This test size was viewed as being adequate to achieve approximate one dimensional heat transfer through the thickness of the sample, and hence would be a reasonable approximation of the heat transfer which would be observed in a test performed on a much larger sample. In reality some differences in test results would be observed between the size of test performed in the authors research, and those obtained in a full scale fire test (exposed area of 3.0x3.0m). One influencing factor would be the heat lost from the sample to the surrounding ambient, room temperature, laboratory atmosphere from the edges of the sample under test. This effect was minimised in the phase II furnace setup by mounting the samples within a highly insulating door, rather than clamping them to the front of the furnace. Other factors which would effect test results are discussed and investigated in chapter 6.

As Vermiculux was seen to be the state-of-the-art material available for fire situations it was decided to adopt this material as a reference point for all material developments. It should be noted that the formulation of Vermiculux was changed by Cape Boards Ltd. during the authors research. The first formulation will be referred to as Vermiculux I, and the new formulation as Vermiculux II. Figure 4.4.1 shows the test results for a cellulosic fire test on a Vermiculux I, and figure 4.4.2 the test results for a hydrocarbon fire test on the same material. In both cases the material under test had been dried to constant mass at 110°C followed by a period of 24 hours at ambient laboratory conditions prior to testing. From figure 4.4.1 it can be seen that Vermiculux I

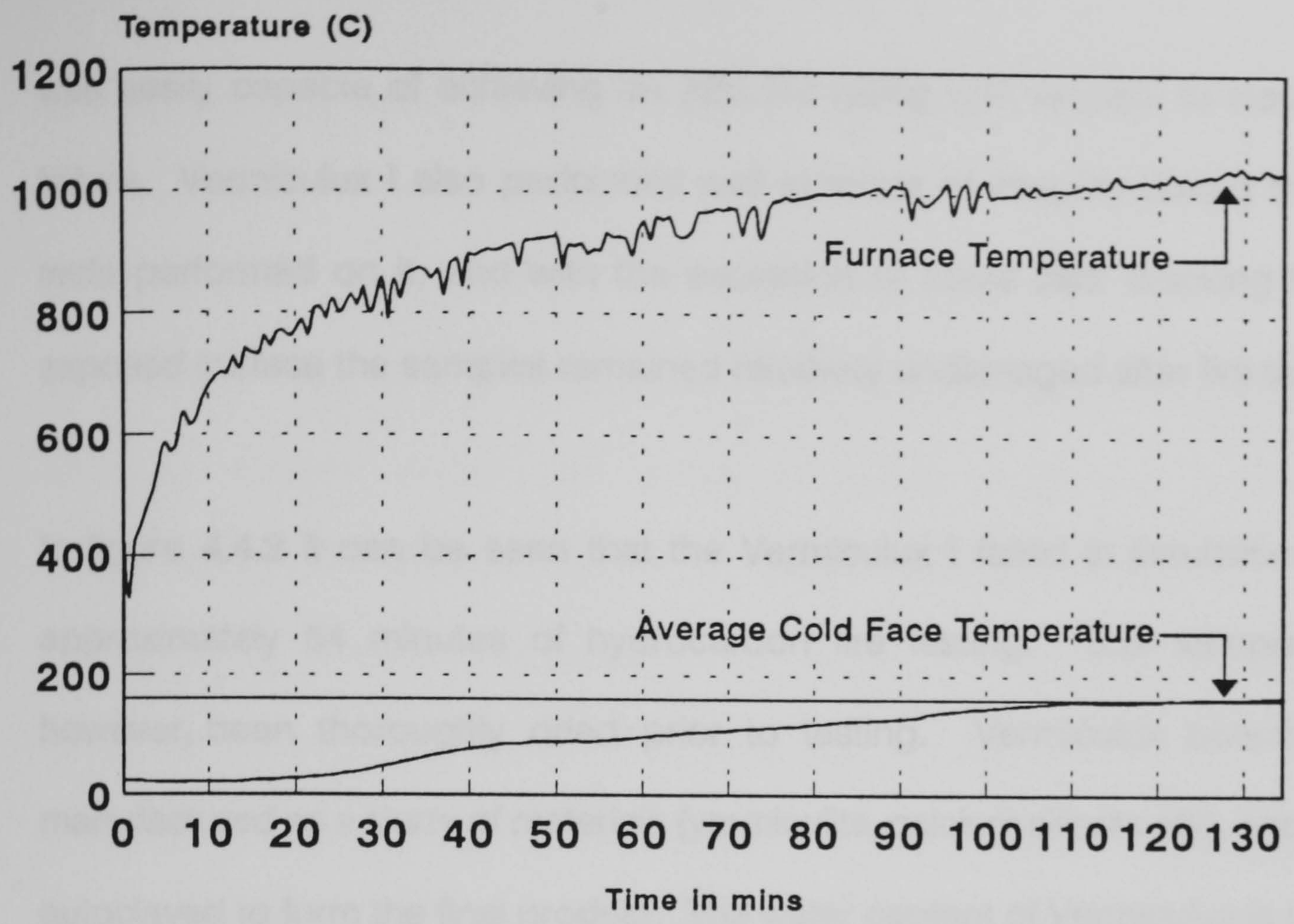

Figure 4.4.1 - BS476 Cellulosic Fire Test
Core Material - Vermiculux I 50mm thick
No hot or cold faces, sample dried prior to test

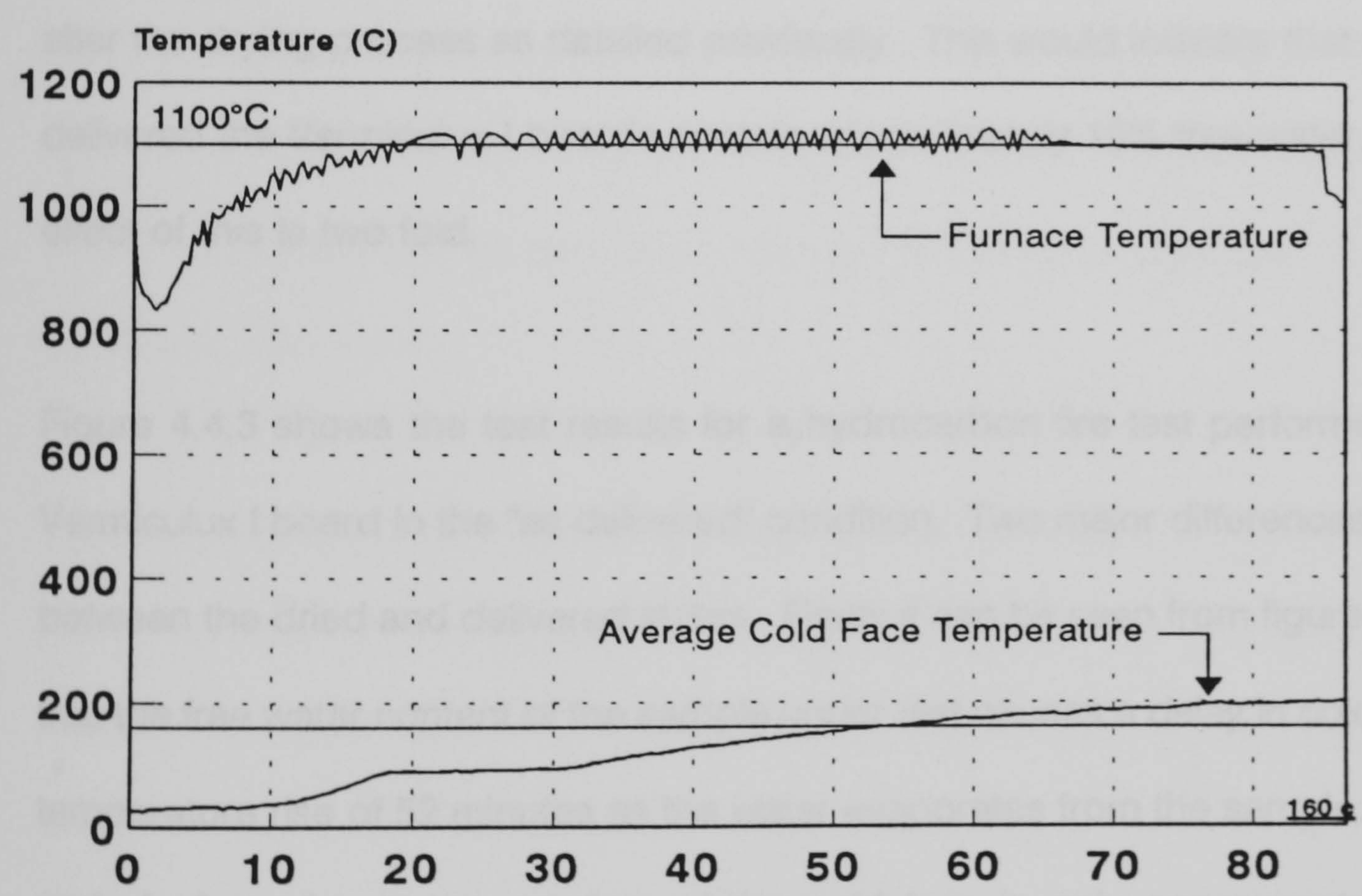

Figure 4.4.2 - DoE Hydrocarbon Fire Test
Core Material - Vermiculux I 50mm thick
No hot or cold face, sample dried prior to test

was easily capable of achieving an A60 fire rating with respect to insulation failure. Vermiculux I also performed well in terms of integrity during the fire tests performed on it, and with the exception of some faint cracking in the exposed surface the samples remained relatively undamaged after fire testing.

In figure 4.4.2 it can be seen that the Vermiculux I failed in insulation after approximately 54 minutes of hydrocarbon fire testing. This sample had, however, been thoroughly dried prior to testing. Vermiculux boards are manufactured as a slurry of materials (vermiculite, calcium silicate etc), and then autoclaved to form the final product. The water content of Vermiculux is rather substantial in its "as delivered" state. In this comparison a 300x300x50mm thick sample of Vermiculux I weighed 2319g in the as delivered state and only 2081g after the drying process as detailed previously. This would indicate that when delivered the Vermiculux I boards contain approximately 10% free water. The effect of this is two fold.

Figure 4.4.3 shows the test results for a hydrocarbon fire test performed on Vermiculux I board in the "as delivered" condition. Two major differences exist between the dried and delivered states. Firstly it can be seen from figure 4.4.3 that the free water content of the sample under test causes a delay in cold face temperature rise of 52 minutes as the water evaporates from the sample. This period of no rise in temperature of the cold face is only approximately 12 minutes for the dried sample in figure 4.4.2. The 12 minute period for the dried sample may represent the evaporation of water within the sample, however, it

is likely that this water will be chemically combined rather than free within sample.

The second effect of a high moisture content of the core is not as readily detected, however if the initial period of testing of the two samples is considered it can be seen that for the dried Vermiculux I sample it takes approximately 17 minutes of testing for the cold face temperature to reach the "dwell" at approximately 100°C. The test on the wet (as delivered) Vermiculux shows that the same cold face temperature is reached after only 13 minutes of testing. This increase in heat transfer to the cold face is due to the moisture content, as water has a high thermal conductivity when compared to the Vermiculux I board. However, the overall effect of a high moisture content is obviously beneficial with respect to insulation failure time. In the case of Vermiculux I a 10% free water content effectively increases the insulation failure time, when exposed to the simulated hydrocarbon fire resistance test, from 54 minutes to 86 minutes.

Voidfill was described in section 3.4. Figures 4.4.4 and 4.4.5 show the fire test results for Voidfill 7D in the dried condition tested to cellulosic and hydrocarbon conditions respectively. From these tests it can be seen that in cellulosic conditions the insulation failure time was approximately 140 minutes, and in hydrocarbon conditions approximately 80 minutes. These failure times compare well with those for Vermiculux I. Hence, the Voidfill 7D mix was considered to be a viable alternative to Vermiculux I.

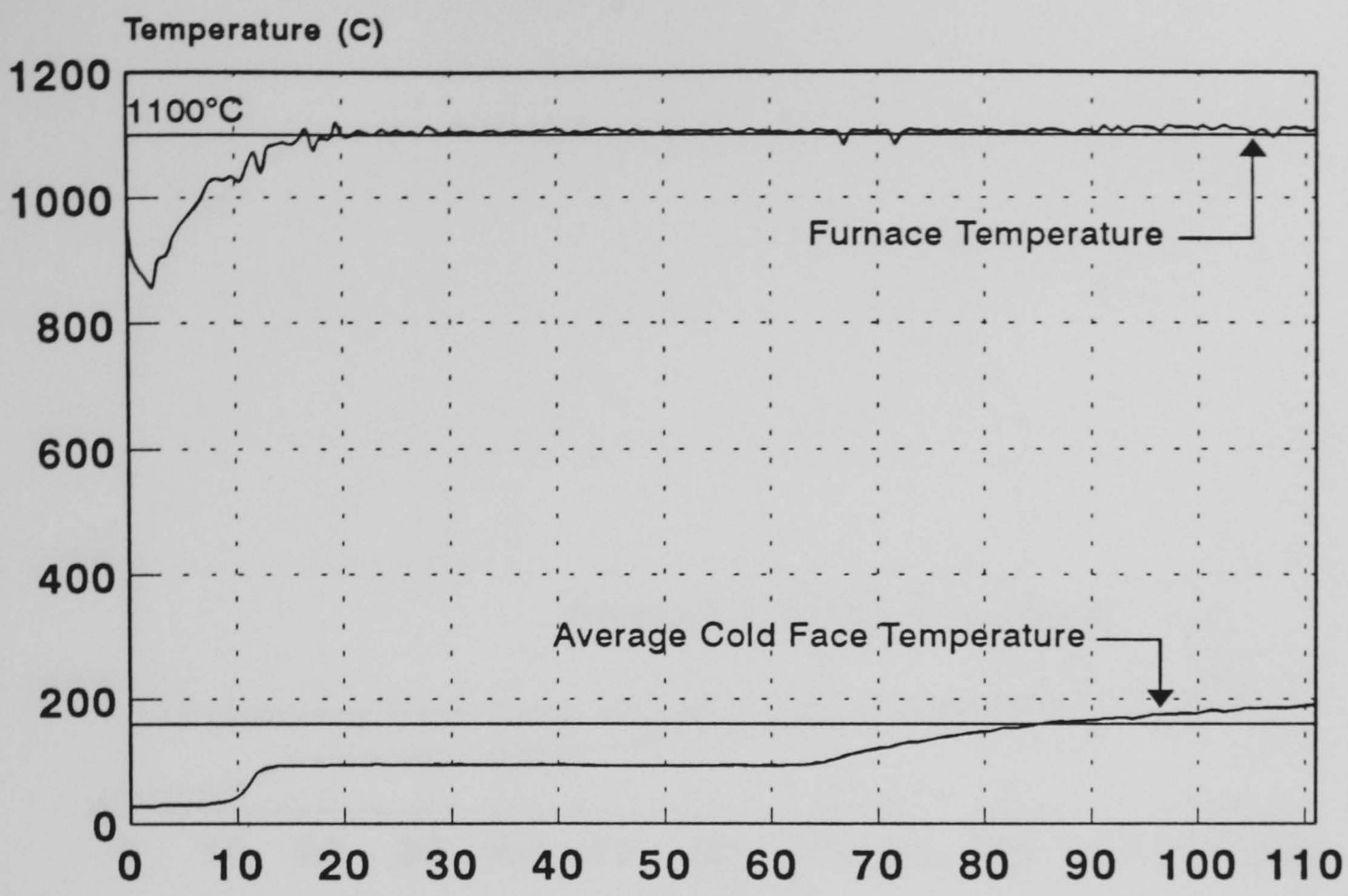

Figure 4.4.3 - DoE Hydrocarbon Fire Test
Core Material - Vermiculux I 50mm thick
No hot or cold faces, tested in "as delivered" condition

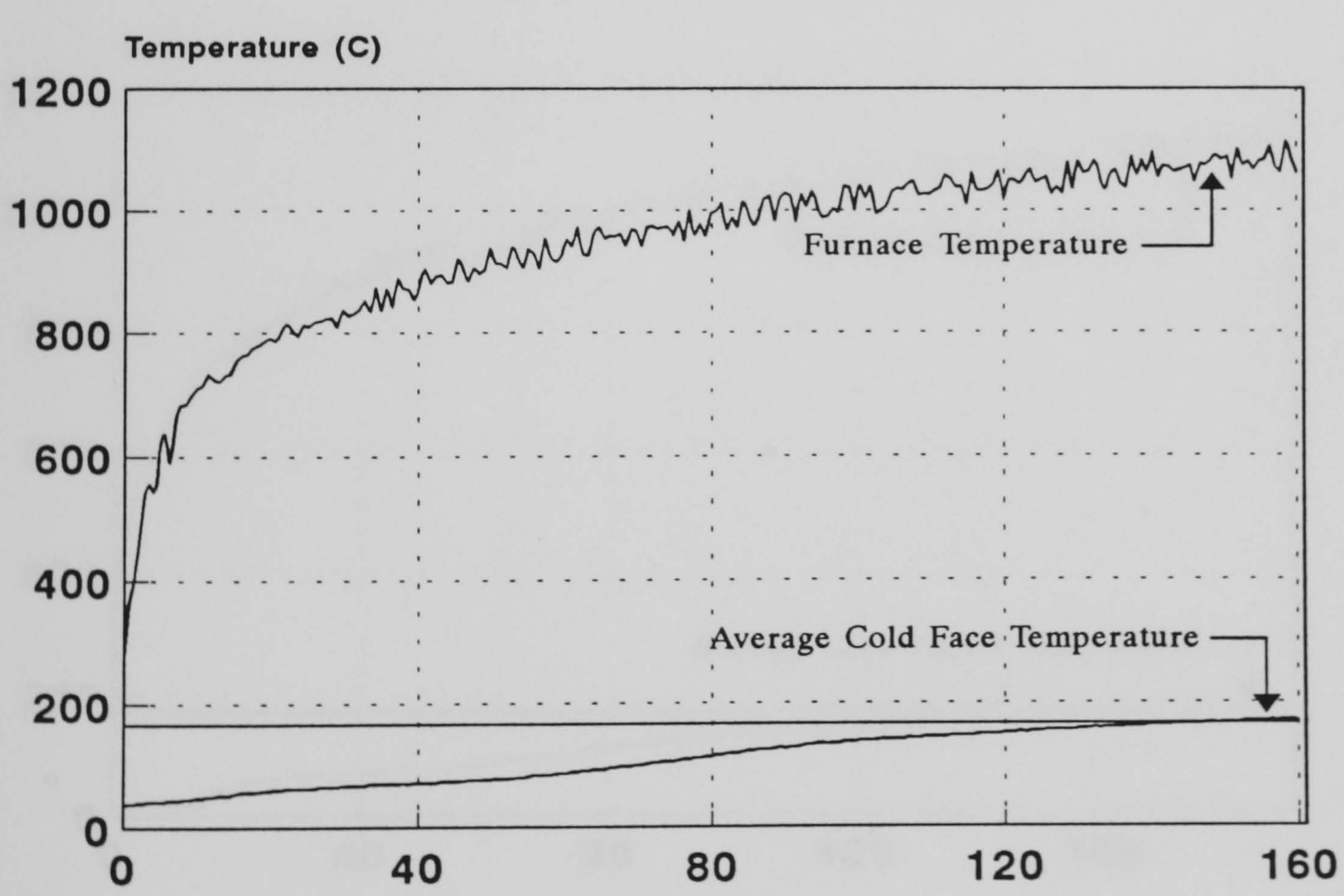

Figure 4.4.4 - BS476 Cellulosic Furnace Test
Core Material - Voidfill 7D
No hot or cold faces

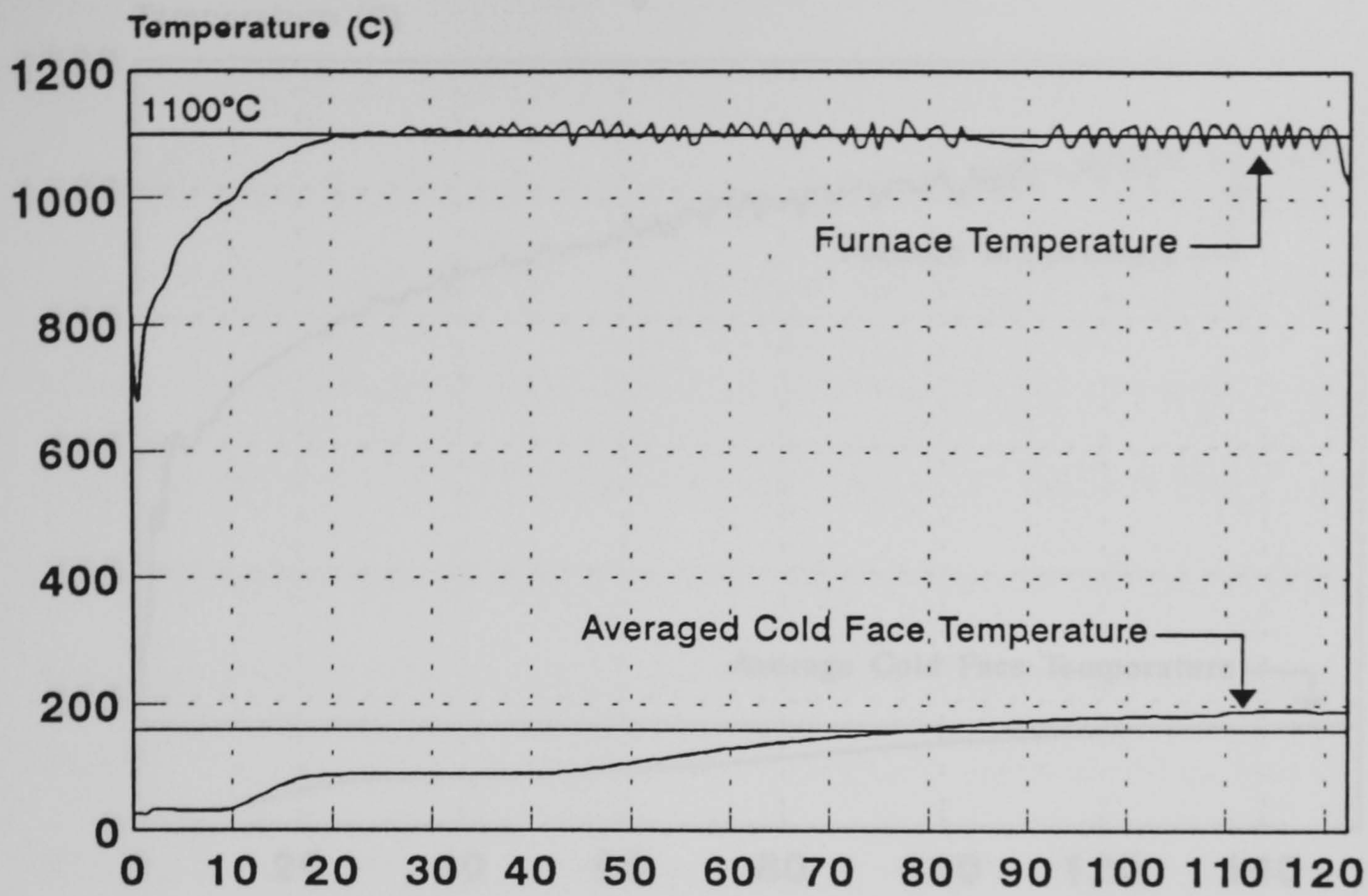

Figure 4.4.5 - DoE Hydrocarbon Fire Test
Core Material - Voidfill 7D 50mm thick
No hot or cold faces

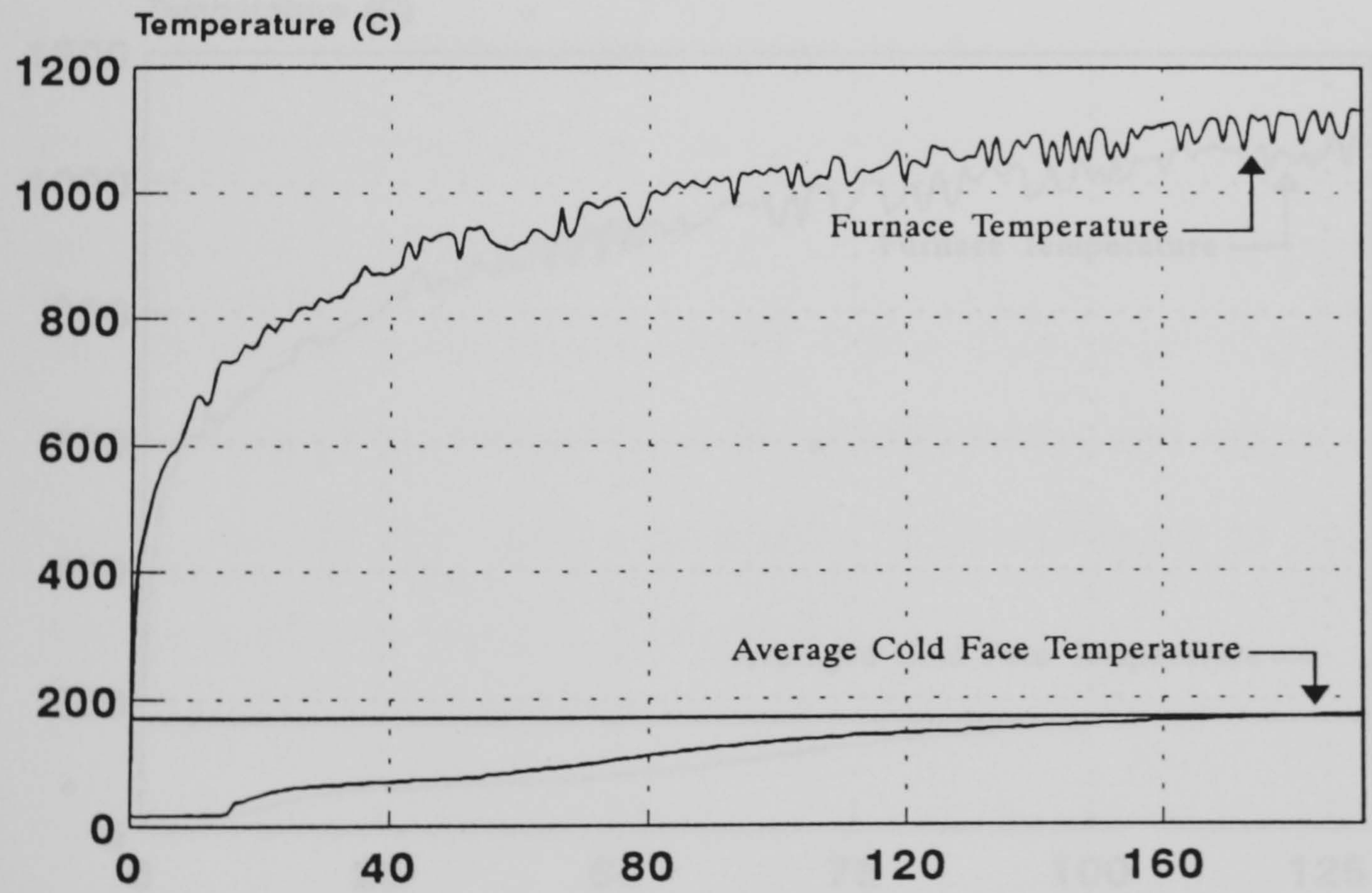

Figure 4.4.6 - BS476 Cellulosic Fire Test
Core Material Vodfill 7D-51
No Hot and Cold Faces

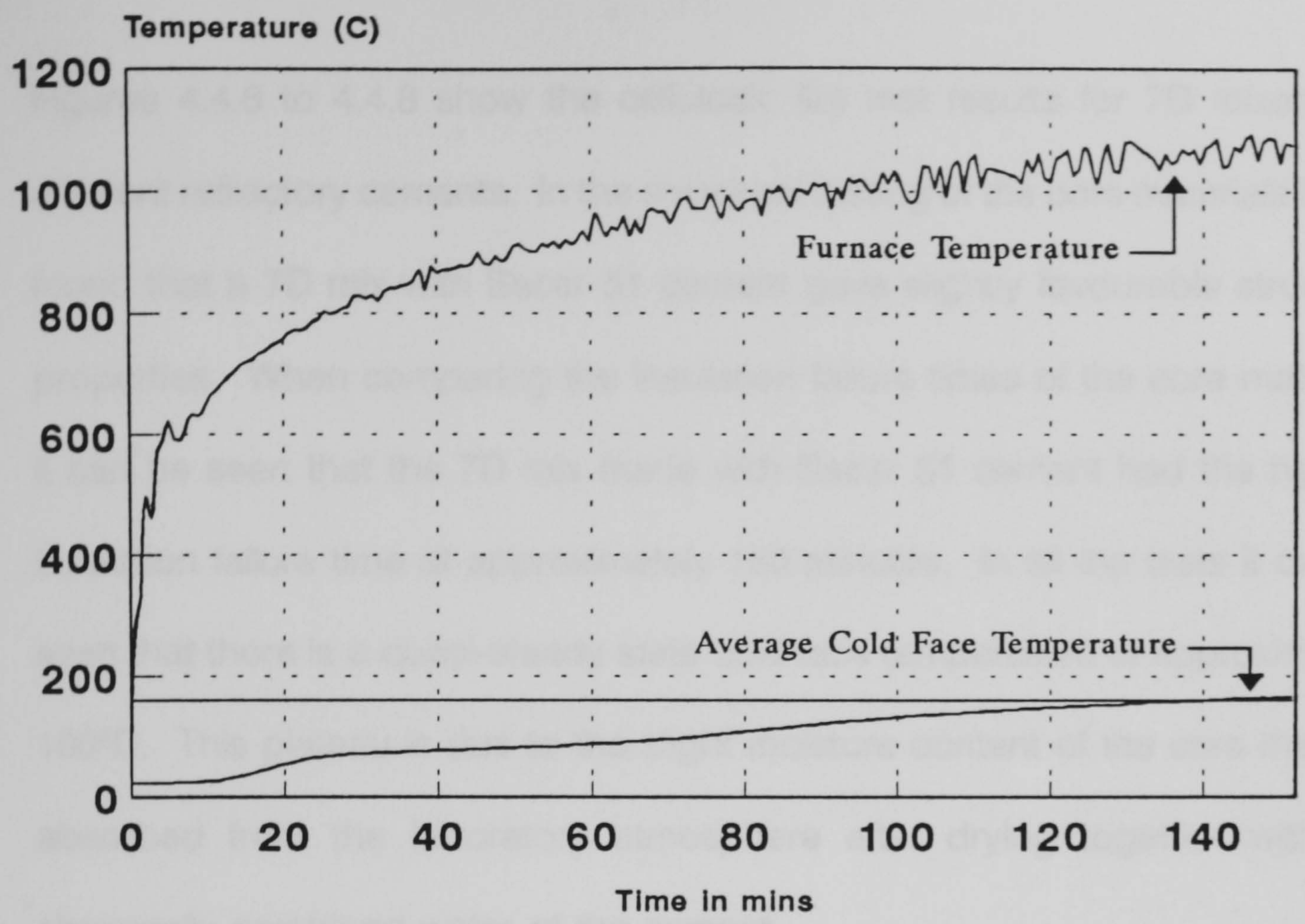

Figure 4.4.7 - BS476 Cellulosic Fire Test
Core Material - Voidfill 7D-71
No Hot or Cold Faces

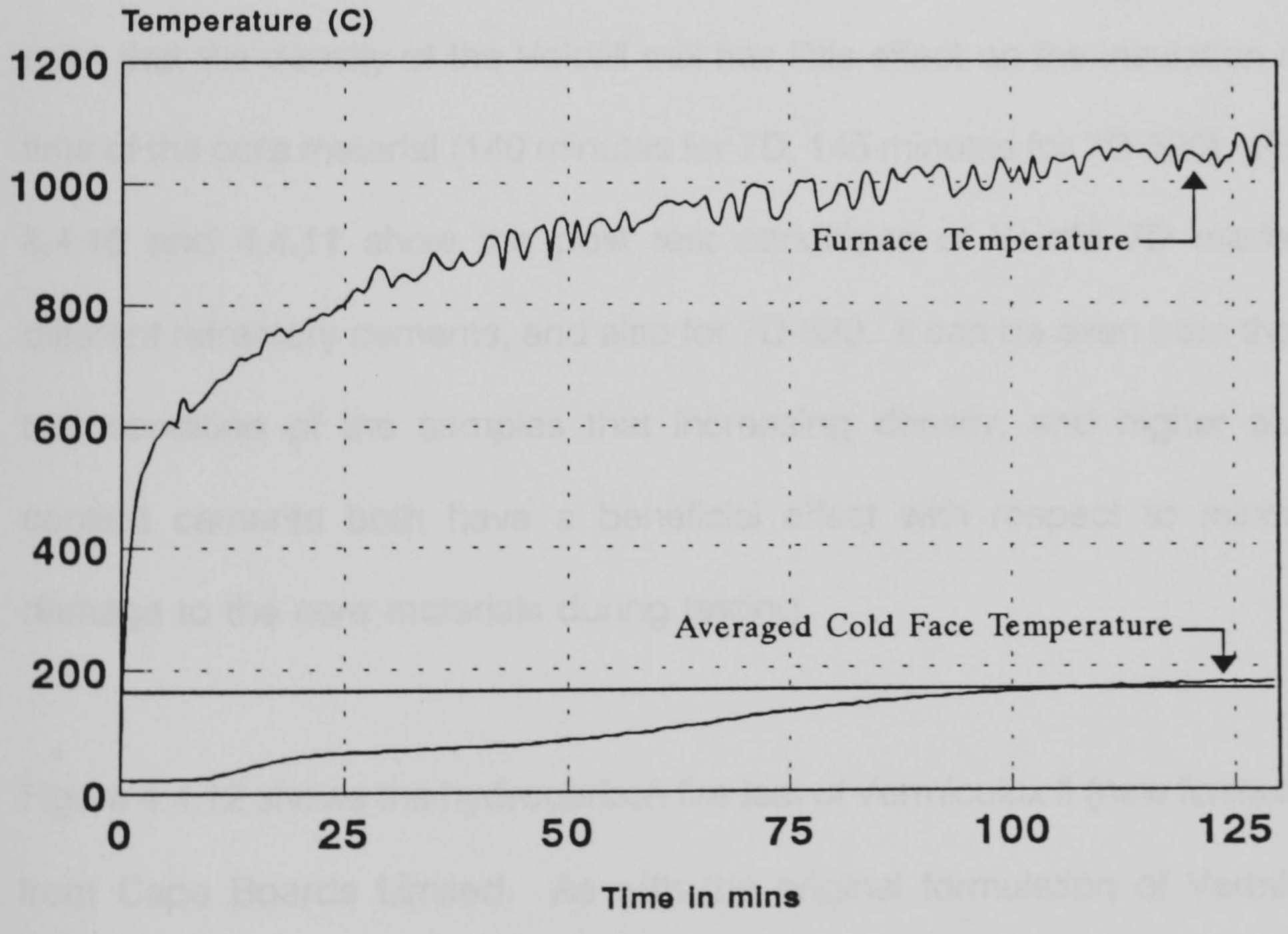

Figure 4.4.8 - BS476 Cellulosic Fire Test
Core Material - Voidfill 7D-80
No Hot or Cold Faces

Figures 4.4.6 to 4.4.8 show the cellulosic fire test results for 7D mixes with different refractory cements. In the structural testing of the core materials it was found that a 7D mix with Secar 51 cement gave slightly favourable structural properties. When comparing the insulation failure times of the core materials it can be seen that the 7D mix made with Secar 51 cement had the highest insulation failure time at approximately 180 minutes. In all the tests it can be seen that there is a quasi-steady state cold face temperature of approximately 100°C. This plateau is due to the slight moisture content of the core material absorbed from the laboratory atmosphere after drying together with the chemically combined water of the cement.

Figure 4.4.9 shows the cellulosic fire test of Voidfill mix 7D-520. Here it can be seen that the density of the Voidfill mix has little effect on the insulation failure time of the core material (140 minutes for 7D, 145 minutes for 7D-520). Figures 4.4.10 and 4.4.11 show the post test conditions of Voidfill 7D made with different refractory cements, and also for 7D-520. It can be seen from the post test condition of the samples that increasing density, and higher alumina content cements both have a beneficial effect with respect to minimising damage to the core materials during testing.

Figure 4.4.12 shows the hydrocarbon fire test of Vermiculux II (new formulation) from Cape Boards Limited. As with the original formulation of Vermiculux, Vermiculux II had a substantial free water content in the "as delivered" state. Samples were dried carefully to constant mass prior to fire testing.

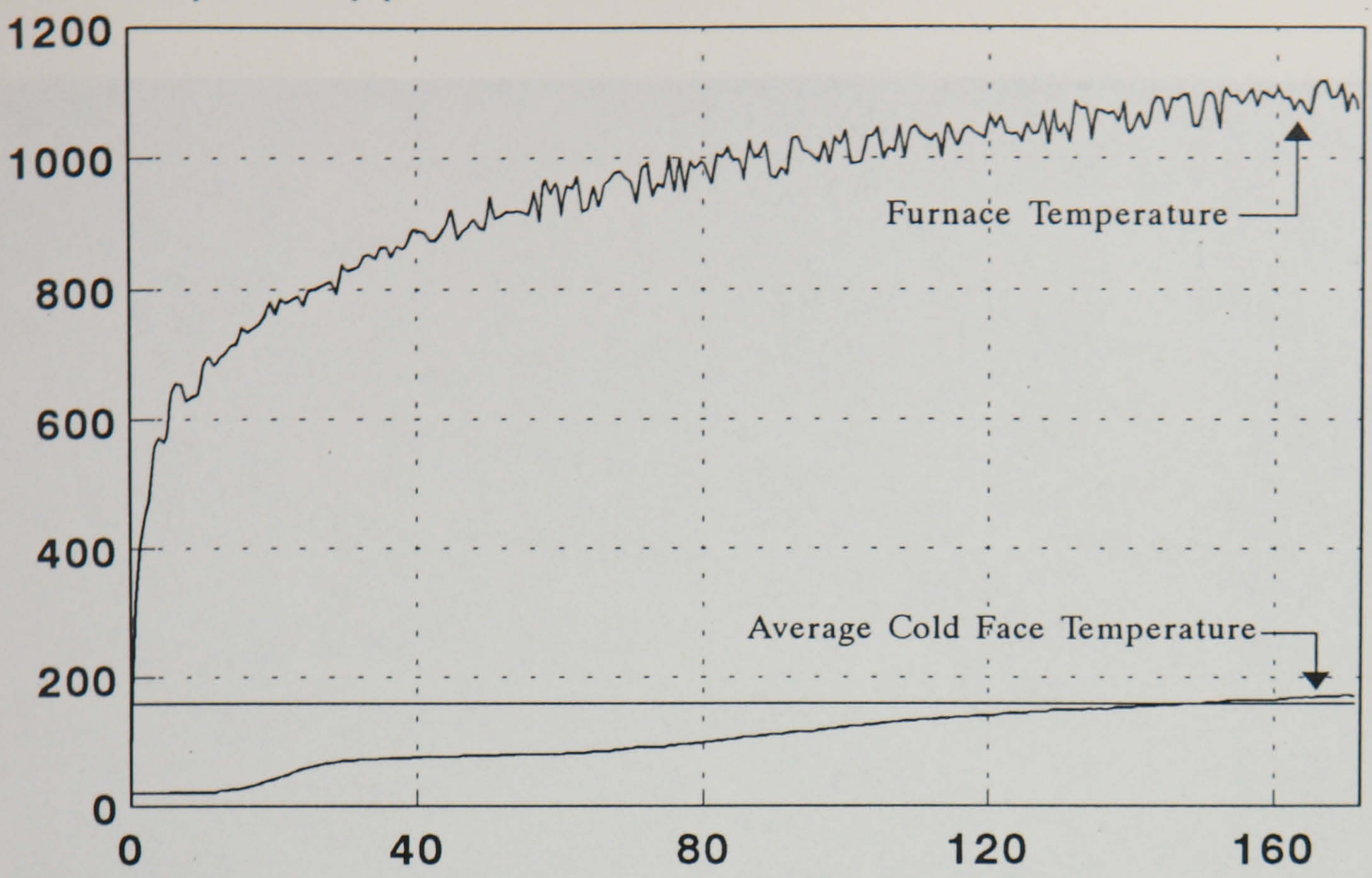

Figure 4.4.9 - BS476 Cellulosic Fire Test
Core Material - Voidfill 7D-520
No hot or cold faces

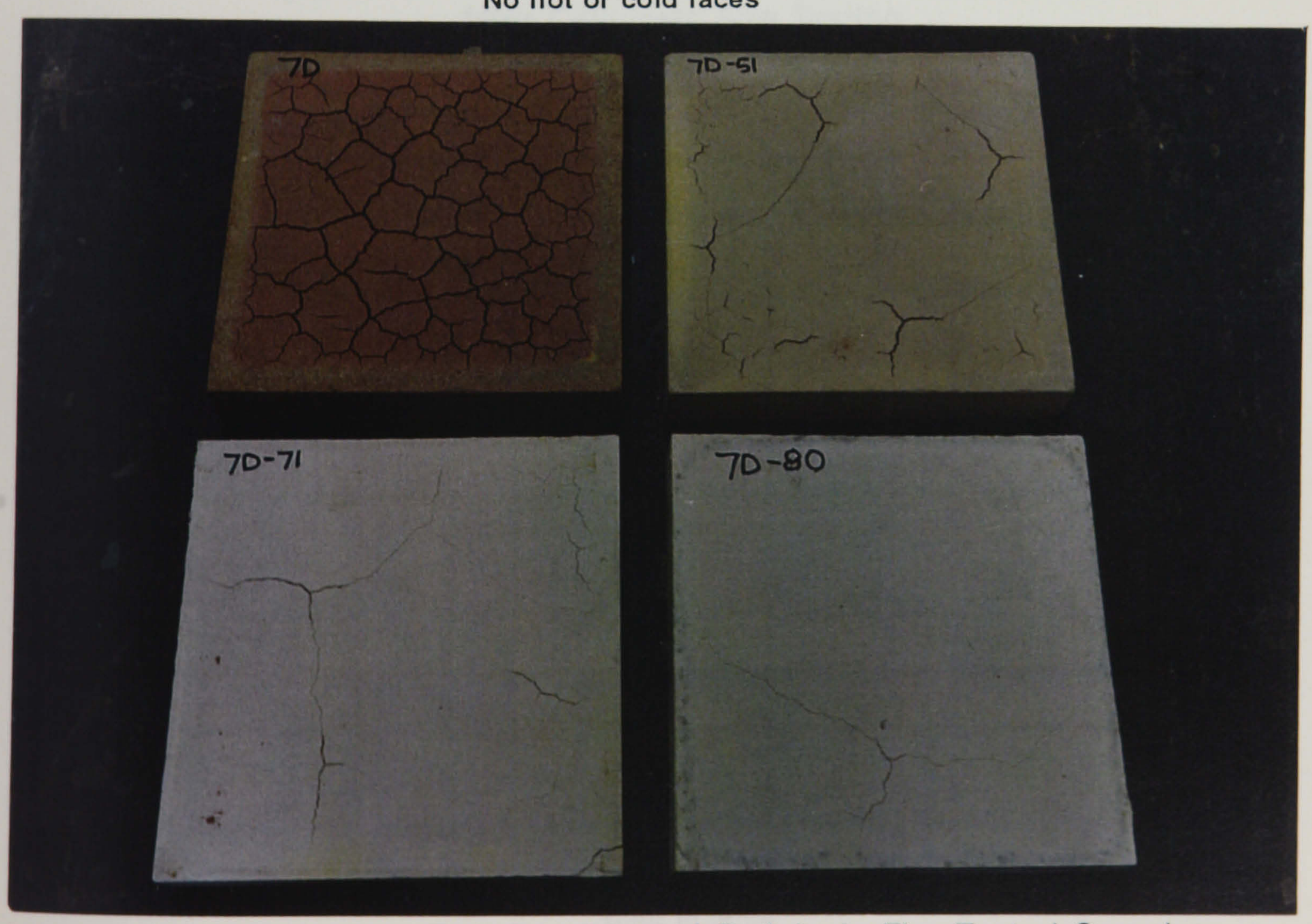

Figure 4.4.10 - Post Test Condition of Cellulosic Fire Tested Samples of Voidfill 7D made with Different Refractory Cements

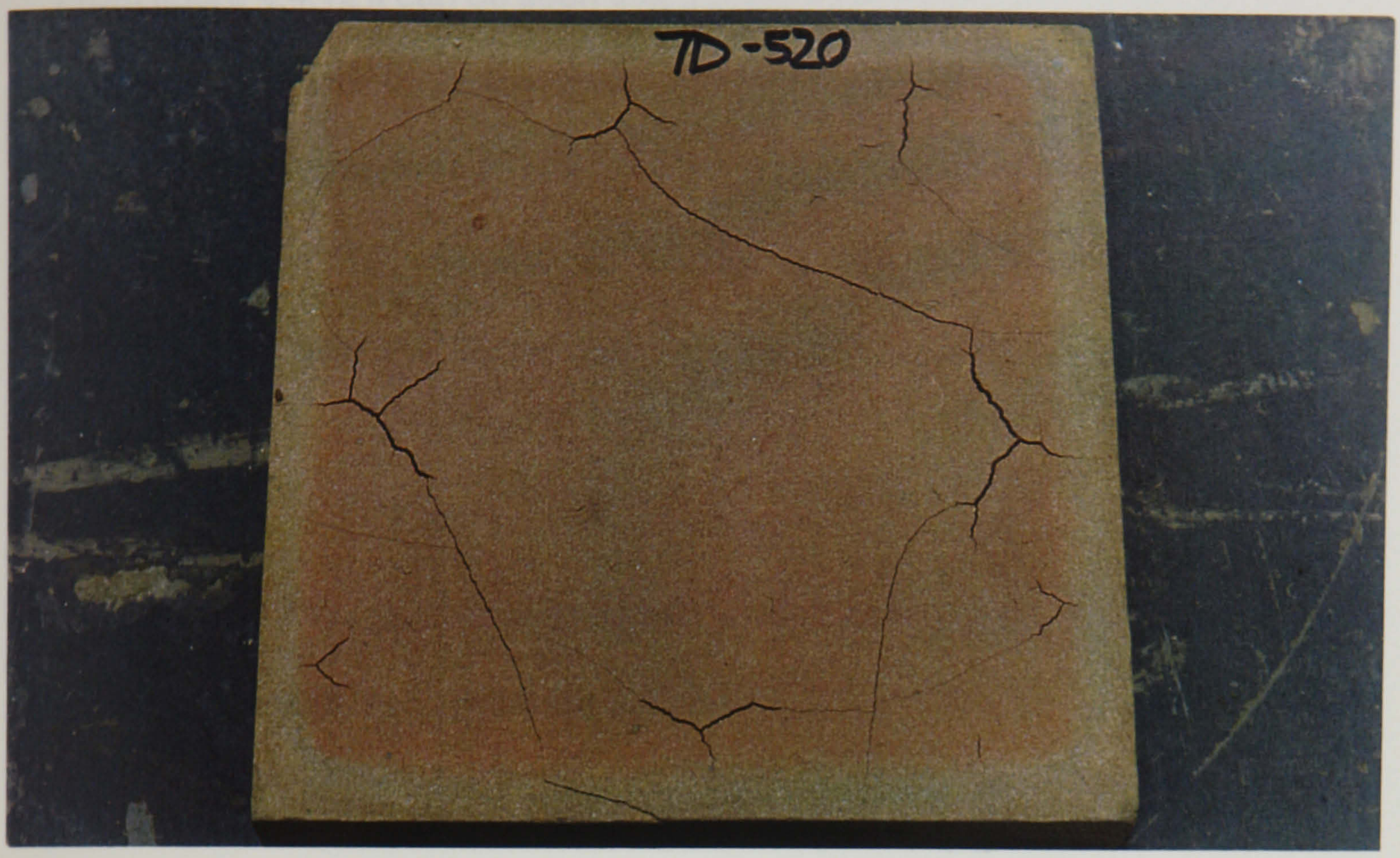

Figure 4.4.11 - Post Test Condition of Voidfill 7D-520
After Cellulosic Fire Testing

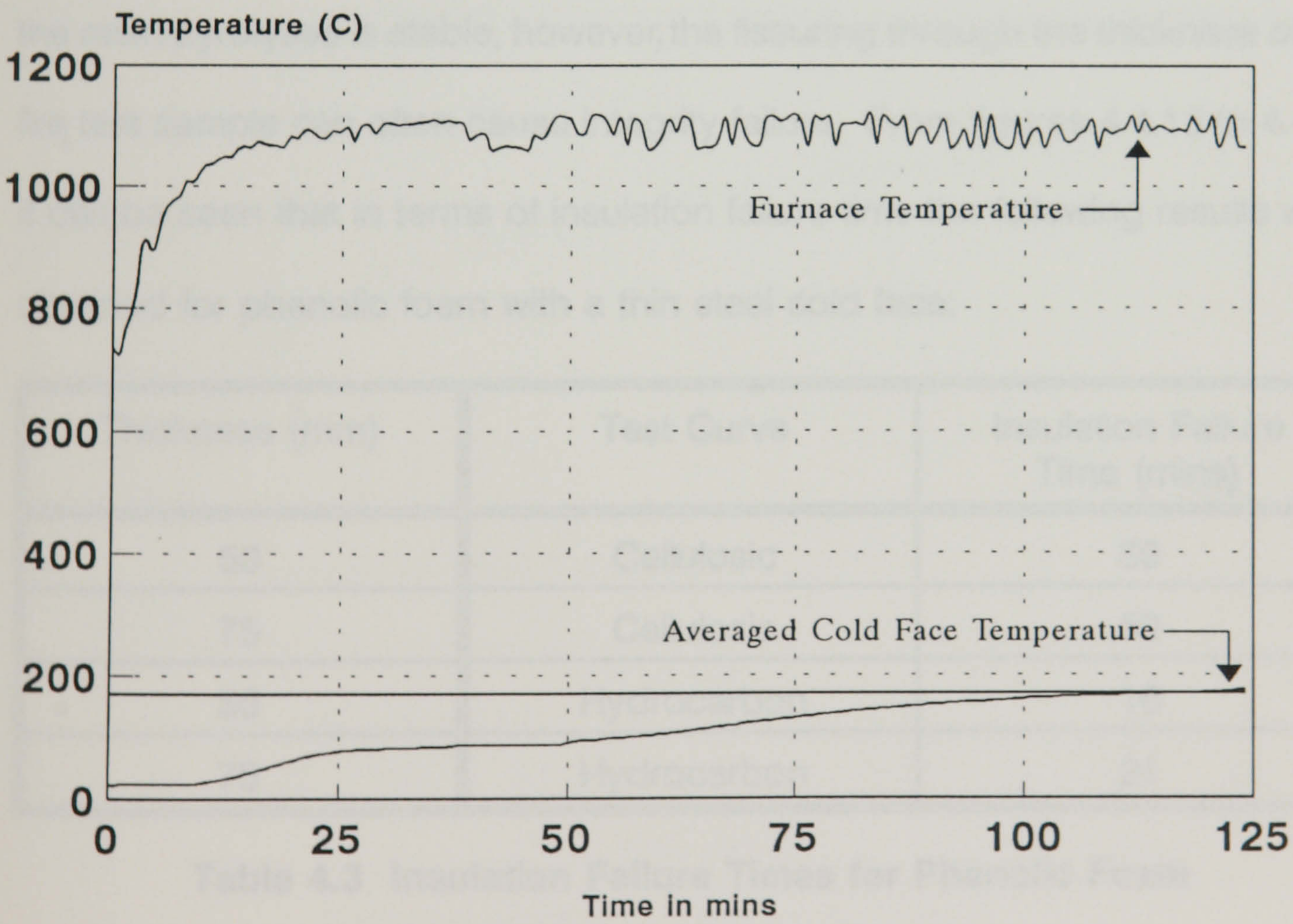

Figure 4.4.12 - DoE Hydrocarbon Fire Test
Core Material - 60mm Vermiculux II
No Hot or Cold Faces

From figure 4.4.12 it can be seen that the increased thickness of the Vermiculux II and its' new formulation gives excellent performance in the simulated hydrocarbon fire resistance test. The sample under test failed in insulation after approximately 115 minutes of testing in the dried condition, a great improvement over the Vermiculux I at 50mm thick which failed after only 54 minutes.

Figures 4.4.13 to 4.4.16 show the cellulosic and hydrocarbon fire test results for phenolic foam (from Permali Ltd, Gloucester). The tests performed included a thin (1.0mm) steel cold face in order to obtain an average cold face temperature. Phenolic foam samples fissure during fire testing due to the high shrinkage of phenolic resin at temperatures above 600°C. The char formed as the resin pyrolyses is stable, however, the fissuring through the thickness of the fire test sample can often cause integrity failure. From figures 4.4.13 to 4.4.16 it can be seen that in terms of insulation failure time the following results were obtained for phenolic foam with a thin steel cold face:

Thickness (mm)	Test Curve	Insulation Failure Time (mins)
50	Cellulosic	39
75	Cellulosic	50
50	Hydrocarbon	16
75	Hydrocarbon	21

Table 4.3 Insulation Failure Times for Phenolic Foam

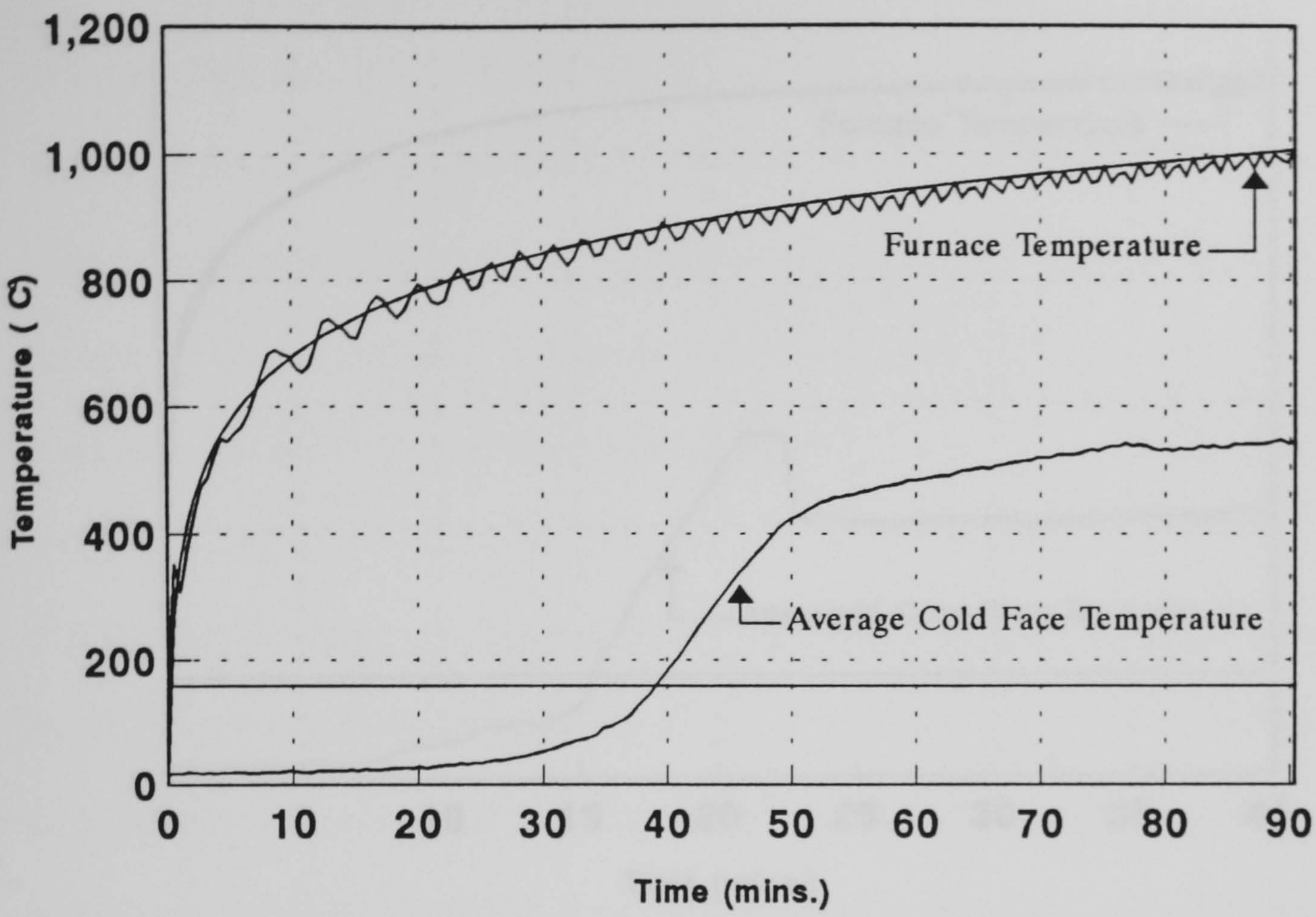

Figure 4.4.13 - BS476 Cellulosic Fire Test
Core Material - Phenolic Foam 50mm thick
No hot face, steel cold face

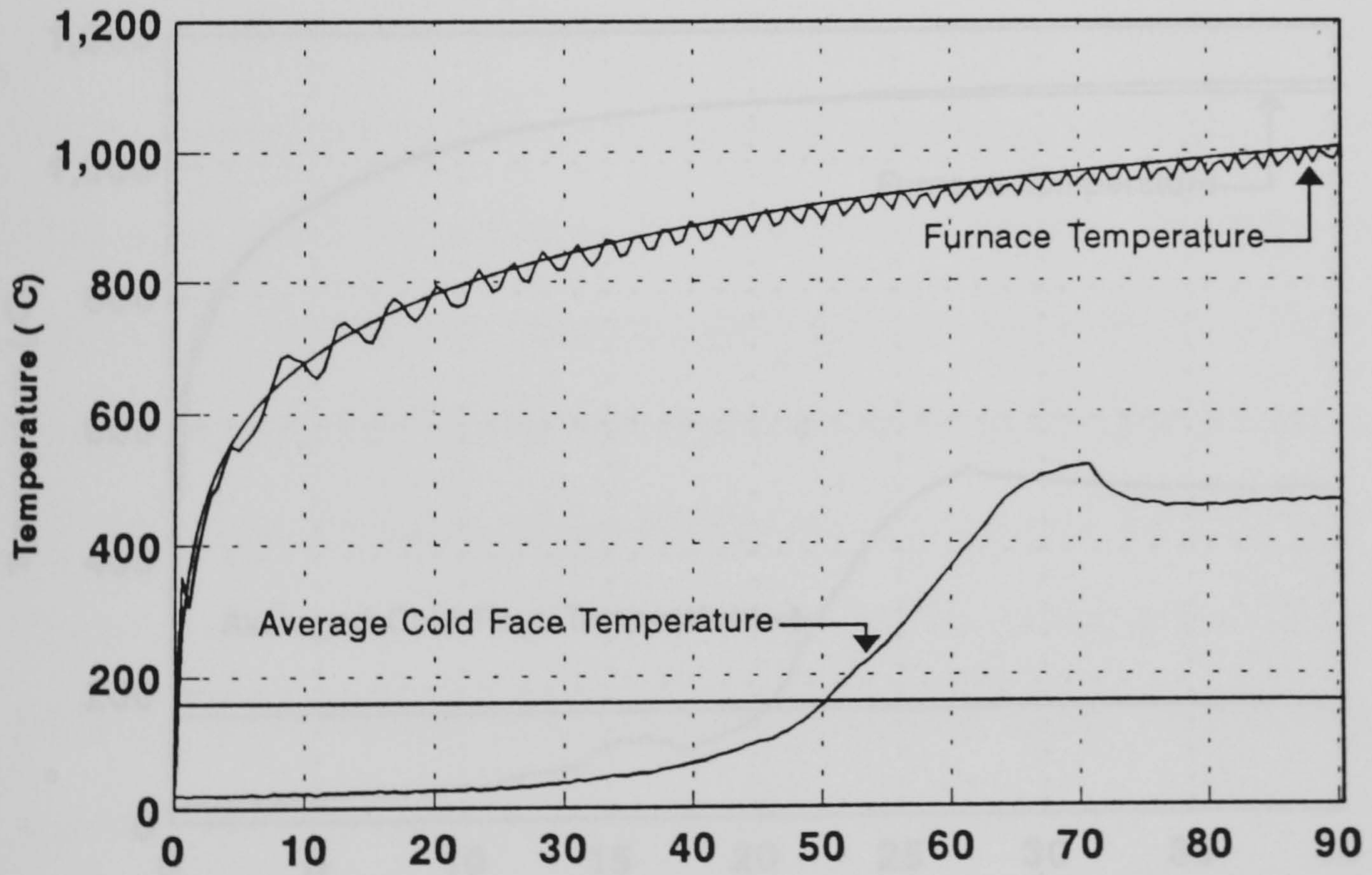

Figure 4.4.14 - BS476 Cellulosic Fire Test
Core Material - Phenolic Foam 75mm Thick
No hot face, steel cold face

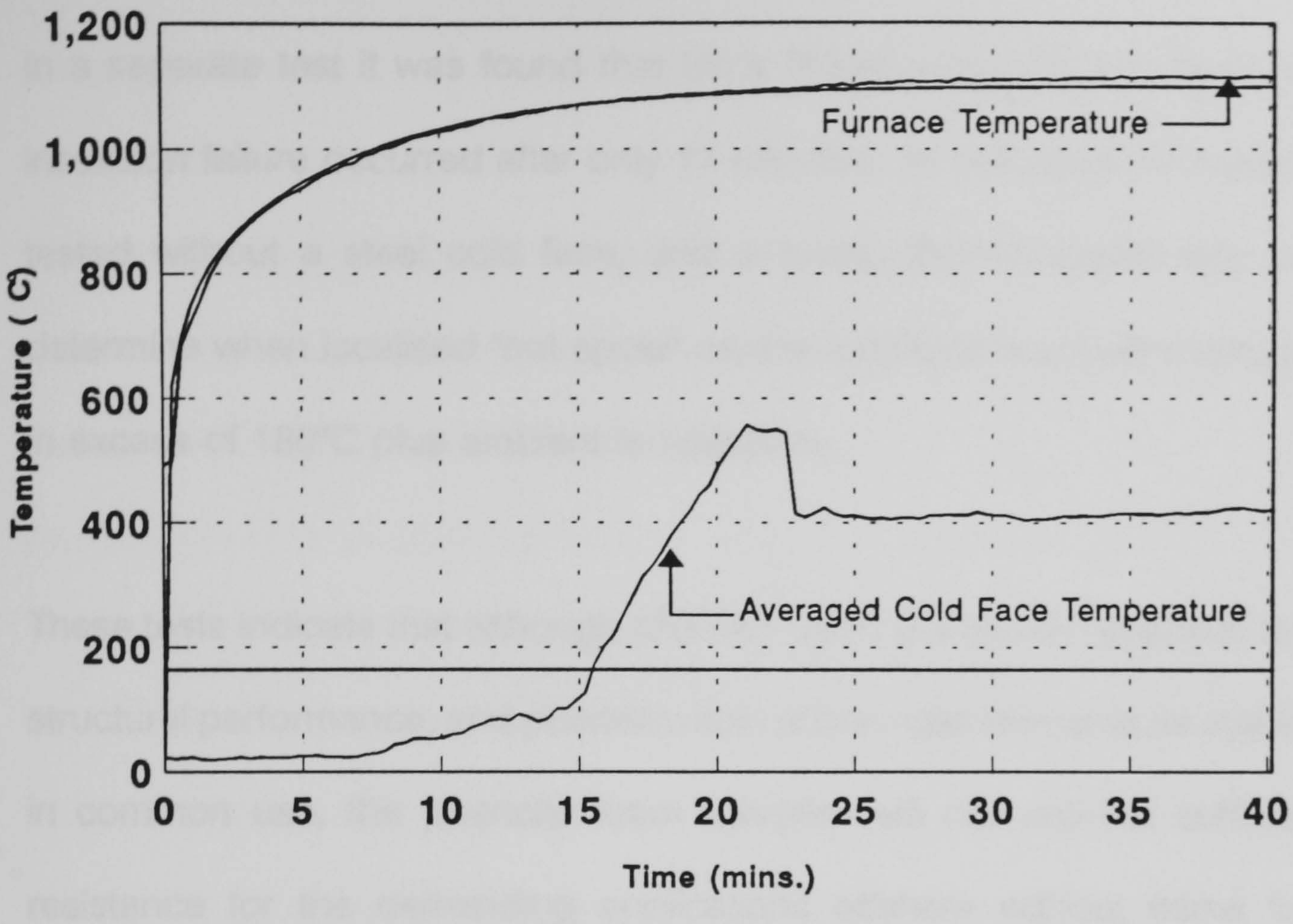

Figure 4.4.15 - DoE Hydrocarbon Fire Test
Core Material - Phenolic Foam 50mm thick
No hot face, steel cold face

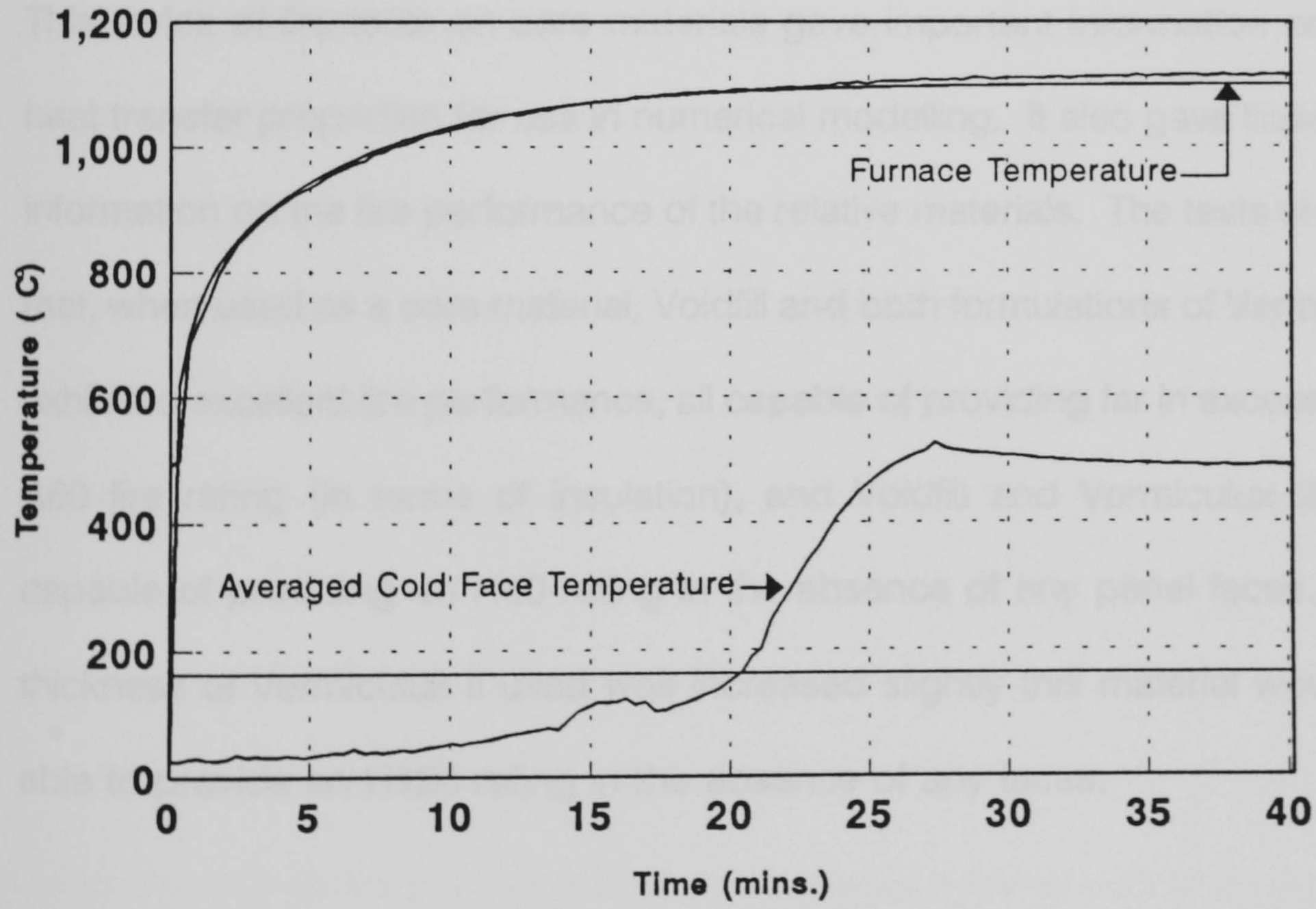

Figure 4.4.16 - DoE Hydrocarbon Fire Test
Core Material - Phenolic Foam 75mm thick
No hot face, steel cold face

In a separate test it was found that for a 75mm thick phenolic foam sample insulation failure occurred after only 17 minutes. In this case the sample was tested without a steel cold face, and a roving thermocouple was used to determine when localised "hot spots" on the cold face reached a temperature in excess of 180°C plus ambient temperature.

These tests indicate that although phenolic foam is a good material in terms of structural performance, and phenolic resin is the most temperature stable resin in common use, the phenolic foam samples will not provide sufficient fire resistance for the demanding applications offshore without some form of additional fire protection.

This series of fire tests on core materials gave important information on their heat transfer properties for use in numerical modelling. It also gave base level information on the fire performance of the relative materials. The tests showed that, when used as a core material, Voidfill and both formulations of Vermiculux exhibited excellent fire performance, all capable of providing far in excess of an A60 fire rating (in terms of insulation), and Voidfill and Vermiculux II were capable of providing an H60 rating in the absence of any panel faces. If the thickness of Vermiculux II used was increased slightly this material would be able to provide an H120 rating in the absence of any faces.

4.4.2 Fire testing of steel faced sandwich panels

The preliminary fire tests performed on steel faced sandwich panels were for Voidfill mixes 7D and 7DW2. It was relatively certain from panel fire resistance tests performed on Voidfill 7D in the absence of faces that an A60 fire resistance would be easily achieved, however, it was uncertain as to the effect of changing the surface properties of the panel (i.e. including steel sheets). Figure 4.4.17 shows the result for a cellulosic fire test performed on a Voidfill 7D core material with thin steel faces. As can be seen, the insulation failure time of 140 minutes compares very well with the test performed in the absence of faces. This inferred that the inclusion of steel faces had little effect on the heat transfer through the sample. Voidfill mix 7DW2 (figure 4.4.18) showed a slight improvement in cellulosic fire conditions over the original mix of Voidfill 7D with an insulation failure time of approximately 155 minutes.

It was decided from these tests that there was little need to test either of the Vermiculux formulations or Voidfill mixes tested previously to hydrocarbon fire conditions in the steel faced condition as very similar fire test results would be obtained.

In the research performed to improve the structural properties of the Voidfill mixes the impregnation or premixing of the Voidfill material with phenolic resin was investigated. Figures 4.4.19 and 4.4.20 show the hydrocarbon fire test results for mixes of 7D-20 (a Voidfill 7D mix with a notional inclusion of 20%

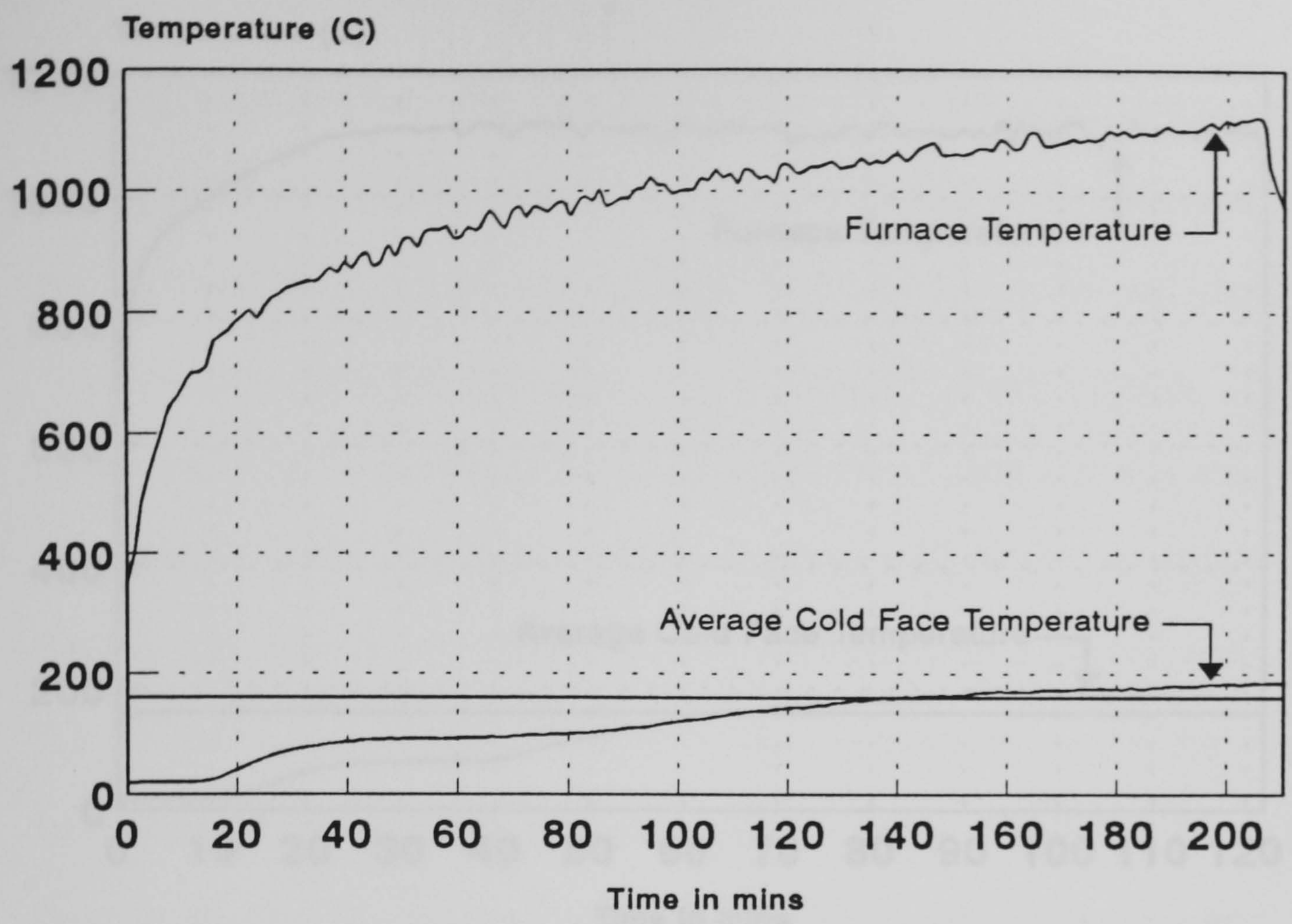

Figure 4.4.17 - BS476 Cellulosic Fire Test
Core Material - Voidfill 7D 50mm thick
Steel hot and cold faces

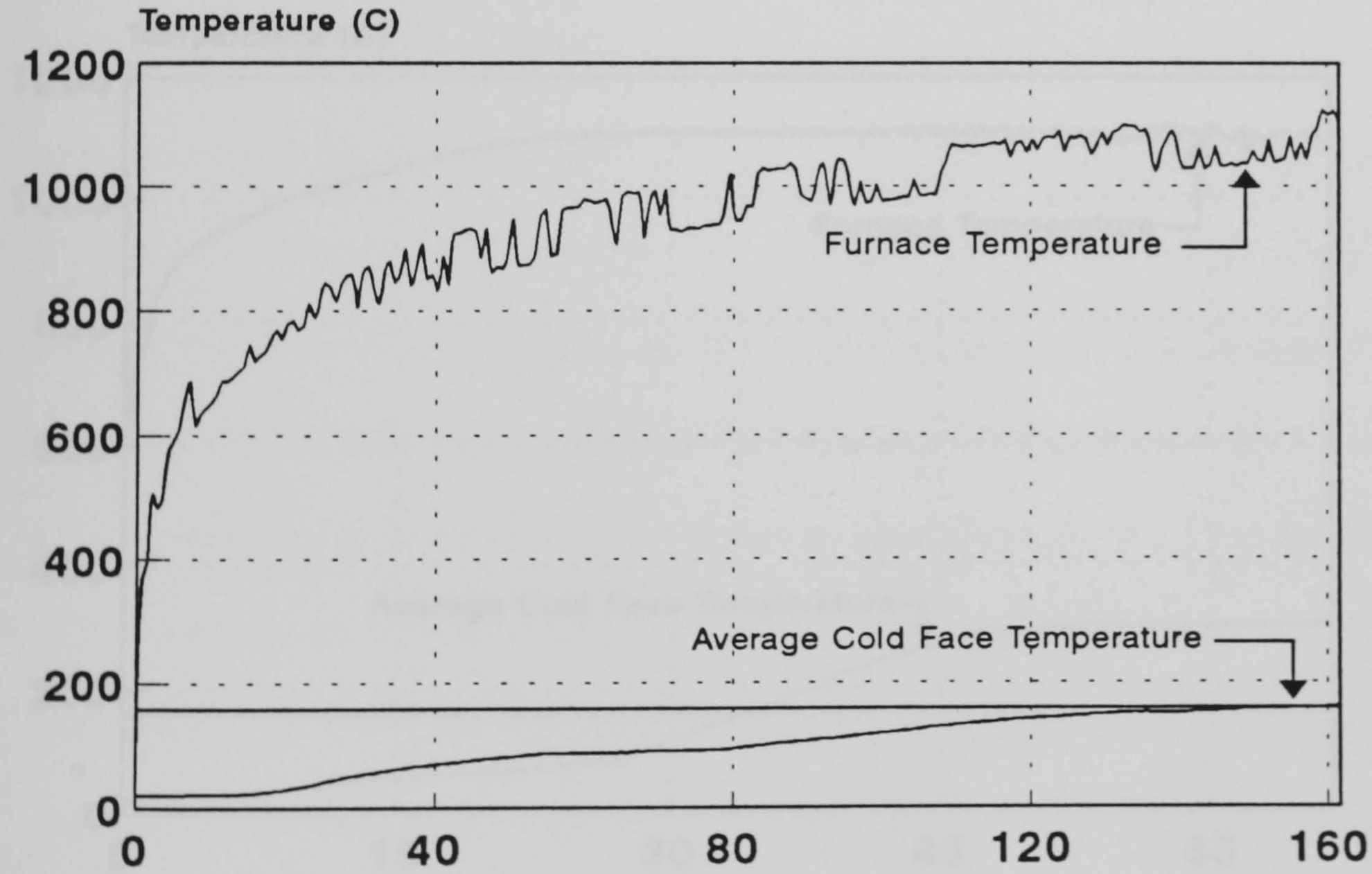

Figure 4.4.18 - BS476 Cellulosic Fire Test
Core Material - Voidfill 7DW2 50mm thick
Steel hot and cold faces

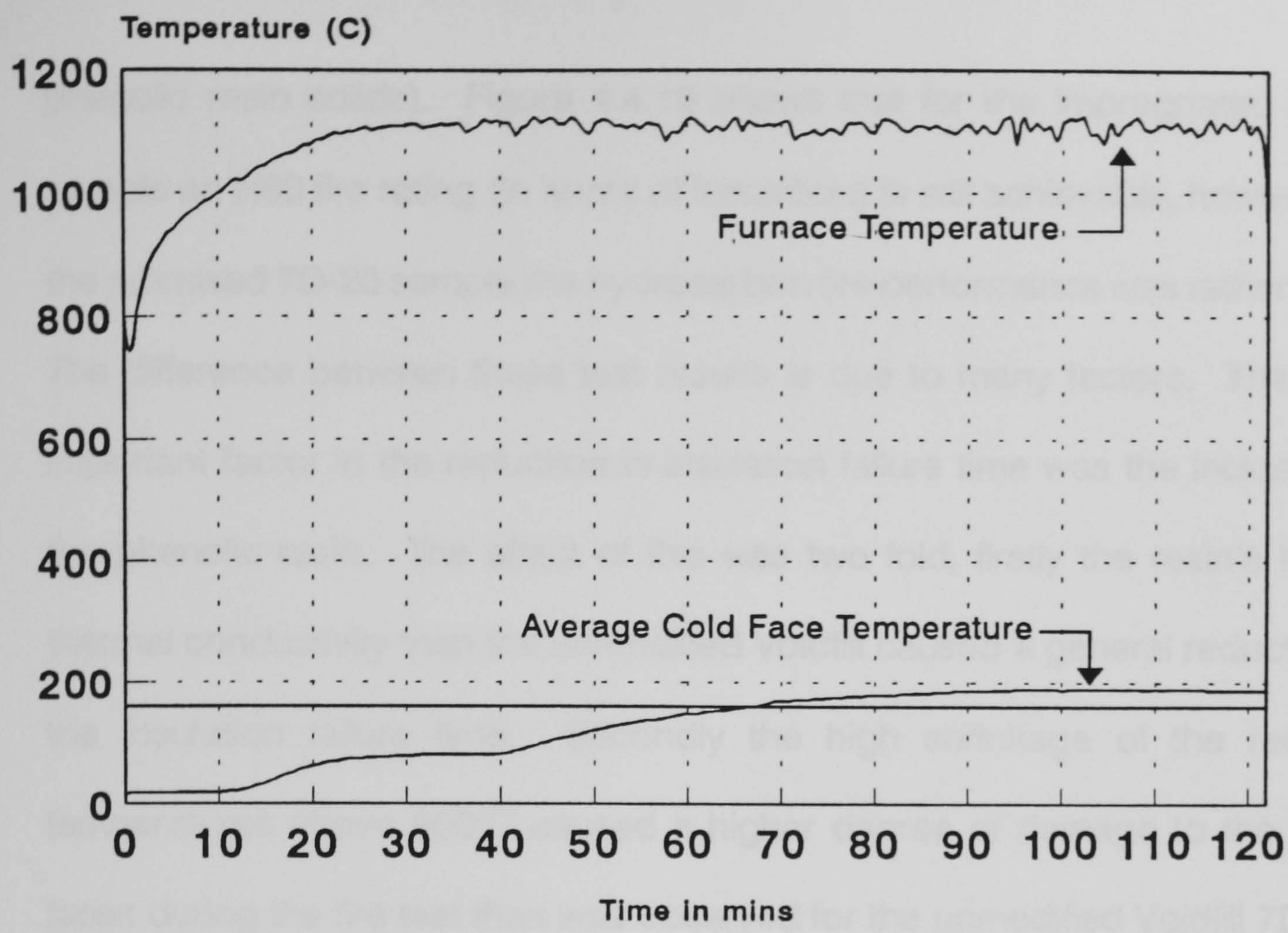

Figure 4.4.19 - DoE Hydrocarbon Fire Test
Core Material - Voidfill 7D-20 (meths)
Steel hot and cold faces

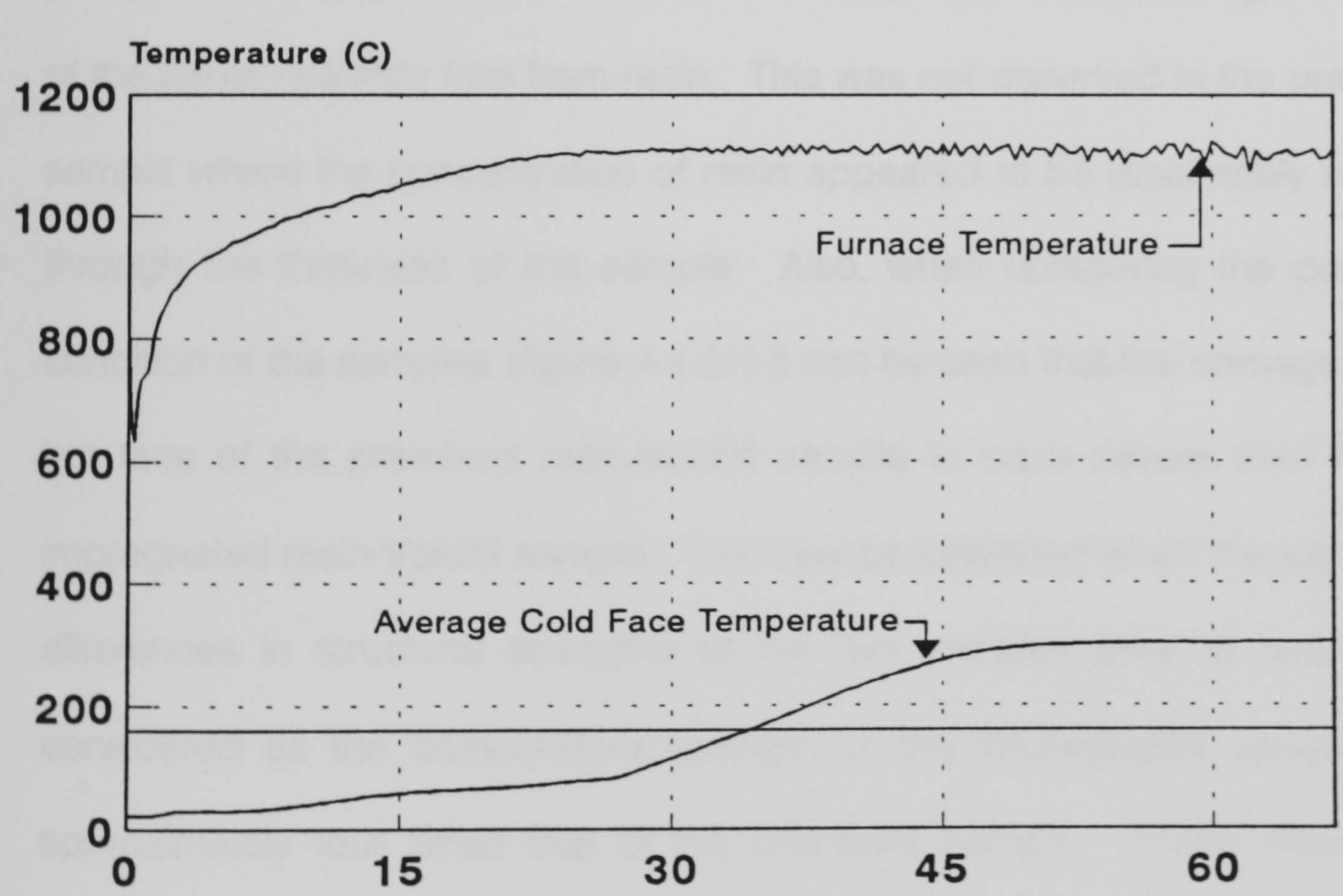

Figure 4.4.20 - DoE Hydrocarbon Fire Test
Core Material - Voidfill 7D-20 (water based resin)
No hot or cold faces

phenolic resin solids). Figure 4.4.19 shows that for the impregnated 7D-20 sample an H60 fire rating (in terms of insulation) is still achievable, however,for the premixed 7D-20 sample the hydrocarbon fire performance was rather poor. The difference between these test results is due to many factors. The most important factor in the reduction in insulation failure time was the inclusion of the phenolic resin. The effect of this was two fold, firstly the resin's higher thermal conductivity than the unmodified Voidfill caused a general reduction in the insulation failure time. Secondly the high shrinkage of the resin at temperatures above 600°C caused a higher degree of damage to the panel faces during the fire test than was observed for the unmodified Voidfill 7D mix. In the impregnated Voidfill sample there was a tendency for migration of the phenolic resin solids towards the faces of the panel, hence leaving the centre of the panel relatively free from resin. This was not observed in the premixed sample where the concentration of resin appeared to be reasonably uniform through the thickness of the sample. Also, when comparing the post test condition of the samples (figure 4.4.21) it can be seen that the damage to the hot face of the premixed resin-Voidfill sample is more severe than for the impregnated resin-Voidfill sample. This may be explained when the significant differences in structural strengths of the two samples prior to testing are considered as the compressive strength of the impregnated sample was approximately four times that of the premixed sample. These differences between the two core materials explain the dramatic difference in the fire test results. However, both tests indicate that the inclusion of phenolic resin within the Voidfill mix produces a reduction in the fire resistance of the sample. This

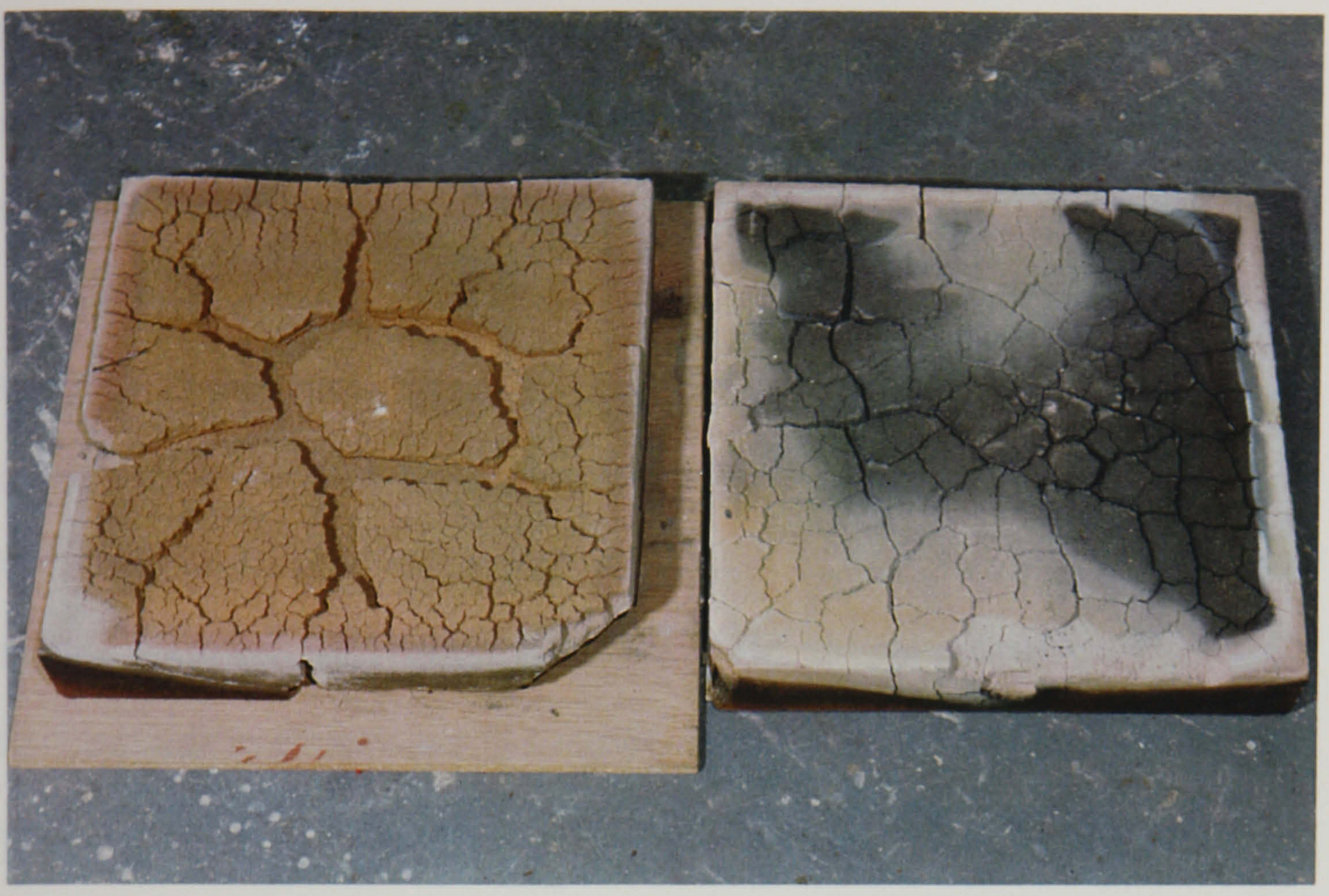

Figure 4.4.21 - Post Test Condition of Samples
of Voidfill 7D-20 (left-premixed, right-impregnated)

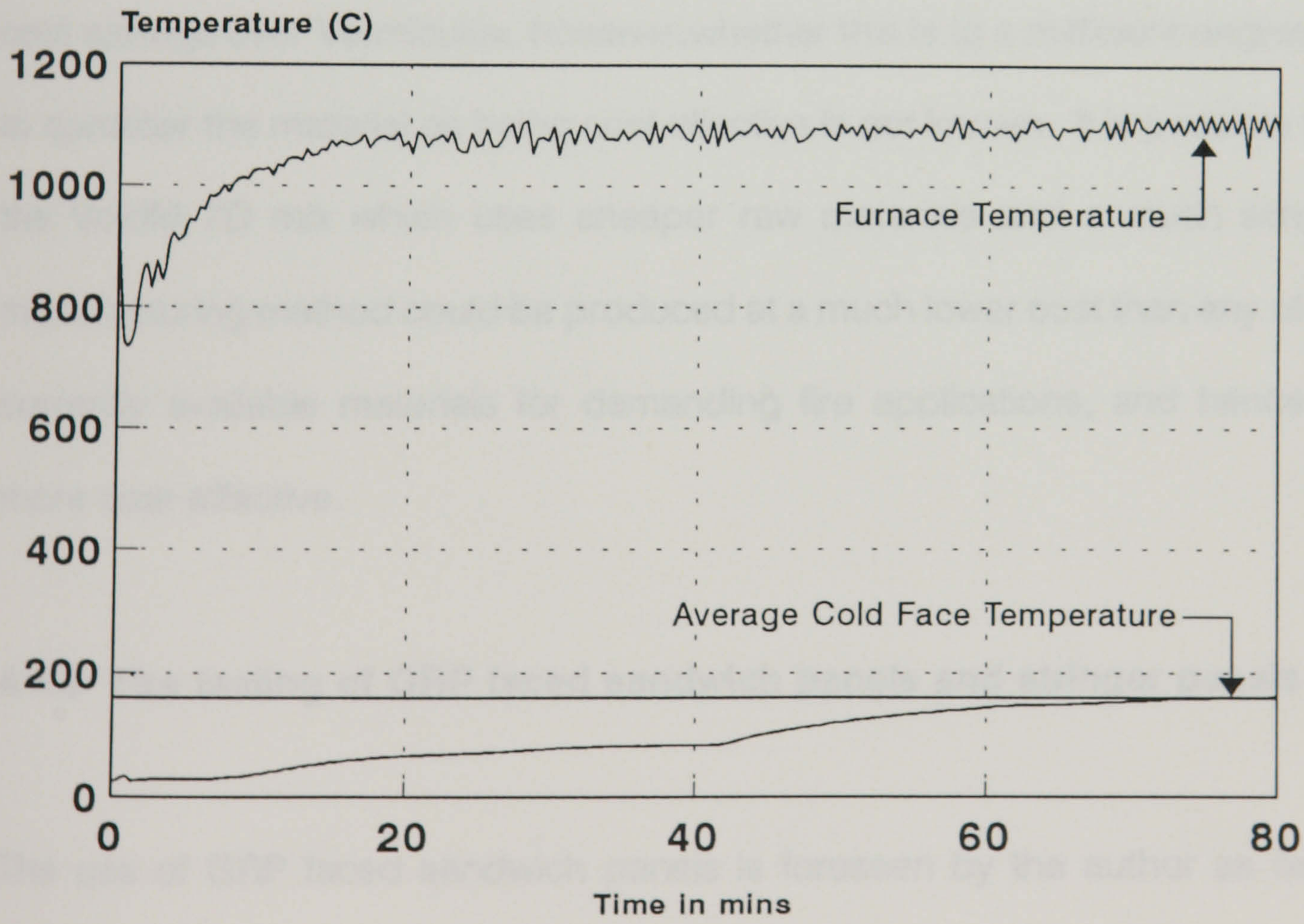

Figure 4.4.22 - DoE Hydrocarbon Fire Test
Core Material - Newtherm 50mm thick
Steel Hot and Cold Faces

reduction of fire resistance is an undesirable effect, but may be an acceptable one where high structural performance is required in areas where fire risk, and fire load will be low.

Figure 4.4.22 shows the hydrocarbon fire test of Newtherm from Cape Boards Limited tested with mild steel panel faces. Newtherm is a cheaper version of Vermiculux, and is produced in a similar manner, but is structurally weaker, and shows a lower insulation failure time in the fire test. The insulation failure time in the test was approximately 75 minutes, and hence as a steel faced sandwich panel Newtherm easily achieves the H60 fire rating. Figure 4.4.23 shows the post-test condition of the fire tested sample. As can be seen there is little damage to the material after the fire exposure. The material does have inherent cost savings over Vermiculux, however, whether this is to a sufficient degree as to consider the material as being cost effective is not known. It is possible that the Voidfill 7D mix which uses cheaper raw materials and a much simpler manufacturing method could be produced at a much lower cost than any of the currently available materials for demanding fire applications, and hence be more cost effective.

4.4.3 Fire testing of GRP faced sandwich panels and stringer panels

The use of GRP faced sandwich panels is foreseen by the author as being limited to areas which demand a combination of high structural strength with a high degree of fire resistance. It has been shown in chapter 3 that GRP

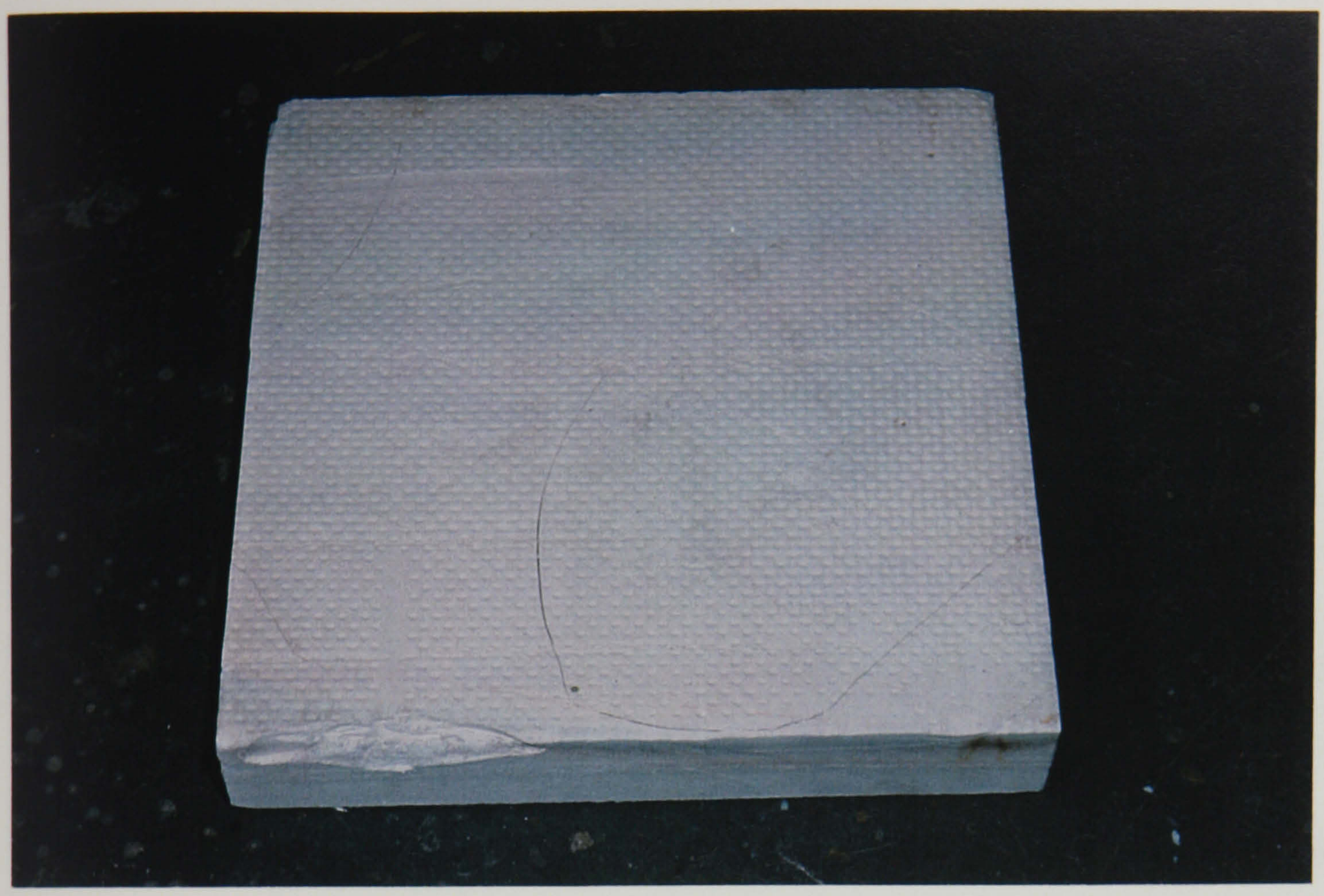

Figure 4.4.23 - Post Test Condition of Newtherm After Hydrocarbon Fire Testing

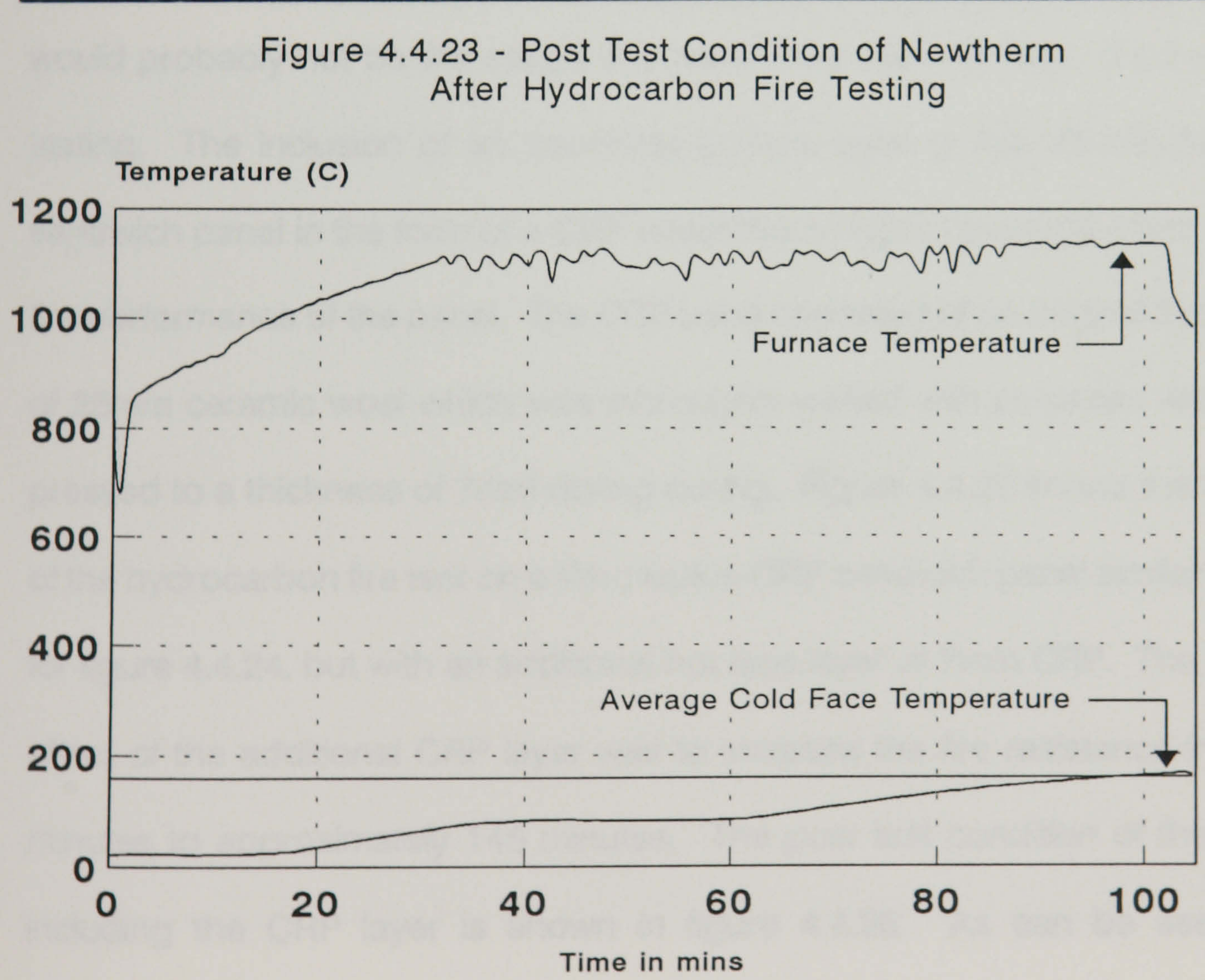

Figure 4.4.24 - DoE Hydrocabon Fire Test
Core Material - Vermiculux I 50mm thick
6mm GRP (polyester) Hot and Cold Faces

faced sandwich panels, and GRP stringer panels can both be adequate in terms of structural strength for offshore loading conditions. The inherent corrosion resistance of the GRP faces is also extremely beneficial in the aggressive marine offshore environment. As has been mentioned previously the primary fire barrier of a GRP faced sandwich panel is the fire resistant structural core. However, there is a beneficial effect of GRP faces and GCRP faces (see section 3.2.3).

Figure 4.4.24 shows the hydrocarbon fire test results for a sandwich panel consisting of 6mm thick polyester GRP skins and a dried 50mm Vermiculux I core. As can be seen the panel fails to achieve an H120 fire resistance. This would probably not be the case if the panel core had not been dried prior to testing. The inclusion of an insulating surface layer to the Vermiculux-GRP sandwich panel in the form of a CRP sheet has a highly beneficial effect on the fire performance of the panel. The CRP used consisted of an original thickness of 25mm ceramic wool which was thoroughly wetted with polyester resin and pressed to a thickness of 7mm during curing. Figure 4.4.25 shows the results of the hydrocarbon fire test on a Vermiculux-GRP sandwich panel similar to that for figure 4.4.24, but with an additional hot face layer of 7mm CRP. The overall effect of the additional CRP layer was to increase the fire resistance from 95 minutes to approximately 145 minutes. The post test condition of the panel including the CRP layer is shown in figure 4.4.26. As can be seen, the additional layer of resin encapsulated ceramic wool protected the glass fibre of the hot face, which was still fully intact after test termination. The results

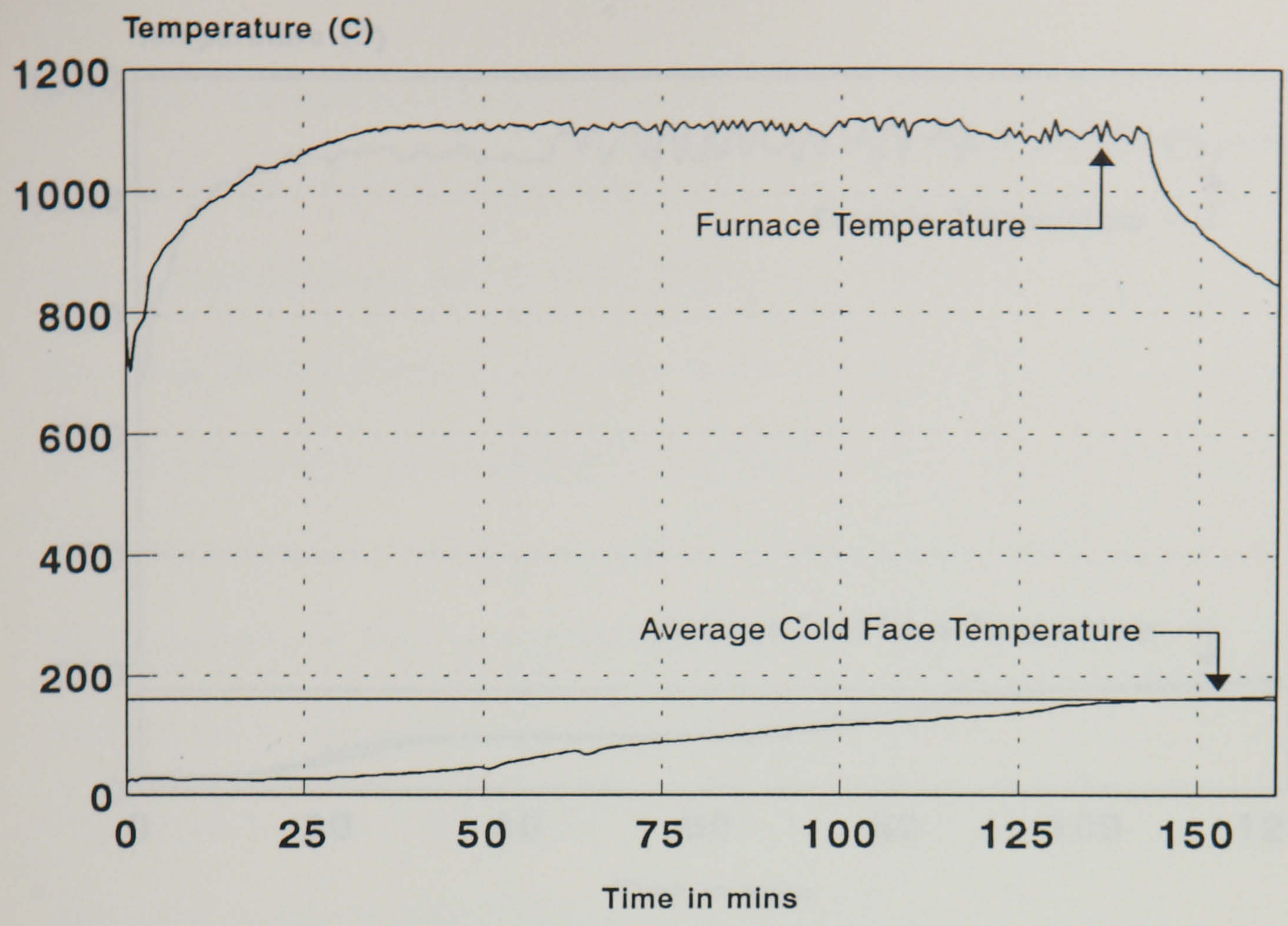

Figure 4.4.25 - DoE Hydrocarbon Fire Test
Core Material - Vermiculux I 50mm thick
6mm GRP (polyester) Hot and Cold Faces + CRP Hot Face

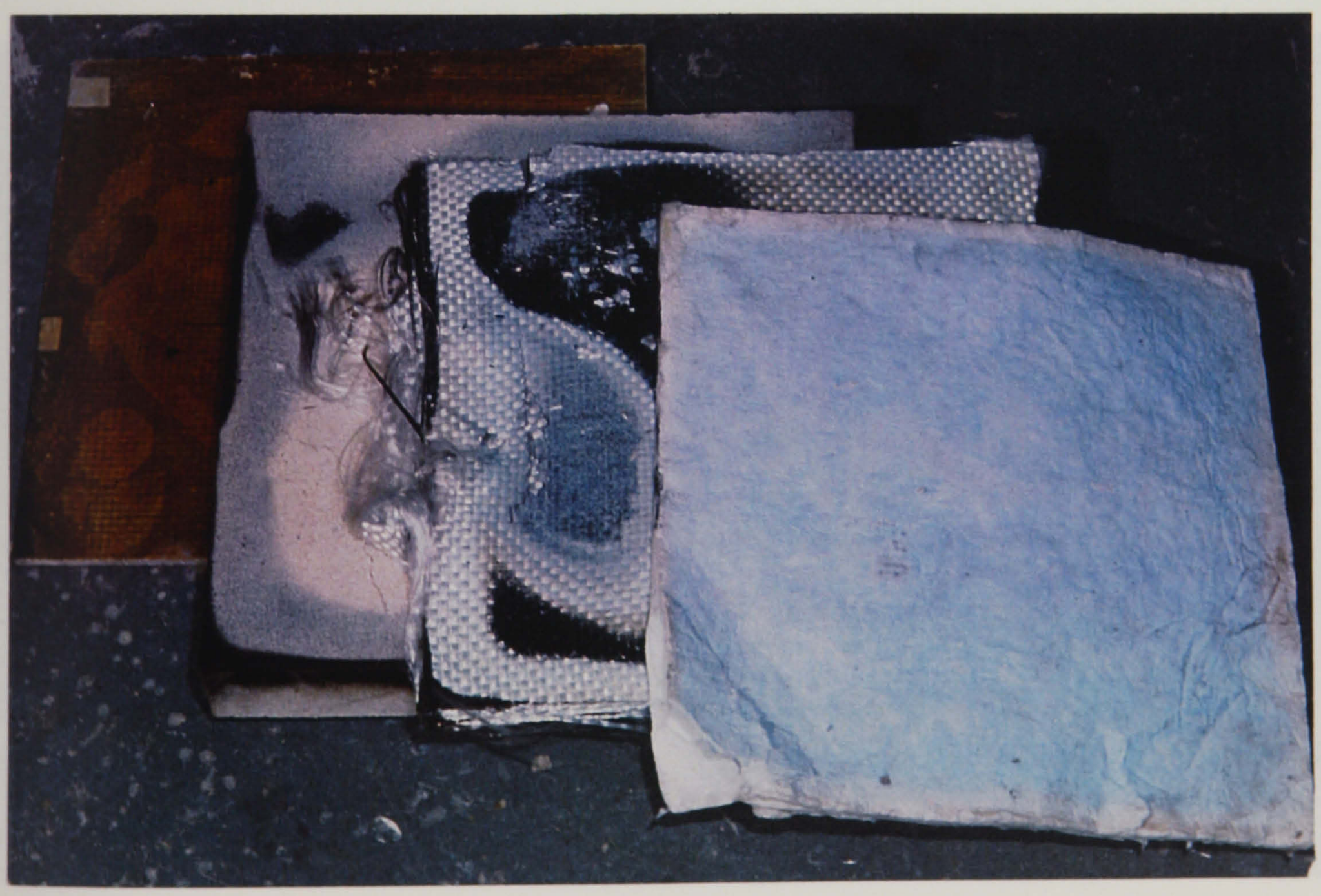

Figure 4.4.26 - Post Test Condition of Sandwich Panel Consisting of Voidfill I Core, 6mm GRP Skins, and additional 7mm CRP Hot Face

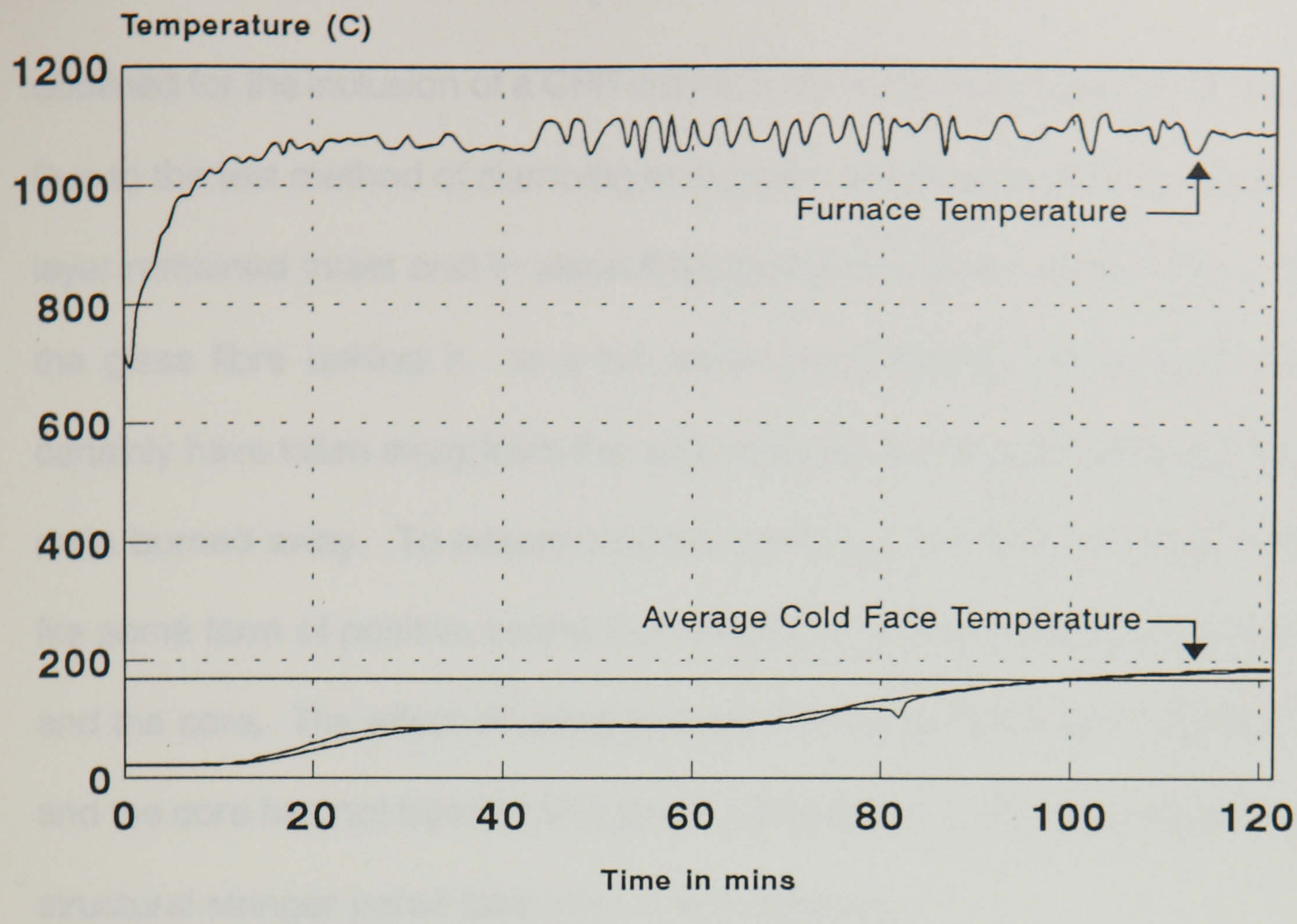

Figure 4.4.27 - DoE Hydrocarbon Fire Test
Core Material - Vermiculux I 50mm thick
6mm GRP (polyester) hot and cold faces, lap jointed

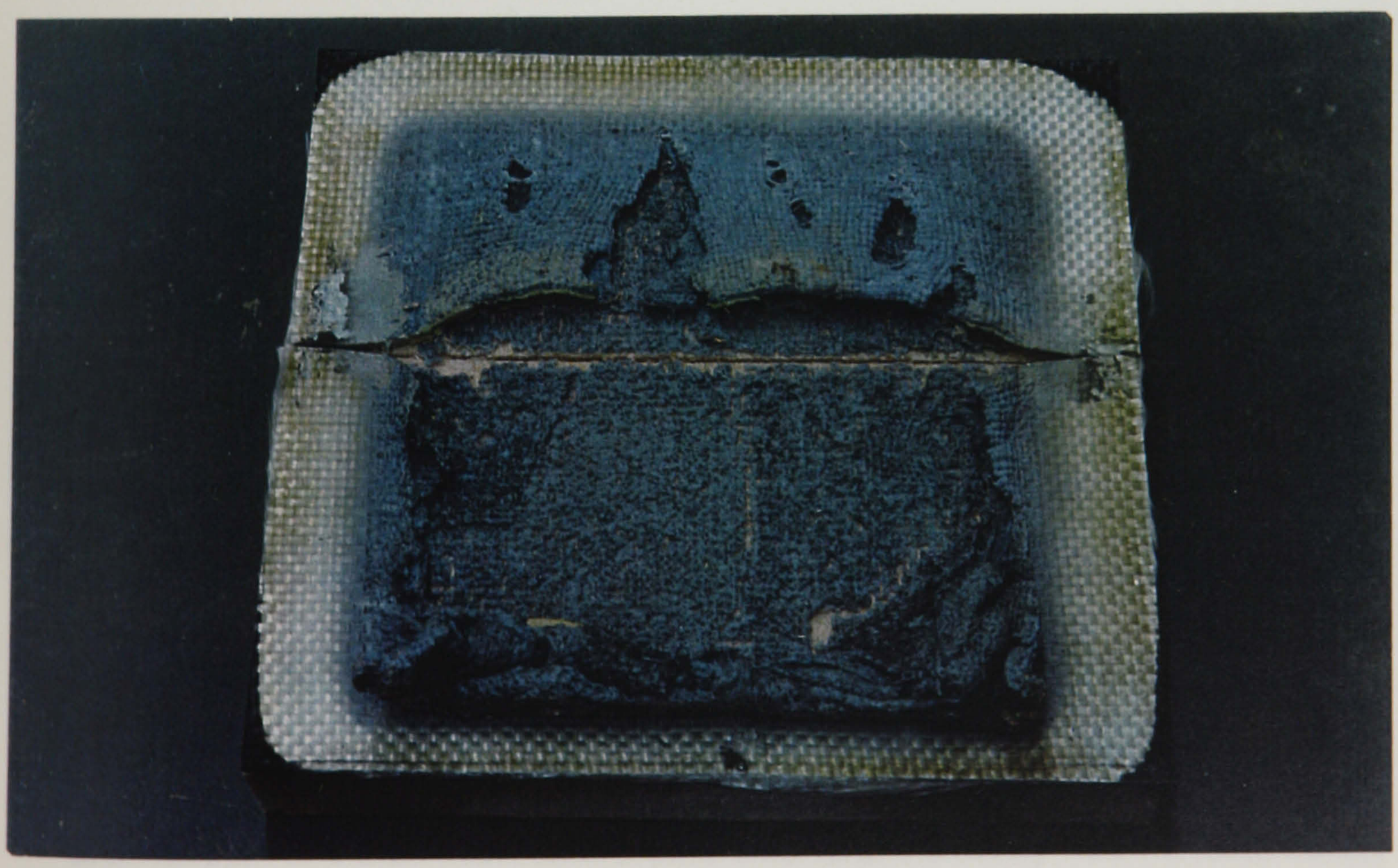

Figure 4.4.28 - Post Test Condition of Lap Jointed Sandwich Panel
Vermiculux I Core with 5mm GRP Faces

obtained for the inclusion of a CRP hot face are somewhat misleading however. Due to the test method of clamping to the front of the furnace the ceramic wool layer remained intact and in place throughout the whole test duration, as did the glass fibre behind it. In a full scale panel the hot faces would almost certainly have fallen away from the core material due to their self weight as the resin burned away. To ensure that the hot faces remained in place during a fire some form of positive connection would be required between the hot face and the core. The effect of using positive connections between the hot faces and the core has not been investigated, partially due to the development of the structural stringer panel (see later in this chapter).

A brief investigation was made into the effect of joint systems on the hydrocarbon fire resistance of Vermiculux. The joint system employed was a simple lap joint, 25mm wide at the mid-depth of the panel. The GRP faces were jointed also, directly above the lap joint at the hot and cold surfaces of the core. The lap joint was bonded together with a mixture of sodium silicate and ball clay. The mixture of sodium silicate and ball clay was found to be an effective fire cement due to the slightly intumescent properties of sodium silicate in fire and the ball clay forming a ceramic solid at high temperatures as the sodium silicate softened. Figure 4.4.27 shows the results of the hydrocarbon fire resistance test on the lap jointed Vermiculux I panel with 5mm polyester GRP faces. The insulation failure time was approximately 100 minutes which compares well with the test result for the unjointed sample. Hence it can be seen that simple joint designs may be sufficient when using non-flammable

structural sandwich panel core materials. Figure 4.4.28 shows the post-test condition of the jointed panel, and the location of the joint on the hot face can be clearly seen.

Figure 4.4.29 shows the hydrocarbon fire test result for Voidfill mix 7D with 6mm polyester GRP faces. As can be seen, the panel easily achieves the H120 fire rating. It should be noted however that, as with all the small scale fire tests performed, the method of mounting the fire test sample to the furnace provided very beneficial conditions with respect to retention of the hot face. In the absence of positive connection between the GRP face and the core it is likely that as the resin of the hot face burns the fixity between the GRP face and the core would reduce, and eventually the hot face would fall away from the core leaving it exposed to the fire. The effect of the hot face falling away from the core during a fire has been investigated using a numerical model and is presented in section 4.5.3.

Figures 4.4.30 and 4.4.31 show the results of hydrocarbon fire tests on cores of 75mm phenolic foam and 60mm Vermiculux II respectively. These figures show comparisons of the effect the hot face has on the fire test results. In the case of the phenolic foam, no cold face was used for the tests. A series of four thermocouples were mounted to the cold face of the phenolic foam, and the cold face temperature was taken as an average of those four temperatures. For the tests performed with a Vermiculux II core, the cold face used was the same as used for the hot face, and the cold face temperature was taken as

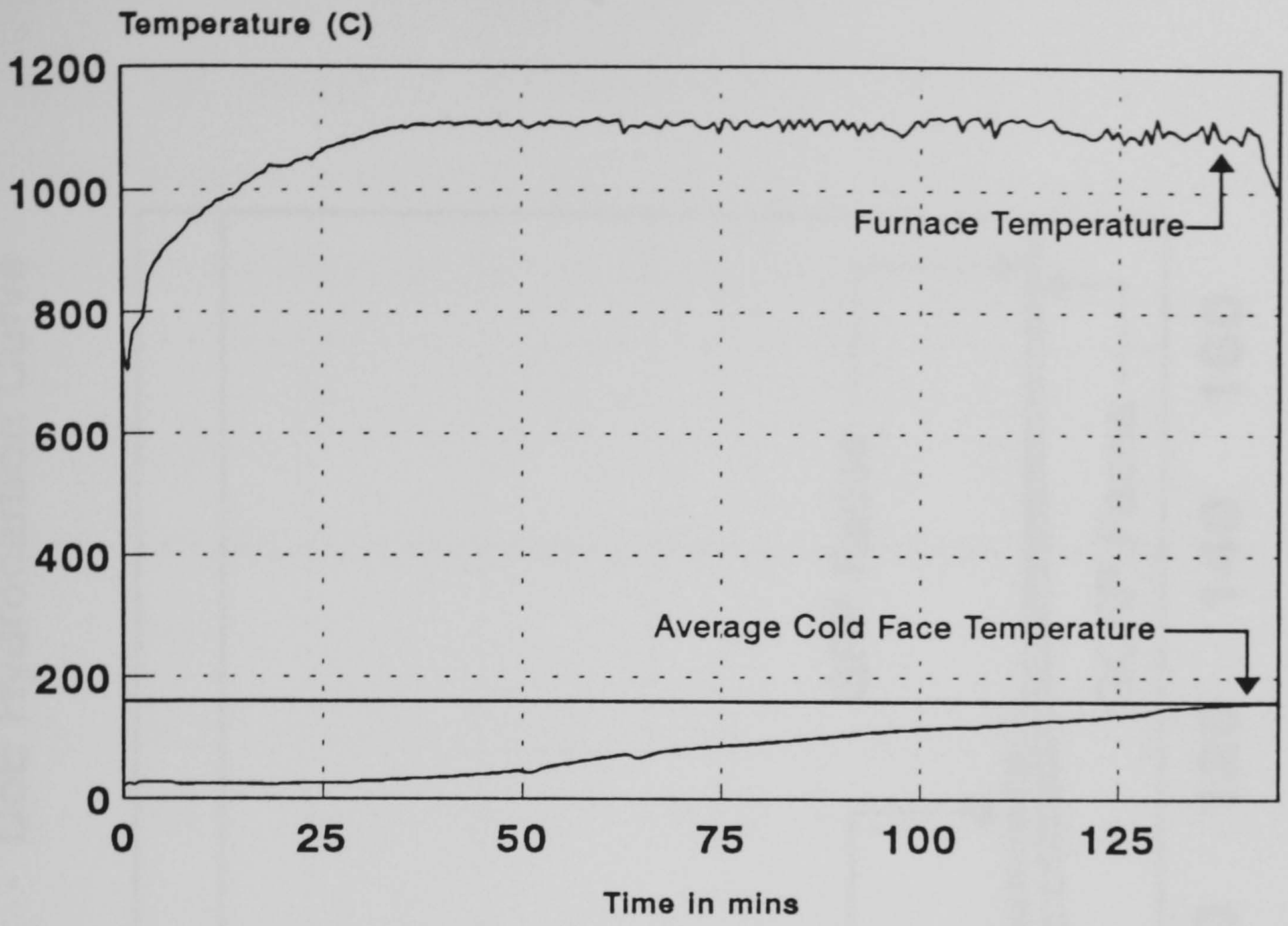

Figure 4.4.29 - DoE Hydrocarbon Fire Test
Core Material - Voidfill 7D 50mm thick
6mm GRP (polyester) hot and cold faces

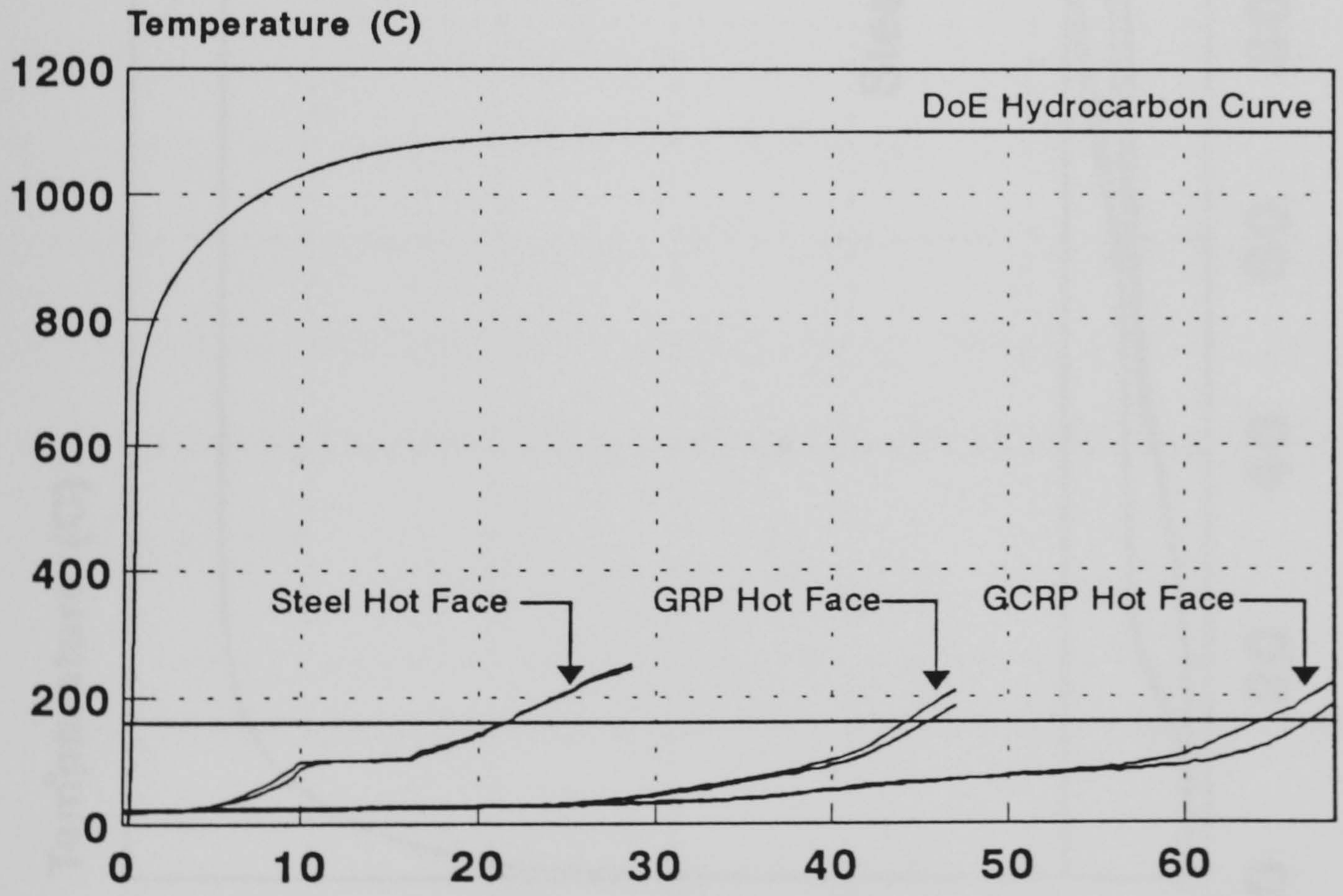

Figure 4.4.30 - DoE Hydrocarbon Fire Test
Core Material - Phenolic Foam 75mm thick
Face materials vary

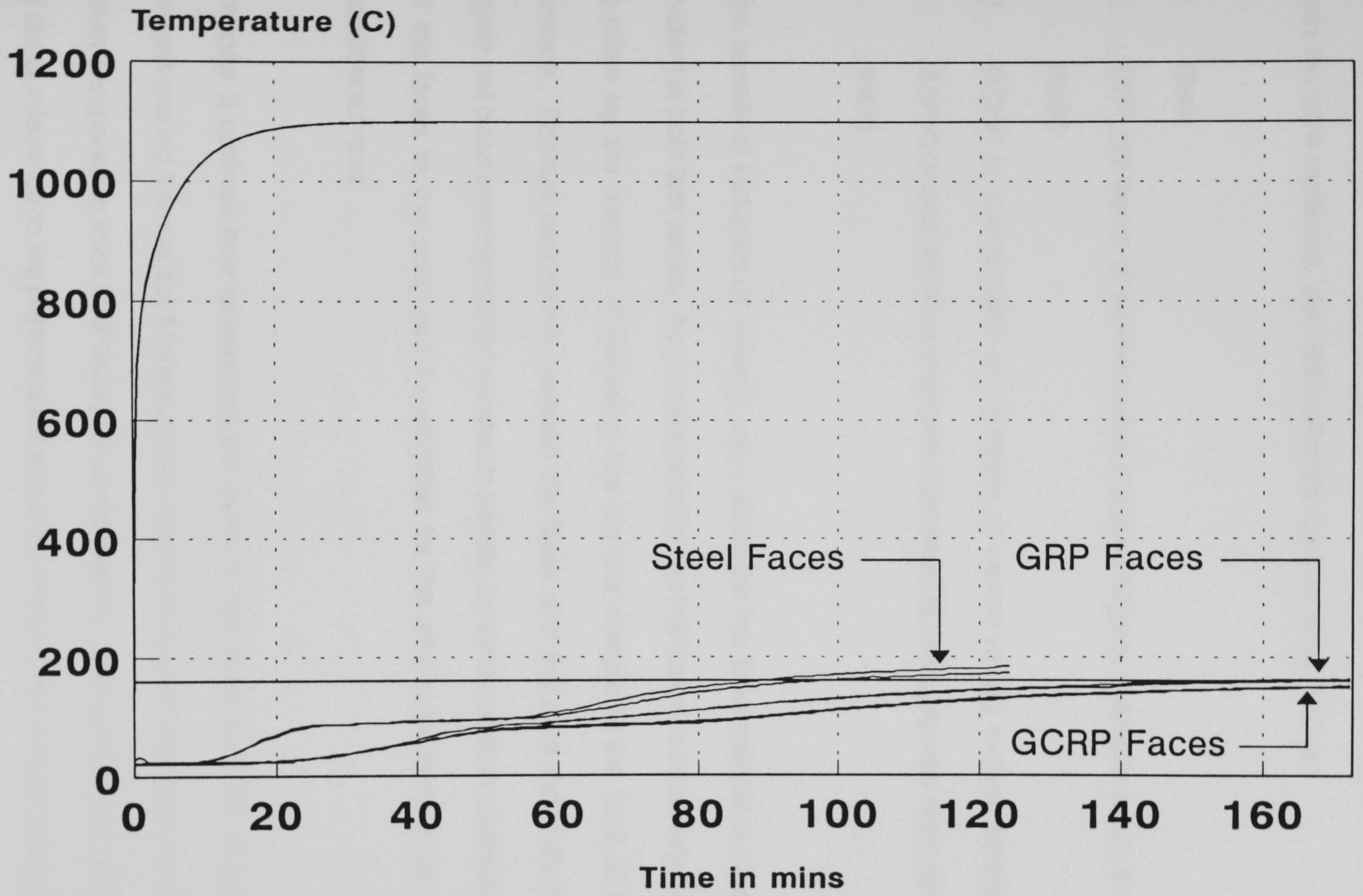

Figure 4.4.31 - DoE Hydrocarbon Fire Test
Core Material - Vermiculux II 60mm Thick
Face materials vary

being the average of the temperatures measured by two cold face thermocouples located near the centre of the exposed area of the panel. For both the core materials, the face materials used were as follows:

a) Steel

b) GRP (12 layers of woven roving e-glass 600gsm, polyester resin, 6mm thick)

c) GCRP (a combination of 10 layers of woven roving e-glass 600gsm, 3.5mm original thickness ceramic fibre blanket, and polyester resin, 6mm thick)

The benefit of inclusion of ceramic wool within the hot face material is clearly evident in both test series. As in previous tests the hot face was effectively held in place by the method of mounting the fire test sample to the front of the furnace. Positive connection between the faces and the core materials has again not been investigated for sandwich panels, however, positive connection of the faces to the core was investigated for the structural stringer panels considered next.

Chapter 3 outlined how connecting the faces of the panel by GRP stringers formed around Vermiculux II formers gave a much improved structural solution when compared to thick GRP faced sandwich panels. A secondary advantage of direct relevance to fire performance is that the faces of the stringer panel can be connected to the GRP and former material of the stringer by mechanical

means. Where the panel faces incorporate a thin layer of ceramic fibre blanket, and the faces are mechanically connected to the stringers, the ceramic fibre blanket and the glass fibre behind it will remain in place during a fire as the resin matrix burns away.

In the original stringer panel designs a steel stringer insulated from the panel faces by thin strips of Vermiculux II was used. This steel stringer, and the difficulty in forming the panel led to disappointing results. STRING 1 and STRING 2 (as detailed in section 3.6) gave hydrocarbon fire resistances of H60, with String 2 having the higher failure time at approximately 75 minutes.

STRING 3 differed from the original stringer panel designs in that it encompassed a GRP wrapped stringer, GCRP faces, and a non-structural core infill of compressed ceramic blanket. The GCRP faces and the stringer were connected together by steel wood screws. The overall weight of STRING 3 was calculated at approximately 31.5kg/m^2. Figure 4.4.32 shows the simulated hydrocarbon fire resistance test result for STRING 3. As can be seen, the insulation failure time was in excess of 130 minutes, and therefore the H120 fire rating was easily achieved. Post test inspection of the tested sample showed the glass and ceramic fibre of the hot face to be relatively undamaged, and the mechanical connection between the face and the stringer was still in good condition. The materials only cost of the stringer panel investigated would be approximately £75 per square metre (1996 prices), and when compared to an approximate cost of £170 per square metre (1996 prices) for the steel-mineral

fibre traditional panel it would appear to be a cost effective alternative (allowing £75 per square metre for manufacture, transport and profit margins).

Further structural investigation has shown that a panel of only 27kg/m² weight may be possible whilst maintaining the same fire performance - it was assumed that if the overall thickness of the panel was maintained then fire performance should not be effected unduly. These assumptions are yet to be proved by testing.

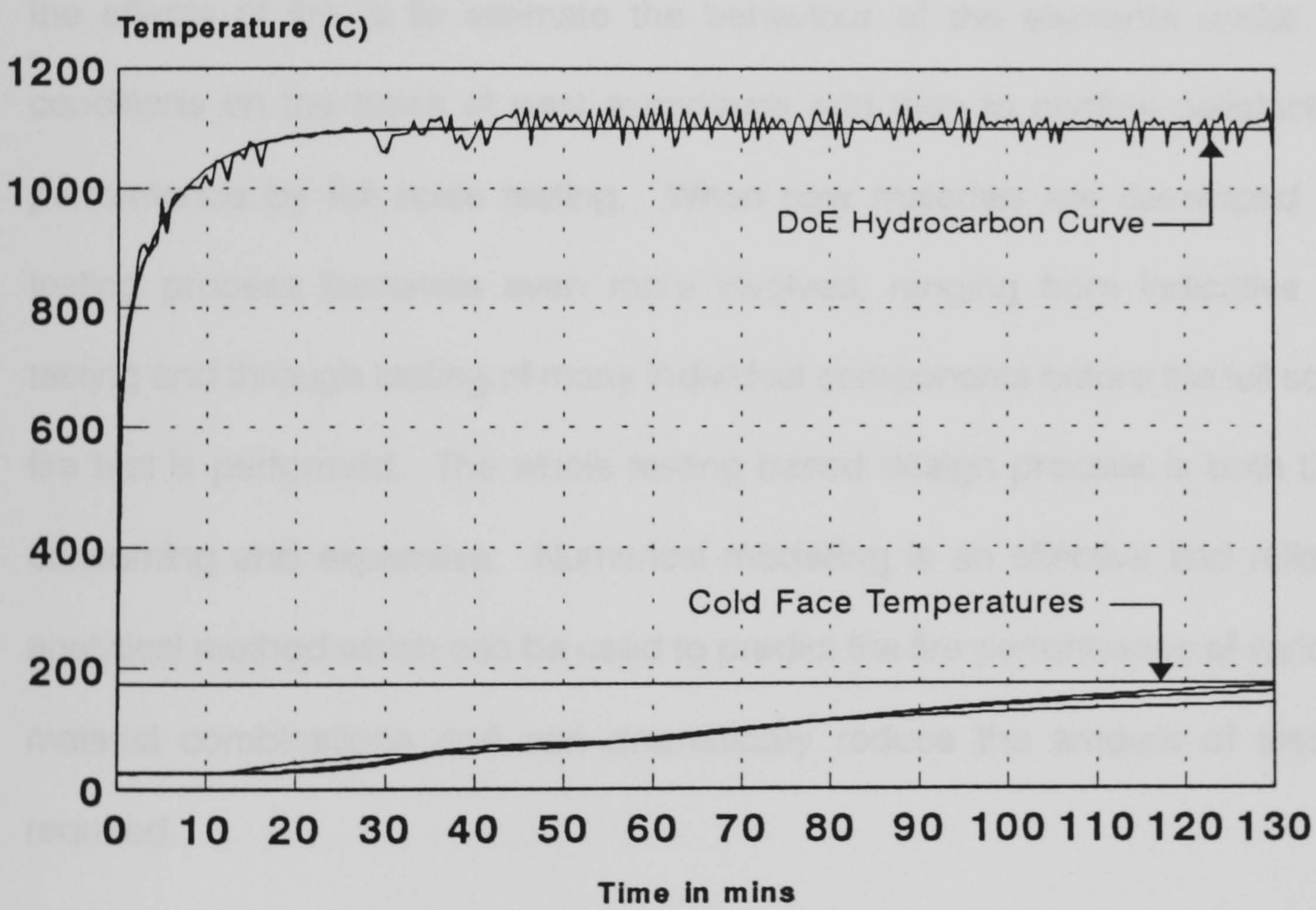

Figure 4.4.32 - DoE Hydrocarbon Fire Test
GRP Stringer Panel - STRING 3
GCRP Hot and cold faces, Ceramic Wool Core

4.5 Numerical modelling of fire test results

The fire testing results of both GRP laminates and core materials as well as their various combinations provided a great deal of information not only on their relative fire performance, but also to aid the development of a numerical model, produce a database of material heat transfer properties, and provide accurate data sets against which to verify the model.

The most widespread approach to designing building components to withstand the effects of fire is to estimate the behaviour of the elements under fire conditions on the basis of past experience and then to confirm satisfactory performance by full scale testing. When new materials are developed the testing process becomes even more involved, ranging from indicative fire testing and through testing of many individual components before the full scale fire test is performed. The whole testing based design process is both time consuming and expensive. Numerical modelling is an effective and reliable analytical method which can be used to predict the fire performance of various material combinations and can dramatically reduce the amount of testing required.

The following text shows how a simple one dimensional model can accurately predict the fire behaviour of the different materials used and developed within the author's research. The accuracy of the numerical modelling is, however, heavily dependant on the accuracy of the derivation of the thermal properties

of the constituent materials at elevated temperatures.

Where the thickness of a panel is small compared to the other dimensions the heat transfer through the panel can be considered as one dimensional (i.e. the only heat flow through the sample is through the thickness). This case is not strictly true for the small scale fire tests performed within the authors research. However, it can be assumed to be a reasonable approximation.

A natural starting point for the calculation of heat transfer through the sample under test is Fourier's Partial Differential Equation for heat flow by conduction. The general unsteady-state equation governing heat conduction in cartesian coordinates[44] is three dimensional, and can be reduced to the one dimensional transient equation:

$$\rho C_p \frac{\partial T(x,t)}{\partial t} = \frac{\partial}{\partial x}\left(k(T)\frac{\partial T(x,t)}{\partial x}\right) \quad for\ 0 \le x \le L,\ t > 0 \qquad (4.5.1)$$

Where

T(x,t) is the temperature (°C)

k(T) is the temperature dependant thermal conductivity (W/m°C)

ρ is the density (kg/m^3)

C_p is the specific heat (J/kg°C)

t is time (s)

x is a cartesian coordinate (through thickness for 1D case)

The right hand side of equation 4.5.1 represents the net heat conduction in a solid, while the left hand term represents the energy accumulated. The materials are assumed to be homogenous and isotropic . Where complicated geometries or boundary conditions are evident the solution to equation 4.5.1 can only be obtained by an approximate numerical method.

Finite difference methods are reasonably simple in conception and are well suited to the approximate solution of heat conduction through sections which are subjected to a prescribed heating rate. Finite difference solutions are based upon replacing derivatives with approximations of finite sized differences between values at particular locations.

Wang[44] used the physical energy balance technique for the solution of the finite difference equations due to its ease of use, and its convenience for cases with variable grids and convective boundary conditions. The energy balance method considers a control cell at a particular time step, and the temperature of the cell is calculated by considering the heat flow into and out of the cell. An explicit scheme is obtained when the heat flow is calculated from the temperature of the adjacent cells at the previous time step. The change of temperature at any particular point can be calculated by:

Net heat flow to cell = Mass of cell x Specific Heat x Rate of change of node temperature

There are two classifications of approach to finite difference methods for heat

transfer problems. These are the implicit and explicit methods. The implicit method solves a simultaneous system of algebraic equations at any particular time step, whilst the explicit method calculates temperature at a given time directly from the previous time steps' calculated values. The explicit finite difference method is an especially effective procedure although it suffers from a stability criterion[45] which necessitates small time steps to be used. With current computer capabilities the large number of calculations which can be required for the explicit method pose little problem. Furthermore, a small time step is required to accurately model the fire tests performed due to the very rapid temperature increase of the hot face during testing.

Equation 4.5.1 is subject to boundary conditions at $x = 0$ or $x = L$ for $t > 0$.

(i) For the boundary exposed to the prescribed temperature:

$$T = T_g(t) \tag{4.5.2}$$

(ii) For boundaries exposed to ambient conditions (gaining or losing heat)

$$k(T)\frac{\partial T}{\partial n} = h(T)(T_\infty - T) + FE\sigma[(T_\infty+273)^4 - (T+273)^4] \tag{4.5.3}$$

(iii) The initial boundary condition within the panel is:

$$T = T_o(x) \quad for\ t = 0,\ 0 \le x \le L \tag{4.5.4}$$

Where:

T	is the temperature (°C)
$T_g(t)$	is the known time-dependant temperature at the boundary (°C)
T_∞	is the ambient temperature (°C)
h(T)	is the surface heat transfer coefficient ($W/m^{2o}C$)
F	is a configuration factor for radiation
E	is the emissivity
σ	is the Stefan-Boltzman constant (5.67×10^{-8} $W/m^2 K^4$)

In equation 4.5.3 the first term on the right hand side represents the convective heat transfer, and the second term represents the radiative heat transfer. Three finite difference equations (FDE's) are required for the numerical modelling of a sandwich panel exposed to fire[46]. The three FDE's required represent:

(1) A typical internal node, m, within one layer

$$T_m^{i+1} = F_o\left[\frac{2(k_{m-1,m}T_{m-1}^i)}{k_{m-1,m} + k_{m+1,m}} + T_m^i\left(\frac{1}{F_o} - 2\right)\right] \qquad (4.5.5)$$

where: superscript i indicates the time step level
F_o is the fourier number which is defined by:

$$F_o = \frac{(k_{m-1,m} + k_{m+1,m})\Delta t}{2\rho C_p(\Delta x)^2} \qquad (4.5.6)$$

To preserve the stability of the explicit method, and not to violate thermodynamic principles, the coefficient $(1/F_o - 2)$ of T_m^i in equation 4.5.5 must be greater than zero, and F_o should be less than 0.5. The conductivity $k_{m-1,m}$ (similar to $k_{m+1,m}$) is evaluated at each time step as:

$$k_{m-1,m} = k\left[\frac{T_{m-1}^i + T_m^i}{2}\right] \qquad (4.5.7)$$

(2) An interface node, m, between two different material layers

$$T_m^{i+1} = F_o\left[2\frac{k_1\Delta x_2 T_{m-1}^i + k_2\Delta x_1 T_{m+1}^i}{k_1\Delta x_2 + k_2\Delta x_1} + T_m^i\left(\frac{1}{F_o} - 2\right)\right] \qquad (4.5.8)$$

where subscripts 1 and 2 represent the different materials

$$F_o = \frac{k_1\Delta x_2 + k_2\Delta x_1}{\Delta x_1\rho_1 C_{p1} + \Delta x_2\rho_2 C_{p2}} \cdot \frac{\Delta t}{\Delta x_1\Delta x_2} \qquad (4.5.9)$$

(3) A boundary node, for instance node 1, which when it corresponds to the boundary condition in 4.5.3

$$T_1^{i+1} = 2F_o\left[T_2^i + \frac{h(T_1^i)\Delta x}{k_1}T_\infty + \left(\frac{1}{2F_o} - 1 - \frac{h(T_1^i)\Delta x}{k_1}\right)T_1^i\right] \qquad (4.5.10)$$

$$+ FE\sigma\left[(T_\infty+273)^4 - (T_1^i + 273)^4\right]\frac{2\Delta t}{\rho C_p \Delta x}$$

$$F_o = \frac{k_1\Delta t}{\rho C_p(\Delta x)^2} \qquad (4.5.11)$$

This scheme is called the explicit method because the temperature at an arbitrary node, m, at time step i+1 is determined solely from equations 4.5.5, 4.5.8 and 4.5.10 where the temperature of the node m, and its neighbouring nodes are known at the previous time step.

The heat transfer from the furnace to the panel under test can be considered in one of two ways:

- As a boundary condition represented by equation 4.5.5 using the appropriate heat transfer parameters. T_∞ can be assumed to be the mean furnace temperature, and E the resultant emissivity at that temperature.

- By using the measured temperatures of the hot face during the fire test. These can be used in two ways, firstly to verify the heat transfer parameters as used in the previous method, and secondly to be directly applied as a boundary condition (eq. 4.5.2)

At the unexposed surface of the panel (the cold face) the heat transfer coefficient h(T) is calculated according to the following equation for natural convection adjacent to a vertical heated panel:

$$h(T) = 0.59\frac{k_{air}}{H}(G_{rL}P_r)^{0.25} \qquad for\ G_{rL}P_r < 10^9 \tag{4.5.12}$$

Where:

k_{air} is the temperature dependant thermal conductivity of air
$k_{air} = 0.23 + (7.43 \times 10^{-5}T) - (1.56 \times 10^{-8}T^2)$

H is the vertical height of the panel

G_{rL} is the Grashof number ($< 1.4 \times 10^9$)

P_r is the Prandtl number of air (which is approximately 0.7)

A typical value of h(T) is 7 W/m² K for a 300x300mm² vertical panel.

It has been shown that the actual heat conduction finite difference equations are relatively simple, and easy to use. However, the effect of moisture content of core materials, and resin decomposition and ablation of face materials has not been considered. Also, it should be noted that factors such as thermal conductivity and specific heat are temperature dependant. The transient material properties required for numerical modelling of fire test results from samples with GRP faces, or core materials with significant water content are

discussed in sections 4.5.1 and 4.5.2 following.

4.5.1 Numerical modelling of polymer composite materials

Due to the considerable complexity it is not possible to form a complete model of the physical and chemical processes occurring as a polymer composite degrades in fire. There is an almost complete absence of information concerning the majority of the material parameters involved. A promising approach is to form a mathematically viable but relatively simple model[47] which can capture the main features of the pyrolysis process and the consequent heat transfer behaviour. To simplify the model, several idealizations have to be made:

a) The GRP material is assumed to be homogenous, and the transport of heat and mass is perpendicular to the face of the panel only.

b) There is thermal equilibrium between the decomposition gasses and the solid material and there is no accumulation of these volatile gasses within the solid material.

c) The feedback of energy from the flaming of released volatiles by the GRP is ignored due to its small contribution when compared to the high heat flux created by the furnace. It may be the case in large scale tests, or in the case of sustained combustion after the ignition source has been removed, that it is not possible to ignore this energy feedback.

Wang[47] followed principles developed by several authors[65,66,67,68] in his development of an analytical model which was based upon the governing principles of conservation of mass and conservation of energy. The one dimensional energy equation in a panel subject to thermal degradation was expressed as a balance between the transient energy accumulation rate, with the sum of the rates of conduction, pyrolysed convection, and the energy sink due to decomposition:

$$\frac{\partial}{\partial t}(\rho h) = \frac{\partial}{\partial x}\left(k\frac{\partial T}{\partial x}\right) - \frac{\partial}{\partial x}\left(m_g' h_g\right) - Q\frac{\partial \rho}{\partial t} \qquad (4.5.13)$$

Where:

ρ	is density (kg/m^3)
h	is the enthalpy (J/kg)
t	is time (s)
T	is the temperature (°C)
k	is the thermal conductivity (W/m°C)
x	is the spacial variable (m)
h_g	is the enthalpy of the gasses
m'_g	is the mass flux of the gasses (kg/m^2 -s)
Q	is the heat of decomposition (J/kg)

The specific enthalpies of the solid and volatiles are:

$$h = \int_{T_o}^{T} C_p dT \;,\; h_g = \int_{T_o}^{T} C_{pg} dT \qquad (4.5.14)$$

Equation 4.5.13 must be solved simultaneously with equations for the rate of decomposition and the mass flux of the gasses. The rate of decomposition of the resin is assumed to conform to a mean reaction which is described by a single first-order Arrhenius function:

$$\frac{d\rho_r}{dt} = -A\rho_r \exp\left(\frac{-E_A}{RT}\right) \qquad (4.5.15)$$

Where ρ_r is the instantaneous density of the partially pyrolysed resin, E_A is the activation energy (J/mol), R is the gas constant (8.314 J/K.mol) and T is the

temperature (K). Experimental results show that the thermal degradation process of the resin materials is highly endothermic. The endothermic nature of the resin decomposition reaction slows heat transmission through the sample, and preserves the integrity of the laminate.

If accumulation of gases is ignored, the conservation of mass may be written:

$$\frac{\partial \dot{m}_g}{\partial x} = -\frac{\partial \rho}{\partial t} \qquad (4.5.16)$$

and the mass flux m_g at any spatial location and time may be calculated by integration of equation 4.5.16.

Hence, equation 4.5.14 can be modified into its final form by expanding the first three terms, substituting in the specific heat and the continuity equations, and rearranging, resulting in:

$$\rho C_p \frac{\partial T}{\partial t} = k\frac{\partial^2 T}{\partial x^2} - \dot{m}_g C_{pg}\frac{\partial T}{\partial x} - \frac{\partial \rho}{\partial t}(Q + h - h_g) \qquad (4.5.17)$$

Where

C_p is the specific heat of the material (J/kg/°C)

C_{pg} is the specific heat of the gasses (J/kg°C)

Equations 4.5.15, 4.5.16 and 4.5.17 form a set of non-linear partial differential equations which may be solved simultaneously for ρ, m_g, and T respectively.

4.5.2 Numerical modelling of hygroscopic materials

It has been shown earlier in this chapter, from comparison of experimental results, that the moisture content of fire test samples has a significant effect on the failure times, heating rates, and hence heat transfer. During the heating of a moist material the water is lost by a process of evaporation and migration. For the moisture to be evaporated a certain amount of energy is needed, and the absorption of this energy retards the rise in temperature.

A reasonably simple approach to modelling this process is to consider the effect of the moisture content on specific heat and thermal conductivity separately. Assuming that the evaporation of the water will take place over a temperature interval of 85°C to 135°C then the latent heat of evaporation can be added to the heat capacity of the material over that temperature range. The heat energy of evaporation[48] can be taken as 2.26×10^6 J/kg and the additional specific heat obtained from:

$$DC_p = \frac{2.26 \times 10^6 \, e}{DT} \; (J/kg^\circ C) \qquad (4.5.18)$$

Where: DC_p is the specific heat

e is the moisture content expressed as % by weight

DT is the magnitude of the given temperature interval

The following improvements have been made to this simplified approach within the modelling, and have been shown to give good correlation with experimental

results:

a) The latent heat of evaporation is introduced when the temperature at the unexposed side of the panel reaches the critical temperature. The critical temperature has been deduced from experimental results as being 85°C.

b) The evaporation-condensation mechanism of moisture migration requires additional energy in addition to that originally allowed for in the model. This additional energy can vary between 20% and 80% of the latent heat of evaporation depending on the material.

The value of thermal conductivity generally increases as temperature increases under conditions of constant moisture content. However, during a fire test the moisture content of the hygroscopic material will gradually reduce as the test progresses. As a result of this it is essential that both factors are allowed for in the calculation of the thermal conductivity. Jakob[49] recommended the following empirical formula for inorganic materials:

$$k_M = k(1.0819 + 0.17675M - 8.7812x10^{-3}M^2 + 1.7617x10^{-5}M^3)$$

Where M is the moisture content percentage by volume.

This equation allows the conductivity k_M of a moist material to be estimated for any arbitrary moisture level when the thermal conductivity is known for a given moisture content.

4.5.3 Comparison of experimental results with numerical modelling

The model as developed by H.B.Wang has been used to both predict and replicate experimental results during the course of the authors research. The primary area of interest within the authors research was for the modelling of a hydrocarbon fire resistance test on a sandwich panel consisting of GRP faces and a hygroscopic core.

The accuracy of the computer model is obviously heavily dependant on the accuracy of the material parameters used in the heat transfer calculations. The conventional thermal properties required for the modelling of heat transfer through a substrate are the materials thermal conductivity, specific heat and emissivity. These three factors are generally temperature dependant, and in order to determine them directly and explicitly various delicate experimental procedures are required. This makes the direct experimental measurement of these properties complicated and time consuming.

A much more attractive solution is to extract material properties by numerical techniques. This involves systematically "fitting" numerical predictions to the results of standard fire resistance tests. The initial numerical model is run using assumed figures, or manufacturers data, and the given scope for variation with the temperature, moisture and decomposition as described in sections 4.5.1 and 4.5.2. Once the thermal properties have been determined they are stored in a database of material properties for future reference and use.

The model, once the material properties are known, can be used to mimic test results, or can be used to predict the effect of variations from the test sample used to either increase fire resistance if under designed, or decrease fire resistance if over designed. Another use for numerical modelling can be to predict the effect of different face materials for a particular core material with respect to fire resistance for instance.

Figures 4.5.1 and 4.5.2 show comparisons of the numerical model out put with experimental results. Figure 4.5.1 shows a cellulosic fire test performed on a hygroscopic Voidfill 7D core material. Figure 4.5.2 shows the hydrocarbon fire test results for Vermiculux II with GRP faces (of slightly different thicknesses). Both these comparative figures show the accuracy of the numerical model, and reinforce its effectiveness as a design tool. The use of numerical modelling is likely to reduce the need for fire testing during the development and selection of materials stage of designing for fire. However, it is unlikely that numerical modelling will ever replace the need for final full scale fire testing of elements. These full scale tests are required to include joints, and standard fixings etc. and are more likely to fail due to stability or integrity than indicative fire test samples. These structural aspects of fire resistance are not allowed for in the numerical modelling at present due to the complexity of the problem.

A Numerical model employing the finite difference technique was used to determine the point at which a fire exposed GRP panel face would be expected to disintegrate or fall away from the core. Small scale and indicative samples

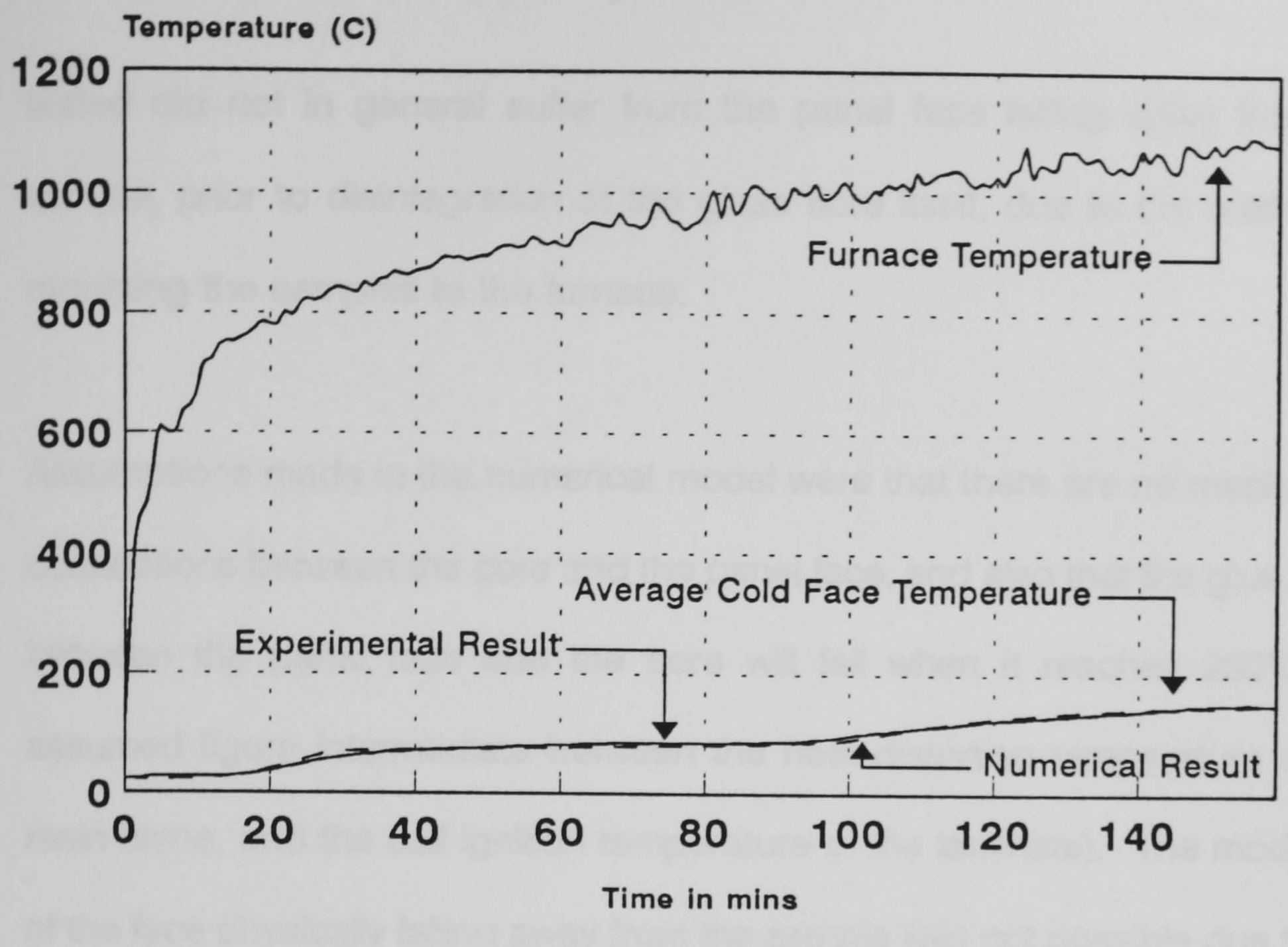

Figure 4.5.1 - BS476 Cellulosic Fire Test
Core Material - Voidfill 7D
Comparison of Experimental and Numerical Results

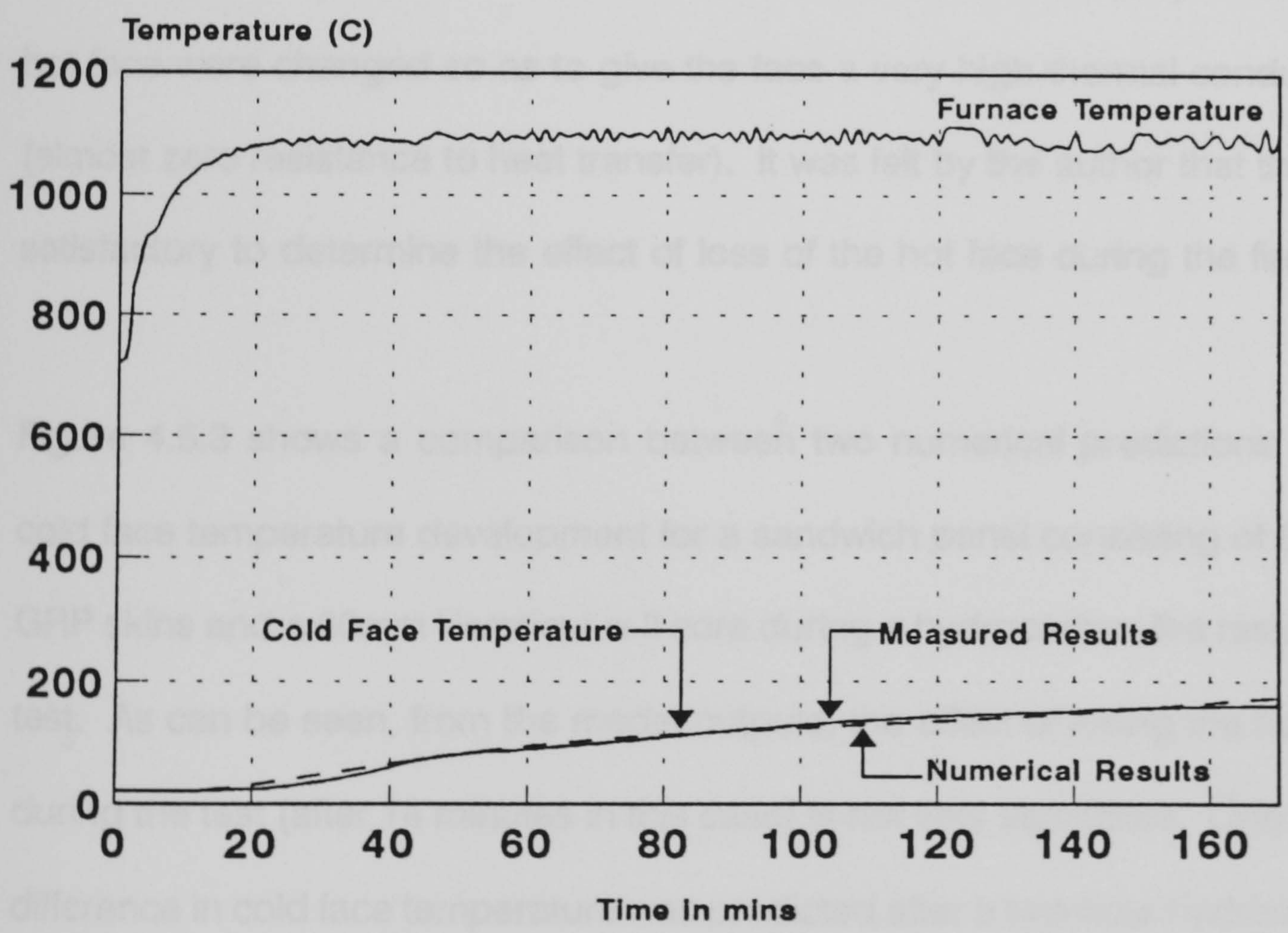

Figure 4.5.2 - DoE Hydrocarbon Fire Test
Core Material - Vermiculux II, Faces GRP (6mm)
Comparison of Experimental and Numerical Results

tested did not in general suffer from the panel face falling away from the sample, prior to disintegration of the glass fibre itself, due to the method of mounting the samples to the furnace.

Assumptions made in the numerical model were that there are no mechanical connections between the core and the panel face, and also that the glue bond between the panel face and the core will fail when it reaches 250°C (an assumed figure intermediate between the heat distortion temperature of the resin alone, and the self ignition temperature of the laminate). The modelling of the face physically falling away from the sample was not possible due to the explicit method of the model. Instead, at the time step when the bond layer between the face of the panel and the core reached 250°C the properties of the hot face were changed so as to give the face a very high thermal conductivity (almost zero resistance to heat transfer). It was felt by the author that this was satisfactory to determine the effect of loss of the hot face during the fire test.

Figure 4.5.3 shows a comparison between two numerical predictions of the cold face temperature development for a sandwich panel consisting of 8.5mm GRP skins and a 60mm Vermiculux II core during a hydrocarbon fire resistance test. As can be seen, from the model outputs, the effect of losing the hot face during the test (after 14 minutes in this case) is not very significant. Only a 5°C difference in cold face temperature was predicted after a two hour hydrocarbon exposure.

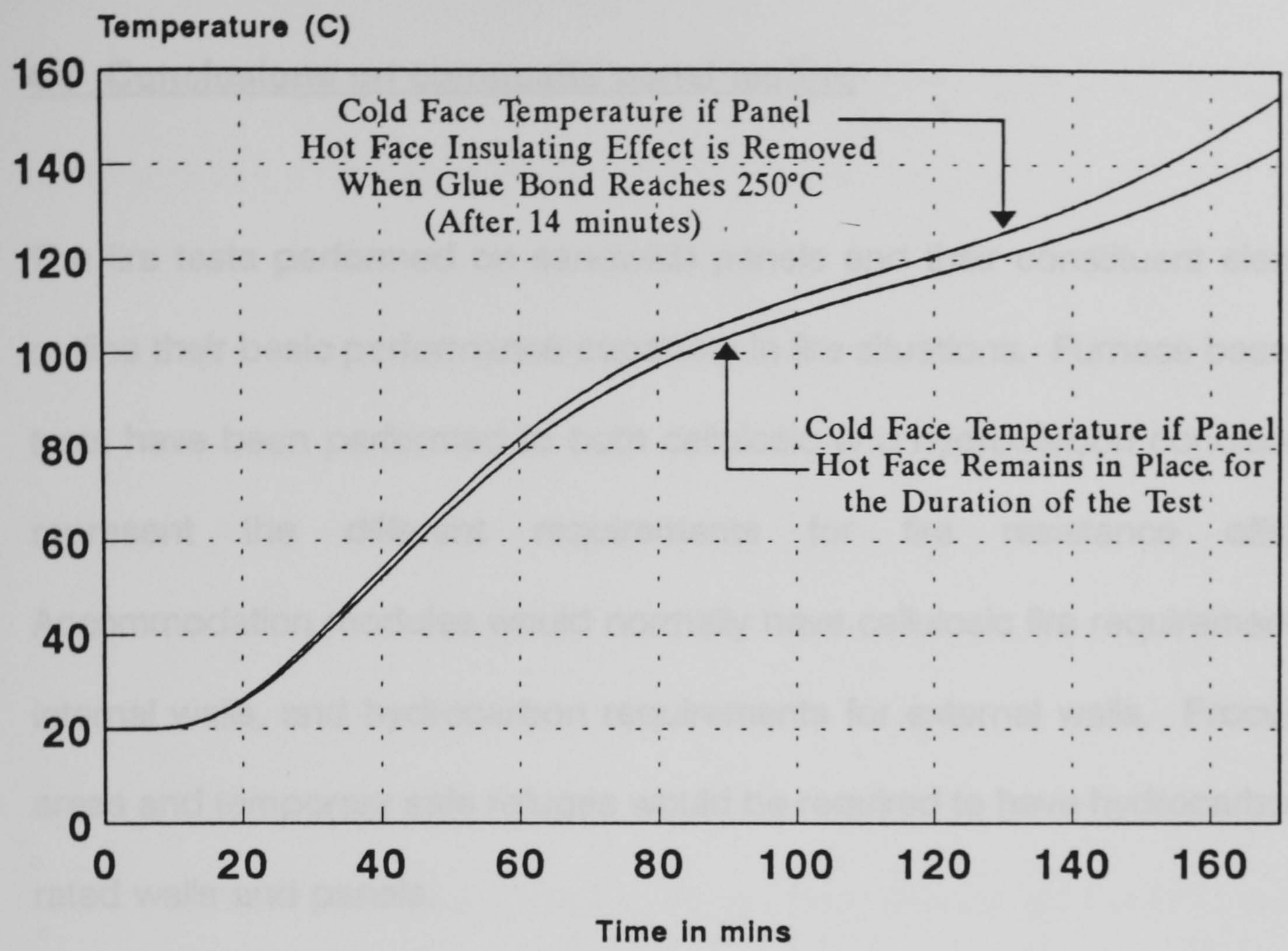

Figure 4.5.3 Numerical Prediction of the Effect of Loss of the Hot Face During a Hydrocarbon Fire Resistance Test of a GRP-Vermiculux Sandwich Panel (Face=8.5mm, Core=60mm)

4.6 Conclusions on composite panel testing

The fire tests performed on sandwich panels and their constituent elements outline their basic performance capability in fire situations. Furnace based fire tests have been performed to both cellulosic and hydrocarbon conditions to represent the different requirements for fire resistance offshore. Accommodation modules would normally have cellulosic fire requirements for internal walls, and hydrocarbon requirements for external walls. Processing areas and temporary safe refuges would be required to have hydrocarbon fire rated walls and panels.

Fire tests have been performed on the state of the art core materials selected for the authors research. It has been shown from these fire tests that the free water content, and the chemically combined water content of these materials has a big effect upon their fire resistance. High free water contents increase the thermal conductivity of the material initially, however, more energy is required to evaporate the water. It was seen that with Vermiculux I, a free water content of approximately 10% increased the insulation failure time from 54 minutes to 86 minutes in DoE hydrocarbon fire test conditions.

In the author's research all hygroscopic core materials were dried to constant mass prior to fire testing. This may not represent realistic conditions, however, it was decided that this represented the "worst case" scenario, and thus would give the minimum possible fire resistance for each material. Hydrocarbon fire

tests performed on core materials alone have shown Voidfill 7D to have good fire properties, and a reasonable fire resistance.

All materials tested to cellulosic fire conditions, with the exception of phenolic foam, have been shown to easily provide an A60 fire rating. The use of materials such as Vermiculux in either of its' formulations may not be economically viable for these low fire performance requirements. The foreseen cost of Voidfill in its standard form, mix 7D, is much lower than that of either Vermiculux or Newtherm, and may make it a viable material for accommodation modules offshore. Investigation into using different refractory cements showed that the best cellulosic fire performance for a Voidfill 7D mix was achieved when Secar-51 cement was used. The post fire test damage observed on the core materials appeared to reduce with increasing alumina content of the cement.

Voidfill 7D, Newtherm and Vermiculux II were all found to be able to provide an H60 fire resistance in the form of steel faced panels. The inclusion of phenolic resin within the Voidfill mix was shown to have a detrimental effect on the materials fire resistance. However, for a nominal 20% resin impregnation an H60 fire resistance was shown to be still possible. Where phenolic resin was included within the Voidfill mix by premixing a substantial reduction in fire performance was observed. Premixed resin Voidfill samples not were considered to be economically viable materials, or suitable materials for panel cores.

Within the research it was found that none of the core materials being investigated were capable of providing an H120 fire resistance alone (at the thicknesses tested). Vermiculux II was almost capable of providing and H120 fire resistance as a core material alone. Vermiculux II (60mm thick) and Voidfill 7D (50mm thick) were both shown to be easily capable of providing and H120 fire rating when used as a panel core between two 6mm thick polyester FRP faces.

The inclusion of ceramic wool within the FRP laminates has been shown to significantly increase the fire performance of a sandwich panel. In the case of a 75mm thick phenolic resin core, the inclusion of 3mm ceramic wool within the face laminate increased the fire resistance from 45 minutes to 65 minutes. It is thought that this ceramic wool inclusion would be most effective if some means of mechanical connection existed between the panel faces and the core material to prevent loss of the hot face during a fire.

It has been shown in the author's research that the apparently superior structural panel design of connecting the faces by means of structural stringers can also achieve an H120 fire rating. It was found that an H120 fire rating could be achieved at a stringer panel weight of 31.5kg/m^2. This panel design represents substantial weight and cost savings over the traditional steel and mineral/ceramic fibre panel design, and also over foreseen panel weights for sandwich panels consisting of thick GRP skins and fire resistant cores such as Vermiculux.

Many different FRP laminates have been fire resistance tested to the DoE hydrocarbon curve, and comparison of these test results shows that phenolic resin laminates have superior performance in fire to the polyester resin laminates as used throughout the authors research. Phenolic resin laminates can suffer from explosive delamination in fire situations due to the formation of high interlaminar pressures from its degradation products. These delaminations can considerably reduce the integrity failure times of phenolic resin laminates in fire tests.

Cone calorimetry has shown that the 6mm polyester FRP laminates used by the author have a positive extinction sensitivity index, and a thermal sensitivity index of greater than one. These together would imply that if 6mm laminates were to be used in fire situations they could be expected to propagate the fire, and would require no external heat source to maintain flaming. Research has shown that using thicker laminates can alleviate this problem, and current thinking is that laminates used should be a minimum of 10mm thick. This could have implications as to the validity of the structural stringer panel design which is designed for relatively thin faces (<5mm).

The thermal decomposition of both polyester and phenolic resins is highly endothermic. The endothermic decomposition reaction of the resins is an important factor in limiting the rate of heat transfer through an FRP laminate, and also limiting the degradation of the laminate itself. Furnace based fire testing has shown that for a 6mm thick polyester-glass laminate the time taken

to complete resin decomposition under hydrocarbon fire test conditions can be in excess of 30 minutes.

Numerical modelling utilising the finite difference method has been shown to be a simple, effective and accurate design tool for the prediction of the heat transfer through FRP laminates, hygroscopic cores, and sandwich panels combining the two. The accuracy of the numerical model is highly dependant on how accurately the material thermal properties are known. It has been shown that systematic curve fitting of numerical predictions to the results of standard fire resistance tests is an effective manner of determining the thermal properties of materials.

Numerical modelling of a 8.5mm thick GRP faced sandwich panel with a 60mm thick Vermiculux II core has shown that the bond line between the laminate and the core material would reach a temperature of 250°C after approximately 14 minutes when exposed to the simulate hydrocarbon fire curve. It was assumed by the author that at this temperature the fire exposed face would fall away from the core. The effect of this loss of the hot face was only marginal on the cold face temperature development.

Chapter 5, following, discusses the fire performance of GRP pipes with different internal conditions (i.e. empty and dry, stagnant water filled, flowing water filled). Chapter 5 also contains information regarding possible methods of fire protecting GRP pipes and the effectiveness of those methods. Further use is

made of the numerical model in chapter 5, and the basic equations for one dimensional heat transfer through the GRP pipe wall are presented together with graphical comparisons of experimental fire test results and numerical predictions.

CHAPTER 5 - FRP PIPES IN FIRE SITUATIONS

5.1 Scope of test variations and methodologies

There has been an abundance of fire testing of GRP pipes over the last twenty years, the main reason behind this being the desire to introduce lightweight corrosion resistant pipe systems into ships and offshore oil rigs, not least in Norway. Within these tests a vast array of test methodologies has been used ranging from furnace testing to the relatively benign heating regimes of SOLAS (Safety Of Life At Sea) and ASTM E-119 to other tests incorporating configurations of multi-burners of either gaseous or liquid fuel, or pool fires.

The testing of pipes to a cellulosic temperature regime is insufficiently aggressive for pipe systems which are to be located in situations where hydrocarbon fires may occur. The heat load to the sample during the test must obviously be in question as must the temperature to which the sample is subjected. These factors warrant an investigation as to what relationship the heat flux and temperature have to the degradation of an FRP pipe. However, that is beyond the scope of this thesis.

The tests in the various available test reports have considered pipes with vastly different internal conditions ranging from open ended and empty to containing nitrogen at low pressure, or from being stagnant water filled at atmospheric pressure to containing flowing water under various pressures. The variety of

failure criteria adopted ranges from post test pressure testing of fire tested samples, time to first leakage to time to complete failure (inability to hold pressure) or even collapse.

In the case of considering pipe failure as the time to first leakage, particularly when considering pipes filled with water under pressure, this could be a vast underestimate to the period of time for which a pipe could operate at or near its design pressure. The failure of the pipe wall in a fire appears to be a progressive mechanism during which the resin matrix burns off, and several micro-cracks form through which small amounts of water can pass and hence cool the remaining unburnt resin. This quasi-steady state acts to generally prolong the endurance of the sample to fire. The progressive failure mechanism acts to reduce the risk of sudden and explosive failure of a pipe containing water, should the sprinkler heads become blocked and the water start to boil, building up significant overpressures very rapidly.

It has been found in a few of the reports that the break down of the resin matrix occurs rapidly at temperatures above 200°C. It has also been reported that the type of resins used for GRP pipes has little effect on the fire performance[50], in particular there is little difference between polyester and epoxy, also that the addition of flame retardants in the resin have little effect.

The effect of different manufacturing methods (i.e. filament winding, centrifugal casting etc) and hence glass volume percentage has only been commented on

briefly in the available test results[51]. Useful comparisons are not readily obtained from comparisons between different investigators due to differing test methods. Bonavent[51] found that filament wound polyester pipe of 100mm internal diameter, 5mm wall thickness could provide similar performance in gasoline sheet fire conditions to centrifugally cast epoxy resin pipes of 7mm wall thickness, and 9mm walled vinyl ester pipes. These samples were also subjected to a propane blowtorch flame for 5 minutes, however, under these conditions, the only sample to maintain its functionability was the 9mm walled vinyl ester pipe. This is almost certainly due to the increased wall thickness. All other samples failed due to total resin combustion. It has been suggested that the higher the glass content the better fire endurance due to the insulating protection of tissue-like layers of glass fibre after the resin has been burned away. This has not been investigated in any literature known to the author, and indeed may not always be the case due to the endothermic nature of the thermal degradation of most resins.

A variety of insulation systems have been used in tests[52,53,54,55,56] and several of the insulation systems have shown more than adequate degrees of protection. There has, however, been no report on how these systems will perform in an aggressive marine environment, or if they are required in the majority of offshore situations.

There is limited information of flame spread and smoke toxicity and obscuration however in those reports containing information on this matter[50,57] have shown

that nearly all the samples passed the requirements of the various standards to which they were tested, and as such GRP piping should cause no problem with respect to these aspects.

In pipe systems exposed to fire conditions, the critical aspects appear to be the performance of the joints, and the internal condition of the pipes. The effects of joints within the pipe loop has been shown in test results or commented on in the conclusions of some of the tests[52,53,55]. It has been shown that with the joints sufficiently insulated they should have no detrimental effect on the overall performance of the pipe system. Belason[55] showed that with pipe loops tested to the ASTM E-119 regime with an 815°C "hot start" even a thin (2.5mm) layer of intumescent coating given to a bolted flanged joint increased its fire resistance from 4-5 minutes to 17-20 minutes. When a 2.5mm intumescent coating was given to the pipe, and a 6.3mm mesh reinforced intumescent coating given to the bolted flange joint, the serviceability of the pipe was extended to 41 minutes, and some degree of integrity was still maintained after that with the pipe/flange being capable of maintaining an internal pressure of 3 bar.

The effect of various internal conditions of the pipes has been investigated in reasonable detail[51,53,54,58]. Bonavent[51] found that a 5mm thick walled filament wound polyester pipe of 100mm internal diameter could survive 15 minutes in the stagnant water filled condition when subjected to a gasoline sheet fire (800-1000°C), but the fire resistance was increased dramatically in the flowing water

condition to 100 minutes. Marks[54] found a similar increase in fire performance between gas filled and stagnant water filled conditions of fire protected filament wound epoxy pipes.

Many tests have been carried out recently on behalf or by the large FRP piping companies such as Ameron or Wavin. These tests tend to be targeted towards the suitability of a product for a particular application. Many tests performed are regarded as commercially sensitive and hence obtaining results may be found difficult. Test results which are readily available include gasoline sheet fires, blow-torch tests, furnace tests, propane multi-burner tests, liquid propane fire tests, propane jet fire tests and alcohol burner fire tests. None of these (with the exception of propane jet fires) would be considered to be as aggressive a test as the simulated hydrocarbon fire furnace based test used for the categorisation of panels. It was decided that there was no reason why FRP pipes should not be exposed to this aggressive test, and different systems of firing and cooling were devised to investigate the performance in different internal conditions.

5.2 The fire testing of dry, empty FRP pipes

5.2.1 Dry unprotected pipes

The preliminary investigation carried out by the author was to investigate the performance of empty and dry pipes exposed to the simulated hydrocarbon regime. Ameron Bondstrand 2000M filament wound epoxy pipes of 3" and 4" internal diameter, 4.3-4.6mm wall thickness, and 53% glass by volume were selected as typical samples. One end of the sample was sealed with a Vermiculux bung and a mixture of sodium silicate and ball clay. The sealed end of the pipe was inserted into a cold furnace through a circular aperture cut in a blanking panel to a depth of 1m.

The furnace used for the dry pipe testing reported in this chapter was the 1.5x1.5x1.5m active volume furnace as described in chapter 4. The furnace temperature was computer controlled to follow the hydrocarbon curve (the target temperature is referred to as the "set point" in this thesis). After the required exposure time, the pipe sample was drawn from the furnace whilst being smothered with a fire blanket and also subject to a carbon dioxide fire extinguisher. Once any flames had been extinguished, the pipe was filled with water taking care not to wet the outside of the pipe. This method was used to simulate the sudden cooling effect of a fire water system starting up, and also served to freeze in time the condition of the pipe wall. After the pipe was fully cooled it was pressurised to the working pressure or the maximum pressure

achievable. Tests were performed of increasing duration to determine the limit of fire exposure of the pipe whilst retaining its serviceability. Exposures of 40, 60, 80, 90 and 120 seconds were performed and figure 5.2.1 shows the furnace output for a 4" pipe hydrocarbon exposure. Graphical outputs showed that the furnace temperature did not achieve the hydrocarbon curve in the first 60 seconds due to an unavoidable time delay between the computer signal and the full opening of a motor driven gas valve. Comparison of the set point and the actual furnace temperature showed that it would be reasonable to assume that the datum time (the effective start time of the test) should be taken as +20 seconds. That is, if a sample failed after 100 seconds it should be considered as only having had an effective exposure of 80 seconds.

After cooling of the pipes they were pressure tested to a maximum static internal pressure of 16 bar (the original rating of the pipes). The pipes exposed to the simulated hydrocarbon curve for 80 seconds withstood this pressure with no leakage, however, pipes which had longer exposures would not hold the pressure.

These initial tests suggested that the safe fire resistance of unprotected GRE pipes under these conditions could be as low as 60 seconds, and that functionality of the pipe was lost after the internal wall temperature exceeded about 200°C (the internal temperature corresponding to an effective exposure time of 60 seconds). This "200°C" failure criterion is extensively used later in this chapter. The deluge system of an offshore platform would be expected to

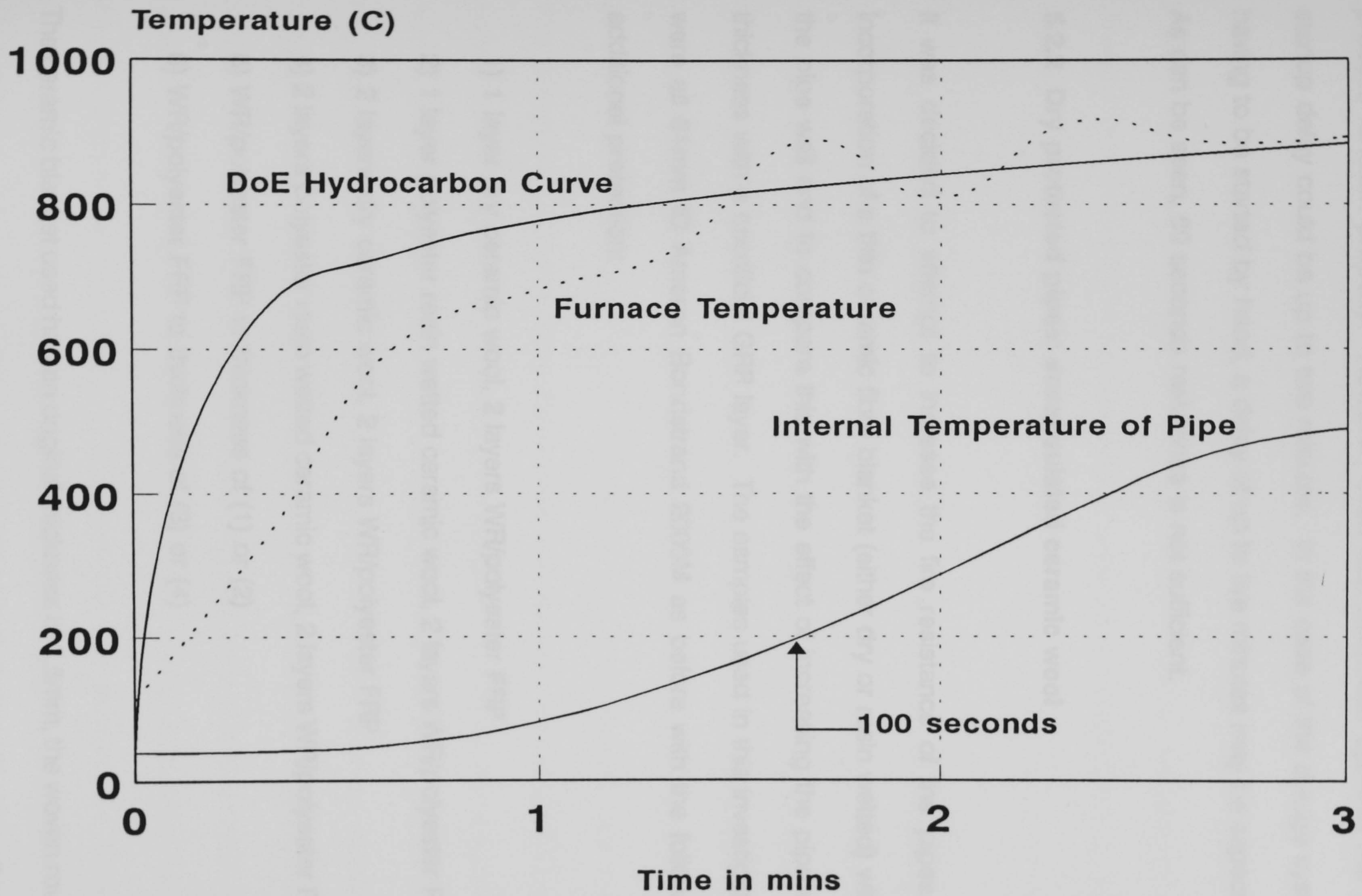

Figure 5.2.1 Ameron 2000M 4" Epoxy Pipe Hydrocarbon Fire Test, Empty and Dry

run within the first 30 seconds should the automatic detection and startup process function properly. However, even with automatic systems the true startup delay could be up to two minutes. In the case of the deluge system having to be started by hand, a delay of up to five minutes may be expected. As can be seen, 60 seconds resistance is not sufficient.

5.2.2 Dry protected pipes: encapsulated ceramic wool

It was decided to attempt to increase the fire resistance of the pipes by incorporation of a thin ceramic fibre blanket (either dry or resin wetted) within the pipe wall and to compare this with the effect of increasing the pipe wall thickness with a sacrificial GRP layer. The samples used in this investigation were all 81mm ID Ameron Bondstrand 2000M as before with the following additional protection:

1) 1 layer dry ceramic wool, 2 layers WR/polyester FRP

2) 1 layer polyester resin wetted ceramic wool, 2 layers WR/polyester FRP

3) 2 layers dry ceramic wool, 2 layers WR/polyester FRP

4) 2 layers polyester resin wetted ceramic wool, 2 layers WR/polyester FRP

5) WR/polyester FRP to thickness of (1) or (2)

6) WR/polyester FRP to thickness of (3) or (4)

The ceramic blanket used had an original thickness of 3.5mm, the woven roving was 600gsm and in all cases the resin used to form the protection was Crystic

489 polyester resin with catalyst M. Arrangements 5 and 6 were control samples to investigate whether the protection improvement was due to the ceramic inclusion or the general increase in thickness of the pipe wall. When the ceramic blanket was wetted with polyester resin and pressed in place the thickness of each layer was reduced to approximately 1.5mm. The subsequent layers of resin wetted woven roving glass fibre were to produce a hard, durable finish to the pipes.

The pipes were tested using the same method as described previously for dry, unprotected filament wound epoxy pipes. Figures 5.2.2 and 5.2.3 following show the fire test results for three and five minute hydrocarbon fire tests on the protected pipes. Post cooling pressure tests showed that an increase in the pipe wall thickness alone was not as major factor in the increase in fire resistance as the material used. The pipes were instrumented with three thermocouples, each touching the internal wall surface, and located at the centre of the one metre exposed length of the pipe. A single layer of ceramic wool in either the dry or resin wetted condition, plus two finishing layers of GRP wrap was sufficient to increase the functionality of the pipe after cooling from 60 seconds fire testing to three minutes, however, the corresponding thickness of GRP alone was not, and the post fire test pipes were unable to hold any pressure. Two layers of the resin wetted ceramic wool plus finishing layers would preserve the functionality of the pipes for five minutes fire testing. However, when ceramic wool was used in the dry condition, some integrity of the pipes was lost, and the maximum maintainable internal pressure was only

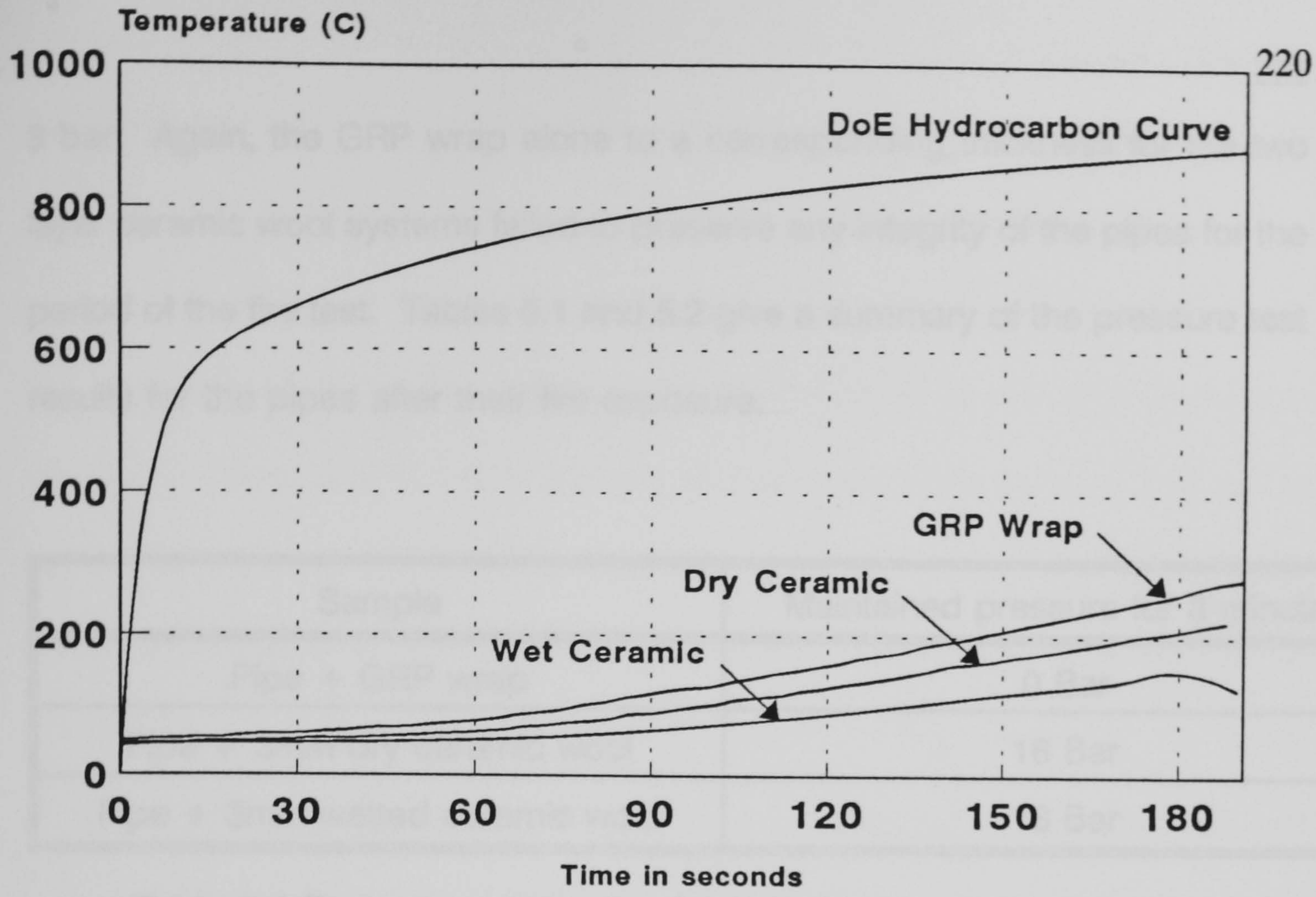

Figure 5.2.2 - Internal wall temperatures of Ameron GRE pipes fire tested for 3 minutes

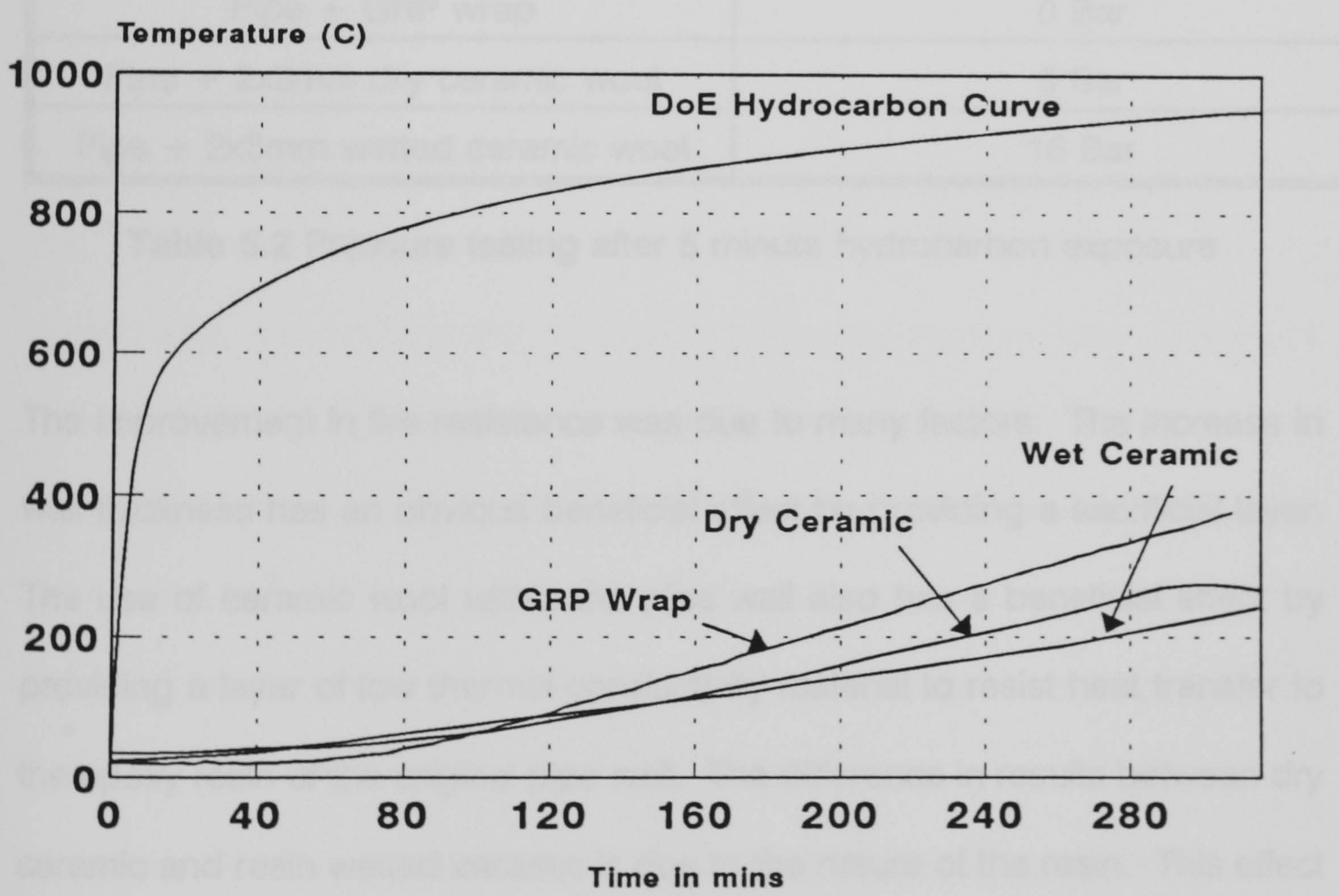

Figure 5.2.3 - Internal wall temperatures of Ameron GRE pipes fire tested for 5 minutes

8 bar. Again, the GRP wrap alone to a corresponding thickness for the two layer ceramic wool systems failed to preserve any integrity of the pipes for the period of the fire test. Tables 5.1 and 5.2 give a summary of the pressure test results for the pipes after their fire exposure.

Sample	Maintained pressure for 3 minutes
Pipe + GRP wrap	0 Bar
Pipe + 3mm dry ceramic wool	16 Bar
Pipe + 3mm wetted ceramic wool	16 Bar

Table 5.1 Pressure testing after 3 minute hydrocarbon exposure

Sample	Maintained pressure for 3 minutes
Pipe + GRP wrap	0 Bar
Pipe + 2x3mm dry ceramic wool	8 Bar
Pipe + 2x3mm wetted ceramic wool	16 Bar

Table 5.2 Pressure testing after 5 minute hydrocarbon exposure

The improvement in fire resistance was due to many factors. The increase in wall thickness has an obvious beneficial effect by providing a sacrificial layer. The use of ceramic wool within the pipe wall also has a beneficial effect by providing a layer of low thermal conductivity material to resist heat transfer to the epoxy resin of the original pipe wall. The difference in results between dry ceramic and resin wetted ceramic is due to the nature of the resin. This effect is due to the thermal degradation of polyester resin being highly endothermic, this in effect keeps the pipe wall cool during the fire test. It is possible that with

resins other than polyester the wetting of the ceramic blanket may be more, or less, effective in increasing the fire resistance of the composite pipe.

If the ceramic wrapping of pipes were to be performed as part of an industrial process it is likely that the resin used would need to be the same as that of the pipe itself. Due to this Ameron supplied some of the appropriate resin for further investigations. It was not realised at the time that the resin needed to be pre-heated before it could be used, due to its high viscosity. At room temperature the resin was too viscous to penetrate the ceramic blanket, an hence the resulting wrap was effectively "dry". Again, the pipe was finished with two layers of woven roving glass and resin to provide a hard finish to the system.

These epoxy-ceramic dry wraps were each approximately 3.5mm in thickness. One, two and three layer systems were used, and the appearance of the finished pipe was rather bulky compared to the polyester system. The pipes again were instrumented with three internal thermocouples touching the internal wall surface, half way along the 1 metre length of the pipe. In these tests however, due to previous experience with burning epoxy pipes it was decided that both ends of the pipe should be sealed, and the entire pipe be fully immersed within the furnace. The hydrocarbon test was run until the internal temperature of the pipe reached 200°C at which point it was assumed that the pipe had failed. The pipes were not able to be pressure tested after their fire exposure due to the nature of the fire test method. Figure 5.2.4 shows the time

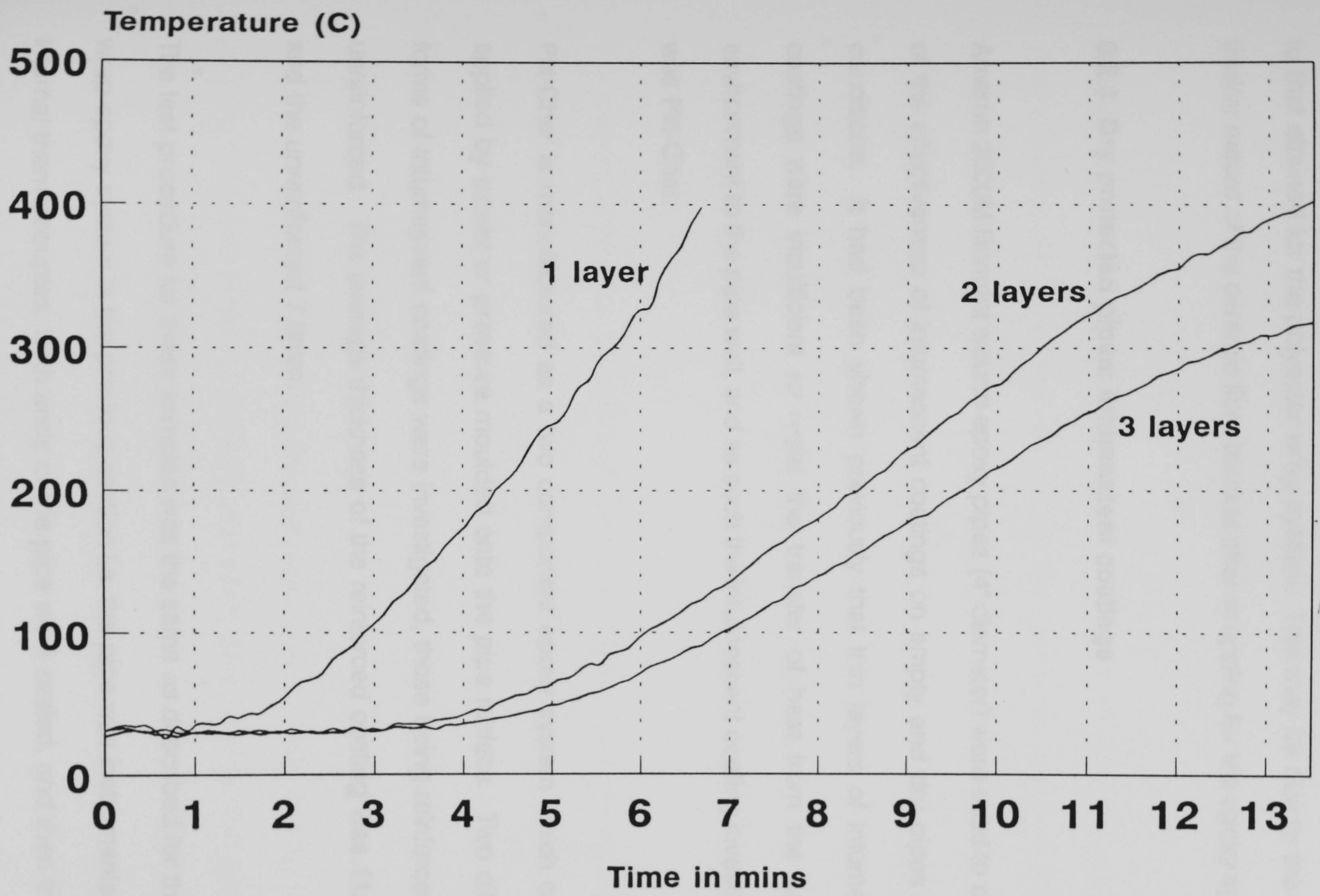

Figure 5.2.4 Ameron Epoxy Pipes Protected by Ceramic Fibre and WR Glass Mat Hydrocarbon Fire Tests

temperature data for one, two and three layers of wrap. As can be seen, the performance of the dry wrap system with epoxy resin appears to be superior to that attained for the polyester wrap system. This may be due to the rather thicker nature of the ceramic fibre blanket after wrapping for the epoxy system.

5.2.3 Dry protected pipes: Intumescent coatings

Ameron 2000M filament wound epoxy pipes (4" diameter) were used to assess of the effectiveness of intumescent coatings on empty and dry pipes in fire conditions. It had been shown previously that thin layers of intumescent coatings were insufficient to resist the transfer of heat from the furnace environment to the pipe wall, and as such the intumescent coating investigated was Pitt-Char.

Pitt-Char is manufactured as a two component epoxy system which can be applied by trowel or pressure moulded onto the pipe surface. Two different forms of intumescent coatings were investigated, those being reinforced and unreinforced. The average thickness of the reinforced coating was 11.6mm, and the unreinforced 7.6mm.

The test procedure for these samples was the same as described for the dry-wrap epoxy system in the previous section i.e. the pipe was instrumented with internal thermocouples, both ends of the pipe were sealed, and then the test section was fully immersed within the furnace. The failure criterion as before

was when the internal wall temperature of the pipe rose above 200°C. Figure 5.2.1 (previously) shows the fire test result of a 4" Ameron 2000M filament wound epoxy pipe when exposed to hydrocarbon fire test conditions. This is a typical result and has been used for the basis of all subsequent comparisons.

Figures 5.2.6 and 5.2.7 show typical test results for the reinforced and unreinforced systems respectively. It can be seen from these that the two systems perform very similarly with respect to increase of internal wall temperature when exposed to the simulated hydrocarbon fire test. The use of the intumescent coating increased the time to 200°C of the internal wall temperature from 100 seconds for the bare pipe to approximately 11 minutes for each of the two intumescent systems, more than a factor of 6 increase.

The similar insulation performance of the two coatings, despite the significantly different thicknesses (7.6mm .v. 11.6mm) was probably due to the intumescence of the reinforced coating being restrained by the reinforcement. Post test inspection of the two different Pitt-Char systems showed that the unreinforced system exhibited a much higher degree of expansion, however,it was heavily fissured compared to the reinforced system. Another point of note was that the unreinforced coating was quite easily detached from the pipe wall. This combination of higher degree of expansion, balanced by greater fissuring also could explain why the fire performance of the two coatings was so similar.

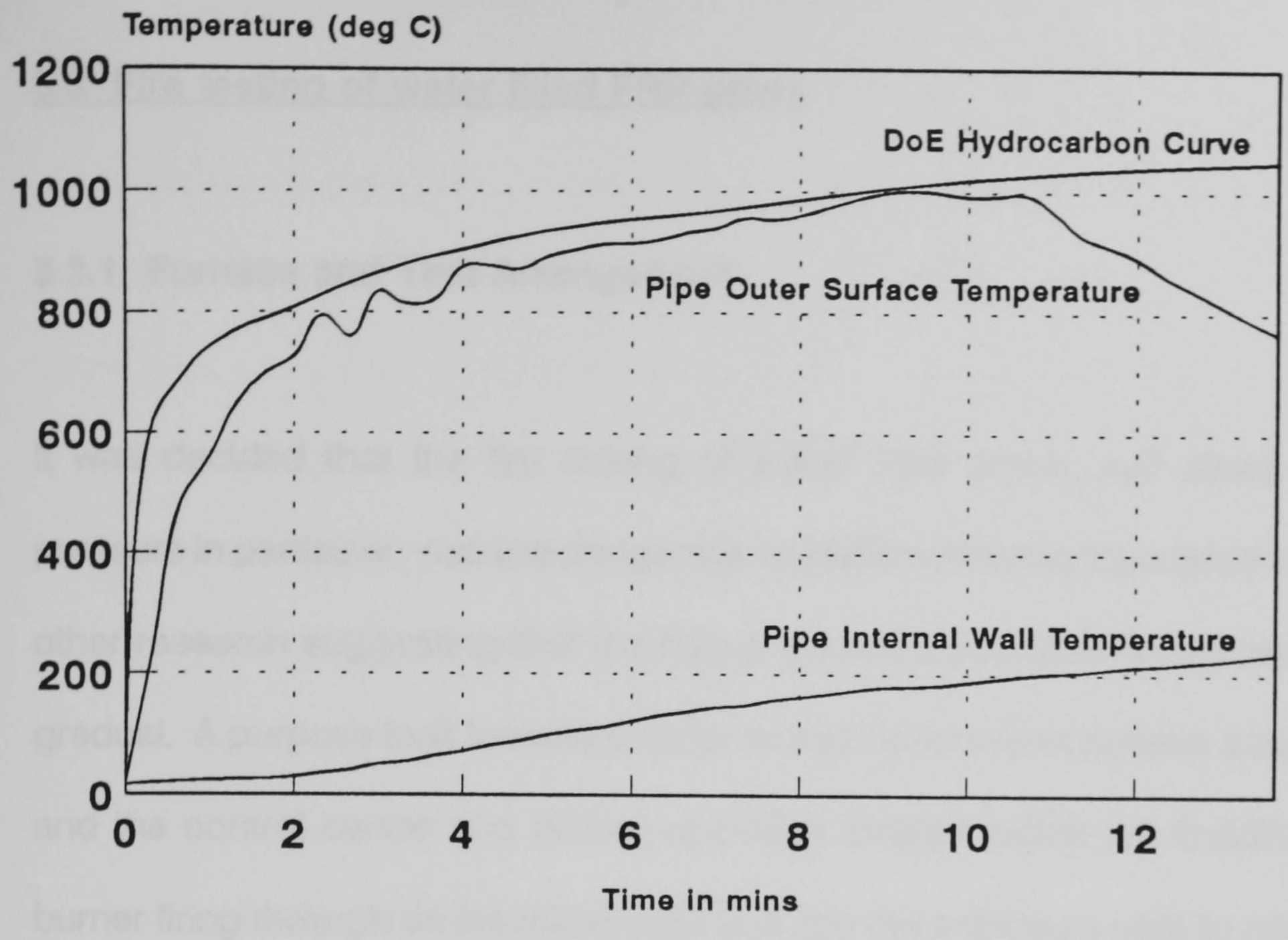

Figure 5.2.5 Ameron 4" 2000M Epoxy Pipe with Intumescent Pitt-Char (7.5mm) Coating Hydrocarbon Fire Test

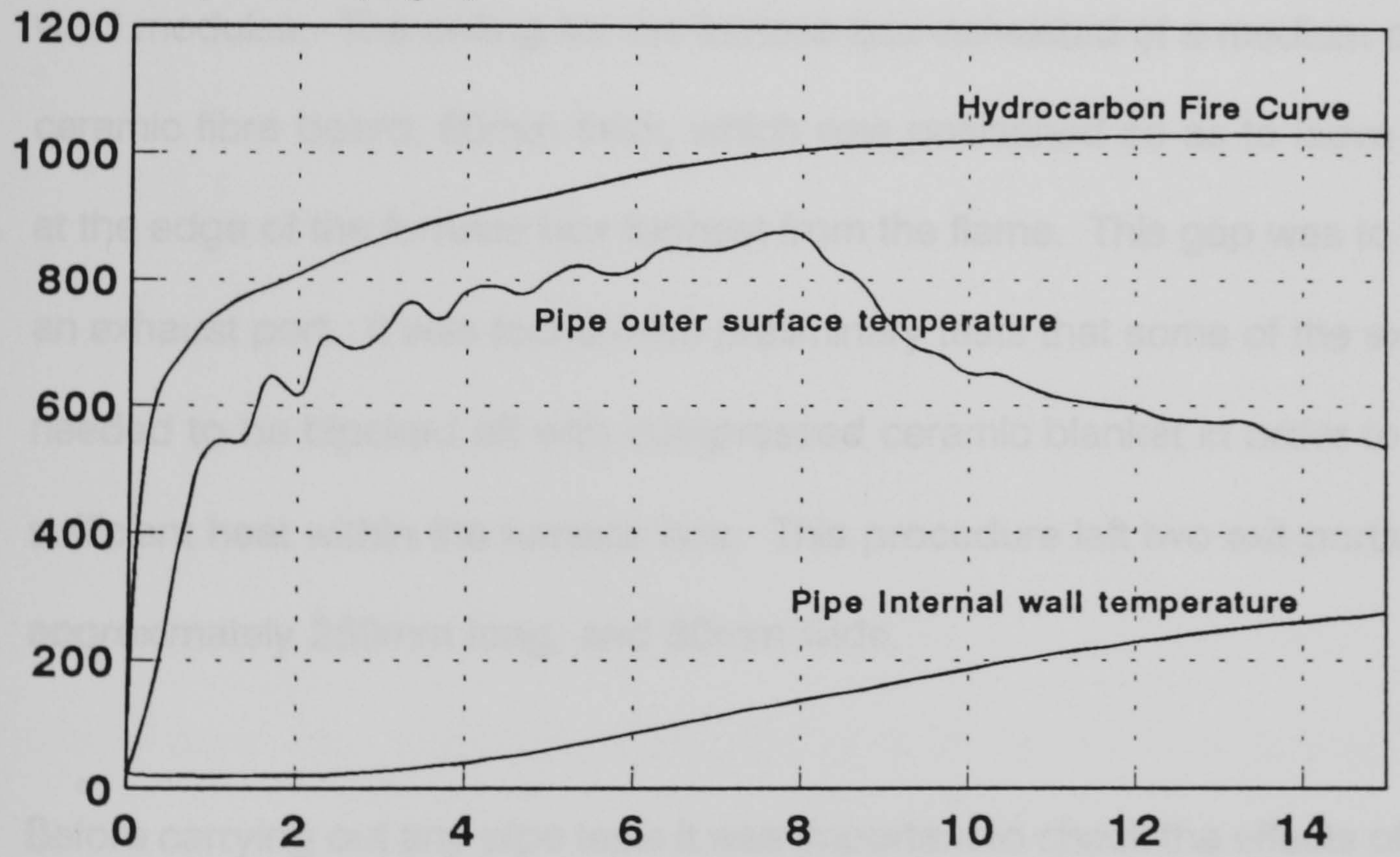

Figure 5.2.6 Ameron 4" 2000M Epoxy Pipe with Reinforced Pitt-Char (11.5mm) Hydrocarbon Fire Test

5.3 Fire testing of water filled FRP pipes

5.3.1 Furnace and Test Arrangement

It was decided that the fire testing of water filled pipes, and pipes under pressure in particular, was too dangerous to perform within a laboratory despite other research suggesting that the failure mechanism of GRP in fire was very gradual. A purpose built furnace enclosure was constructed outside a building, and the control centre and burner unit were located inside the building (the burner firing through an insulated steel wall into the enclosure unit) to minimise danger. The furnace itself was constructed from concrete blocks which were dry fitted together (no mortar), and lined with a 200mm thick layer of ceramic wool modules. The ceiling for the furnace box consisted of a medium density ceramic fibre board, 60mm thick, which was positioned so as to leave a gap at the edge of the furnace box furthest from the flame. This gap was to act as an exhaust port. It was found from preliminary tests that some of the exit port needed to be blocked off with compressed ceramic blanket in order to retain sufficient heat within the furnace box. This procedure left two exit ports, each approximately 250mm long, and 50mm wide.

Before carrying out any pipe tests it was important to check the effects of water being spilled into a hot furnace. This scenario was likely to occur if a water filled pipe burst or burned through during testing. Accordingly, the furnace was fired and heated to 1100°C, and water was deliberately introduced through the

furnace lid at increasing rates from 2 litres/minute up to 18 litres/minute. Figure 5.3.1 shows the decline in furnace temperature which occurred with the introduction of water to the furnace. No explosive effect was observed from the water being suddenly transformed into steam, and as the water input was increased, excess water could be seen flowing from the bottom of the block walls. No damage occurred to the lining other than some local contraction of thickness and some staining. Subsequently it took a long time to dry the furnace lining out.

For practical reasons, it was necessary that the water system should be run under low flow and low pressure conditions. The water system was open ended using a stand pipe at the input and output of the furnace to maintain a head of approximately 1.2m of water. Figures 5.3.2 and 5.3.3 show cross sections through the furnace. The test pipe was fitted with flanges for convenience in connecting it to the permanent standpipe structures. After the test the fire damaged pipe complete with flanges could be removed from the furnace for pressure testing. The 10° inclination of the pipe was to reduce steam formation, and hence localised hot-spots. K type inconnel sheathed thermocouples to measure internal wall temperatures and mean water temperature were supported within the pipe by means of a polycarbonate spring. In addition to these, the external pipe wall temperature was measured, and also input and output water temperature. Figure 5.3.4 gives the locations of thermocouples used. A drain outlet was provided at the lowest point of the system so that after cooling the water could be emptied from the pipe system

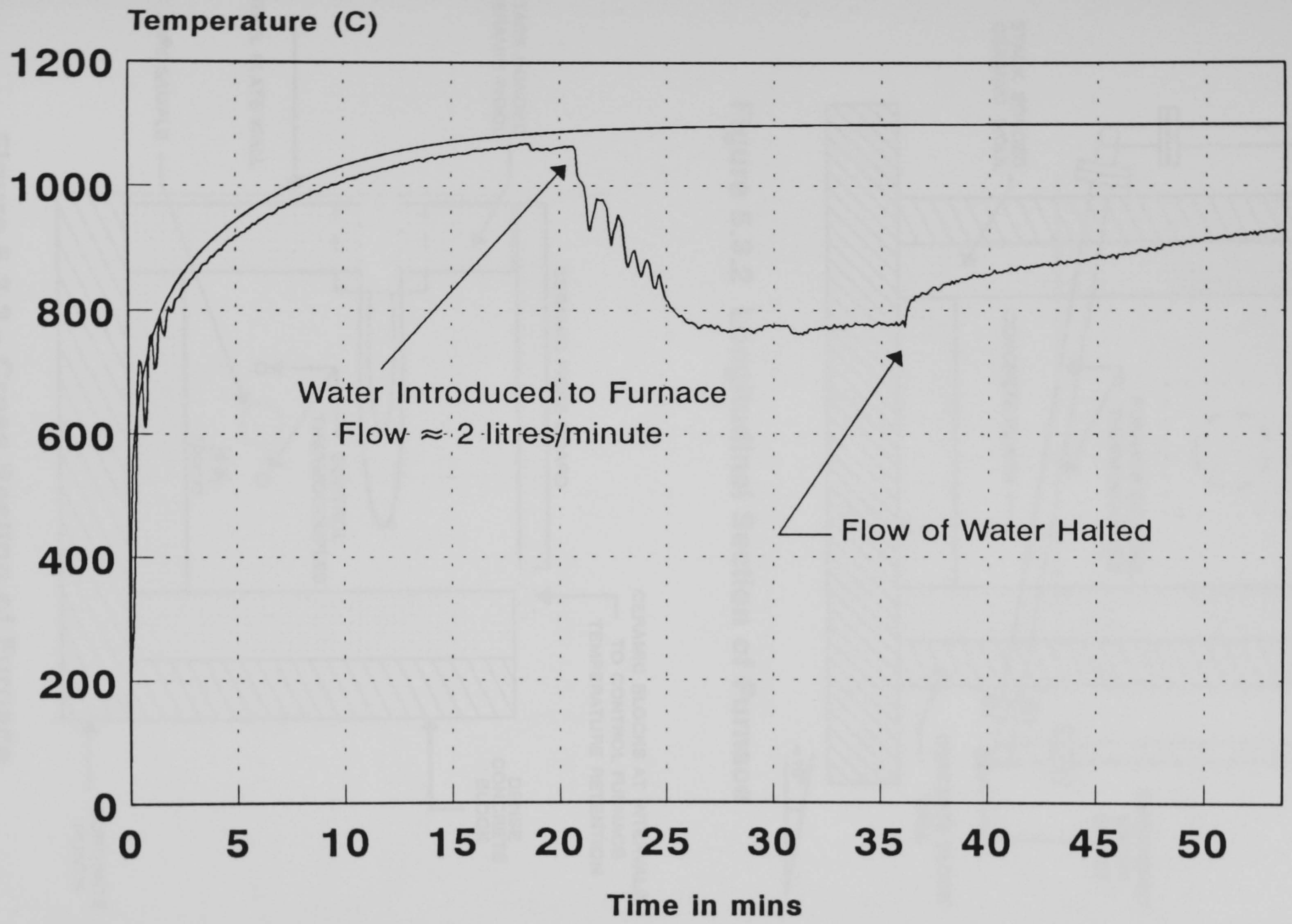

Figure 5.3.1 - Furnace Reaction to Water Spill at high temperature

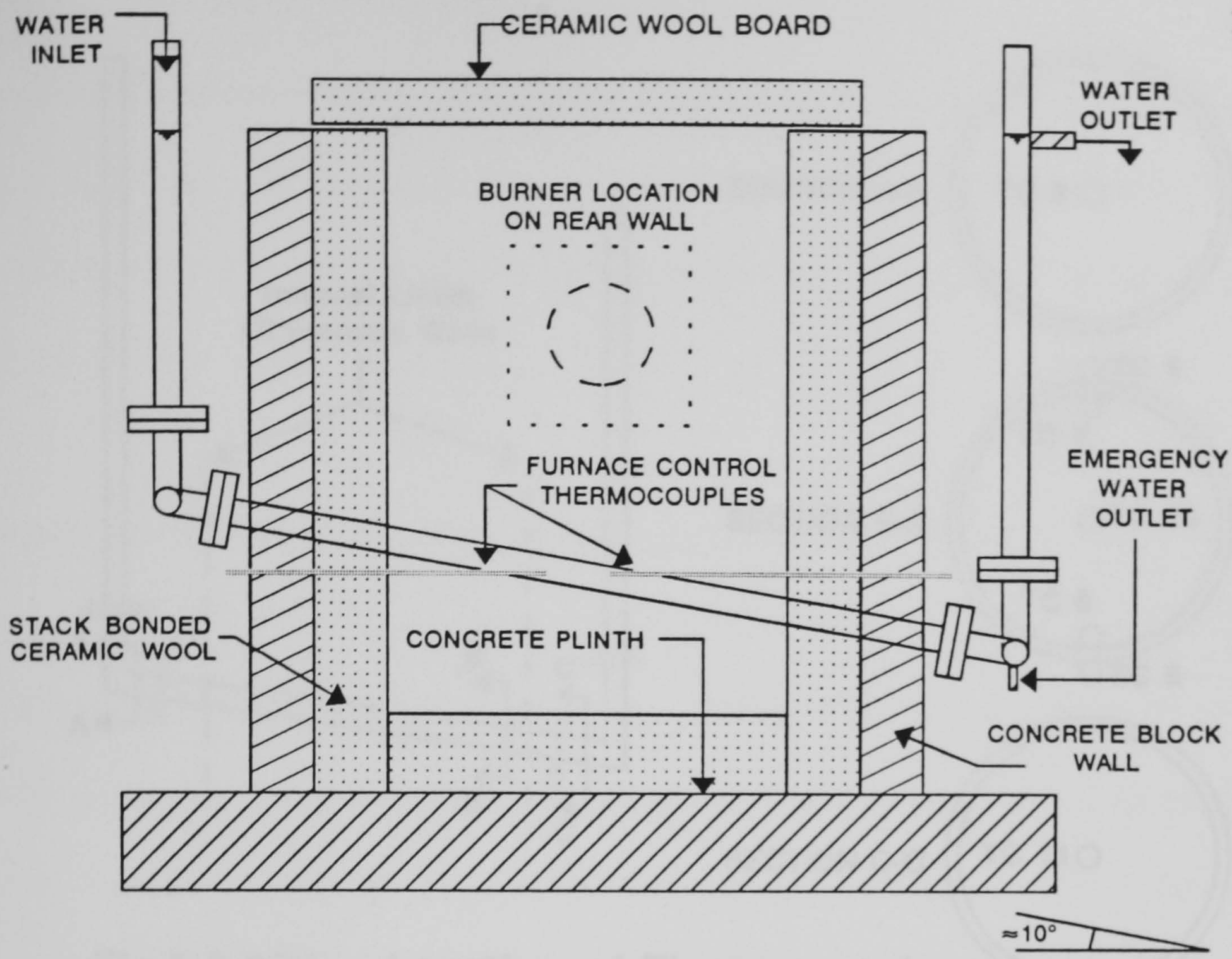

Figure 5.3.2 Longitudinal Section of Furnace

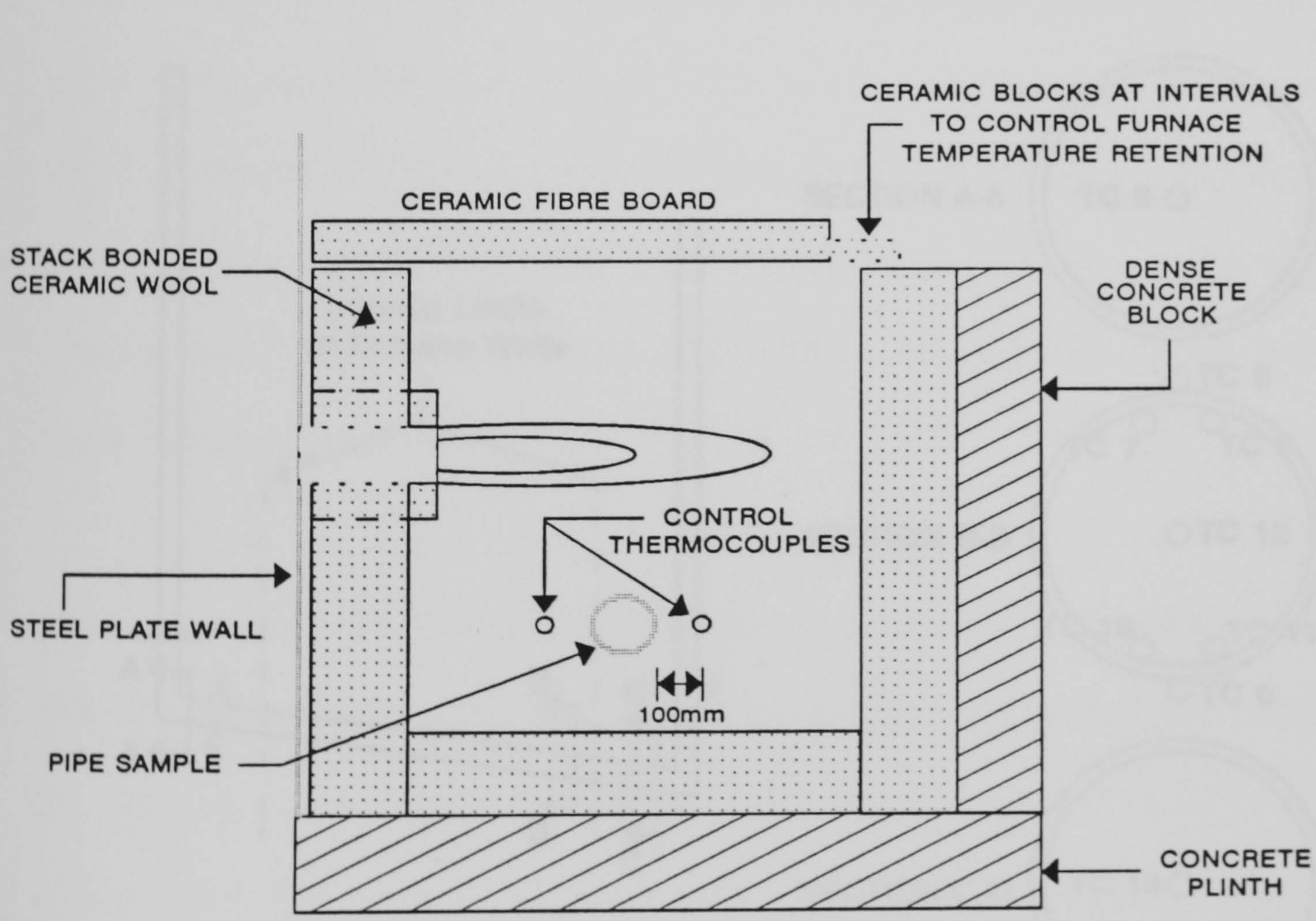

Figure 5.3.3 - Cross Section of Furnace

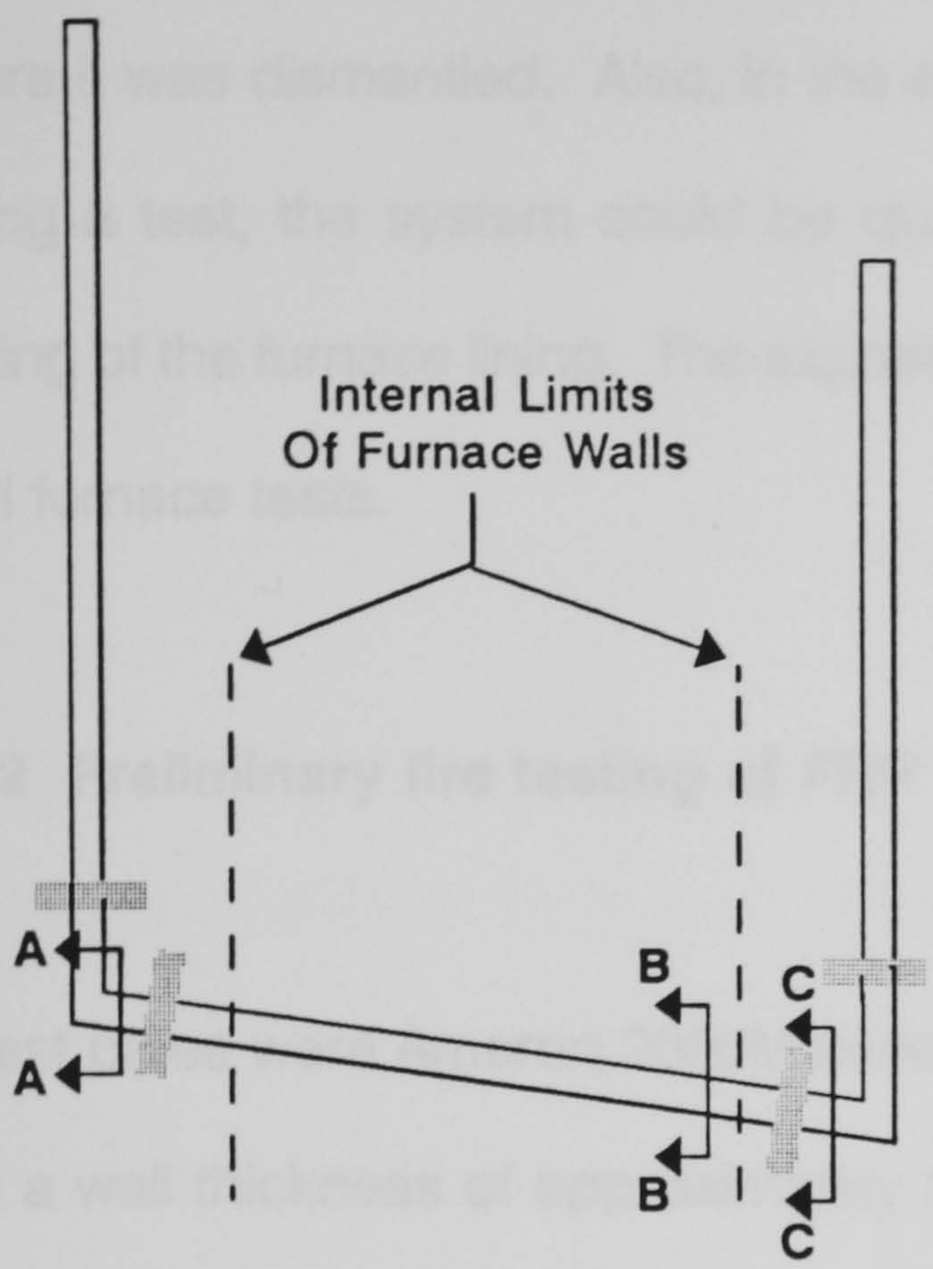

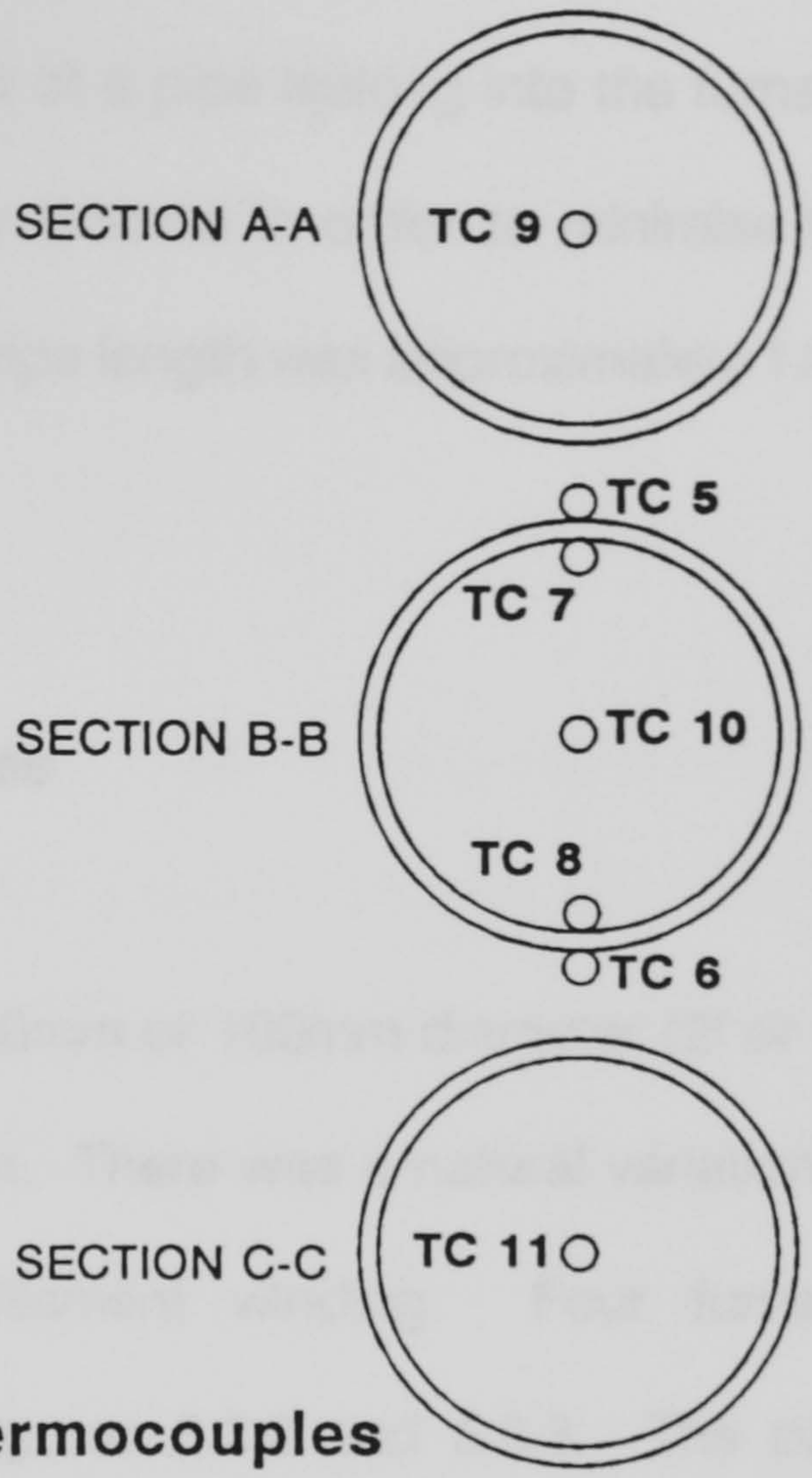

Fig 5.3.4(a) - Location of Thermocouples

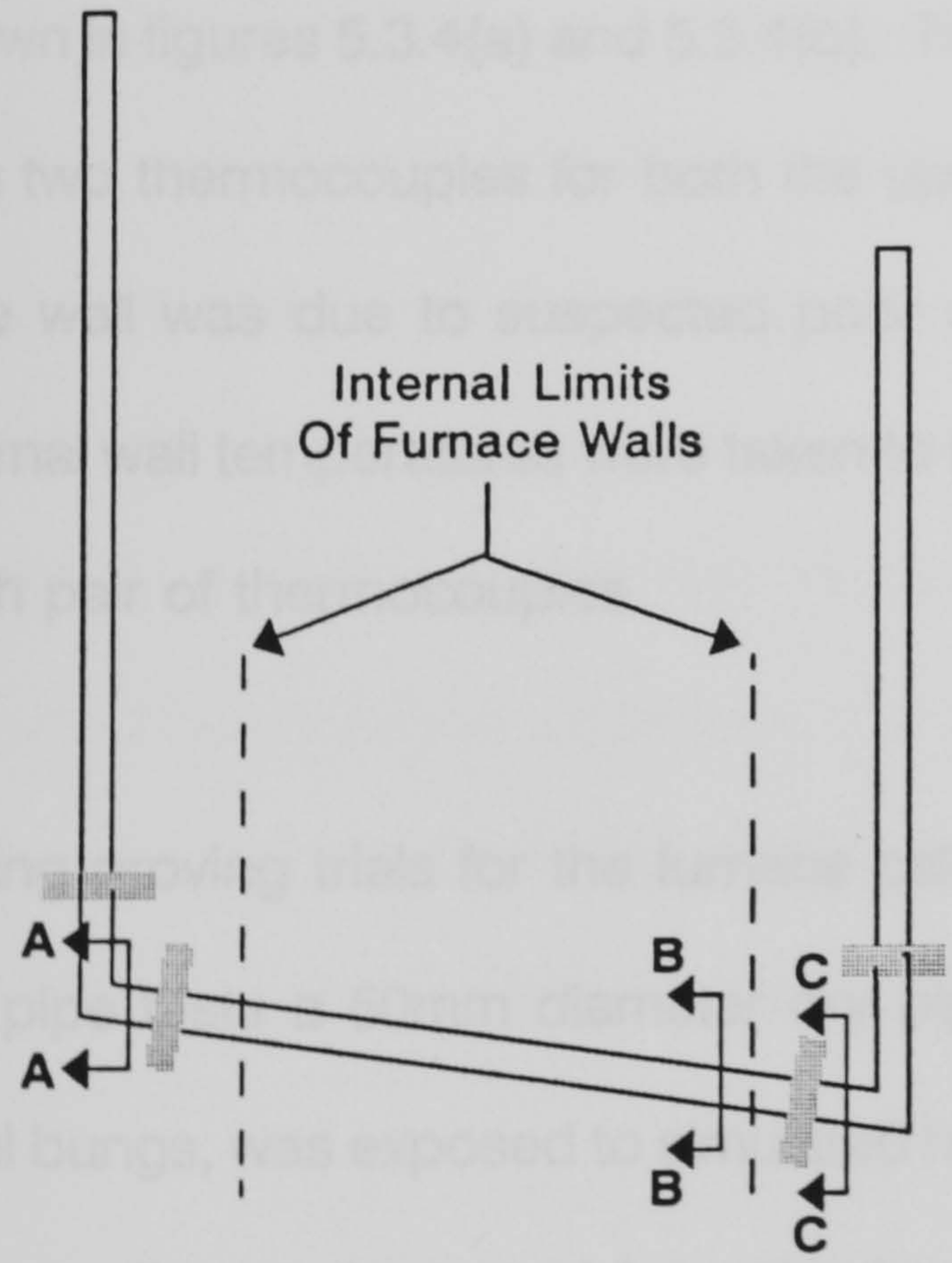

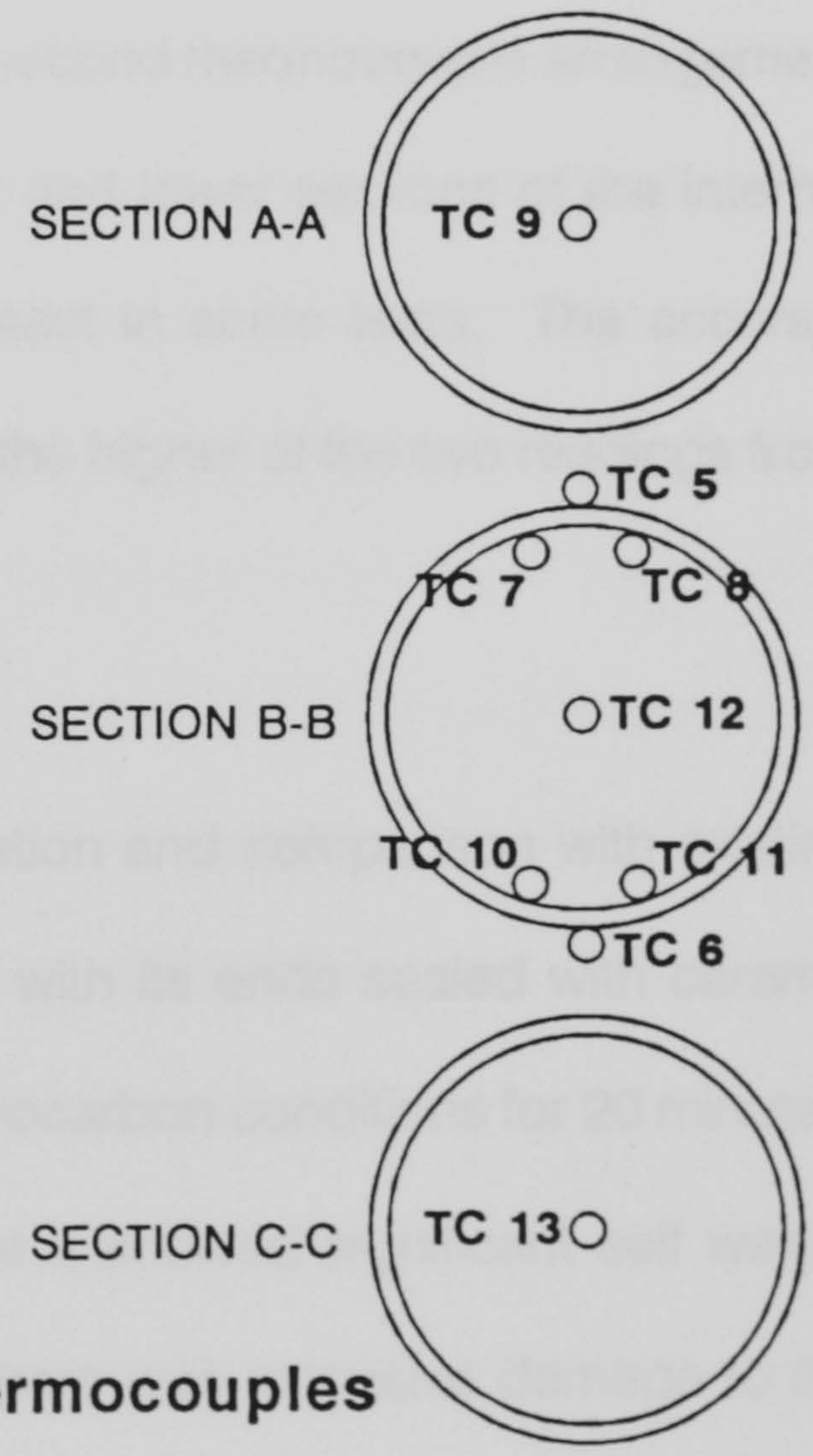

Fig 5.3.4(b) - Location of Thermocouples

before it was dismantled. Also, in the event of a pipe leaking into the furnace during a test, the system could be quickly drained in order to minimise the wetting of the furnace lining. The exposed pipe length was approximately 1.0m in all furnace tests.

5.3.2 Preliminary fire testing of FRP pipes

All test pipes were Ameron 2000M series, 50mm or 100mm diameter (2" or 4") with a wall thickness of approximately 5mm. There was a natural variation in wall thickness due to the pattern of filament winding. Four furnace thermocouples were used as shown in figures 5.3.2 and 5.3.3. The pipe section instrumentation was located at the most critical position, and the layouts shown in figures 5.3.4(a) and 5.3.4(b). The second thermocouple arrangement with two thermocouples for both the upper and lower sections of the internal pipe wall was due to suspected poor contact in some tests. The accurate internal wall temperatures were taken to be the higher of the two readings from each pair of thermocouples.

During proving trials for the furnace calibration and comparison with existing dry pipe tests a 50mm diameter dry pipe, with its ends sealed with ceramic wool bungs, was exposed to simulated hydrocarbon conditions for 20 minutes. After cooling and removal from the furnace it showed significant self weight deflection but was structurally coherent. There was extensive damage to the internal bore of the pipe and it was unable to hold water at atmospheric

pressure. The internal temperature reached 200°C after 1 minute and 35 seconds. Allowing the +20s datum as for previous dry pipe tests, this compared well with the 80 second dry functionability limit as determined previously.

A second 50mm diameter pipe was tested under flowing water internal conditions on each of three days. On the first day the flow rate was 18 litres per minute and the exposure time was 33 minutes (hydrocarbon curve). Figures 5.3.5 and 5.3.6 show the test results for this exposure of the pipe. The water flow was maintained until the furnace had cooled to below 150°C at which time it was left in the stagnant water condition. The same test piece was then re-tested on the second day. Over a 2 hour exposure to the hydrocarbon curve the flow of water through the pipe was reduced in stages from 18 to 7 litres per minute (figures 5.3.7 and 5.3.8). Figure 5.3.6 shows that during the test the internal temperature of the pipe exceeded 100°C for two short periods as the water flow was adjusted. The cooled pipe still appeared to be in good condition, and on the third day the same test piece was again exposed to simulated hydrocarbon conditions, this time with a flow rate of 3.5 litres/minute (figures 5.3.9 and 5.3.10). Figure 5.3.10 shows that the critical area of the pipe was isolated by steam from the cooling effects of the water for the majority of the test.

After cooling of the 50mm pipe after its third exposure it was removed from the furnace and pressure tested to 16 bar. The pipe maintained its functionability

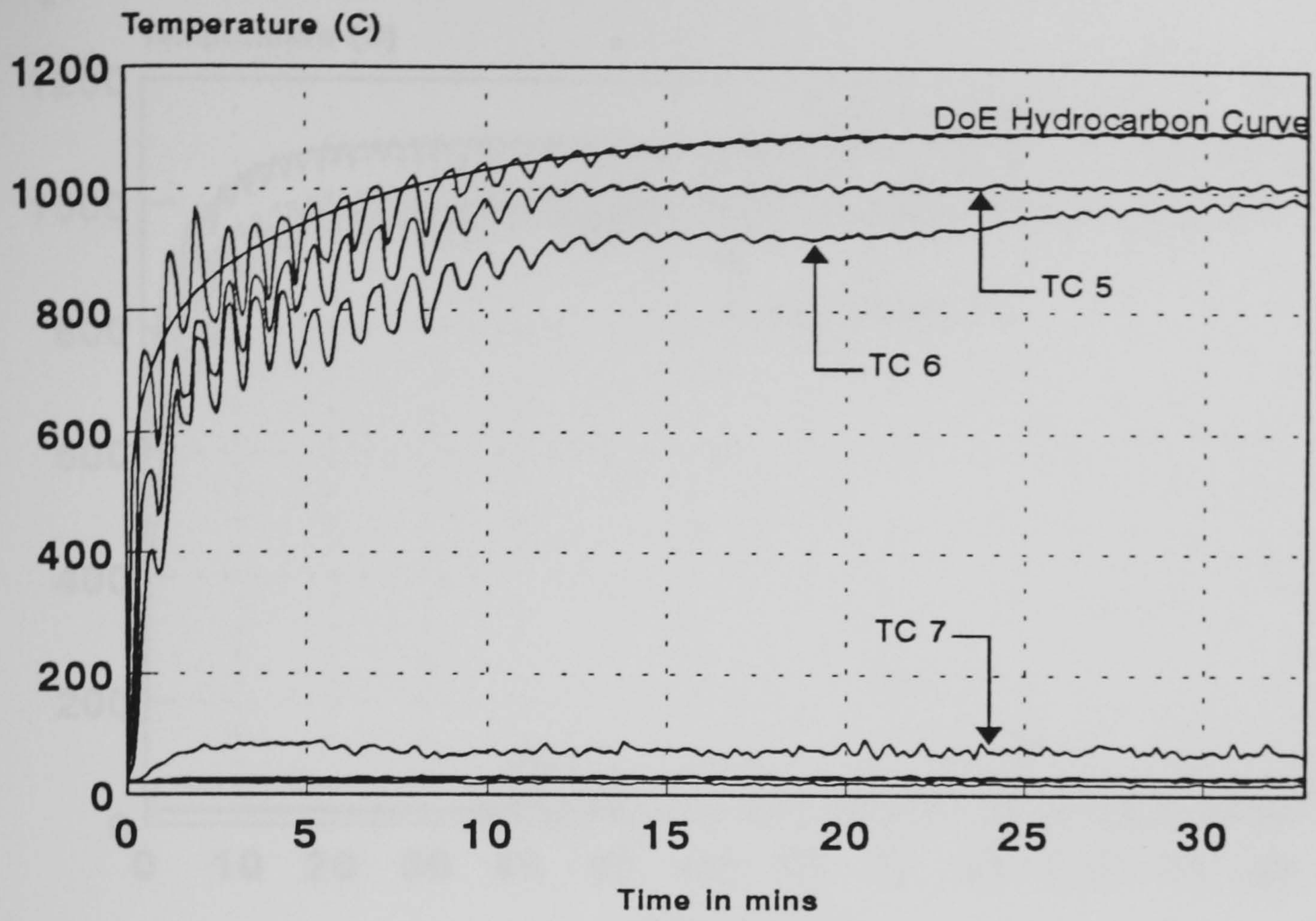

Figure 5.3.5 - Ameron Bondstrand 2000M, 2" GRE Pipe
Flowing Water at 18 l/min, Hydrocarbon Fire Test
All Thermocouples

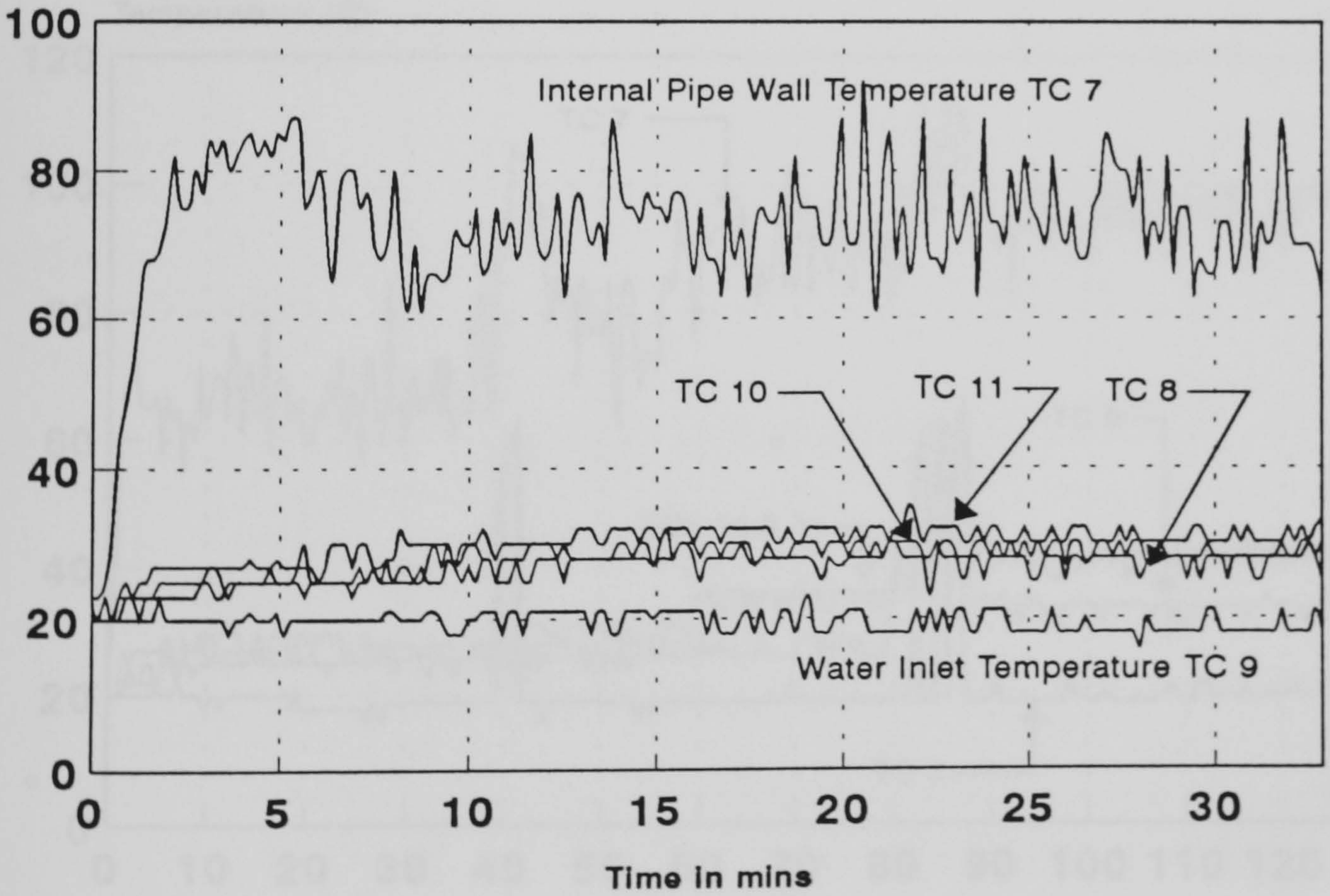

Figure 5.3.6 - Ameron Bondstrand 2000M, 2" GRE Pipe
Flowing Water at 18 l/min, Hydrocarbon Fire Test
Internal Thermocouples Only

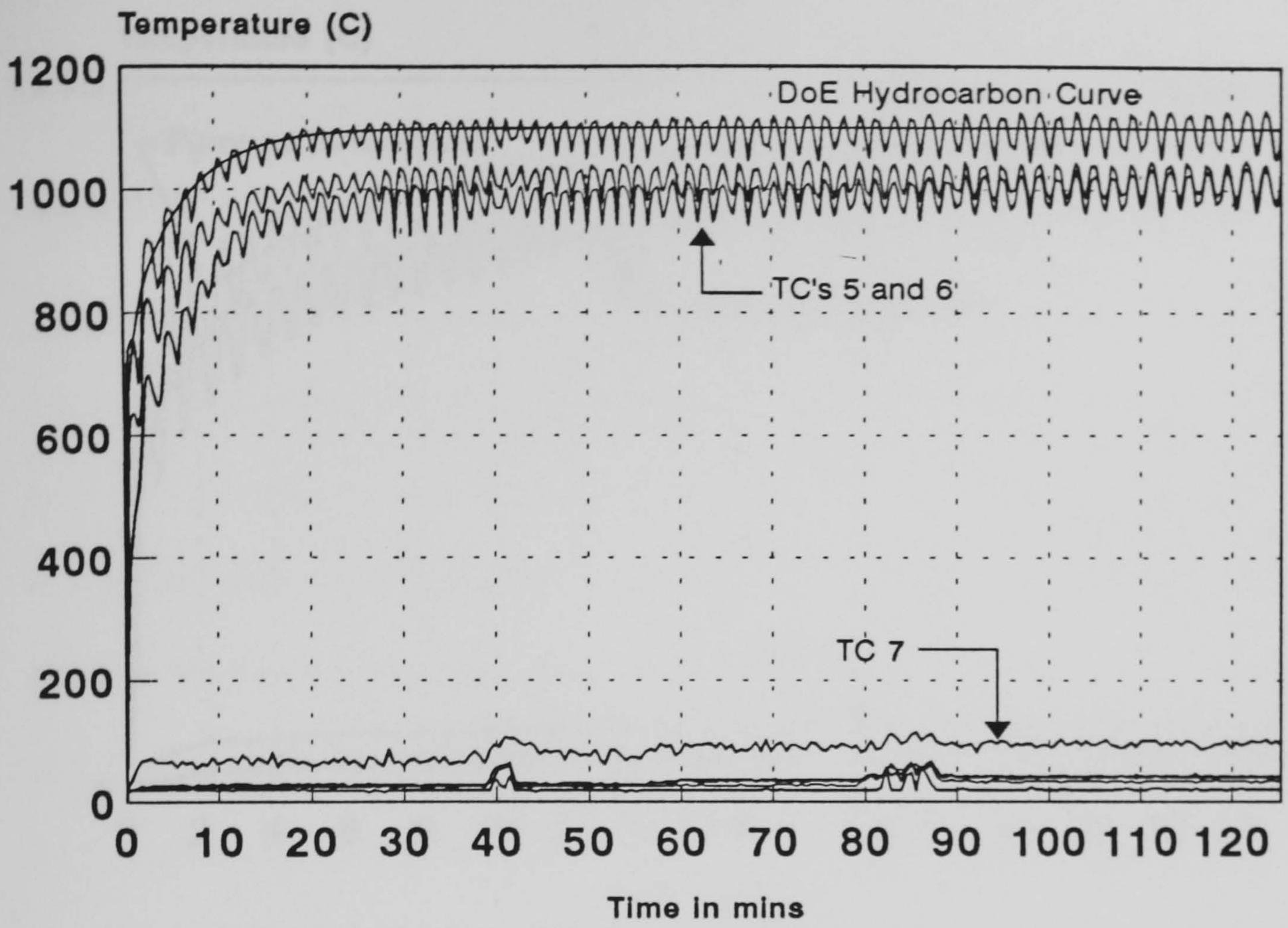

Figure 5.3.7 - Ameron Bondstrand 2000M, 2" GRE Pipe
Pipe with Varying Water Flows, Tested Previously
All Thermocouples

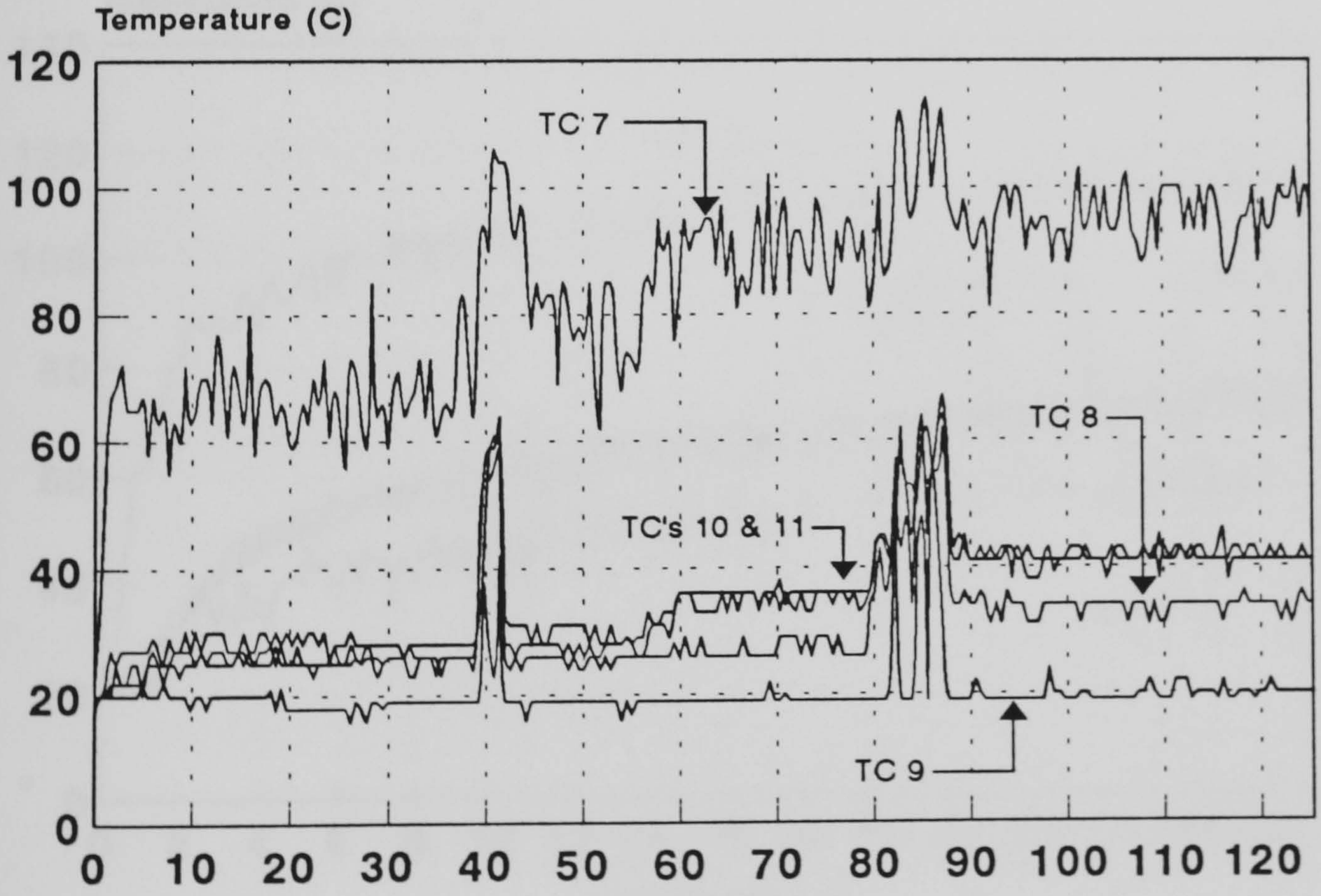

Figure 5.3.8 - Ameron Bondstrand 2000M, 2" GRE Pipe
Pipe with Varying Water Flows, Tested Previously
Internal Thermocouples Only

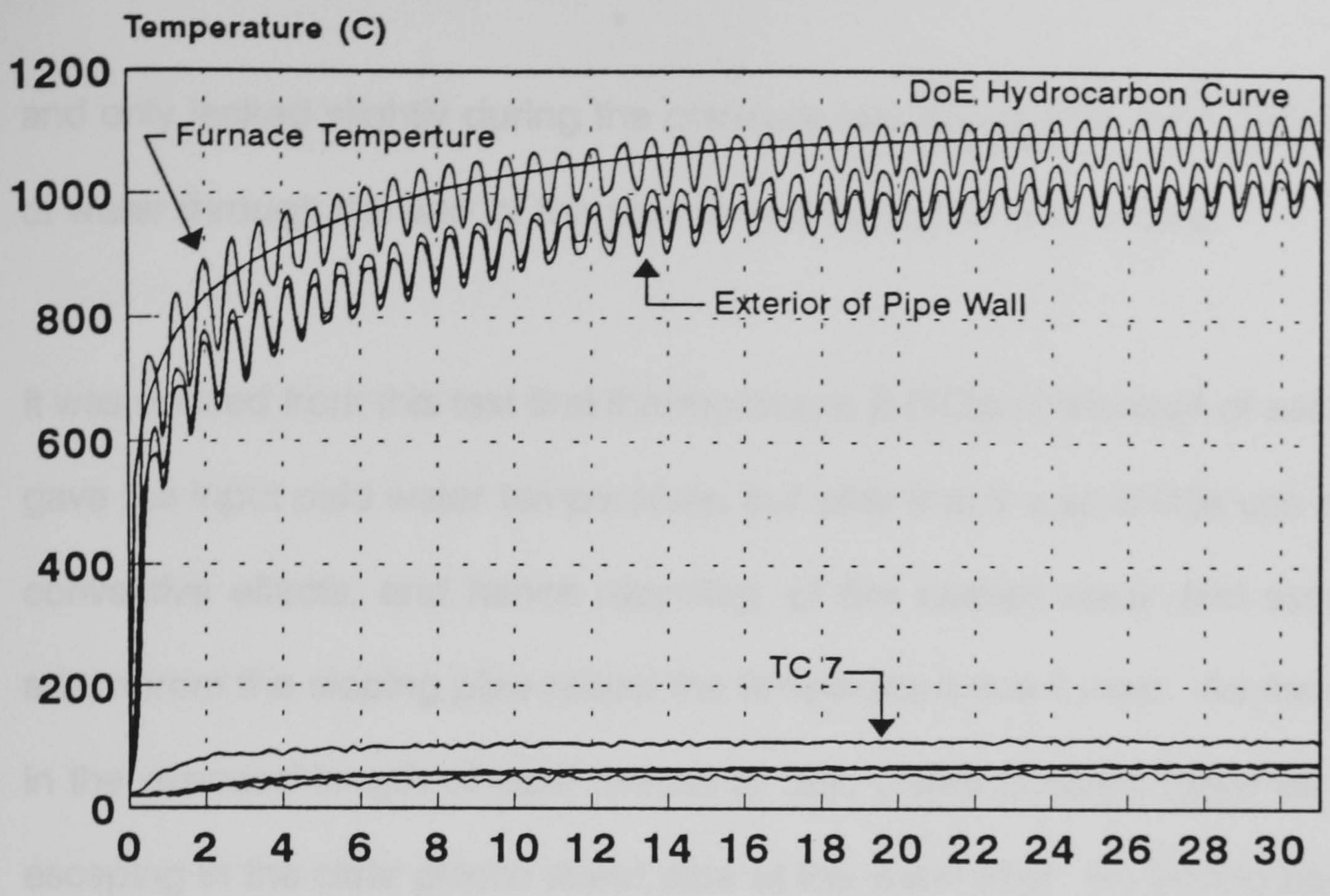

Figure 5.3.9 - Ameron Bondstrand 2000M, 2" GRE Pipe
Flowing Water at 3.2l/min, Hydrocarbon Fire Test
All Thermocouples

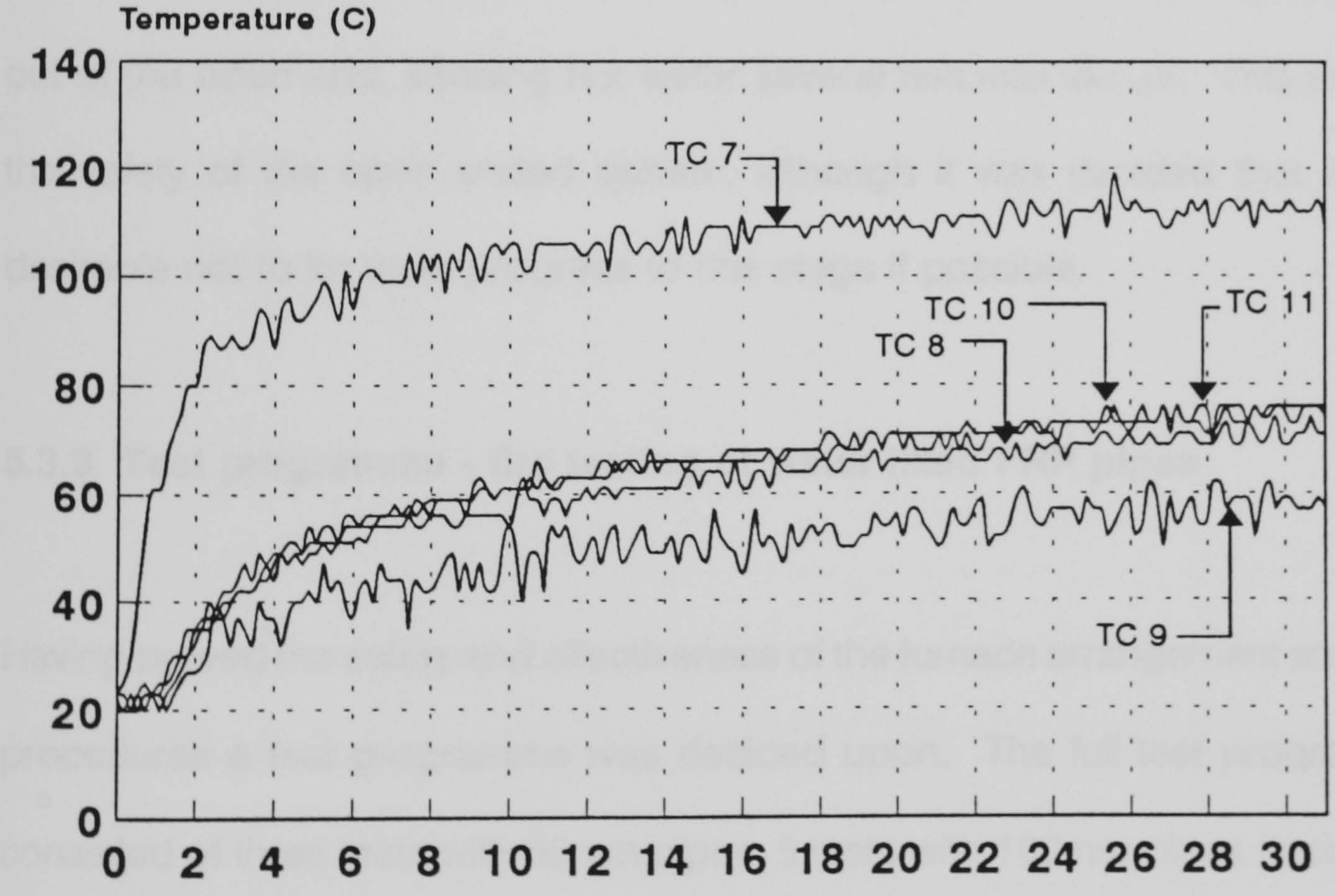

Figure 5.3.10 - Ameron Bondstrand 2000M, 2" GRE Pipe
Flowing Water at 3.2l/min, Hydrocarbon Fire Test
Internal Thermocouples Only

and only leaked slightly during the pressure test losing only 30cc (0.03 litres) of water through the wall of the pipe over a period of one minute.

It was noticed from this test that thermocouple 9 (TC9) at the start of each test gave the input cold water temperature, but after that it was of little use as the convective effects, and hence recycling, of the heated water and escaping steam from the sloping pipe raised the temperature that it read. As the water in the exposed length of pipe started to boil, steam bubbles could be seen escaping in the clear plastic stand pipe at the water inlet. As boiling became more vigorous steam bubbles could be seen escaping in both standpipes. If the pipe was allowed to be heated further it was found in subsequent tests that the formation of steam was so rapid that it forced the water in both stand pipes out of the open end, sending hot water several feet into the air. This proved the safety of the open ended system, although it was decided that it was desirable not to let tests progress to this stage if possible.

5.3.3 Test programme - fire testing of water filled FRP pipes

Having proved the safety and effectiveness of the furnace arrangement and test procedures a test programme was decided upon. The full test programme consisted of three tests with 50mm pipes, 5 tests with 100mm pipes (including one repeated test) and two tests on 100mm pipes with intumescent coatings. The tests performed are detailed in table 5.3. The start condition in one test was dry for 2 minutes, but the rest of the tests had a stagnant water start of 2,

5 or 10 minutes. The empty or stagnant water condition of 2 minutes represents the expected maximum time for the start-up of a deluge system offshore if the pumps start automatically. The 5 minute stagnant condition represents the maximum expected time to start-up of the deluge system if the pumps were to be started manually. The 10 minutes stagnant initial condition was intended to investigate the time that the pipe could remain in the stagnant water condition whilst still maintaining functionability. In all cases the start condition was followed by flowing water at 18 litres/minute. In the preliminary test of a flowing water filled pipe as described previously in section 5.3.2 it was observed that steady state conditions were reached in approximately 15 minutes. Due to this it was decided that a minimum standard run time was to be fixed at 30 minutes.

Test no.	Pipe Dia. (mm)	Orientation (to horiz.)	Dry Minutes	Stagnant Minutes	Flowing Minutes
1	50	-10°	2	-	28
2	50	"	-	2	28
3	50	"	-	5	25
4	100	"	-	2	28
5	100	"	-	5	25
6	100	"	-	10	20
7	100	"	-	2	58
8	100c	"	-	5	25
9	100c	"	-	60	-

Table 5.3 Test programme - unpressurised water filled pipes

Notes:
1) Flowing water rate was constant 18l/min
2) 100c - 100mm dia pipe with Patcher intumescent coating

5.3.4 Fire testing of flowing water filled GRE pipes: 50mm diameter

Figures 5.3.11 and 5.3.12 show the results for test 1. In this particular test the pipe system was fitted with a head water tank of approximately 2500 litres capacity fitted with a wide bore supply pipe in addition to the normal running water supply. The thermocouple arrangement for this test was as shown in figure 5.3.4(b). This was used to rapidly fill the pipe system after the required empty and dry exposure. It was of note that after 100 seconds exposure the rate of temperature climb of the internal wall of the pipe was over 100°C per ten second interval. There was a time delay of approximately 15 seconds for the pipe to fill with water once the fast supply had been started. At this point water could be seen running freely through the pipe wall, a point which was also indicated by the cooling of the thermocouples measuring the external wall temperature. This test reinforced earlier findings that the GRE pipes being investigated were not capable of resisting a simulated hydrocarbon fire for the required two minutes duration in the empty condition. Post test inspection of the pipe showed extensive damage to the internal bore. Due to this the pipe was not pressure tested.

Test 2 consisted of a 50mm diameter pipe, originally in the stagnant water filled condition, the sample thermocouple arrangement was as shown in figure 5.3.4(a). Figures 5.3.13 and 5.3.14 show the test results. It can be seen from the test results that after a period of 2 minutes in the stagnant water filled condition the internal temperatures of the pipe wall were rising rapidly. The

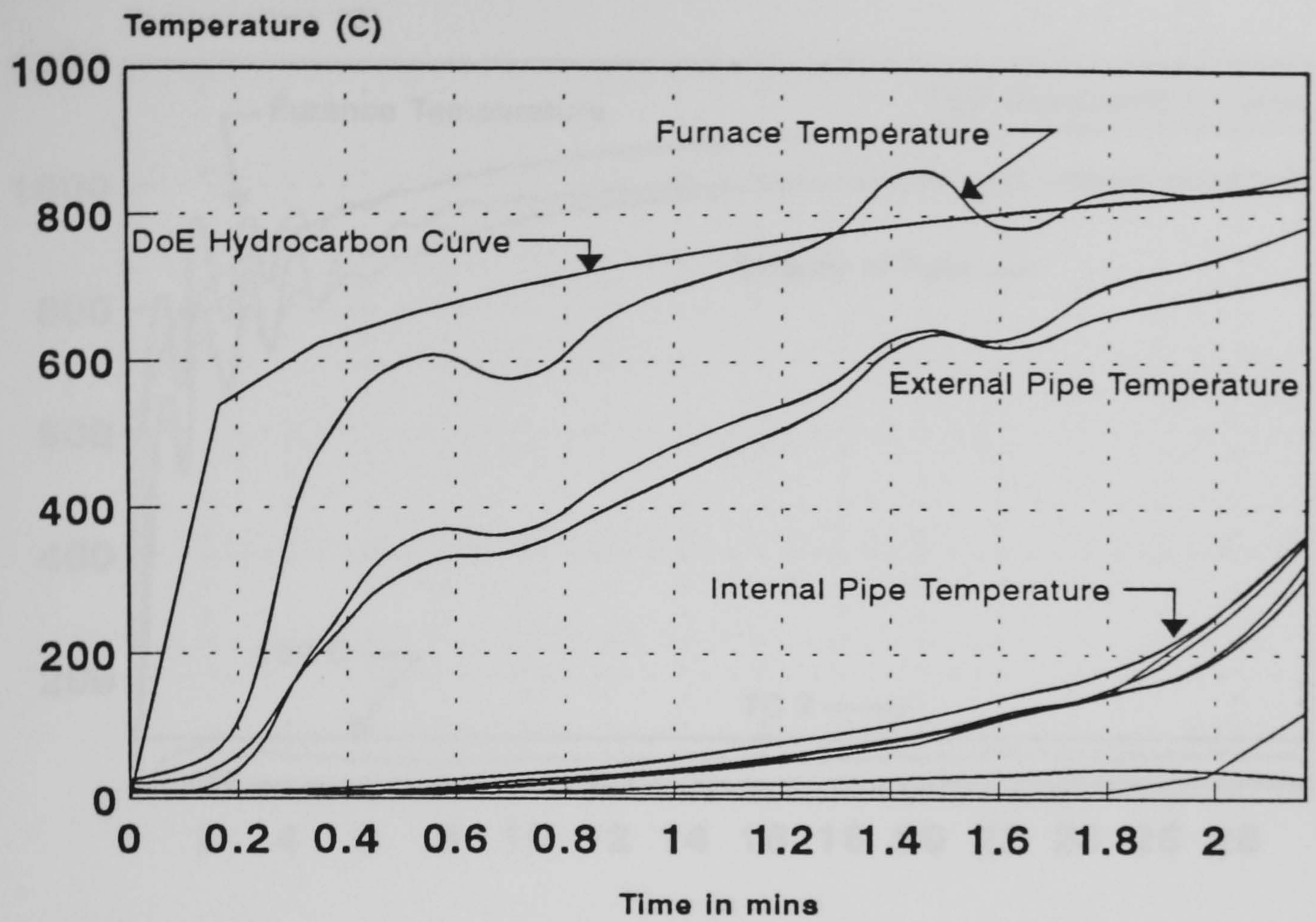

Figure 5.3.11 - Ameron Bondstrand 2000M, 2" GRE Pipe
2 Minute empty, 28 min flowing water, hydrocarbon fire test
All Thermocouples

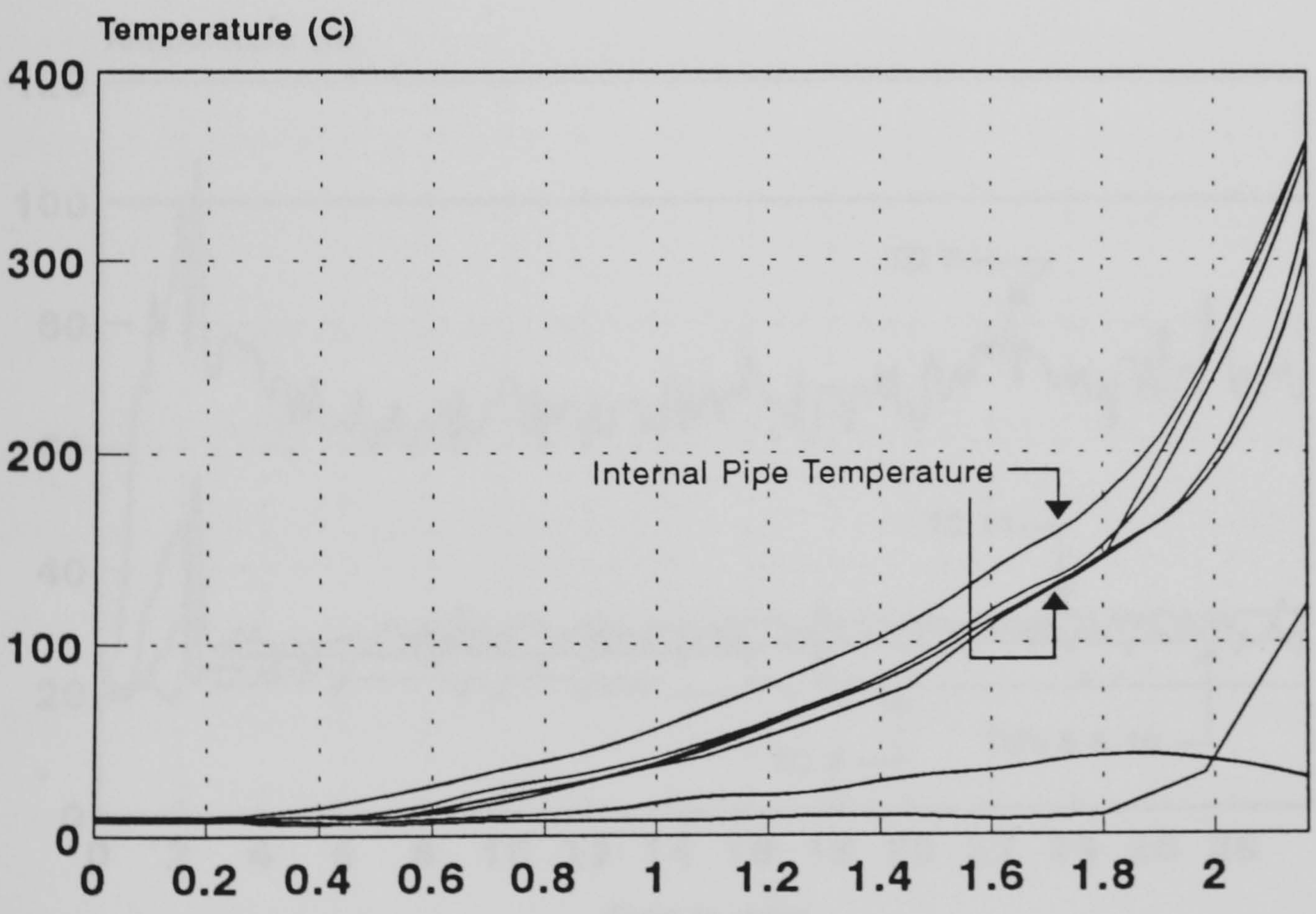

Figure 5.3.12 - Ameron Bondstrand 2000M, 2" GRE Pipe
2 Minute empty, 28 min flowing water, hydrocarbon fire test
Internal Thermocouples Only

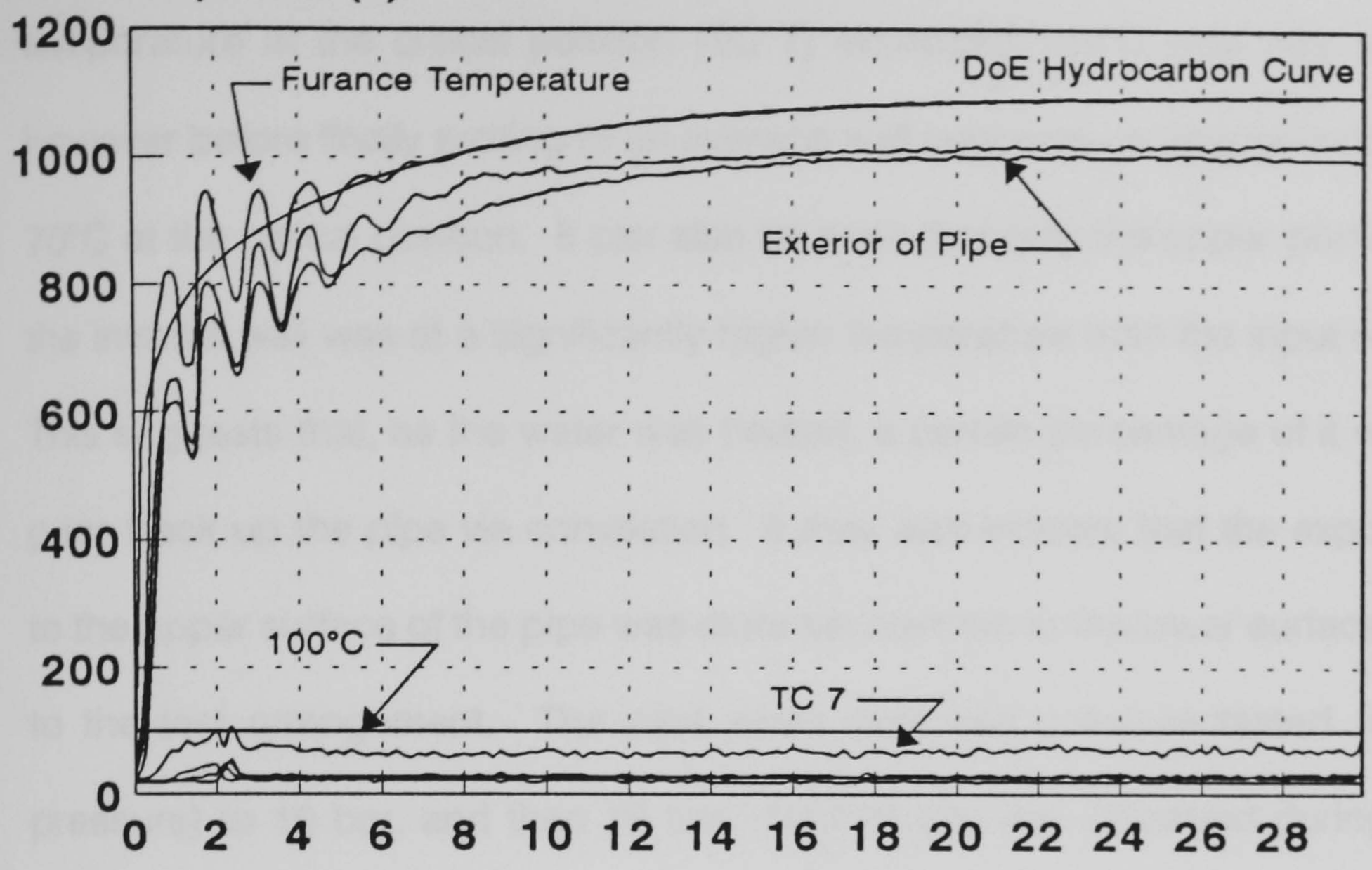

Figure 5.3.13 - Ameron Bondstrand 2000m, 2" GRE Pipe (2 minute stagnant)
Flowing water at ≈18l/min, Hydrocarbon Fire Test
All Thermocouples

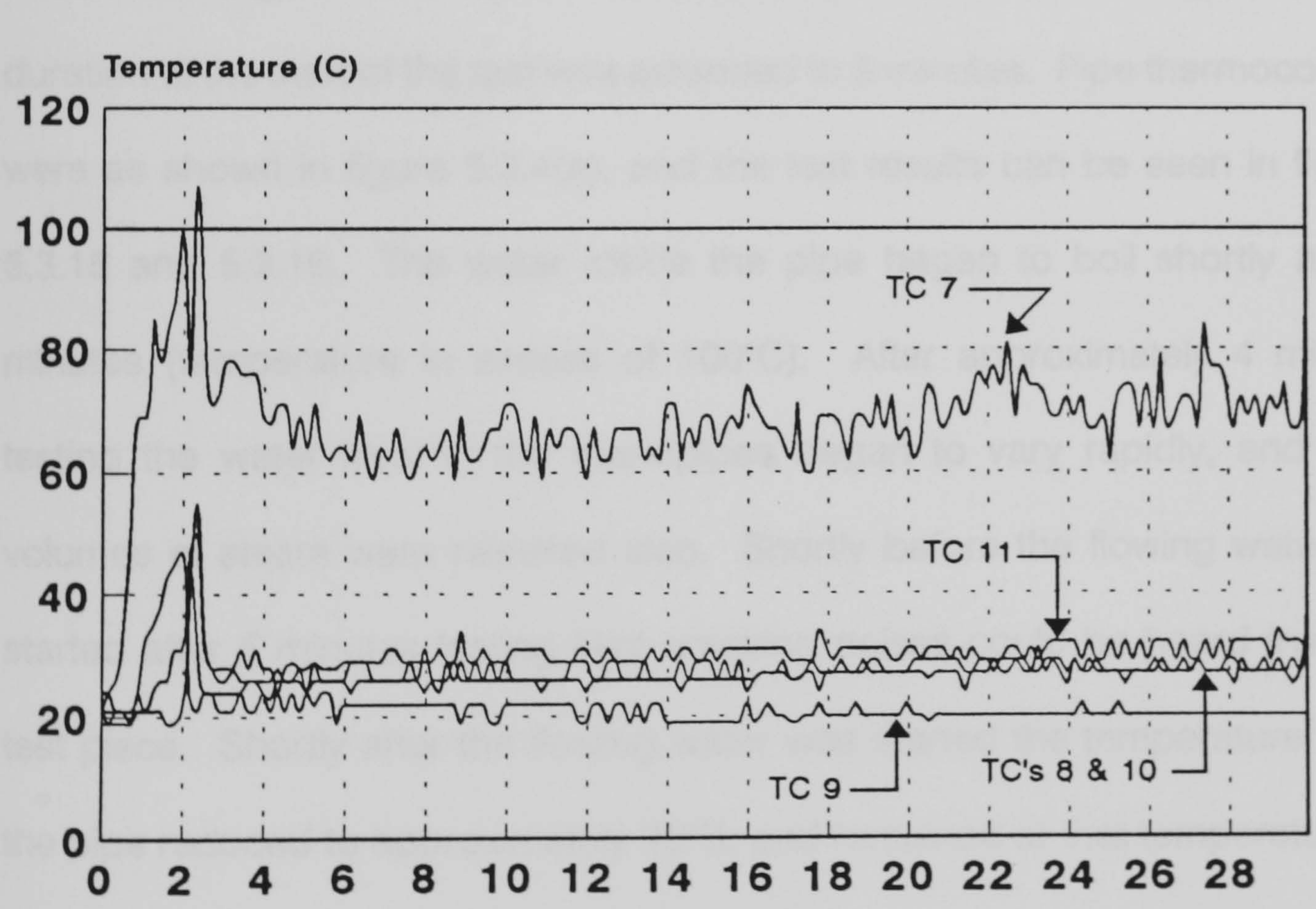

Figure 5.3.14 - Ameron Bondstrand 2000M, 2" GRE Pipe (2 minute stagnant)
Flowing water at ≈18l/min, Hydrocarbon Fire Test
Internal Thermocouples Only

temperature at the critical position (TC 7) exceeded 100°C only very briefly however before finally settling to an average wall temperature of approximately 70°C at the critical position. It can also be seen that only the upper portion of the internal wall was at a significantly higher temperature than the input water. This suggests that, as the water was heated, a certain percentage of it would pass back up the pipe via convection. It may also indicate that the exposure to the upper surface of the pipe was more severe than to the lower surface due to the test arrangement. The pipe when cool was pressure tested (static pressure) to 10 bar, and then 16 bar. No leakage was observed during the pressure test.

Test 3 was again on a 50mm diameter pipe, however the stagnant water duration at the start of the test was extended to 5 minutes. Pipe thermocouples were as shown in figure 5.3.4(a), and the test results can be seen in figures 5.3.15 and 5.3.16. The water inside the pipe began to boil shortly after 2 minutes (temperature in excess of 100°C). After approximately 4 minutes testing the water level in the standpipes began to vary rapidly, and large volumes of steam were released also. Shortly before the flowing water was started after 5 minutes testing faint cracking noises could be heard from the test piece. Shortly after the flowing water was started the temperature within the pipe reduced to approximately 70°C, and remained at that temperature for the remainder of the test duration. Post test examination of the pipe revealed that some damage to the bore, and this was reinforced by static pressure testing. Leakage first occurred at 3 bar, however, a pressure of 7 bar was

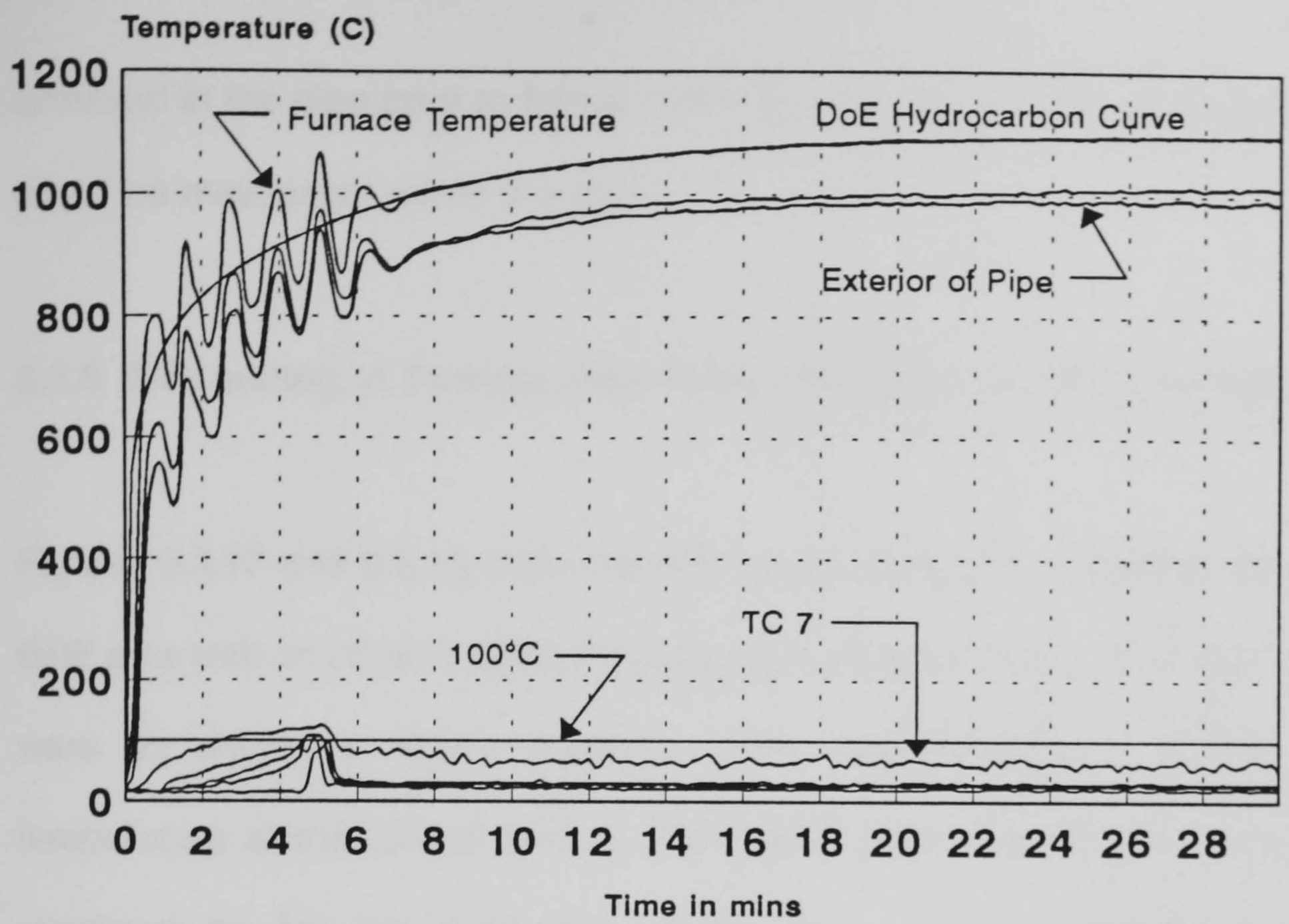

Figure 5.3.15 - Ameron Bondstrand 2000M, 2" GRE Pipe, 5 minute stagnant
Flowing Water ≈ 18l/min, Hydrocarbon Fire Test
All Thermocouples

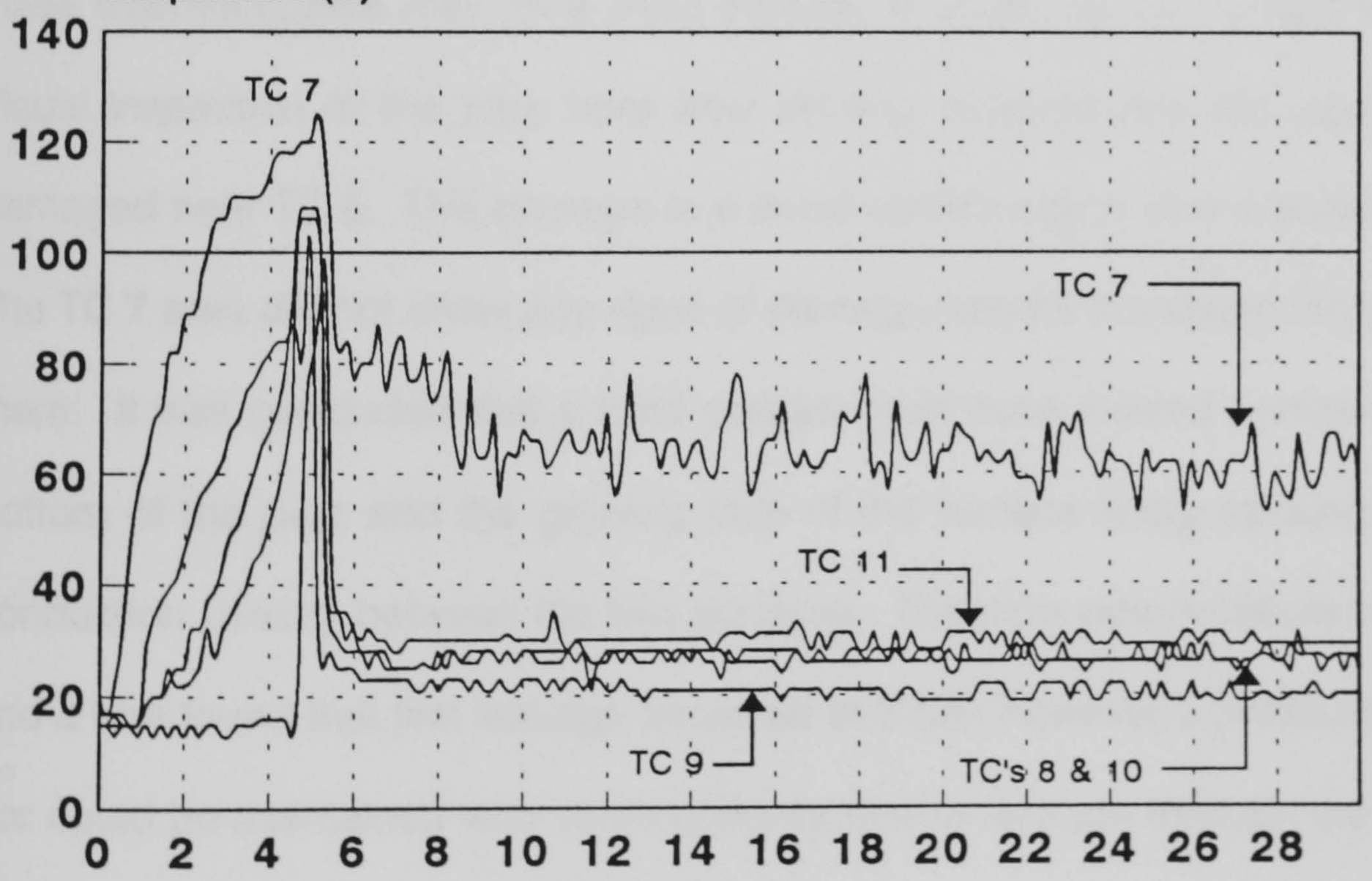

Figure 5.3.16 - Ameron Bondstrand 2000M, 2" GRE Pipe, 5 minute stagnant
Flowing Water ≈ 18l/min, Hydrocarbon Fire Test
Internal Thermocouples Only

achieved in the pipe prior to failure. After the pipe failed at 7 bar no pressure could be maintained within the pipe.

5.3.5 Fire testing of flowing water filled GRE pipes: 100mm diameter

Figures 5.3.17 and 5.3.18 show the test results for test 4, a 100mm diameter GRE pipe with an initial condition of 2 minutes stagnant water. Thermocouples were as shown in figure 5.3.4(a). After approximately 3 minutes the temperature at the critical section of the pipe were in excess of 100°C and remained so for the remainder of the test. It was noticed that the thermocouples on the outside of the pipe (TC 5 and 6) were measuring substantially lower temperatures than for previous tests, and was thought that these thermocouples may have been partially shielded by the furnace lining. Visual inspection of the pipe bore after cooling revealed that the pipe was damaged near TC 8. This damage in a water cooled region was unexpected. The TC 7 area did not show any signs of damage despite the steam formation there. It was concluded that a hard contact must have existed between the bottom of the pipe and the glowing face of the furnace lining causing heat conduction directly between the two surfaces. The pipe was pressure tested and it was found that first leakage occurred at 3 bar, however, a pressure of 9 bar could be maintained with some difficulty due to leakage through the pipe wall and its corresponding loss in pressure.

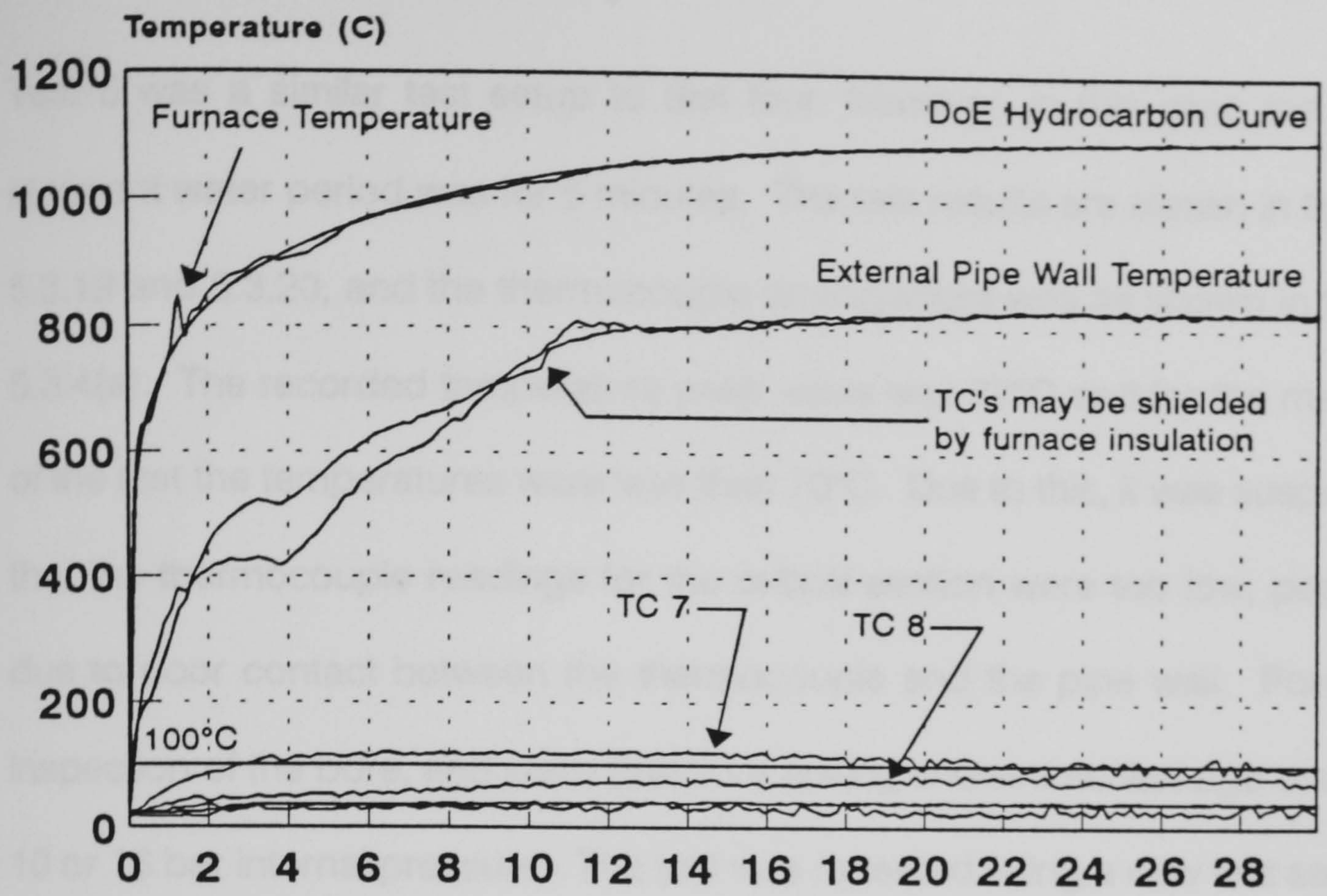

Figure 5.3.17 - Ameron Bondstrand 2000M, 4" GRE Pipe, 2 minutes stagnant
Flowing water ≈ 18l/min, Hydrocarbon Fire Test
All Thermocouples

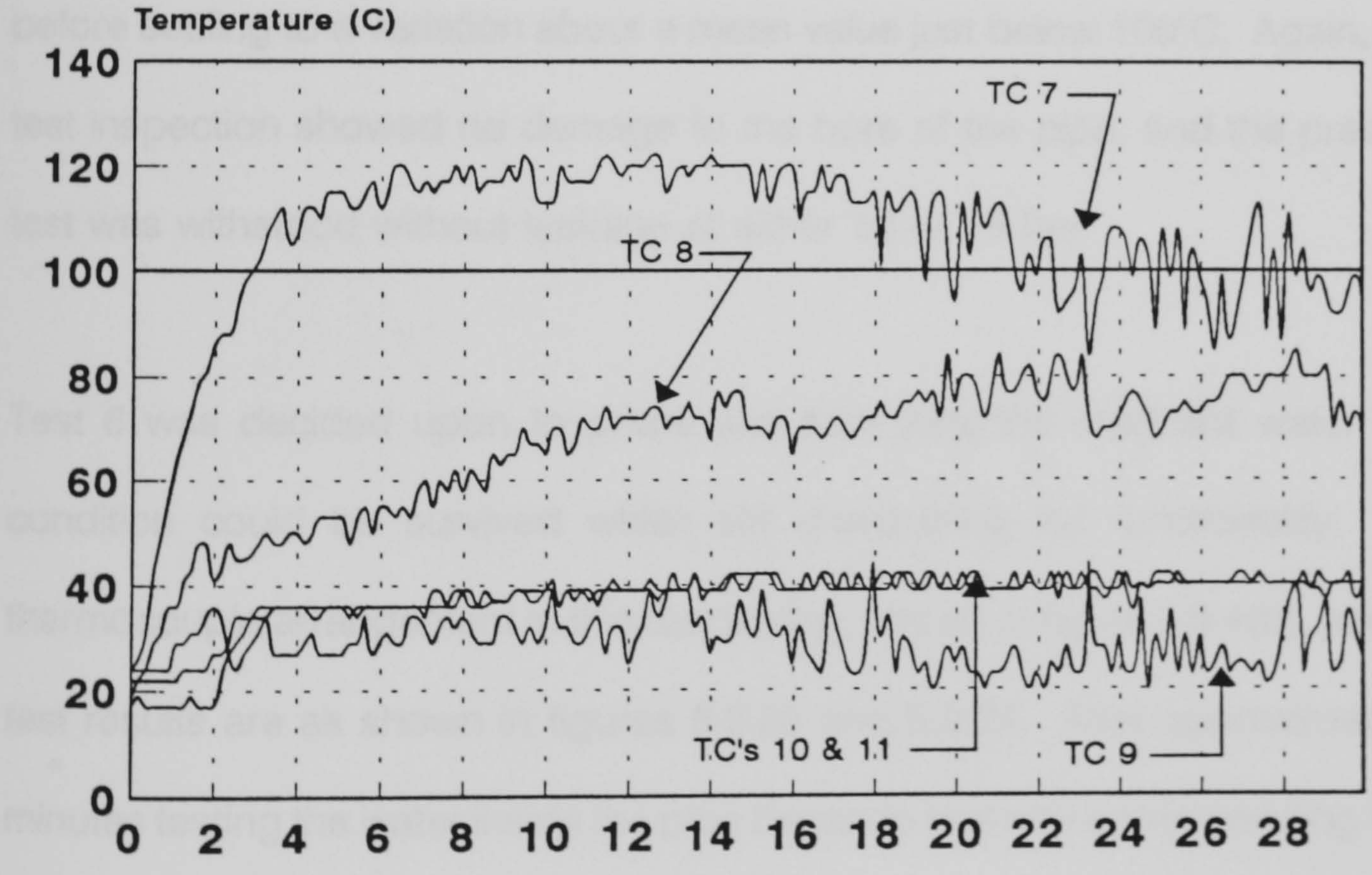

Figure 5.3.18 - Ameron Bondstrand 2000M, 4" GRE Pipe, 2 minutes stagnant
Flowing water ≈ 18l/min, Hydrocarbon Fire Test
Internal Thermocouples Only

Test 5 was a similar test setup to test four, however, in this case the initial stagnant water period was for 5 minutes. The test results are shown in figures 5.3.19 and 5.3.20, and the thermocouple arrangement was as shown in figure 5.3.4(a). The recorded temperature peak value was 77°C and for the majority of the test the temperatures were less than 70°C. Due to this, it was suspected that the thermocouple readings for the critical section were too low, possibly due to poor contact between the thermocouple and the pipe wall. Post test inspection of the bore, and static pressure testing showed no leakage at either 10 or 16 bar internal pressure. The test was repeated using a new test sample to gain accurate temperature measurements for the critical section, and this data is shown in figures 5.3.21 and 5.3.22. This set of test results showed that the temperature at the position of TC 7 exceeded 100°C for almost 12 minutes before settling to a variation about a mean value just below 100°C. Again, post test inspection showed no damage to the bore of the pipe, and the pressure test was withstood without leakage at either 10 or 16 bar.

Test 6 was decided upon to probe just how long the stagnant water filled condition could be survived whilst still maintaining full functionality. The thermocouple arrangement in this test was as shown in figure 5.3.4(b), and the test results are as shown in figures 5.3.23 and 5.3.24. After approximately 8 minutes testing the water inside the pipe began to boil with corresponding large steam releases through the vertical stand pipes. By the time that flowing water was started after 10 minutes testing the water within the pipe was boiling vigorously. The air-lock effect of the pipe system resulted in large amounts of

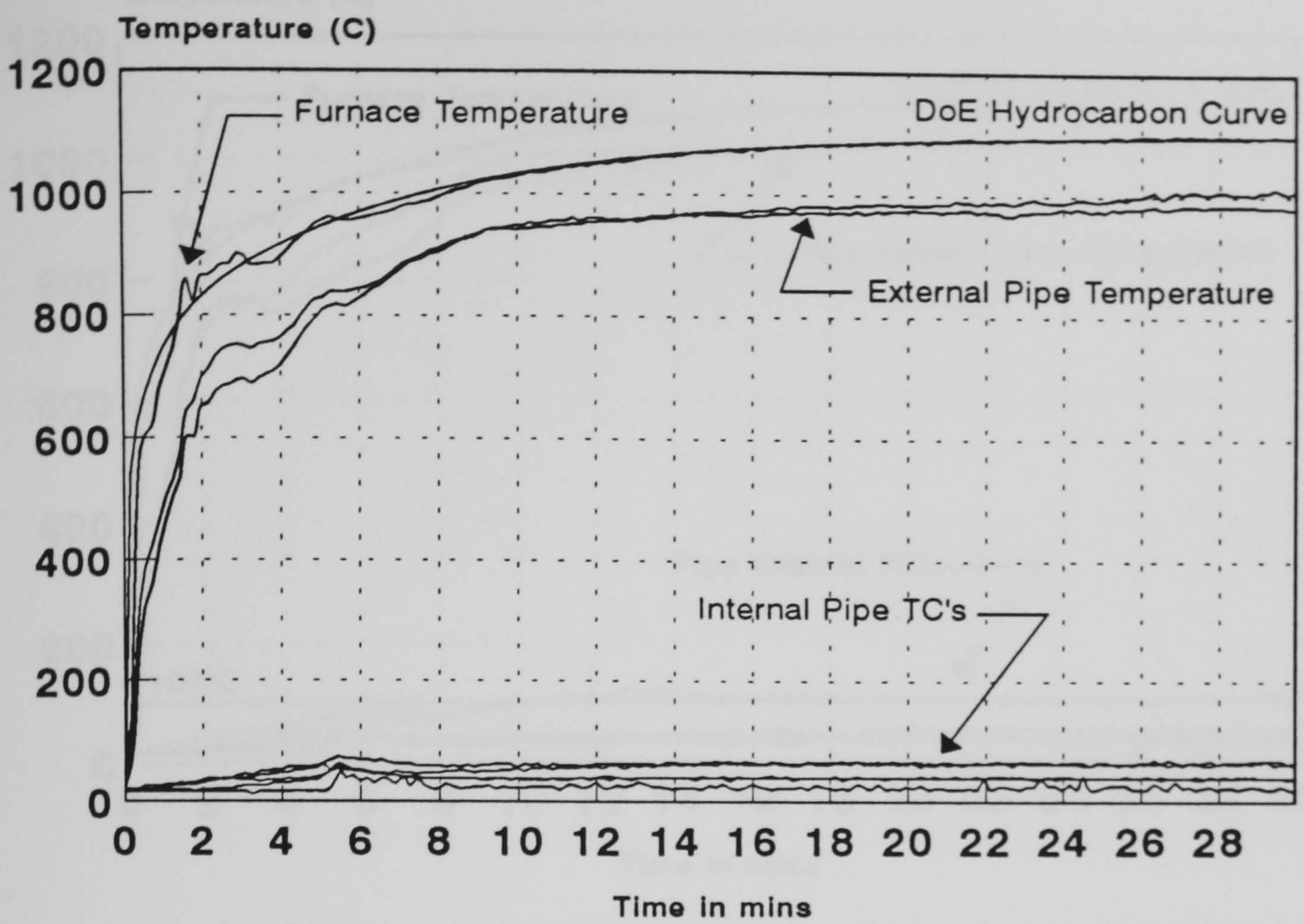

Figure 5.3.19 - Ameron Bondstrand 2000M, 4" GRE Pipe, 5 minute stagnant
Flowing water ≈18l/min, Hydrocarbon Fire Test
All Thermocouples

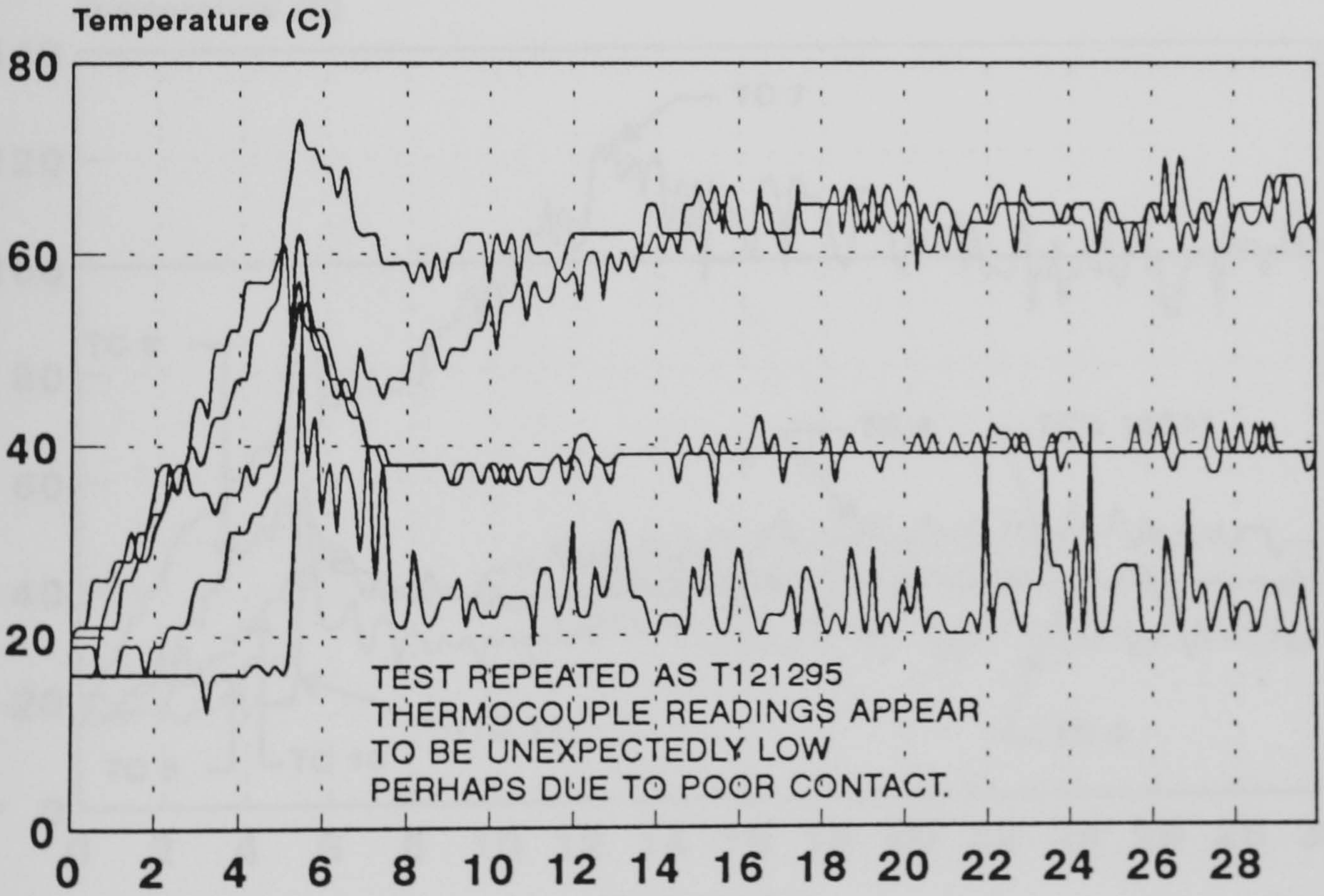

Figure 5.3.20 - Ameron Bondstrand 2000M, 4" GRE Pipe, 5 minute stagnant
Flowing water ≈18l/min, Hydrocarbon Fire Test
Internal Thermocouples Only

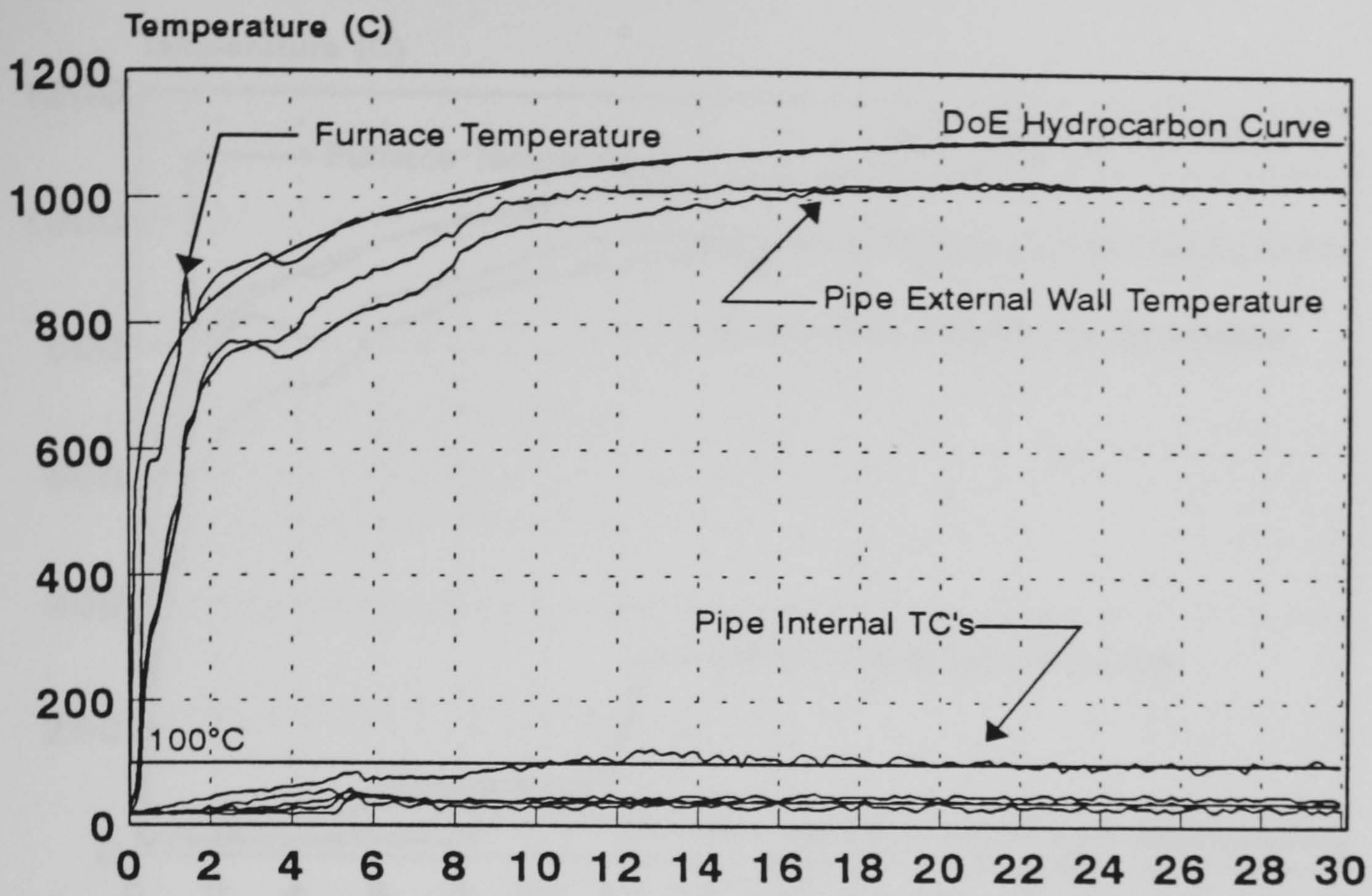

Figure 5.3.21 - Ameron Bondstrand 2000M, 4" GRE Pipe, 5minute stagnant Flowing Water at 18l/min, Hydrocarbon Fire Test All Thermocouples

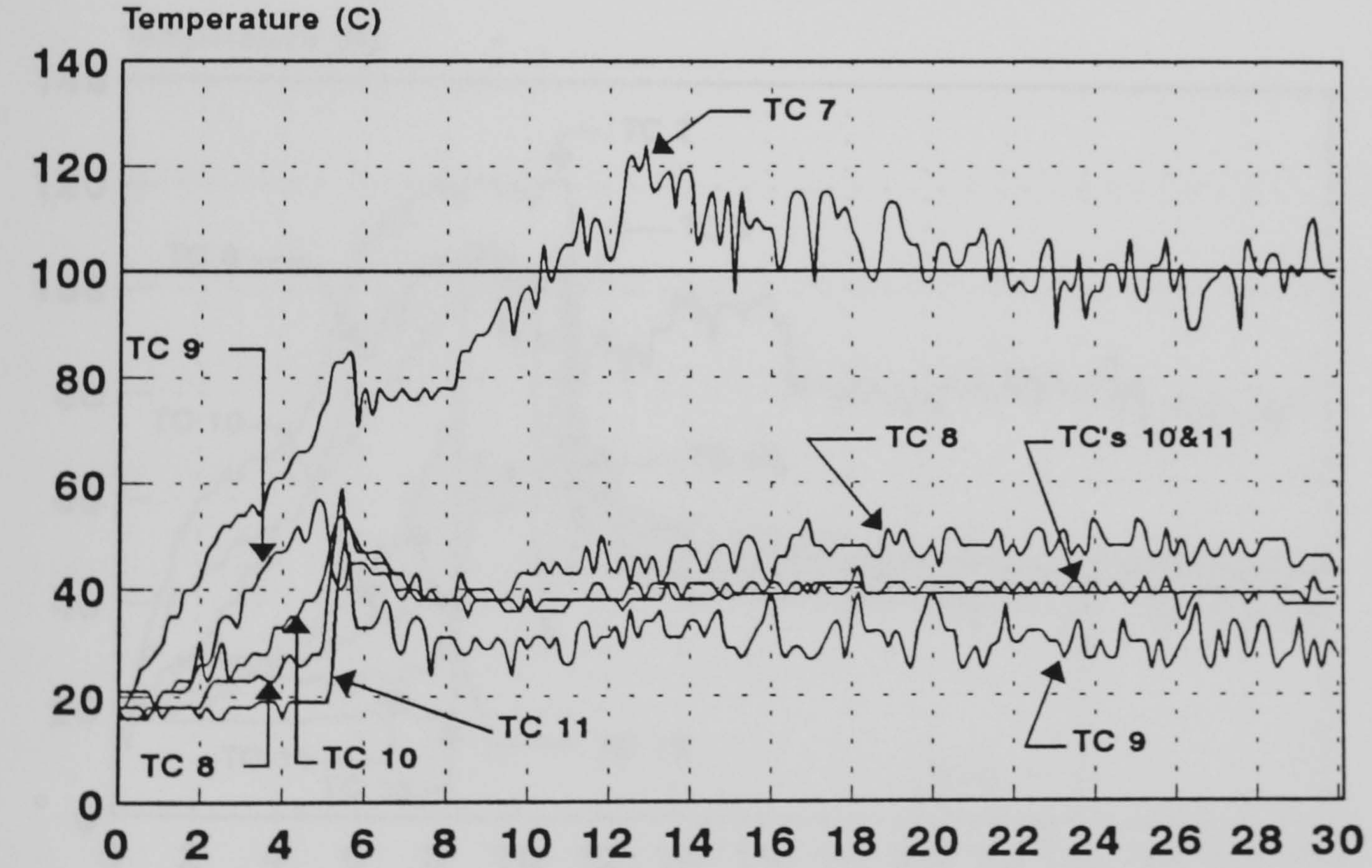

Figure 5.3.22 - Ameron Bondstrand 2000M, 4" GRE Pipe, 5minute stagnant Flowing Water at 18l/min, Hydrocarbon Fire Test Internal Thermocouples Only

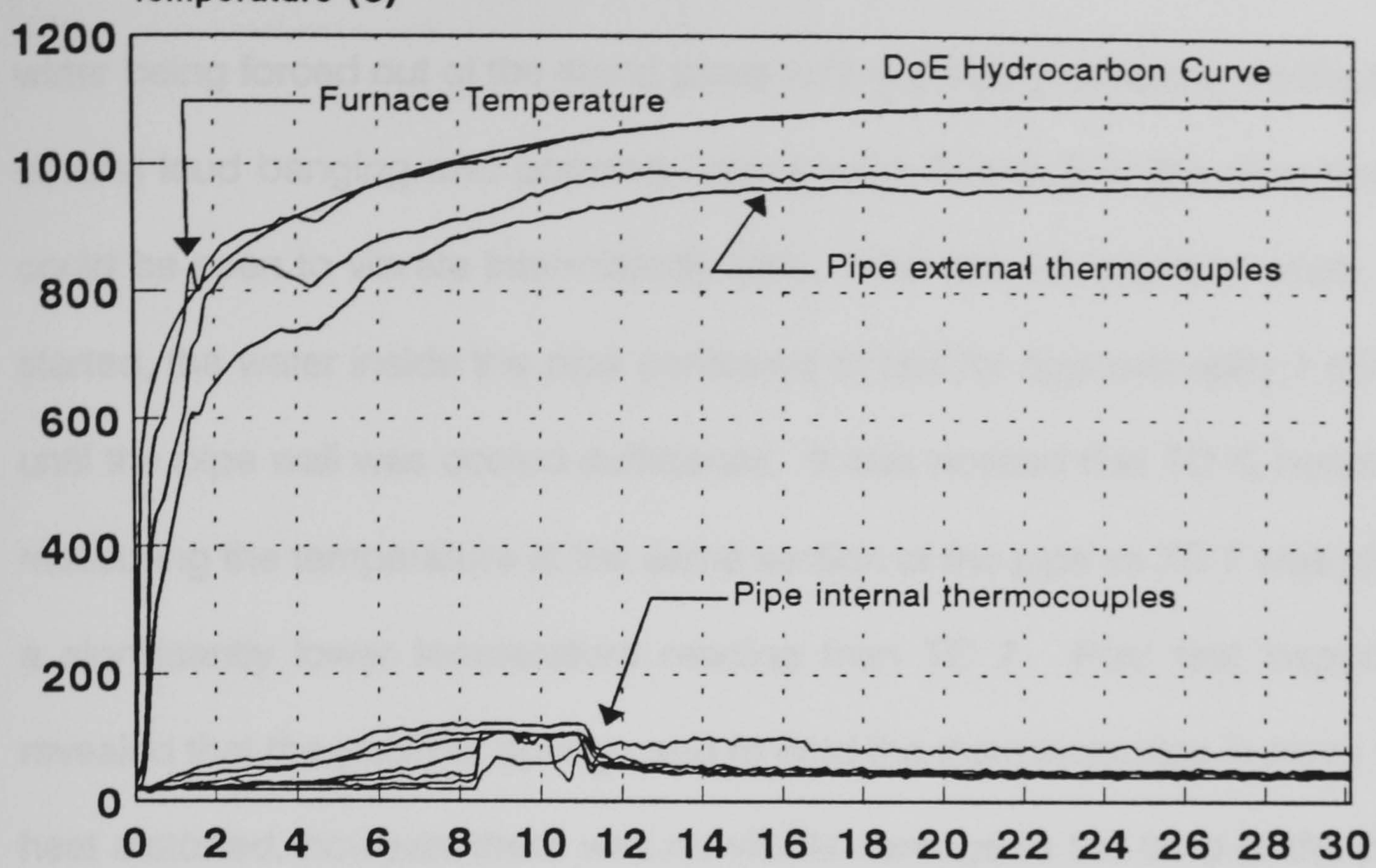

Figure 5.3.23 - Ameron Bondstrand 2000M, 4" GRE Pipe
10 minute stagnant, 20 minute flowing (18l/min) water. Hydrocarbon Test.
All Thermocouples

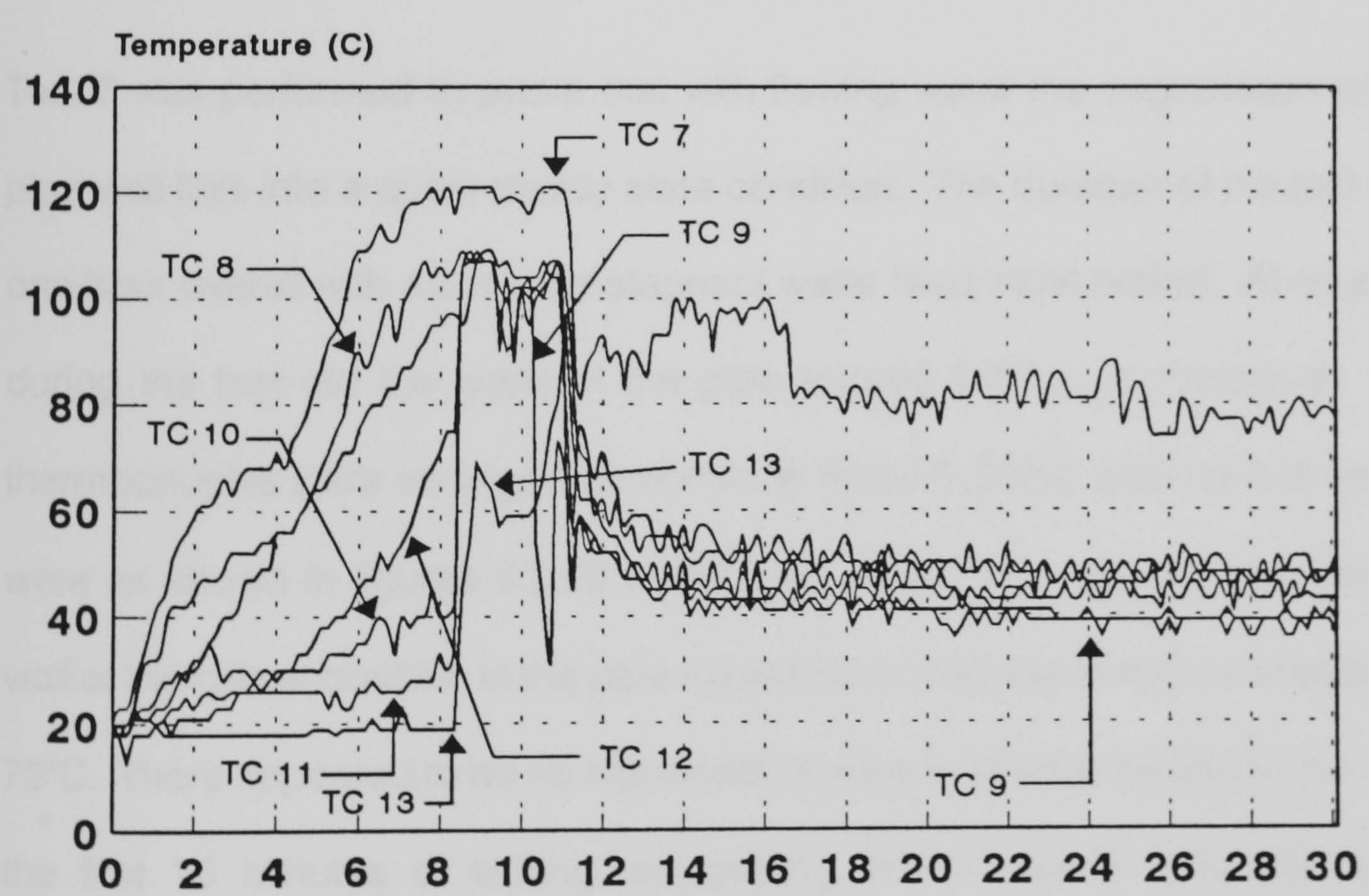

Figure 5.3.24 - Ameron Bondstrand 2000M, 4" GRE Pipe
10 minute stagnant, 20 minute flowing (18l/min) water. Hydrocarbon Test
Internal Thermocouples Only

water being forced out of the stand pipes with the steam releases. At this time several loud banging and popping noises were heard, and the pipe system could be seen to vibrate intermittently also. After the running cold water was started, the water inside the pipe continued to boil for approximately 1 minute until the pipe wall was cooled sufficiently. It was noticed that TC 8, notionally measuring the temperature at the same section of the pipe as TC 7 was giving a significantly lower temperature reading than TC 7. Post test inspection revealed that the polymer spring used to hold the thermocouples in place was heat distorted, however, there was no visible damage to the bore of the pipe. Pressure testing showed no leakage at 10 or 16 bar internal pressure over a sustained period of time.

Test 7 was performed to prove that with flowing water the degradation of the pipe wall falls into a quasi steady state condition. The duration of the test was one hour overall with a 2 minute stagnant water filled initial period. At no point during the test did the water in the pipe exceed 80°C in temperature. The thermocouples were arranged as shown in figure 5.3.4(b) and the test results were as shown in figures 5.3.25 and 5.3.26. The temperature of the internal wall at the critical position in the pipe appeared to stabilise at approximately 70-75°C. There appeared to be no significant change in internal temperatures after the first 15 minutes of testing, suggesting that a steady state had been achieved. Post test inspection of the pipe showed no damage to the bore, and no leakage was observed at 10 or 16 bar during the pressure test.

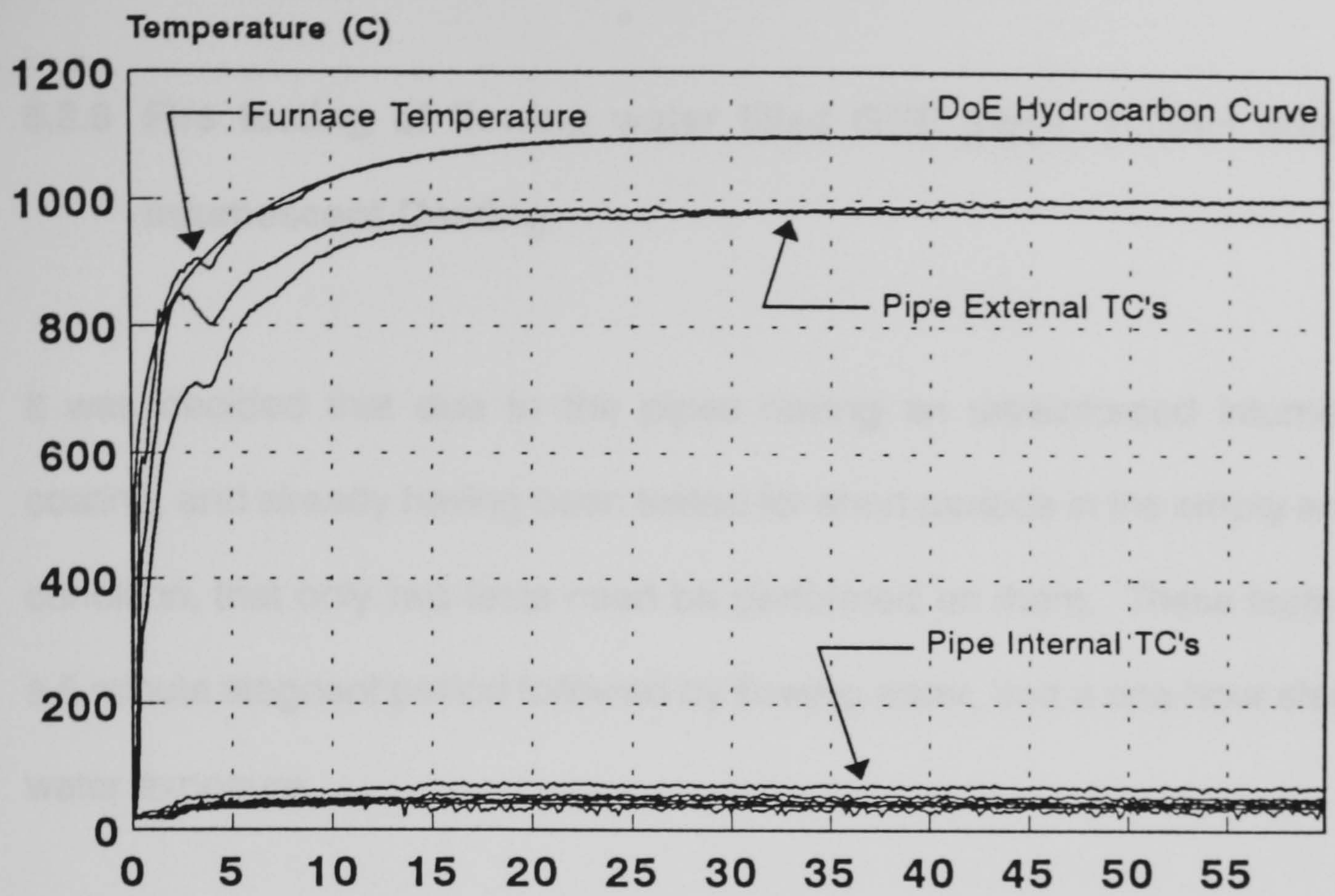

Figure 5.3.25 - Ameron Bondstrand 2000M, 4" GRE Pipe
2 Minute stagnant, 58 minute flowing (18l/min) water, hydrocarbon fire test
All Thermocouples

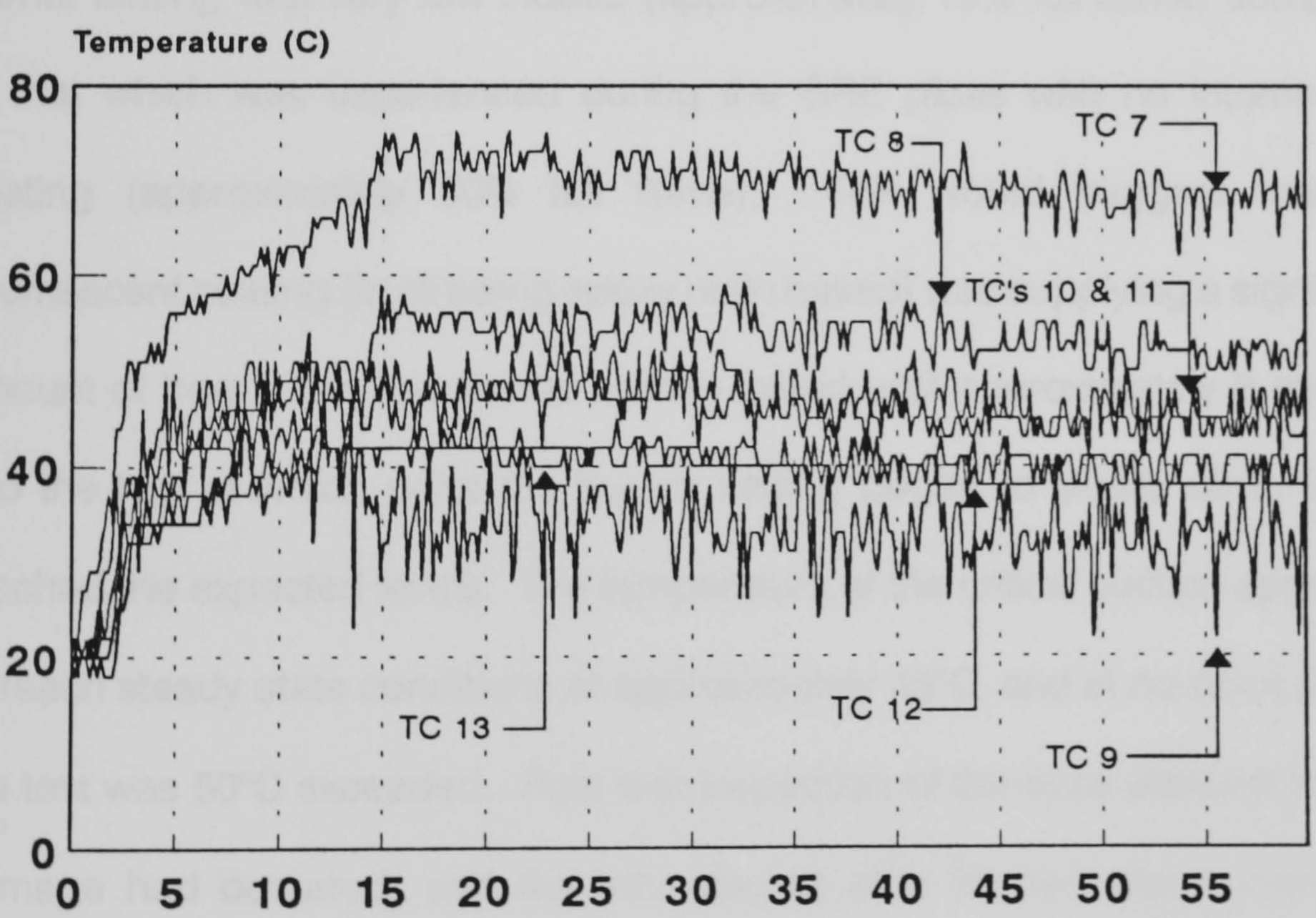

Figure 5.3.26 - Ameron Bondstrand 2000M, 4" GRE Pipe
2 Minute stagnant, 58 minute flowing (18l/min) water, hydrocarbon fire test
Internal Thermocouples Only

5.3.6 Fire testing of flowing water filled GRE pipes: 100mm diameter, Intumescent Coating

It was decided that due to the pipes having an unreinforced intumescent coating, and already having been tested for short periods in the empty and dry condition, that only two tests need be performed on them. These tests were a 5 minute stagnant period followed by flowing water, and a one hour stagnant water exposure.

Figures 5.3.27 and 5.3.28 show the results for test 8, the thermocouples are located as shown in figure 5.3.4(b). It was noticed that during the test the burner setting was very low indeed (approximately 15% full flame) compared to that which was experienced during the GRE pipes with no intumescent coating (approximately 60% full flame). This would suggest that the intumescent coating (itself being epoxy resin based) was supplying a significant amount of heat. This low burner setting lasted until approximately 8 minutes into the test at which point the burner setting began to slowly climb until it reached the expected levels. The temperature at the critical section appeared to reach steady state conditions at approximately 45°C, and at no point during the test was 50°C exceeded. Post test inspection of the bore showed that no damage had occurred, and the intumescent char formed was surprisingly cohesive. There were expansion cracks within the char, however, the tested pipe could still be handled without damaging the intumescent char. The pipe was pressure tested at 10 bar and 16 bar, and no leakage was observed.

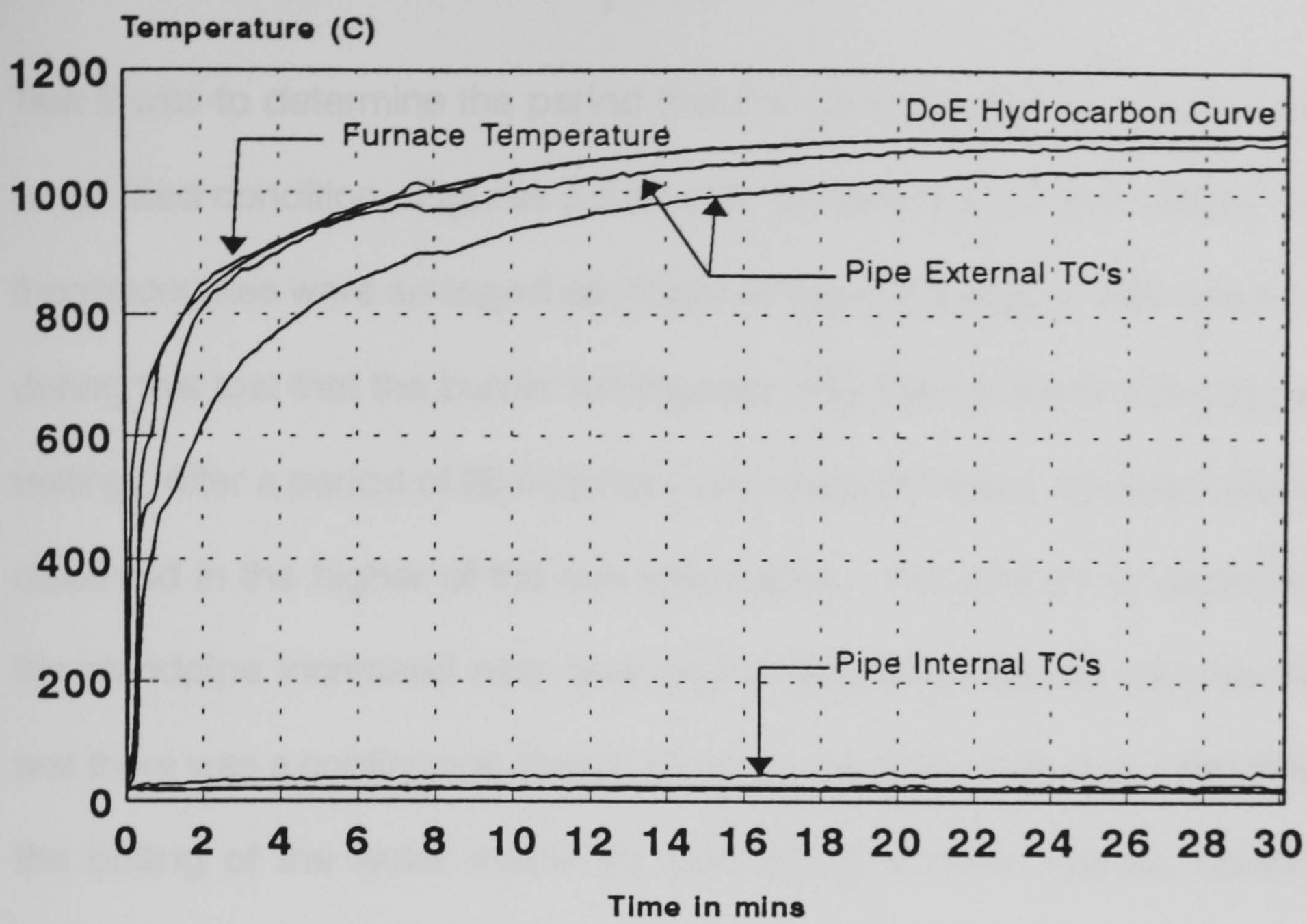

Figure 5.3.27 - Ameron Bondstrand 2000M, 4" Pitt-Char coated GRE Pipe
5 minute stagnant, 25 minute flowing (18l/min), Hydrocarbon Fire Test
All Thermocouples

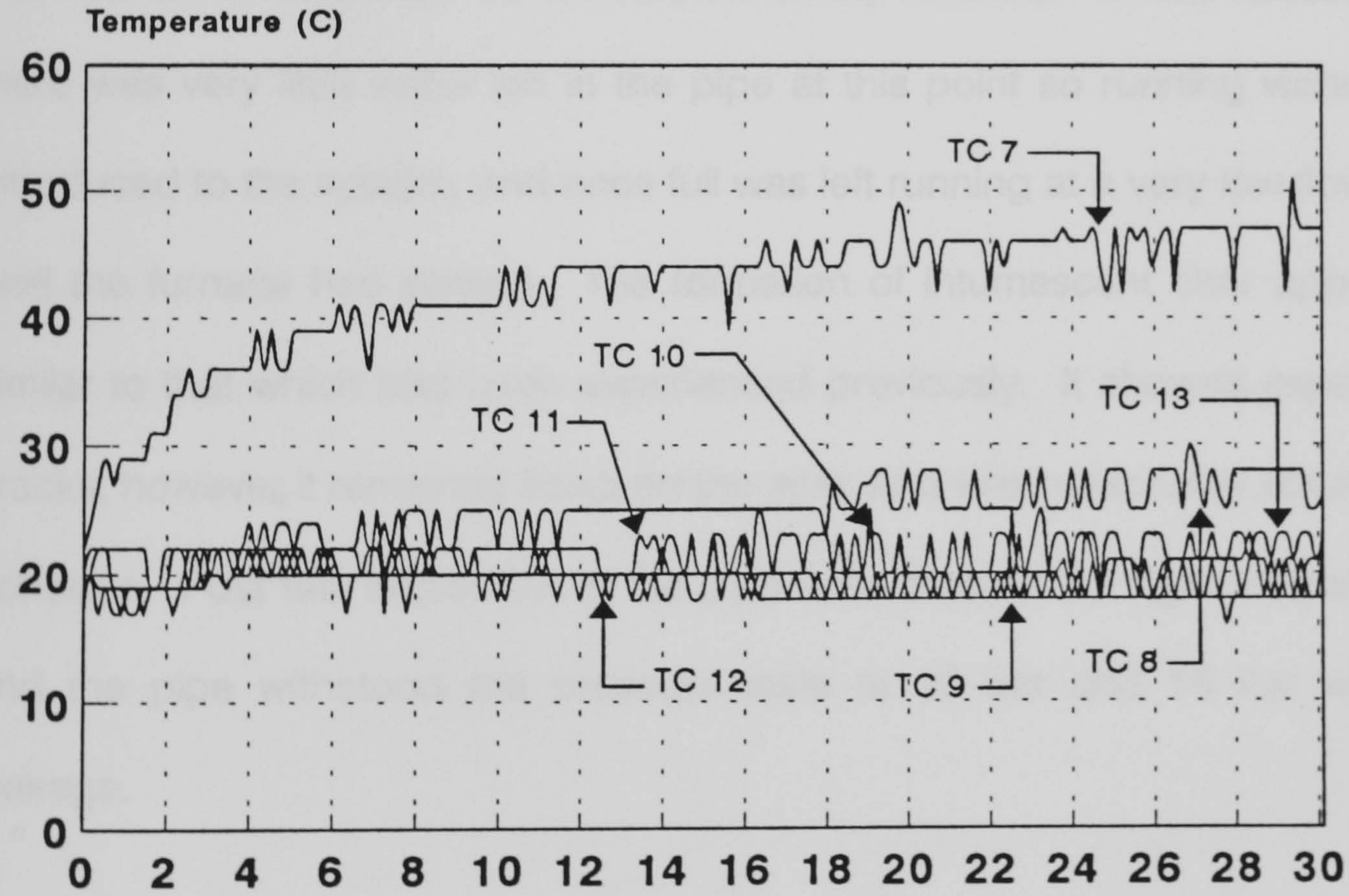

Figure 5.3.28 - Ameron Bondstrand 2000M, 4" Pitt-Char coated GRE Pipe
5 minute stagnant, 25 minute flowing (18l/min), Hydrocarbon Fire Test
Internal Thermocouples Only

Test 9 was to determine the period that the pipe could survive in the stagnant water filled condition. Figures 5.3.29 and 5.3.30 show the test results, and the thermocouples were arranged as shown in figure 5.3.4(a). It was again noticed during this test that the burner setting was very low for the first few minutes of testing. After a period of 26 minutes in the stagnant water condition steam was observed in the higher of the two standpipes. The amount of steam seen in the standpipe increased over time until at approximately 45 minutes into the test there was a continuous stream of steam bubbles observed. After this point the boiling of the water inside the pipe became more intense, causing air-locked steam pockets to force boiling water out of the standpipes. This became increasingly violent, to the point of shaking the entire pipe loop. The test was terminated after 49 minutes for safety reasons. It was noticed that there was very little water left in the pipe at this point so running water was introduced to the system, and once full was left running at a very low flow rate until the furnace had cooled. The formation of intumescent char appeared similar to that which had been experienced previously. It showed expansion cracks, however, it remained intact on the pipe, and was reasonably stable and cohesive. Post test inspection of the pipe bore showed no signs of damage, and the pipe withstood the pressure tests at 10 bar and 16 bar without leakage.

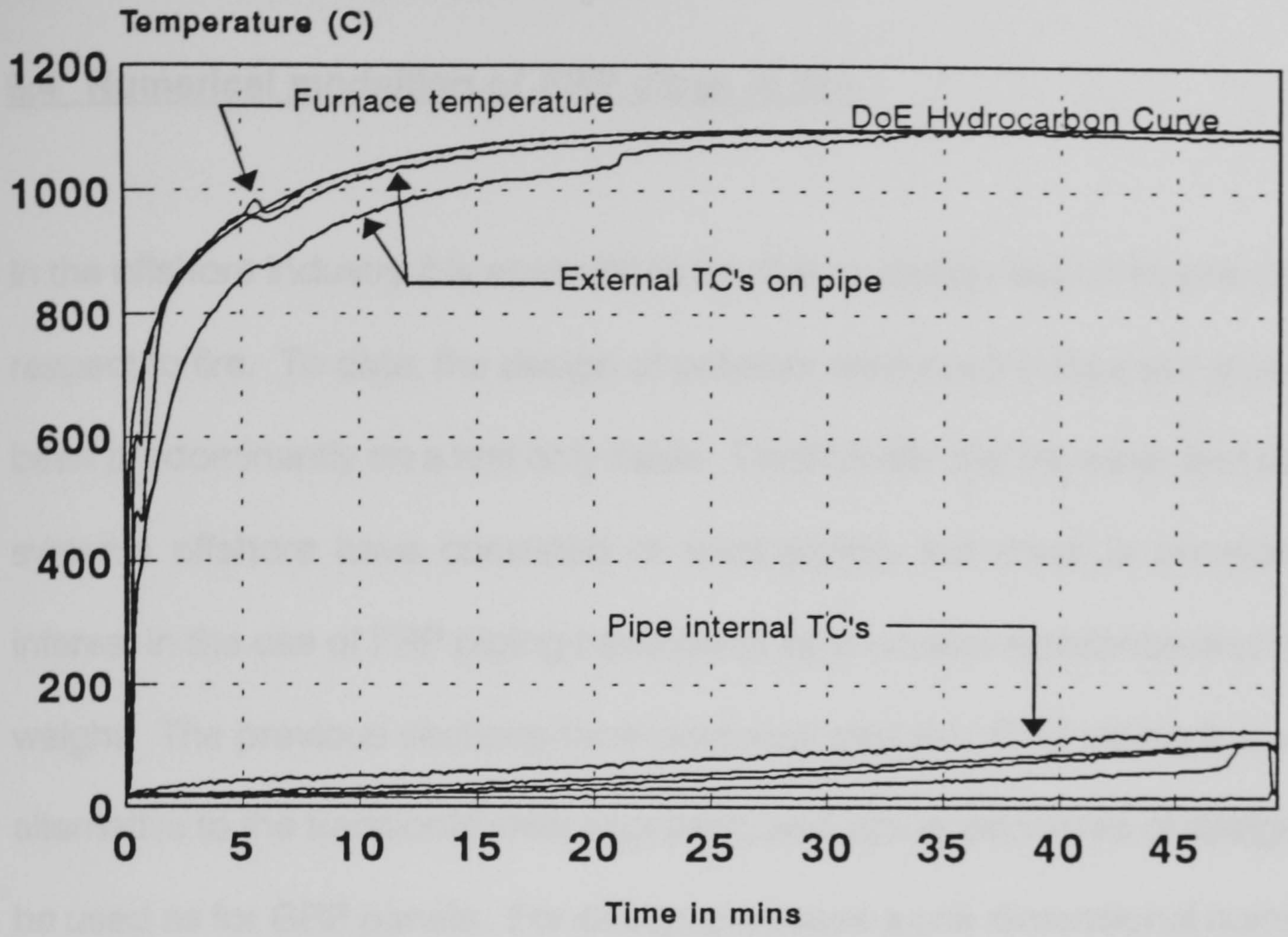

Figure 5.3.29 - Ameron Bondstrand 2000M, 4" Pitt-Char Coated GRE Pipe
Stagnant Water Filled Hydrocarbon Fire Test
All Thermocouples

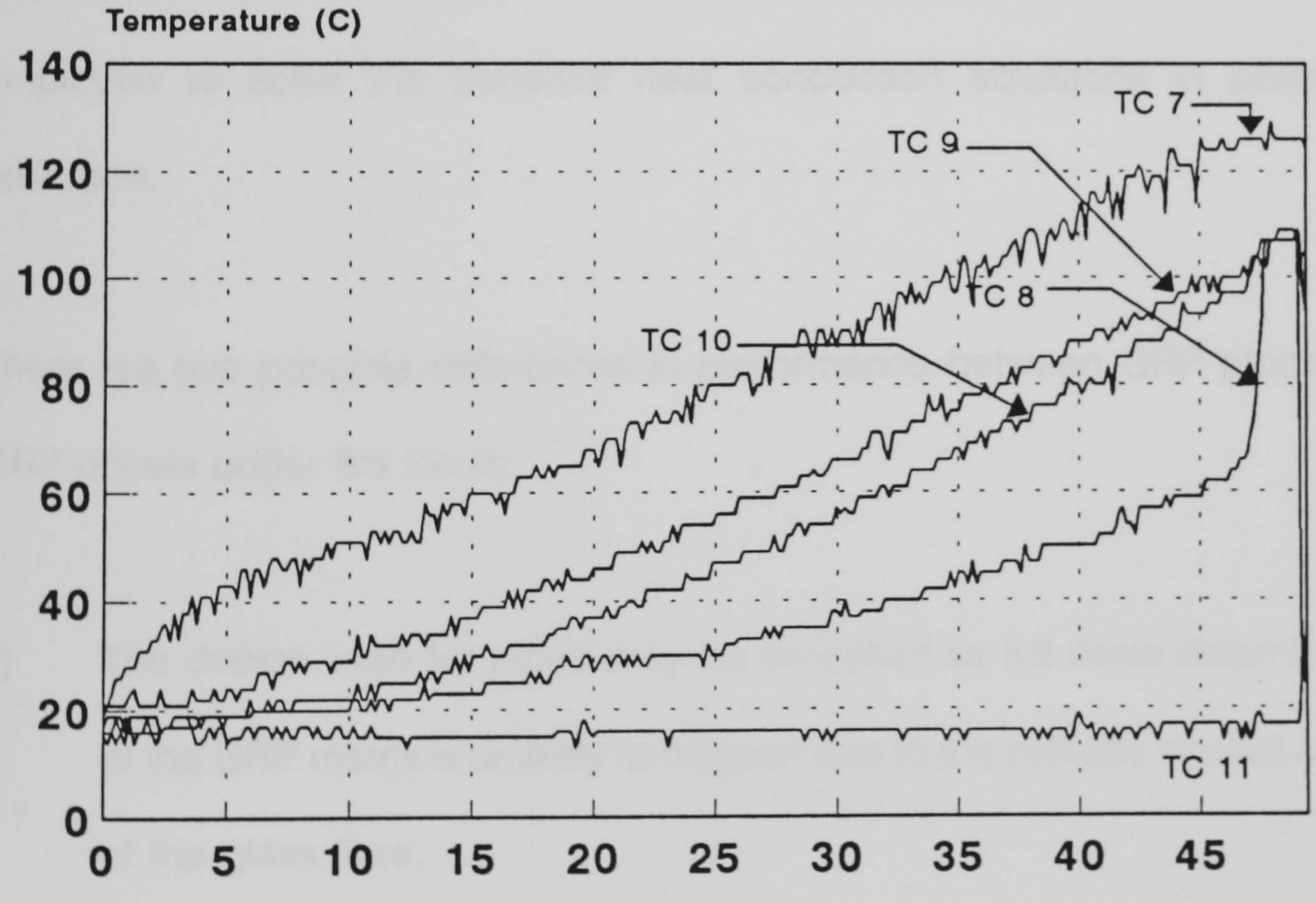

Figure 5.3.30 - Ameron Bondstrand 2000M, 4" Pitt-Char Coated GRE Pipe
Stagnant Water Filled Hydrocarbon Fire Test
Internal Thermocouples Only

5.4 Numerical modelling of FRP pipes in fire

In the offshore industry it is essential to be able to design key components with respect to fire. To date, the design of polymer reinforced composite pipes has been predominantly on a test only basis. Traditionally the fire water and deluge systems offshore have consisted of steel piping, but there is considerable interest in the use of FRP piping because of its corrosion resistance and lighter weight. The previous sections have demonstrated that GRP piping is a viable alternative to the traditional steel approach, and similar principles of design can be used as for GRP panels. For design purposes a one dimensional numerical model for GRP pipes subjected to a prescribed time-temperature history within a furnace has been developed. The explicit finite difference method has been employed to solve the transient heat conduction equations in polar co-ordinates.

There are two possible differences in performance between GRP pipes and GRP panels under fire insult:

1) The design case for pipes may be simplified as full scale delamination of the GRP matrix is unlikely to happen due to the helically wound nature of the glass fibre.

2) The loss of heat from the cold surface (i.e. the inside of the pipe) may be restricted due to the nature of a pipe. This will lead to a more rapid

increase in the temperature of the cold surface than would be observed for a panel.

The fundamental assumptions and principles as used for GRP panels are still applicable for pipes. However, it is necessary to recast the equations into a polar coordinate system. Mass and heat transport is assumed to take place solely in the radial direction. The one dimensional energy equation in a pipe undergoing thermal decomposition, expressed as a balance between the transient energy accumulation rates, with the sum of the rates of conduction, pyrolysed convection, energy sink due to pyrolysis, and heat feedback by combustion of volatiles now becomes[59]:

$$\frac{\partial}{\partial t}(\rho h) = \frac{1}{r}\frac{\partial}{\partial r}\left[k_r(T) r \frac{\partial T}{\partial r}\right] - \frac{\partial}{\partial r}(m'_g h_g) - \phi\frac{\partial \rho}{\partial t} \qquad (5.4.1)$$

in which $R_1 \leq r \leq R_2$, for $t > 0$.

Where:

ρ	is the density (kg/m^3)
h	is the solid enthalpy (J/kg)
t	is time (s)
r	is the polar coordinate (m)
T	is the temperature (°C)
K_r	is the thermal conductivity on the radial direction (W/m°C)
h_g	is the enthalpy of gas (J/kg)
m'_g	is the mass flux of gas (kg/m^2 -s)
ϕ	is the heat of reaction (J/kg)

R_1 and R_2 are the inside and outside radii of the pipe respectively. It was found that the heat release by combustion of volatiles was significant, this being possibly due to the enclosure of the pipe within the furnace. The heat of

reaction is therefore defined as the offset of the endothermal heat of decomposition and the heat feedback by volatile combustion.

Equation 4.1 when solved simultaneously with the equations for the rate of decomposition and the mass flux of the volatiles can be expanded and re-arranged into its final form:

$$\rho C_p \frac{\partial T}{\partial t} = \frac{1}{r}\frac{\partial}{\partial r}\left[k_r(T) r \frac{\partial T}{\partial r}\right] - m'_g C_{pg} \frac{\partial T}{\partial r} - \frac{\partial \rho}{\partial t}(\phi + h - h_g) \qquad (5.4.2)$$

As previously, this equation can be solved simultaneously with the equations for the rate of decomposition of the resin (eq. 4.5.15) and conservation of mass (eq. 4.5.16) for ρ, m'_g, and T respectively. Equation 5.4.2 was solved by the 1-D explicit finite difference method. Allowances are made for the spatial interval between nodes to change due to temperature rise and hence thermal expansion. However, for simplicity it is assumed that the internal surface does not move during expansion at high temperature. Finite difference equations for the nodes are obtained by using the energy balance technique.

Following the formation of the finite difference equations they can be implemented together with the material properties of the samples under test (determined experimentally) to give highly accurate predictions of the thermal response of the sample to the time-temperature regime it is exposed to. Figures 5.4.1 and 5.4.2 show comparisons of the numerical model predictions against actual test data for a 4" diameter GRE pipe tested in the empty and dry condition, and for a 2" diameter GRE pipe tested in the flowing water condition.

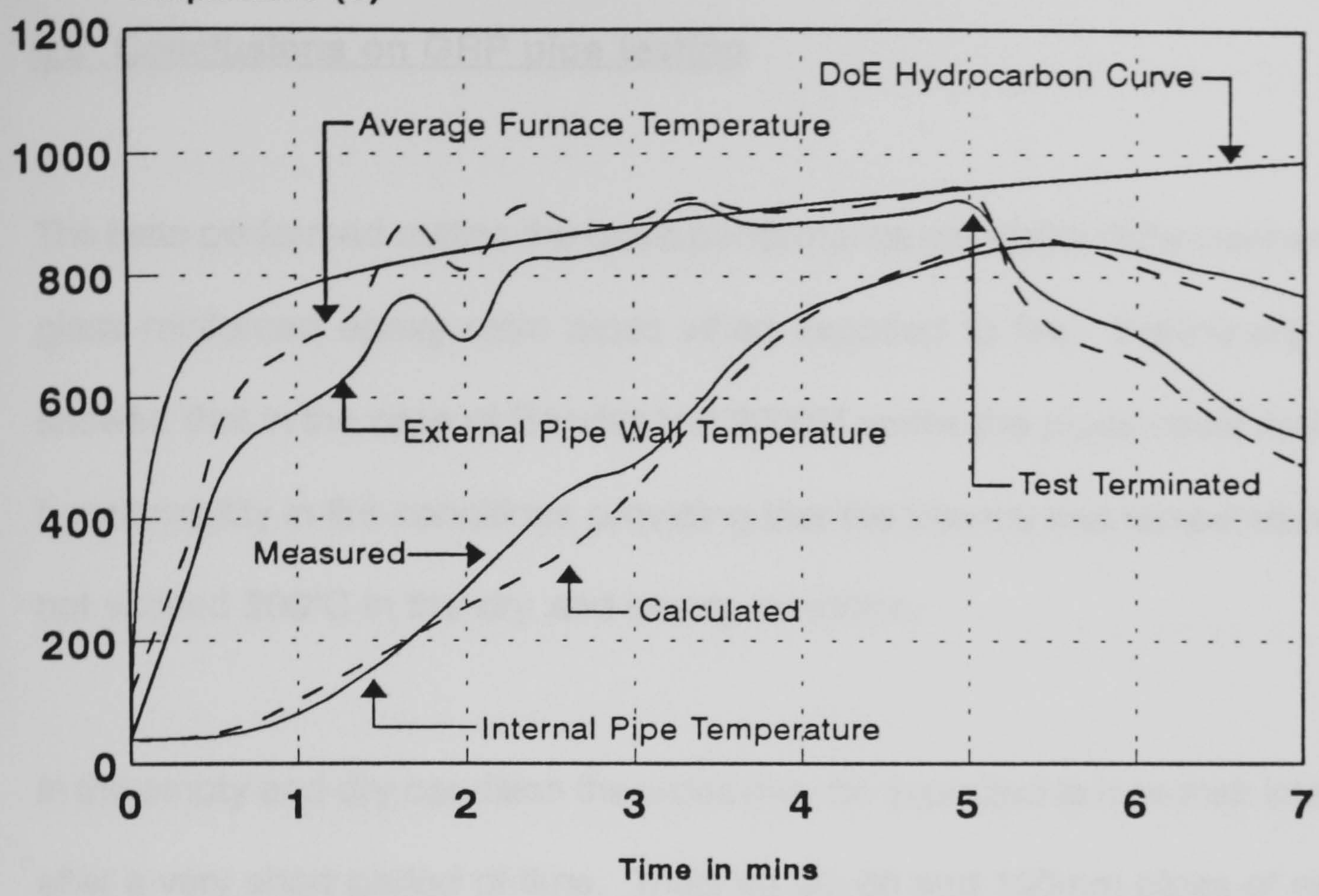

Figure 5.4.1 - DoE Hydrocarbon Fire Test
Ameron Bondstrand 4" GRE Pipe - Empty
Comparison of Experimental and Numerical Results

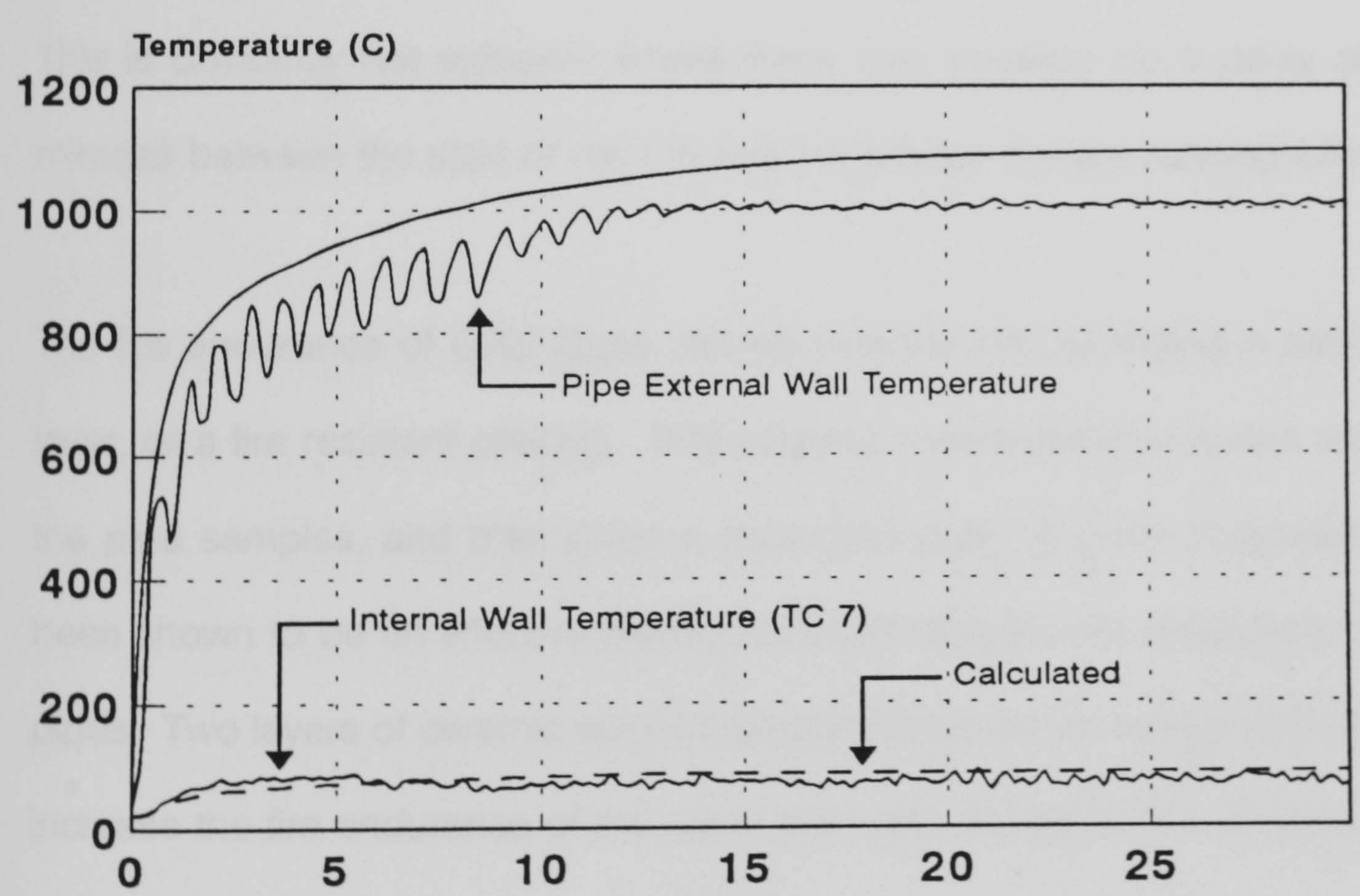

Figure 5.4.2 - DoE Hydrocarbon Fire Test
Ameron Bondstrand 2" Pipe, Flowing water @ 18l/min
Comparison of Experimental and Numerical Results

5.5 Conclusions on GRP pipe testing

The tests performed outline the basic performance capability of filament wound glass reinforced epoxy resin pipes when exposed to fire. Preliminary trials showed that in the case of Bondstrand 2000M series the pipes could maintain functionability in fire conditions providing that the internal wall temperature did not exceed 200°C in the dry and empty condition.

In the empty and dry condition the pipes may be expected to lose their integrity after a very short period of time. Trials on 50, 80 and 100mm pipes of similar wall thickness have shown that under simulated hydrocarbon conditions the pipe can lose some degree of integrity, and possibly all in just 80 seconds. This is obviously not sufficient where there may possibly be a delay of five minutes between the start of the fire and the deluge system running fully.

The fire endurance of GRE pipes can be extended by providing a sacrificial layer, or a fire resistant coating. Thin ceramic wool blanket wrapped around the pipe samples, and then given a protective layer of glass fibre/resin has been shown to be an effective method of increasing the fire resistance of the pipes. Two layers of ceramic wool (originally 3.5mm thick) can be sufficient to increase the fire endurance of the pipes from one minute to five minutes.

Intumescent coatings can also improve the fire endurance of GRE pipes exposed to fire. In tests, a 7.6mm coating of Pitt-Char intumescent epoxy

increased the failure time of a 100mm GRE pipe (5mm wall) from 100 seconds to 11 minutes (a factor of 6). These coatings are very effective in fire situations, but carry a significant cost premium, and are also less durable in an aggressive environment than the original pipe wall material.

By far the cheapest and easiest manner of increasing the performance of GRE pipes in fire is to maintain them in a water filled condition. This would be easy to achieve in an offshore environment. Maintaining the deluge system in the water filled condition is not currently practised offshore, as the water can corrode the steel piping, this however, would not pose a problem to glass fibre reinforced plastics.

For the 50mm pipe samples tested, a 2 minute dry start and a five minute stagnant water start caused leakage failures. A 2 minute stagnant start followed by flowing water at 18 litres/minute will give and extended functional life in hydrocarbon fire conditions. If a five minute stagnant start is required it would be possible to achieve this by increasing the pipe wall thickness, or adding a thin additional layer of fire protection. As can be seen from this, the effectiveness of maintaining GRP pipes in the water filled condition is a function of the pipe volume, and hence the volume of water acting as a heat sink.

For 100mm diameter pipes it has been shown that 2, 5, and 10 minute stagnant water starts, followed by flowing water at 18 litres/minute will give extended functional life in hydrocarbon fire conditions. It would appear that should the

pipes be maintained in the water filled condition that no additional fire protection is needed, but may be required for more demanding fire scenarios (eg jet fires).

For the test method used a period of 30 minutes testing overall was sufficient to achieve steady state conditions. This research has not considered the effect of high water flow rates (which may limit steam formation), or the length effect of the exposed pipe loop (longer pipes will allow water to be heated more as it passes through the loop). These two effects will serve to cancel each other out to some extent, however, to what degree is not known at this point in time.

The research would suggest that even at modest water flow rates GRE pipes may have an indefinite life in hydrocarbon fire conditions, providing that there is no erosion effect.

Utilising the explicit finite difference method it has been shown that the thermal response of filament wound GRP pipes to fire can be predicted with great accuracy. This method is an effective design tool for polymeric composite materials and may lead to a substantial reduction in the testing requirements for new materials.

CHAPTER 6 - FURNACE CHARACTERISATION AND THE VALIDITY OF FIRE RESISTANCE TEST RESULTS.

6.1 The Variability of Fire Test Results.

As there are an infinite number of "real fire" scenarios each giving rise to different conditions, furnace fire resistance testing of construction elements is based on a standardised furnace test in which there are prescribed time-temperature regimes. These may be related to cellulosic or hydrocarbon fires and standard time-temperature relationships are specified in various documents such as ISO834/BS476 (cellulosic) or DoE/NPD (hydrocarbon). The thermal severity of a furnace fire resistance test, however, may be influenced by more factors than just the time-temperature regime. Many factors which could affect the thermal severity of the fire resistance test are not subject to regulation. These include type, colour and condition of the furnace lining, the furnace geometry, the fuel type, burner type and location, the test piece orientation, the location of the exhaust duct, and the gas velocities adjacent to the test piece. When testing combustible materials possibly the most important factor is the amount of free air within the furnace. A low free air content within the furnace combustion products will act to suppress flaming of a combustible sample and hence encourage a general heat up-take rather than heat release. A consequence of these factors is that different test results are obtained from different test furnaces for nominally identical material samples. As can be seen,

if all the variables which may influence the thermal severity of a fire resistance test are taken into account then the mechanisms of heat transfer would be complex and difficult to quantify. It has been thought that the difference in thermal severity between furnaces could be limited by:

a) Lining all furnaces with a highly efficient low density lining material such as ceramic wool.

b) Using temperature measuring devices which more realistically measure the energy that the test piece "sees" during the test. Plate thermometers have been investigated for this purpose.

Assessing the benefits of these two possible solutions will aid in the production of accurate and reproducible data sets for numerical modelling of the heat transfer mechanism from a furnace to a test specimen. If the exact furnace test conditions were known and referenced against fire resistance test results it would be more reliable to determine material properties for numerical modelling. In addition this approach should also lead to more appropriate methods of furnace control or correction factors when the reference conditions cannot be achieved.

Similar work to this was performed by Cooke[18] however inherent differences in the accuracy of control between the different furnaces into which he installed his calibration elements leads to an uncertainty about the degree of effect that

the furnace variations had. Cooke's test programme consisted of eleven furnace tests in total, using three different furnaces. All the furnaces used were full scale floor furnaces of approximately 4.0 x 4.0 x 1.7m (there were some slight dimensional differences between the furnaces). Each furnace was fitted with a heavily insulated standard test rig which supported the calibration elements in the furnace environment below it. The calibration elements used within Cooke's experimental programme were calibration plate elements, calibration rods and spheres and a copper pipe containing flowing water. The temperature measurement devices were either plate thermometers, or standard k type thermocouples (either bare wire or sheathed).

6.1.1 The reason for plate thermometer use

The differences mentioned previously in furnace design, namely furnace dimensions, furnace wall materials and conditions, fuel types etc are at present not controlled by the national standards for fire testing. Cooke[18] reported that to bring only the European officially approved furnaces in to line with an adopted "standardised" design would realistically cost in the region of £50 million. This does not account for the numerous furnaces used for research and development. It can be seen from this that there is no clear incentive for the construction of "standard" furnaces due to the cost that this would incur.

The philosophy behind the use of plate thermometers is that it may be possible by using these instruments that the significant differences in test results between different furnaces may be reduced without the costly process of rebuilding furnaces. In a correspondence between Dr Vytenis Babrauskas and Dr Gordon Cooke, Dr Babrauskas outlined that during a fire resistance test, the sample under test is only sensitive to the heat flux imposed on its hot face. Thus in an ideal case the fire test would be controlled via flux meters mounted flush with the sample face. This is impractical as mounting a flux meter through the specimen would modify its behaviour from that originally intended.

The Wickström[60] design plate thermometer (figure 6.1.1) consists of a thin inconnel sheet folded to leave a face area of 100x100mm. A fast reacting thermocouple is spot welded to the unexposed side of the inconnel, and the

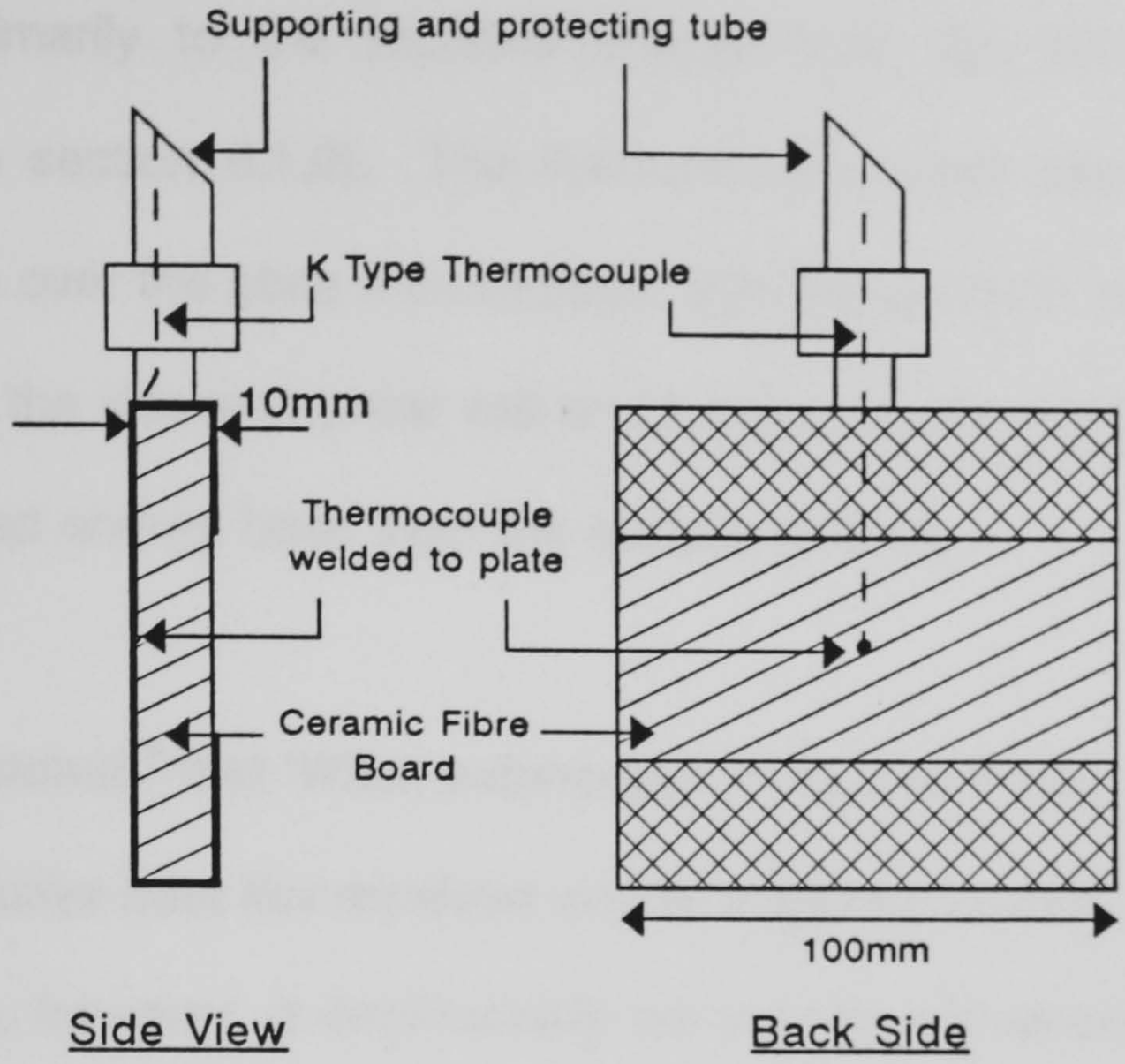

Figure 6.1.1 - The Wickström Design Plate Thermometer

back side of the plate thermometer is insulated with ceramic fibre board to prevent direct radiative influence from the test specimen. The plate thermometer is located 100mm away from the face of the sample under test, in positions as would be used for control thermocouples. The plate thermometer is aligned within the furnace to face away from the sample under test. This arrangement allows the plate thermometer to receive the same radiation as the sample under test.

Theoretically the plate thermometer has several advantages when considering it over standard thermocouples for furnace temperature control. Primarily the small bead of the thermocouple is sensitive to convective heat, and whilst this is acceptable for control at low furnace temperatures where radiative energy from the walls of the furnace is low, at high temperatures the sample under test

responds primarily to the radiative energy from the furnace walls (see discussion in section 6.1.2). The thermocouple bead also has a second disadvantage over the plate thermometer, that being that it "sees" the energy not only from the side walls, rear wall and furnace gases, but it also is affected by the radiated energy back from the sample surface.

Babrauskas stated[18] that "*When submerged in the same environment, the per unit area radiative heat flux received will be identical for both small and large objects. This, however, is emphatically not true for convective heat flux. For a spherical object, this convective heat flux varies* $\propto D^{-1/2}$ *(for a planar wall, the variation is also inversely proportional to size, but scaling as* $\propto L^{-1/5}$*)*". In Babrauskas's statement D refers to the diameter of the spherical object, and L refers to the length of the planar wall. From this it can be seen that a small spherical object will be much more sensitive to convective heat flux than a relatively large square plate.

Following this statement through to it's conclusion, this would suggest that a thermocouple bead would be much more sensitive to the gas flow and convective heating from the furnace gases than the specimen under test. Conversely should large differences exist between the furnace linings and their emissivities, and hence radiative energy emitted, the specimen under test would be greater affected than would be registered by the thermocouples.

Given that the temperature measuring device should be shielded from the

response of the specimen under test we arrive at the guiding principles behind the design of the plate thermometer:

The plate thermometer has a large surface area when compared to a thermocouple bead:

This minimises over-representation of the convective heat flux for temperature measurements where the specimen under test is relatively insensitive to it.

It is shielded from any reactions the sample may have to the furnace test by the ceramic fibre board backing:

This avoids mis-representation of the heat energy that the sample in effect "sees" - for instance a burning sample may effect a thermocouple temperature measurement by providing localised convective energy sources (ie flames), whilst the sample itself may not be effected unduly by this.

It is still sufficiently thin to have a fast reaction rate to changes in furnace environment:

By keeping the mass of the inconnel sheet as low as possible the thermal mass of the plate thermometer is hence minimised. Using

thicker sheets or spheres would cause the effective response time to be increased, hence reducing the ability to accurately control the furnace environment.

Analysis of experimental results and numerical predictions of the effect of using plate thermometers for furnace temperature control systems has also been performed by Twilt and Van de Heur[61]. The experimental programme of their research showed that there was no systematic reduction in differences between test results when using plate thermometer control. In their numerical simulations the temperatures in all the calibration elements were higher under plate thermometer control than they were under bare wire thermocouple control. This numerical prediction was not systematically supported by their experimental results.

Twilt and Van de Heur also found that there was an inconsistency in the difference between plate thermometer and thermocouple measured temperatures. Furnaces with a large depth showed only small differences in the measured temperatures of the thermocouples and plate thermometers, however, the effect was reversed for shallow furnaces where large differences in measured temperature existed.

Twilt and Van de Heurs' final conclusions were that plate thermometer control increases the severity of the fire resistance test, and tends to improve the reproducibility of results between furnaces, although not to the extent of

expectations. They also stated that the resulting improvement "drowns" in the effects of other parameters such as furnace lining, furnace depth, and burner types, locations and number.

6.1.2 Use of a highly efficient furnace lining.

As mentioned previously, it has been thought that lining all furnaces with a highly efficient additional lining layer (i.e. ceramic fibre) would go some way towards minimising the differences between test results from different test centres and furnaces. Some data from testing carried out at the National Fire Laboratory is presented by Cooke[18] in addition to the test programme of the occasional paper itself.

Dr M Sultan of the National Fire Laboratory, NRC, Canada stated "*For a furnace heated with a liquid fuel....the specimen's exposed surface sees only flames.*" Comparing two test results, both in liquid fuel fired furnaces, one fire brick lined, the second lined with Fiberfrax (mineral wool) he said "*The differences...(between results)...are small because the specimen sees only the luminous flames and, thus, the furnace walls have little effect on the specimens exposed surface. A similar trend at the unexposed surface is also indicated.....*"

Sultan's limited data serves well to show that the furnace lining may be a governing factor only in certain cases. "*.....in a large furnace...whether you*

use a gas fuel or liquid fuel, the overall heat severity on the specimen would be comparable. This might not be the case for small depth furnaces.....The size of the furnace is a controlling factor...."

Further experimental work as to the effect of varying furnace linings, and in particular the effect of the furnace lining surface emissivity has been performed by several other authors. Elliston et al.[62] showed in their calculations and experimental work that the heat transferred from a furnace to a specimen varied by only 2% as the furnace lining emissivity was increased from 0.5 to 0.9. Further calculative work showed that when considering the convective heat transfer from the combustion products to the specimen the total heat transfer increased by a further 5% of the radiative contribution. This further reinforces the thought that convective heat transfer plays only a small role in the total heat transfer during a fire resistance test.

Sultan et al.[63] investigated heat transmission within furnaces with respect to an acceptable "test efficiency". The research did not appear to be aimed at standardising furnace fire resistance tests, but at prescribing a minimum acceptable performance level based on the normalized heat load to a specimen.

The normalized heat load, H, was calculated from the maximum temperature rise in a slab of known thermal properties as:

$$H = 2.3 \frac{a}{\kappa^{1/2}}(T-T^{o})_{m}$$

Where κ is the thermal diffusivity of the slab, and a is a distance below the surface of the slab such that $0.8 < a/\kappa^{1/2} \tau^{1/2} < 1.2$, and τ is the test duration in seconds. $(T-T^{\circ})_m$ is the maximum temperature rise above the original temperature T° at the depth a after the termination of the test.

The research experimental work was performed on a full size floor furnace (3.66x4.58m) but the furnace depth was not reported. A typical floor furnace would have a depth of between 1.5 and 2.0m. Two different fuels, diesel oil and propane gas, were used to heat the furnace to follow a prescribed time-temperature regime. It was reported that the value of $(T-T^{\circ})$ did not seem dependent on the nature of the fuel, and hence the heat load to the test piece did not appear to be dependent on the fuel used. This was despite the fact that the emissivities of the fuel combustion products were substantially different. The emissivity of the flames and combustion products for the diesel oil was approximately 0.8, and for the propane approximately 0.3.

The recommendations for improving fire test efficiency were to increase the furnace volume, reduce the excess air for combustion, and to use fuels which yield combustion products of higher absorption coefficient.

When considering these three options with reference to standardising the fire resistance test the first option of increasing the furnace depth would incur large capital expenditure and hence would be the least attractive solution. Reduction of the excess air for combustion would, in the case of hydrocarbon gases, produce a "dirtier" and hence more radiant flame. This would effectively reduce the effect of variation in furnace linings between different furnaces as the sample under test would "see" only the flame. However, there are two further considerations to be made when reducing the excess oxygen for combustion. Firstly, reduction in excess oxygen may represent a reduction in furnace pressure also which cannot go below a certain limit according to national standards. Secondly, and perhaps more importantly, if there is little or no excess oxygen during the test then combustible materials, such as fibre reinforced plastics, will have significantly different performance to that which may be observed in "real" fire situations.

If the available theoretical and experimental evidence is all taken into consideration at the same time, it can be seen that:

1) If the furnace used for fire resistance testing is fired by "dirty" fuels, i.e. those typical of fuel oils, or incomplete combustion of hydrocarbon gases, then the furnace volume and nature of the furnace lining has little effect on the thermal severity of the fire resistance test.

2) If the furnace volume is large, particularly with respect to furnace depth,

then the heat load to the specimen under test will be similar, regardless of the nature of the fuel type used to heat the furnace.

3) The effect of furnace wall emissivity is low where the furnace is relatively deep. For instance, in a methane fired furnace 1.6m deep and 6.5m^3 total volume, the effect of varying furnace wall emissivity from 0.5 to 0.9 resulted only in a 2% increase in heat load. It was noted also that convective heat transfer within this furnace accounted for only 5% of the total heat transfer to the stock.

From the above findings it can be seen that, predominantly, the largest effects due to wall properties would be for shallow furnaces of small volume which are fired by clean burning fuels.

6.2 The Experimental Furnace and Instrumentation

A test regime was used to investigate in more detail some of the factors described previously. It was decided that initially just one furnace should be used, and only two variables be investigated in detail, those being the furnace lining and the method of temperature control. The $1m^3$ active volume furnace at Salford was decided upon due to the ease with which the lining could be altered, and also as it would appear to be ideal in terms of furnace size and fuel type.

The gas flow to the burner heads was computer controlled with a simple PID control routine with a sample rate typically of less than one second. Typical furnace errors were generally less than 1.5% and below 0.5% after the first thirty minutes of testing. This manner of furnace control ensured that the desired furnace temperature (set point) could be accurately reproduced between independent tests. Figure 6.2.1 shows a comparison between two identical tests carried out several days apart, and shows the accuracy of the reproduction of the test conditions.

Due to the fundamental nature of this research it was decided that an alternative family of furnace time-temperature regimes should be adopted, on the basis that linear variations of temperature with time would make it easier to determine significant differences in results. The new control curves are shown in figure 6.2.2 and are based on a linear rise in temperature from room

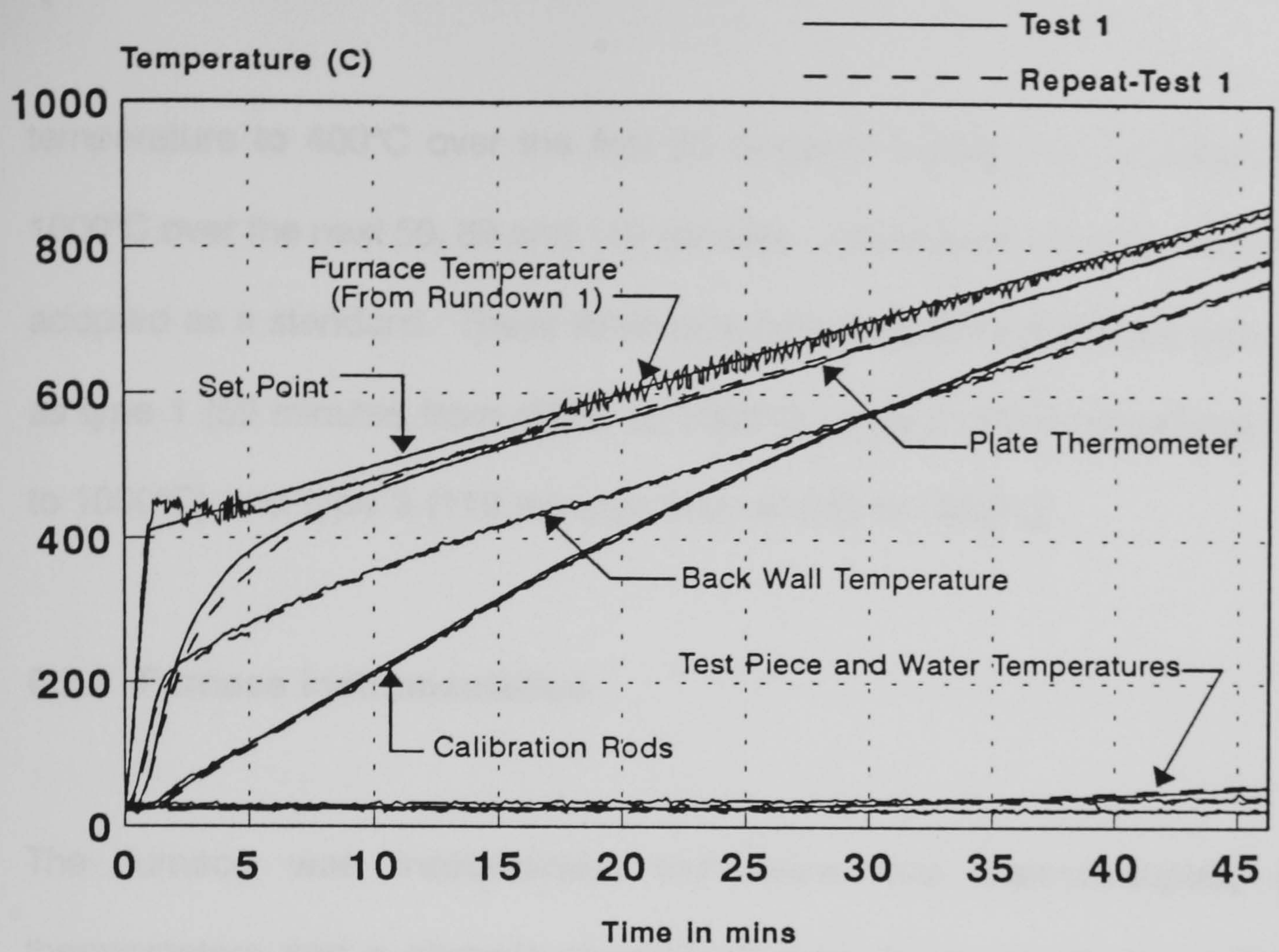

Figure 6.2.1 - Furnace Characterisation
Comparison of Test 1 and Repeat-Test 1
Over First 45 Minutes of Testing

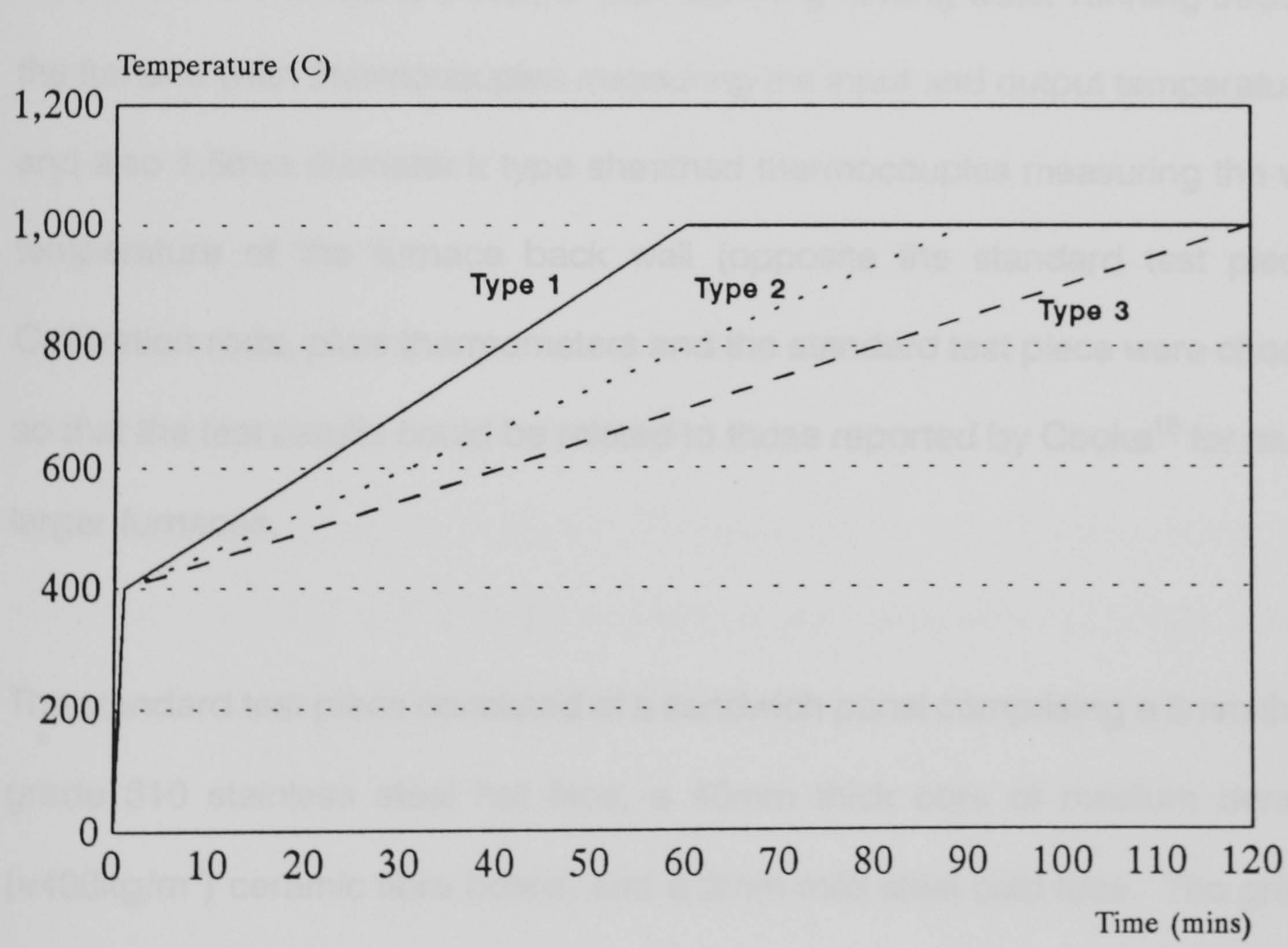

Figure 6.2.2 - New Linear Control Curves
Adopted for Furnace Characterisation Work

temperature to 400°C over the first 60 seconds followed by a linear rise to 1000°C over the next 59, 89 and 119 minutes. A test duration of two hours was adopted as a standard. These three time-temperature regimes are referred to as type 1 (59 minutes from 400°C to 1000°C), type 2 (89 minutes from 400°C to 1000°C) and type 3 (119 minutes from 400°C to 1000°C).

6.2.1 Furnace instrumentation

The furnace was instrumented with bare wire thermocouples, plate thermometers and a ceramic sheathed R type thermocouple in addition to having a standard test piece (mounted to the front of the furnace), calibration rods within the furnace, a copper pipe carrying flowing water running through the furnace (with thermocouples measuring the input and output temperature), and also 1.5mm diameter k type sheathed thermocouples measuring the wall temperature of the furnace back wall (opposite the standard test piece). Calibration rods, plate thermometers and the standard test piece were chosen so that the test results could be related to those reported by Cooke[18] for much larger furnaces.

The standard test piece consisted of a sandwich panel comprising a 5mm thick grade 310 stainless steel hot face, a 40mm thick core of medium density ($\approx$400kg/m^3) ceramic fibre board, and a 2mm mild steel cold face. The grade 310 stainless steel hot face to the panel was heated to a temperature of 1000°C in excess oxygen prior to use. This encouraged the formation of a stable black

oxide layer on the stainless steel, the properties of which would not alter during the progression of the test. The hot face temperature was measured using a k type inconnel sheathed contact thermocouple, and the cold face temperature was measured with two copper disk k type thermocouples covered with insulating pads.

The calibration rods were 500mm long 50mm diameter grade 310 stainless steel which had been precision drilled to mid section to accommodate an inconnel sheathed 1.5mm diameter k type thermocouple 50mm either side of mid depth of the rod. These rods had also been heated in excess oxygen in order to form the stable black oxide layer.

Plate thermometers[60] were constructed from 1.2mm thick inconnel sheet, folded to leave an exposed surface area of 100x100mm. A fast responding K type sheathed thermocouple was carefully spot welded to the centre of the unexposed surface of the inconnel, and was supported at the edge of the sheet with spot welded wire loops. The construction of the plate thermometers for the research followed the Wickström[60] original design in all matters apart from the actual thickness of the inconnel sheet. It was not possible to obtain 0.7mm thick sheet, and therefore the thinnest gauge available was used, namely 1.2mm.

A copper pipe filled with flowing water was fitted through the furnace along its centreline. The pipe was of notional 12mm OD with a right angle bend at the

outflow end of the pipe. The pipe was fed with flowing water from a three phase pump which in turn was supplied by two water tanks connected together by a syphon. The outflow velocity of the pump could be regulated directly by a gate valve, and was fed directly into a metric rotameter containing a stainless steel float, from which the water flow velocity could be measured. The flow from the rotameter was then fed to the copper pipe via garden hose. The outflow from the pipe was then taken back to the first of the two tanks also via garden hose. Precision holes, 1.5mm diameter, were drilled in the hose to pipe connectors at both the inflow and outflow into which thermocouples were mounted at the mid-depth level of the copper pipe. The reason behind using a copper pipe filled with flowing water is that the difference in water temperature between the input and outflow could be assumed to be directly proportional to available heat flux within the furnace. This is a reasonable assumption as the thermal conductivity of water changes very little between the minimum and maximum temperatures observed during any of the tests (minimum $\approx$ 18°C, maximum $\approx$ 60°C). Knowing the specific heat capacity and density of the pipe and the water, and also the rate of water flow through the pipe, it should also be possible to calculate the available heat flux within the furnace with a reasonable degree of accuracy. In transient conditions (i.e. during the heating of the furnace) assuming that the copper pipe wall temperature is uniform (due to the high thermal conductivity of copper), and that the pipe wall temperature increases at the same rate as furnace temperature, the heat flux available can be approximated as:

$$q \approx \frac{\dot{m}_w C_{p_w} (T_{1_w} - T_{0_w}) + m_{Cu} C_{p_{Cu}} \left(\frac{\partial T_{Cu}}{\partial \tau_{Cu}} \right)}{2 \pi r l}$$

where:

$$\dot{m}_w = \rho_w A_w V_w$$

q = heat flux (kW/m^2)
C_p = Specific heat capacity ($J/kg°C$)
ρ = Density (kg/m^3)
r = radius of the pipe, l = length of the pipe
$\partial T/\partial \tau$ = Rate of change of temperature with time ($°C/s$)
A = Cross section of the pipe (m^2), V = Velocity of water flow (m/s)

In steady state conditions this reduces to the simpler approximation (as the copper pipe wall should be at notionally steady state temperatures):

$$q \approx \frac{\dot{m}_w C_{p_w} (T_{1_w} - T_{0_w})}{2 \pi r l}$$

Figure 6.2.3 shows both the cross section and longitudinal section of the furnace indicating the relative positions of the furnace instrumentation.

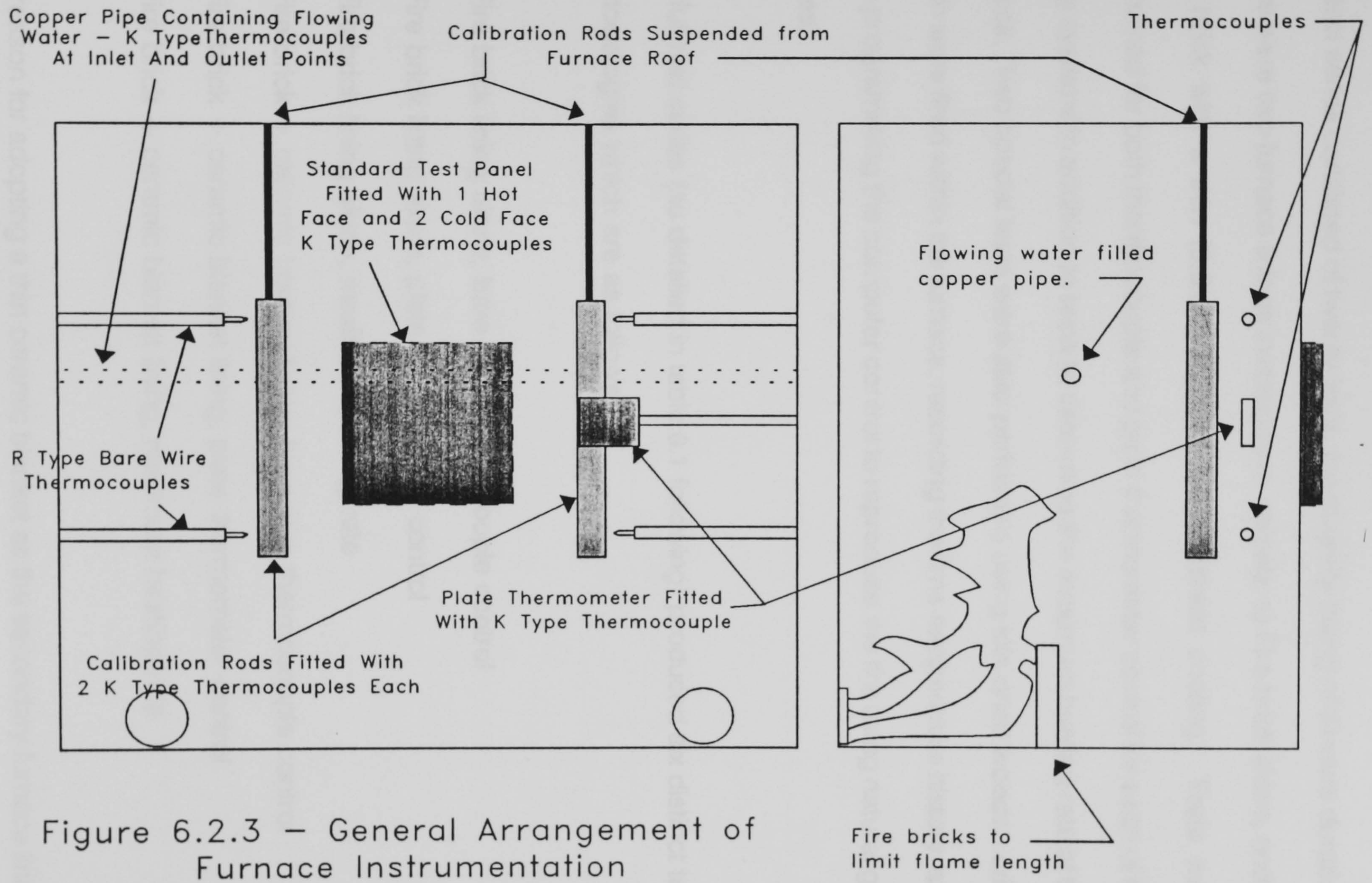

Figure 6.2.3 – General Arrangement of Furnace Instrumentation

(R Type Thermocouples and Plate Thermometers Reversed for Plate Thermometer Control Method)

6.3 Furnace Characterisation Test Programme

The test series consisted of twenty tests, the majority being of 2 hours duration.

There were two furnace linings investigated, namely, a) Fire brick alone, and b) Fire brick with a thin (3.5mm) ceramic wool blanket coating. Tests were performed for both thermocouple and plate thermometer control for each of the lining systems in addition to tests to determine the maximum heating rate of the furnace. Two special tests were also performed using kiln dried wooden cribs which were fired within the furnace, recording the time-temperature history, and then programming the computer control to reproduce the fire using natural gas flames.

The full test series (as detailed in table 6.1 following) produced six distinct test methodologies which are as follows:

1) Fire brick lining alone, bare wire thermocouple control
2) Fire brick lining alone, plate thermometer control
3) Fire brick lining alone, maximum heating rate
4) Fire brick + ceramic blanket lining, bare wire thermocouple control
5) Fire brick + ceramic blanket lining, plate thermometer control
6) Fire brick + ceramic blanket lining, maximum heating rate

The reason for adopting a thin ceramic blanket as the secondary furnace lining was that the volume of the furnace box, the burner and exhaust positions, and

instrumentation positions with respect to the walls all remained essentially unchanged. This eliminated all possible factors affecting fire resistance except the wall lining itself.

Test Run	Control Method	Furnace Lining	Time to 1000°C	Duration
1	TC	Fire Brick	60	120
2	TC	Fire Brick	90	120
3	TC	Fire Brick	120	120
4	TC	Fire Brick	60	120
5	TC	Fire Brick	90	120
6	TC	Fire Brick	120	120
7	PT	Fire Brick	60	120
8	PT	Fire Brick	90	120
9	PT	Fire Brick	120	120
10	PT	Fire Brick	90	120
11	None	Fire Brick	Max Heat Rate	51
12	None	Brick + Ceramic	Max Heat Rate	36
13	TC	Brick + Ceramic	120	120
14	TC	Brick + Ceramic	60	120
15	TC	Brick + Ceramic	90	120
16	PT	Brick + Ceramic	120	120
17	PT	Brick + Ceramic	90	120
18	PT	Brick + Ceramic	60	120
19	None	Brick + Ceramic	"Real Fire"	30
20	TC	Brick + Ceramic	"Real Fire" Sim.	25

Table 6.1 - Full Test Programme

6.4 Results of Furnace Characterisation Study

For clarity of the text the graphical representations of individual test results are presented in appendix D, and the comments in this chapter will refer specifically to comparisons between different tests. The comparisons drawn between test results will be for the two different furnace linings and the two different temperature measuring devices. At the end of this section there is a discussion of the test results and their relevance and meaning.

The comparative graphs, and test result comparisons made in this chapter are as follows:

1) Fire Brick Alone Furnace Lining

Comparison of the effect of different control methods for the three different heating regimes. Comparisons made are between thermocouple and plate thermometer read temperatures and also between calibration rod and standard test piece cold face temperature response.

2) Fire Brick plus Ceramic Wool Furnace Lining

Comparison of the effect of different control methods for the three different heating regimes. Comparisons made are between thermocouple and plate thermometer read temperatures and also between calibration rod and standard test piece cold face

temperature response.

3) R type Bare Wire Control Thermocouples

Comparison of the effect of different lining systems for the three different heating regimes. Comparisons are made between thermocouple and plate thermometer read temperatures and also between calibration rod and standard test piece cold face temperature response.

4) Plate thermometer Control

Comparison of the effect of different lining systems for the three different heating regimes. Comparisons are made between thermocouple and plate thermometer read temperatures and also between calibration rod and standard test piece cold face temperature response.

6.4.1 Fire brick alone furnace lining

Figures 6.4.1 and 6.4.2 show comparisons between the measured temperatures within the furnace and in the calibration elements for the fire brick alone furnace lining. The furnace control was for either R type bare wire thermocouples (TC's) or plate thermometers (PT's) and followed the type 1 furnace time-temperature regime.

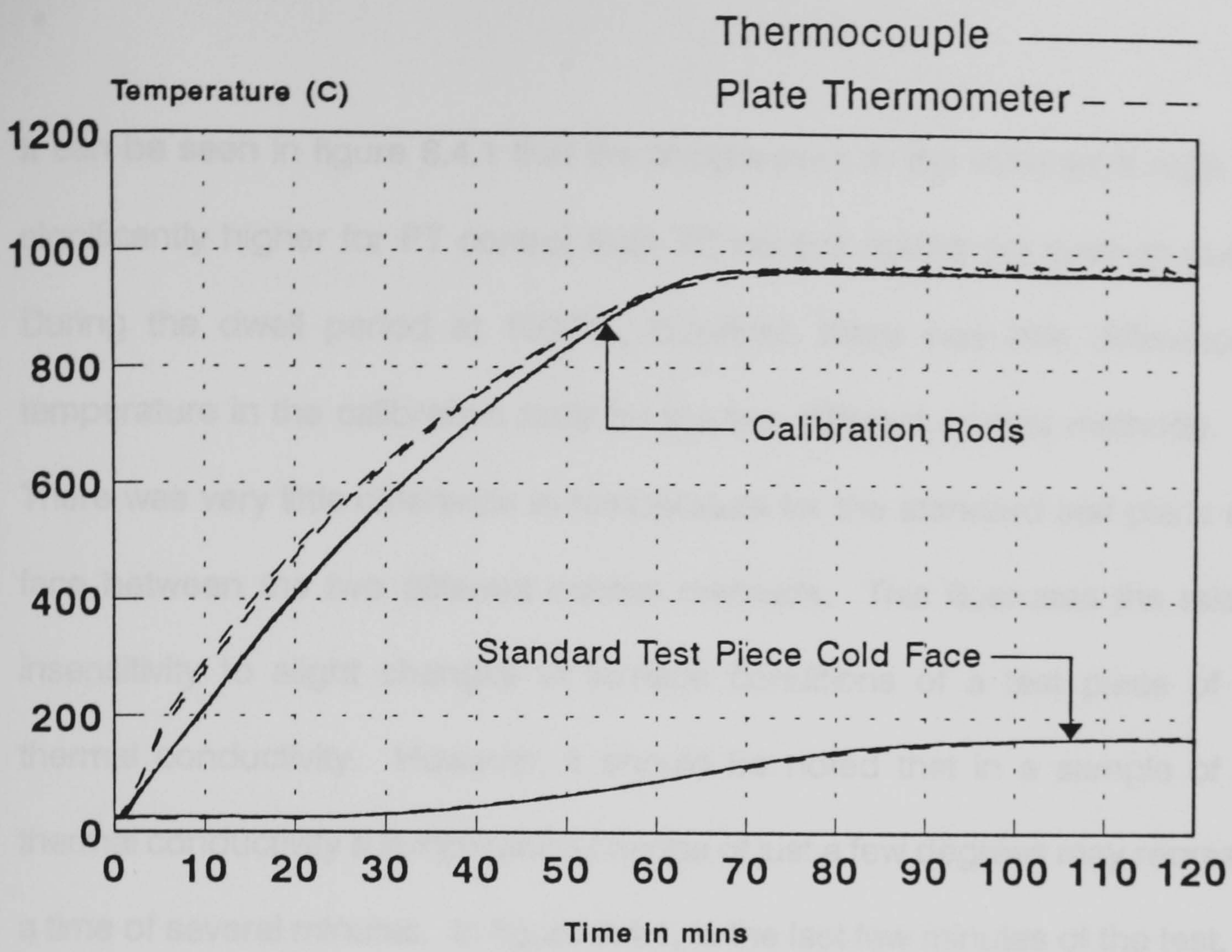

Figure 6.4.1 - Comparison of Response of Calibration Rods, and Standard Test Piece between Thermocouple and Plate Thermometer Control Systems. Fire Brick Alone Furnace Lining.

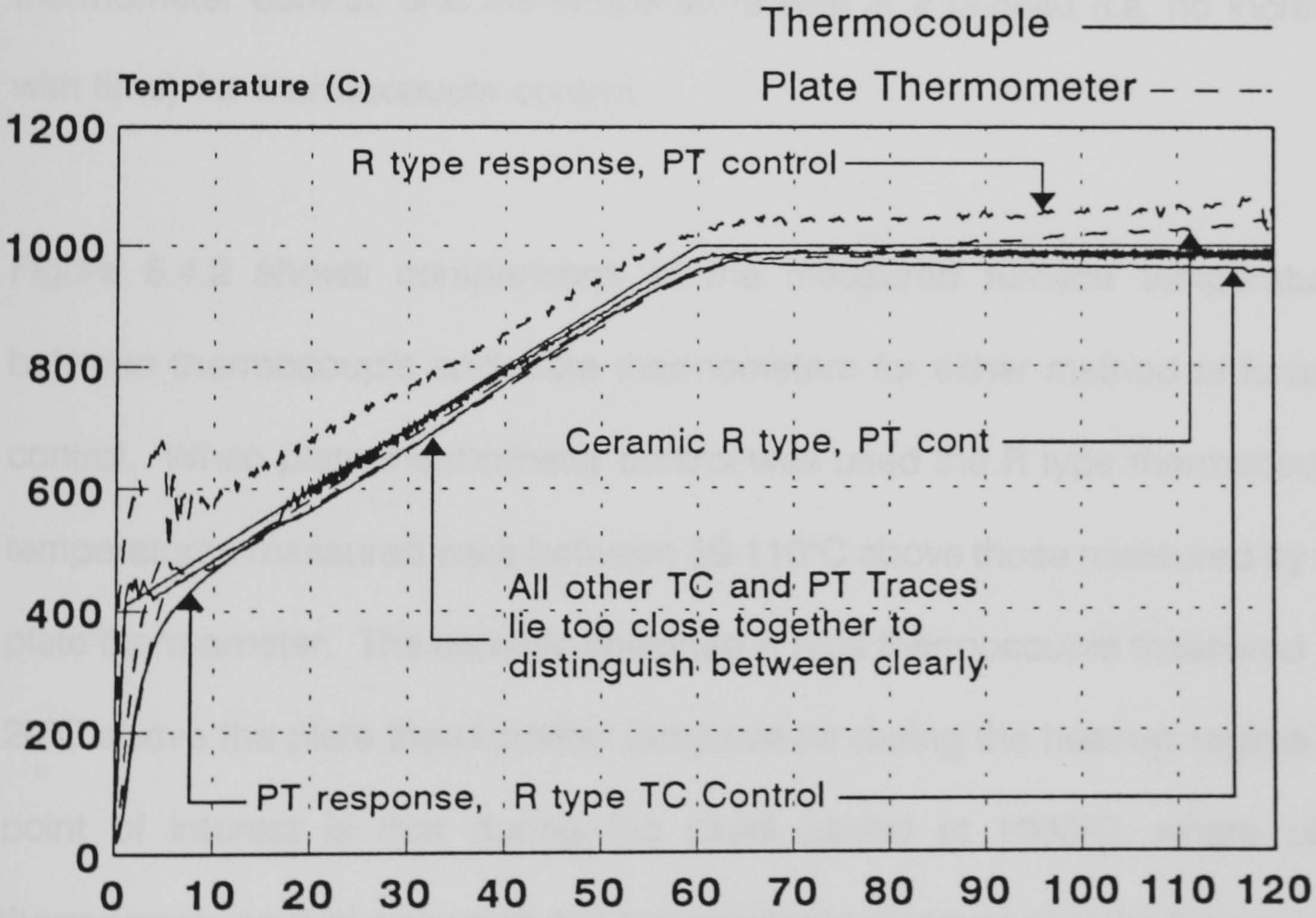

Figure 6.4.2 - Comparison of Furnace Temperature as Measured by R type Thermocouple or Plate Thermometer for both Control Methods. Fire Brick Alone Furnace Lining.

It can be seen in figure 6.4.1 that the temperature in the calibration rods was significantly higher for PT control than TC control during the heat-up period. During the dwell period at 1000°C, however, there was little difference in temperature in the calibration rods for the two different control methods.

There was very little difference in temperature for the standard test piece cold face between the two different control methods. This illustrates the relative insensitivity to slight changes in furnace conditions of a test piece of low thermal conductivity. However, it should be noted that in a sample of low thermal conductivity a temperature change of just a few degrees may represent a time of several minutes. In figure 6.4.1, in the last few minutes of the test, the cold face temperature increase was approximately 0.5°C per minute for plate thermometer control, and the temperature was at a plateau (i.e. no increase with time) for thermocouple control.

Figure 6.4.2 shows comparisons of the measured furnace temperatures between thermocouple and plate thermometers for either method of furnace control. When plate thermometer control was used the R type thermocouple temperatures measured were between 80-110°C above those measured by the plate thermometer. The ceramic sheathed R type thermocouple measured 10-20°C above the plate thermometer temperature during the heat-up regime. A point of interest is that during the dwell period at 1000°C, where plate thermometer control was used, the temperatures measured by the R type bare wire and ceramic sheathed thermocouples continued to rise steadily.

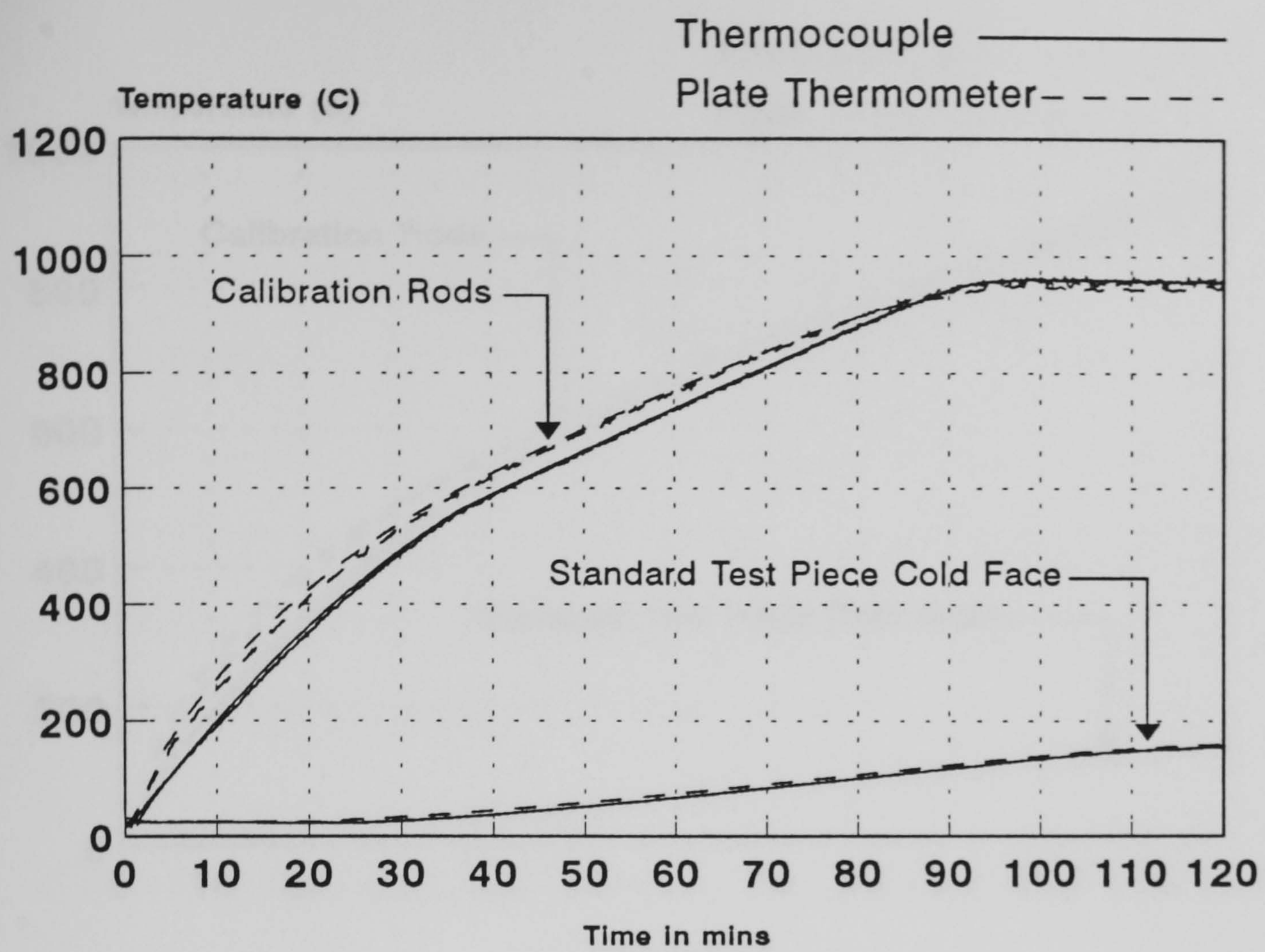

Figure 6.4.3 - Comparison of Response of Calibration Rods and Standard Test Piece between Thermocouple and Plate Thermometer Control Systems. Fire Brick Alone Furnace Lining.

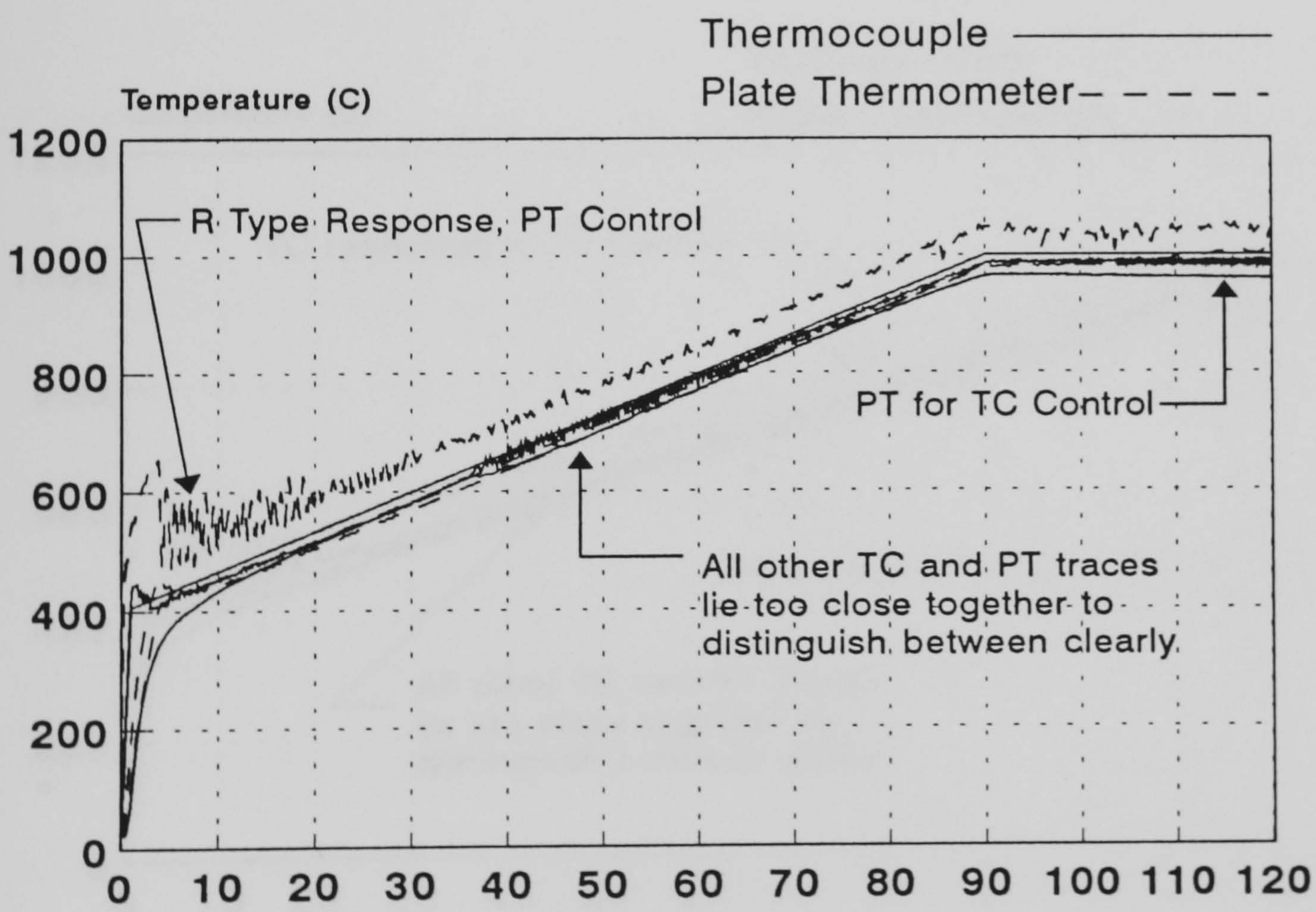

Figure 6.4.4 - Comparison of Furnace Temperature as Measured by Thermocouple or Plate Thermometer for both Control Methods. Fire Brick Alone Furnace Lining.

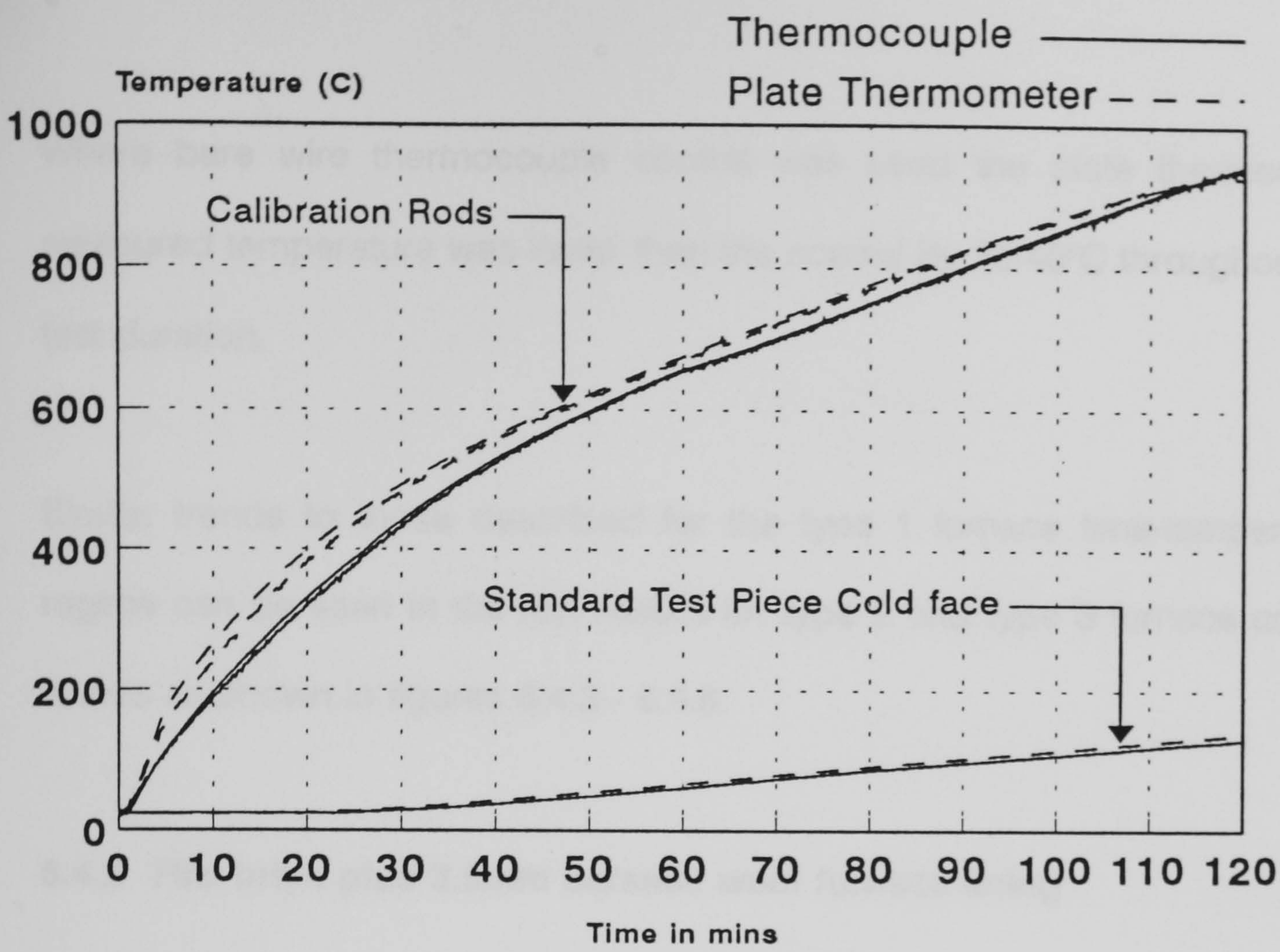

Figure 6.4.5 - Comparison of Response of Calibration Rods and Standard Test Piece between Plate Thermometer and Thermocouple Control Systems. Fire Brick Alone Furnace Lining.

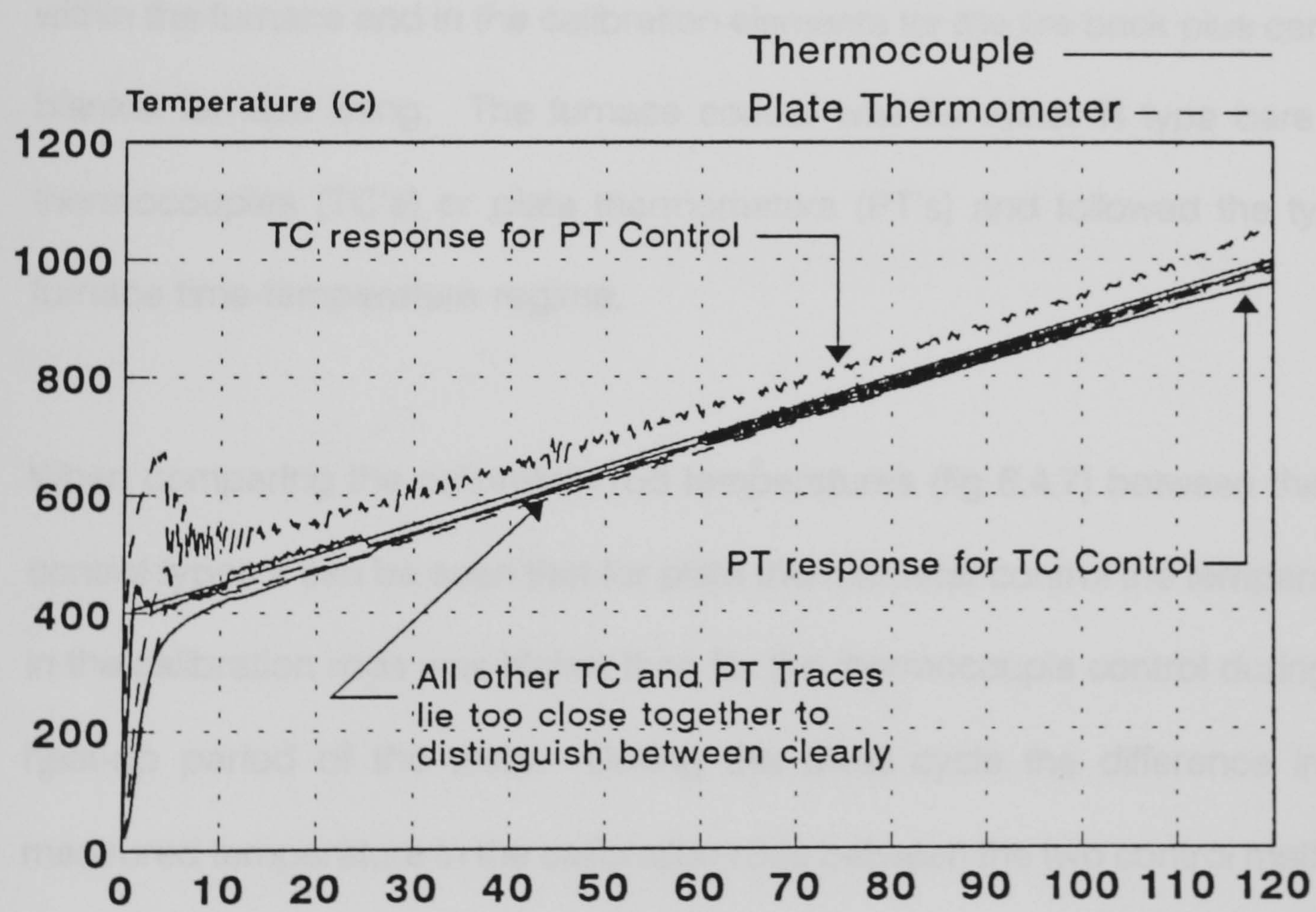

Figure 6.4.6 - Comparison of Furnace Temperature as Measured by R Type Thermocouple or Plate Thermometer for both Control Methods. Fire Brick Alone Furnace Lining.

Where bare wire thermocouple control was used the plate thermometer measured temperature was lower than the control by 30-40°C throughout the test duration.

Similar trends to those described for the type 1 furnace time-temperature regime can be seen in the test results for type 2 and type 3 furnace control curves as shown in figures 6.4.3 - 6.4.6.

6.4.2 Fire brick plus 3.5mm ceramic wool furnace lining

Figures 6.4.7 and 6.4.8 show comparisons between the measured temperatures within the furnace and in the calibration elements for the fire brick plus ceramic blanket furnace lining. The furnace control was for either R type bare wire thermocouples (TC's) or plate thermometers (PT's) and followed the type 1 furnace time-temperature regime.

When comparing the calibration rod temperatures (fig 6.4.7) between the two control types it can be seen that for plate thermometer control the temperature in the calibration rods was higher than for the thermocouple control during the heat-up period of the tests. During the dwell cycle the difference in the measured temperature in the calibration rods between the two control methods was very small.

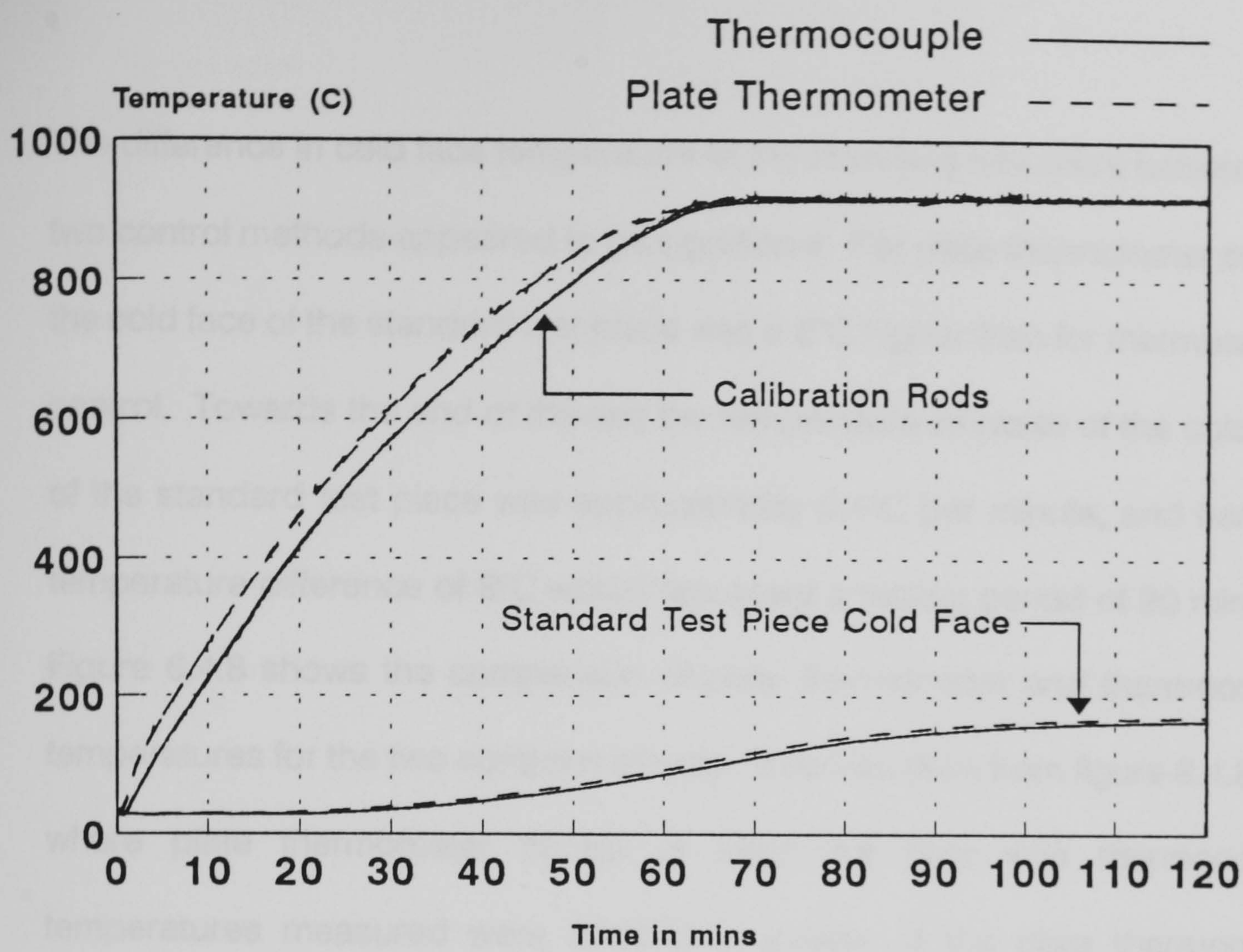

Figure 6.4.7 - Comaprison of Response of Calibration Rods and Standard Test Piece Between Thermocouple and Plate Thermometer Control. Fire Brick + 3.5mm Ceramic Wool Furnace Lining.

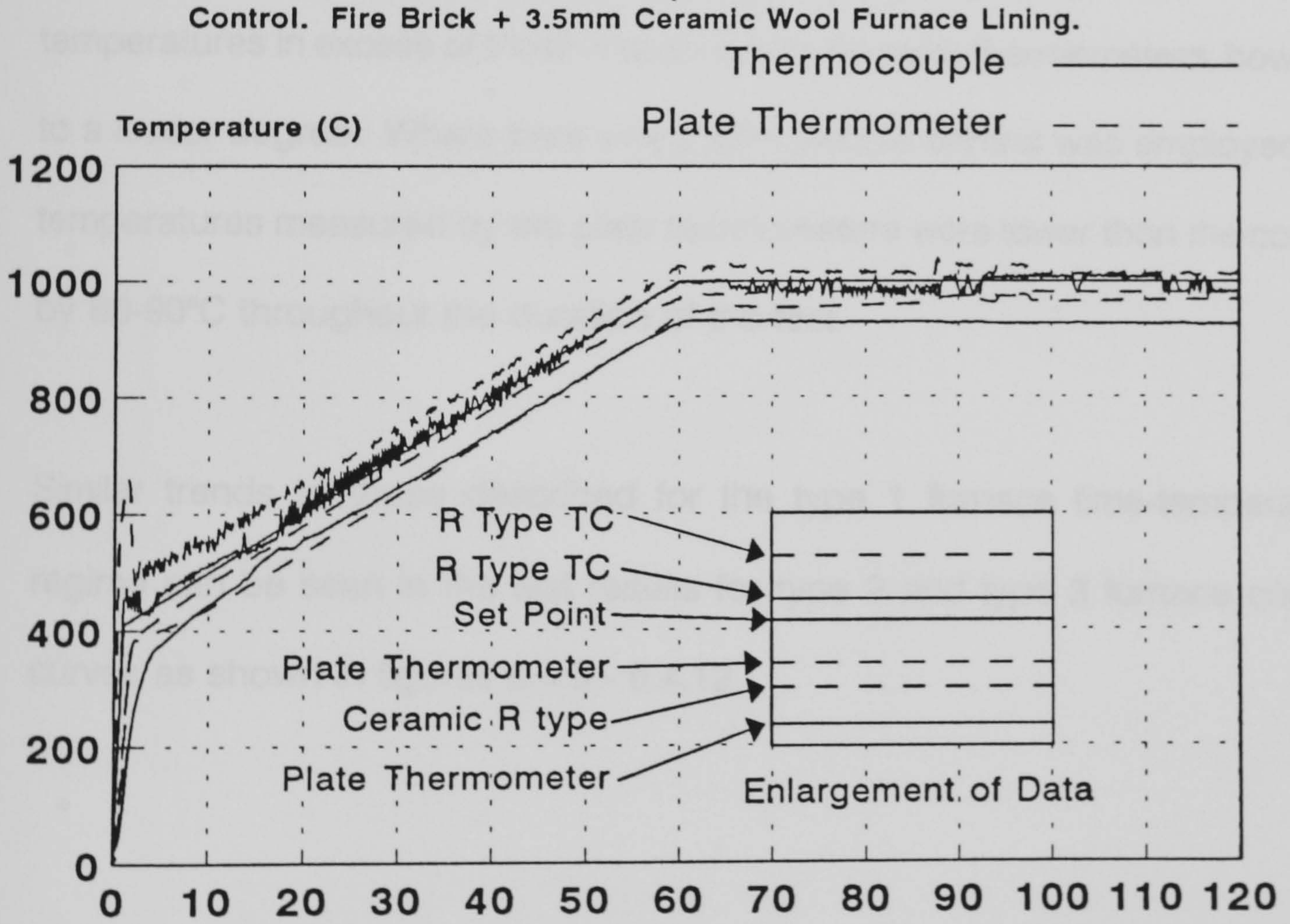

Figure 6.4.8 - Comparison of Furnace Temperature as Measured by R Type Thermocouple or Plate Thermometer for both Control Methods. Fire Brick + 3.5mm Ceramic Wool Furnace Lining.

The difference in cold face temperature of the standard test piece between the two control methods appeared to be significant. For plate thermometer control the cold face of the standard test piece was 6-8°C higher than for thermocouple control. Towards the end of the test the temperature increase of the cold face of the standard test piece was approximately 0.4°C per minute, and hence a temperature difference of 8°C would represent a testing period of 20 minutes. Figure 6.4.8 shows the comparison of plate thermometer and thermocouple temperatures for the two control methods. It can be seen from figure 6.4.8 that where plate thermometer control is used the bare wire thermocouple temperatures measured were 35-60°C in excess of the plate thermometer temperatures. The ceramic sheathed R type thermocouple also measured temperatures in excess of those measured by the plate thermometers, however to a lesser degree. Where bare wire thermocouple control was employed the temperatures measured by the plate thermometers were lower than the control by 60-90°C throughout the duration of the test.

Similar trends to those described for the type 1 furnace time-temperature regime can be seen in the test results for type 2 and type 3 furnace control curves as shown in figures 6.4.9 - 6.4.12.

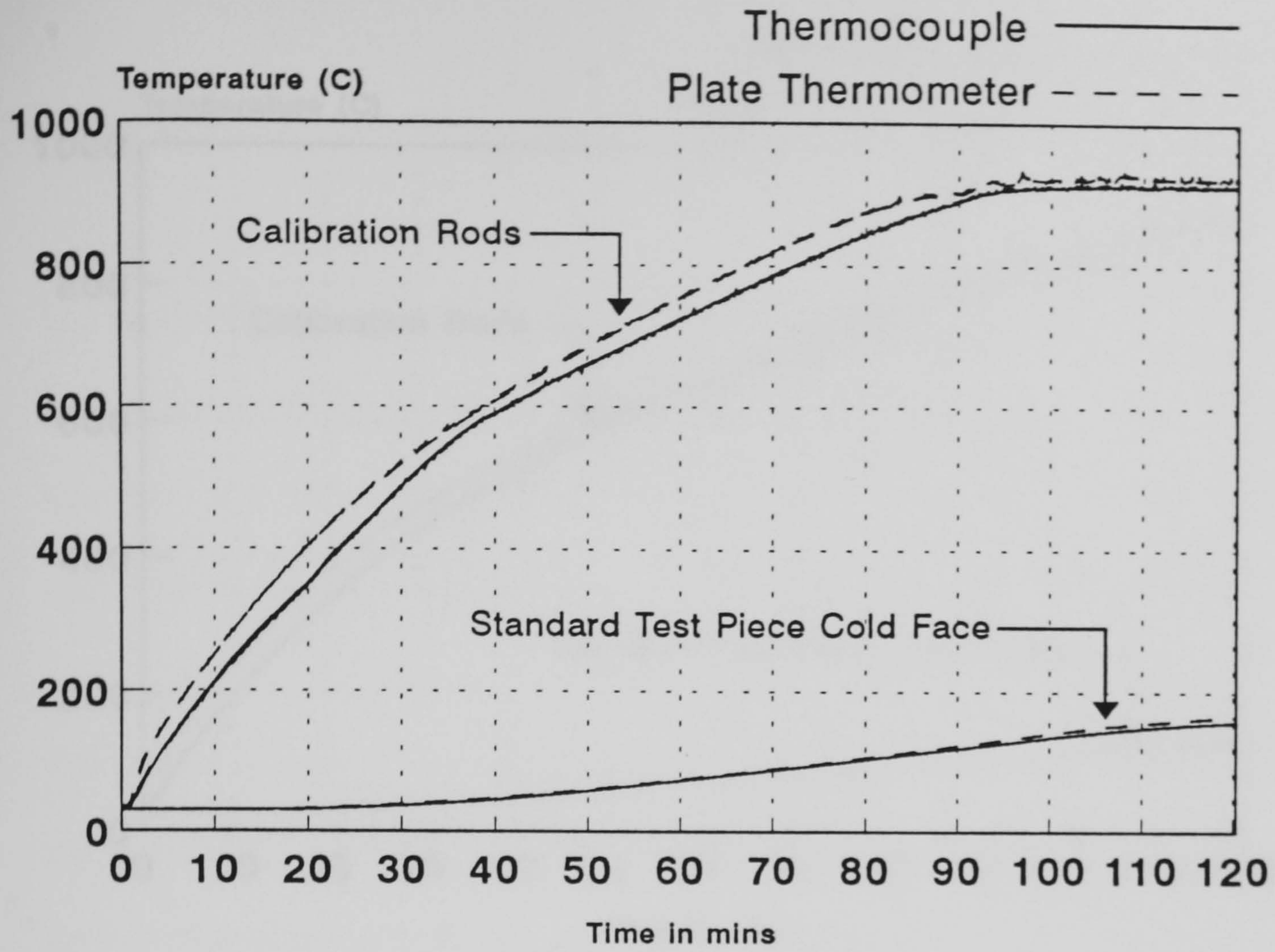

Figure 6.4.9 - Comparison of Response of Calibration Rods and Standard Test Piece between Thermocouple and Plate Thermometer Control Systems. Fire Brick + 3.5mm Ceramic Wool Furnace Lining

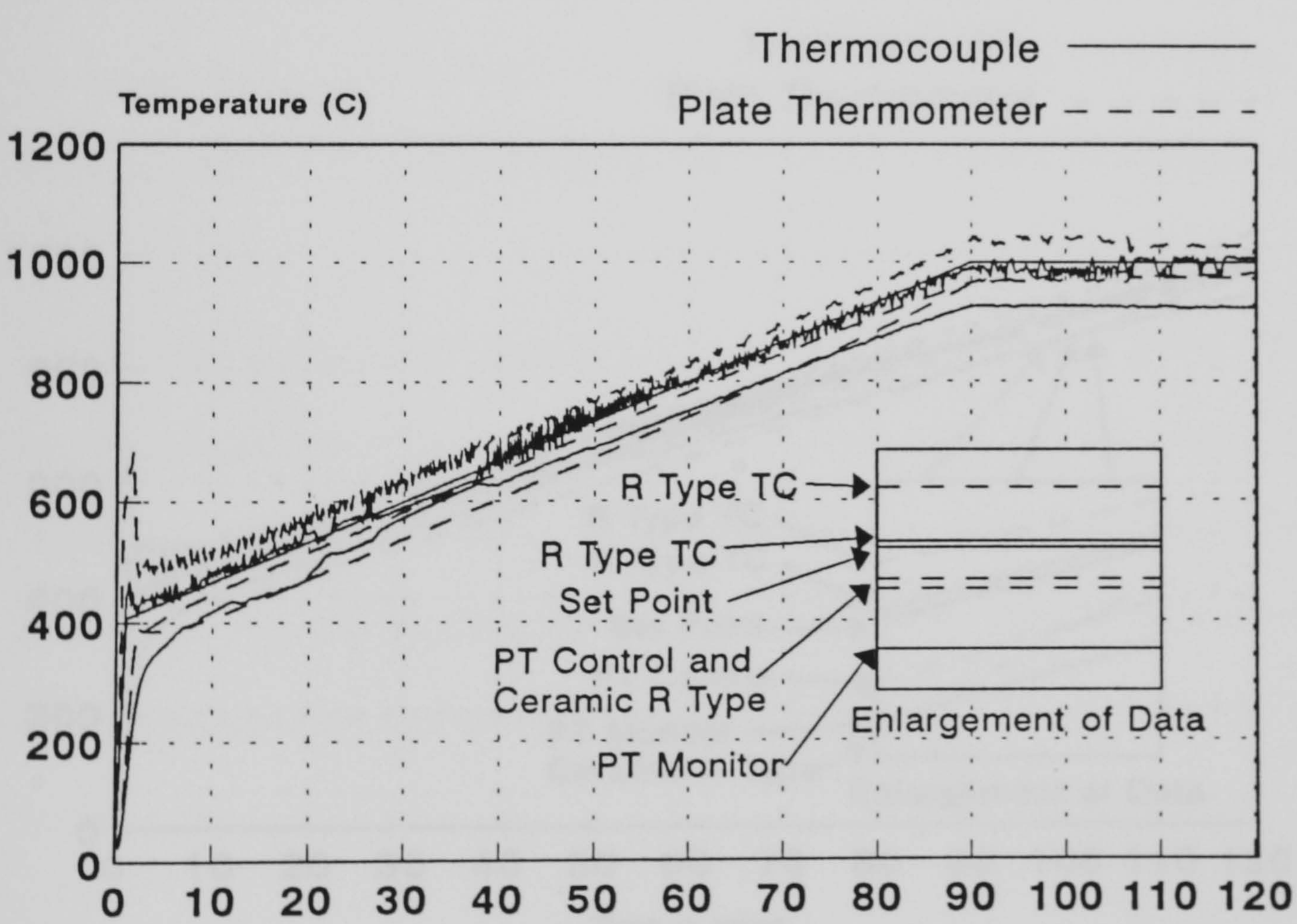

Figure 6.4.10 - Comparison of Furnace Temperature as Measured by R Type Thermocouple or Plate Thermometer for both Control Methods. Fire Brick + 3.5mm Ceramic Wool Furnace Lining

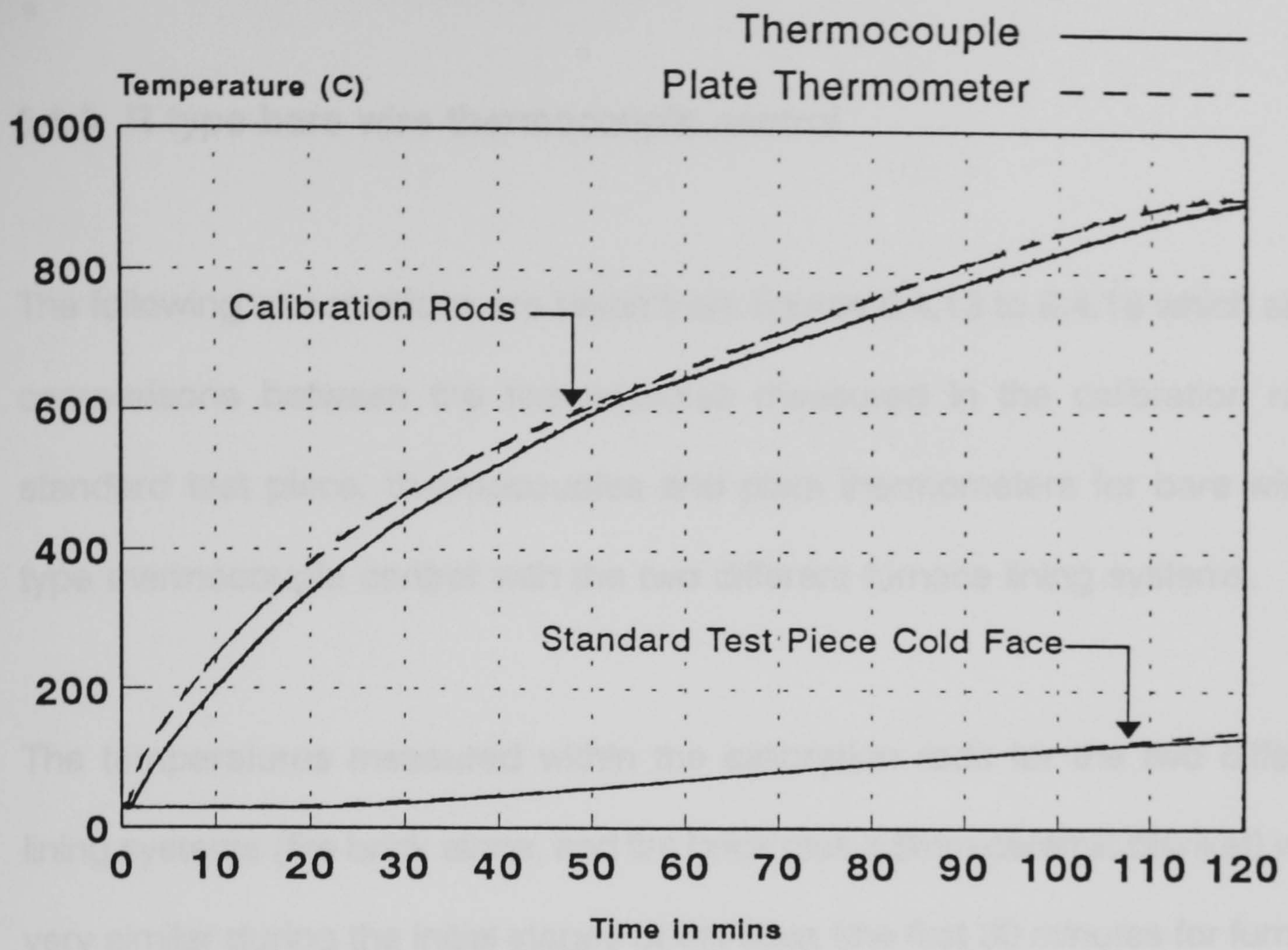

Figure 6.4.11 - Comparison of Response of Calibration Rods and Standard Test Piece between Thermocouple and Plate Thermometer Control Systems. Fire Brick + 3.5mm Ceramic Wool Furnace Lining

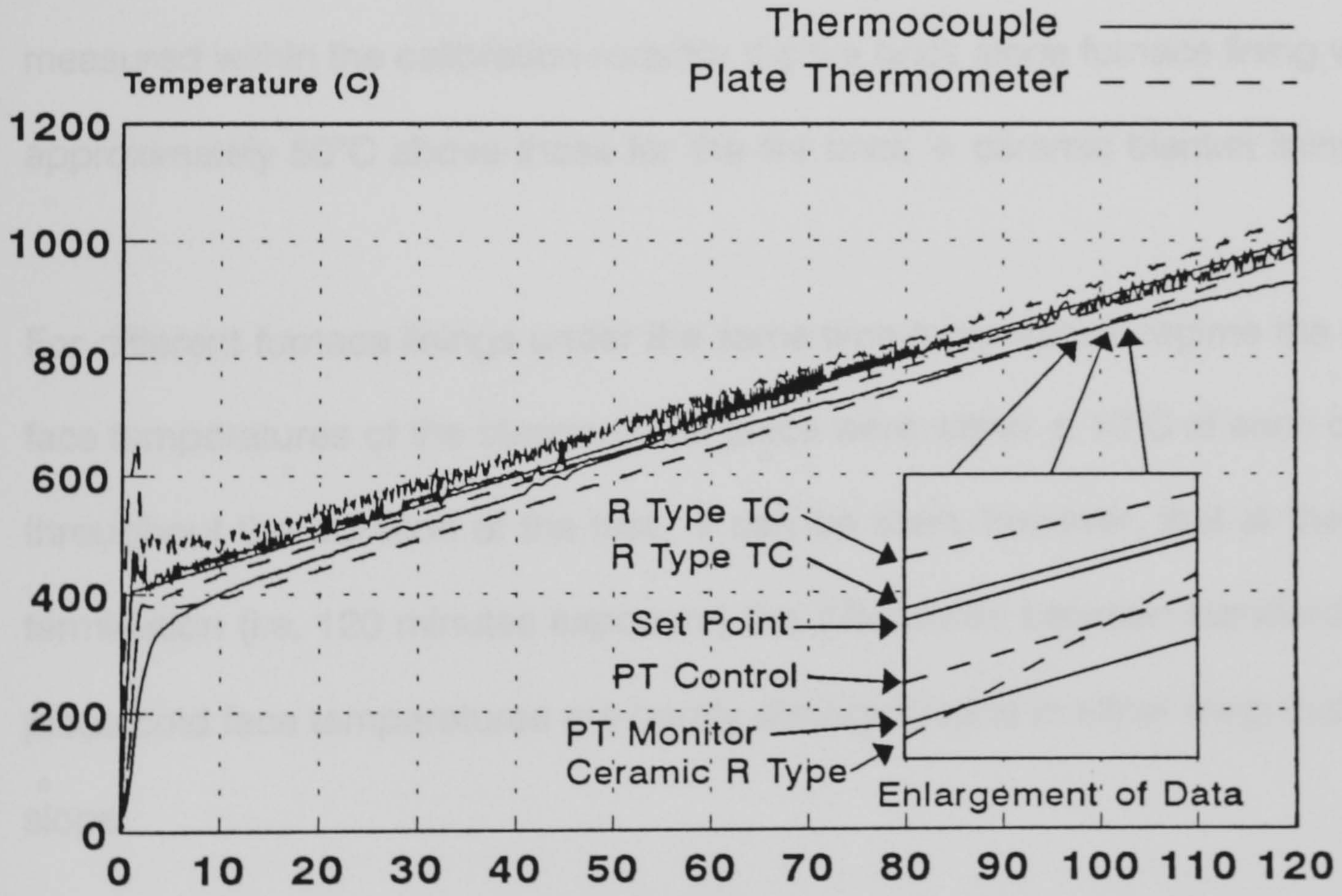

Figure 6.4.12 - Comparison of Furnace Temperature as Measured by R Type Thermocouple or Plate Thermometer for both Control Methods. Fire Brick + 3.5mm Ceramic Wool Furnace Lining

6.4.3 R type bare wire thermocouple control

The following observations are taken from figures 6.4.13 to 6.4.18 which show comparisons between the temperatures measured in the calibration rods, standard test piece, thermocouples and plate thermometers for bare wire R type thermocouple control with the two different furnace lining systems.

The temperatures measured within the calibration rods for the two different lining systems (fire brick alone, and fire brick plus 3.5mm ceramic blanket) were very similar during the initial stages of the tests (the first 30 minutes for furnace curve type 1, first 50 minutes for furnace curve type 2, and first 70 minutes for furnace curve type 3). At the termination of the tests the temperatures measured within the calibration rods for the fire brick alone furnace lining were approximately 50°C above those for the fire brick + ceramic blanket lining.

For different furnace linings under the same time-temperature regime the cold face temperatures of the standard test piece were within ± 10°C of each other throughout the duration of the test. It can be seen, however, that at the test termination (i.e. 120 minutes exposure) the differences between standard test piece cold face temperatures are barely distinguishable in either magnitude or slope.

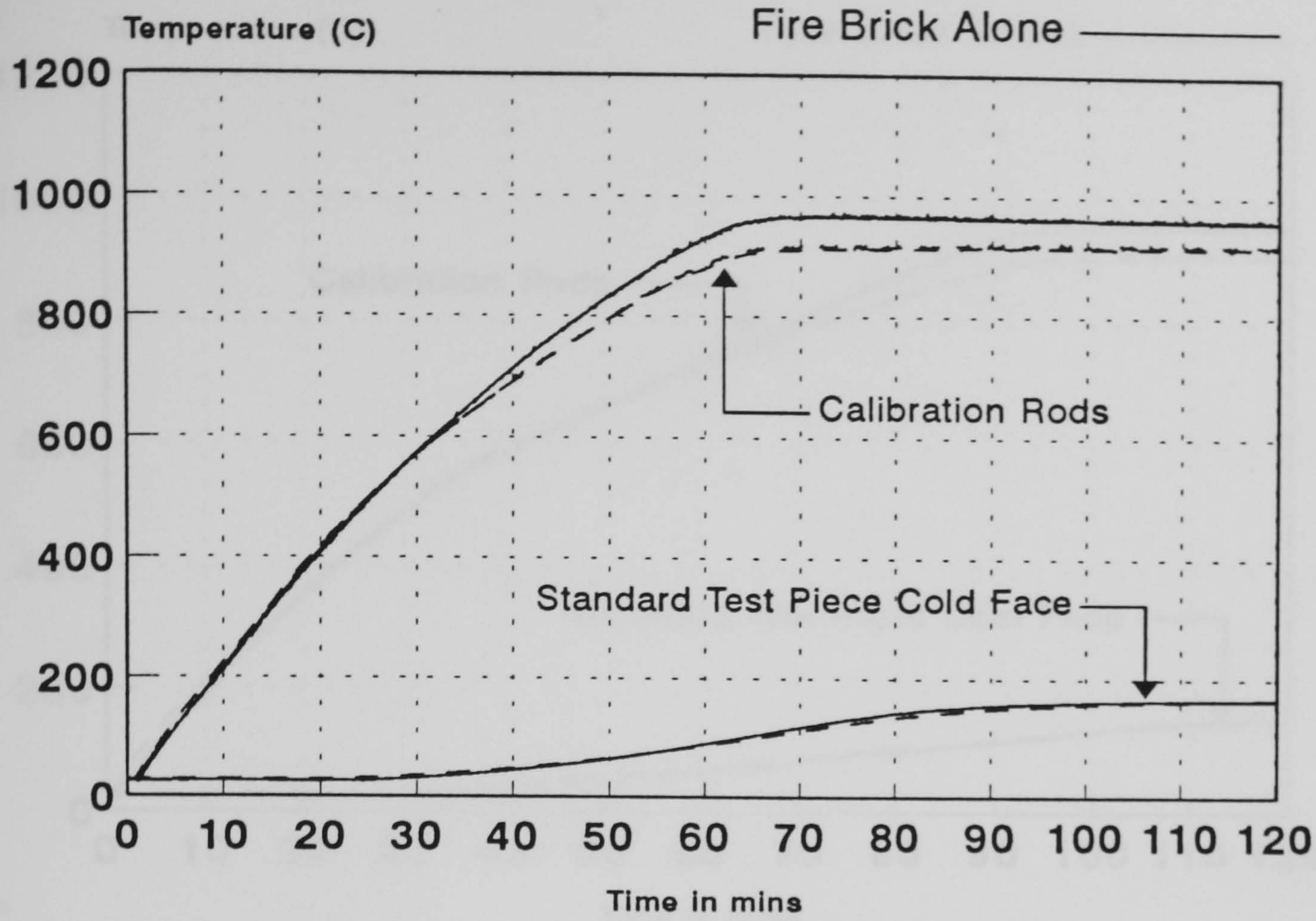

Figure 6.4.13 - Comparison of Response of Calibration Rods and Standard Test Piece between Fire Brick alone and Fire Brick + 3.5mm Ceramic Wool Furnace Lining. R Type Thermocouple Control.

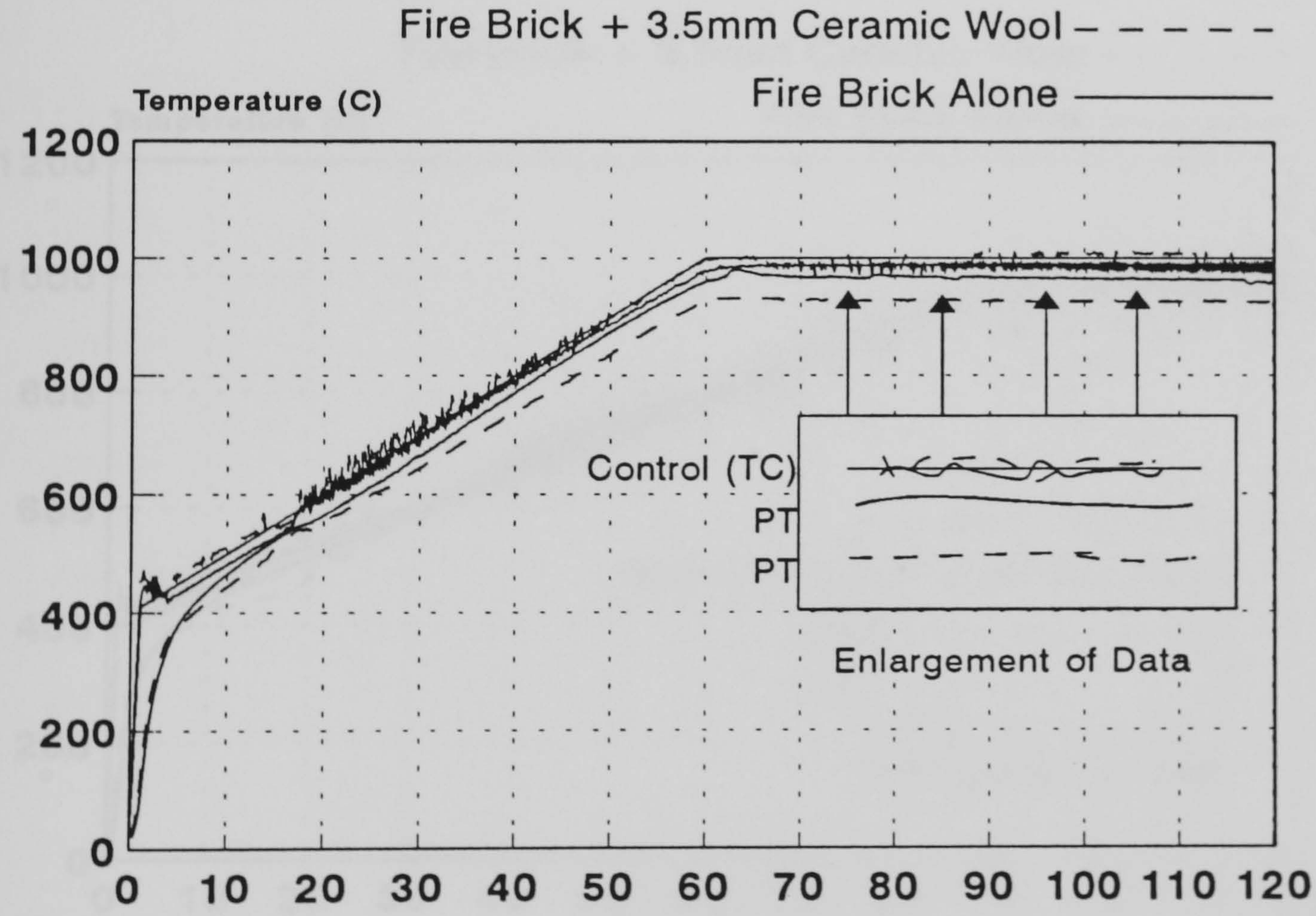

Figure 6.4.14 - Comparison of Response of Plate Thermometer and R Type Thermocouple for Fire Brick alone and Fire Brick + 3.5mm Ceramic Wool Furnace Lining. R Type Thermocouple Control.

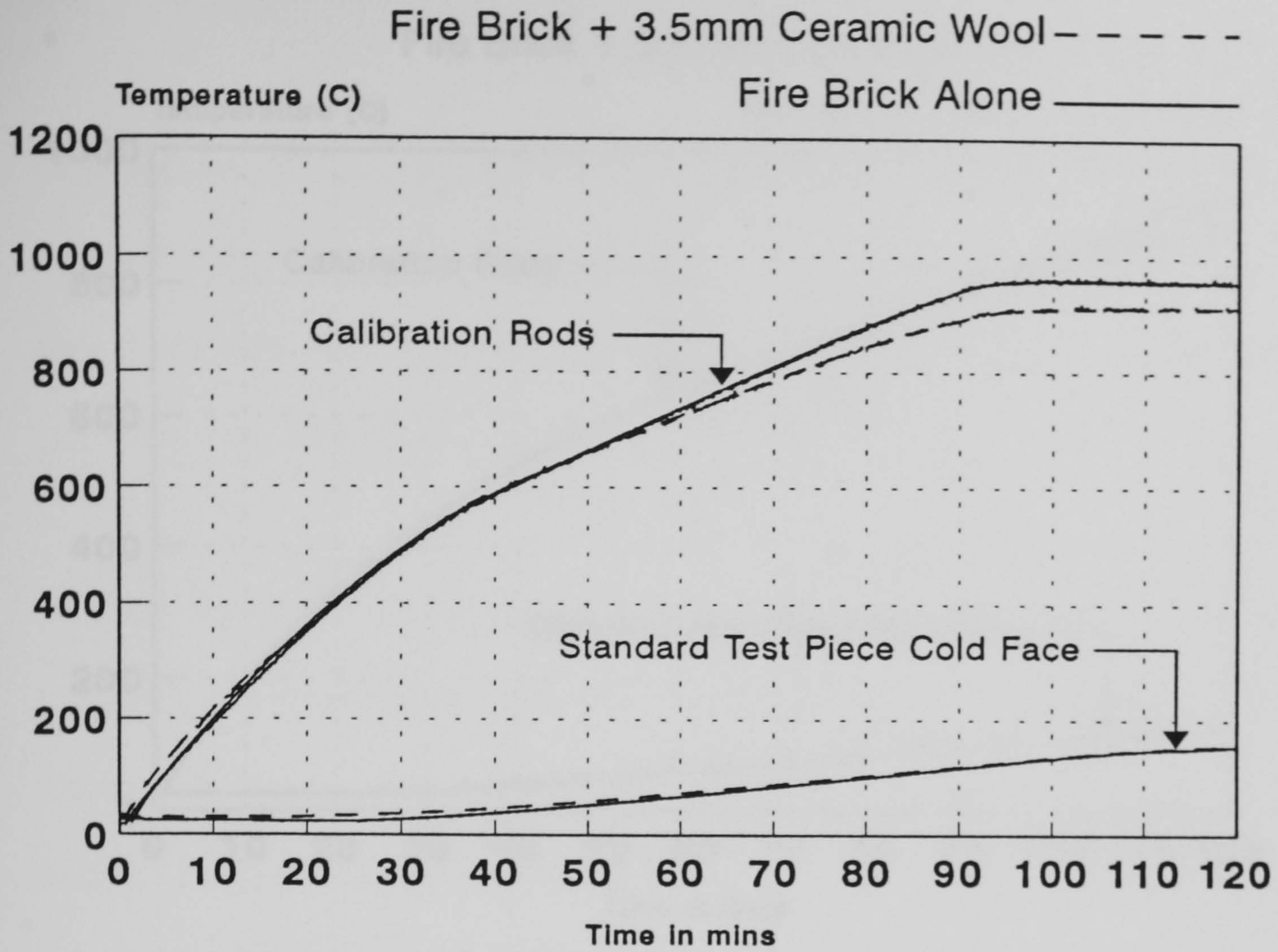

Figure 6.4.15 - Comparison of Response of Calibration Rods and Standard Test Piece between Fire Birck alone and Fire Brick + 3.5mm Ceramic Wool Furnace Lining. R Type Thermocouple Control.

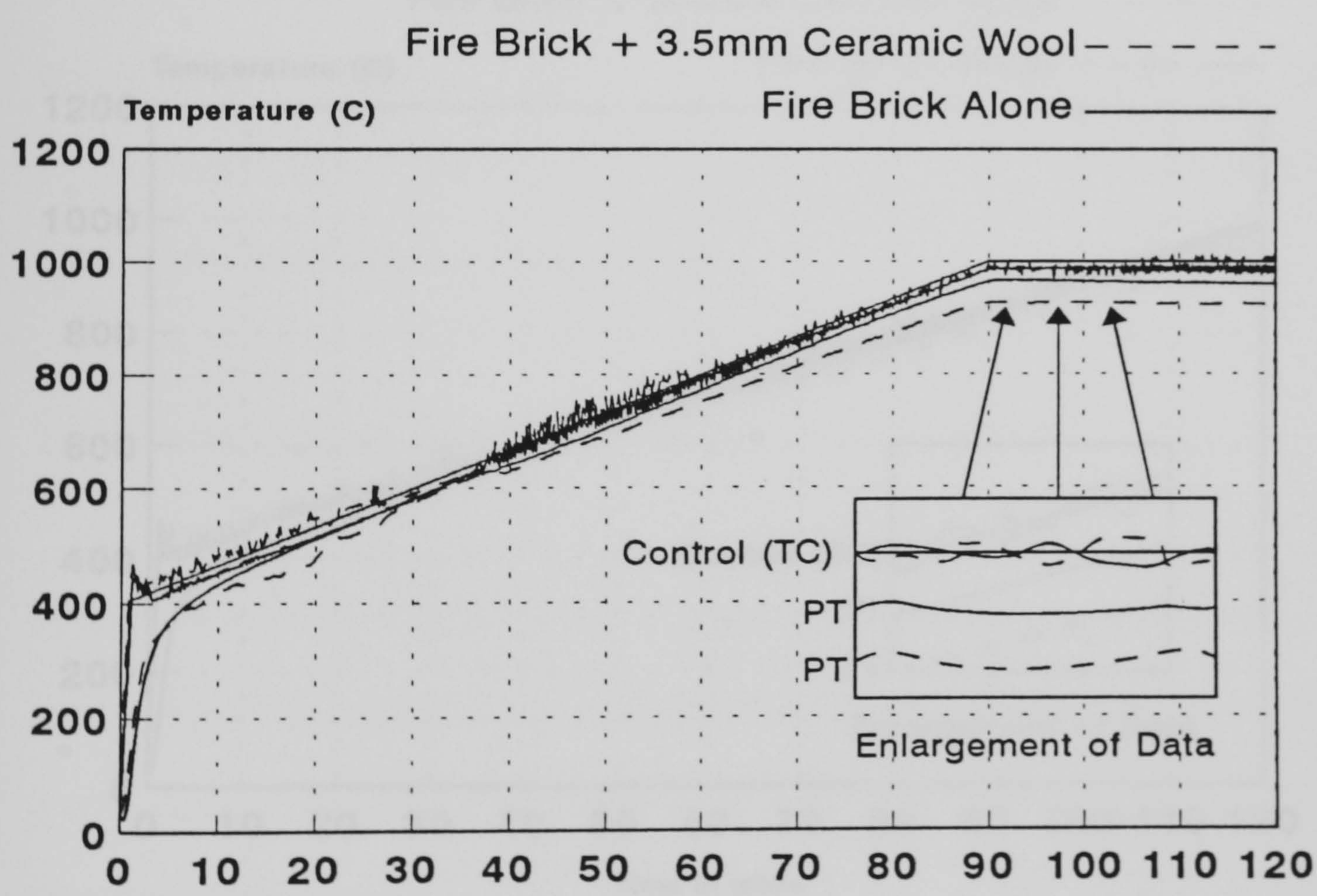

Figure 6.4.16 - Comparison of Response of Plate Thermometer and R Type Thermocouple for Fire Brick Alone and Fire Brick + 3.5mm Ceramic Wool Furnace Lining. R Type Thermocouple Control.

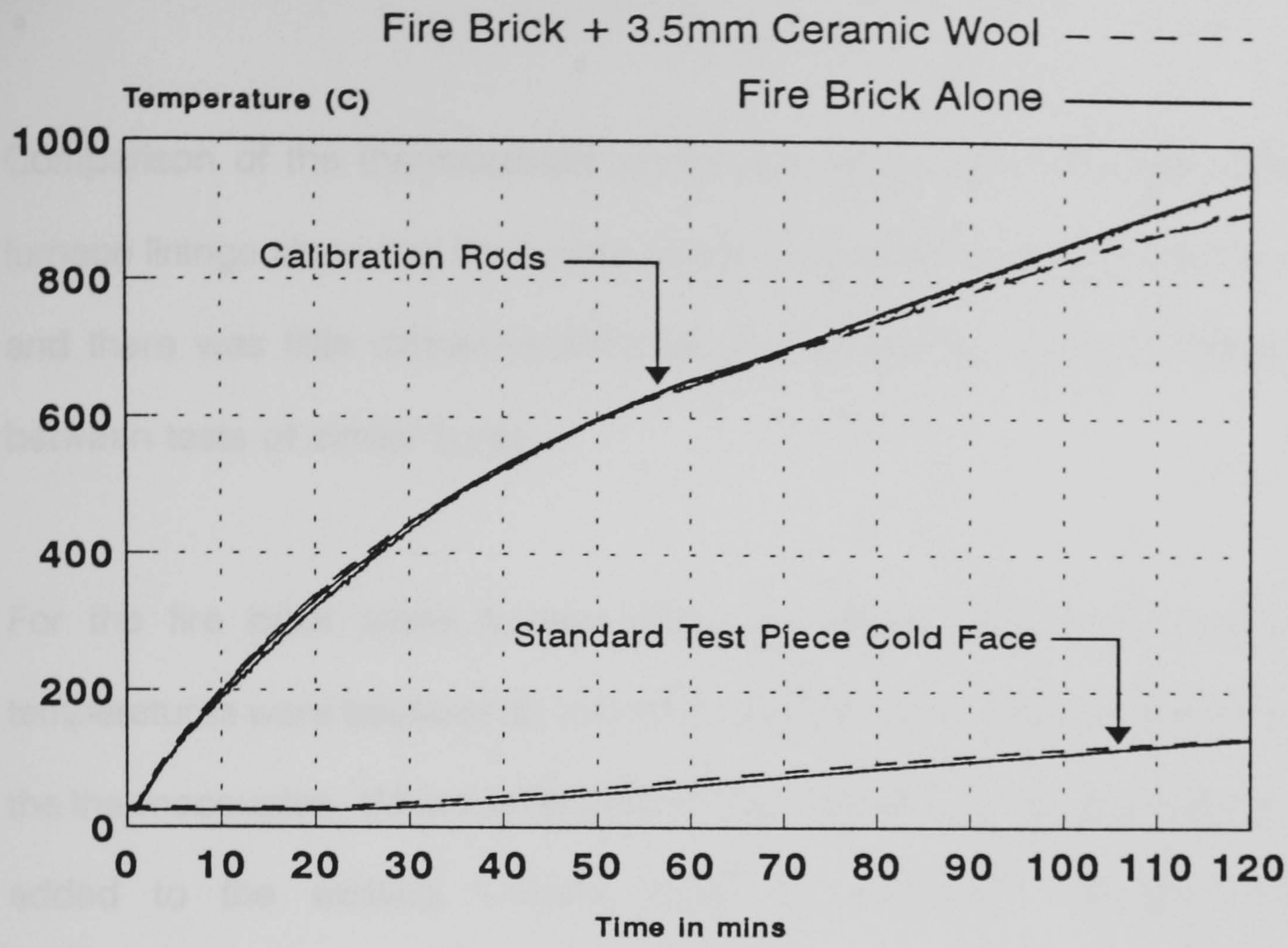

Figure 6.4.17 - Comparison of Response of Calibration Rods and Standard Test Piece Between Fire Brick alone and Fire Brick + 3.5mm Ceramic Wool Furnace Lining. R Type Thermocouple Control.

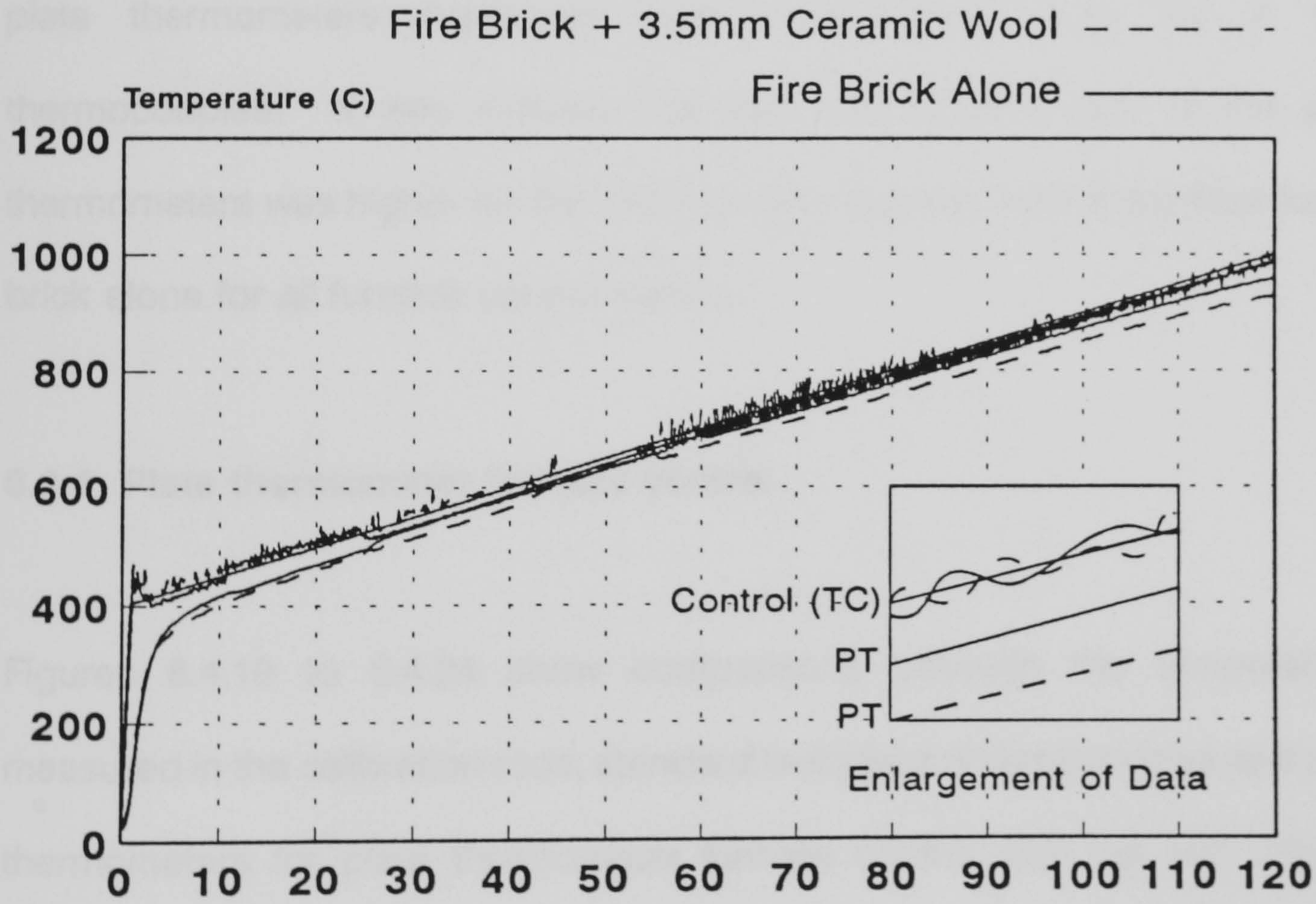

Figure 6.4.18 - Comparison of Response of Plate Thermometer and R Type Thermocouple for Fire Brick alone and Fire Brick + 3.5mm Ceramic Wool Furnace Lining. R Type Thermocouple Control.

Comparison of the thermocouple control temperatures for the two different furnace linings show that there was a high degree of accuracy in the control, and there was little difference between the measured control temperatures between tests of similar types.

For the fire brick alone furnace lining the plate thermometer measured temperatures were between 20 and 30°C below the temperatures measured by the thermocouples. Where an additional thin layer of ceramic fibre blanket was added to the existing furnace lining this difference between control (thermocouple measured) temperature and the plate thermometer measured temperature was substantially greater at approximately 50-70°C. In all tests the plate thermometers measured lower temperatures than the R type thermocouples. It was noticed that the initial heating rate of the plate thermometers was higher for the fire brick plus ceramic wool lining than for fire brick alone for all furnace control curves.

6.4.4 Plate thermometer furnace control

Figures 6.4.19 to 6.4.24 show comparisons between the temperatures measured in the calibration rods, standard test piece, thermocouples and plate thermometers for plate thermometer furnace control with the two different furnace lining systems.

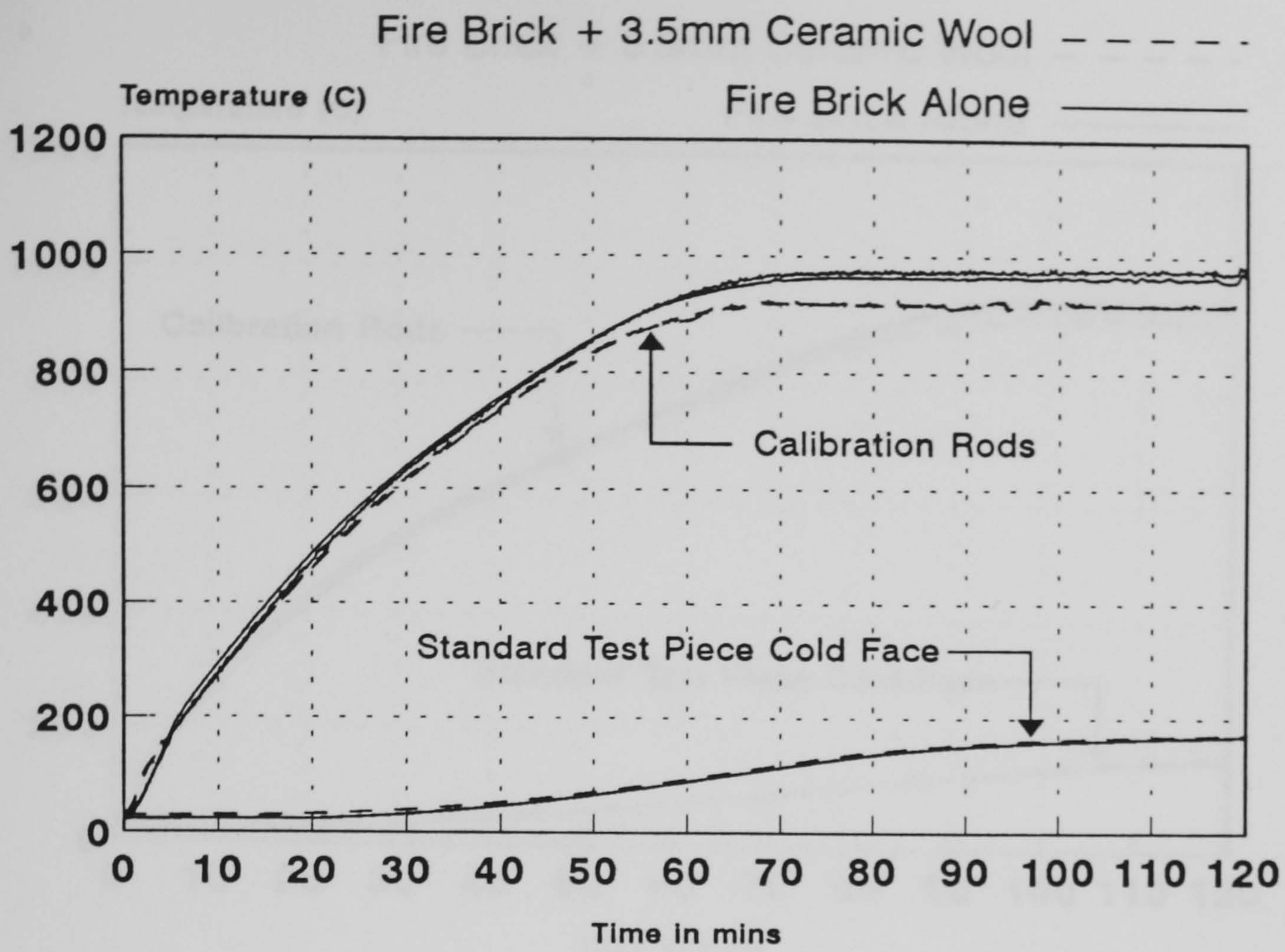

Figure 6.4.19 - Comparison of Response of Calibration Rods and Standard Test Piece between Fire Brick Alone and Fire Brick + 3.5mm Ceramic Wool Furnace Lining. Plate Thermometer Control.

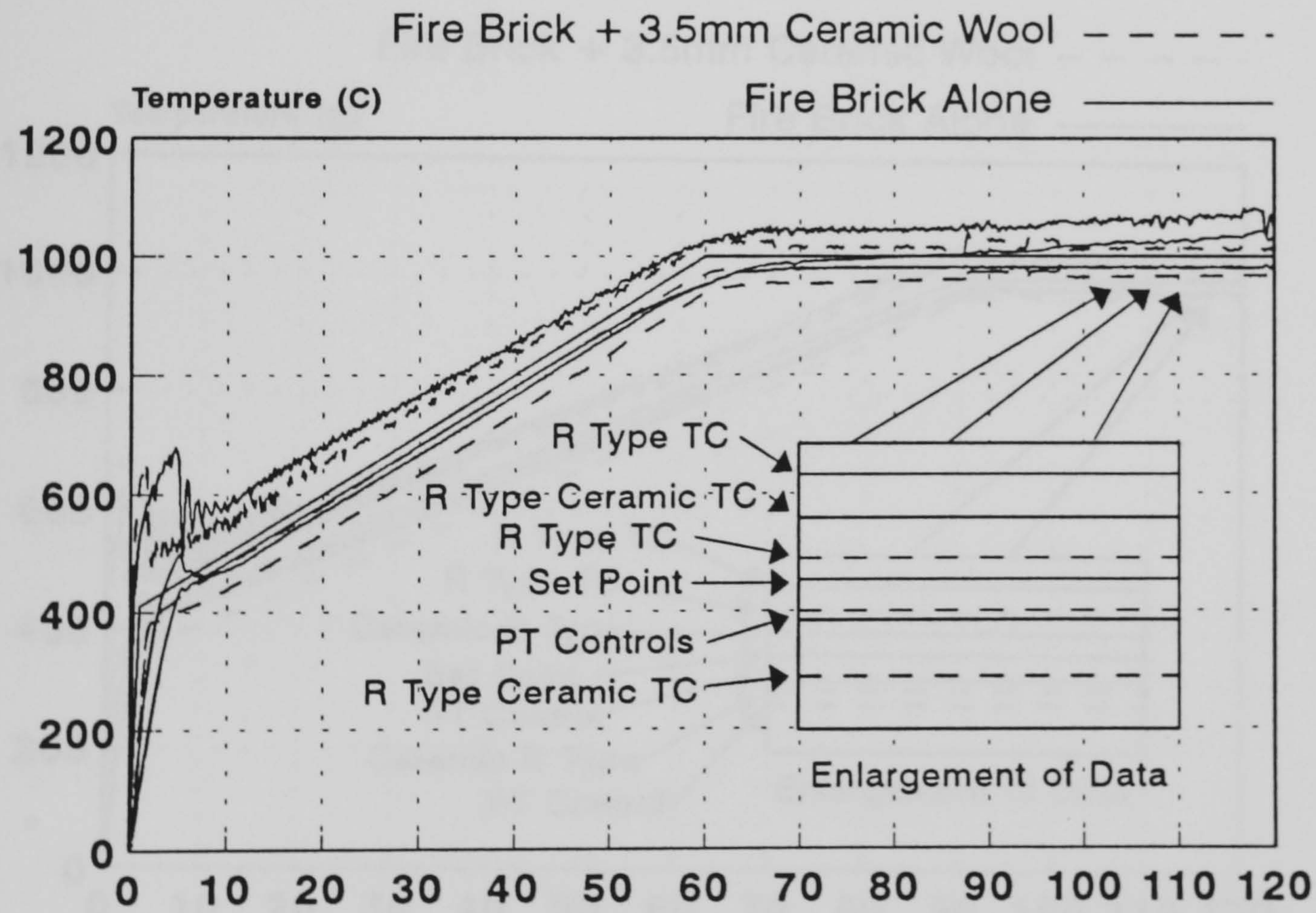

Figure 6.4.20 - Comparison of Response of Plate Thermometer and R Type Thermocouple for Fire Brick Alone and Fire Brick + 3.5mm Ceramic Wool Furnace Lining. Plate Thermometer Control.

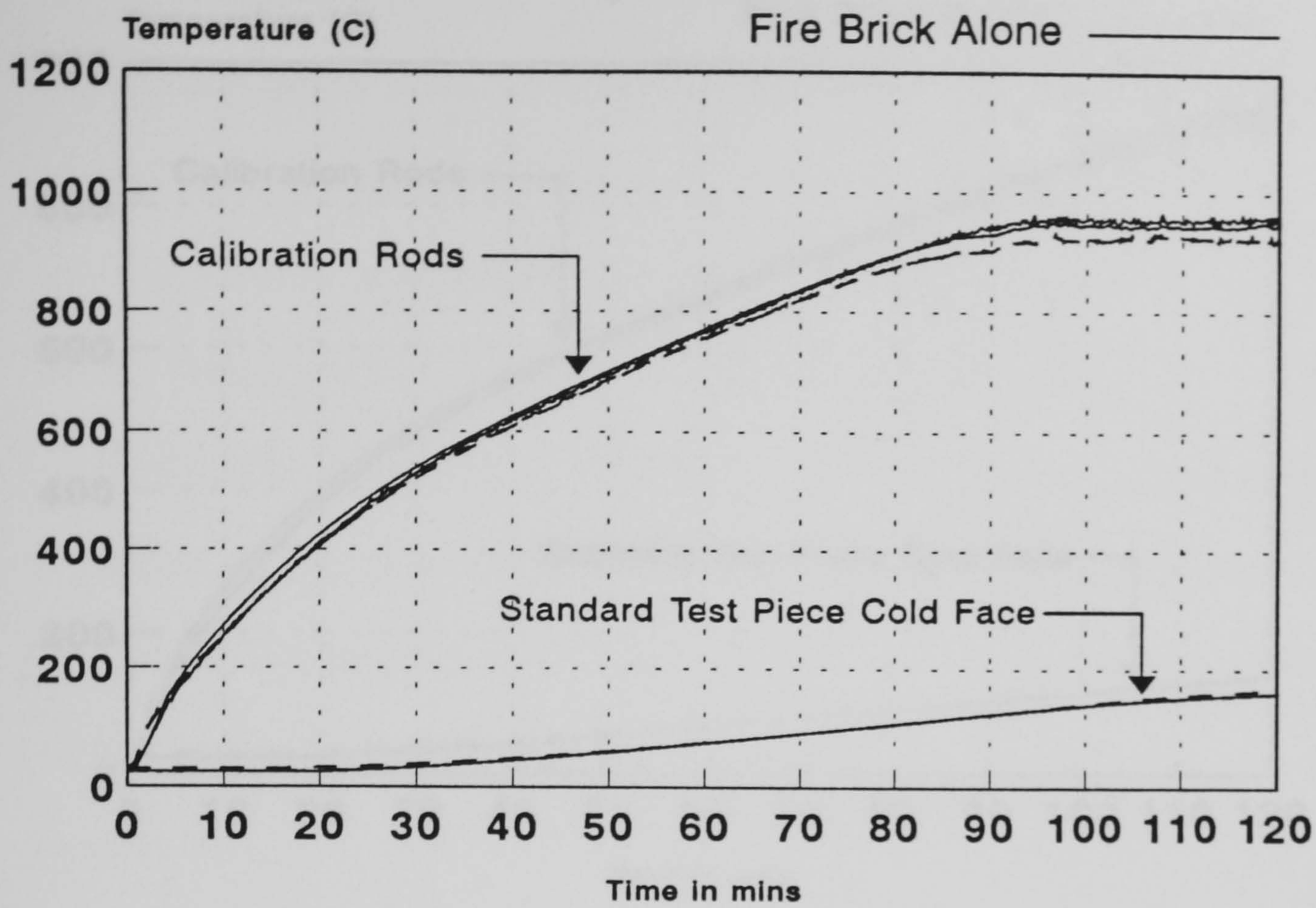

Figure 6.4.21 - Comparison of Response of Calibration Rods and Standard Test Piece between Fire Brick alone and Fire Brick + 3.5mm Ceramic Wool Furnace Lining. Plate Thermometer Control.

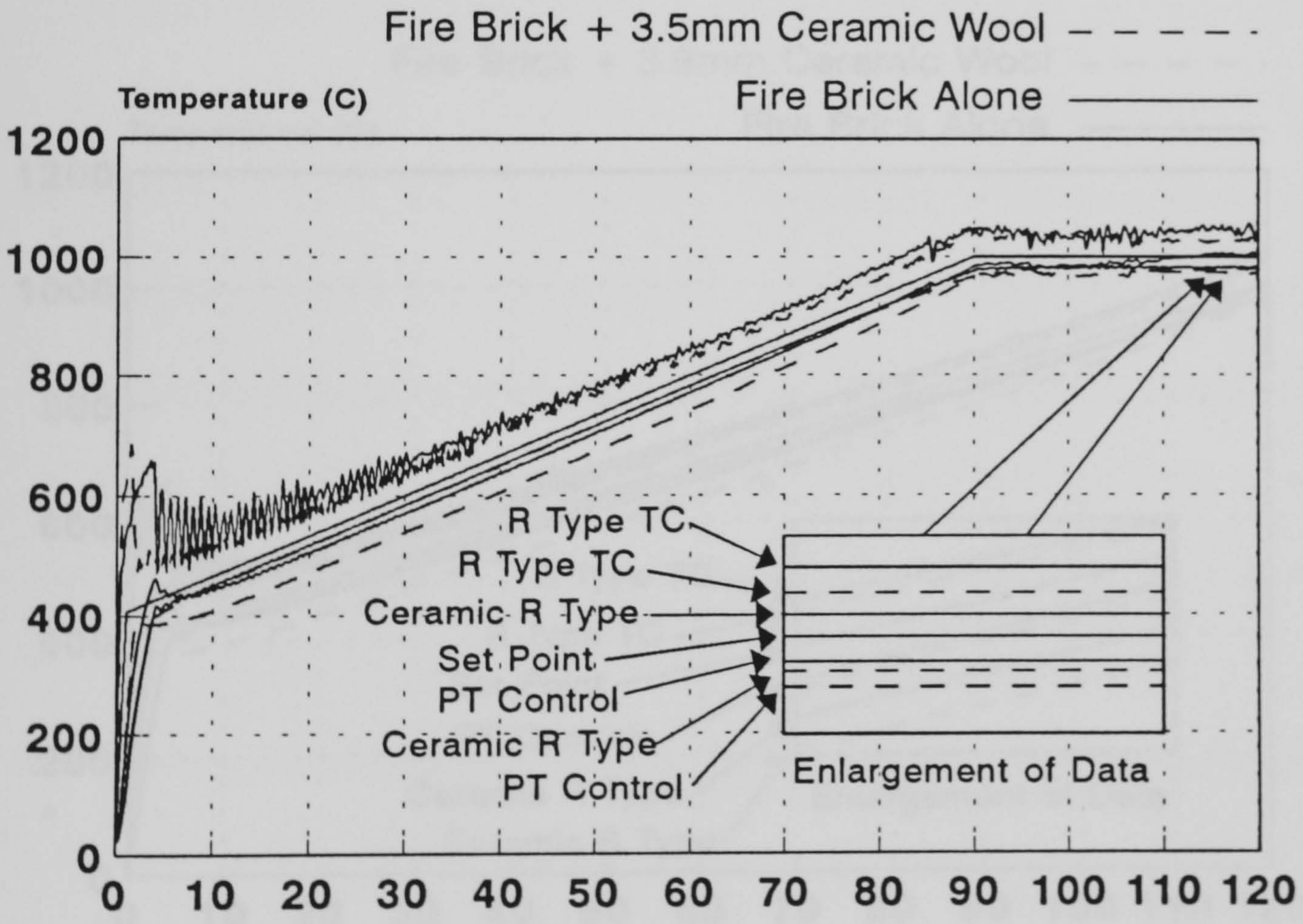

Figure 6.4.22 - Comparison of Response of Plate Thermometer and R Type Thermocouples for Fire Brick alone and Fire Brick + 3.5mm Ceramic Wool Furnace Lining. Plate Thermometer Control.

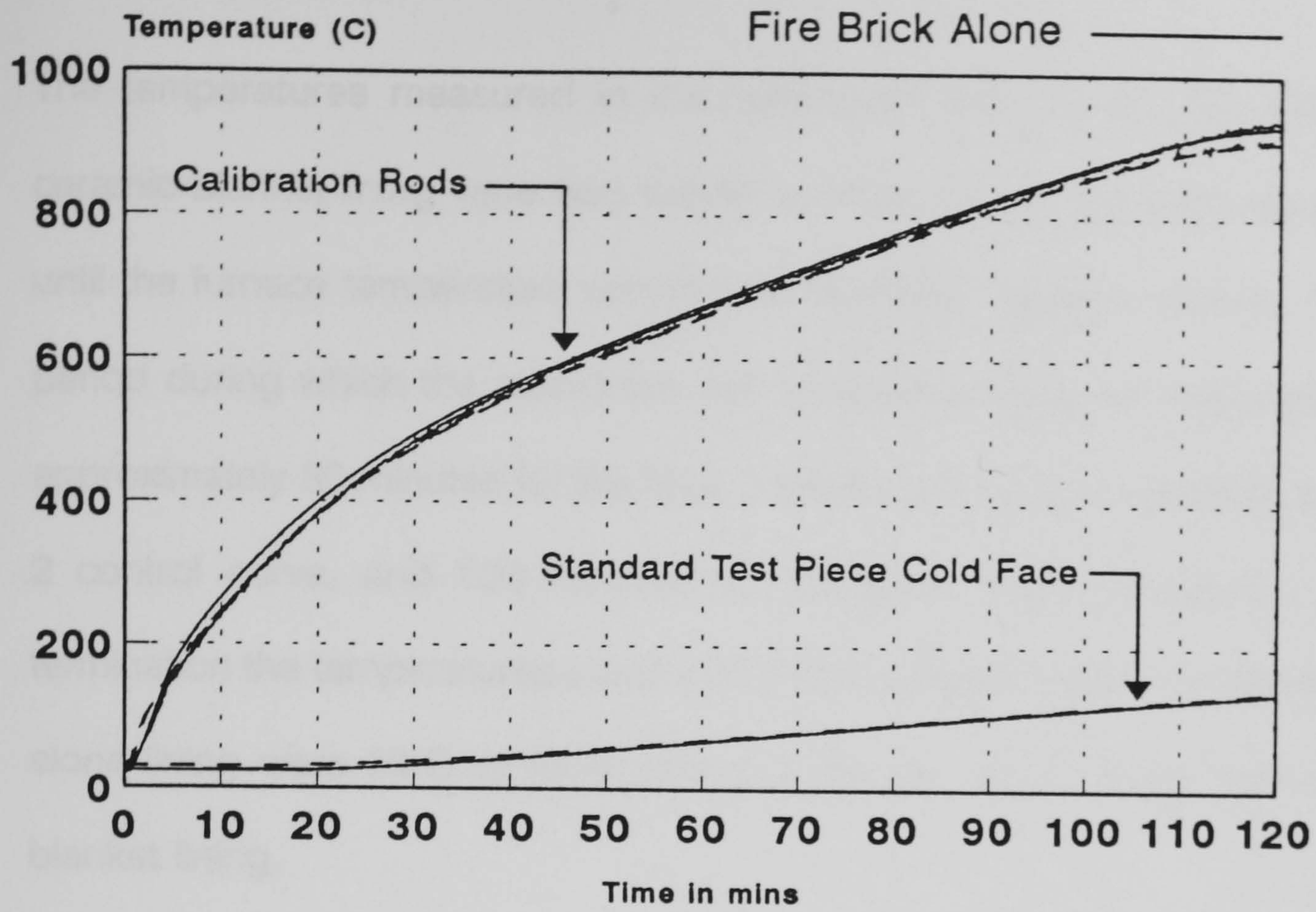

Figure 6.4.23 - Comaprison of Response of Calibration Rods and Standard Test Piece between Fire Brick Alone and Fire Brick + 3.5mm Ceramic Wool Furnace Lining. Plate Thermometer Control.

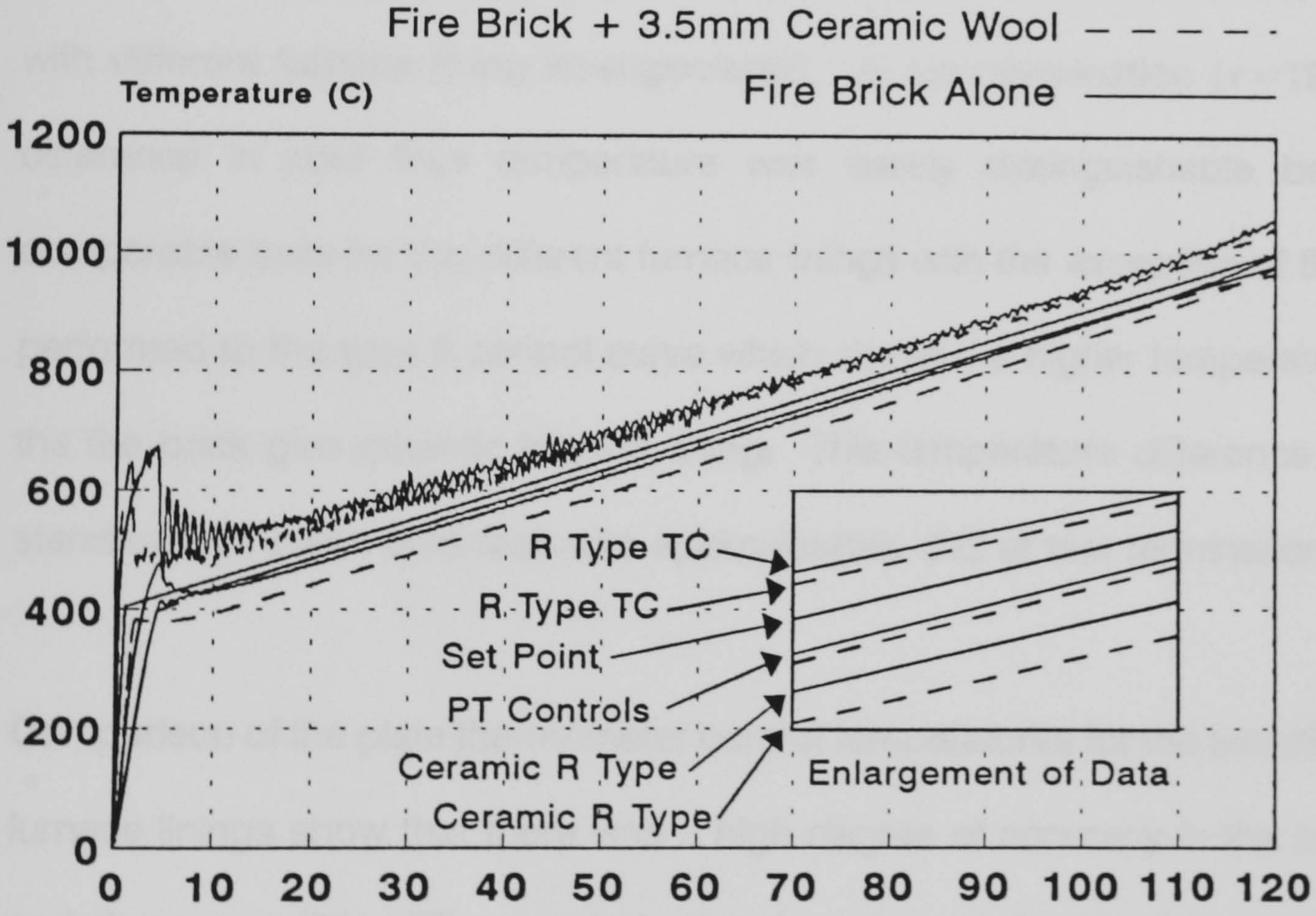

Figure 6.4.24 - Comaprison of Response of Plate Thermometer and R Type Thermocouples for Fire Brick Alone and Fire Brick + 3.5mm Ceramic Wool Furnace Lining. Plate Thermometer Control.

The temperatures measured in the calibration rods for the fire brick plus ceramic blanket lining were very similar to those for the fire brick alone lining until the furnace temperature was in the 700-800°C range or above. The test period during which the calibration rod temperatures were comparable were approximately 30 minutes for the type 1 control curve, 60 minutes for the type 2 control curve, and 100 minutes for the type 3 control curve. At test termination the temperatures measured in the calibration rods for the fire brick alone lining were 30°C or more above those for the fire brick plus ceramic blanket lining.

The standard test piece cold face temperatures were within ± 10°C of each other throughout the duration of the test (for comparable test control curves with different furnace lining arrangements). At test termination ($\tau = 120$) the difference in cold face temperature was barely distinguishable between comparable tests for the different furnace linings with the exception of the test performed to the type 2 control curve which showed a higher temperature for the fire brick plus ceramic blanket lining. This temperature difference in the standard test piece cold face was approximately 6°C at test termination.

Comparison of the plate thermometer control temperatures for the two different furnace linings show that there was a high degree of accuracy in the control, and there was little difference between the measured control temperatures between tests of similar types.

For the fire brick alone furnace lining the plate thermometer measured temperatures were between 70 and 90°C below the temperatures measured by the thermocouples. Where an additional thin layer of ceramic fibre blanket was added to the existing furnace lining this difference between control (plate thermometer measured) temperature and the bare wire R type thermocouple measured temperature was slightly lower at approximately 50-70°C. In all tests the plate thermometer measured control temperatures were lower than the measured temperature by R type thermocouples.

6.4.5 Calculated heat flux during furnace testing

To aid comparisons and analysis of the temperature measurements in the previous sections the approximate heat flux within the furnace was calculated as outlined in section 6.2.1. The inlet and outlet temperatures of the flowing water filled copper pipe were measured by fast response inconnel sheathed K type thermocouples. Table 6.2 shows the calculated approximate heat flux available within the furnace during the tests at 30 minute intervals for the different lining systems and control methods.

The heat fluxes in table 6.2 are represented graphically in figures 6.4.25 and 6.4.26. Figure 6.4.25 shows a comparison of the calculated heat flux within the furnace for thermocouple control and different furnace linings. Figure 6.4.26 shows the calculated heat flux within the furnace for plate thermometer control and the different furnace lining systems. It can be seen from figures 6.4.25 and

6.4.26 that the calculated heat flux within the furnace increases with time regardless of whether the elapsed time represents an increase in the furnace temperature or it represents a dwell period at 1000°C. This is as expected as even during the dwell period of the control curve more energy is being supplied to the furnace in order to maintain the temperature, and hence more energy is available within the furnace (in the form of radiative energy from the furnace walls).

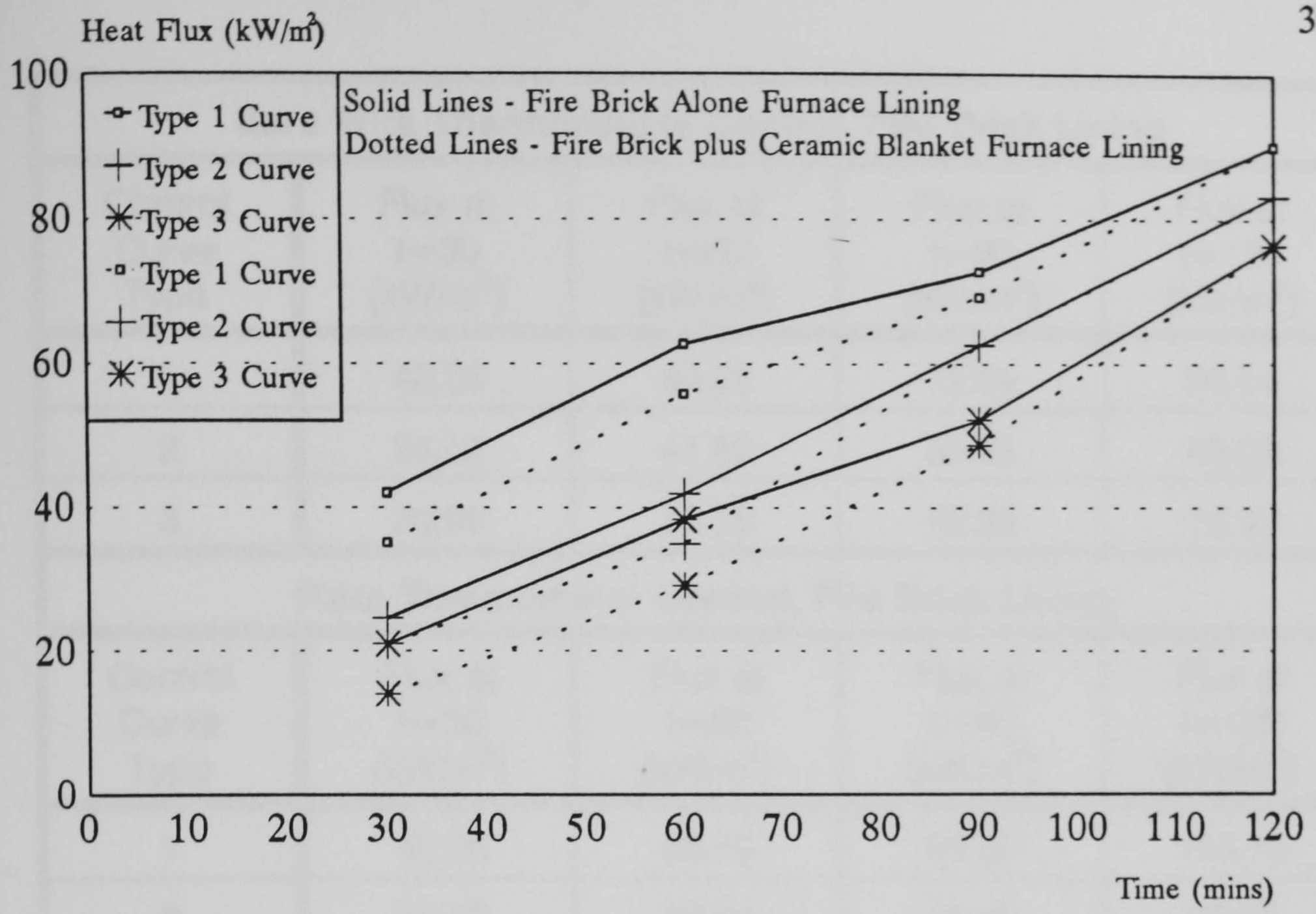

Figure 6.4.25 - Comparison of Calculated Heat Flux from Flowing Water Temperature Measurements. Bare Wire Thermocouple Control, Different Furnace Linings.

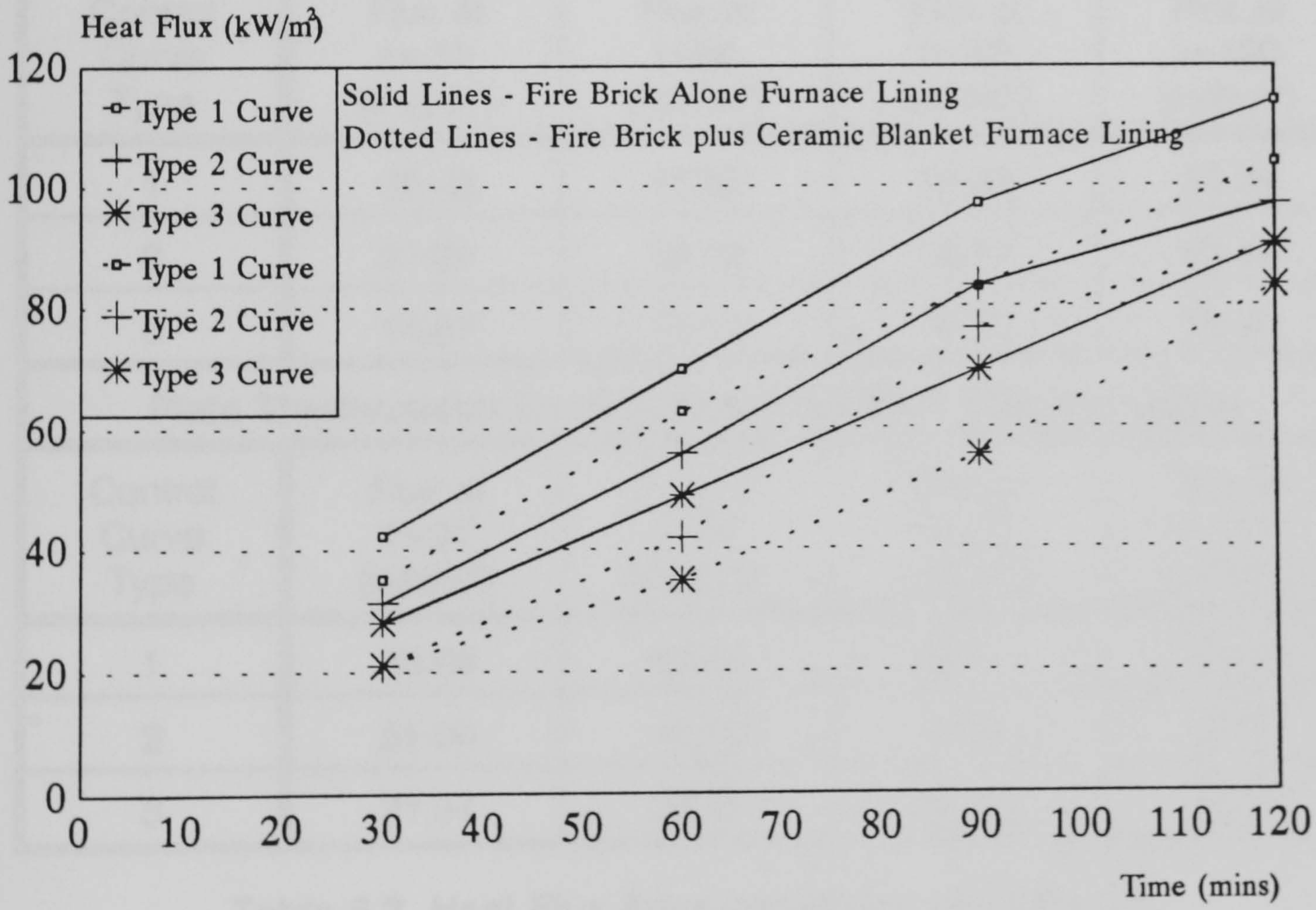

Figure 6.4.26 - Comparison of Calculated Heat Flux from Flowing Water Temperature Measurements. Plate Thermometer Control, Different Furnace Linings.

Bare Wire Thermocouple Control, Fire Brick Lining				
Control Curve Type	Flux at t=30 (kW/m^2)	Flux at t=60 (kW/m^2)	Flux at t=90 (kW/m^2)	Flux at t=120 (kW/m^2)
1	42.05	62.82	72.84	90.14
2	24.57	41.89	62.66	83.23
3	20.99	38.35	52.23	76.43
Plate Thermometer Control, Fire Brick Lining				
Control Curve Type	Flux at t=30 (kW/m^2)	Flux at t=60 (kW/m^2)	Flux at t=90 (kW/m^2)	Flux at t=120 (kW/m^2)
1	42.26	69.76	97.09	114.13
2	31.22	55.80	83.45	97.03
3	28.01	48.78	69.54	90.31
Bare Wire Thermocouple Control, Fire Brick plus Ceramic Lining				
Control Curve Type	Flux at t=30 (kW/m^2)	Flux at t=60 (kW/m^2)	Flux at t=90 (kW/m^2)	Flux at t=120 (kW/m^2)
1	35.08	55.85	69.32	90.09
2	21.04	34.92	62.57	83.14
3	14.07	29.12	48.75	76.42
Plate Thermometer Control, Fire Brick Plus Ceramic Lining				
Control Curve Type	Flux at t=30 (kW/m^2)	Flux at t=60 (kW/m^2)	Flux at t=90 (kW/m^2)	Flux at t=120 (kW/m^2)
1	35.08	62.76	83.17	103.97
2	21.04	41.80	76.37	90.09
3	21.04	34.84	55.46	83.34

Table 6.2 Heat Flux Approximations for Different Furnace Linings and Control Methods

The maximum calculated heat flux within the furnace during the tests was 114kW/m² . This figure was comparable to the heat flux measurements taken at high temperature for the furnace as used for the GRP "wet" pipe fire testing as described in chapter 5. In this furnace, the heat flux was calculated from the maximum rate of temperature climb of a thin walled copper pipe after being inserted into the hot furnace. The calculated received heat flux for the furnace used for the GRP "wet" pipe tests was in the order of 90kW/m² after 30 minutes exposure to the DoE hydrocarbon curve.

From figures 6.4.25 and 6.4.26 it can also be seen that the heat flux within the furnace depends significantly on the furnace lining material. There is a distinct trend in the results showing that the heat flux for the fire brick alone lined furnace is significantly higher than that for the fire brick plus ceramic blanket furnace lining. This difference must be attributed to the lining alone as all other furnace variables such as furnace volume and dimensions, heating regime, fuel type, burner locations etc were kept as constants between the test series. The reason for lower heat fluxes in the furnace when lined with a thin layer of ceramic wool can be attributed directly to the ceramic wool lining. The low thermal conductivity of the ceramic wool would mean that less energy would be required to maintain the temperature within the furnace, and that less energy would be stored in, and hence radiated from, the furnace walls.

6.4.6 Special case tests

During the furnace characterisation studies there were two special case tests considered. The first special case test was a comparison of the maximum heating rate of the furnace between the two lining systems. In both tests the furnace computer control was programmed to achieve the temperature of 1000°C in as short a time as possible (this was done by using a furnace control set point of 1500°C so that burners would be set to 100% capacity from the start of the test until the test was terminated manually). It was decided that the furnace temperature should be considered as that measured by bare wire thermocouples.

Figures 6.4.27 and 6.4.28 show the test results for the fire brick alone furnace lining, and fire brick plus ceramic blanket lining respectively. As can be seen, the time to 1000°C for the fire brick alone furnace lining at the maximum burner settings was approximately 47 minutes. When the furnace was given an additional layer of thin ceramic fibre blanket the time taken to reach 1000°C at the maximum heating rate was much lower, at only 30 minutes. Thus it can be seen that the inclusion of only a very thin layer (3.5mm) of ceramic fibre blanket has a very significant effect on the heating rate of the furnace. When comparing the temperatures measured in the calibration rods, it can be seen that at the point where the measured furnace temperature was 1000°C the temperatures in the calibration rods were approximately 900°C, for both furnace lining systems (and hence heating durations). However, if the temperature of

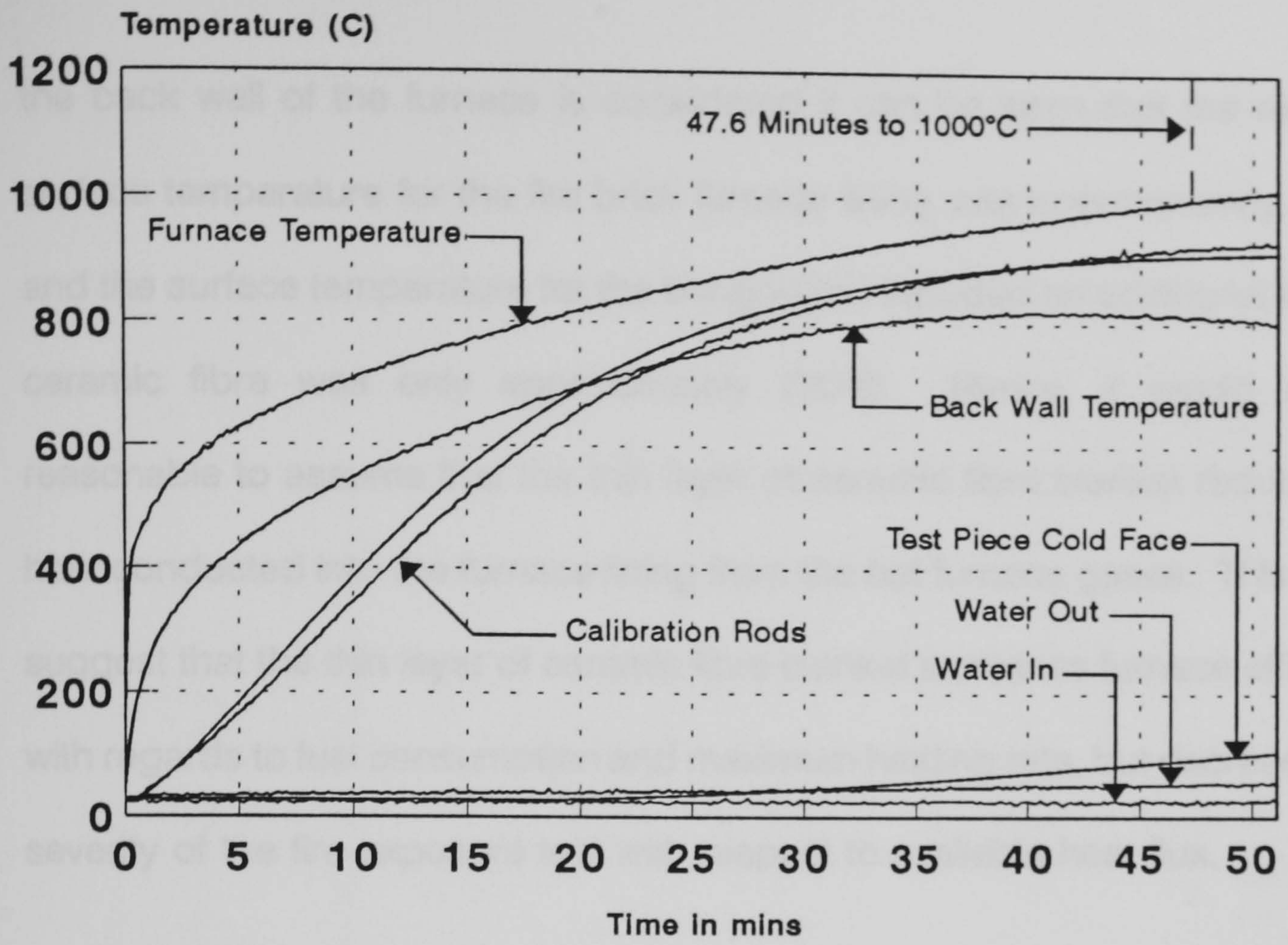

Figure 6.4.27 - Furnace Characterisation Test Run 11
Maximum Furnace Heating Rate - Fire Brick Lining Alone
R Type Furnace Temperature, All Thermocouples, 21-07-95

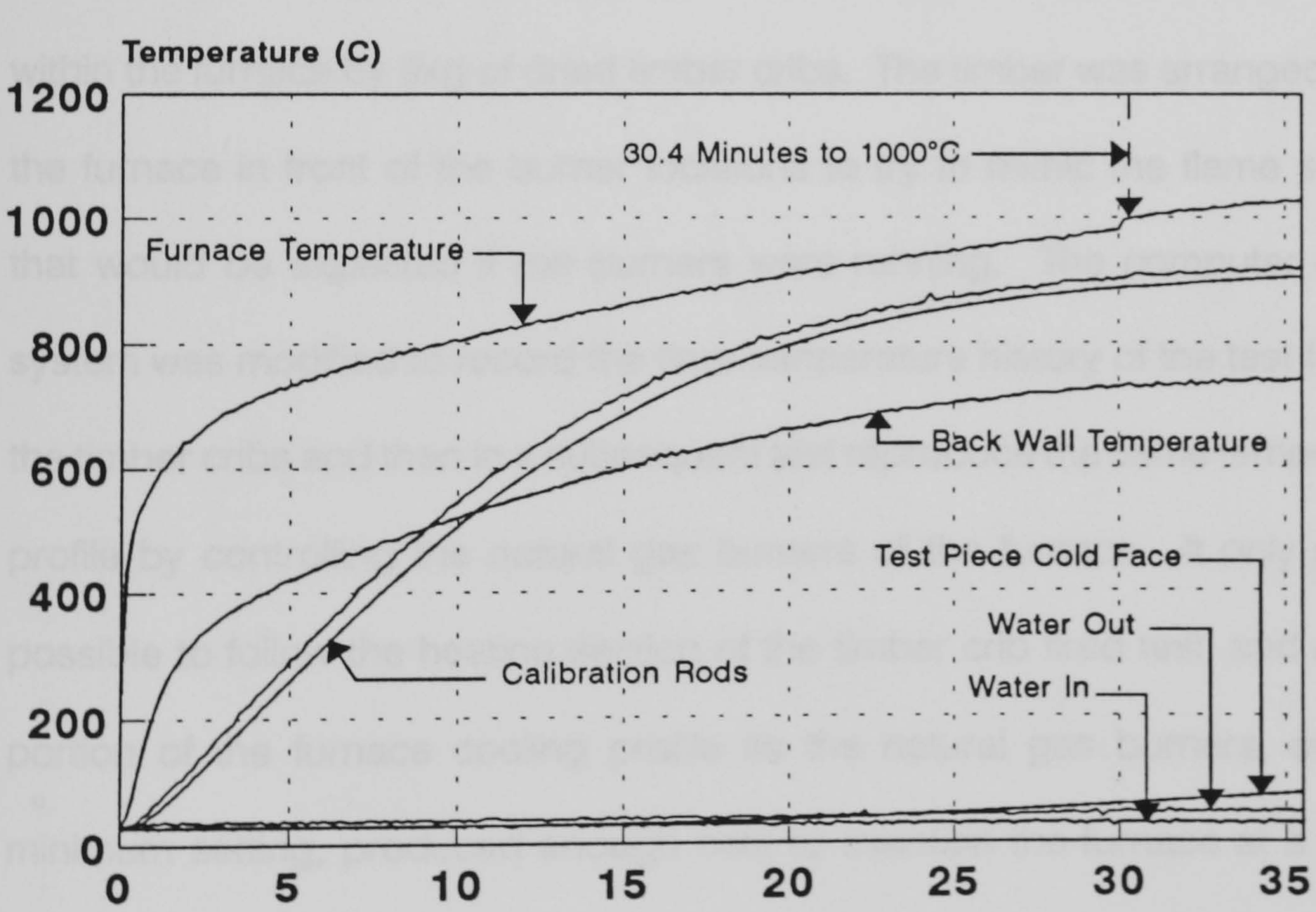

Figure 6.4.28 - Furnace Characterisation Test 12
Maximum Furnace Heating Rate - Fire Brick + 3.5mm Ceramic
R Type Furnace Temperature, All Thermocouples, 27-07-95

the back wall of the furnace is considered it can be seen that the rear wall surface temperature for the fire brick furnace lining was approximately 810°C, and the surface temperature for the lining which included an additional layer of ceramic fibre was only approximately 720°C. Hence, it would appear reasonable to assume that the thin layer of ceramic fibre blanket reduces the heat conducted into the furnace lining from the hot furnace gases. This would suggest that the thin layer of ceramic fibre blanket increases furnace efficiency with regards to fuel consumption and maximum heating rate, but decreases the severity of the fire exposure test with respect to available heat flux.

Figure 6.4.29 shows a comparison of the measured temperatures between identical test arrangements with different fuel sources. The initial test was fired within the furnace by 9kg of dried timber cribs. The timber was arranged within the furnace in front of the burner locations to try to mimic the flame sources that would be expected if the burners were running. The computer control system was modified to record the time-temperature history of the test fired by the timber cribs and then in a subsequent test reproduce the same temperature profile by controlling the natural gas burners of the furnace. It only proved possible to follow the heating section of the timber crib fired test, and a small portion of the furnace cooling profile as the natural gas burners, even on minimum setting, produced enough heat to maintain the furnace at a steady temperature of approximately 400°C.

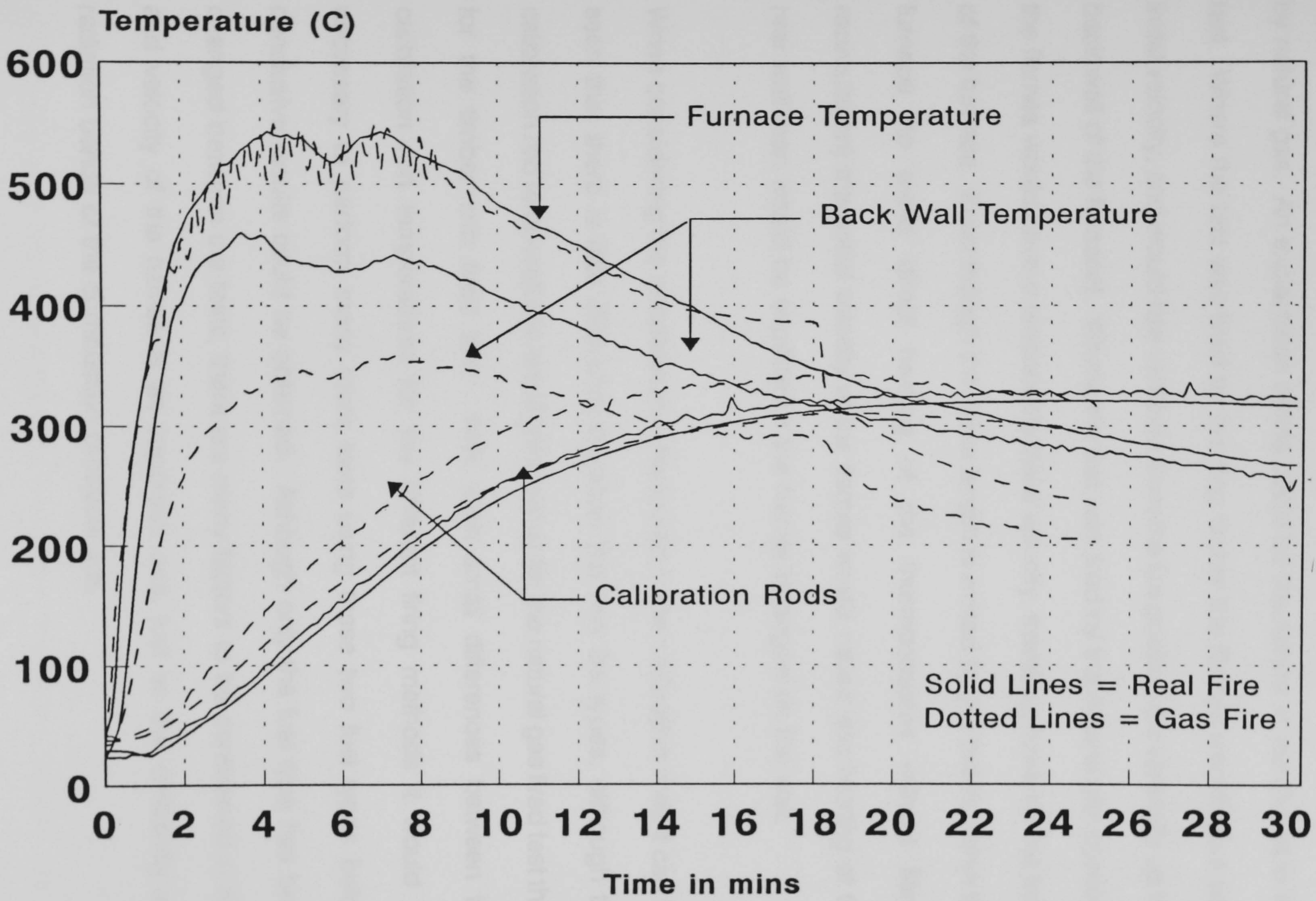

Figure 6.4.29 - Furnace Characterisation Tests 19 and 20
Comparison of Real Fire and Gas Fired Test

It can be seen from figure 6.4.29 that for the test heated by burning timber cribs the back wall temperature was significantly higher than for the test fired by natural gas. An explanation of this could be the nature of the flames in the test. Where the test was fired by burning timber the flames would have zero initial velocity, and would rise vertically from the fire position (i.e vertically up the back wall of the furnace). Where the test was fired by the natural gas burners, the flames would have a reasonable initial velocity, travelling towards the front of the furnace. Even though the flame length is limited by fire bricks within the furnace (to avoid direct heating of the thermocouples without flame recirculation) this initial velocity of the flames would cause less heating of the rear wall than would be expected if the flames impinged on the wall.

When considering the temperatures measured in the calibration rods it can be seen that there is little difference between the two fire types, although the calibration rod temperatures are slightly higher for the natural gas fired test than for the timber crib fired test. With such small differences between the calibration rod temperatures for the different firing methods it would be necessary to perform many more tests using these two fuel types before conclusive results could be obtained. Although only the fuel type has been changed between the tests, there are many factors to be considered in this, and velocity of the flames is an important one, just as the emissivity and radiation bands of the combustion products are.

6.5 Discussion of the Furnace Characterisation Study Results

The use of plate thermometer control gave noticeably higher temperatures in the calibration rods during the heating regime of the test cycle (due to the thermal inertia of the control temperature measuring devices). However, there was generally little or no difference in the temperature of the calibration rods when compared between tests carried out on the two lining systems. The use of plate thermometers for the control also appeared to make the test more aggressive with respect to the cold face temperature of the standard test piece, this observation is reinforced by the calculation of heat flux within the furnace which shows heat flux to be significantly higher where plate thermometer control was used. The cold face temperature difference between plate thermometer and bare wire thermocouple control methods was less than 10°C in all tests. Although this temperature difference may not be considered excessive, it could represent an elapsed time of 20 minutes or more for this increase to take place (assuming a cold face temperature rise of 0.5°C/min or less as observed towards the final stages of the tests).

In the majority of cases, the use of plate thermometers for the furnace control system appeared to reduce the temperature difference between the calibration rods for the different lining systems. This is similar to the effects as found in Cooke's research, however, the use of plate thermometers for control systems on its own may not be sufficient to harmonise fire testing results. In the author's research the use of plate thermometer control appeared to *increase*

the difference in the cold face temperatures of the standard test piece between the two lining systems.

In the authors research, significant differences were observed between the temperatures as measured by plate thermometers and bare wire thermocouples during any particular test. These can be explained as being partly due to the shallow furnace being used, and the small furnace volume, and this may not be the case for furnaces of larger depth. However, for the small furnace depth, and small furnace volume used, the measured temperature by the plate thermometer was lower than the bare wire thermocouple control temperature by up to 30°C for the fire brick alone furnace lining, and between 50-90°C for the fire brick plus ceramic wool lining. In all cases of plate thermometer control the temperature measured by the bare wire thermocouple was well in excess of the averaged control temperature (70-110°C for the fire brick alone lining, and 35-80°C for the fire brick plus ceramic blanket lining).

The temperatures measured in the calibration rods towards the end of the test with bare wire thermocouple control were approximately 50°C higher for the fire brick alone furnace lining than for the fire brick plus ceramic wool lining system. This trend of the temperatures in the calibration rods being higher at test termination for the fire brick alone lining was also observed with plate thermometer control. However, the difference between the calibration rod temperatures for the two lining systems was less for plate thermometer control

than for thermocouple control at approximately 30°C.

The temperature differences in the calibration rods between the two lining systems can be explained by comparing the calculated measured heat flux within the furnace. It can be seen in all tests that the heat flux in tests using the fire brick alone furnace lining is significantly higher than in the similar tests using the fire brick plus ceramic blanket lining system.

Giving the fire brick lined furnace an additional lining layer of 3.5mm ceramic wool reduced the heating time from room temperature to 1000°C from 47 to 30 minutes. The additional furnace lining layer improved the efficiency of the furnace with respect to maximum heating rate, which would have an associated reduction in fuel consumption for furnace tests, however, it also reduced the heat transfer within the furnace, and hence the severity of the furnace test. In a fully developed hydrocarbon pool fire the incident heat flux can be as high as 350kW/m^2 [11]. The maximum calculated heat flux within the furnace during any of the tests in the series was 114kW/m^2, and hence it may be that for hydrocarbon fire conditions furnace based tests are not sufficiently severe. Although the furnace based fire resistance test would still provide a valid platform for comparison of the relative fire performance of materials, it may be that the fire tests do not represent a realistic value of expected fire resistance. Hence, actual fire resistance could be much less than the classification obtained from fire testing regardless of whether or not test results are harmonized between different furnaces.

A full investigation into furnace characterisation is outside the scope of this thesis. However, the research provides information about the relative performance of furnaces, particularly with respect to small furnace volumes. To prove conclusively the benefit of using plate thermometer control or highly efficient furnace linings for the harmonisation of furnace fire resistance testing would require a much more extensive study of different furnaces, and cover all the furnace variables in much greater detail. From the small study undertaken by the author, and from other research performed in this field, it would appear that using plate thermometer control does go some way towards harmonisation of fire resistance tests. However, use of plate thermometer control alone will not bring different fire test furnaces into harmonisation.

The authors research found the use of a highly efficient furnace lining to reduce dramatically the available heat flux within the furnace. The use of the highly efficient furnace lining layer may or may not aid harmonisation between different furnaces, further research investigating furnaces of different dimensions would be required before this could be commented on accurately. The reduction in heat flux within the furnace may further reduce the aggressiveness of the furnace based fire resistance test which would appear to be insufficiently aggressive when comparing the available heat flux expected in "real" hydrocarbon fires.

There are many factors which must be addressed, particularly fuel type, burner types and locations, furnace volume and furnace lining materials, before the

harmonisation of fire resistance testing may be achieved. The use of an additional lining of ceramic fibre blanket, or the use of plate thermometer control alone are insufficient to harmonise fire resistance testing, however, they may go some way towards that goal.

It is thought by the author that a more important route towards the harmonisation of fire resistance tests may be to develop empirical correction factors for specific testing cases, or numerical models to "correct" the fire test results to ones which would be expected in a test performed on a "standard" design of furnace. The author feels that the empirical correction factors for furnaces should be based on the testing of different materials, both flammable and non-flammable chosen to incorporate many aspects of materials performance. Materials which may be suitable for this purpose could be steel, a hygroscopic material such as concrete or a particulate composite, and a flammable material such as GRP. Comparing the failure times and failure mechanisms of these types of materials with reference to those obtained in the furnace design which is to be adopted as the "standard" furnace would give a series of correction factors. The decision of whether to take an average correction factor, or to adopt different correction factors for different material characteristics (i.e. Flammable, High Thermal Conductivity, Low thermal conductivity with chemically combined water etc) is one which needs to be researched. The numerical modelling and correction of test results would be an ideal solution, however, the complexities of the modelling of the effects of burner locations, flue ports, and combustion product velocities within the

furnace may make this solution somewhat unlikely. The use of sophisticated computational fluid dynamics (CFD) models is one possibility for modelling the fluid flow and gas velocities within the furnace during a test. However, even using very sophisticated computer packages, the modelling of all the factors effecting a furnace fire resistance test would still be an extremely difficult task. It would also be necessary to investigate fully the effects of all the variables and assess the importance of their effect on the fire test results before such a model could be verified.

At present the results obtained from different fire resistance test furnaces are not harmonised. This is likely to remain the case until regulatory bodies specify either a "standard" furnace design, or specify acceptance criteria for furnace design, and correction factors (including the method of obtaining them) for furnaces which vary from the standard design. Without necessitating this course of action through regulatory requirements there is little or no incentive for commercial testing sites to bring all fire test results into harmonisation.

CHAPTER 7 - CONCLUSIONS AND RECOMMENDATIONS FOR FURTHER WORK

7.1 Conclusions

The author has performed an extensive experimental programme into the performance of FRP and other compatible materials in fire situations. Within the work presented in this thesis the following aspects have been investigated:

1) Structural design and optimisation of GRP faced sandwich panels and stringer panels;

2) The development of new and cost effective fire resistant core materials for sandwich construction with FRP faces;

3) The performance of FRP and FRP-faced sandwich panels in fire situations, encompassing many standard fire resistance tests, and also the consideration of finite difference numerical modelling as an effective design tool for the prediction of the fire performance of FRP and FRP-faced sandwich panels;

4) The fire performance of FRP pipes in standard hydrocarbon fire resistance tests in the empty and dry, stagnant water-filled, and flowing water-filled conditions including the effect of a sacrificial, insulating, or

intumescent layer on the fire resistance for the empty and dry condition;

5) The applicability of standard fire resistance testing, and the harmonisation of fire resistance tests between different furnaces. Consideration has been given to the use of highly efficient furnace linings, and also the use of plate thermometers for furnace control temperature measuring devices. An alternative method of achieving furnace fire resistance test harmonisation has also been proposed.

The following main conclusions can be drawn from the author's research:

7.1.1 Structural aspects of sandwich construction

1) The structural design methods for both thin and thick faced sandwich panels are readily available and, with current computation capabilities, reasonably easy to implement.

2) The governing design criterion for sandwich panels utilising GRP faces is generally one of allowable deflection. The implication from this research is that the allowable deflection design criteria, and corresponding low face stresses, suggest that GRP face materials for sandwich construction would not be susceptible to creep and fatigue problems.

3) Current panel designs incorporating relatively thick GRP faces and fire resistant cores are attractive alternatives to traditional construction materials in terms of corrosion resistance and ease of installation. However, at the present time, this design philosophy suffers from the lack of a core material that is sufficiently light in weight while still possessing adequate mechanical properties. These panel designs, therefore, become less attractive when their weight is taken into consideration.

4) GRP Stringer panels appear to exhibit superior structural performance to GRP faced sandwich panels, and can offer significant weight savings over both traditional steel-fibre fire resistant panels, and FRP faced sandwich panels for offshore use.

7.1.2 The fire performance of FRP sandwich and stringer panels

5) The fire performance of fibre reinforced plastics is influenced by many factors. In consideration of the tendency of FRP to maintain flaming, and to aid fire growth it appears that the thickness of the laminate used is a critical factor. Current thinking is that laminates of less than 10mm thickness should not normally be used. This has implications with respect to the efficiency of the structural stringer panel design (which incorporates relatively thin panel faces) in terms of weight saving.

6) The thermal decomposition process of most resins in common use is highly endothermic. This endothermic nature slows heat transfer through the GRP laminate and helps preserve the integrity of the laminate with respect to ablation and degradation.

7) Phenolic resin laminates appear to have superior fire performance to other commonly used resin systems. However, the fire performance of phenolic resin laminates can be significantly affected by violent delamination. These delaminations can cause unexpectedly poor performance in terms of integrity and stability of the composite in fire situations.

8) The fire resistance of hygroscopic core materials is highly dependent on their free and chemically combined water content. A high free water content can increase the thermal conductivity of the material. However the latent heat energy required for evaporation of the water content significantly increases insulation failure times, and is the dominant effect of the two.

9) A structural core material termed "Voidfill" has been developed as part of this project. This material exhibits excellent performance in terms of fire resistance. At the present stage of development Voidfill is relatively brittle and weak when compared to state of the art materials such as Vermiculux and Newtherm. Impregnating Voidfill with phenolic resin can

provide substantial improvements in mechanical properties, however, this also sacrifices some degree of fire resistance.

10) With respect to the standard fire resistance test, the use of steel panel faces may give no distinguishable advantage in fire resistance over that of the core alone where non-polymeric core materials are considered. Using GRP panel faces can offer distinct improvements in insulation failure times in fire resistance tests over that of the core alone, and these improvements can be further enhanced where a layer of ceramic fibre blanket is encapsulated within the laminate.

11) With respect to fire resistance, the GRP structural stringer panel may be a viable alternative to traditional panel designs. Structural stringer panels have been shown to be able to offer comparable structural performance to the steel-fibre panel or GRP-faced sandwich panel solutions with a significant weight saving, and offer comparable fire resistance. An additional benefit of structural stringer panels is that positive connection of the faces to the stringer is easily achieved which offers the advantages of maintaining the fire exposed face in place throughout the duration of the fire. This is particularly advantageous where the fire exposed face contains an encapsulated ceramic blanket layer.

12) Numerical modelling using the explicit finite difference method can be an

effective and accurate design tool in predicting the thermal response of polymer composites, hygroscopic core materials, and combinations of the two, to the standard fire resistance test. The accuracy of numerical modelling is highly dependent on the degree of accuracy with which the material thermal properties are known, or are derived, at elevated temperatures.

7.1.3 The fire performance of FRP pipes

13) In an empty and dry condition, GRE pipes are unlikely to have sufficient fire resistance for offshore applications.

14) The fire endurance of GRE pipes is a function of wall thickness and wall composition. The fire resistance of the pipe wall can be extended by increasing the wall thickness (and hence providing a sacrificial layer). Using a sacrificial layer incorporating ceramic fibres appears to be a more effective way to improve fire resistance than to increase the wall thickness of the pipe alone. Using a resin wetted ceramic blanket appears to be more effective at increasing fire resistance than using a "dry" ceramic blanket layer. Thoroughly wetting the ceramic blanket with resin prior to application takes advantage of the highly endothermic nature of the resin decomposition reaction.

15) Thick intumescent coatings can significantly increase the fire resistance

of GRE pipes but can carry a high cost premium, and are also less durable in an aggressive marine environment. Thin-film intumescents do not offer sufficient protection at an early stage.

16) From the research performed it appears that the easiest, cheapest and most effective manner of improving the fire resistance of GRE pipes is to maintain them in a water-filled condition. For small diameter pipes some additional fire protection may be required for offshore applications as the volume of contained water, and hence the size of the heat sink is small.

17) With respect to the test method used in the authors research, even modest water flow rates appear to be able to preserve indefinitely the functionability of the GRE pipes tested.

18) Finite difference modelling can provide accurate predictions of fire test exposure results of FRP pipes with the proviso that accurate material data are known. The modelling technique is effective for differing internal conditions (e.g. empty and dry, stagnant water filled, flowing water filled).

7.1.4 Furnace-based fire resistance testing, and its harmonisation.

19) With respect to the furnace and instrumentation used in the authors research, the use of plate thermometer control appears to make fire resistance tests more aggressive when considering the cold face response of a standard test piece, and calculated values of heat flux available within the furnace.

20) With respect to the furnace and instrumentation used in the authors research, the use of an additional thin layer of highly efficient furnace lining (3.5mm ceramic wool) appears to reduce the heat flux available within the furnace.

21) Due to plate thermometer control apparently increasing the difference in test results between two different furnace linings, it appears that there is no possibility in the systematic harmonisation of furnace test results by simply using plate thermometers to measure the furnace control temperature.

22) From calculating the available heat flux within the furnace during the tests performed, it appears that furnace based fire testing is not sufficiently aggressive, when compared to conditions which may be expected in a developed hydrocarbon fire, to give a reasonable approximation to how a material or construction will perform in a real fire

situation. Furnace fire resistance testing, however, can still provide a means of determining an acceptable level of performance.

23) The failure times of flammable materials in fire resistance tests may be significantly affected by the free oxygen content of the hot furnace gases. This is not controlled in any current standard procedure.

24) It is the author's belief that the development of empirical correction factors for different furnaces would prove a more productive route towards the harmonisation of fire resistance test results. It is proposed that different material compositions should be considered in order to cover aspects of flammability, thermal conductivity, and moisture content. From a series of test results obtained on any particular furnace, correction factors could be derived to standardise the results with those which would be obtained on a "standard design" furnace.

7.2 Future Developments

Standard fire resistance testing plays a vital role in fire engineering. The authors research programme has raised several questions as to the applicability of current testing methods as a means of categorising a materials fire performance. In addition to this there are some aspects in the use of FRP materials for fire risk areas which still require investigation.

Following are the author's recommendations for areas which require further research:

1) It has been discussed briefly that evidence from cone calorimetry suggests that using FRP laminates of less than 10mm thick can encourage fire development and propagation. The author believes that further investigation is warranted into the factors which effect the flammability of FRP. In particular the author feels that the flammability of FRP including ceramic blanket layers should be investigated. This research is key to the validity and efficiency of the structural stringer panel design.

2) The current testing methods used for the fire resistance testing of materials such as fibre reinforced plastics leave many factors which could affect the thermal degradation of the materials not investigated. Primary consideration, in the authors opinion, should be given to the free

oxygen content within a furnace during a standard fire resistance test. The author believes that consideration should also be given to the internal furnace pressure during a fire test. Current regulations require a significant positive pressure to be maintained within the furnace in order to determine the integrity failure time of a specimen. This positive pressure could suppress volatile release and hence reduce the rate of decomposition of a resin matrix.

3) Investigation into the available heat flux within the furnace during a fire resistance test has shown that flux levels may be significantly lower than those which could be expected in a fully developed hydrocarbon fire. The author believes that this warrants an investigation into the effect of higher levels of incident heat flux on heat transfer through a material under test. Of particular interest would be the effect on polymer composites as preliminary investigation has shown that the rate of decomposition is highly dependant on the incident flux levels.

4) There is currently very little information regarding the structural performance of FRP laminates at elevated temperatures. Of particular interest would be the structural response of an FRP laminate or FRP-faced sandwich panel subjected to a standard fire resistance test whilst under load. If the reduction in mechanical properties with elevated temperature (and hence resin matrix degradation) were known, then commercially available finite element packages could be used to

produce a complete thermal-structural response model of a fire exposed element or structure.

5) Filament wound GRE pipes have been shown to perform well in fire under low water flow conditions. The author believes that some important factors still remain to be investigated. Firstly the effect of higher levels of incident flux need to be investigated, preferably in conjunction with realistic flow velocities within the pipe loop. In addition to this, the author believes that it would be prudent to investigate the length effect, if any, of a fire-exposed pipe loop. The author believes that realistic pipe loop lengths require fire testing in fire conditions to determine any functionability limits which the pipe material may have.

6) Another important consideration in the use of FRP pipes offshore would be the significant pressures developed during startup of the deluge system. If the pipe system is maintained in a stagnant water filled condition the pipe wall notionally be at its hottest, and hence weakest condition immediately prior to the starting of the deluge system, as the pipe walls will not have the additional cooling effect of the flowing water. In this "weakest" condition the pipes are subject to the highest pressure during the running of the deluge system - the pressure head of starting the water flow, which can be up to 16 bar. The author believes that investigation into the pipes ability to withstand this combination of factors is of great importance.

7) As has been outlined in this thesis, one of the major drawbacks of standard fire resistance testing is that the exposure regime is specified in terms of temperature control. The amount of available heat flux within the furnace, and particularly the radiated heat flux to the sample appear to be more significant factors than temperature. The author believes that alternative control methods (such as heat flux control) should be further investigated. In addition to this the possibility of harmonising results from different test furnaces by means of testing several samples with different characteristics in fire and applying empirical correction factors should be investigated. An alternative method of harmonising fire resistance tests would be to determine the required time-temperature regime to produce comparable thermal response for specific materials between different furnaces. Numerical modelling of the heat transfer from the furnace to a sample of known properties, and the thermal response of the sample, could be extremely useful in determining the time-temperature exposures required for different furnaces in order to obtain harmonised fire resistance tests.

8) The author believes that further investigation into the applicability of furnace based fire resistance testing should be performed. Brief comparison of the heat flux levels in a furnace based test, and those observed in fully developed fires, show large discrepancies. The author believes that although the furnace based fire resistance test is a means of comparing fire resistance of different materials, elements and

structures, more realistic heat flux levels should be available within the furnace during a fire resistance test. Current test methods and furnace designs may give very optimistic fire ratings for different materials when compared to the performance which they may offer in "real" fire situations. The hydrocarbon fire testing regime is of particular interest due to the very high heat flux levels observed in fully developed fires.

APPENDIX A

Appendix A contains detailed descriptions of the methodologies used and experiments performed in the development of a new, non-fibrous, highly efficient furnace lining.

The work presented was performed as part of a multi sponsor research project in conjunction with the Energy Efficiency Office, Department of the Environment. The research is part of an ongoing project (March 1997), and due to its' commercially sensitive nature is presented in volume 2 of this thesis.

APPENDIX B

Analysis of a thick faced sandwich panel under UDL - MathCad solution

Analysis of sandwich panel under UDL

l= Span length, E= Elastic mod. of faces, qo= UDL, W=Width,t=Facethickness
C=Core thickness, Gs= Core shear modulus, Es=Core elastic modulus
ϵ= spane length ratio, s= sandwich, o=upper face, u=lower face, t=total

$l := 4000 \quad E := 16.0 \cdot 10^{3} \quad qo := 2.0 \cdot 10^{-3} \quad W := 1 \quad t := 8.5 \quad C := 60$

$Gs := 95$

$Es := 2 \cdot Gs \qquad Ac := W \cdot C$

$$A := Gs \cdot W \cdot \frac{(C + t)^2}{C}$$

$$Iu := W \cdot \left[\frac{t^3}{12}\right] \qquad Is := W \cdot \frac{C^3}{12}$$

$Io := Iu$

$$Bs := (E \cdot W \cdot t)^2 \cdot \frac{(C + t)^2}{2 \cdot E \cdot W \cdot t}$$

$Bo := E \cdot Io \qquad Bu := E \cdot Iu$

$B := Bo + Bs + Bu \qquad \alpha u := \frac{Bu}{Bs} \qquad \alpha o := \frac{Bo}{Bs} \qquad \alpha := \alpha u + \alpha o$

$\epsilon := 0, 0.1 \ldots 1$

$$\beta := \frac{Bs}{A \cdot l^2} \qquad \lambda := \left[\frac{1 + \alpha}{\alpha \cdot \beta}\right]^{0.5}$$

$$w1(\epsilon) := qo \cdot \frac{l^4}{B} \cdot \left[\frac{1}{\alpha \cdot \lambda^4} \cdot \frac{\cosh\left[\frac{\lambda}{2}\right] - \cosh\left[\lambda \cdot \frac{1 - 2 \cdot \epsilon}{2}\right]}{\cosh\left[\frac{\lambda}{2}\right]}\right]$$

$$w(\epsilon) := qo \cdot \frac{l^4}{B} \cdot \left[\frac{1}{24} \cdot \epsilon \cdot \left[1 - 2 \cdot \epsilon^2 + \epsilon^3\right] + \frac{1}{2 \cdot \alpha \cdot \lambda^2} \cdot \epsilon \cdot (1 - \epsilon)\right] - w1(\epsilon)$$

$$Ms(\epsilon) := qo \cdot l^2 \cdot \left[\frac{1}{1+\alpha}\right] \cdot \left[0.5 \cdot \epsilon \cdot (1-\epsilon) - \left[\frac{1}{\lambda^2}\right] \cdot \left[\frac{\cosh\left[\frac{\lambda}{2}\right]}{\cosh\left[\frac{\lambda}{2}\right]} - \frac{\cosh\left[\lambda \cdot \frac{1-2\cdot\epsilon}{2}\right]}{\cosh\left[\frac{\lambda}{2}\right]}\right]\right]$$

$$Mu(\epsilon) := qo \cdot l^2 \cdot \left[\frac{\alpha u}{1+\alpha}\right] \cdot \left[0.5 \cdot \epsilon \cdot (1-\epsilon) + \left[\frac{1}{\alpha \cdot \lambda^2}\right] \cdot \left[\frac{\cosh\left[\frac{\lambda}{2}\right]}{\cosh\left[\frac{\lambda}{2}\right]} - \frac{\cosh\left[\lambda \cdot \frac{1-2\cdot\epsilon}{2}\right]}{\cosh\left[\frac{\lambda}{2}\right]}\right]\right]$$

$$Mo(\epsilon) := qo \cdot l^2 \cdot \left[\frac{\alpha o}{1+\alpha}\right] \cdot \left[0.5 \cdot \epsilon \cdot (1-\epsilon) + \left[\frac{1}{\alpha \cdot \lambda^2}\right] \cdot \left[\frac{\cosh\left[\frac{\lambda}{2}\right]}{\cosh\left[\frac{\lambda}{2}\right]} - \frac{\cosh\left[\lambda \cdot \frac{1-2\cdot\epsilon}{2}\right]}{\cosh\left[\frac{\lambda}{2}\right]}\right]\right]$$

$$Qs(\epsilon) := qo \cdot l \cdot \left[\frac{1}{1+\alpha}\right] \cdot \left[0.5 \cdot (1-2\cdot\epsilon) - \left[\frac{1}{\lambda}\right] \cdot \left[\frac{\sinh\left[\lambda \cdot \frac{1-2\cdot\epsilon}{2}\right]}{\cosh\left[\frac{\lambda}{2}\right]}\right]\right]$$

$$Qu(\epsilon) := qo \cdot l \cdot \left[\frac{\alpha u}{1+\alpha}\right] \cdot \left[0.5 \cdot (1-2\cdot\epsilon) + \left[\frac{1}{\alpha \cdot \lambda}\right] \cdot \left[\frac{\sinh\left[\lambda \cdot \frac{1-2\cdot\epsilon}{2}\right]}{\cosh\left[\frac{\lambda}{2}\right]}\right]\right]$$

$$Qo(\epsilon) := qo \cdot l \cdot \left[\frac{\alpha o}{1+\alpha}\right] \cdot \left[0.5 \cdot (1-2\cdot\epsilon) + \left[\frac{1}{\alpha \cdot \lambda}\right] \cdot \left[\frac{\sinh\left[\lambda \cdot \frac{1-2\cdot\epsilon}{2}\right]}{\cosh\left[\frac{\lambda}{2}\right]}\right]\right]$$

$Qt(\epsilon) := Qs(\epsilon) + 2 \cdot Qo(\epsilon)$

$Mt(\epsilon) := Ms(\epsilon) + 2 \cdot Mo(\epsilon)$

$Qs(0) = 3.95$

$Qt(0) = 4$

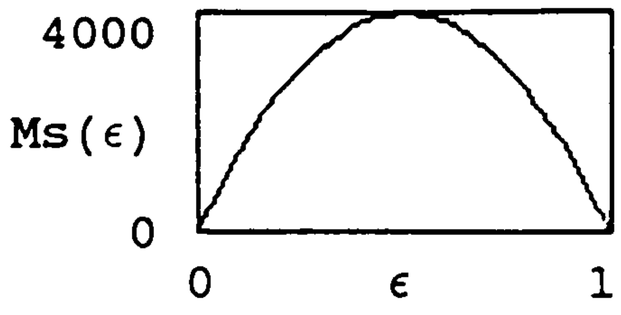

Sandwich bending moment

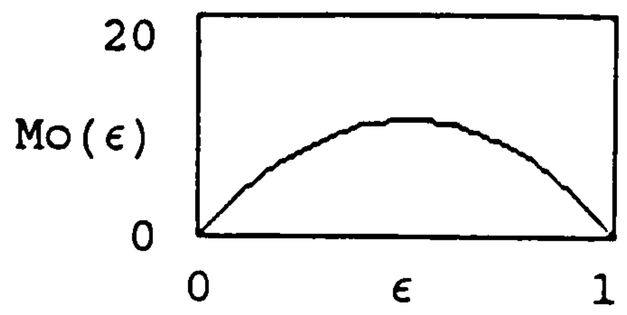

Upper face bending moment

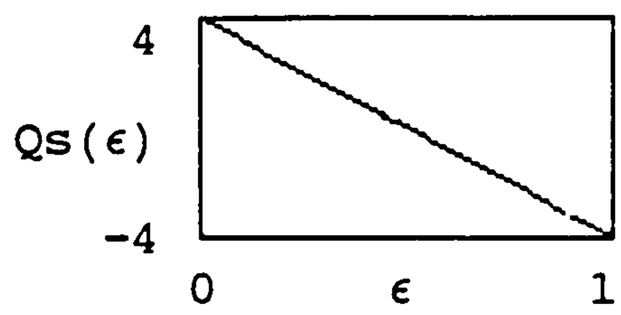

Sandwich Shear Force

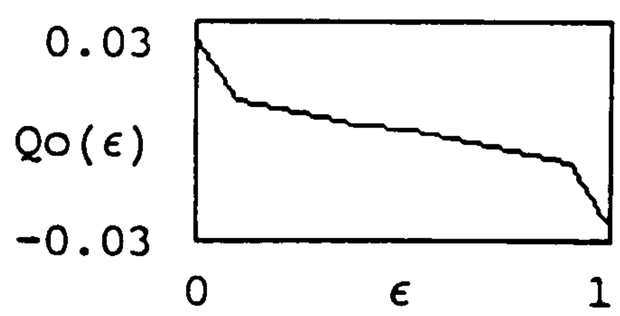

Upper face shear force

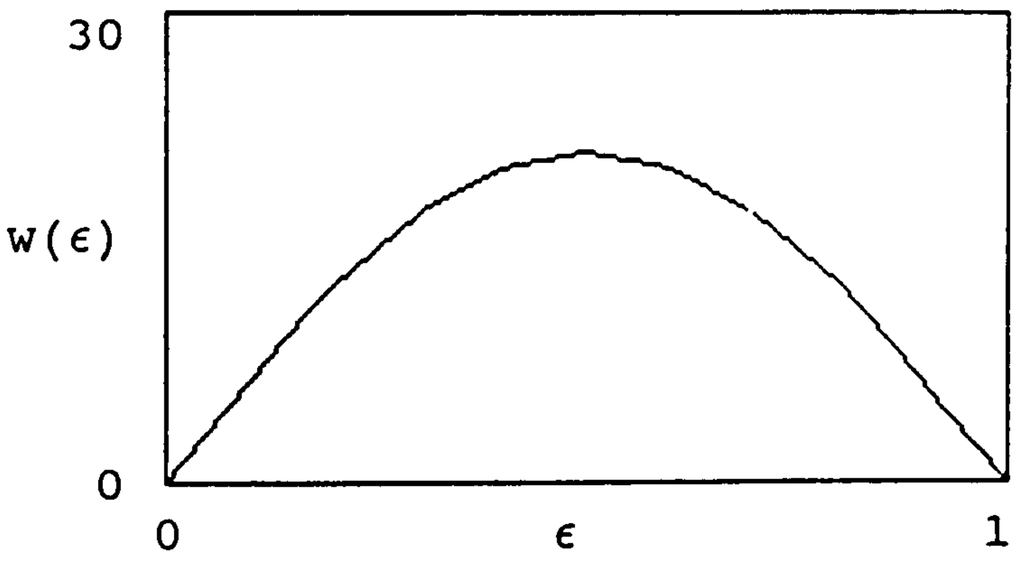

Deflected shape

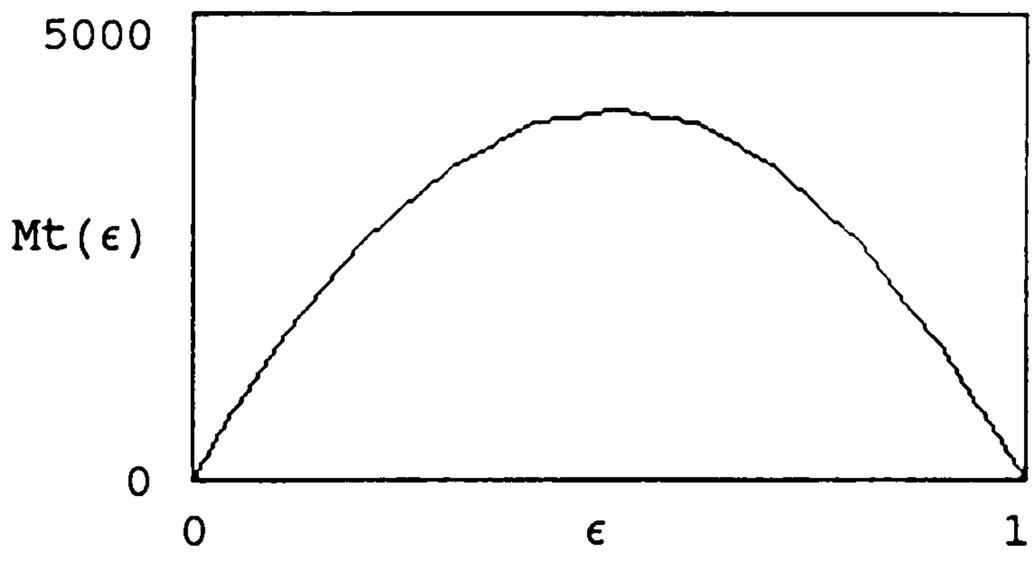

Bending moment Diagram

Stress calculations

$$\sigma o(\epsilon) := \frac{Mo(\epsilon)\cdot\frac{t}{2}}{W\cdot\frac{t}{12}\cdot\frac{t}{3}} - \frac{Ms(\epsilon)}{(C+t)\cdot(W\cdot t)}$$

$$\sigma u(\epsilon) := \frac{Mu(\epsilon)\cdot\frac{t}{2}}{W\cdot\frac{t}{12}\cdot\frac{t}{3}} + \frac{Ms(\epsilon)}{(C+t)\cdot(W\cdot t)}$$

$$\tau s(\epsilon) := \frac{Qs(\epsilon)}{W\cdot(C+t)}$$

$\sigma o(\epsilon)$
0
-2.136
-3.813
-5.01
-5.728
-5.968
-5.728
-5.01
-3.813
-2.136
$-2.122\cdot 10^{-15}$

Upper face
Direct Stress

$\sigma u(\epsilon)$
0
2.783
4.934
6.471
7.393
7.7
7.393
6.471
4.934
2.783
$3.906\cdot 10^{-15}$

Lower face
Direct stress

$\tau s(\epsilon)$
0.058
0.046
0.035
0.023
0.012
0
-0.012
-0.023
-0.035
-0.046
-0.058

Core
shear stress

$w(\epsilon)$
0
6.717
12.687
17.35
20.308
21.32
20.308
17.35
12.687
6.717
$7.62\cdot 10^{-15}$

Panel
deflection

APPENDIX C

Cone calorimeter runtime data for glass fibre reinforced polyester samples

CONE CALORIMETER SINGLE RUN DATA

Material name:	polyester
Sample description:	polyester panel
File name:	POLY32
Date of test:	September 28, 1995
Specimen thickness:	5.7 mm
Specimen initial mass:	180.5 g
Heat flux:	100 kW/m²
Exhaust duct flow rate:	0.024 m³/s (Nominal)
Orientation:	Horizontal
Time to ignition:	15 s
Flameout:	200 s
End of test:	430 s
Total heat evolved:	86.4 MJ/m²
Mass lost:	49.9 g

Observations:

tested to completion
shielded edges started to burn at approx 180s

Comment: 130x130 sample with edge guard

Peak and average values:	**Peak**	**Time(s)**	**Average**
Heat release rate:	308 kW/m²	252	209
Effective heat of combustion:	29.1 MJ/kg	397	17.3
Mass loss rate:	0.359 g/s	26	0.121
Specific extinction area:	1300 m²/kg	42	882
Carbon monoxide yield:	0.0432 kg/kg	44	0.0226
Carbon dioxide yield:	1.44 kg/kg	45	1.09

Average during period from ignition to ignition plus...

	1 min	**2 min**	**3 min**	**4 min**	**5 min**	**6 min**
Heat release rate:	128	172	190	208	219	219
Heat of combustion:	10.5	13.9	14.7	15.1	16.0	16.7
Mass loss rate:	0.122	0.124	0.129	0.138	0.137	0.131
Specific ext. area:	1002	1027	1034	1004	945	904
Carbon monoxide:	0.0301	0.0287	0.0241	0.0221	0.0220	0.0222
Carbon dioxide:	1.04	1.03	1.03	1.06	1.09	1.10

CONE CALORIMETER GRAPHICAL DATA

File name: POLY32
Material name: polyester
Irradiance: 100 kW/m^2
Orientation: Horizontal

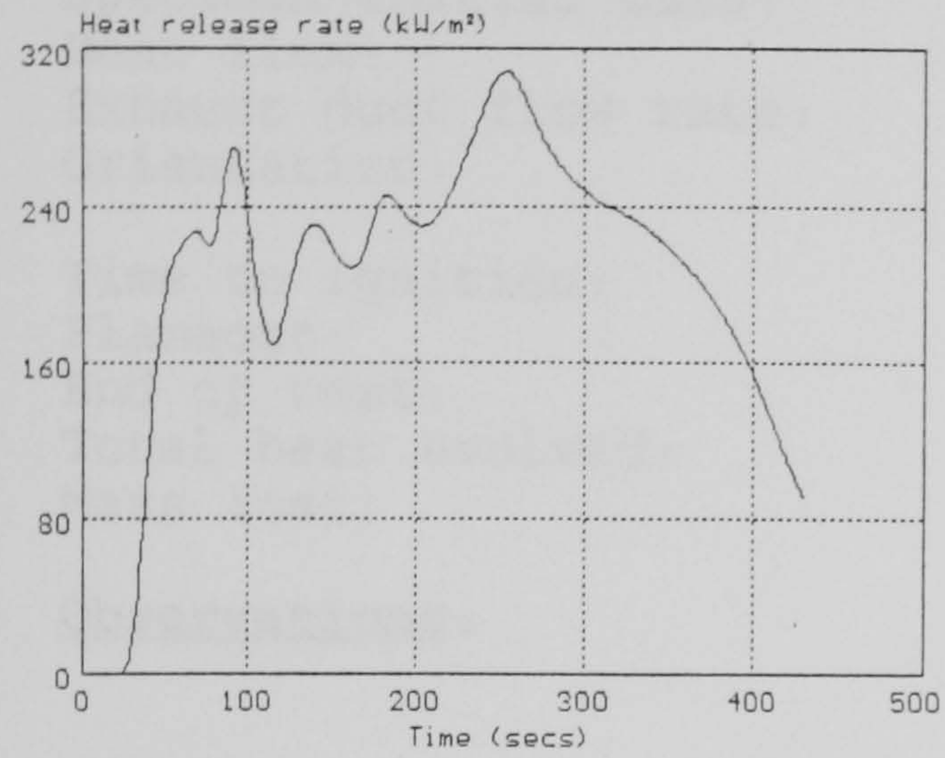

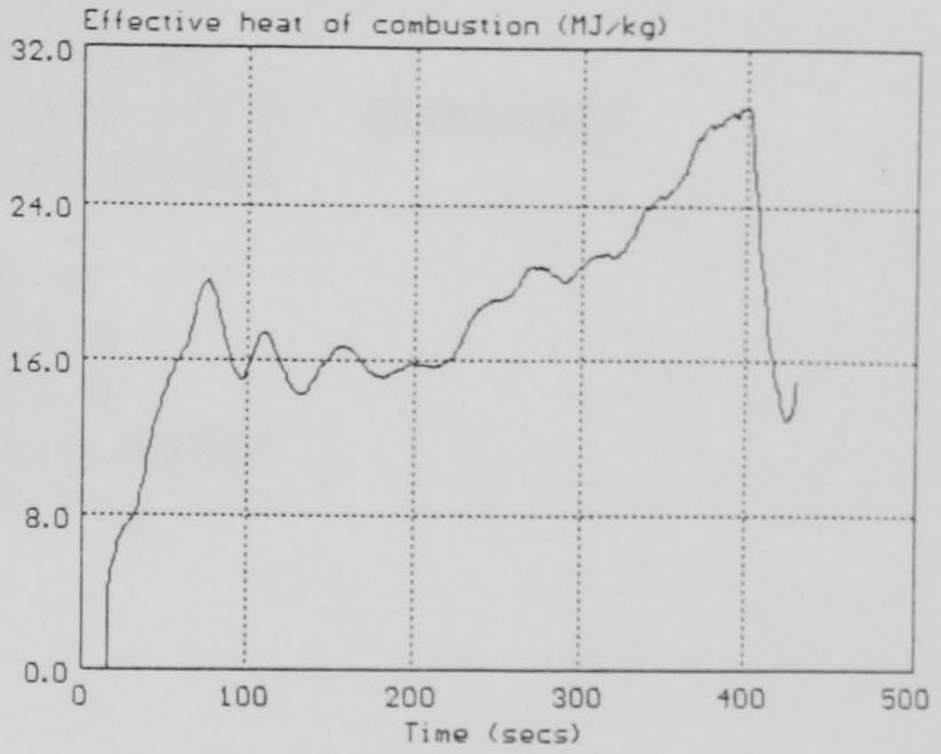

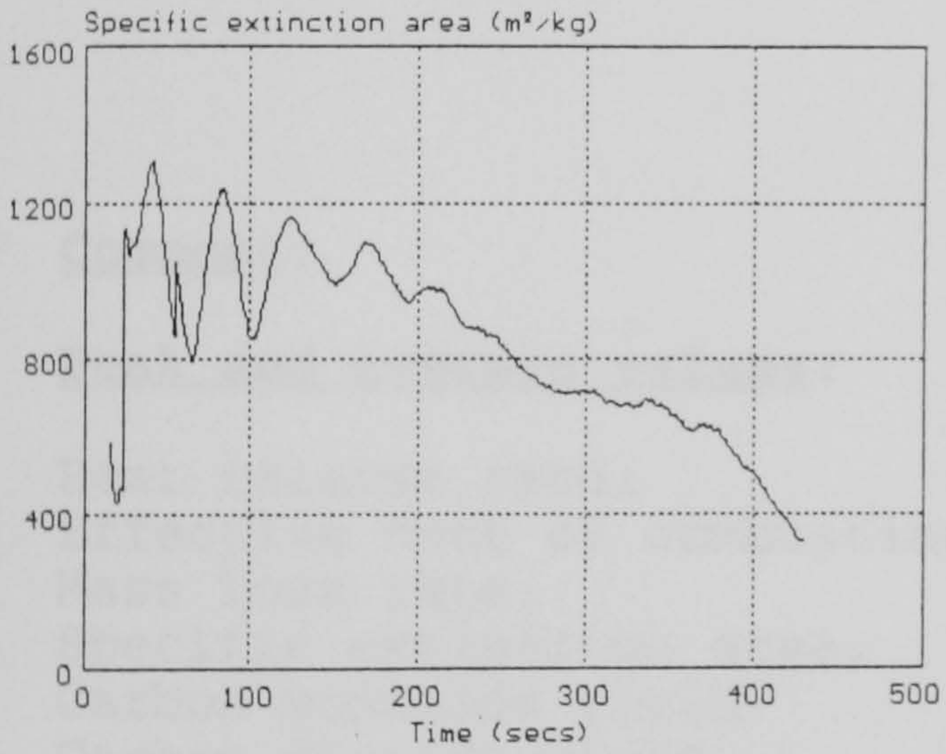

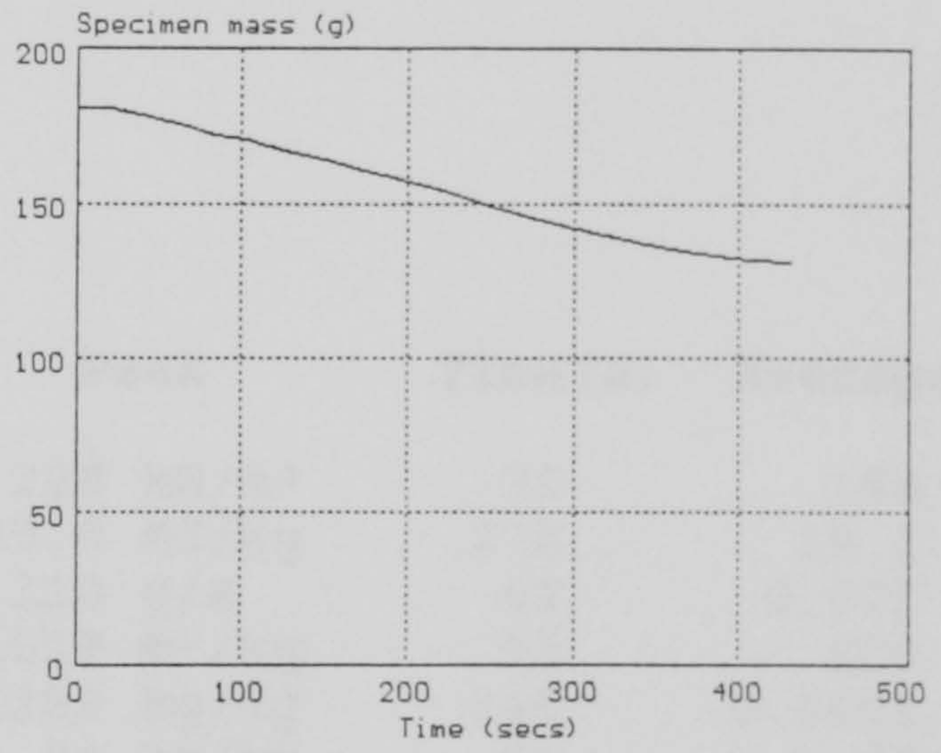

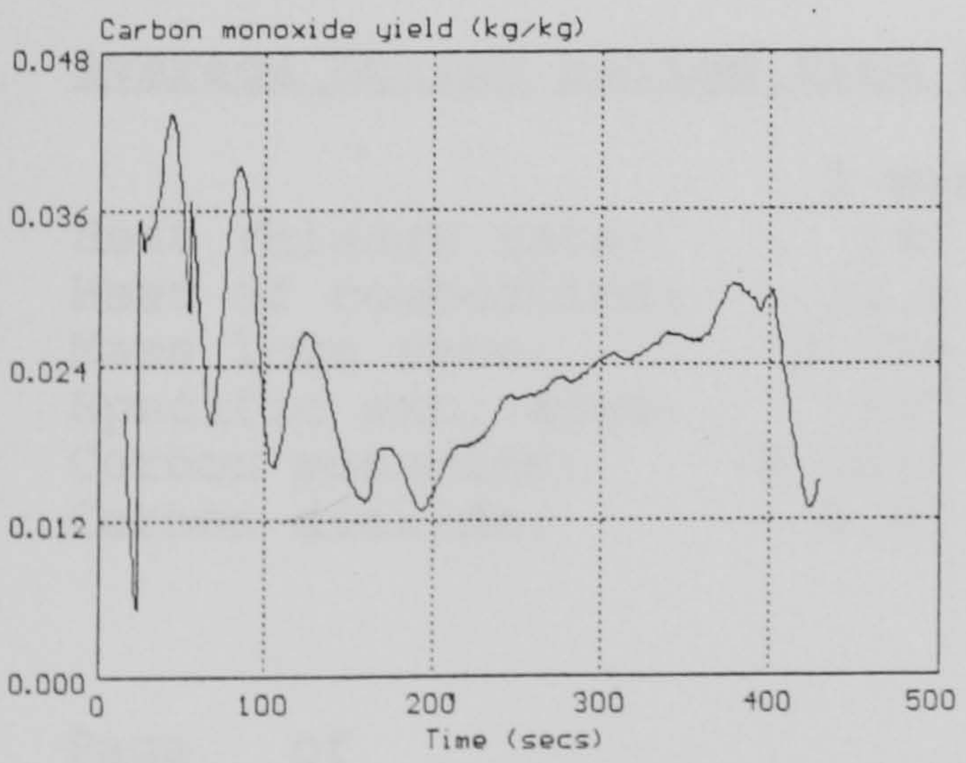

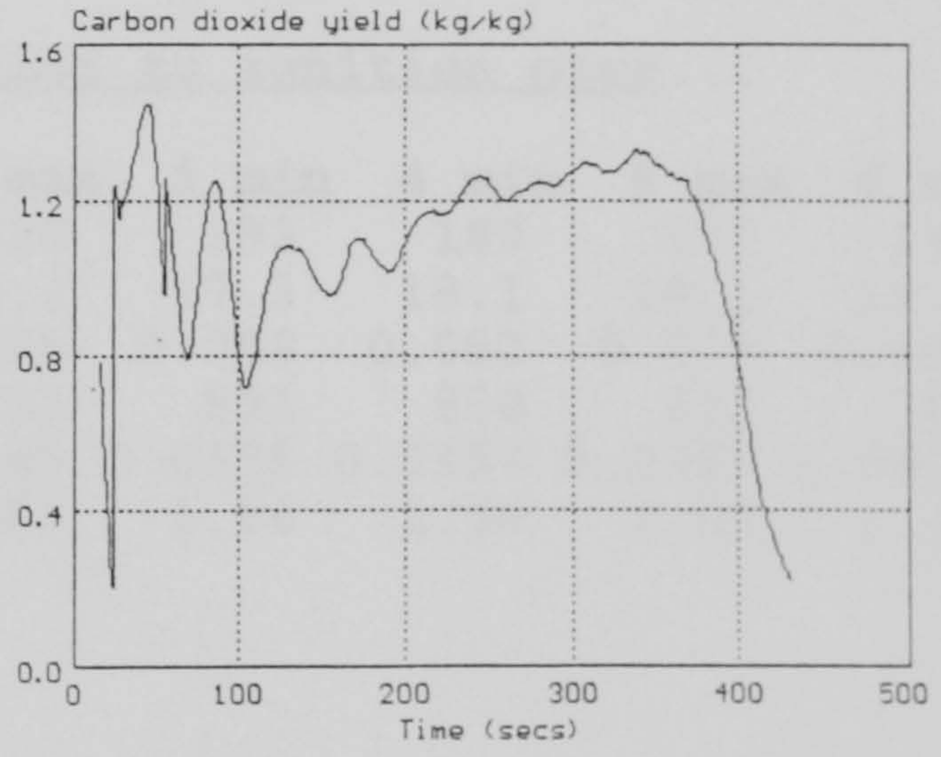

These results relate only to the behaviour of the material under the conditions of the test - they are not intended to be the sole criterion for the assessment of performance under real fire conditions.

CONE CALORIMETER SINGLE RUN DATA

Material name:	polyester
Sample description:	polye pm1
File name:	POLY8
Date of test:	June 20, 1995
Specimen thickness:	5.2 mm
Specimen initial mass:	102.6 g
Heat flux:	75 kW/m²
Exhaust duct flow rate:	0.024 m³/s (Nominal)
Orientation:	Horizontal
Time to ignition:	36 s
Flameout:	359 s
End of test:	357 s
Total heat evolved:	54.3 MJ/m²
Mass lost:	24.0 g

Observations:

Comment:

Peak and average values:	**Peak**		**Time(s)**	**Average**
Heat release rate:	228	kW/m²	76	164
Effective heat of combustion:	29.0	MJ/kg	278	19.2
Mass loss rate:	0.110	g/s	62	0.075
Specific extinction area:	1019	m²/kg	59	800
Carbon monoxide yield:	0.1289	kg/kg	345	0.0401
Carbon dioxide yield:	2.04	kg/kg	61	1.68

Average during period from ignition to ignition plus...

	1 min	**2 min**	**3 min**	**4 min**	**5 min**	**6 min**
Heat release rate:	145	180	193	189	172	149
Heat of combustion:	12.9	16.2	17.3	18.1	19.1	19.4
Mass loss rate:	0.098	0.098	0.098	0.092	0.079	0.068
Specific ext. area:	857	891	891	850	808	788
Carbon monoxide:	0.0340	0.0349	0.0355	0.0357	0.0385	0.0425
Carbon dioxide:	1.69	1.69	1.66	1.66	1.68	1.68

CONE CALORIMETER GRAPHICAL DATA

File name: POLY8
Material name: polyester
Irradiance: 75 kW/m^2
Orientation: Horizontal

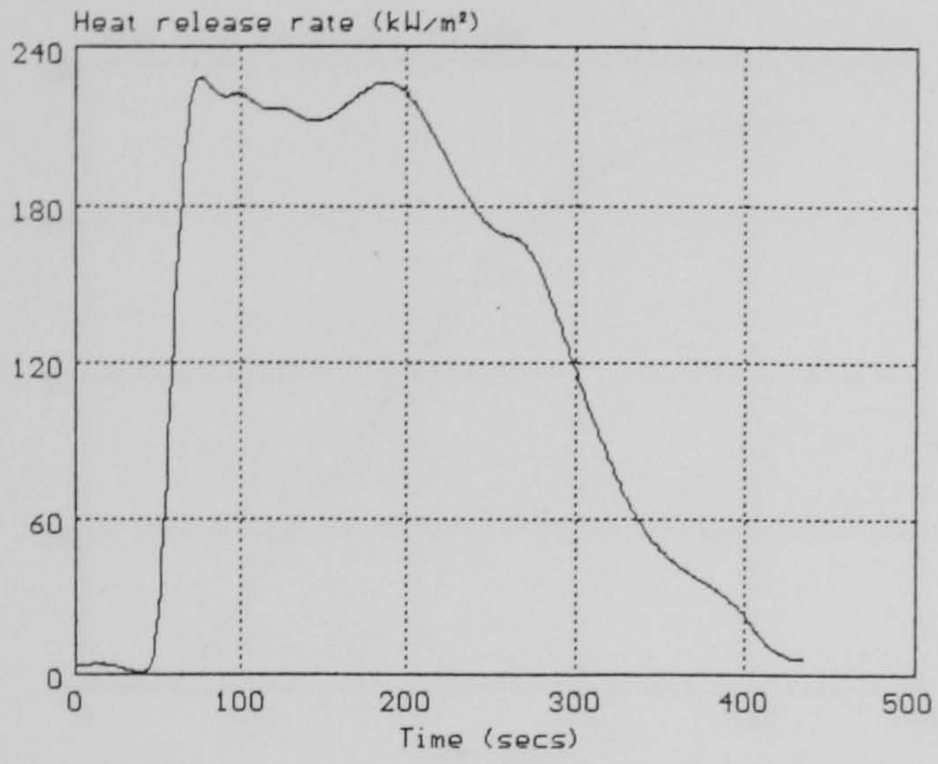

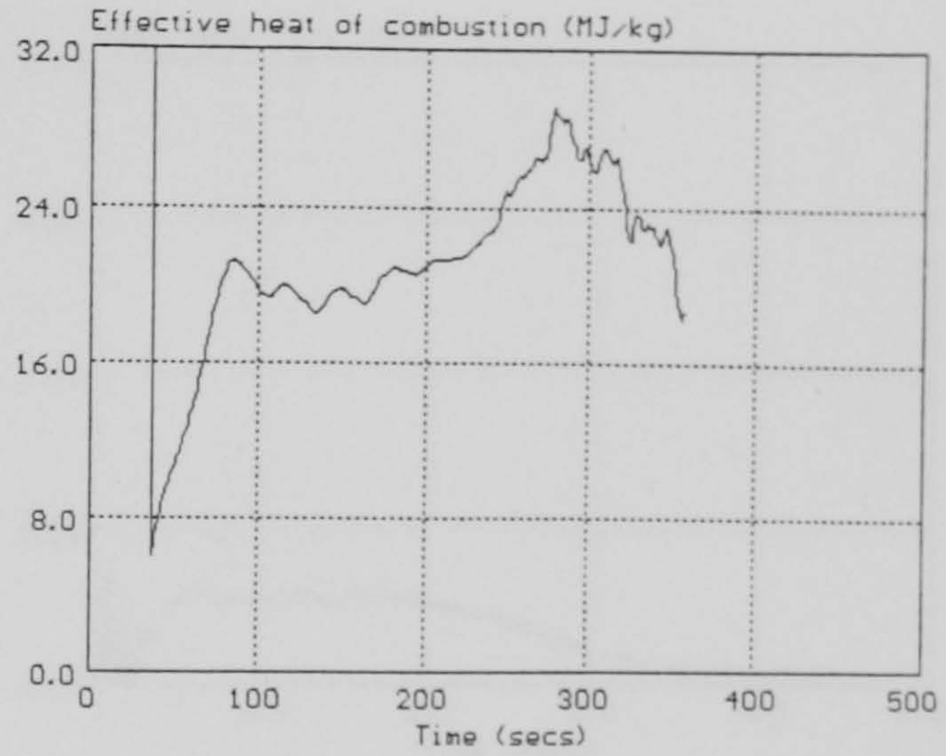

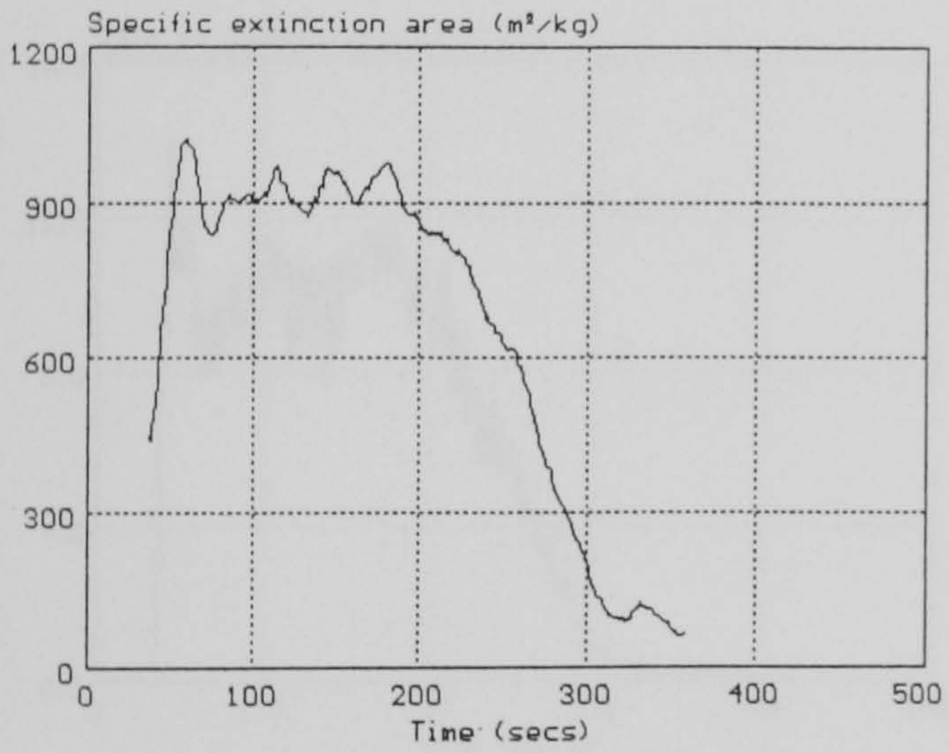

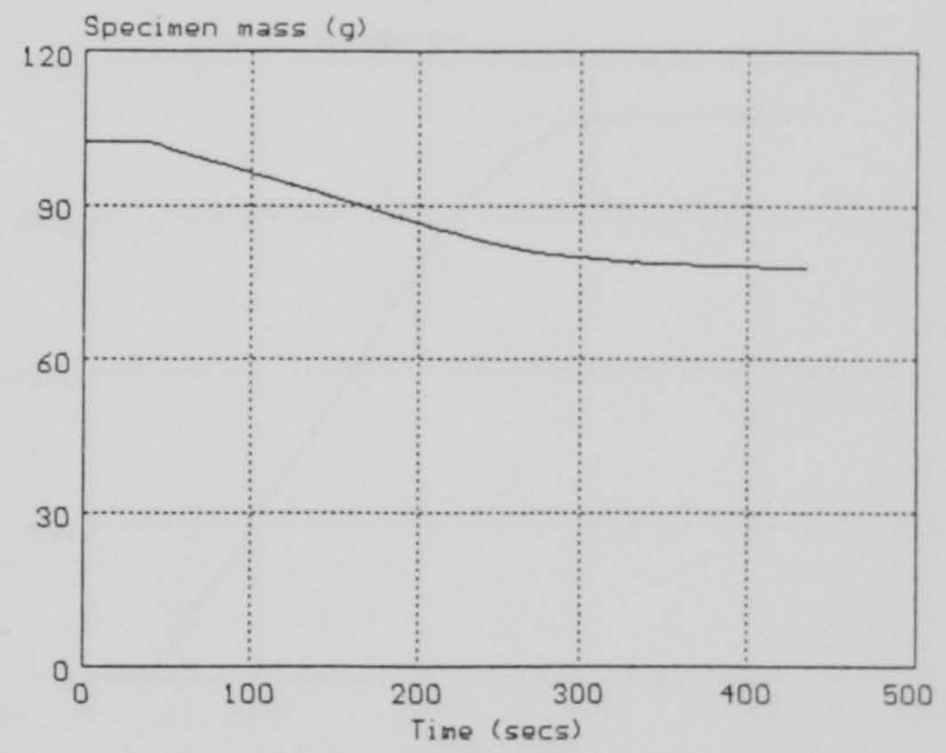

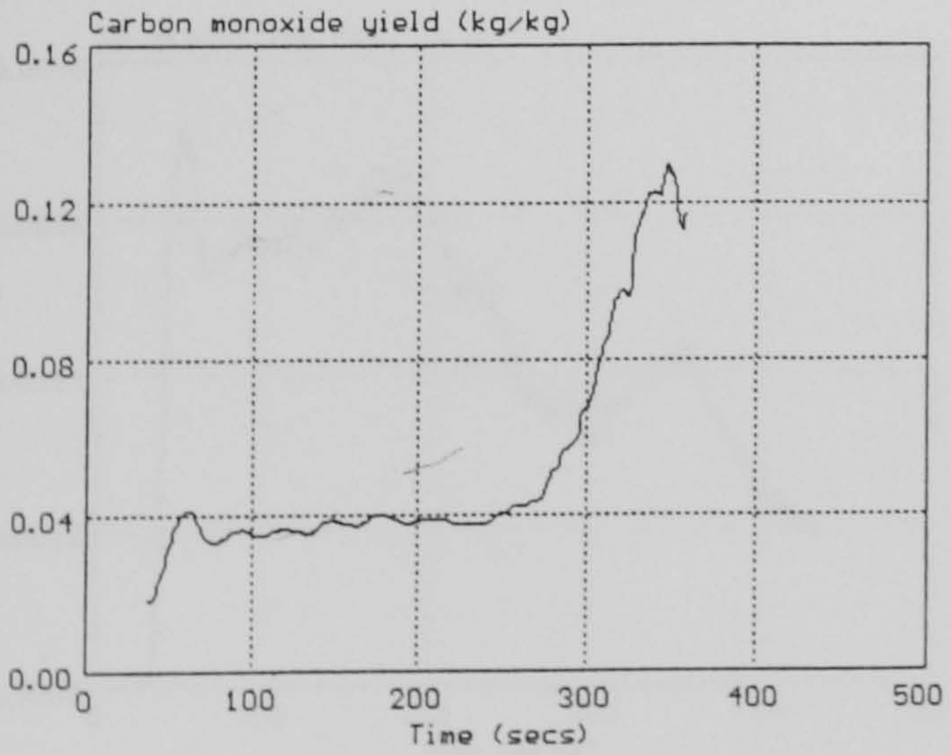

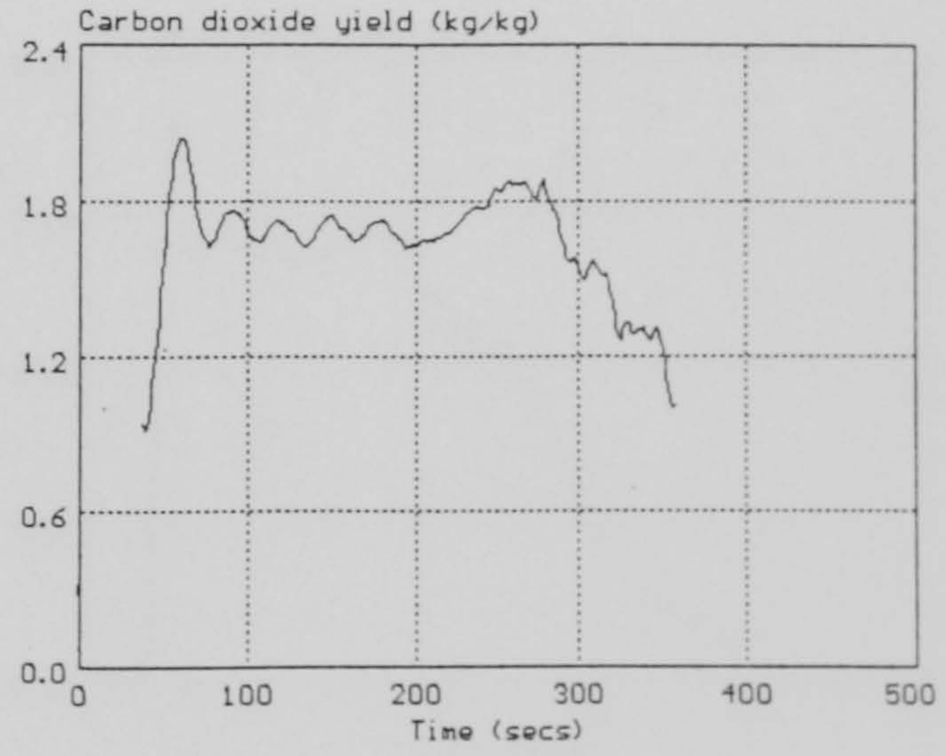

These results relate only to the behaviour of the material under the conditions of the test - they are not intended to be the sole criterion for the assessment of performance under real fire conditions.

CONE CALORIMETER GRAPHICAL DATA

File name: POLY8
Material name: polyester
Irradiance: 75 kW/m^2
Orientation: Horizontal

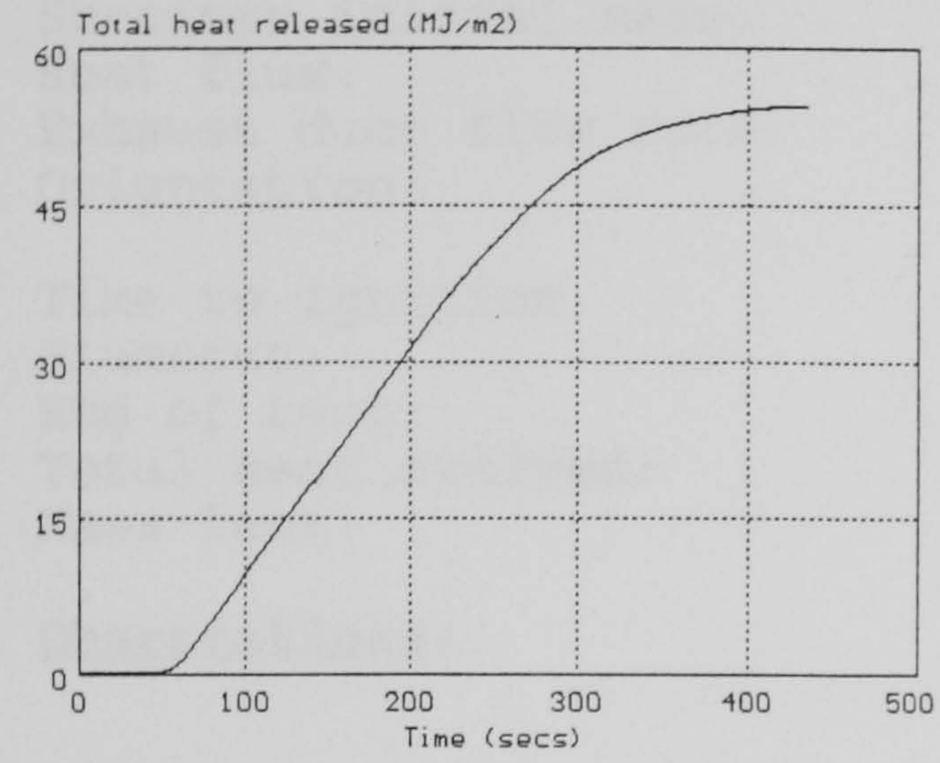

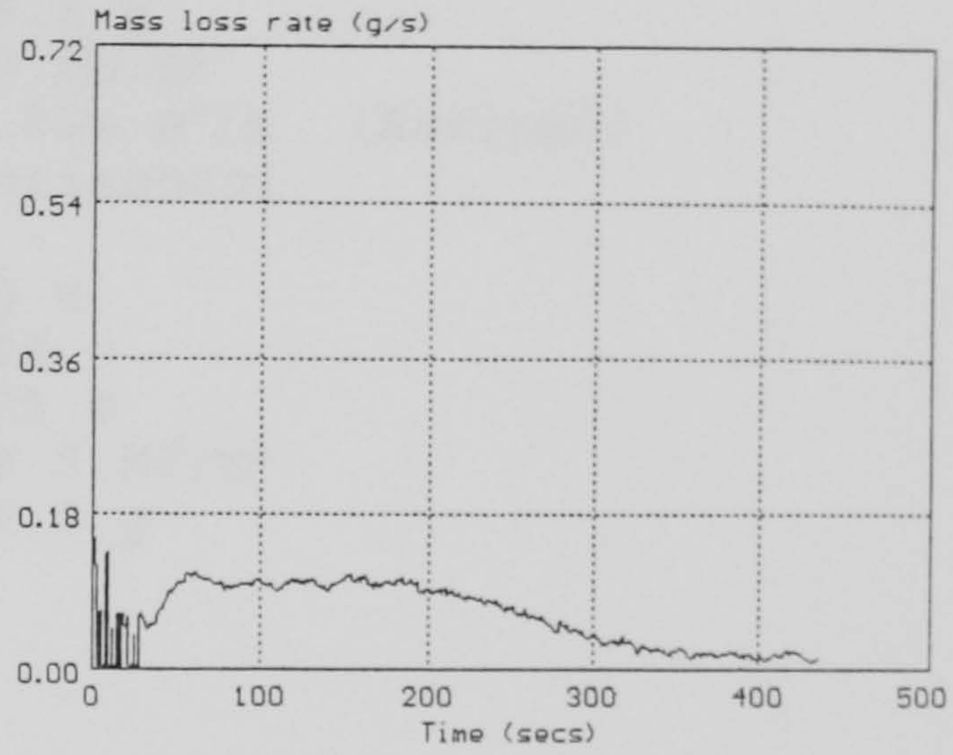

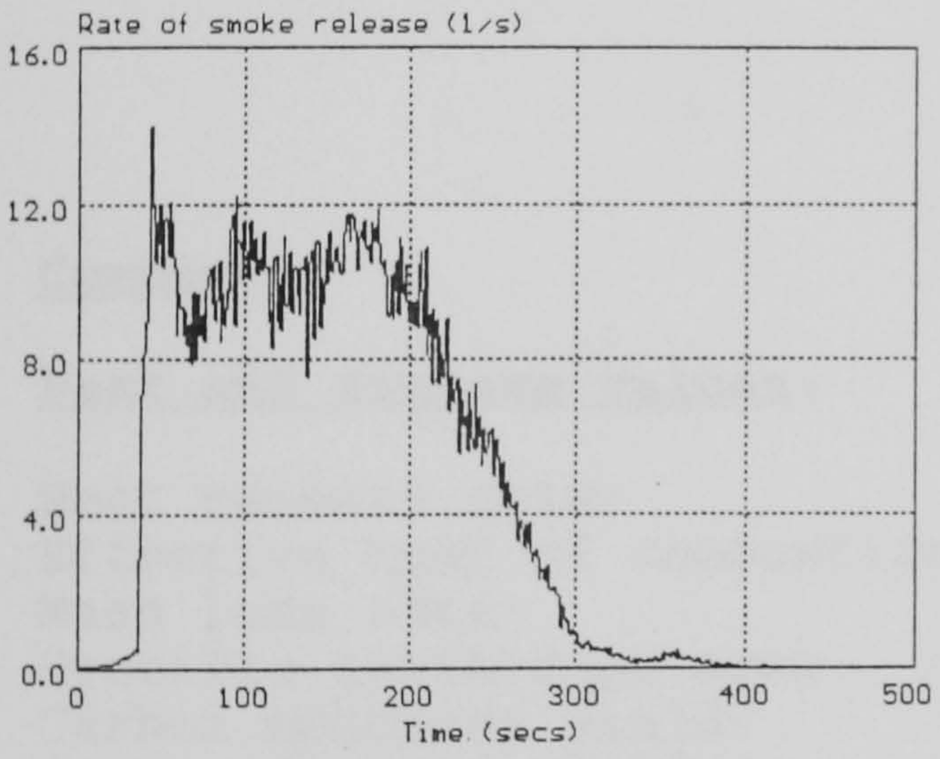

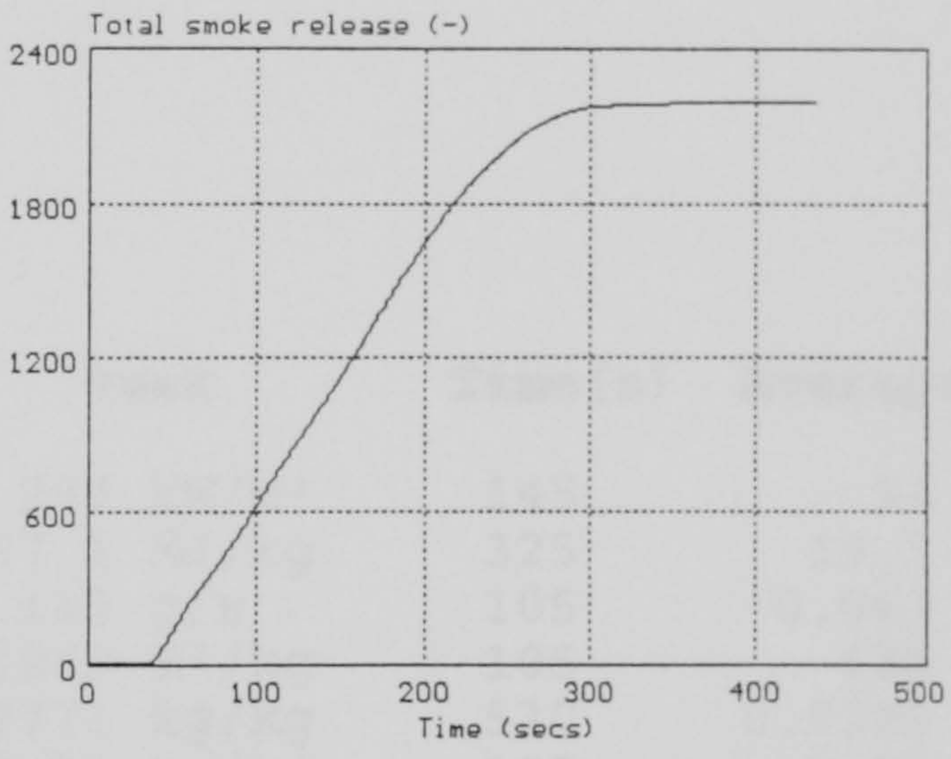

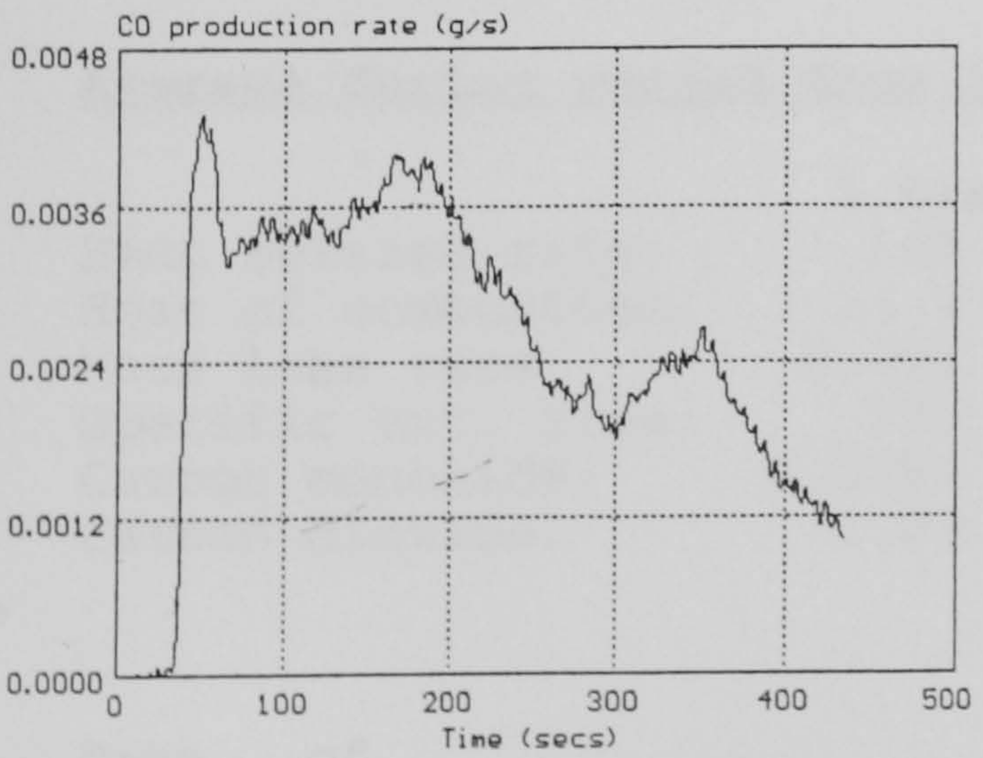

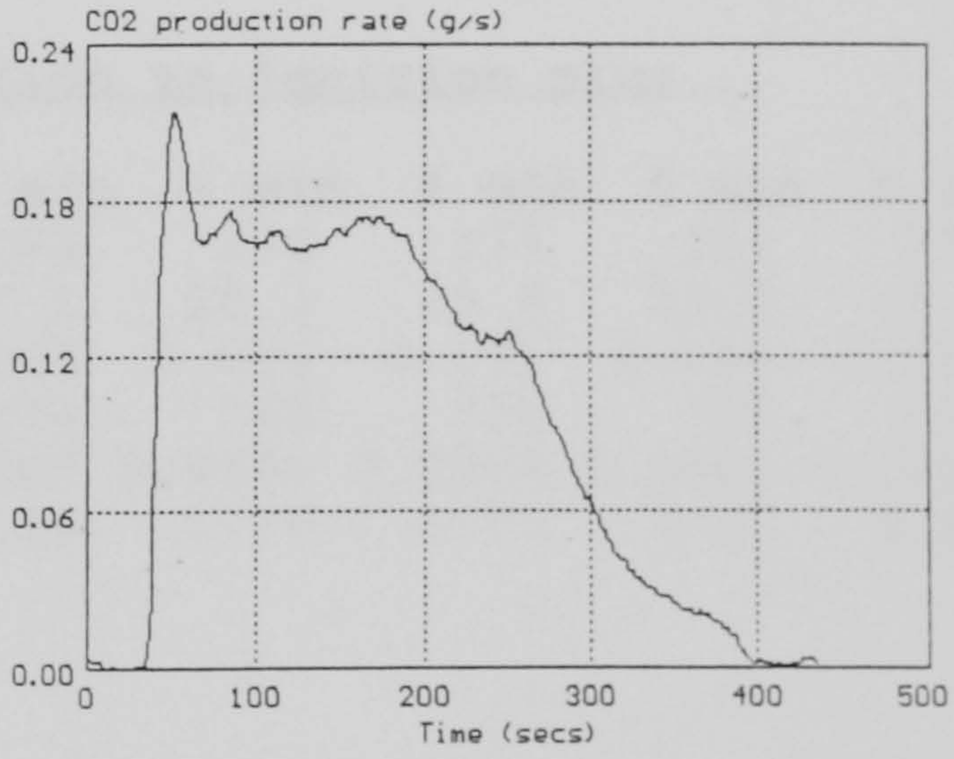

These results relate only to the behaviour of the material under the conditions of the test - they are not intended to be the sole criterion for the assessment of performance under real fire conditions.

CONE CALORIMETER SINGLE RUN DATA

Material name:	polyester	
Sample description:	polyester panel pm1	
File name:	POLY1	
Date of test:	June 16, 1995	
Specimen thickness:	5.0 mm	
Specimen initial mass:	99.5 g	
Heat flux:	50 kW/m²	
Exhaust duct flow rate:	0.024 m³/s	(Nominal)
Orientation:	Horizontal	
Time to ignition:	83 s	
Flameout:	605 s	
End of test:	605 s	
Total heat evolved:	49.0 MJ/m²	
Mass lost:	22.3 g	

Observations:

Comment:

Peak and average values:	**Peak**		**Time(s)**	**Average**
Heat release rate:	208	kW/m²	145	94
Effective heat of combustion:	37.1	MJ/kg	325	19.3
Mass loss rate:	0.113	g/s	105	0.043
Specific extinction area:	1049	m²/kg	105	628
Carbon monoxide yield:	0.0771	kg/kg	530	0.0326
Carbon dioxide yield:	2.28	kg/kg	105	1.58

Average during period from ignition to ignition plus...

	1 min	**2 min**	**3 min**	**4 min**	**5 min**	**6 min**
Heat release rate:	145	172	178	175	154	132
Heat of combustion:	13.9	17.1	18.3	19.4	20.0	19.8
Mass loss rate:	0.092	0.088	0.086	0.079	0.068	0.059
Specific ext. area:	773	774	768	751	708	678
Carbon monoxide:	0.0283	0.0287	0.0296	0.0295	0.0301	0.0309
Carbon dioxide:	1.67	1.69	1.70	1.71	1.69	1.65

CONE CALORIMETER GRAPHICAL DATA

File name: POLY1
Material name: polyester
Irradiance: 50 kW/m^2
Orientation: Horizontal

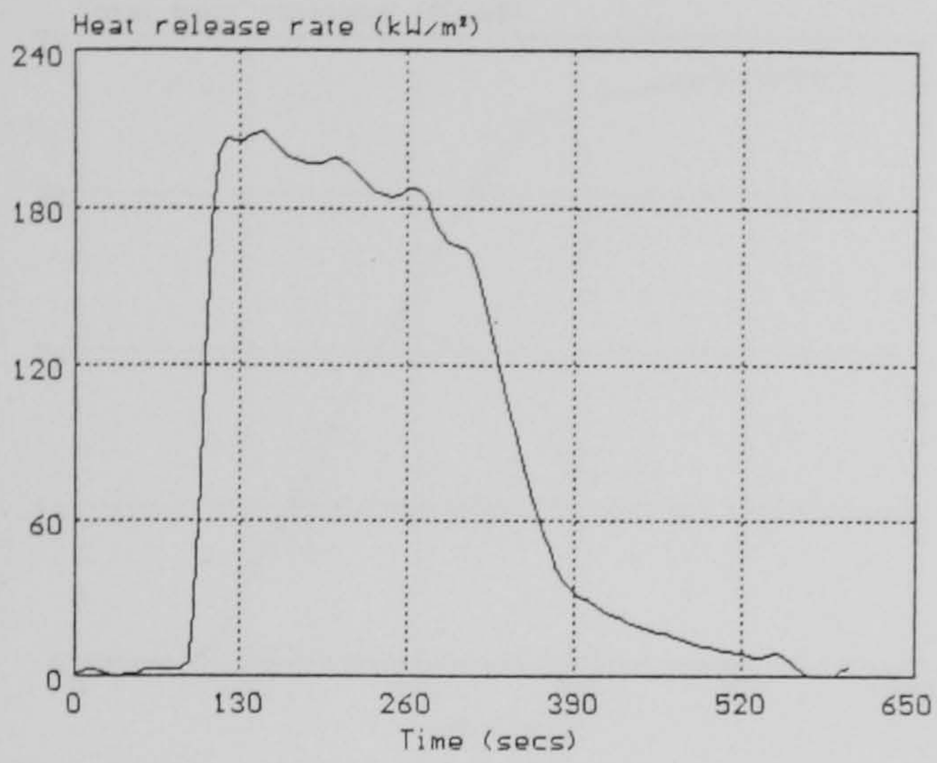

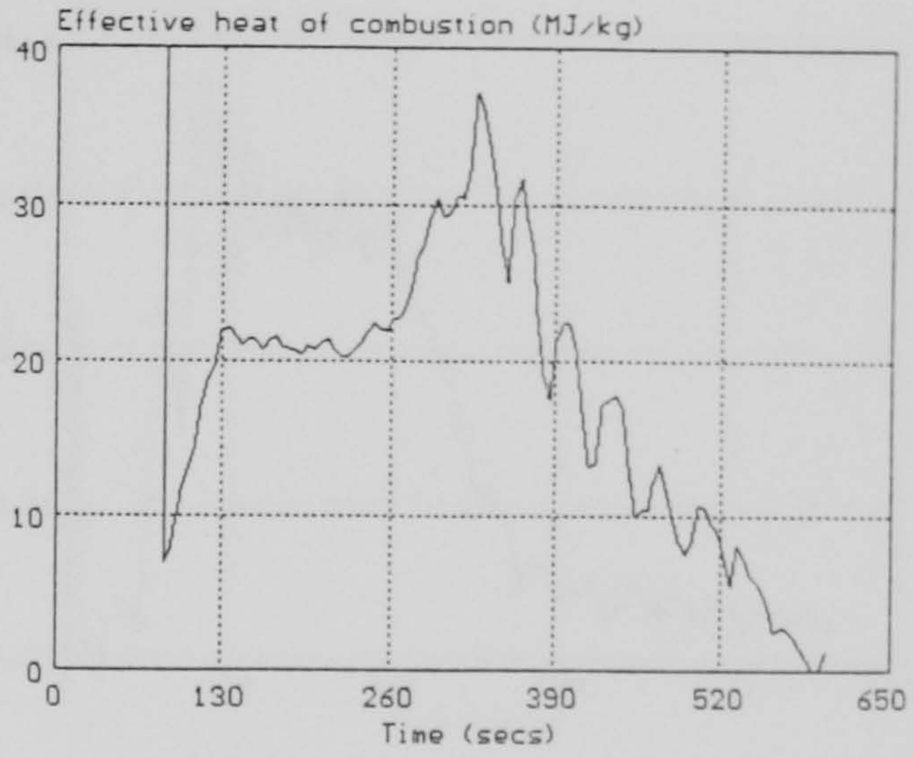

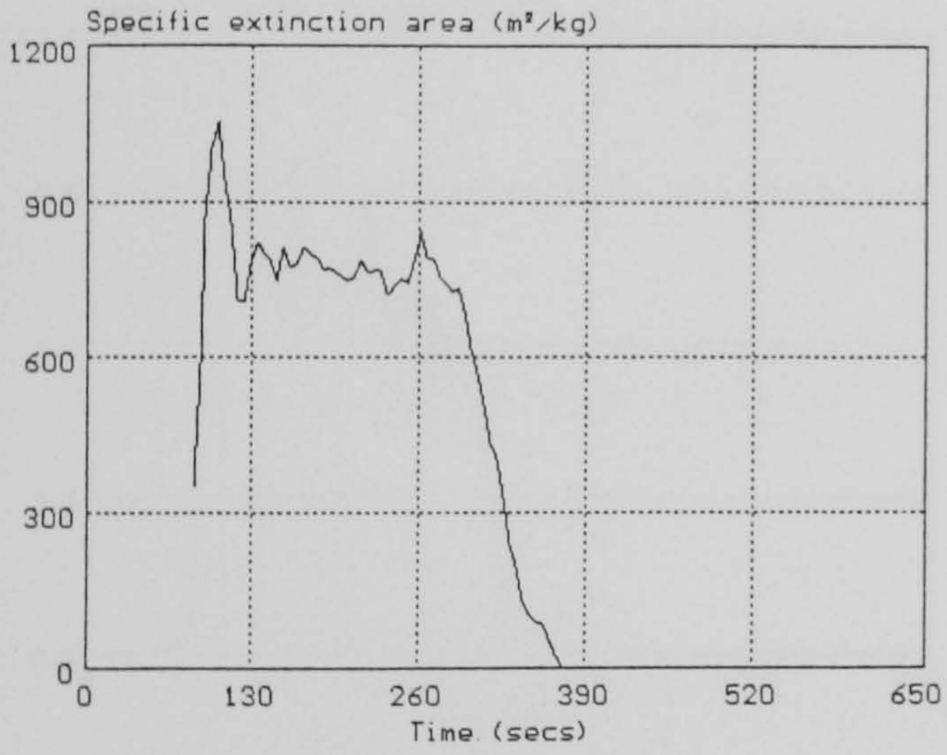

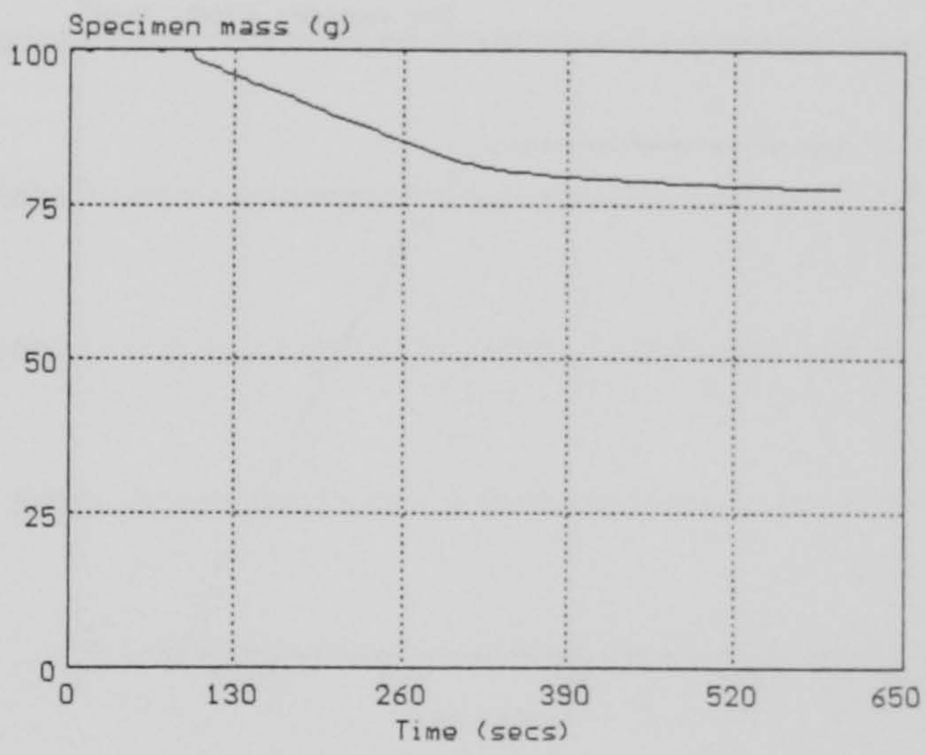

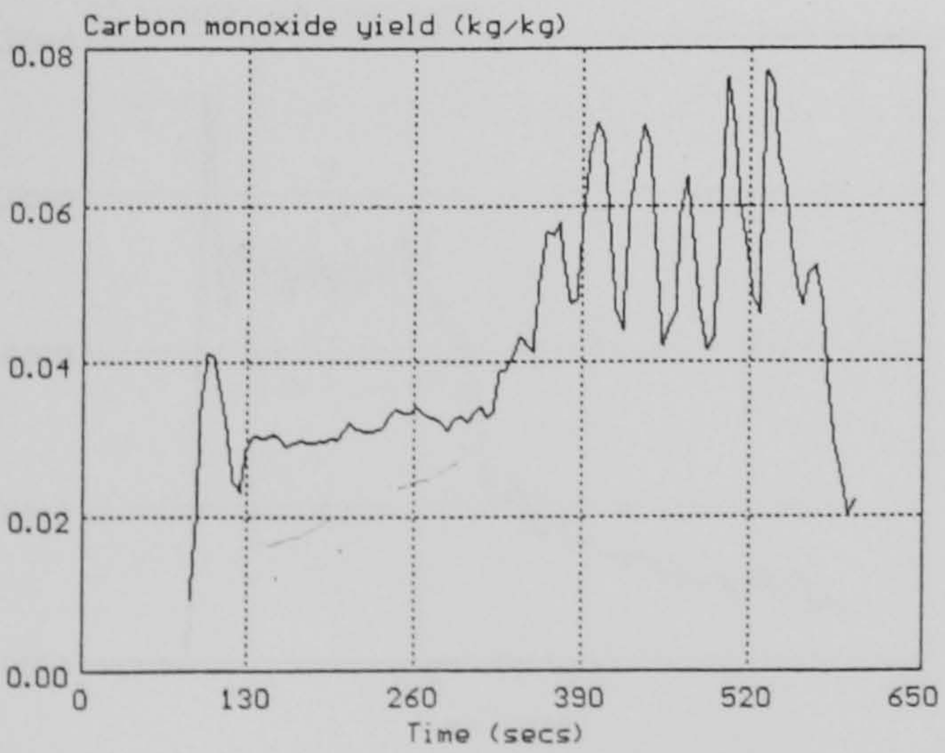

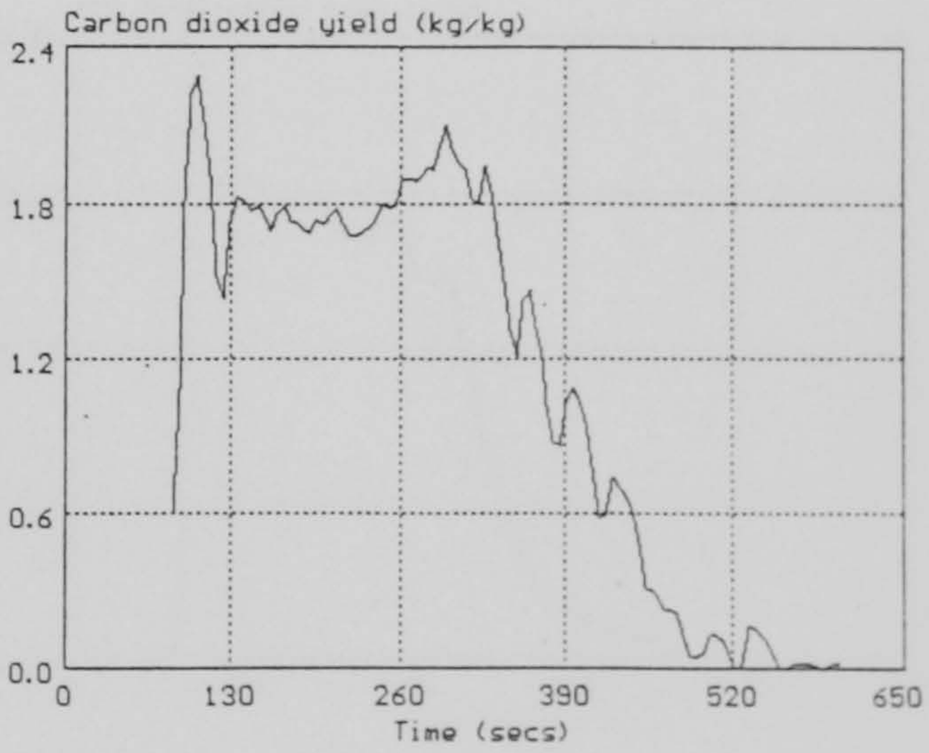

These results relate only to the behaviour of the material under the conditions of the test - they are not intended to be the sole criterion for the assessment of performance under real fire conditions.

CONE CALORIMETER GRAPHICAL DATA

File name: POLY1
Material name: polyester
Irradiance: 50 kW/m^2
Orientation: Horizontal

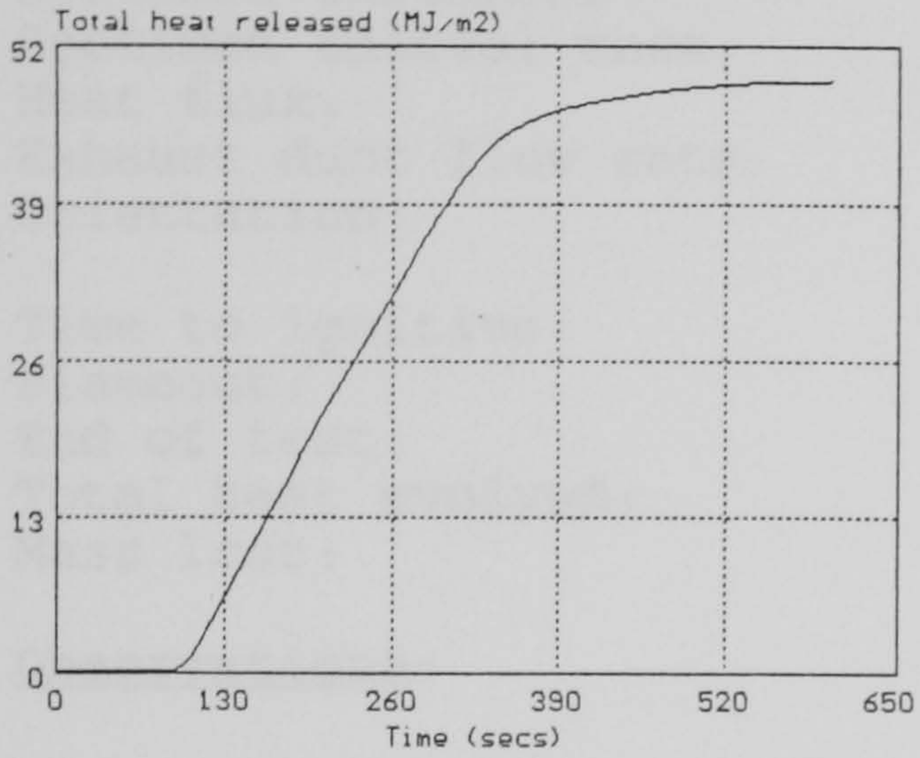

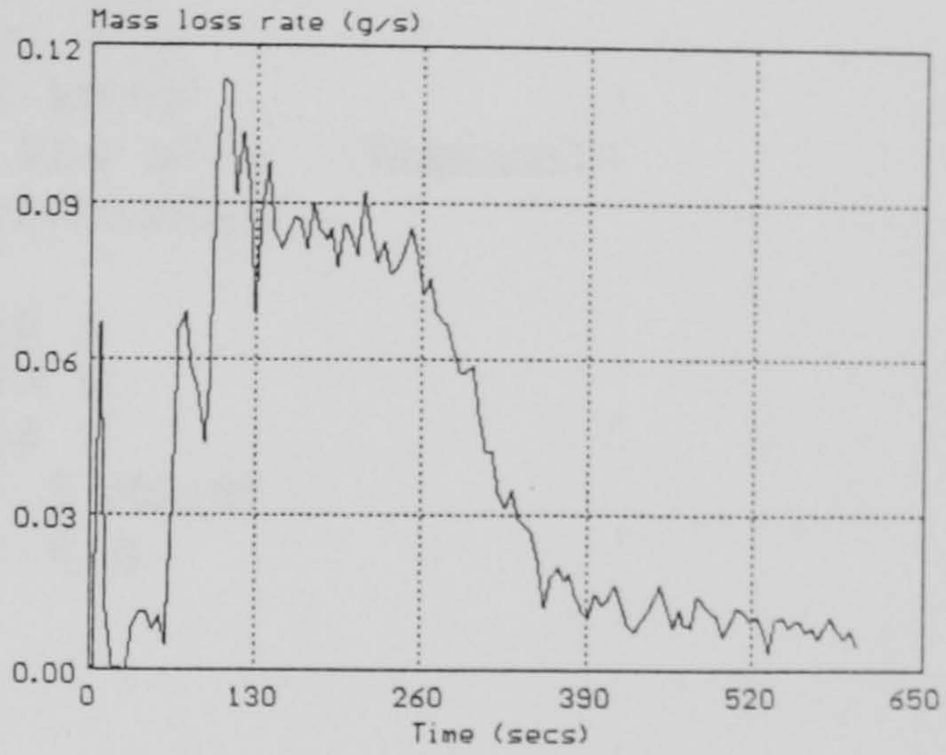

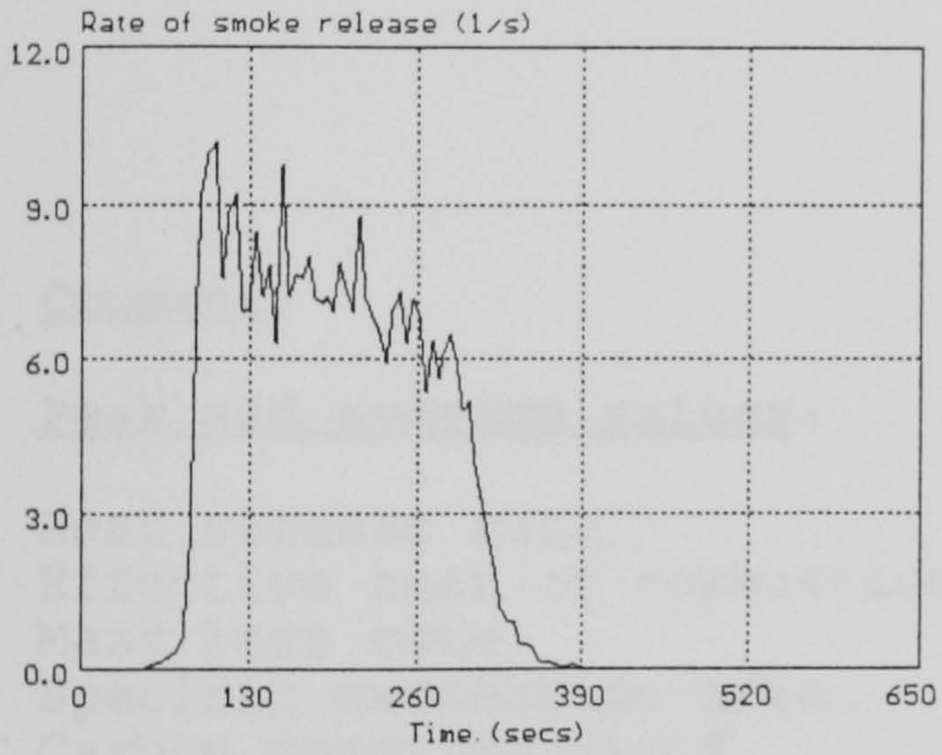

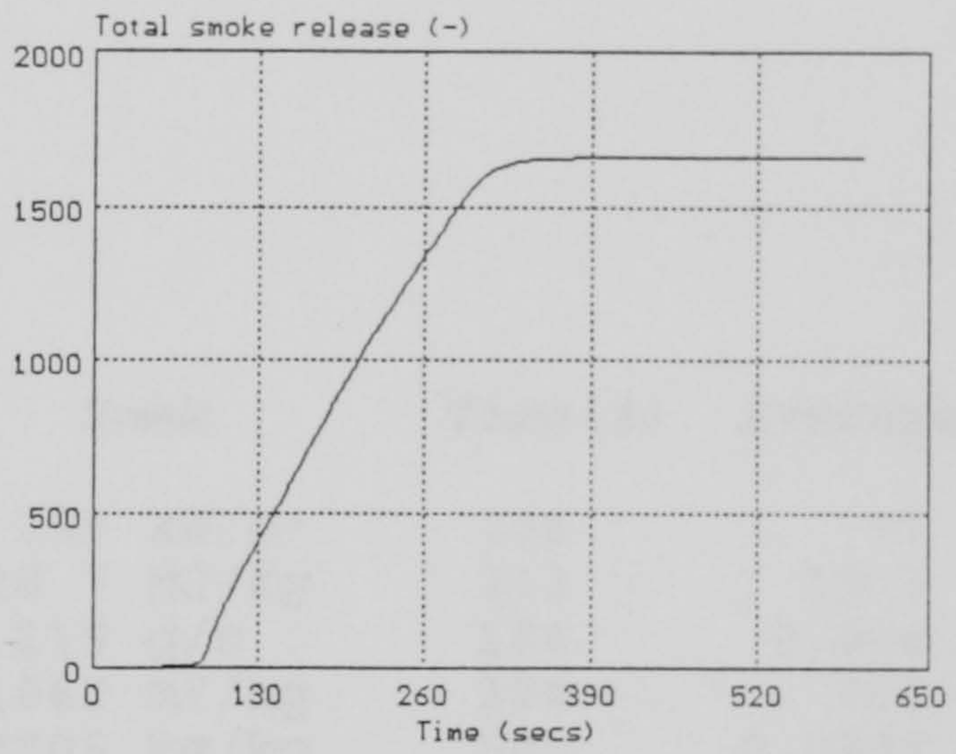

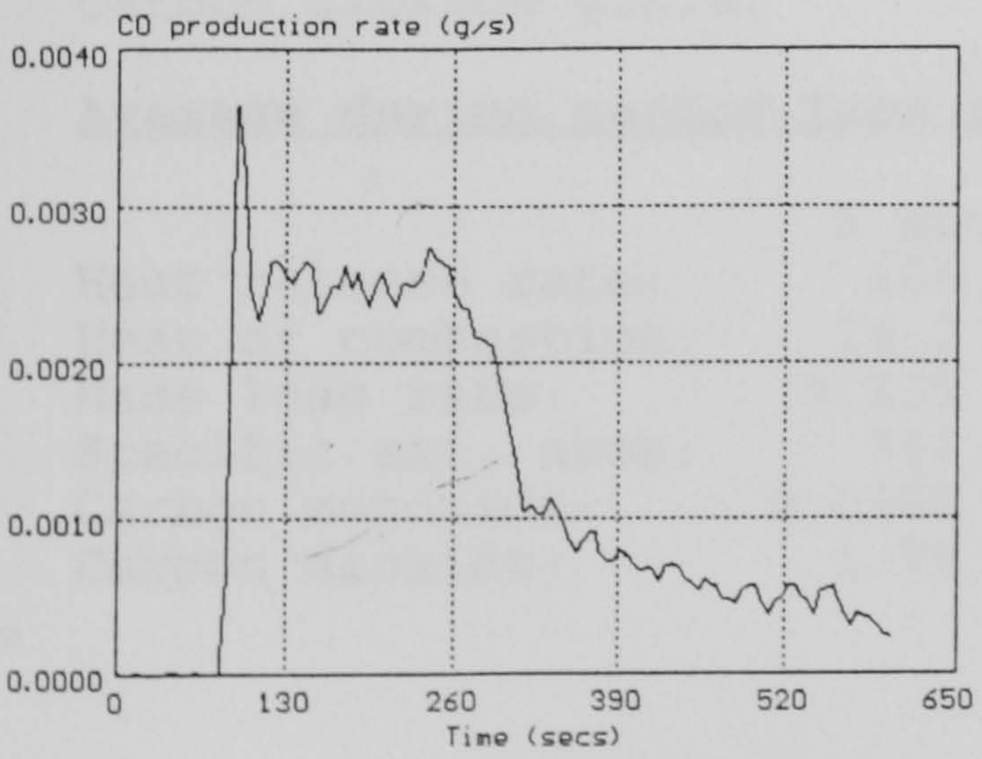

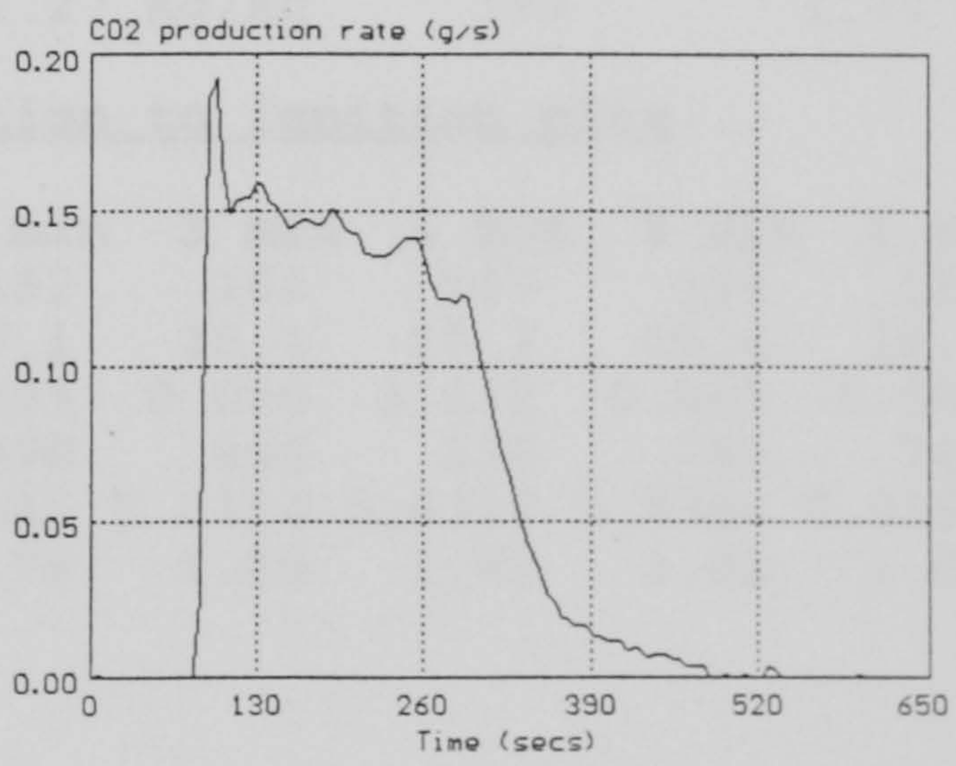

These results relate only to the behaviour of the material under the conditions of the test - they are not intended to be the sole criterion for the assessment of performance under real fire conditions.

CONE CALORIMETER SINGLE RUN DATA

Material name:	polyester
Sample description:	polye pm1
File name:	POLY6
Date of test:	June 20, 1995
Specimen thickness:	5.3 mm
Specimen initial mass:	101.5 g
Heat flux:	35 kW/m²
Exhaust duct flow rate:	0.024 m³/s (Nominal)
Orientation:	Horizontal
Time to ignition:	159 s
Flameout:	648 s
End of test:	648 s
Total heat evolved:	47.5 MJ/m²
Mass lost:	21.6 g

Observations:

Comment:

Peak and average values:	**Peak**		**Time(s)**	**Average**
Heat release rate:	295	kW/m²	206	97
Effective heat of combustion:	28.7	MJ/kg	213	19.3
Mass loss rate:	0.119	g/s	184	0.044
Specific extinction area:	1062	m²/kg	304	707
Carbon monoxide yield:	0.0805	kg/kg	500	0.0397
Carbon dioxide yield:	2.27	kg/kg	187	1.77

Average during period from ignition to ignition plus...

	1 min	**2 min**	**3 min**	**4 min**	**5 min**	**6 min**
Heat release rate:	166	162	164	157	144	129
Heat of combustion:	14.2	17.1	18.1	19.3	19.4	19.7
Mass loss rate:	0.103	0.083	0.080	0.072	0.065	0.058
Specific ext. area:	747	798	846	836	781	742
Carbon monoxide:	0.0368	0.0346	0.0354	0.0346	0.0344	0.0365
Carbon dioxide:	1.79	1.79	1.80	1.82	1.81	1.81

CONE CALORIMETER GRAPHICAL DATA

File name: POLY6
Material name: polyester
Irradiance: 35 kW/m^2
Orientation: Horizontal

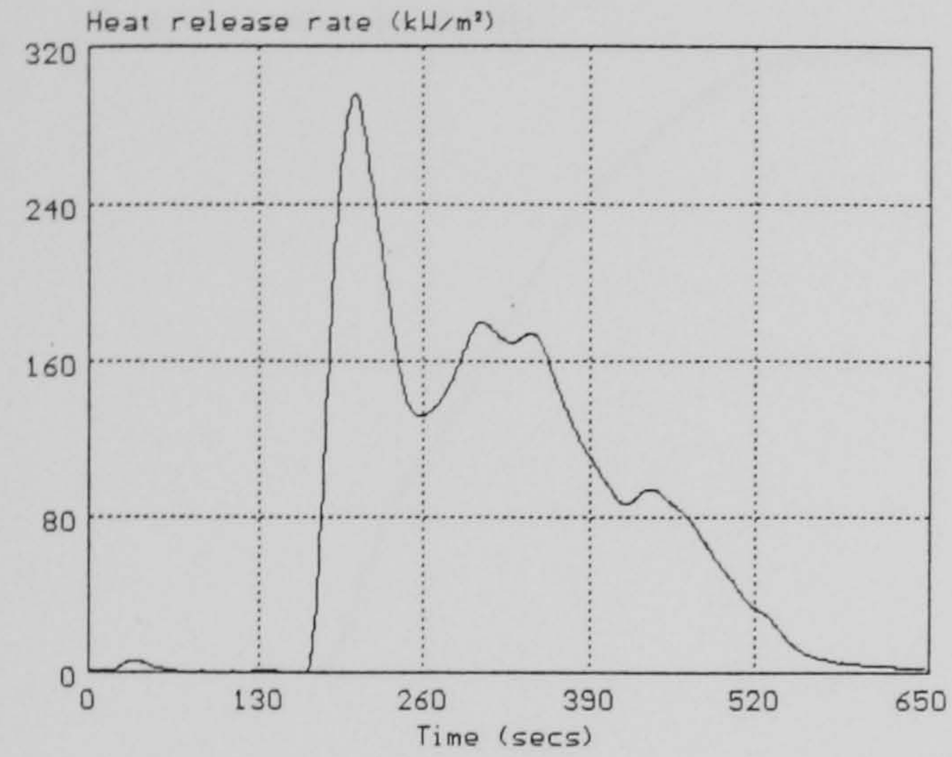

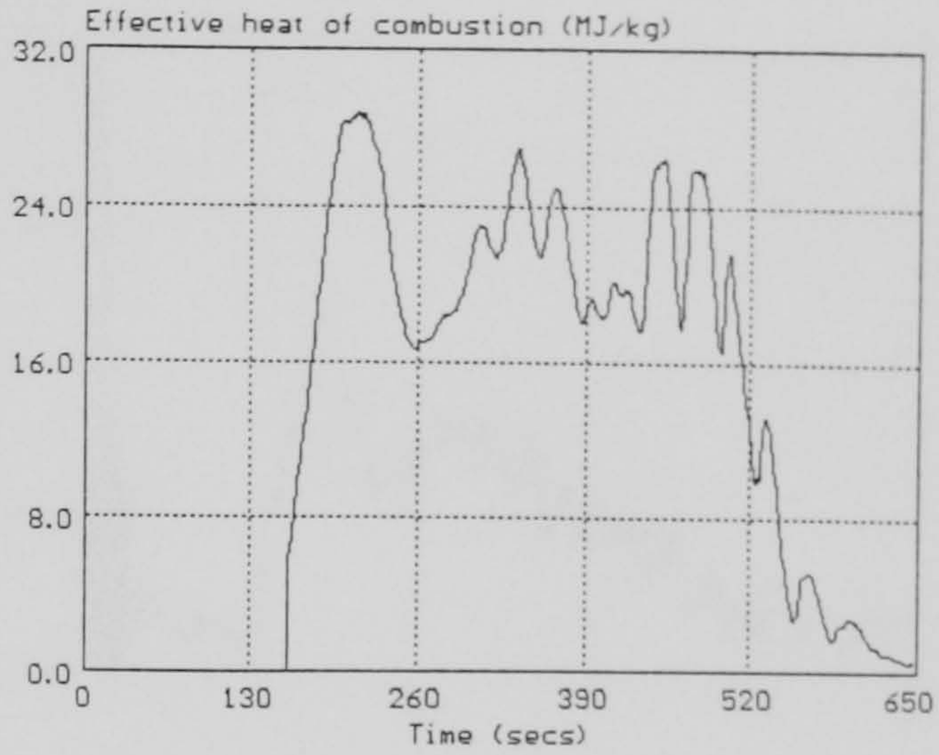

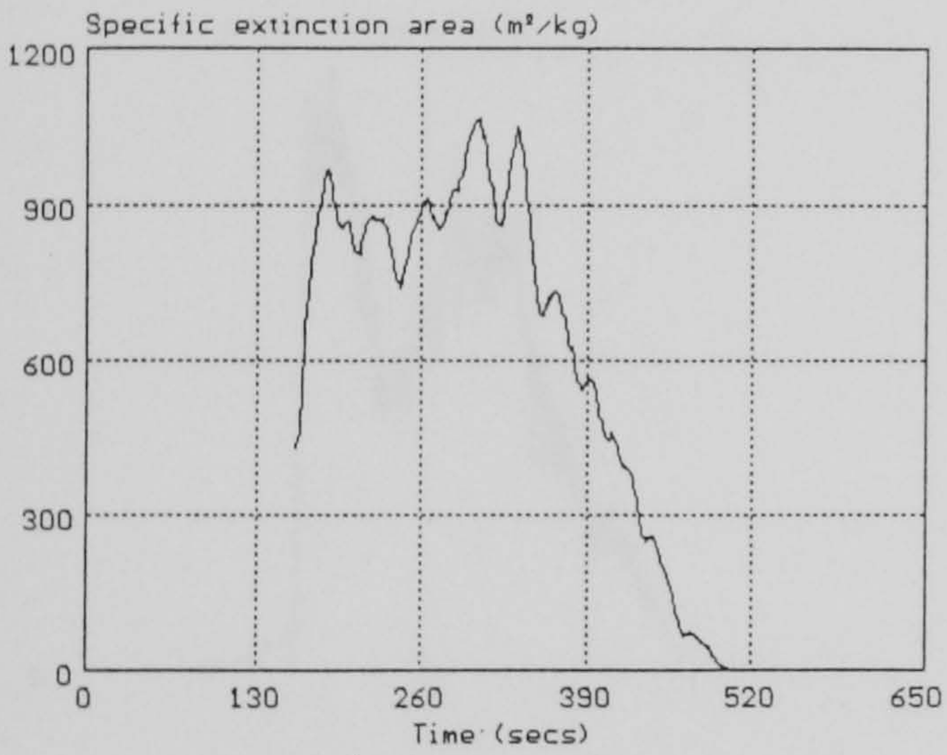

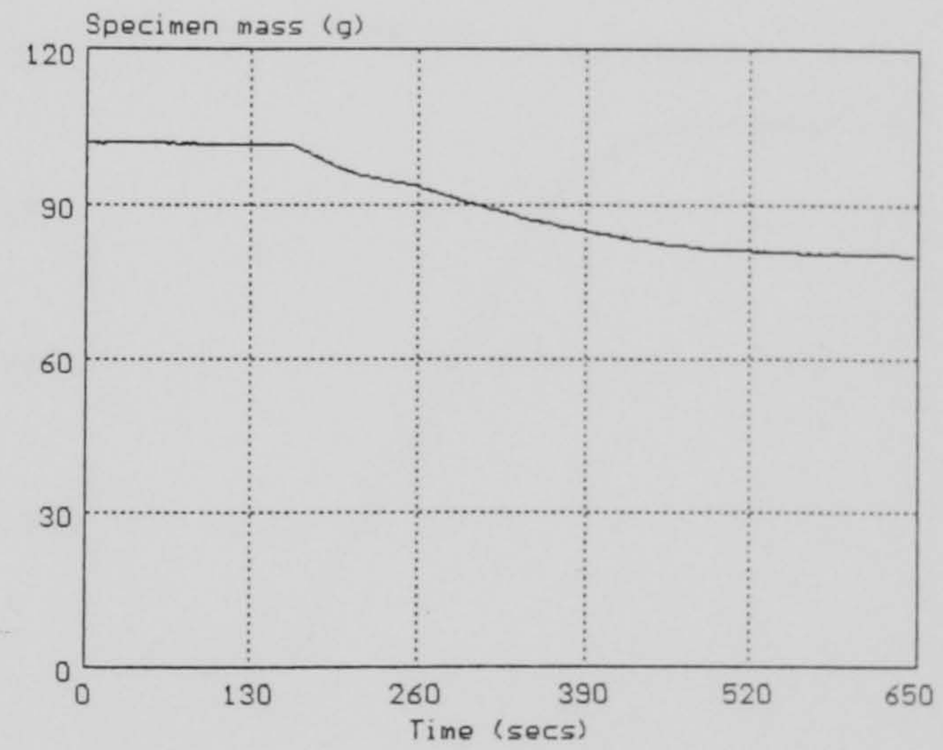

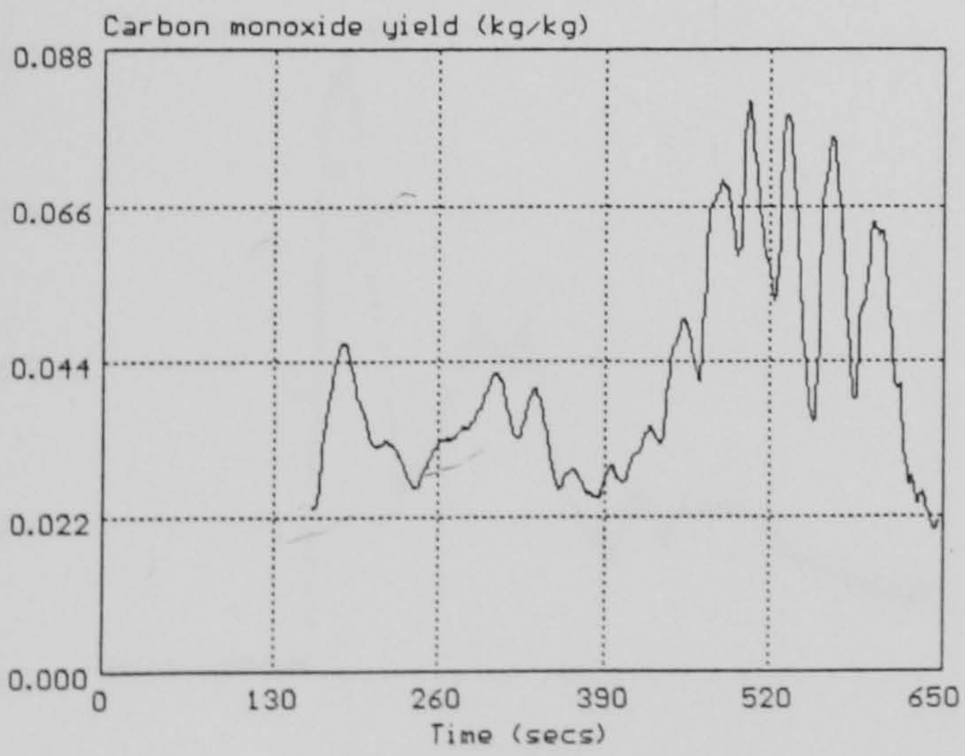

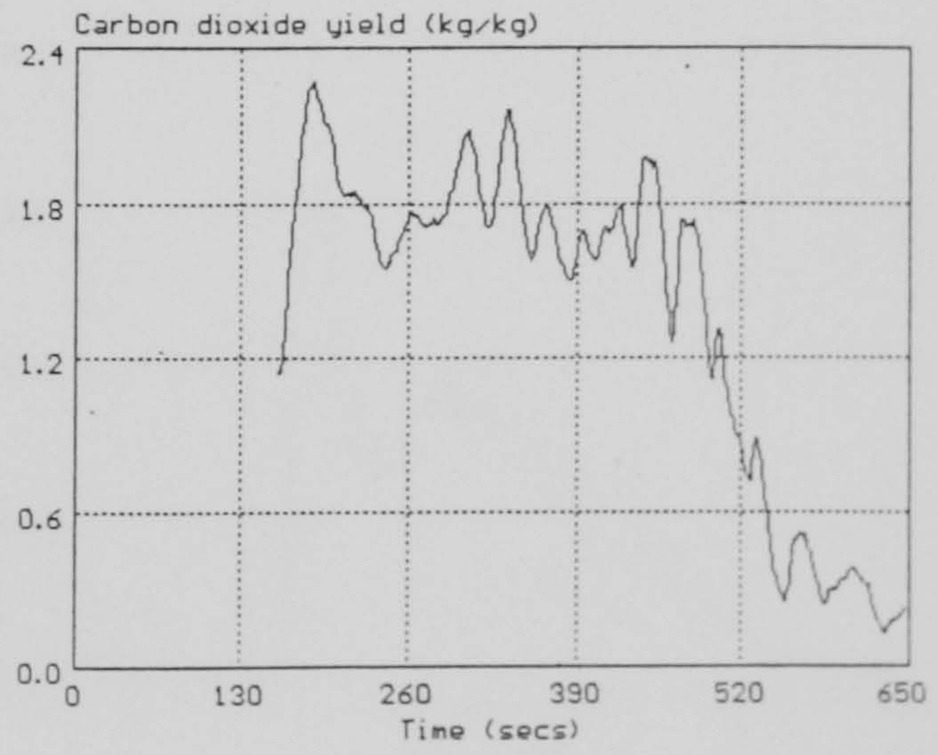

These results relate only to the behaviour of the material under the conditions of the test - they are not intended to be the sole criterion for the assessment of performance under real fire conditions.

CONE CALORIMETER GRAPHICAL DATA

File name: POLY6
Material name: polyester
Irradiance: 35 kW/m^2
Orientation: Horizontal

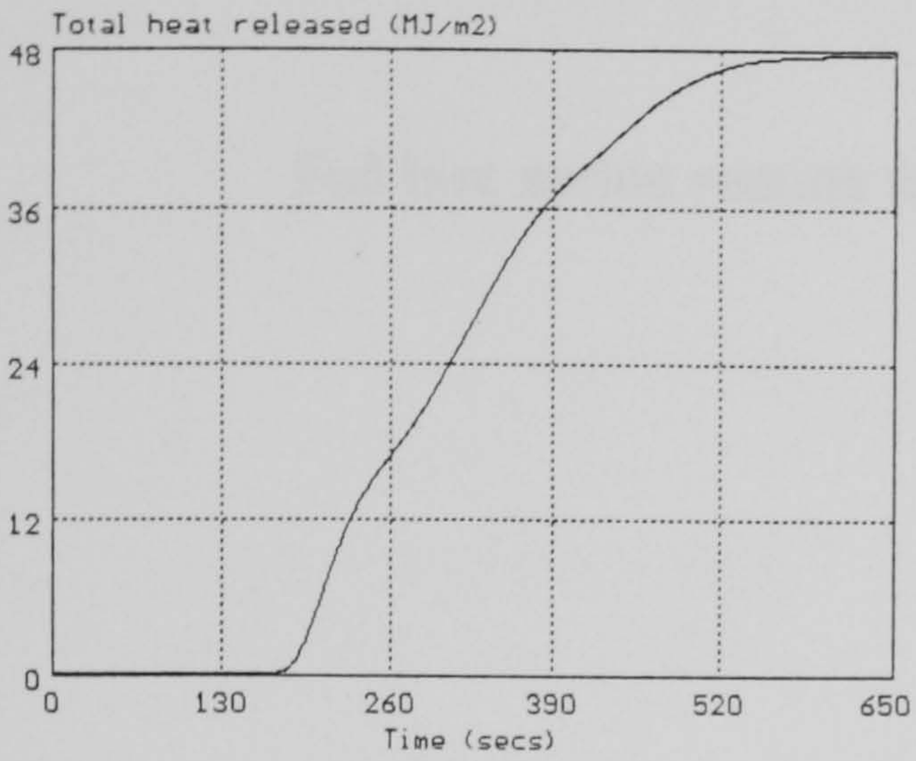

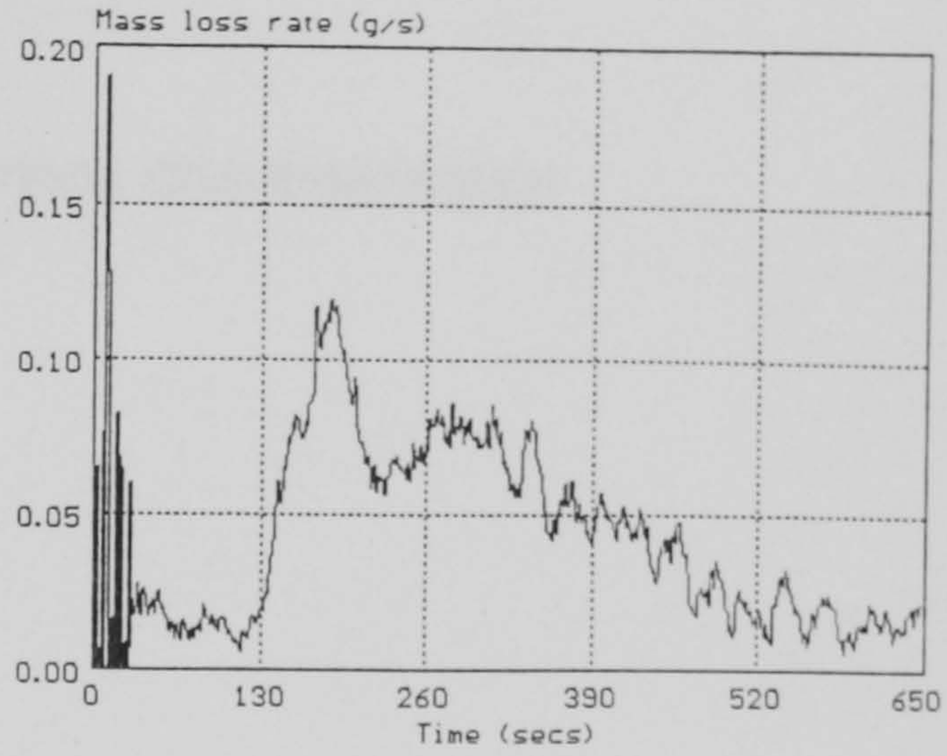

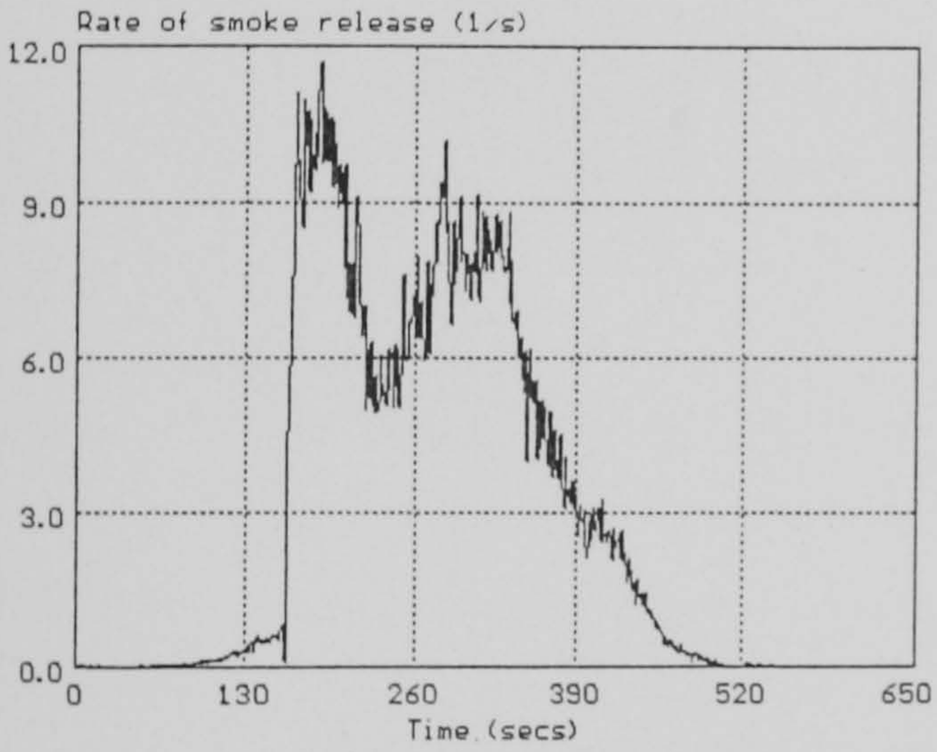

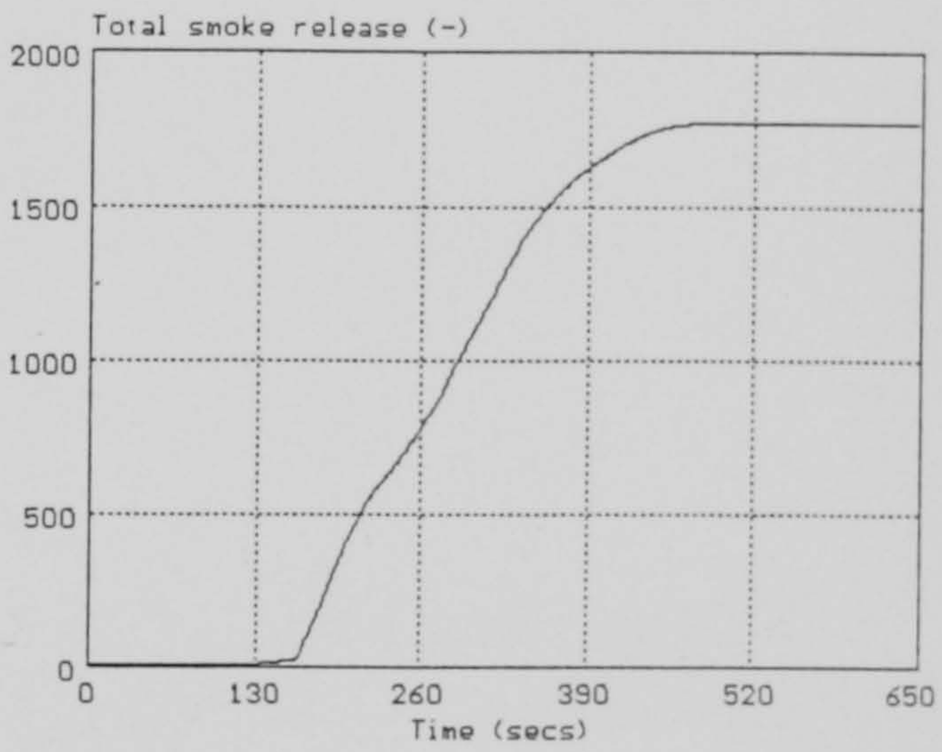

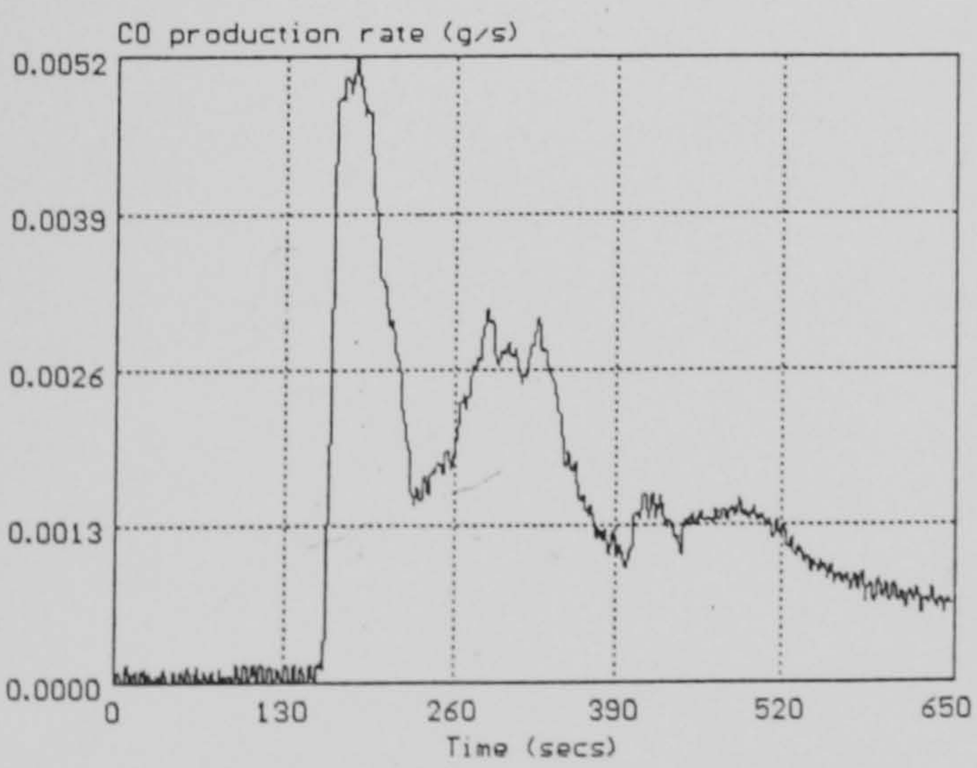

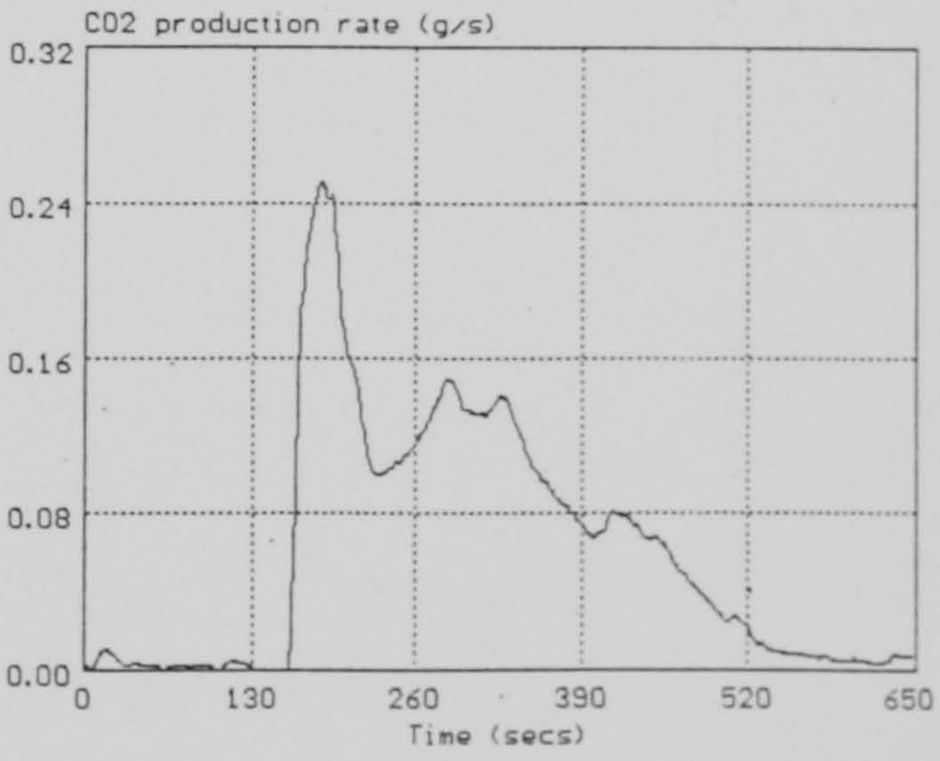

These results relate only to the behaviour of the material under the conditions of the test - they are not intended to be the sole criterion for the assessment of performance under real fire conditions.

APPENDIX D

Full test series results for furnace characterisation

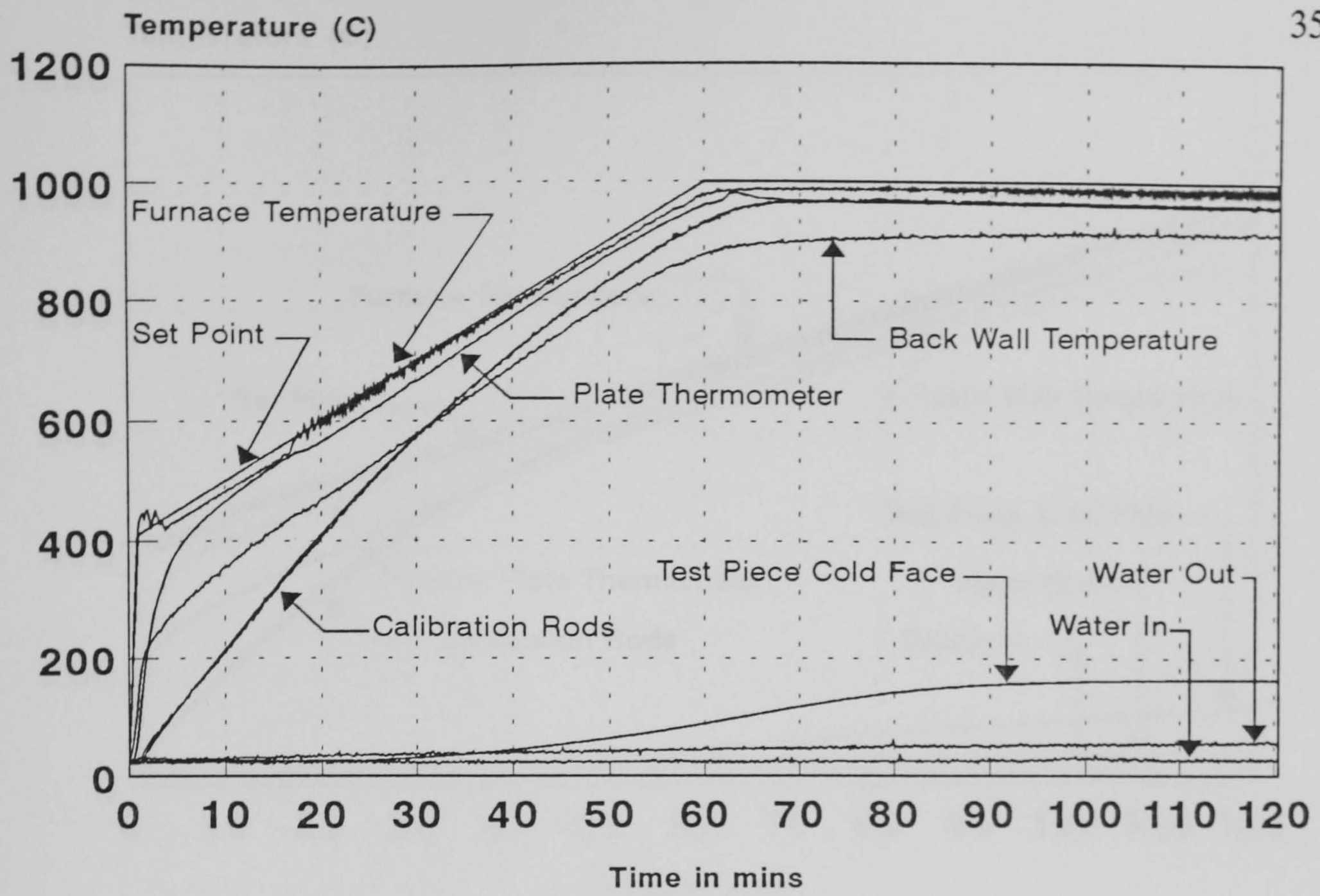

Furnace Characterisation - Test 1
R Type Control, PT Monitor
All Thermocouples 20-06-1995

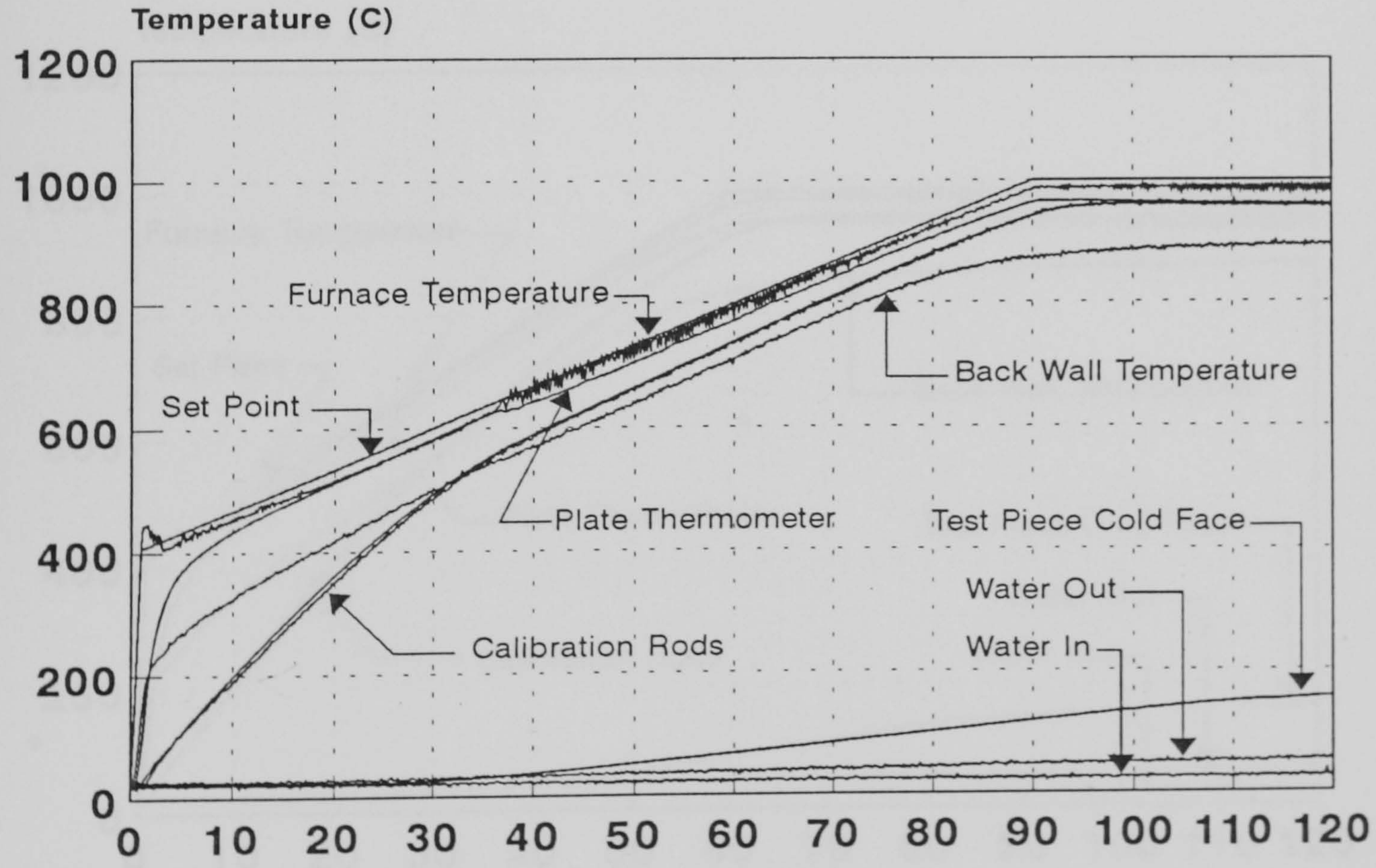

Furnace Characterisation - Test 2
R Type Control, PT Monitor
All Thermocouples 22-06-1995

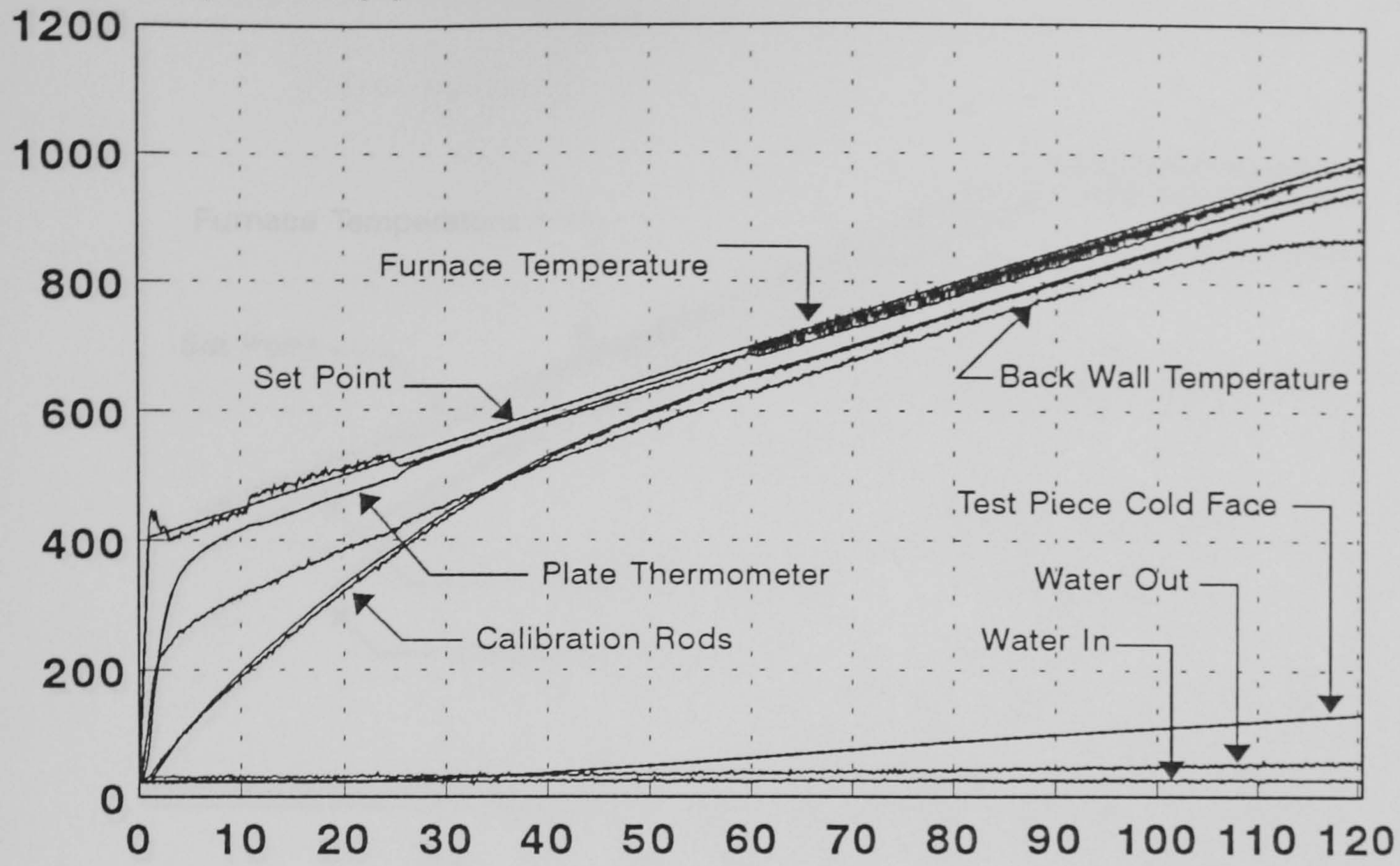

Furnace Characterisation - Test 3
R Type control, PT monitor
All Thermocouples 23-06-1995

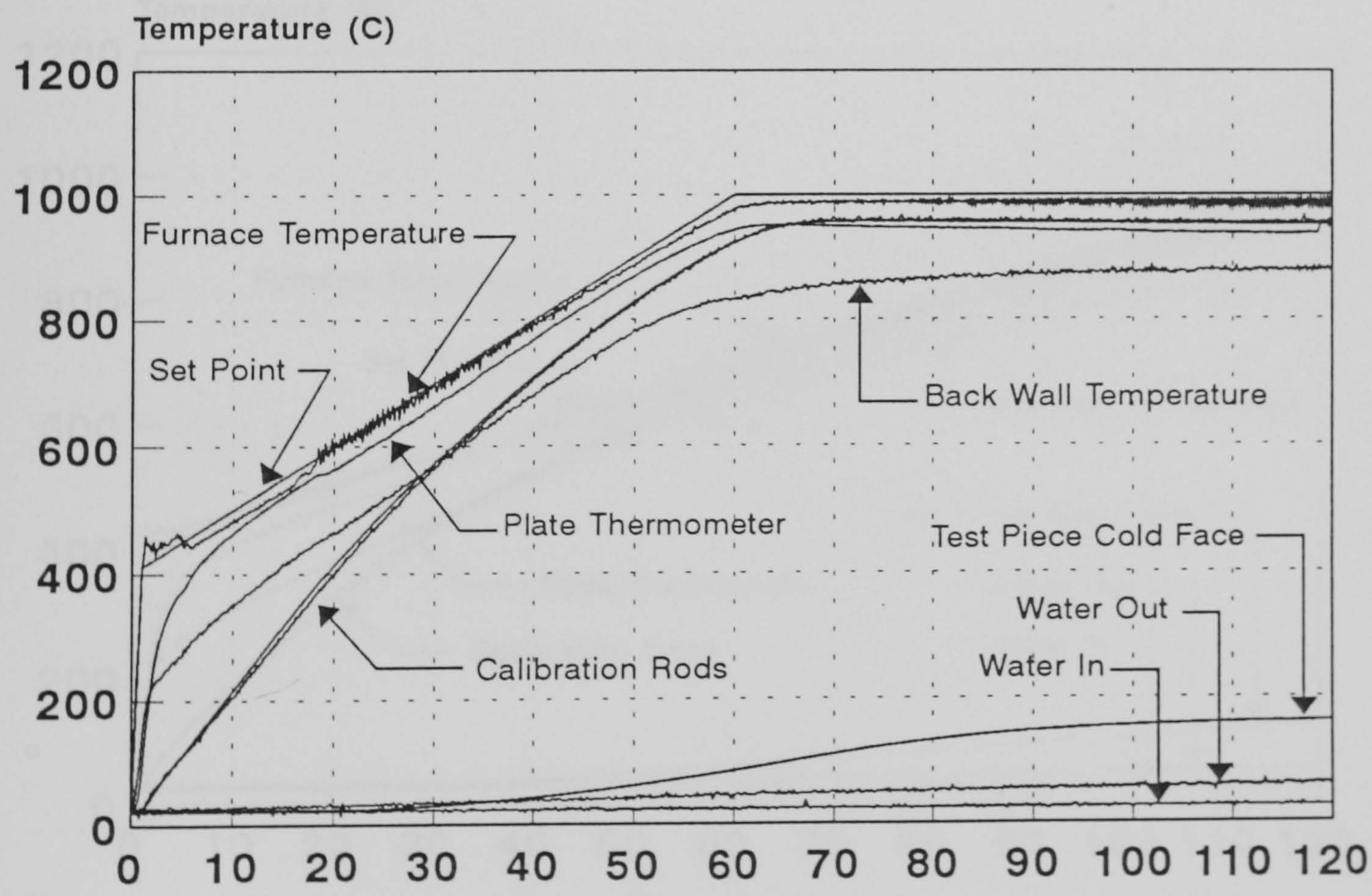

Furnace Characterisation - Test 4
R Type Control, PT Monitor
All Thermocouples, 26-06-95

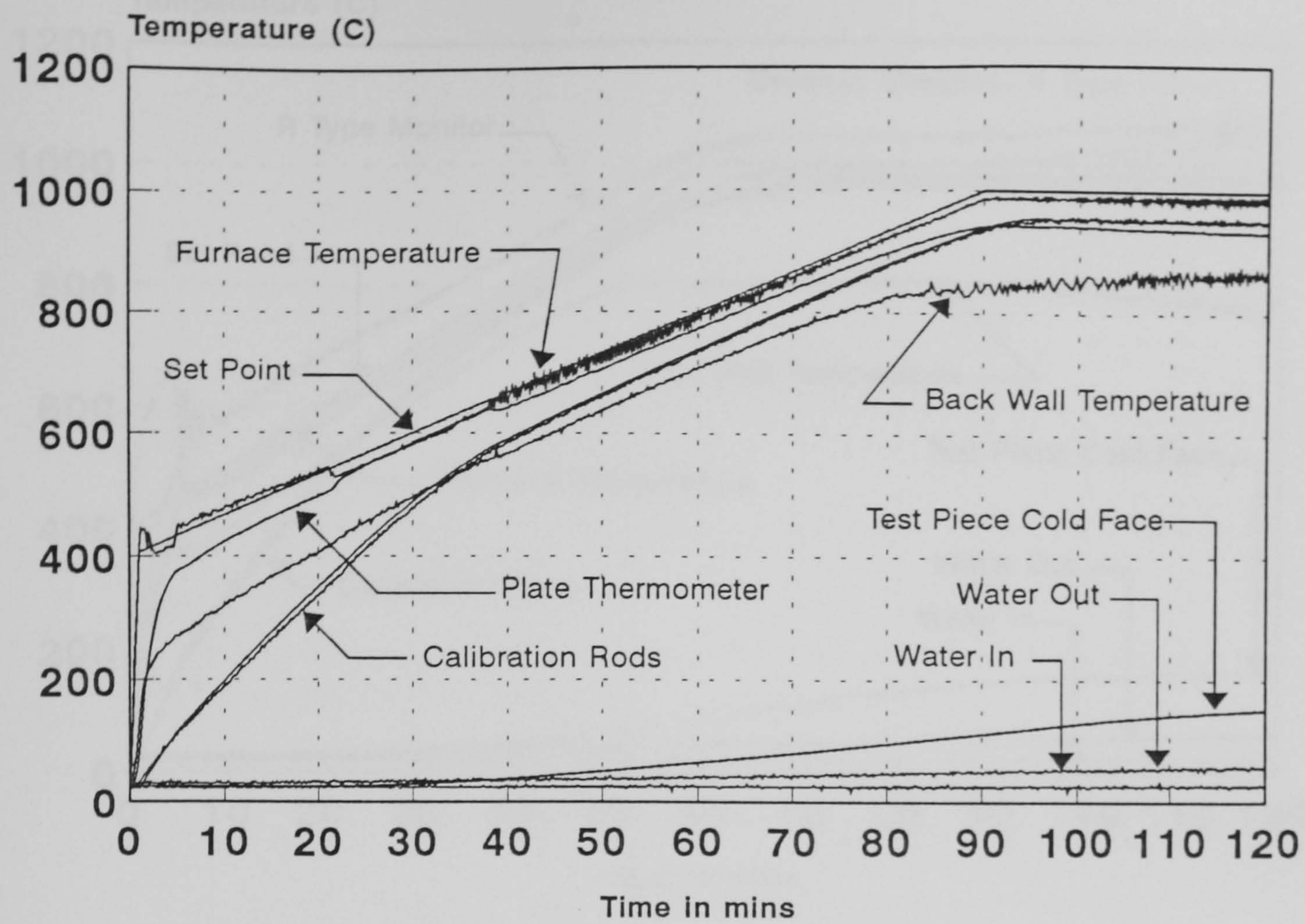

Furnace Characterisation - Test 5
R Type Control, PT Monitor
All Thermocouples 27-06-95

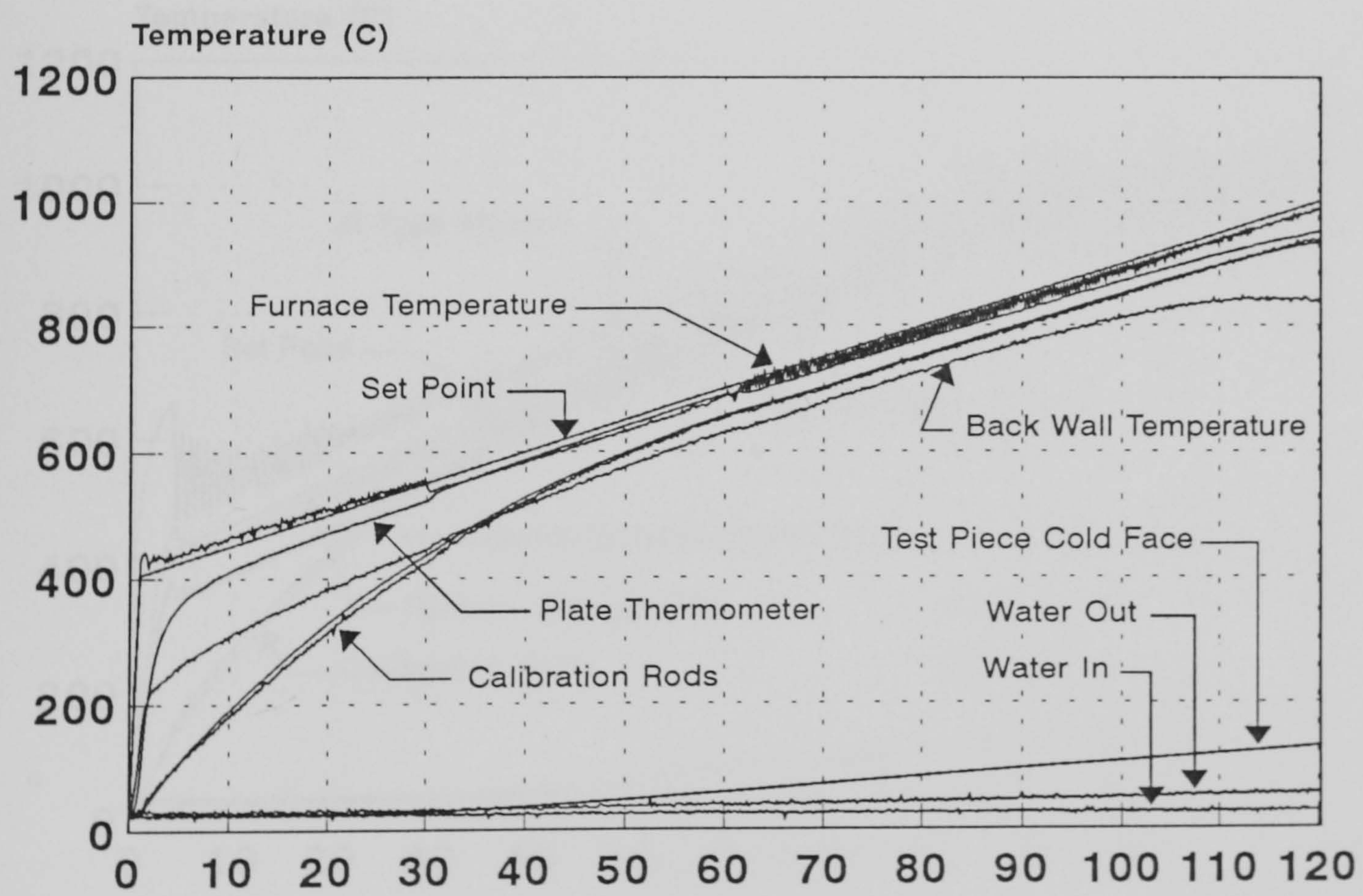

Furnace Characterisation - Test 6
R Type Control, PT Monitor
All Thermocouples 28-06-1995

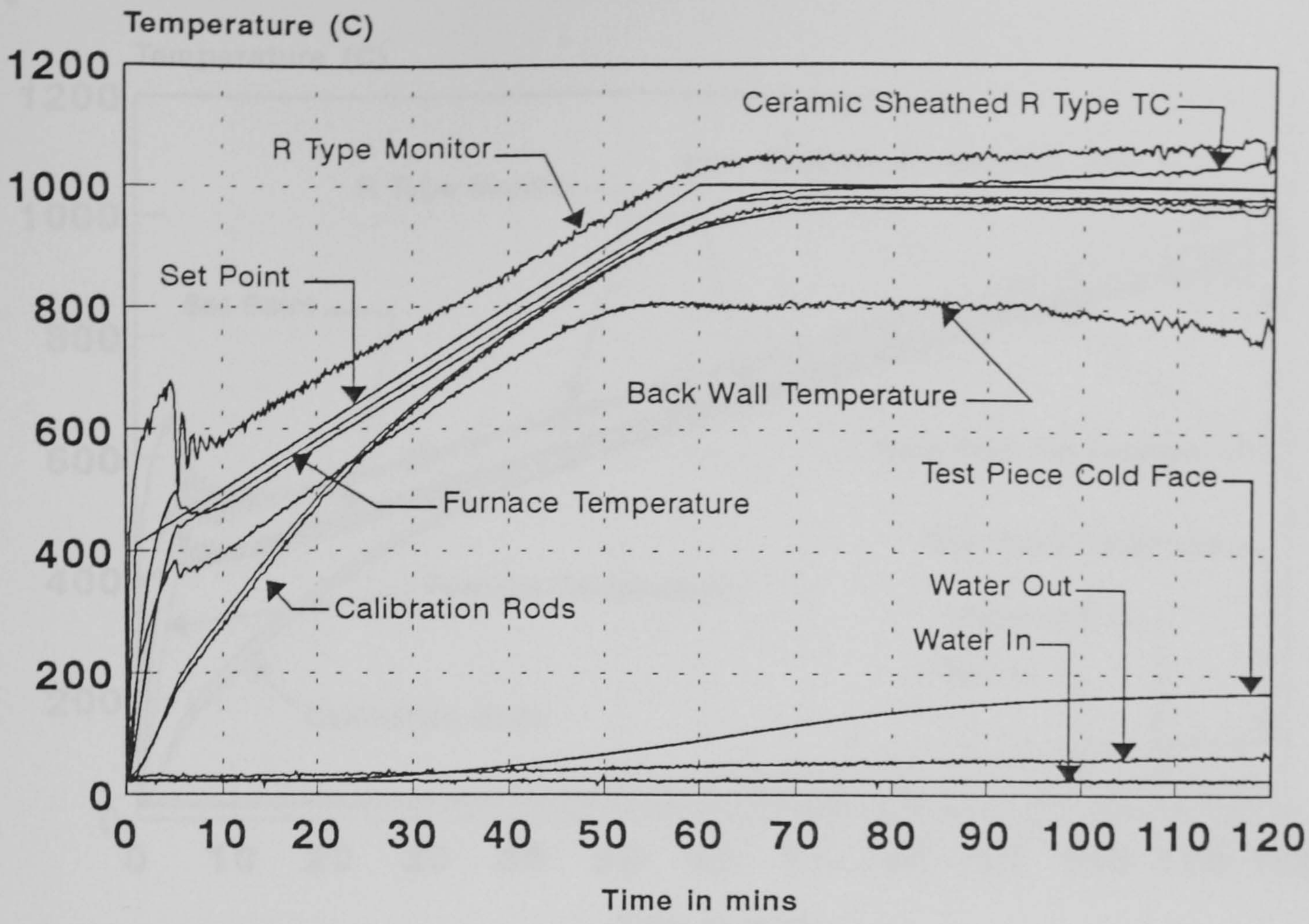

Furnace Characterisation - Test 7
PT Control, R Type Monitor
All Thermocouples, 04-07-95

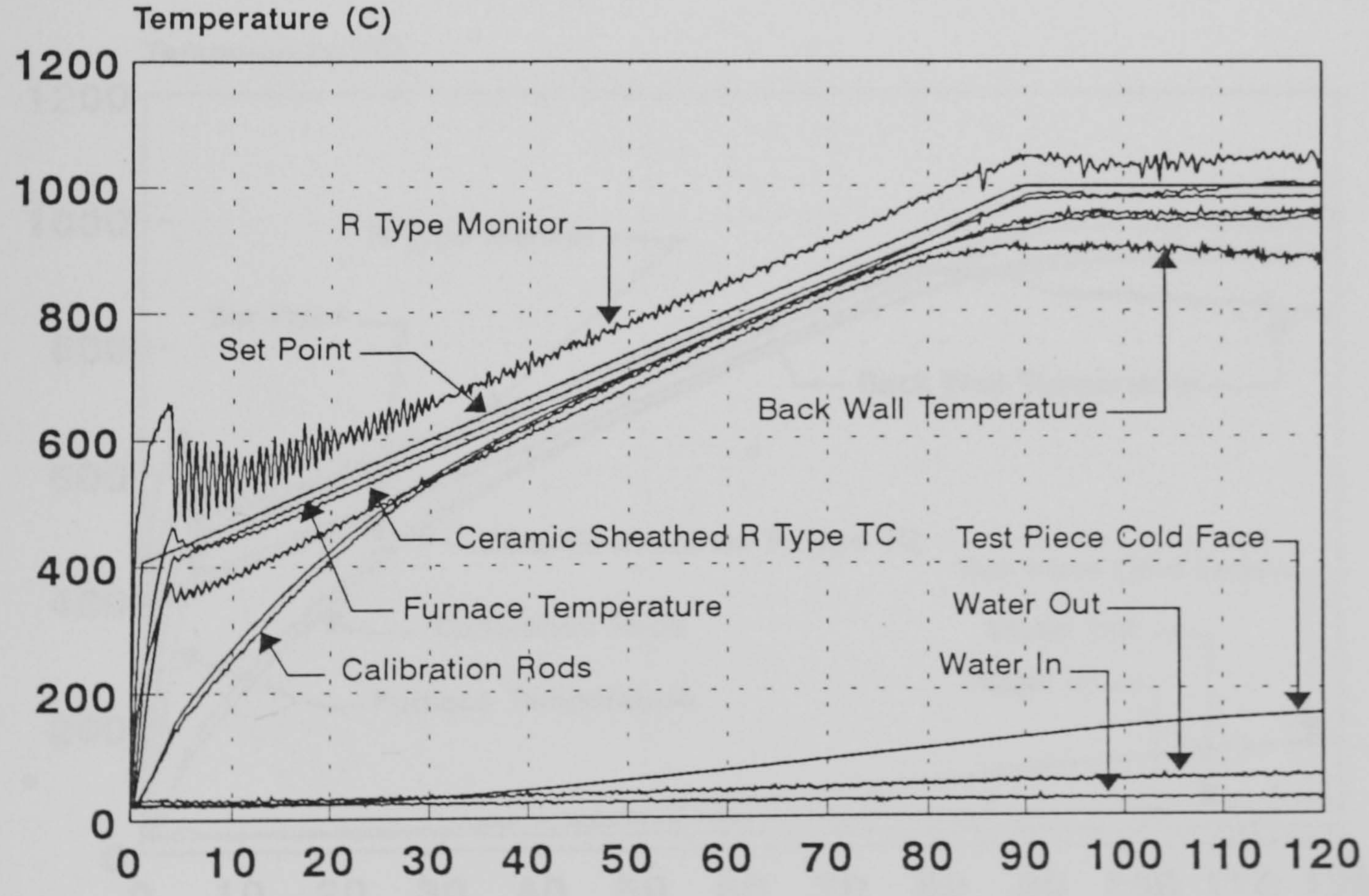

Furnace Characterisation - Test 8
PT Control, R Type Monitor
All Thermocouples, 07-07-95

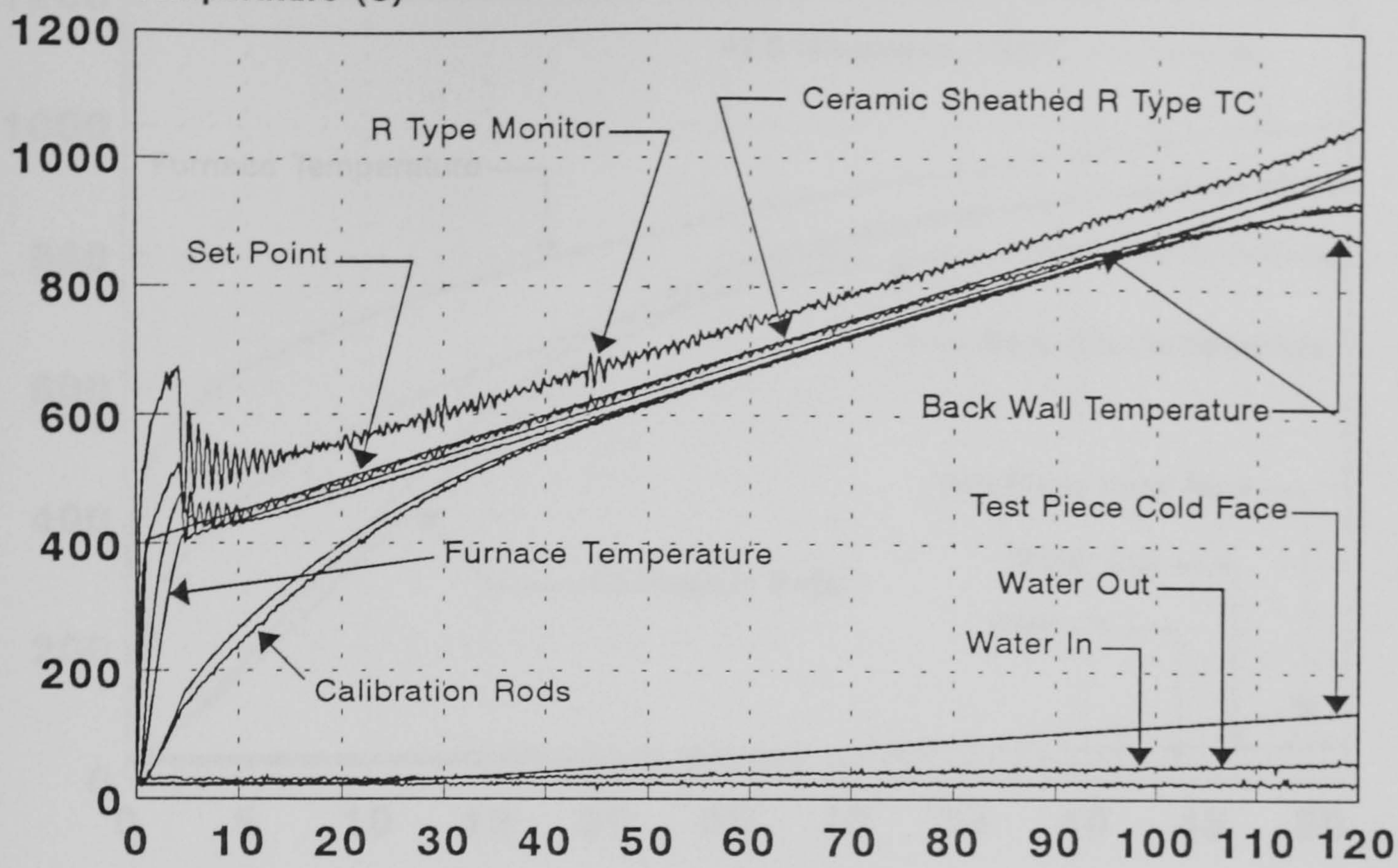

Furnace Characterisation - Test 9
PT Control, R Type Monitor
All Thermocouples, 17-07-95

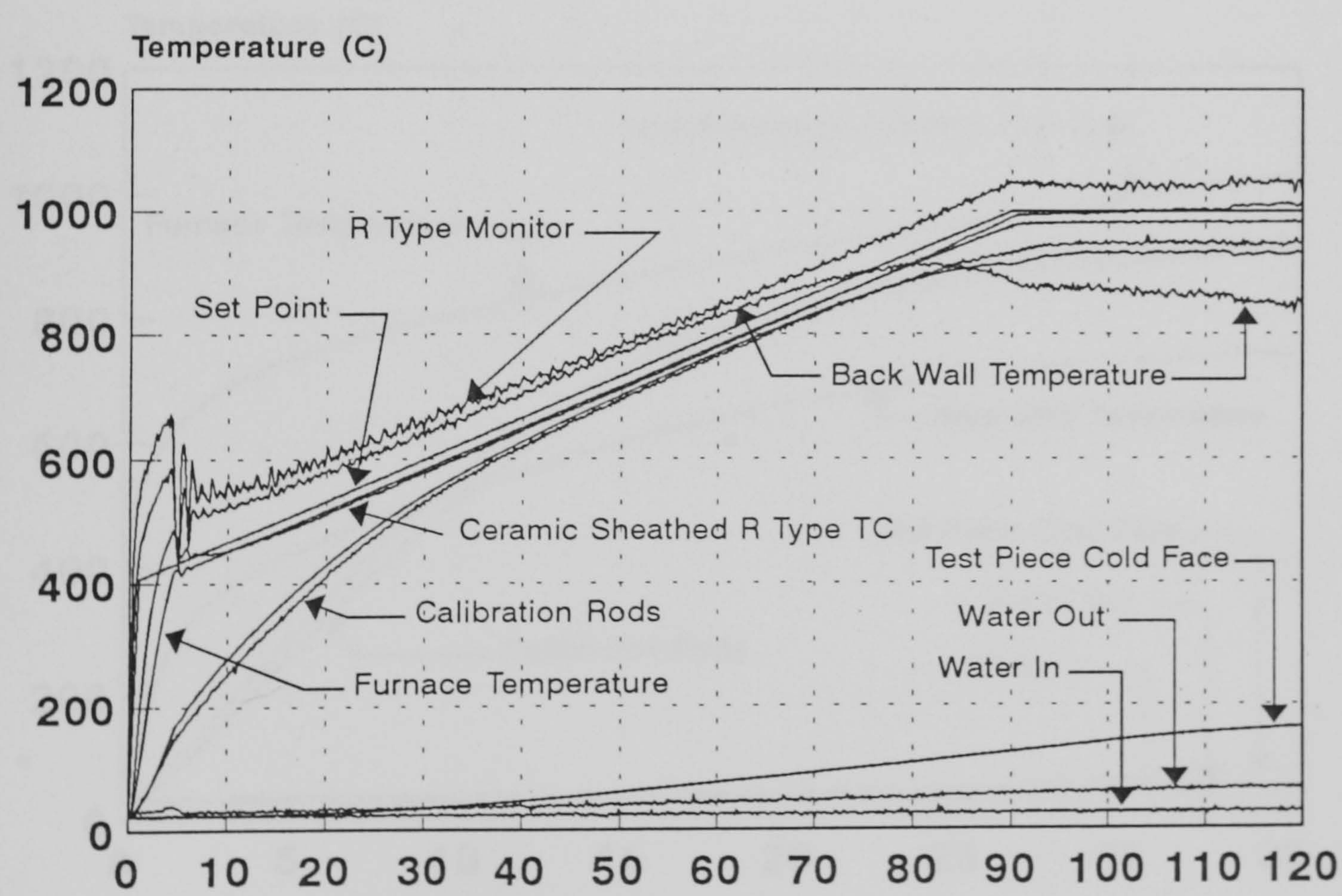

Furnace Characterisation - Test 10
PT Control, R Type Monitor
All Termocouples, 18-07-95

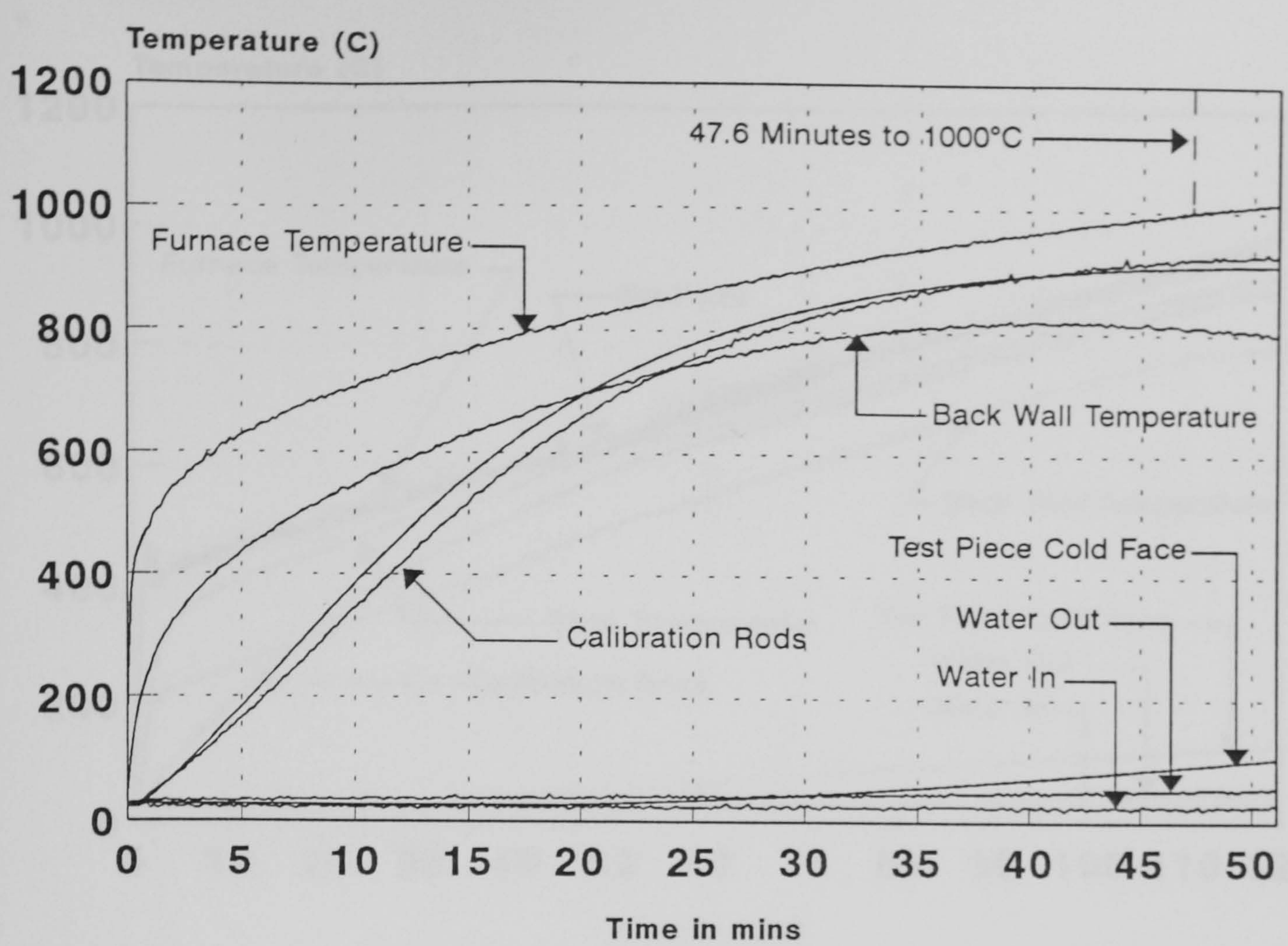

Furnace Characterisation - Test 11
Maximum Furnace Heating Rate - Fire Brick Lining Alone
R Type Furnace Temperature, All Thermocouples, 21-07-95

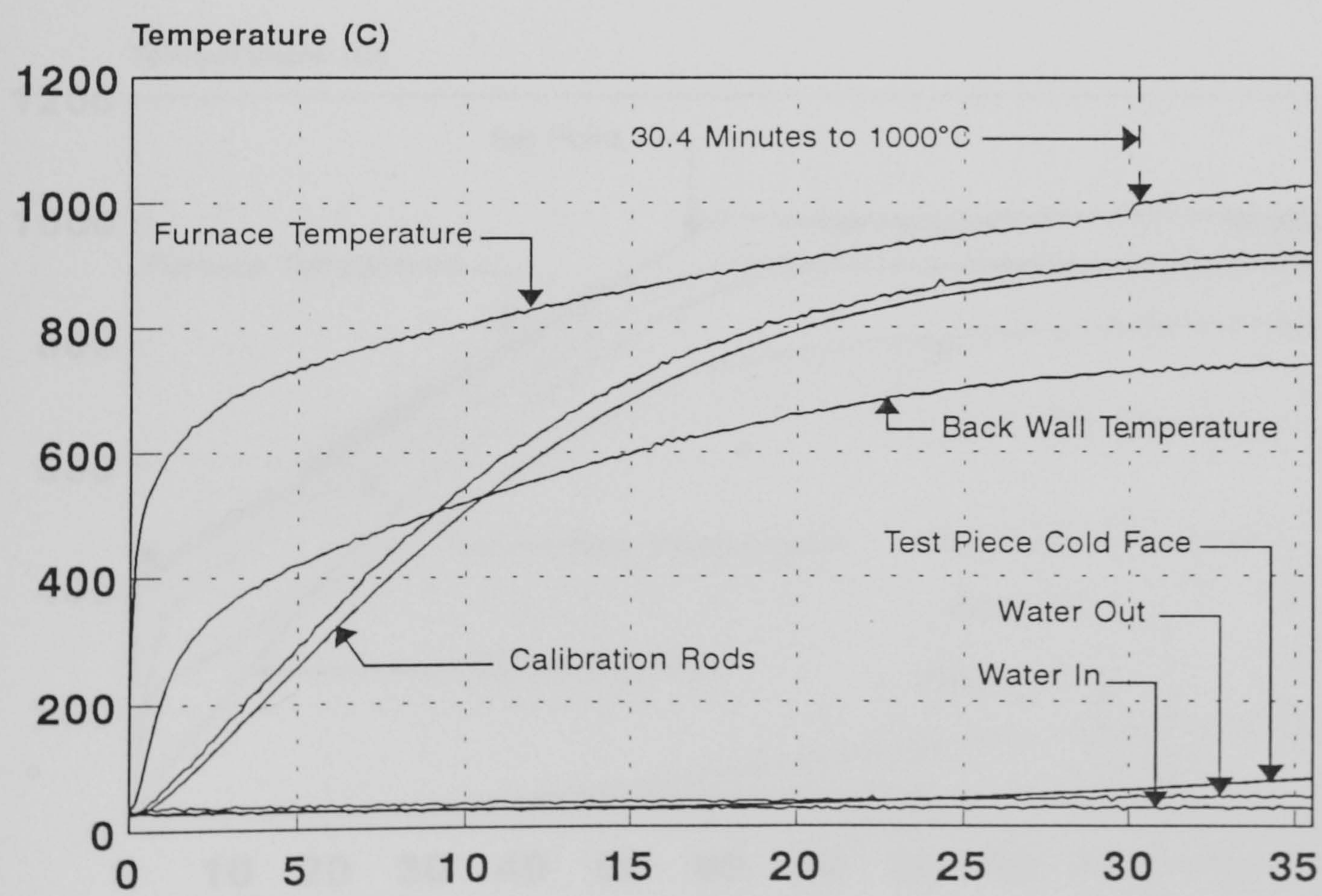

Furnace Characterisation - Test 12#2
Maximum Furnace Heating Rate - Fire Brick + 3.5mm Ceramic
R Type Furnace Temperature, All Thermocouples, 27-07-95

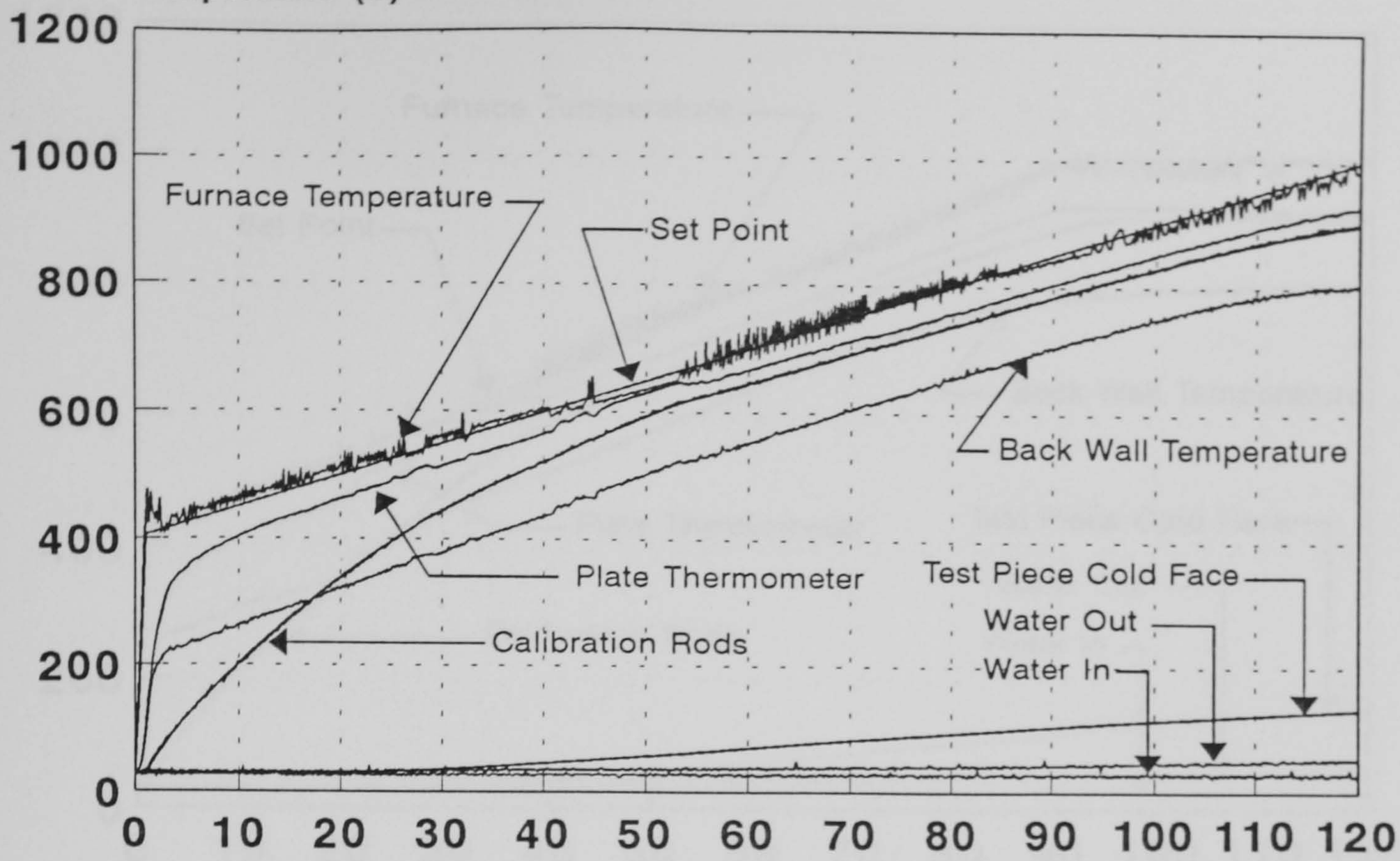

Furnace Characterisation - Test 13
R Type Control, PT Monitor, Ceramic Lined Furnace
All Thermocouples, 28-07-95

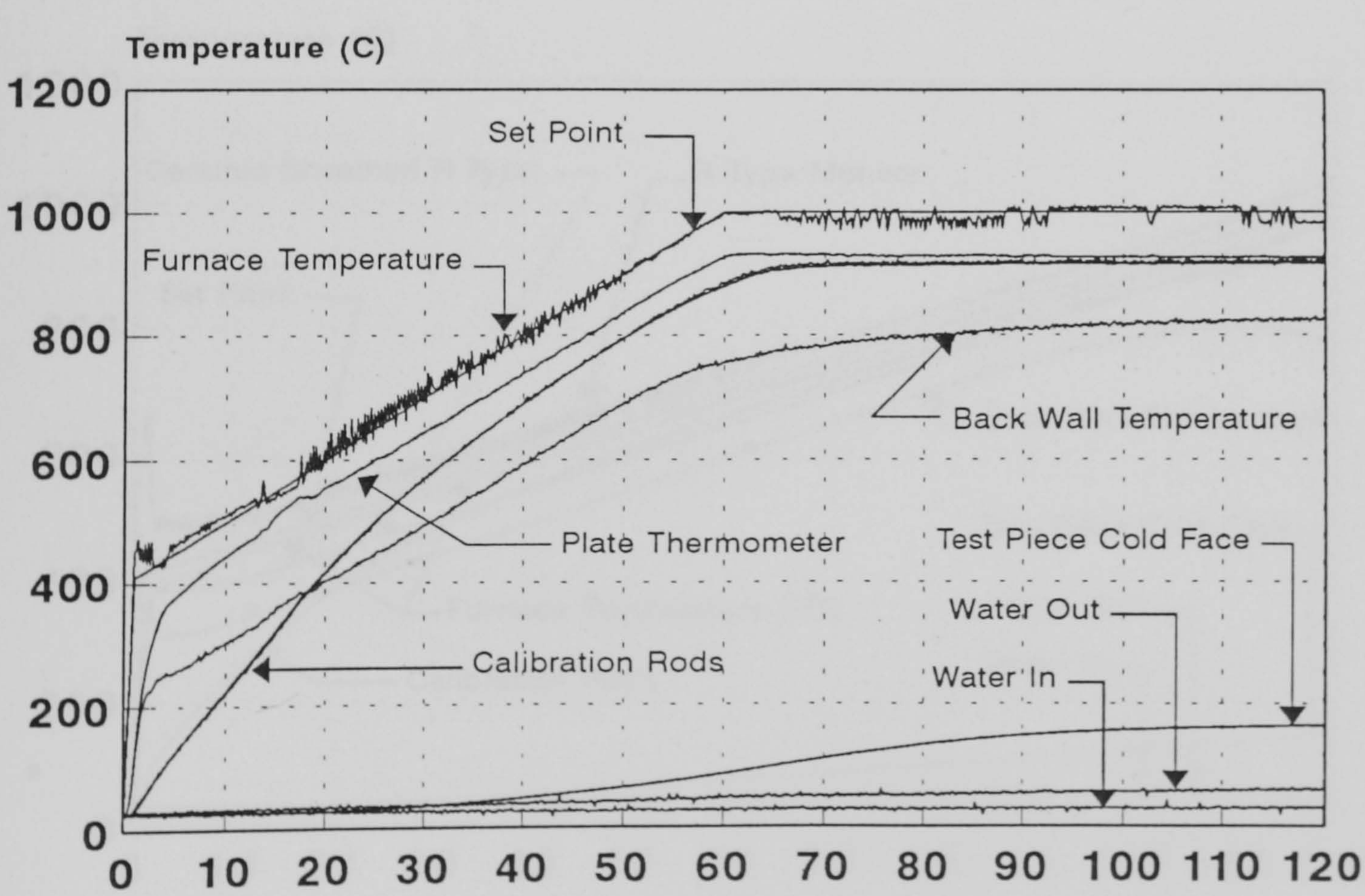

Furnace Characterisation - Test 14
R Type Control, PT Monitor, Ceramic Lined Furnace
All Thermocouples, 31-07-95

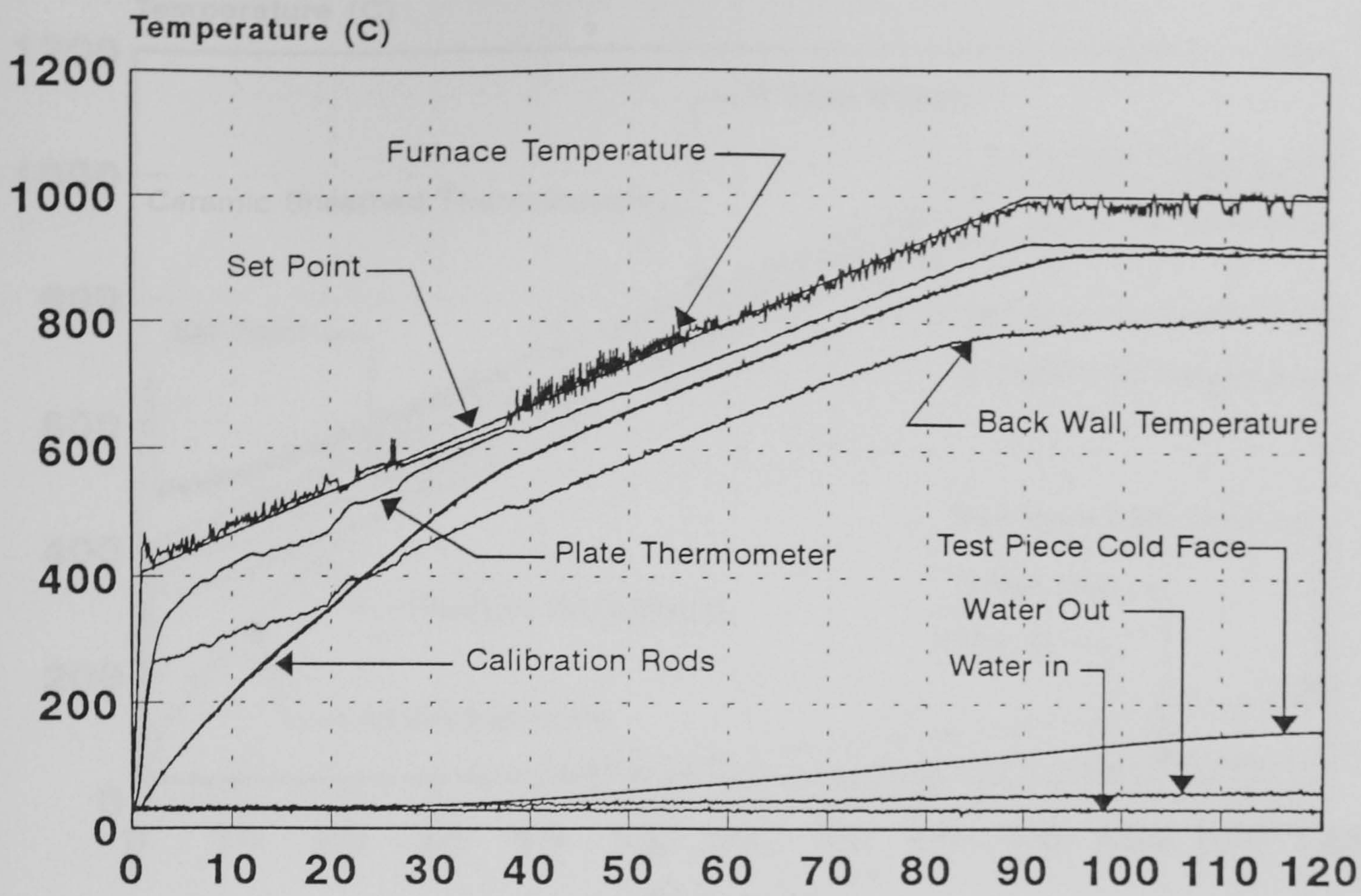

Furnace Characterisation - Test 15
R Type Control, PT Monitor, Ceramic Lined Furnace
All Thermocouples, 01-08-95

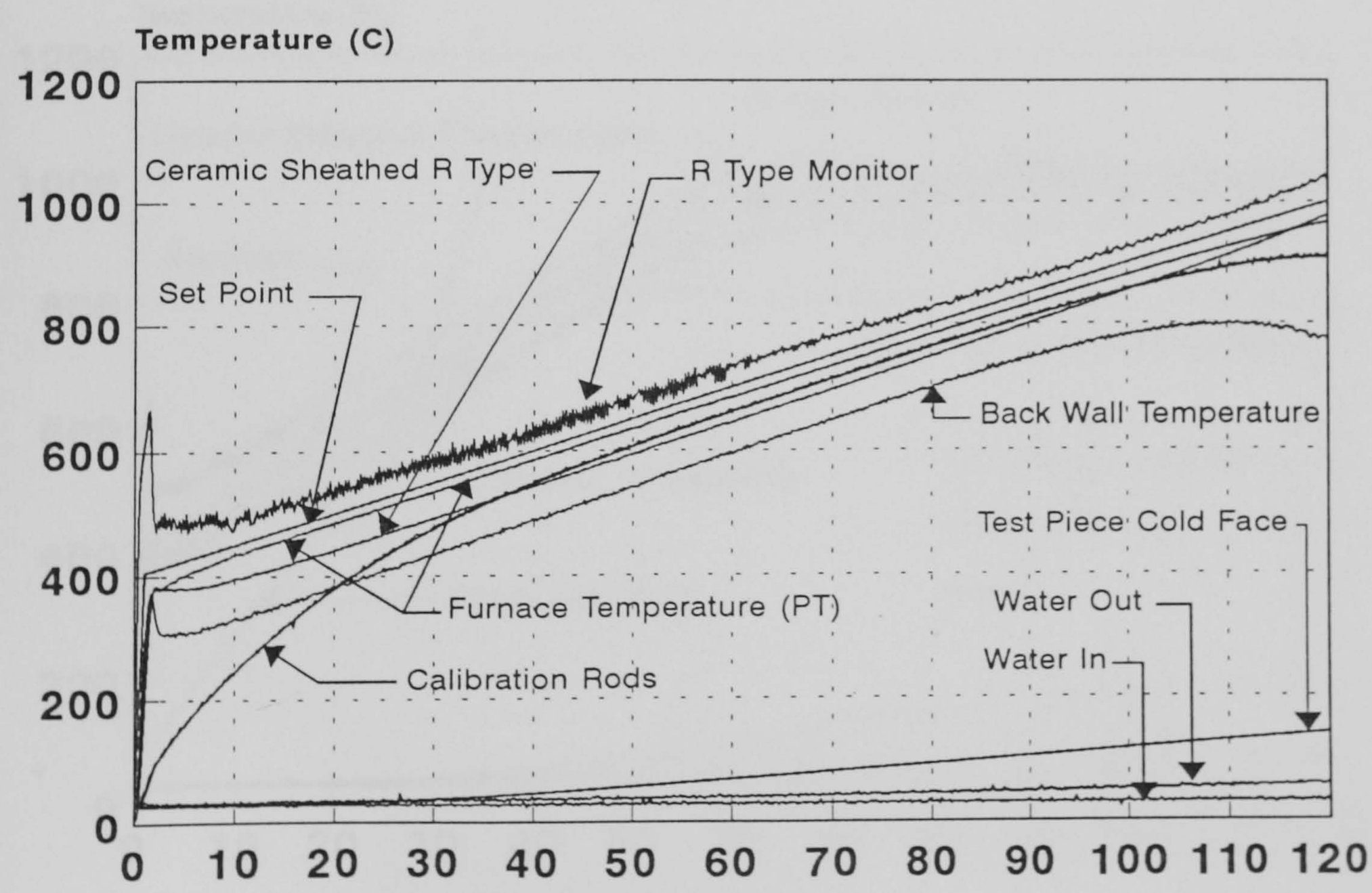

Furnace Characterisation - Test 16
PT Control, R Monitor, Ceramic Lined Furnace
All Thermocouples, 02-08-95

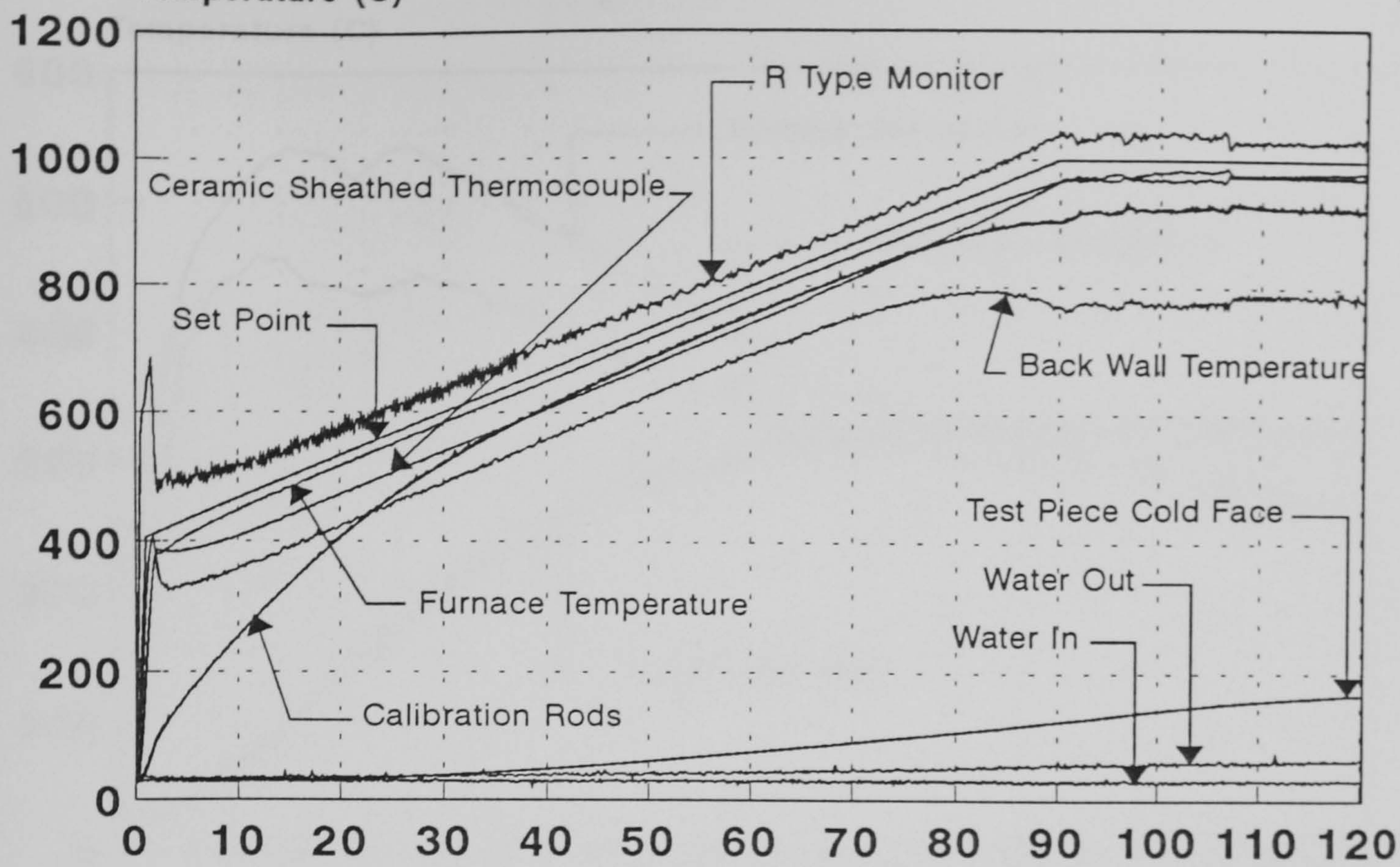

Furnace Characterisation - Test 17
PT Control, R Type Monitor, Ceramic Lined Furnace
All Thermocouples, 03-08-95

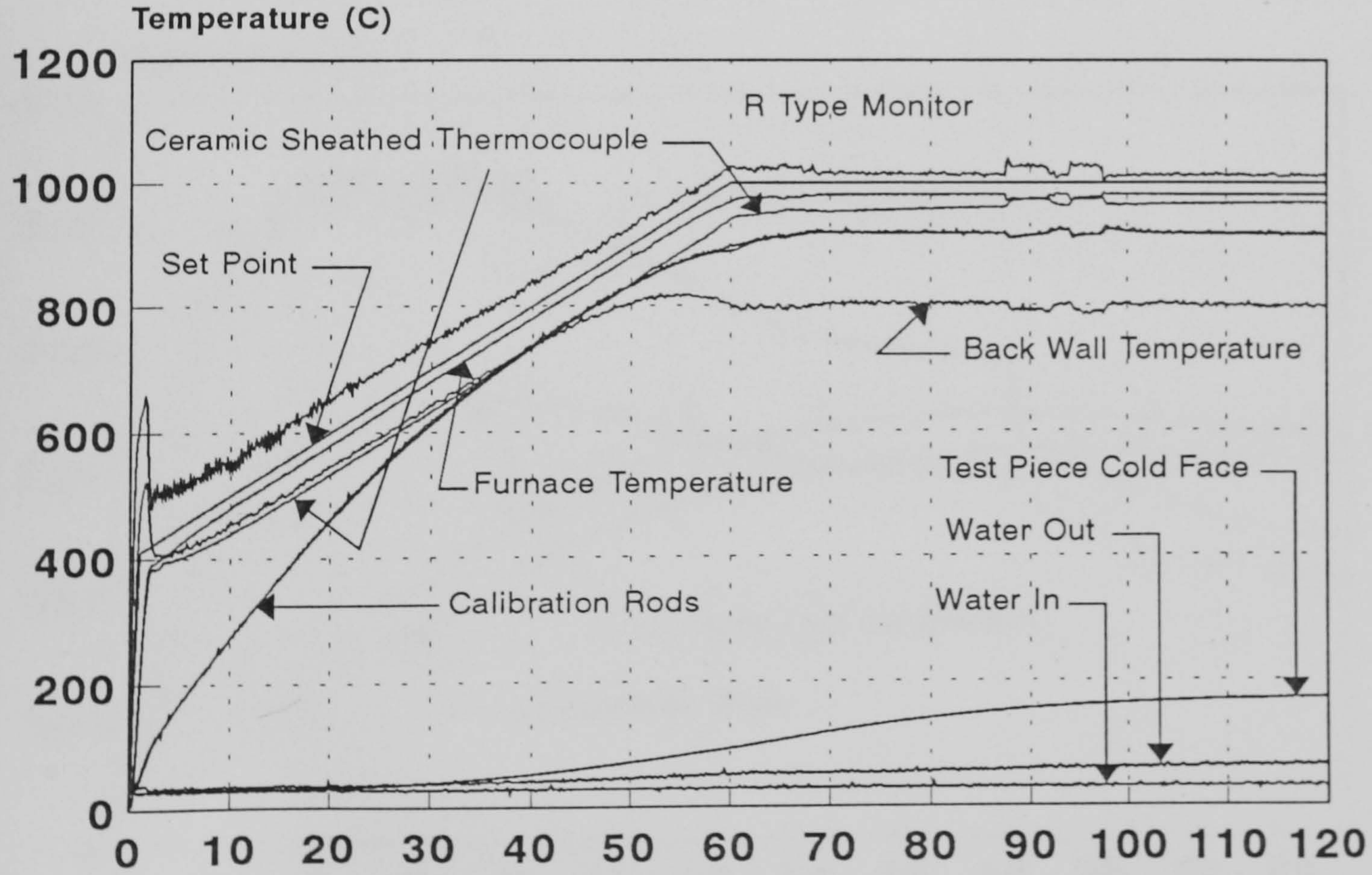

Furnace Characterisation - Test 18
PT Control, R Type Monitor, Ceramic Lined Furnace
All Thermocouples, 04-08-95

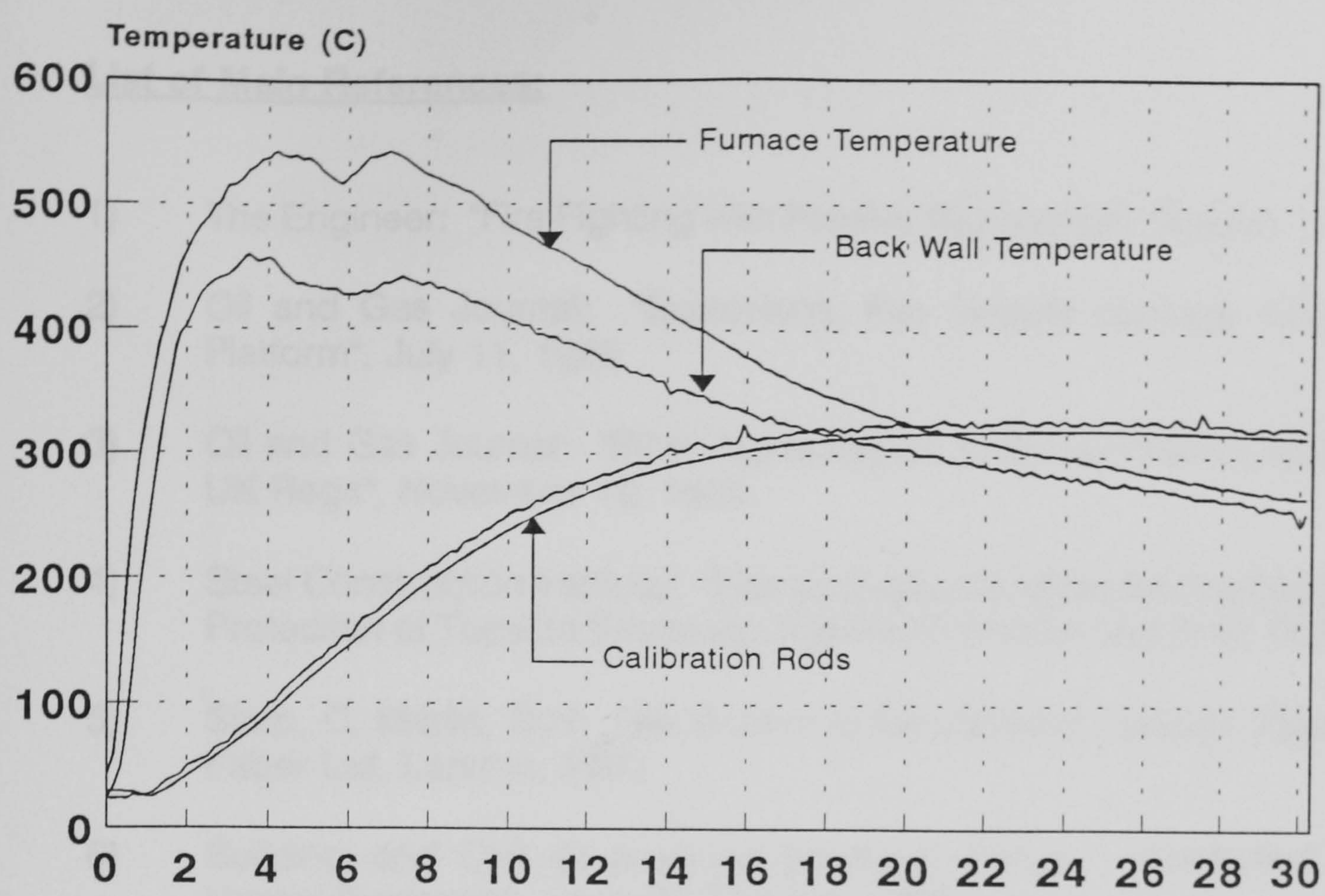

Furnace Characterisation - Test 19
"Real" Fire from 9kg Timber Inside Furnace
09-08-95

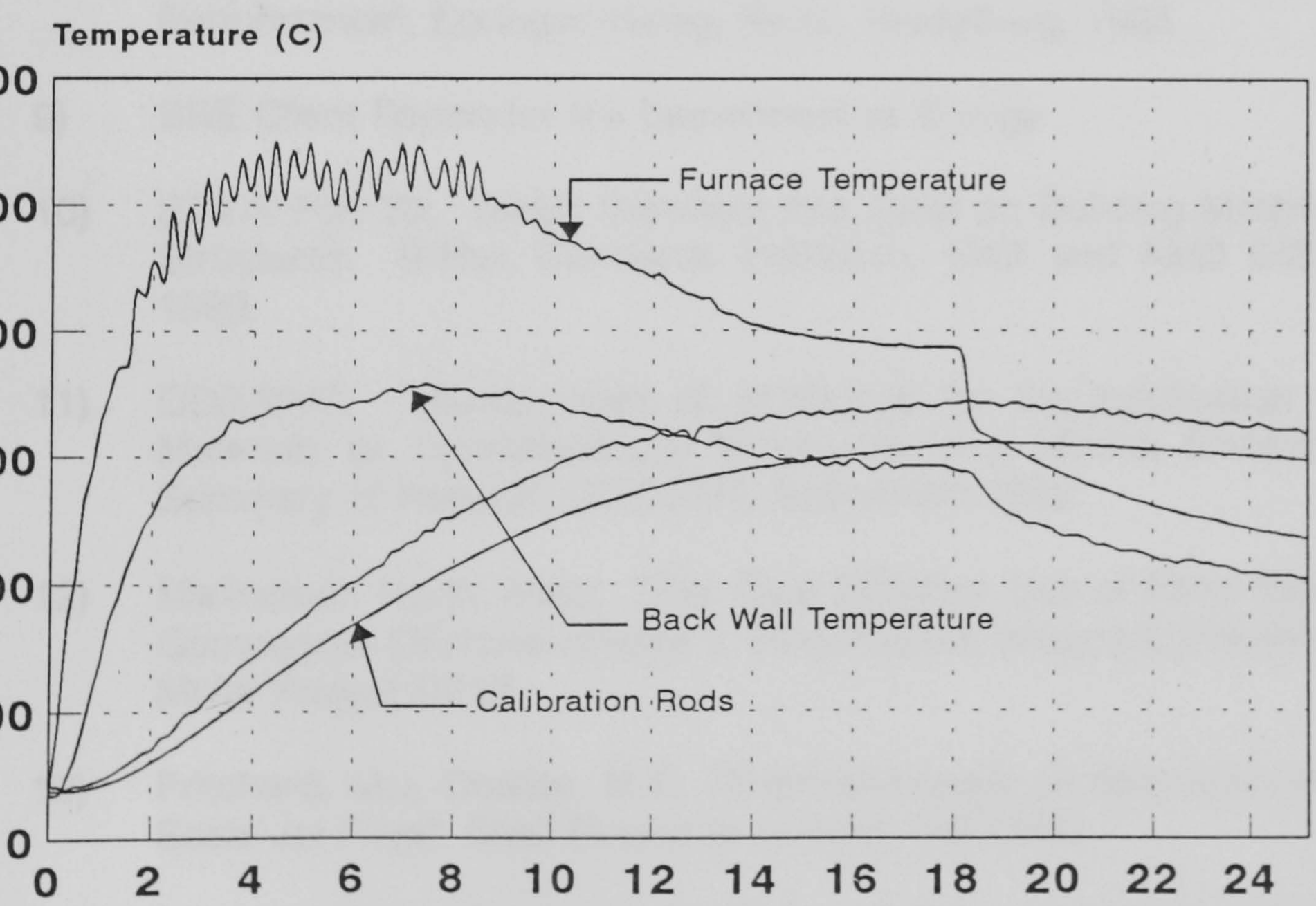

Furnace Characterisation - Test 20
Gas Fired Test to Reproduce "Real Fire" Conditions
18-08-95

List of Main References:

1) The Engineer: "Fire Fighting with Passive Resistance", October 18, 1990

2) Oil and Gas Journal: "Explosions, Fire Heavily Damage North Sea Platform", July 11, 1988

3) Oil and Gas Journal: "Piper Alpha Report to Spawn Many Changes in UK Regs", November 19, 1990

4) Steel Construction Institute: "Interim Guidance Notes for the Design and Protection of Topside Structures Against Explosion and Fire", SCI-P-112

5) Slarp, C, Martin, D.H: "An Outline of De Haviland History", Faber and Faber Ltd, London, 1960

6) Building and Civil Engineering Research Focus: "Controlled Water Heater Explosion", Issue 23, October 1995.

7) Stokke, R: "Glass Fiber Reinforced Plastics (GRP) Offshore - Project Summary", Senter for Industriforskning (SI), December 1988

8) Knop, A, Pilato, L.A: "Phenolic Resins - Chemistry, Applications and Performance", Springer-Verlag, Berlin, Heidelberg, 1985

9) BRE Client Report for the Department of Energy

10) BS476:Part 20: British Standard Fire Tests on Building Materials and Structures. British Standards Institution, 1987 and AMD 6487, April 1990.

11) ODE/BMT: "Development of Guidelines for the Application of FRP Materials to Topsides/Super Structures in a Marine Environment - Summary of Results", ODE-BMT, September 1992

12) Marinetech North West: "The Cost Effective Use of Fibre Reinforced Composites Offshore - Phase 1. Final Report, Volume 2, Fire Elements", MNW Project CP10

13) Pritchard, M.J, Cowley, M.T: "Thermal Impact on Structures of Large Scale Jet Fires", Shell Research Limited, C407/050

14) Ciaraidi, S.W, Alkire, J.D, Huntoon II, G.G: "Fiberglass Fire Water Systems for Offshore Platforms", OTC 6962, 24th Annual Offshore Technology Conference, Houston, Texas, May 1992

15) Pederson, K.S, Drangsholt, G, SINTEF: "Test Procedure to Document the Jet Fire Resistance of Passive Fire Protection", ERA Technology Conference - Structural Design Against Accidental Loads as Part of the Offshore Safety Case, London, September 1992

16) International Maritime Organisation: "Test Method for Fire Endurance Testing of Water Filled Plastic Piping", Guidelines for the Application of Plastic Pipes on Ships - Appendix 2, IMO MSC/Circ. 580, December 1992

17) Stokke, R: "Use of Fiber-Reinfirced Plastics (GRP) in Sea Water Pipe System Offshore", 20th Annual Offshore Technology Conference, Houston, Texas, May 1988

18) Cooke, G.M.E: "Use of Plate Thermometer for Standardising Fire Resistance Furnaces", Building Research Establishment Occasional Paper, March 1994

19) Jones, R.M: "Mechanics of Composite Solids", Hemisphere Publishing Corporation, 1975

20) Smith, C.S: "Design of Marine Structures in Composite Materials", Elsevier Applied Science, New York, 1990

21) Malmo, J: "Long Term Properties of GRP Materials", Norsk Hydro A/S, SI Report 85 02 02 - 9

23) Davies, J.M: "Design Criteria for Structural Sandwich Panels", The Structural Engineer, Vol 65a, No.12, pp435-451, December 1987

24) Basu, A.K: "Zur Herstellung und zum Werkstoffverhalten von Sandwich Tragerken des Werkstoffverbund Systems Stahlfeinblech - Polyurethan - Hartschaum" (The Manufacture and Behaviour of Sandwich Panels Made of the Material Combination of Steel Sheets and Polyurethane Foam), Dr. Ing. Dissertation, Technischen Hochschule Darmstadt, D17, 1976 (in German)

25) BS 2783: Part 3: Methods 320a - 320f: "Plastics, Tensile Strength, Elogation and Elastic Modulus", 1976

26) Allen, H.G: "Analysis and Design of Structural Sandwich Panels", Pergamon Press, 1969.

27) Stamm, K, Witte, H: "Sandwichkonstruktionen - Berechnung, Fertigung, Austurung" (Sandwich Construction, Calculation, Manufacture and Use), Springer-Verlag, Wien and New York, 1974 (in German)

28) Davies, J.M: "The analysis of Sandwich Panels with Profiled Faces", Proc. 8th Internalional Speciality Conference on Cold-Formed Steel Structures, St. Louis, Missouri, USA, November 1986

29) Oleesky, S.S, Mohr, J.G: "Handbook of Reinforced Plastics", Society of the Reinforced Plastics Industry, Reinhold Publishing, pp 292-299, 1966

30) Vorlander, D: Annalen, **280**, 167, 1894

31) Taylor, R, Mottram, J.T: "Thermophysical Property Measurements of Fibre/Phenolic Resin Composites", 1st Asian Thermophysical Properties Conference, China Association for Science and Technology, 1986

32) Ciment Fondu Lafarge, Specialist Cements Technical Data Sheets

33) Givan, G.Y, Hart, L.D, Helich, R.P, Maczura, G: Bulletin of the American Ceramic Society, **54**, 710, 1975

34) George, C.M: Transcript of the British Ceramic Society, **79**, 82, 1980

35) Kula, T.M, Meiser, M.D, Tressler, R.E: Cement and Concrete Research, **10**, 491, 1980

36) Watts, Blake and Bearn: Ball and China Clays Technical Data Sheets and Written Communication

37) Silvaperl Manufacturing Limited: Silvalite Perlite Technical Data Sheets

38) Tilcon Limited: Tilcon Perlite Products Technical Data Sheets

39) Mandolite Limited: Mandolite Vermiculite Technical Data Sheets and Written Communication with Vermiculite Development Officer

40) Dave, N: Building Research Technical Paper, 14, HMSO London, 1933

41) Davies, J.M, Dewhurst, D.W, McNicholas, J.B: "Performance of Sandwich Panels in Fire: (2) Offshore Applications", Third International Conference on Sandwich Construction, Southampton, UK, 12-15the September, 1995

42) ISO 5660: "Fire Tests - Reaction to Fire - Rate of Heat Release from Building Products", International Organization for Standardization, Geneva, 1993

43) Marinetech North West: "Cost Effective use of Fibre Reinforced Composites Offshore - Phase 2", CP205: Fire resistant sandwich panels for offshore structures, 1993.

44) Wang, H.B: "Heat Transfer Analysis of Components of Construction Exposed to Fire - A theoretical, numerical and experimental approach", Thesis presented for the award of Doctor of Philosophy, Department of Civil Engineering and Construction, University of Salford, 1995

45) Özişik, M.N: "Heat Transfer", McGraw-Hill International Editions, 1985

46) Davies, J.M, Hakmi, R, and Wang, H.B: "Numerical Temperature Analysis of Hygroscopic Panels Exposed to Fire", Numerical Methods in Thermal Problems, Vol.VIII Part 2, Proceedings of the 8th International Conference held in Swnasea, July 12-16th, 1993. Pineridge Press, UK

47) Davies, J.M, Wang, H.B: "A Numerical and Experimental Heat Transfer Study of GRP Materials Subject to Standard Cellulosic and Hydrocarbon Fire Tests", (to be published)

48) Incropera, F.P, and Dewitt, D.P: "Fundamentals of Heat and Mass Transfer", 3rd Edition, John Wiley and Sons, 1990

49) Jakob, M: "Heat Transfer", Volume 1, Chapman and Hill, London 1949

50) Sundstrom, B: "Plastic Pipes - Testing for Fire Endurance, and Flame Spread Properties", SP-RAPP 1985, 31 ISSN D-280-2503

51) Bonavent, G: "The Behaviour of Reinforced Plastic Pipes in Hydrocarbon Fires - Case of water filled pipes", French Petroleum Institute, IFP 23-294

52) Dekker, J, Twilt, L: "The Effect of Joints on the Fire Endurance of Glass Fiber Reinforced Plastic Pipes with Stagnant Water", IBBC-TNO B85-52

53) Dekker, J, Twilt, L: "The Effect of Joints on the Fire Resistance of Glass Fiber Reinforced Plastic Pipes Filled with Stagnant Water or Gas", IBBC-TNO B 86-378

54) Marks, P.R: "Non-Metallic Pipeline Materials in Ships - Fire Testing of Glass Reinforced Epoxy Pipes", Shell Research Ltd, Thornton Research Centre, Aug 1985. TNER 85.063

55) Belason, E.B: "Performance of Thermally Protected and Unprotected FRP Pipes in Hydrocarbon Fires: Water Filled Condition", AVCO Systems Division, Wilmington, Mass. 01887. March 1977

56) Boothby, P.J: "Jet Fire Testing of Topside Pipework", ASME Paper OMAE-93-892 M

57) Wilhelmi, G.F, Schab, H.W: "Glass Reinforced Plastic (GRP) Piping for Shipboard Applications", Naval Engineers Journal, April 1977

58) Dekker, J, Twilt, L: "Fire Endurance of Glass Fiber Reinforced Plastic Pipes", IBBC-TNO B 84-4

59) Wang, H.B, Davies, J.M: "Heat Transfer Analysis of Glass Reinforced Plastic Pipes Exposed to Fire", (to be published)

60) Wickström, U: "The Plate Thermometer - a Simple Instrument for Reaching Harmonised Fire Resistance Tests", NORDTEST project 609-86, Swedish National Testing Institute, Borås, 1988

61) Twilt, L, Van de Heur, P.H.E: "Numerical .vs. Experimental Evidence Plate Thermometer .vs. Thermocouple Control", TNO report 94-CVB-R0178

62) Elliston, D.G, Gray, W.A, Hibberd, D.F, Ho, T-Y, Williams, A: "The effect of surface emissivity on furnace performance", Journal of the Institute of Energy, (ISSN 0144-2600), v60, December 1987

63) Sultan, M.A, Harmathy, T.Z, Mehaffrey, J.R: "Heat Transmission in Fire Test Furnaces", Fire and Materials, Vol 10, pp47-55, 1986

64) Gibson, A.G, Hume, J.: "Fire Performance of Composite Panels for Large Marine Structures", Plastics, Rubber and Composites Processing and Applications, Vol 23, No 3, pp175-183, 1995

65) Henderson, J.B, Wiebelt, J.A, Tant, M.R: "A Model for the Response of Polymer Composite Materials with Experimental Verification", J. of Composite Materials, Vol 19, pp579-595, 1985

66) Kung, H.C: "A Mathematical Model for Wood Pyrolysis", Combustion and Flame, Vol 18, p185, 1972

67) Henderson, J.B, Wiecek, T.E: "A Mathematical Model to Predict the Thermal Response of Decomposing, Expanding Polymer Composites", J. of Composite Materials, Vol 21, pp373-393, 1987

68) Barnford, C.H, Crank, J, Mallan, D.H: "The Combustion of Wood. Part 1", Cambridge Phil. Soc. Proc. Vol 42, p166, 1946

The Influence of Fire on the Design of Polymer Composite Pipes and Panels for Offshore Structures

Volume 2 of 2

David W Dewhurst

Telford Research Institute
Department of Civil and Environmental Engineering
University of Salford, Salford, UK

Submitted in Partial Fulfilment for the Degree of
Doctor of Philosophy, April 1997

TABLE OF CONTENTS

ACKNOWLEDGEMENT

The author wishes to express his sincere thanks to Professor John M. Davies and Dr John B. McNicholas for their supervision, guidance and encouragement throughout the period of study.

Sincere thanks are due to Mr D C O'Leary for his supervision after the authors period of active research with The University of Salford.

Also the author wishes to express his thanks to those members of the technical staff of the Department of Civil Engineering and Construction for their assistance in the preparation of experimental work.

DECLARATION

None of the material contained in this thesis has been submitted in support of an application for another degree or qualification of this or any other university or institution of learning.

David W Dewhurst

March 1997

FOREWORD

The following text contains detailed descriptions of the methodologies used and experiments performed in the development of a new, non-fibrous, highly efficient furnace lining.

The work presented here was performed as part of a multi sponsor research project in conjunction with the Energy Efficiency Office, Department of the Environment. This research is part of an ongoing project (March 1997), and should be viewed as being commercially sensitive.

David W Dewhurst

March 1997

APPENDIX A - DEVELOPMENT OF A NEW FURNACE LINING MATERIAL

A.1 Introduction

The following chapters detail the development of a new non-fibrous refractory lining material, Insuline. This lining material has been developed with the aim of replacing ceramic fibre without loss of thermal efficiency. Insuline, due to its' constituent materials is inherently free from fibre-related health hazards, and also provides an energy efficient replacement for insulating fire bricks.

Ceramic fibres have been available for high temperature applications for the last 25 years. These fibres are alumino-silicate fibres made from either naturally occurring high purity clays or from direct combination of alumina and silica[1]. Typical methods of manufacture are from melting the appropriate raw materials in a suitable furnace and either subjecting a molten stream to a blast of air, or allowing it to fall onto a spinning disk. The operating temperature of the fibres can be controlled by the percentage of alumina (the standard 1250°C fibre is approximately 50% alumina, and 94-96% alumina fibres would have an operating temperature of approximately 1600°C). The advantages of using ceramic fibres for furnace linings are that they have very low thermal conductivities and also low heat capacity. This makes them suitable for use in intermittent heating situations. Ceramic fibre installations also have a very high resistance to thermal shock related problems. Recently however the health implications of their use have been considered in detail.

A.2 Health and safety implications

Currently all fibrous materials are being viewed as potential health hazards. It is understood that, with ceramic fibres, crystobalite may be formed in certain circumstances. It is further believed that the exposure of the fibres to high temperature firing may embrittle the fibre tips causing the detachment of fibrous pieces of a respirable length. The current repercussions with regards to exposure to asbestos fibres are naturally making people more considerate of fibre-related health problems. Some countries have begun steps towards the outlawing of ceramic fibres and, due to this, a recent study in America was presented to the United States Environmental Protection Agency which considered the cost impacts of this. The conclusions of the report were that the replacement of ceramic fibres with substitute materials would reduce energy efficiency, increase maintenance costs, increase capital costs (for the rebuilding of furnaces, including the need for an increased number of furnaces due to foreseen reductions in throughput). Also in some applications it is foreseen that product quality would also be reduced. The estimated increased energy consumption in the United States for the replacement of ceramic fibre linings was 48 billion kilowatt-hours annually.

It is noted also that ceramic fibres are not the only high temperature fibres which present possible health hazards. Conversely, non-fibrous linings such as refractory concrete and firebricks have a long history of use. They are typically denser, thicker and more expensive than the comparable ceramic

linings, however there is no apparent health hazard for the use of these materials. There is, therefore, a substantial incentive to develop an alternative material which may replace ceramic fibres without the potential health hazard of fibrous materials. Candidate materials make extensive use of refractory cements.

A.3 High temperature applications of cement based materials

Refractory cements are high purity high alumina cements. Typical alumina (Al_2O_3) contents are of 50% or above, with up to 40% calcium oxide (CaO) and also less than 10% silicon dioxide (SiO_2). The cements are rapid hardening with final set times generally less than 4½ hours and the majority of the final strength attained within 24 hours from casting. Refractory cements are typically pale in colour, ranging from pale grey or cream to white. The paler the colour, generally the higher the alumina content with a corresponding increase in melt/working temperature.

The curing/firing process phase changes, and indeed strength effects are complex, and as such the mineralogical changes will not be reported in any great detail. The aim of this chapter is to give a brief overview of the physical effects of the curing and firing processes on the new furnace lining material. As there is no data available for a composition such as the new lining material data for cements and refractory concretes have been reported.

A.3.1 The curing process

Hydraulic cements develop their hydraulic bonds because of chemical reactions between the cement (calcium aluminate) and water. The mixing and curing temperature can affect the types of hydrates formed in the set cement or concrete.

Set high alumina cements cured at room temperature for long durations consist of unhydrated material, CAH_{10} and some alumina gel[2]. The metastable CAH_{10} experiences a slow reaction at room temperature in the formation of C_3AH_6 and gibbite. This reaction is very rapid at temperatures above 80°C providing sufficient moisture is present. In the presence of sufficient water this reaction may occur during "drying" even at temperatures above 110°C[3]. If this conversion reaction is allowed to take place a diminuation in strength may be observed[2]. Midgley[2] reported a diminuation in compressive strength of high alumina cements cured at room temperature for 6 months of 24,000psi (165N/mm^2) to 11,000psi (76N/mm^2) after drying the samples at 110°C.

Many people[4,5,6] have investigated the effect of curing temperature of a refractory concrete. Despite these investigations the effect of curing temperature upon strength is not established conclusively. Givan et al.[4] studied the effect of curing temperature upon the flexural strength of refractory concrete (caftab 20) after curing, after drying at 110°C, and after firing to 1100°C. **Figure A.3.1** following shows a summary of the results in graphical form.

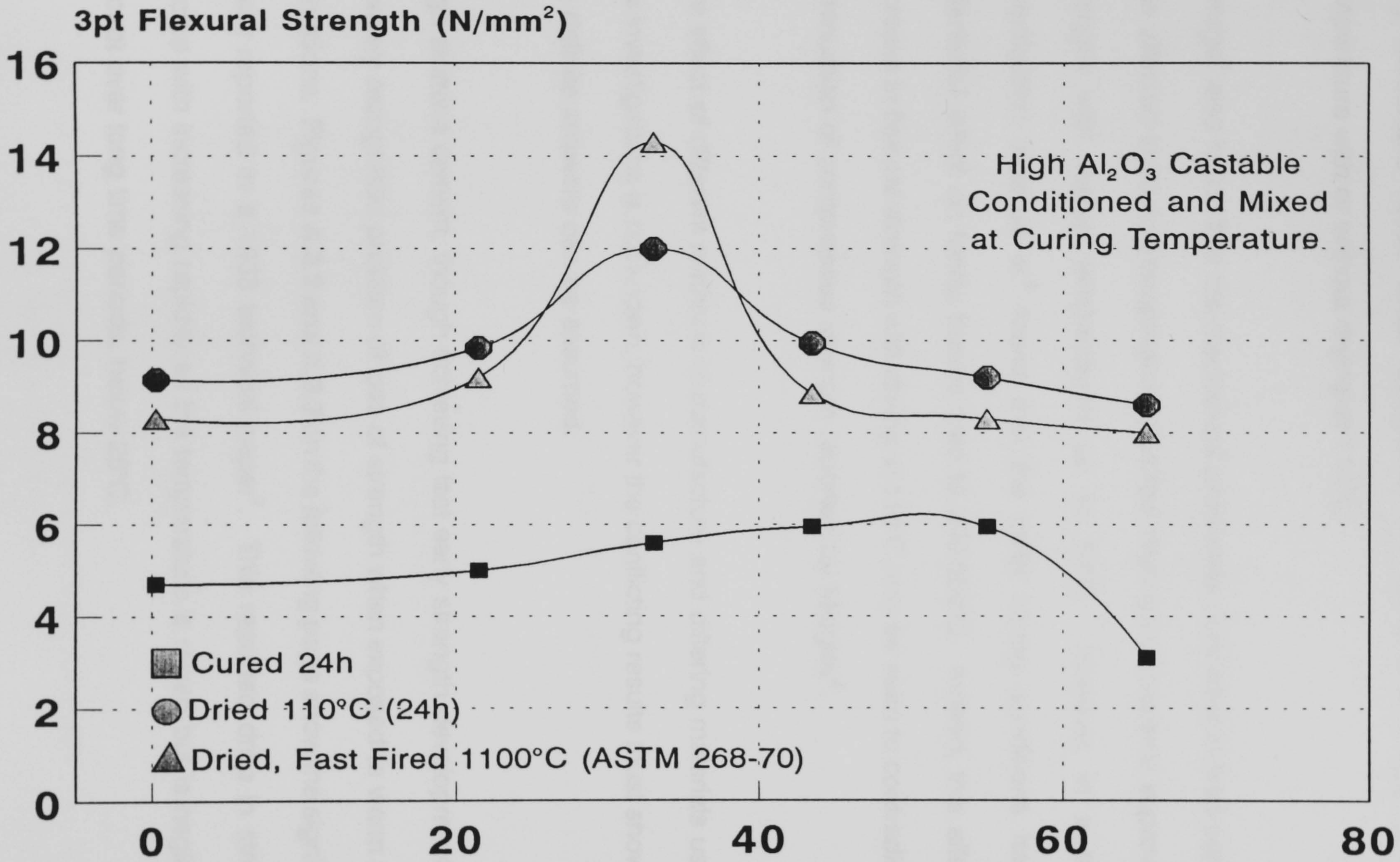

Figure A.3.1 - Flexural Strength of Tabular Alumina High Purity Cement Castable (ASTM C268)

It can be seen that mixing and curing at 30-35°C and drying at 110°C gives a very favourable result when compared to mixing and curing at room temperature with or without drying at 110°C.

George[5] also found that the mechanical properties of dried and fired cements was affected by curing temperature, but that high purity cements improved in strength with curing temperatures up to 54°C. However in a similar investigation Kula et al.[6] found that the initial curing conditions had no differential effect on fondu pastes fired to 300-500°C. Indeed, this effect of increase in flexural strength with drying at 110°C may be seen to contradict the diminuation of compressive strength reported by Midgley[2].

The effect of different methods of manufacture and differing materials used in the investigations is not known, however the conflicting results must show that no definite answers can be assumed.

High alumina cement, though achieving fast early strength development, has a widely recognised problem of loss of strength when exposed to warm moist conditions. **Figures A.3.2 and A.3.3** on the following page show the significant effect reported in a 1933 technical paper[7]. This reported drop in strength occurs with increasing rapidity as the temperature is raised but is negligible, except over long time periods, below 25°C.

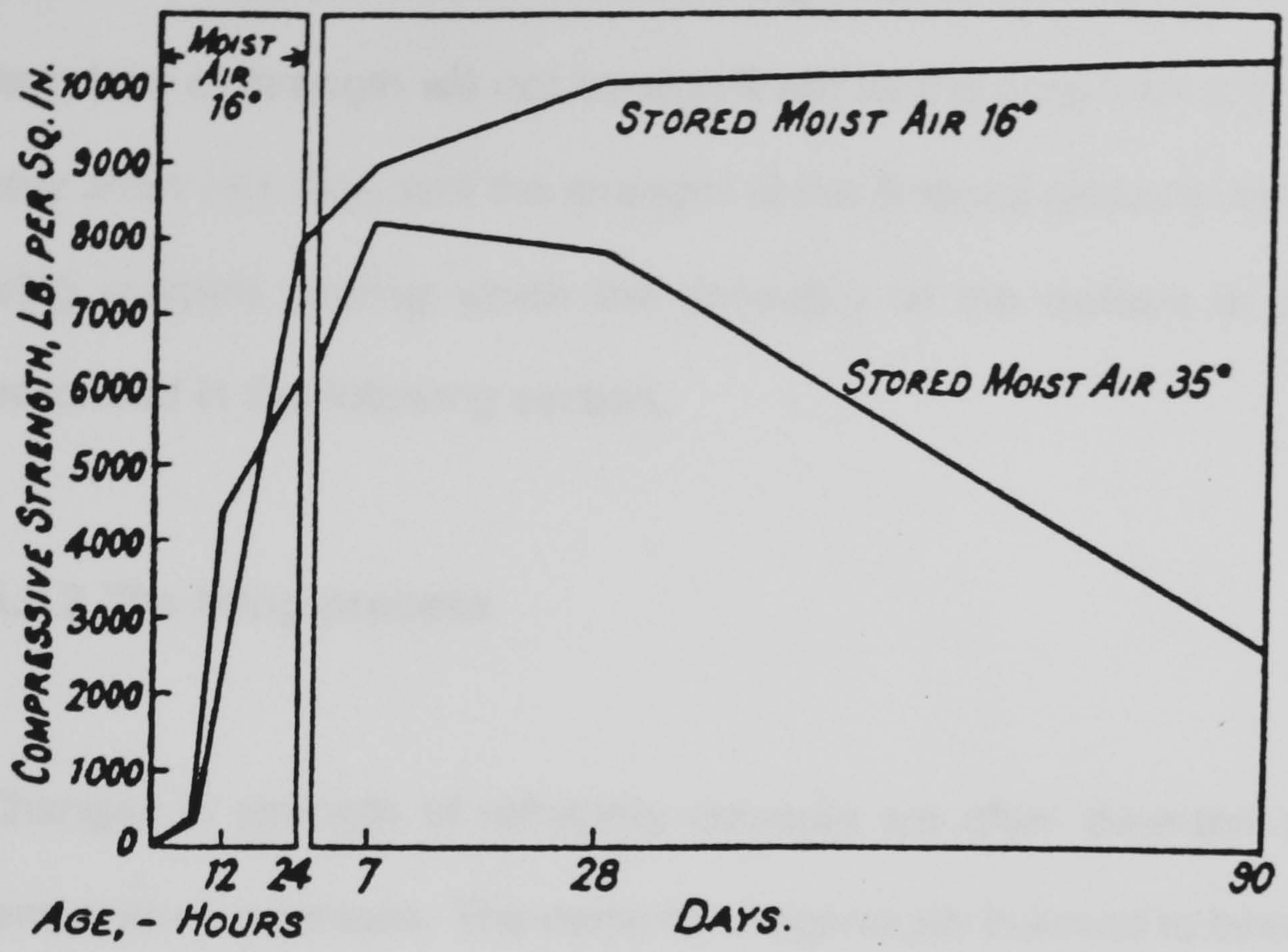

Figure A.3.2 Effect of Air Storage Conditions on Strength of High Alumina Cements

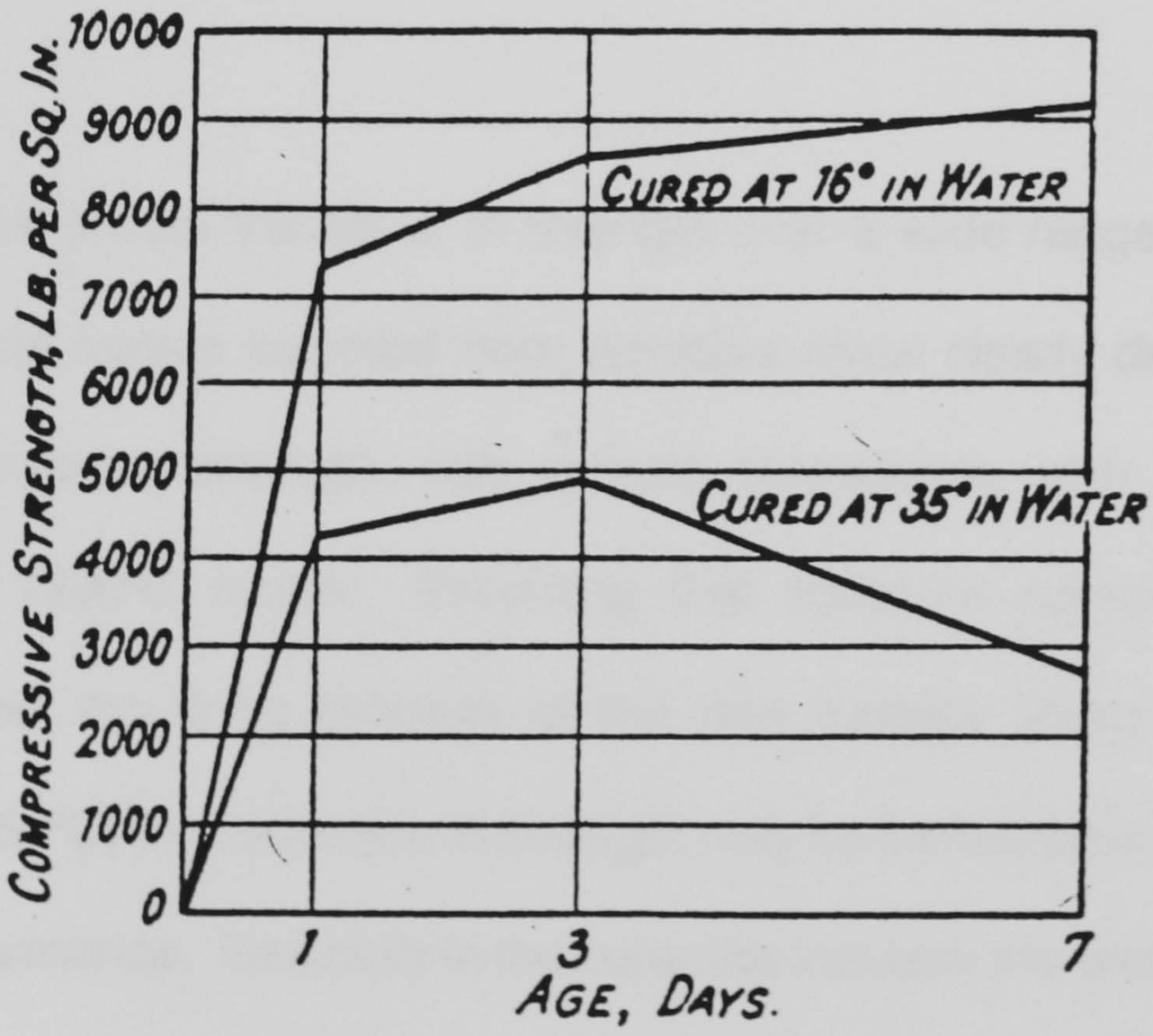

Figure A.3.3 Effect of Curing Conditions on Strength of High Alumina Cement

Due to the nature of the new furnace lining material it is envisaged that this long term loss of strength will not be significant as the cure time of the material is very short (<1 day) and the strength of the finished product comes from the firing process (during which the chemistry of the cement is changed) as described in the following section.

A.3.2 The firing process

Changes in strength of refractory cements are often detected as the firing temperature increases. The cements are generally believed to become weaker between 100°C and 900°C, during the dehydration of the hydraulic bonds, but recover their strength at higher temperatures when "ceramic" bonds begin to form[3].

Figure A.3.4 shows the fall of in strength over a wide range of temperature. These typical curves selected from literature show clearly defined minima of cold compressive strength, with various aggregates, after pre-firing in the 1000°C to 1200°C range. Providing that sufficient compressive strength remains after the firing process of the new furnace lining material (at the moment 1150°C) the reduction in strength may be beneficial in terms of thermal shock performance. Generally in the ceramics industry it is well recognised that by keeping the microstructure poorly bonded a high degree of thermal shock resistance may be achieved.

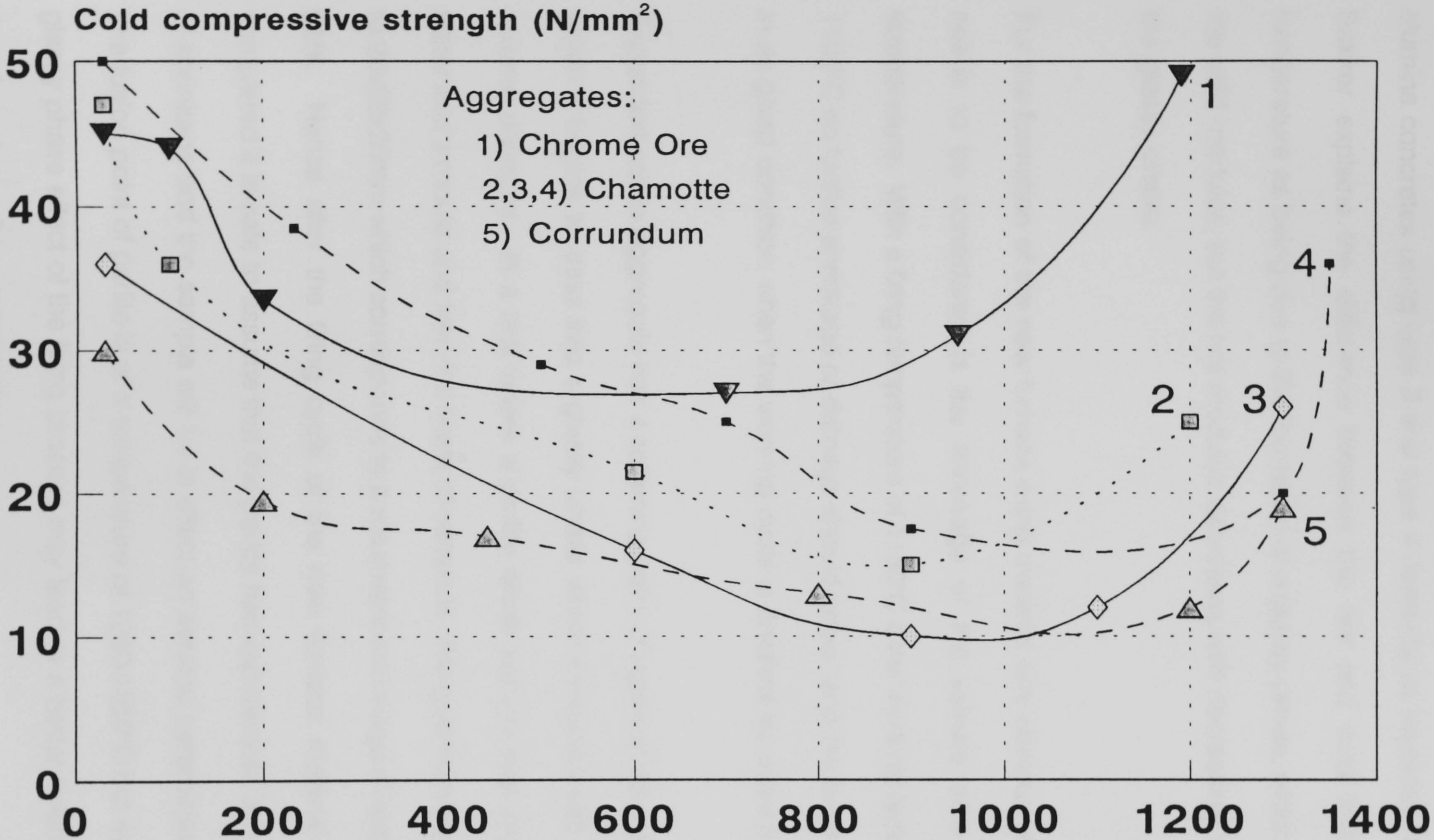

Figure A.3.4 - Variation with temperature of pre-heat of the cold compressive strength of aluminous concretes with various aggregates.

Figures A.3.5 and A.3.6 show the hot and cold moduli of rupture of 40-50% alumina concretes using type 3 and type 4 cements as reported by Bakker[8]. Bakker explains the difference between the hot and cold MOR at high temperature as being due to the formation of a glassy phase, which increases the cold modulus, but the hot modulus decreases with decreasing viscosity of the glassy phase.

For the formation of the new furnace lining material one obvious effect which needs to be considered is the shrinkage of the sample with increased temperature. With a firing temperature of 1150°C if the working temperature is 1100°C no further shrinkage or damage should occur, and the brick should be in as good condition when the working cycle is finished as when it started.

Expanded perlite aggregate has a softening point of approximately 870°C after which it begins to pass into a glassy phase which coincides with very large volume changes. In a test where a perlite alone sample was pressed with water into a mould and fired the linear dimensions changed from 54x52x51mm to 26x26x20mm which corresponds to a volumetric shrinkage of approximately 90%. Hence after the firing cycle of the new furnace material has been completed it is safe to assume that the perlite has experienced a high degree of shrinkage and the sample will be in effect an aerated ceramicised cement. The fusion point of perlite is at a temperature of 1280-1350°C but even so, the glassy phase effect of the firing process may lead to a better finished sample than for a lower firing temperature.

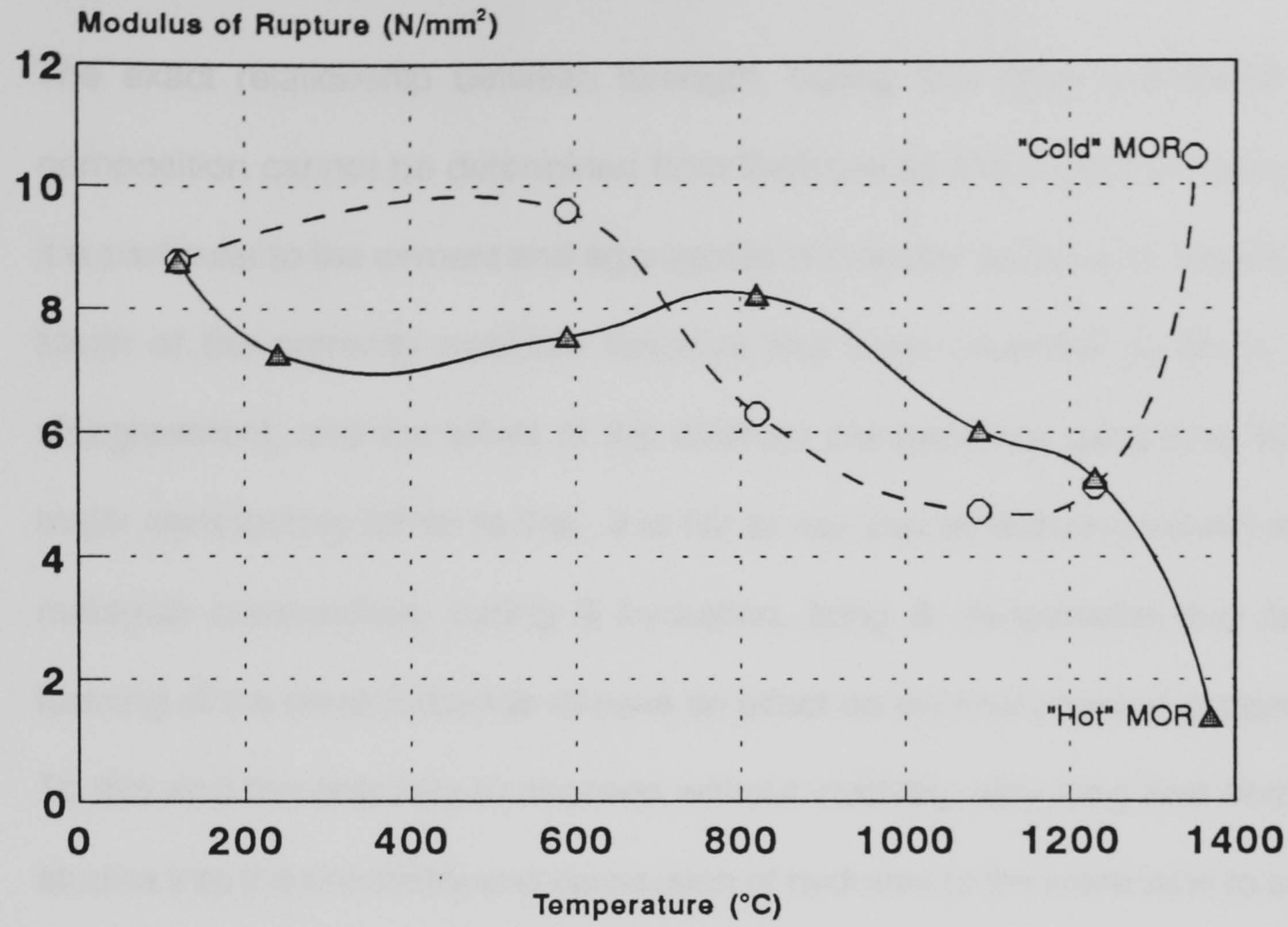

Figure A.3.5 - 45% Al_2O_3 - 55% type 3 refractory cement
Hot and Cold Moduli of Rupture against temperature

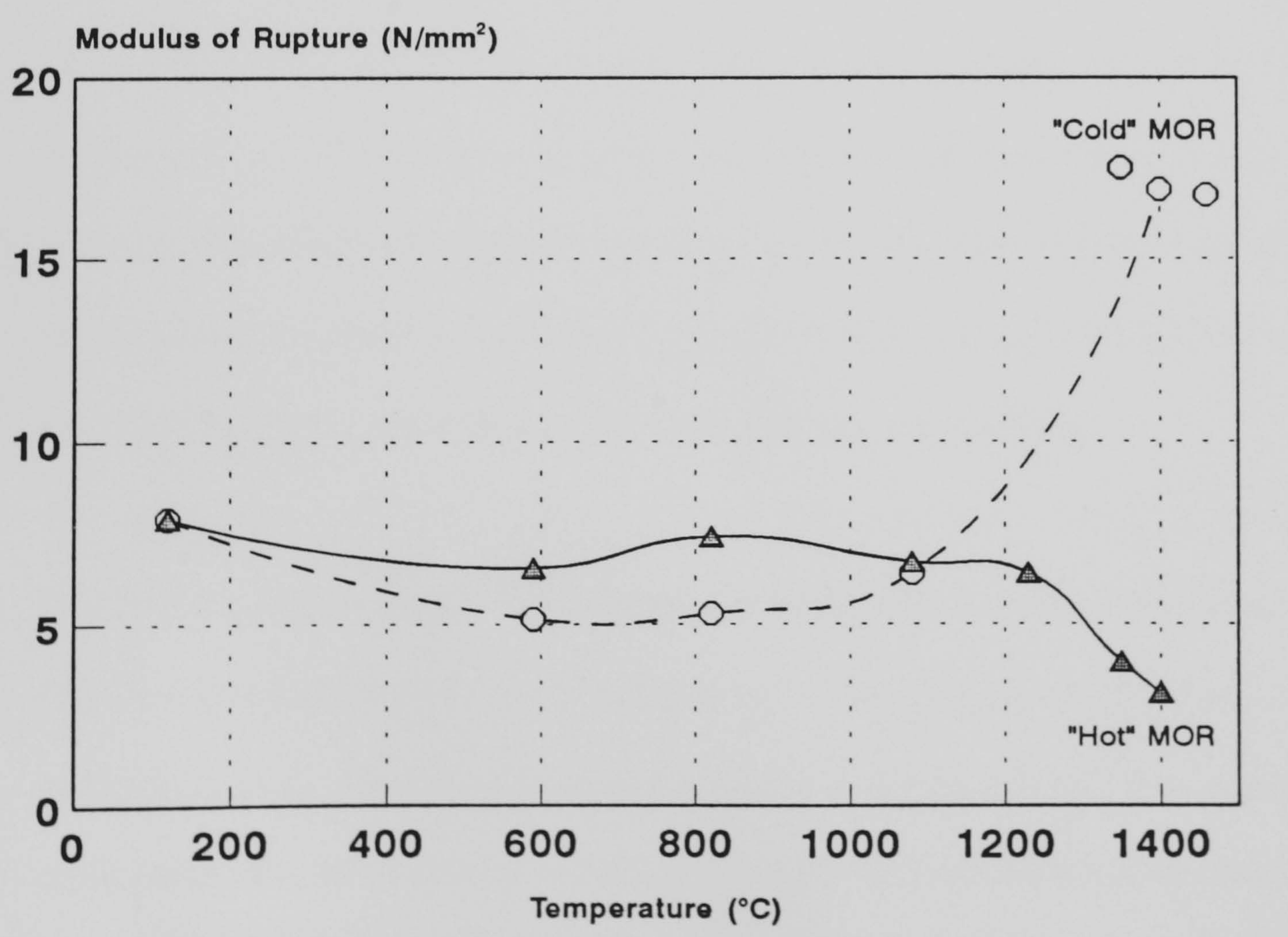

Figure A.3.6 - 50% Al_2O_3 - 50% type 4 refractory cement
Hot and Cold Moduli of Rupture against temperature

The exact relationship between strength, curing and firing conditions and composition cannot be determined from literature as it is more than likely that it is particular to the cement and aggregates chosen for a particular application. Much of the currently available literature has been reported[3] to be in wide disagreement, and the effect of the different compositions used may be the major contributory factor to this. It is fair to say that all factors involved with a materials composition, curing & hydration, firing & dehydration and hence forming of the ceramic bonds all have an effect on the final physical properties. To this end the only way to proceed without involving very long and complex studies into the chemistry and conversion of hydrates of the material is to adopt the long standing research method of "trial and error".

A.4 A new approach to furnace linings.

The objective of the experimental programme was to develop a modular system for furnace linings which had beneficial properties when compared to traditional lining materials such as refractory concrete, fire bricks and ceramic wool. For the purpose of research the manufactured units were brick shaped for ease of production and use. It was proposed that the brick developed would show energy savings at the same thickness as ceramic wool and be inherently free from fibre related problems. The majority of fire bricks are medium density and formed from a fired mixture of fire clay and crushed fire brick as an aggregate. The use of crushed fire brick as an aggregate helps minimise shrinkage during the firing process. Refractory concretes are high density castables which are, as a rule, fired in-situ during the first run of the furnace. The major disadvantages of both these materials with respect to ceramic fibre systems are both their thermal conductivities and density. The new material developed would have the advantages of being non-fibrous and easy to install, but would be relatively light weight and have a low thermal conductivity.

Due to the excellent performance of the cement-perlite panels manufactured for fire testing within the research programme it was decided that this type of composite may provide an excellent furnace lining material if it could be developed with other criteria in mind. In particular the new material should be able to withstand high temperatures without fracturing, distorting or disintegrating. Four cements produced by Lafarge Specialist Cements[9] were

investigated . These were ciment fondu, Secar 51, Secar 71 and Secar 80. The pyrometric cone equivalent (melting point) temperatures of neat cement pastes of these cements are 1270°C, 1440°C, 1680°C and 1750°C respectively. It was anticipated that Secar 51 would be the most suitable material with a maximum continuous operating temperature of about 1350°C.

A.4.1 Initial research

The new material to be developed will be referred to as **Insuline** for the remainder of this appendix. Upon further investigation into the capabilities of the cements it was decided that although Ciment Fondu is the cheapest of the cements, and cost being an important consideration (with respect to capital costs of re-lining a furnace), its iron content would render it unsuitable for reducing atmospheres. It was hence decided that the prime material for investigation should be based around Secar 51, although the advantages of using higher grade cements would also be investigated.

Compositions made from similar raw materials as Insuline have been investigated in great detail as a fire resistant core for sandwich panels. In that particular use (Voidfill) the materials were prone to crazing during the fire test (indicating shrinkage of the sample) and were relatively brittle with low bending strengths. These limitations in strength do not restrict the use of similar compositions for furnace linings. The indicated shrinkage of the materials on exposure to high temperatures would restrict the use of the compositions. It

was first important to devise a method of manufacture which would produce samples free from flaws and defects which would not crack on firing. It was envisaged that the perlite content of the bricks would shrink to a small glassy bead during firing leaving a very finely aerated cement-ceramic body.

Preliminary investigations were made on brick sized samples (≈220 x 110 x 70mm). The materials for the initial specimens were Tilcon perlite pack 3, cements Secar 51, 71 and 80, and water. Pack 3 perlite was a non-graded material typically used for non-demanding applications such as filling timber floor voids. The samples were mixed with care by turning in a polythene bag before mechanical mixing with water to form the pressable material. The mechanical mixing time was kept to a minimum to retain as much volume of material as possible. The brick shaped samples were compressed in a mould to the finished size, although a small degree of "recovery" was noticed when the bricks were released from the mould.

The first samples to be manufactured (mix A) were made to the following mix proportions:

Perlite (729g), Cement (594g), Water (954g)

giving an aggregate-cement ratio of 1.23, and a water-cement ratio of 1.61. The samples were then placed in polythene bags and cured at high humidity for 5 days after which they were air dried for three weeks. The samples were then dried at 110°C in a fan assisted oven to constant temperature. A programmable electric kiln was used for the firing process. The kiln

temperature was programmed to climb at 60°C per hour to a temperature of 1150°C, followed by a dwell of 10 hours, and finally natural cooling to room temperature. The total firing regime is shown in **figure A.4.1** below.

The samples were mounted to a furnace door as shown in **figure A.4.2** and the test results are shown in **figure A.4.3 and A.4.4**. The results from this test were used in a finite difference numerical analysis program was used to predict that the cold face temperatures at 210 and 250mm thick would be 70.6 and 64.2°C respectively. These predictions were very encouraging for the possible use of Insuline as a furnace lining material. Crude measurements taken before and after the firing process indicated that a linear shrinkage of 4-6% could be expected. After the samples were tested they were removed from the furnace door and exposed to thermal cycling between 1100°C and 300°C. The face temperature was monitored with a contact thermocouple. Twenty five heating and cooling cycles were applied, with a typical heating time of six seconds, and a cooling time of twenty four seconds. In the test series there was no apparent damage to the bricks indicating that the thermal shock characteristics were good.

Subsequent samples manufactured by a similar manner (but no air-drying) showed signs of drying shrinkage with very faint cracks being observed on the bricks surfaces. The firing process opened up these cracks to the point where the bricks were rendered useless. Several samples were marked with gauge points and measured carefully during the whole of the manufacturing period.

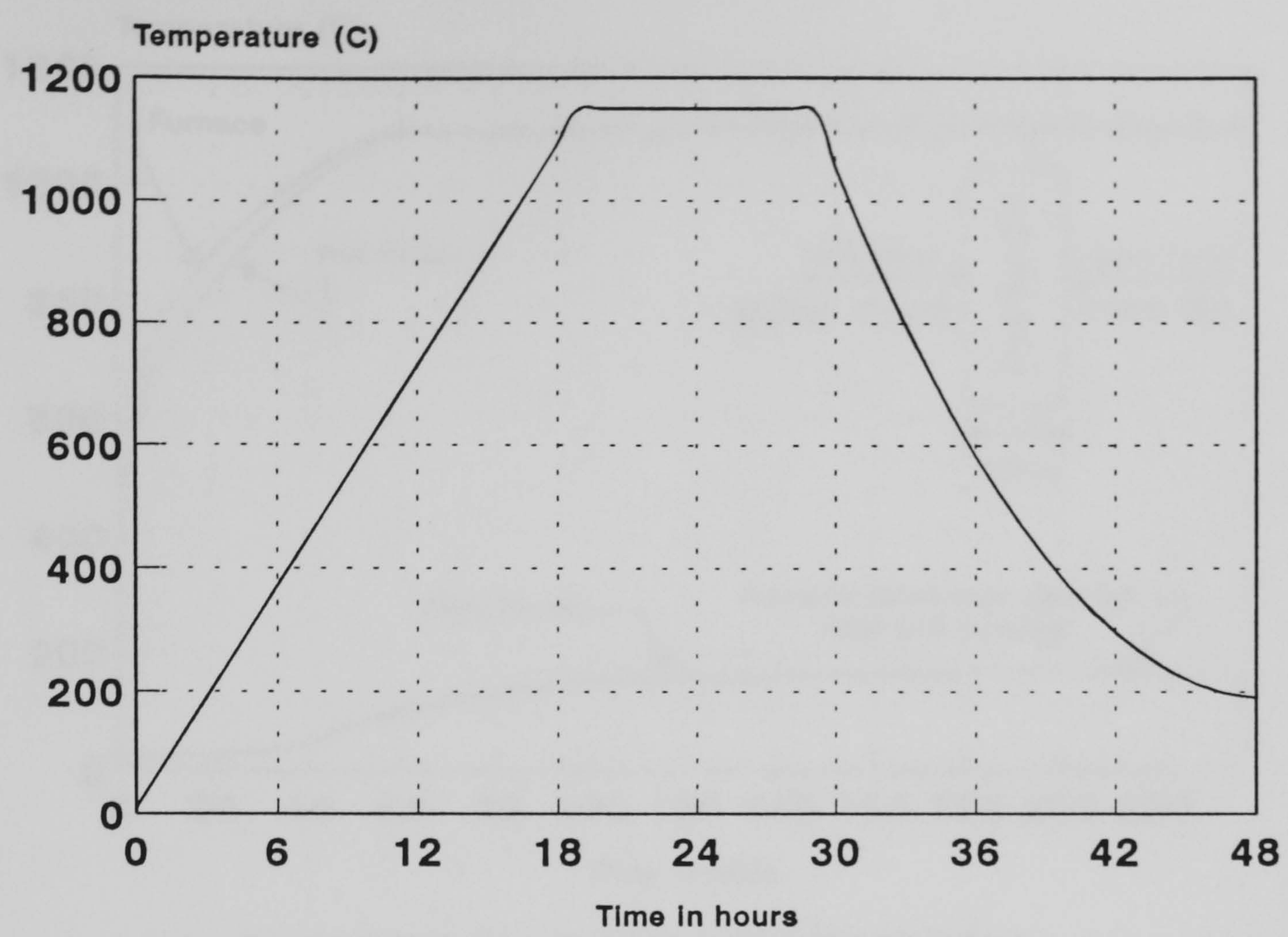

Figure A.4.1 - Carbolite Kiln Firing Cycle for New Furnace Lining Material

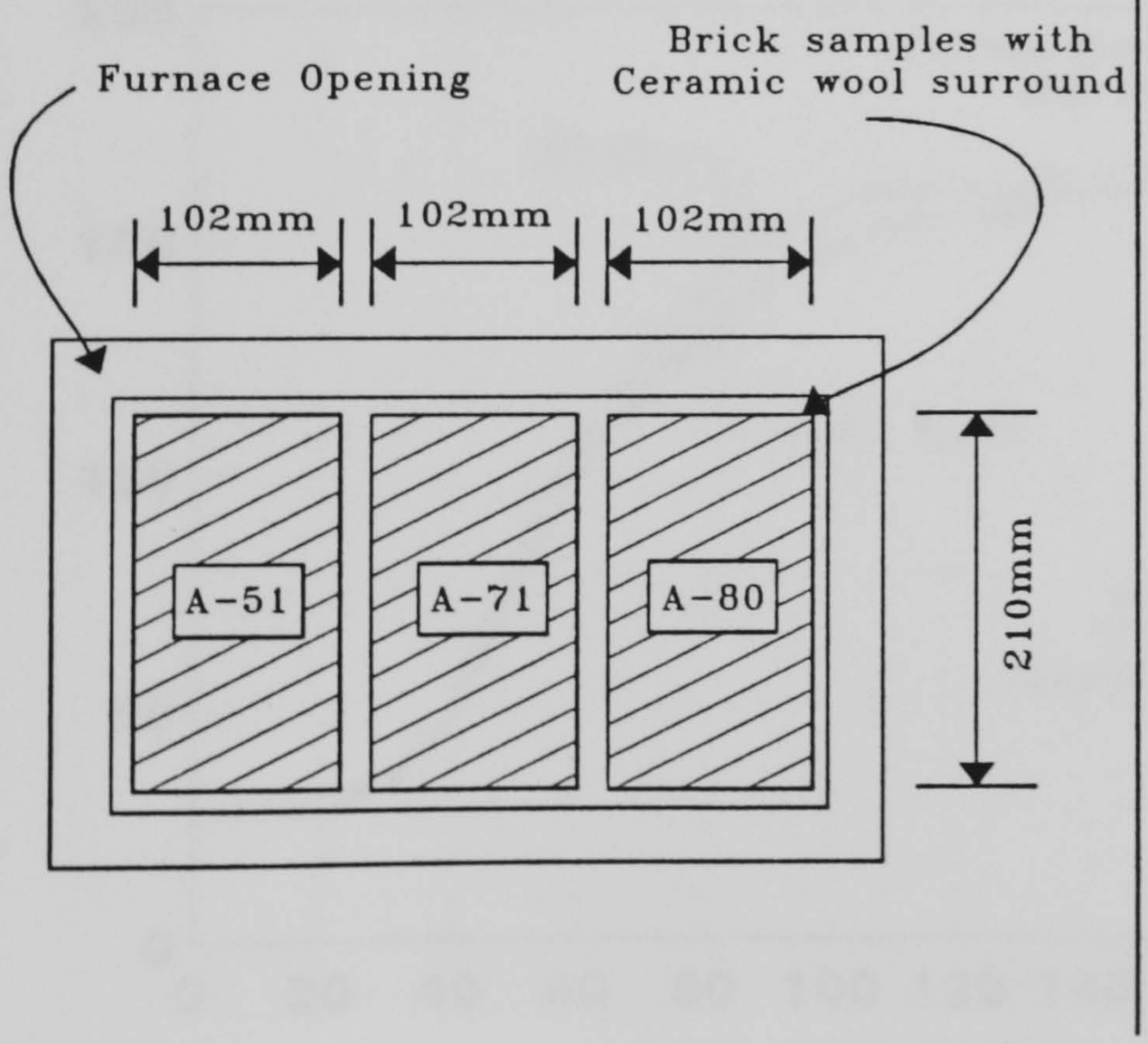

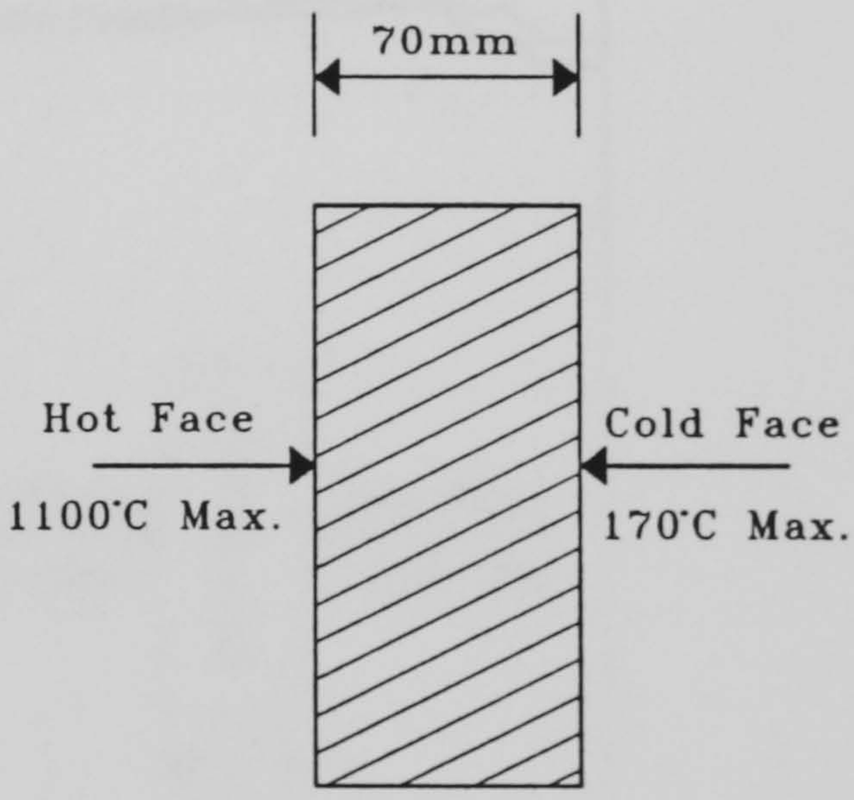

Figure A.4.2 General Arrangement of Preliminary Furnace Test

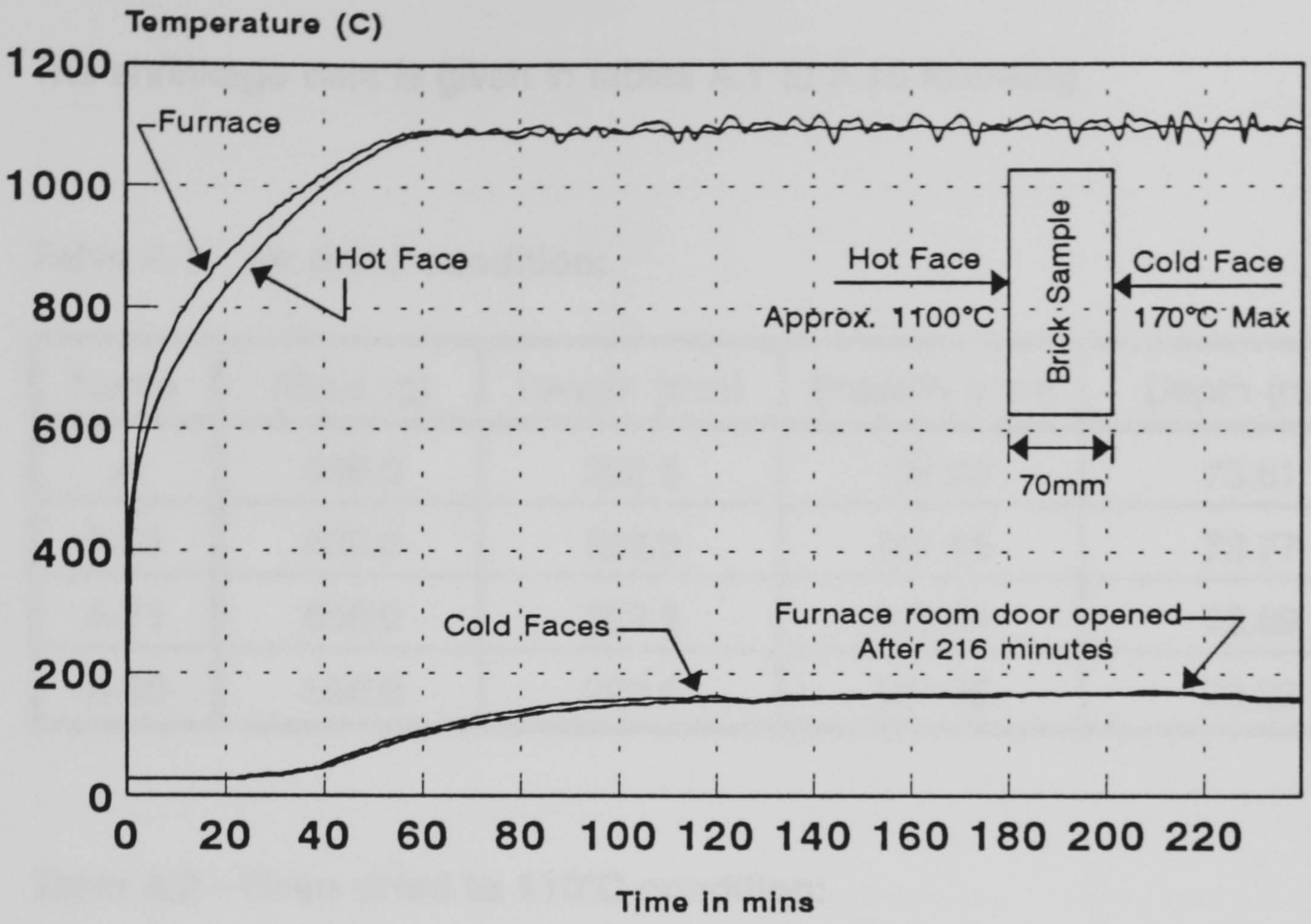

Figure A.4.3 - Insuline Brick Samples Fire Test
25-08-94 Salford University, Small Furnace.
Furnace, hot face and cold face temperatures.

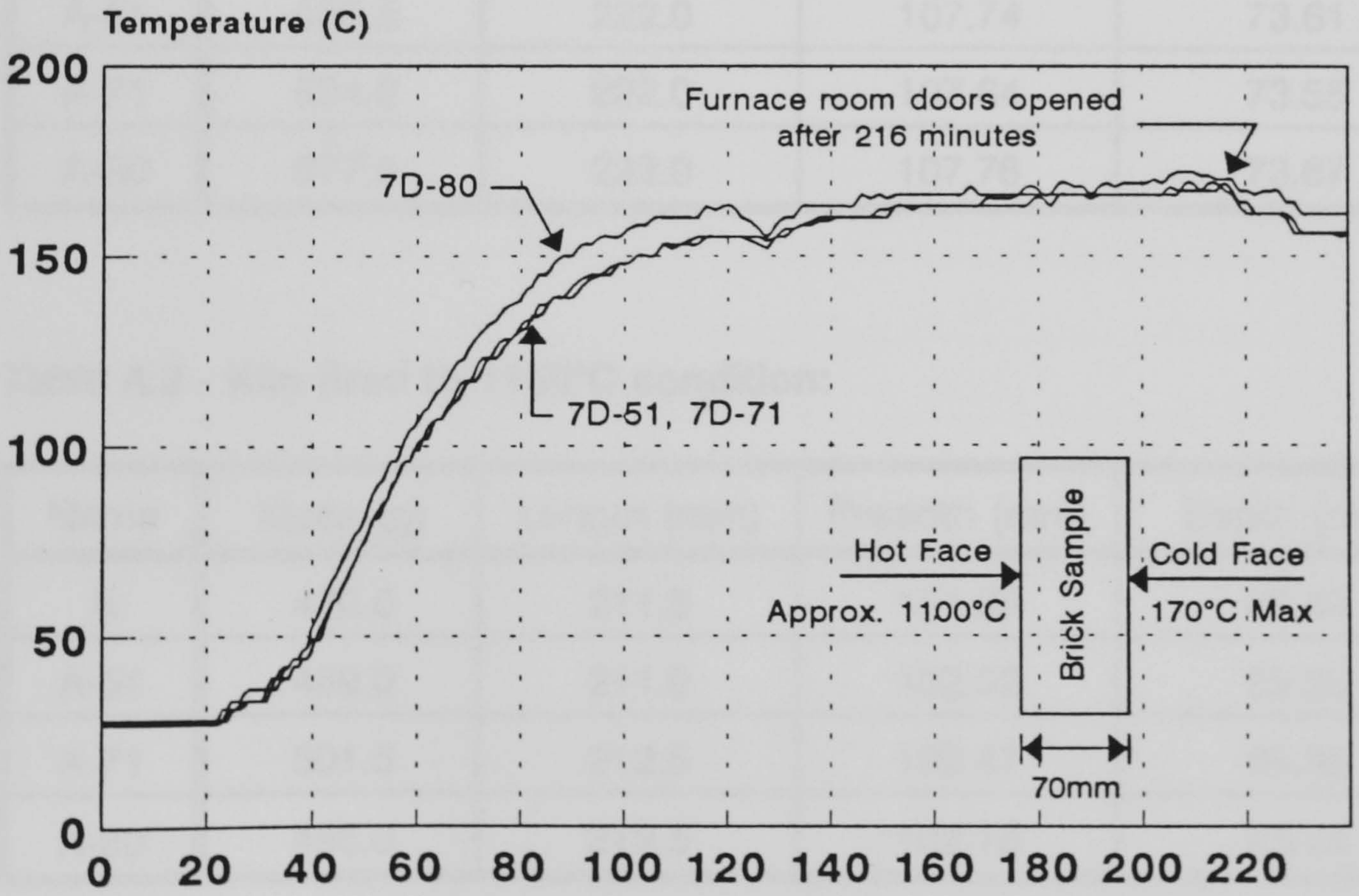

Figure A.3.5 - Insuline Brick Samples Fire Test
25-08-94 Salford University, Small Furnace.
Cold face temperatures only.

The shrinkage data is given in tables A.1 to A.10 following.

Table A.1 **- Air dried condition:**

Name	Mass (g)	Length (mm)	Breadth (mm)	Depth (mm)
A	596.0	222.5	107.99	73.61
A-51	630.0	222.5	107.98	73.77
A-71	656.0	222.5	107.84	73.69
A-80	598.0	222.5	107.98	73.93

Table A.2 **- Oven dried to 110°C condition:**

Name	Mass (g)	Length (mm)	Breadth (mm)	Depth (mm)
A	569.5	222.0	107.79	73.52
A-51	598.5	222.0	107.74	73.61
A-71	634.0	222.0	107.64	73.55
A-80	577.5	222.0	107.76	73.67

Table A.3 **- Kiln fired to 1150°C condition:**

Name	Mass (g)	Length (mm)	Breadth (mm)	Depth (mm)
A	470.0	211.5	101.88	69.40
A-51	489.0	211.0	102.02	69.56
A-71	501.5	212.5	102.47	69.86
A-80	496.0	212.5	102.18	69.44

Breadth and depth measurements made with digital Vernier rule.

Table A.4 **- Brick Densities:**

Condition	A	A-51	A-71	A-80
Cured/Air Dried	336.97	355.46	371.29	336.67
Oven Dried (110°C)	323.71	339.94	360.73	327.68
Air Conditioned	330.62	345.31	365.69	332.28
Fired (1150°C)	314.30	326.57	329.68	328.96

Densities given in Kg/m^3

Table A.5 **- Mix A Brick linear shrinkage (wrt original):**

Condition	Length(%)	Breadth(%)	Depth(%)
Cured/Air Dried	0	0	0
Oven Dried	0.2	0.19	0.12
Air Conditioned	0.2	0.16	0.18
Fired	4.94	5.66	5.72

Table A.6 **- Mix A-51 Brick linear shrinkage (wrt original):**

Condition	Length(%)	Breadth(%)	Depth(%)
Cured/Air Dried	0	0	0
Oven Dried	0.2	0.22	0.22
Air Conditioned	0.2	0.2	0.23
Fired	5.17	5.52	5.71

Table A.7 **- Mix A-71 Brick linear shrinkage (wrt original):**

Condition	Length(%)	Breadth(%)	Depth(%)
Cured/Air Dried	0	0	0
Oven Dried	0.2	0.19	0.19
Air Conditioned	0	0.15	0.18
Fired	4.49	4.98	5.20

Table A.8 - **Mix A-80 Brick linear shrinkage (wrt original):**

Condition	Length(%)	Breadth(%)	Depth(%)
Cured/Air Dried	0	0	0
Oven Dried	0.2	0.2	0.32
Air Conditioned	0.2	0.28	0.31
Fired	4.49	5.37	6.07

After the first firing cycle and subsequent cooling, the bricks were fired again to exactly the same cycle to determine if any further shrinkage or damage would be incurred. The inspection of the samples after the second firing showed that no extra damage had occurred and that the sample dimensions/shrinkages were as shown in the following tables.

Table A.9 - **Brick dimensions after second firing (including densities/shrinkages)**

Name	Mass (g)	Length (mm)	Breadth (mm)	Width (mm)	Density (kg/m^3)
A	470.0	210.0	101.73	69.28	317.6
A-51	487.0	210.0	101.83	69.43	328.0
A-71	500.0	212.5	102.39	69.76	329.4
A-80	495.0	211.5	102.01	69.38	331.1

Table A.10 - **Linear shrinkage after second firing (w.r.t original)**

(Shrinkage after first firing shown in brackets)

Name	Length(%)	Breadth(%)	Depth(%)
A	(4.94) 5.62	(5.66) 5.62	(5.72) 5.76
A-51	(5.17) 5.62	(5.52) 5.70	(5.71) 5.88
A-71	(4.49) 4.49	(4.98) 5.05	(5.20) 5.33
A-80	(4.49) 4.94	(5.37) 5.52	(6.07) 6.15

A.4.2 Further development work

The need to produce fired, crack-free samples was of paramount importance in the development work. For ease of volume retention it was decided to use Tilcon grade 2JS perlite, which has a lower bulk density than pack 3. The standard adopted mix was for an aggregate-cement ratio of 0.8 and a water-cement ratio of 1.35. Slabs of insuline were used for this section of the development work in order to ensure that all samples had the same processing conditions. In this way a slab could be made and have sections removed from it at the required curing duration, for instance 24 hours, 3 days, 7 days etc.

The slabs were manufactured with Secar 51 cement and 2JS. A 300 x 300 x 50mm slab had the following mix proportions (now referred to as mix 1):

Secar 51 - 833g, Perlite 2JS - 667g, Water - 1125g.

After the first cure period the samples were cut in half using a circular saw, and one half returned to its original curing conditions. The other half was cut again, one section being dried at 110°C, the other being placed in a roaster bag and heated at 110°C. The process of sealing in a roaster bag and heating to 110°C will be referred to as "re-heating" in the following text.

The code numbers listed in the results refer in sequence to the mix number, the curing temperature (i.e. RT = room temperature, 40 = 40°C cure temperature), the cure time in days, and the drying condition (R = dried in the bag). Some codes also carry the letter "W" meaning the sample was soaked in water prior to compression testing. The letter "P" means that the sample was tested after curing but without being dried. Edge samples where tested are marked with an asterisk, when making the slab if level grading was used the edge samples were weaker than the internal ones, if more mix was used in the edges they were stronger than the internal samples.

A.4.3 Compression test results for different curing methods.

Notes:

Samples 1-RT-1R correctly processed but air conditioned for 6 days after drying.

Samples 1-RT-3 were air dried after 3 days, then oven dried as normal.

Samples 1-RT-3R were left for 6 days before re-heating.

Samples 1-RT-7R were re-heated in a plastic bag which melted away causing damage to the surfaces of the tested material after being peeled off.

1-RT-1R	Dimensions	Density(kg/m^3)	σ_{cr}(N/mm^2)
A	46.2x49.9x51.1	364	0.556
B	46.2x48.9x51.1	371	0.589
C*	46.2x48.9x49.9	373	0.439

1-RT-3R	Dimensions	Density(kg/m^3)	σ_{cr}(N/mm^2)
A	47.1x50.2x50.0	355	0.410
B	47.1x49.9x50.3	367	0.604
C	47.1x49.9x50.6	395	0.466

1-RT-3	Dimensions	Density(kg/m^3)	σ_{cr}(N/mm^2)
A	46.5x50.3x50.0	368	0.496
B	46.5x50.6x49.8	371	0.599
C	47.5x50.6x50.4	406	0.580

1-RT-7	Dimensions	Density(kg/m^3)	σ_{cr}(N/mm^2)
A	47.7x50.2x50.9	361	0.740
B	47.8x50.1x51.2	380	0.879
C	47.1x50.3x51.3	383	0.765

1-RT-7W	Dimensions	Density(kg/m^3)	σ_{cr}(N/mm^2)
A	50.3x47.8x51.1	374(dry)	0.673
B	51.4x50.4x47.4	369(dry)	0.639
C	50.4x47.3x50.8	363(dry)	0.647

1-RT-7R	Dimensions	Density(kg/m^3)	σ_{cr}(N/mm^2)
A	46.1x50.1x50.6	401	0.755
B	49.4x50.5x51.3	352	0.653
C	49.6x50.0x50.6	377	0.661
D	49.3x50.3x51.1	390	0.599
E	49.6x51.1x51.2	374	0.696
F	46.5x49.9x50.3	386	0.693

1-RT-0R	Dimensions	Density(kg/m^3)	σ_{cr}(N/mm^2)
A	49.2x46.3x51.3	381	0.636
B	49.2x46.0x51.7	381	0.594
C	49.2x46.1x51.8	393	0.616

1-RT-0RW	Dimensions	Density(kg/m^3)	σ_{cr}(N/mm^2)
A	49.2x46.6x51.4	386	0.590
B	49.4x46.3x51.4	376	0.560
C	49.3x46.3x51.7	392	0.556

1-RT-1	Dimensions	Density(kg/m^3)	σ_{cr}(N/mm^2)
A	47.6X47.1x50.6	357	0.520
B	47.4x47.5x50.4	357	0.520
C	47.4x47.1x50.6	359	0.570

1-RT-1R	Dimensions	Density(kg/m^3)	σ_{cr}(N/mm^2)
A	46.2x47.4x50.6	381	0.450
B	47.4x47.2x51.2	385	0.560
C	47.4x47.4x51.0	384	0.550

1-RT-3	Dimensions	Density(kg/m^3)	σ_{cr}(N/mm^2)
A	47.2x47.0x50.4	358	0.530
B	47.4x47.1x50.9	362	0.570
C*	47.3x47.2x50.8	366	0.620

1-RT-3R	Dimensions	Density(kg/m^3)	σ_{cr}(N/mm^2)
A	46.5x47.4x50.7	367	0.580
B	47.6x47.4x50.9	378	0.640
C	46.4x47.5x50.7	363	0.490

1-40-0R	Dimensions	Density(kg/m^3)	σ_{cr}(N/mm^2)
A	49.4x49.1x50.0	351	0.450
B	49.2x49.2x50.1	367	0.460
C	49.2x49.1x50.7	364	0.450

1-40-1	Dimensions	Density(kg/m^3)	σ_{cr}(N/mm^2)
A	46.1x47.6x50.8	391	0.720
B	47.6x45.0x50.8	377	0.790
C	47.3x47.2x50.3	374	0.670

1-40-1R	Dimensions	Density(kg/m^3)	σ_{cr}(N/mm^2)
A	48.2x47.4x50.6	377	0.570
B	47.2x47.9x50.1	349	0.540
C	47.3x47.5x50.3	363	0.510

1-40-3	Dimensions	Density(kg/m^3)	σ_{cr}(N/mm^2)
A	47.2x47.3x50.8	363	0.570
B	47.3x47.3x50.8	370	0.600
C*	47.1x46.6x51.2	382	0.770

1-40-3R	Dimensions	Density(kg/m^3)	σ_{cr}(N/mm^2)
A	46.7x47.4x50.4	368	0.610
B	46.9x47.4x50.7	373	0.730
C	47.6x47.4x50.5	369	0.660

1-40-7	Dimensions	Density(kg/m^3)	σ_{cr}(N/mm^2)
A*	47.7x47.7x51.0	413	0.980
B	47.7x45.9x50.7	374	0.830
C	47.9x45.9x50.5	361	0.700

1-40-7R	Dimensions	Density(kg/m^3)	σ_{cr}(N/mm^2)
A	47.1x47.1x50.8	365	0.760
B	47.2x47.4x50.6	367	0.800
C*	47.2x46.8x50.5	390	0.810

1-40-7P	Dimensions	Density(kg/m^3)	σ_{cr}(N/mm^2)
A	47.3x47.6x50.9	510(wet)	0.550
B	47.5x47.4x50.8	516(wet)	0.630
C	47.3x47.3x50.5	491(wet)	0.530

As expected it can be seen from the results that dried samples are stronger than damp or saturated specimens. Heating to 110°C in a roaster bag appeared to have a detrimental effect on compressive strength in all cases. This could possibly be due to accelerated conversion of the high alumina cements. Also for both curing temperatures the compressive strengths are not consistent. The one day cure strengths are higher than the three day, and the seven day strength higher than the one day.

A.4.4 Investigation into the Effect of Density and Curing time on Strength of Samples.

In the following tables the samples were made brick shaped (220x110x70mm) and tested without cutting to get a more representative set of results for expected strength.

In *Table A.11*, all bricks were made to mix 1 ratios (aggregate-cement ratio = 0.8, water-cement ratio = 1.35), with varying quantities of wet-mix used for the target densities stated. In all cases the cement used was Secar 51, aggregate was perlite 2JS. Samples were cured for 24 hours, bagged at room temperature.

Table A.11 - **Compressive Strength Variation with Density for 2JS, Mix 1 Bricks.**

Target Density (kg/m^3)	Actual Density (kg/m^3)	Comp. Strength (N/mm^2)
400	437	1.07
400	409	0.82
400	419	0.91
375	399	0.75
375	392	0.76
375	406	0.81
350	371	0.57
350	376	0.69
350	374	0.61
325	351	0.41
325	350	0.41

The compression test results are shown in **Figure A.4.5** on a following page.

Table A.12 following shows the fast gain of strength which can be promoted by mixing the constituents in warm conditions (ie warmed cement and aggregates, hot water, and warm cure - bagged - at 40°C) The results of this experiment would tend to indicate that a very fast turn around of the samples may be possible as the brick units need have very little compressive strength in their own right. The samples were dried in a preheated oven at 110°C immediately after the quoted drying time was finished.

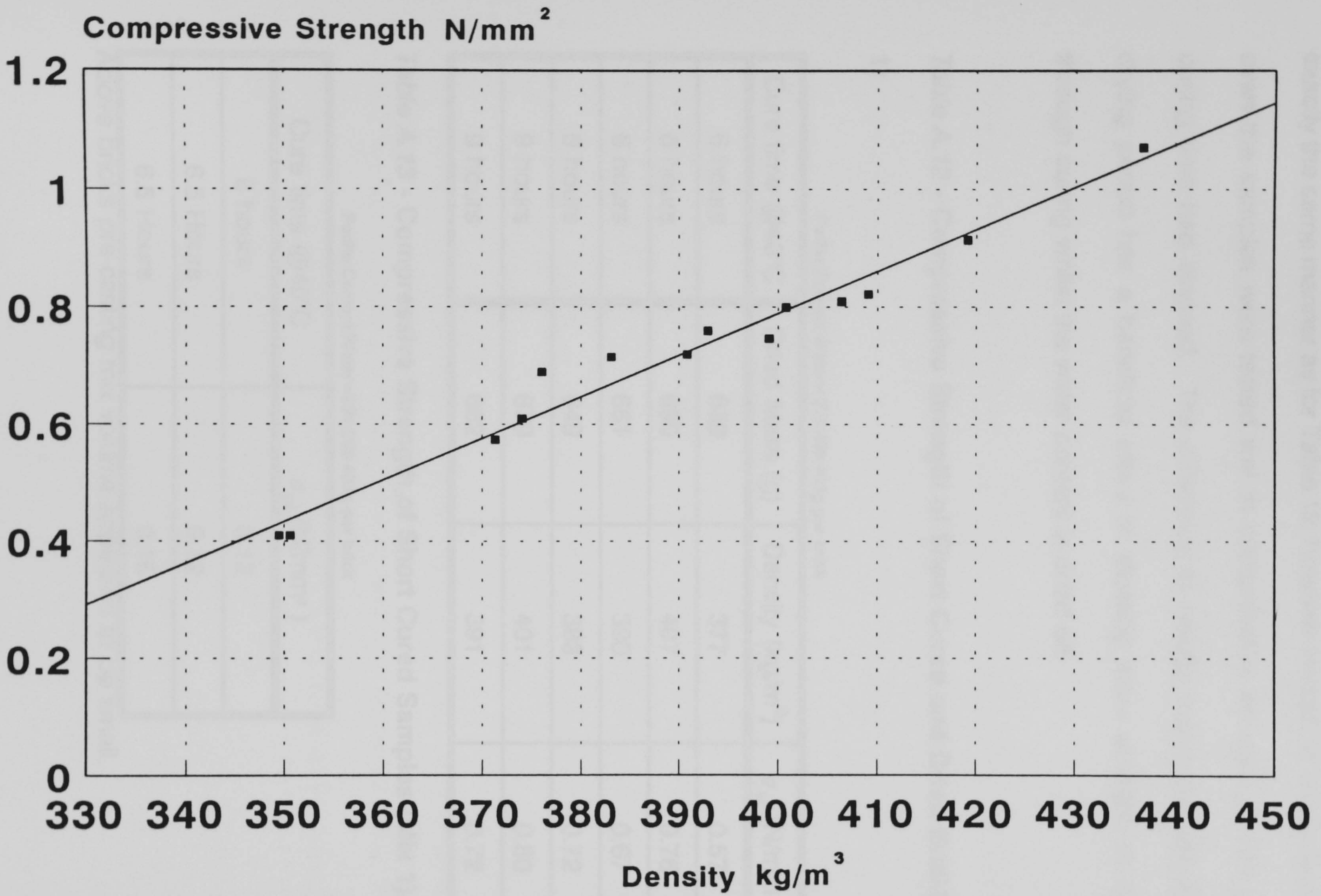

Figure A.4.5 - Brick Compressive Strength .v. Density
Perlite Grade 2JS
Mix 1 - Densities 330-450 kg/m³

Table A.13 following gives the results for the brick samples manufactured in exactly the same manner as for Table 12, however instead of being dried in the oven the samples were tested wet in compression as soon as the quoted curing time had elapsed. The difference in results would indicate that the drying period has a beneficial effect of allowing more strength to develop through curing whilst the water content is dried off.

***Table A.12* - Compressive Strength of Short Cured and Dried BrickS (Mix 1)**

Perlite:Cement:Water=239:298:403g per brick

Cure time @40°C	Dried Mass (g)	Density (kg/m^3)	σ_{cr} (N/mm^2)
6 hours	639	377	0.57
6 hours	690	407	0.76
6 hours	661	390	0.67
9 hours	649	383	0.72
9 hours	679	401	0.80
9 hours	662	391	0.72

***Table A.13* - Compressive Strength of Short Cured Samples (Mix 1).**

Perlite:Cement:Water=239:298:403g per brick

Cure time @40°C	σ_{cr} (N/mm^2)
6 hours	0.12
6.5 Hours	0.12
6.5 Hours	0.16

Above bricks pre-casting mix volume appeared to be small.

Due to the wet mix volume being particularly low for the low end densities with perlite 2JS it was decided to use a grade with a lower bulk density, this grade

was 2JL. *Table A.14* following shows the compressive strengths for bricks made with perlite 2JL, and 3JS (a much higher bulk density) which were made to investigate the effect on Perlite grade and density to higher extremes. The figure after the perlite grade in the sample name is the predicted density of the dried sample.

Samples 3JS-600 cured at room temperature had very poor edges due to the mix being over wet when moulding, hence faces being pulled away when the mould was released.

Samples 3JS-600 and 3JS-700 cured at 40°C had a reduced water content (due to the reduction of perlite surface area with using a coarser aggregate). The aggregate-cement ratio was unchanged, however the water-cement ratio was reduced to 0.89 from 1.35 (i.e. was reduced by one third).

After curing for the time stated in *table A.14* all samples were oven dried at 110°C for approximately 5 hours prior to testing - some samples had not reached a stable water content (i.e. fully oven dried) however the rate of water loss was slow for the hour prior to structural testing.

Table A.14 **- Compressive Strengths and Densities for 2JL and 3JS Bricks**

Sample	Approx. Cure Time (Hours)	Cure Temp (°C)	Density (kg/m^3)	σ_{cr} (N/mm^2)
2JL-300	48	20	339	0.21
2JL-300	48	20	343	0.21
2JL-300	48	20	347	0.22
3JS-600	48	20	659	1.16
3JS-600	48	20	687	1.17
3JS-600	24	40	609	1.31
3JS-600	24	40	613	1.48
3JS-700	24	40	712	2.43
3JS-700	24	40	701	1.80

As can be seen from *table A.14* a very high compressive strength may be obtained at still relatively low density. These brick densities have not been pursued further due to the obvious increase in cost of raw materials, and the likelihood that the distinct increase in density would lead to a much poorer material with regards to thermal efficiency.

Due to the seeming success in manufacturing bricks at the low end of the density range with perlite 2JL it was decided to manufacture a series of samples in the density range of 275-350kg/m^3. These bricks were manufactured once again to mix 1 proportions (aggregate:cement = 0.8, water:cement = 1.35) and were all mixed at elevated temperature using hot water (notionally 50°C). All samples were cured for 24 hours at 40°C in polythene bags to maintain a high humidity atmosphere, followed by immediate

drying at 110°C in a pre-heated oven. After the drying period all samples were inspected thoroughly and all samples appeared to be free from cracks. The compression test results for these bricks are shown in *table A.15*.

A further set of 2JL samples were mixed and cured at room temperature as a comparative sample. The samples were given a longer curing period of 48 hours, once again in polythene bags to maintain a high humidity atmosphere. The samples were tested in the wet state (ie no drying to promote the hydration of the cement and formation of the C_3AH_6/AH_6 structure). The compression test results for these samples are given in *table A.16*.

Table A.15 **- Compression test results for 2JL bricks (275-350kg/m^3)**

Sample	Approx. Cure Time (Hours)	Cure Temp (°C)	Density (kg/m^3)	σ_{cr} (N/mm^2)
2JL-275	24	40	284	0.37
2JL-275	24	40	270	0.31
2JL-275	24	40	275	0.34
2JL-300	24	40	297	0.36
2JL-300	24	40	289	0.32
2JL-300	24	40	308	0.40
2JL-325	24	40	334	0.52
2JL-325	24	40	320	0.46
2JL-325	24	40	310	0.44
2JL-350	24	40	362	0.71
2JL-350	24	40	343	0.60
2JL-350	24	40	332	0.55

Table A.16 - **Compression Test Results for 2JL Room Temperature Cured Bricks**

Sample	Approx. Cure Time (Hours)	Cure Temp (°C)	Density (kg/m^3)	σ_{cr} (N/mm^2)
2JL-300	48	20	339	0.21
2JL-300	48	20	343	0.21
2JL-300	48	20	347	0.22

The compression test results for the 2JL bricks cured at 40°C are shown on the following page in graphical form. **Figure A.4.6** shows the straight line trend of the compression test results.

A.4.5 Investigation of the Factors Effecting Drying and Firing Shrinkage and Cracking.

The problem of samples cracking during drying and firing was a distinct hindrance to the research development. If samples were to be evaluated fully it was necessary to investigate the effects of density, mix proportions, manufacturing methods and firing times on cracking of the samples, and to be able to manufacture crack free samples in good condition (i.e. a viable material from a mass production point of view).

The following sections describe samples made in order to evaluate the correct method required for production. In many cases, if a material was cracked after the drying cycle it was not fired as the effect would only be to open the fault

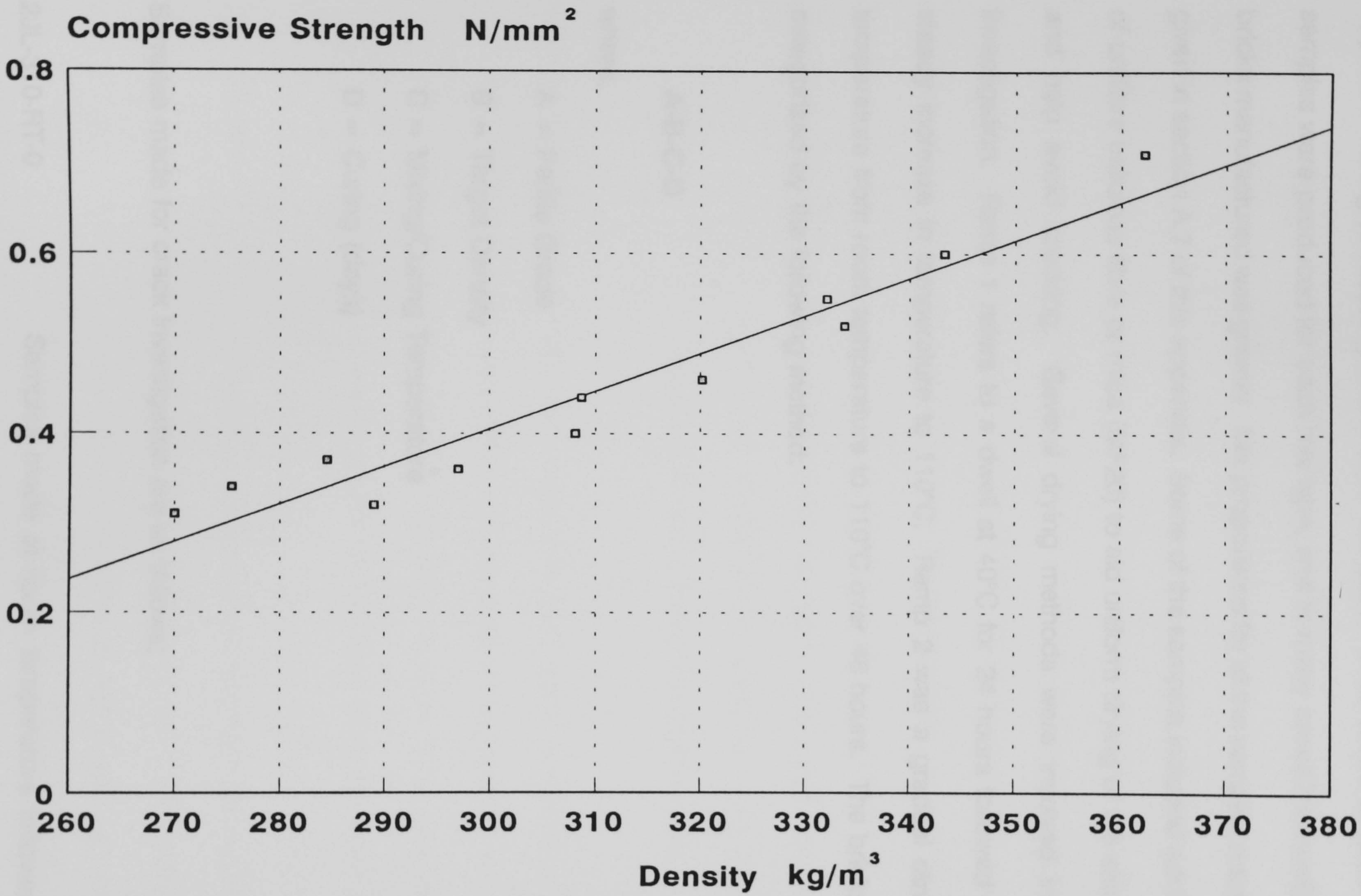

Figure A.4.6 - Brick Compressive Strength .v. Density
Perlite Grade 2JL
Mix 1 - Densities 270-370 kg/m³

further. An attempt has been made to describe the flaws (if any) which were apparent during processing of the brick samples. In all cases at least three samples were produced for each mix type, and in many cases the number of bricks manufactured was greater. Mix proportions for all the samples made are given in section A.7 of this appendix. Some of the samples included additions of unifibre cellulose fibre or mica (MF20) to aid uniform drying of the samples and help avoid cracking. Several drying methods were involved in this investigation. Ramp 1 refers to a dwell at 40°C for 24 hours followed by a steady increase in temperature to 110°C. Ramp 2 was a gradual climb in temperature from room temperature to 110°C over 48 hours. The bricks are categorized by the following method:

A-B-C-D

where,

A = Perlite Grade

B = Target Density

C = Mixing/Curing Temperature

D = Curing (days)

Samples made for crack investigation are as follows;

2JL-310-RT-0	Samples made at room temperature followed by drying immediately in a fan assisted oven at 110°C.

3 no. bricks appeared undamaged during this drying method. When the method was repeated with another 6 no. bricks all samples appeared to have cracked during drying.

2JL-310-RT-0(AIR)	Samples were made at room temperature and allowed to air dry at RT for 24 hours before drying in the oven at 110°C. All samples appeared to be uncracked after the drying cycle.
2JL-310-40-0	Samples made with warm water and immediately dried at 110°C after moulding. All samples appeared to crack during the drying cycle.
2JL-310-40-0(AIR)	Samples made with warm water and allowed to air dry at RT for 24 hours before being dried at 110°C. All samples had very slight cracking after drying, however edges were noticed to be extremely poor
2JL-275-RT-1	Samples made at room temperature followed by 24 hours bagged at room temperature. Samples were then dried immediately at 110°C and all samples appeared to have a slight degree of cracking/damage after drying.

2JL-310-RT-1	Curing/drying process same as 2JL-275-RT-1 above. Again, after drying all samples appeared to have some slight degree of damage.
2JL-350-RT-1	Curing/drying process same as 2JL-275-RT-1 above. All samples appeared to have cracked during the drying cycle.
2JL-310-RT-1(C2%)	Samples contained an addition of 2% weight of dry components of cellulose fibre which was dispersed in water prior to mixing. The curing/drying process was the same as 2JL-275-RT-1 above. All samples appeared to be damaged or cracked after the drying cycle.
2JL-310-RT-1(M2%)	Samples contained an addition of 2% weight of dry components of Mica (MF-20) which was dispersed by mixing dry prior to addition of water. The curing/drying process was the same as 2JL-275-RT-1 above. All samples appeared to be undamaged after the drying cycle.
2JL-310-RT-1(M4%)	Samples contained an addition of 4% weight of dry components of Mica (MF-20) which was dispersed

by mixing dry prior to addition of water. The curing/drying process was the same as 2JL-275-RT-1 above. All samples appeared to be slightly cracked after the drying cycle.

2JL-310-RT-1(RAMP1)	Samples were made at RT, followed by 24 hours bagged at room temperature. The sample were then dried at 40°C for 24 hours followed by a ramped climb from 40-110°C over 24 hours. All samples appeared to be undamaged after drying.
2JL-310-RT-0(RAMP2)	Samples were made at RT followed by immediate drying, unbagged, on a ramped temperature climb from RT to 110°C over 48 hours. All samples were cracked on the underside edges where the drying path had been obstructed by the moulding board/plastic sheet.
2JL-310-RT-0(RAMP1)	Samples were made at RT followed by immediate drying, unbagged, on a ramped temperature climb from RT to 110°C over 48 hours. All samples were cracked on the underside edges where the drying path had been obstructed by the moulding board/plastic sheet.

2JL-310-RT-1(RAMP1)	12 samples were made exactly as the 2JL-310-RT-1(RAMP1) samples previously. Bricks were measured carefully prior to drying cycle to get shrinkage data. Samples were dried to ramp 1 as described previously. After the drying cycle had been completed, inspection of the bricks showed severe cracking both longitudinal and across the bricks.
2JL-310-RT-5(RAMP1)	Samples made at room temperature as described previously, bagged and cured at room temperature for 5 days (to give a fuller curing period), removed from bags and dried to ramp 1. After drying, all samples were cracked on all faces.
2JL-310-RT-1(RAMP1)(P)	It was decided that the variation of particle size distribution may make a difference to the cracking of samples. To this effect 10, 20 and 30% of grade 2JL perlite was replaced by a corresponding mass of grade 2JS perlite in different samples. These samples were manufactured at room temperature and cured (bagged) at room temperature for 24 hours prior to drying to ramp 1. All samples were

cracked after the drying cycle.

2JL-310-RT-1(V) Samples were similar to those described for the grade 2JS perlite substitution above, however in this case fine grade vermiculite was used instead. Samples were cure for 24 hours (bagged) at room temperature followed by drying in a pre-heated oven at 110°C. Some samples showed faint drying cracks, but others appeared to be undamaged.

2JL-310-RT-1(V10)(M) Samples were manufactured with a 10% vermiculite substitution and also an addition of 4% Mica (MF20). The samples were mixed and cured (24hrs) at room temperature. The bricks were then transferred to a hot oven at 110°C and dried for 24 hours. All samples appeared to be undamaged after drying.

Throughout the investigation into different mix proportions and manufacturing method described above several bricks were chosen (when undamaged) and fired either to the cycle described in section A.4.1 or a faster cycle in a small cylindrical kiln. The faster cycle consisted of a ramp to 1150°C of 230°C/hr followed by a 5 hour dwell and natural cooling. **Figure A.4.7** on the following page shows a comparison of the two cycles. In all cases up to this point the

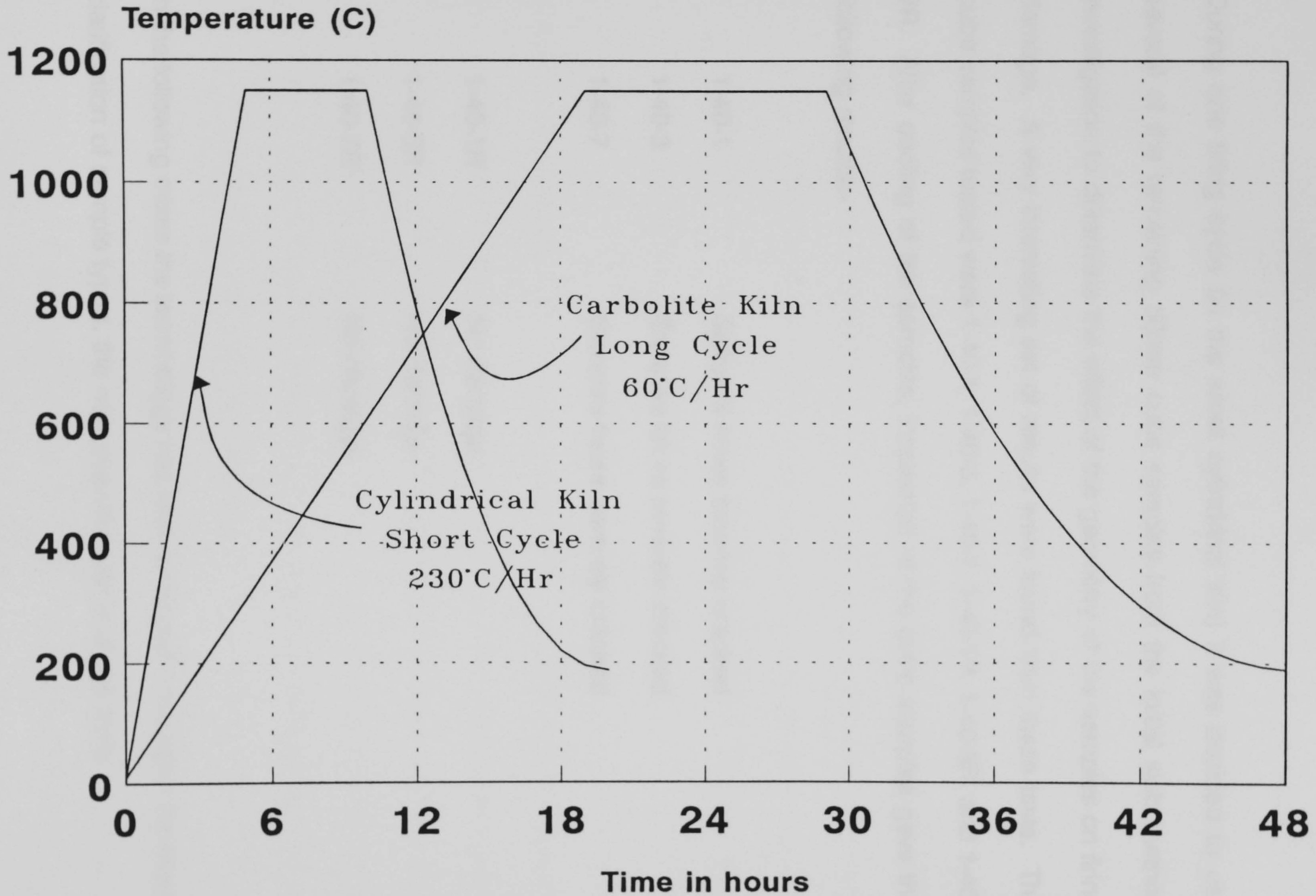

Figure A.4.7 - Comparison of the two firing cycles for New Furnace Lining Material

bricks were severely cracked after the firing cycle and the mix and manufacturing method was modified further.

During one firing cycle (in the small cylindrical kiln) it was decided to use several of the remaining 50mm cube samples from the initial slab method investigation to determine the effect of the geometry of the samples on firing damage. A very interesting set of results were found from these tests. The cube samples tested were 1-40-1, 1-40-3, 1-40-7, 1-40-1R, 1-40-3R, and 1-40-7R. After cooling of the samples, inspection of the cube samples gave the following results:-

1-40-1	Samples faces severely cracked
1-40-3	Samples faces severely cracked
1-40-7	Samples faces severely cracked
1-40-1R	No damage
1-40-3R	No damage
1-40-7R	No damage

In the following mixes the terminology has been changed once again for easier clarification of sample types, the new classification is of the form:

Perlite grade - Curing temperature - Days curing - #Mix number

2JL-RT-1-#2 Cracking problems may have been due to insufficient supply of cement to wet the perlite surfaces. It was decided to make a mix at the envisaged extremes: Aggregate:cement ratio = 0.5, water:cement = 1.35. Samples were made and cured at room temperature. After curing samples were dried in a pre-heated oven at 110°C. All samples were cracked after drying.

2JL-RT-1-#3 Samples were made the same as 2JL-RT-1-#2 above, however the aggregate:cement ratio used was increased to 0.65. After curing the samples were placed to dry in a pre-heated oven at 110°C for 24 hours. After the drying period approximately half of the 12 samples made were carrying minor cracks, other appeared undamaged.

2JL-RT-1-#4 Samples made were exactly the same as #3 above, however the bricks were left in the mould, covered with paper towelling and had an extra 200g water poured onto the sample. The samples were then covered with a plastic sheet and left to cure for 24 hours. Samples were dried as for #3 above, and after drying, no signs of cracking could be seen.

2JL-RT-1-#3(R) 9 no. samples were made as mix #3 above and cured for 1 day at room temperature. The samples were then placed in roaster bags and placed in the oven at 110°C

(i.e. re-heated). The samples were dry after 48 hours re-heating after which they were removed from the oven and removed from the bags. 4 no. of the samples were measured and placed in the large kiln for the firing cycle, 4no. samples were fired in the small kiln. After firing it was found that the samples were undamaged by the firing cycles.

The eight reheated 2JL-RT-1-#3 were fired to a temperature in excess of their service temperature, 4 in the small cylindrical kiln and 4 in the larger kiln. Of these samples no cracking appeared to have taken place during the firing cycle. The small kiln was programmed for a very rapid rise in temperature (230°C/Hr) where as the larger kiln was programmed for a slower rise in temperature (60°C). The samples in the larger kiln were carefully measured before and after firing to get shrinkage and density change information. The dimensions were as shown in the tables below.

Table A.17 **- Pre-Fired dimensions of #3-R bricks**

Brick No.	Length (mm)	Width (mm)	Depth (mm)	Density(kg/m^3)
1	221.0	111.3	72.3	329.8
2	221.0	111.2	72.4	335.3
3	221.0	111.4	72.2	338.4
4	221.0	111.2	72.6	336.0

Table A.18 - **Post-Fired dimensions of #3-R bricks**

Brick No.	Length (mm)	Width (mm)	Depth (mm)	Density(kg/m^3)
1	211.0	103.50	68.16	323.8
2	211.0	103.92	68.14	328.6
3	211.0	103.26	68.68	330.8
4	211.0	103.50	68.22	334.3

Table A.19 - **Shrinkages and density changes of #3-R bricks during firing cycle**

Brick No.	Length (%)	Width (%)	Depth (%)	Density (%)
1	4.52	7.00	5.73	1.82
2	4.52	6.55	5.88	2.00
3	4.52	7.31	4.88	2.24
4	4.52	6.92	6.03	0.51

Although the samples were uncracked after the firing cycle the fired samples were extremely friable to the touch (ie could be eroded easily, and may not perform well in a high velocity flame situation) and had poor edges and corners. This however could be worked upon, and it seemed that the re-heat method of drying was essential for the manufacture of uncracked samples.

Further samples were made using the re-heat method of drying in order to manufacture a full thickness (210mm) test panel in order to be able to compare the performance of the new lining material with an equivalent thickness of ceramic wool. In addition to the #3-R samples made the following samples were manufactured:

2JS-RT-1-#5R Perlite grade 2JS was adopted for this sample due to a

temporary shortage of grade 2JL. Aggregate-cement ratio = 0.8, water-cement ratio = 1.35. Samples were mixed and cured for 24 hours at room temperature (bagged) then re-heated in a pre-heated oven for 48 hours at 110°C. Samples were fired in the small kiln to the short firing cycle. No visible damage had occurred after the firing cycle.

#5-R bricks were fire tested to the hydrocarbon curve on the small furnace to a similar test arrangement as shown in **figure A.4.2** previously. The test results are shown in **figures A.4.8 and A.4.9** which indicate a steady state cold face temperature of approximately 190°C.

2JL-350-RT-3R — Aggregate-cement ratio of 0.8, Water-cement ratio of 1.35, target density 350kg/m^3. Mixed and cured (3 days) at room temperature, re-heated for 24 hours at 110°C. No sign of damage after the drying cycle upon inspection. Samples fired to the fast cycle in the small kiln and showed faint cracks and distortion after firing.

2JL-RT-1-#6R — Aggregate-cement ratio of 0.73, water-cement ratio of 1.35. Samples were mixed and cured for 24 hours at room temperature followed by re-heat drying at 110°C for 24

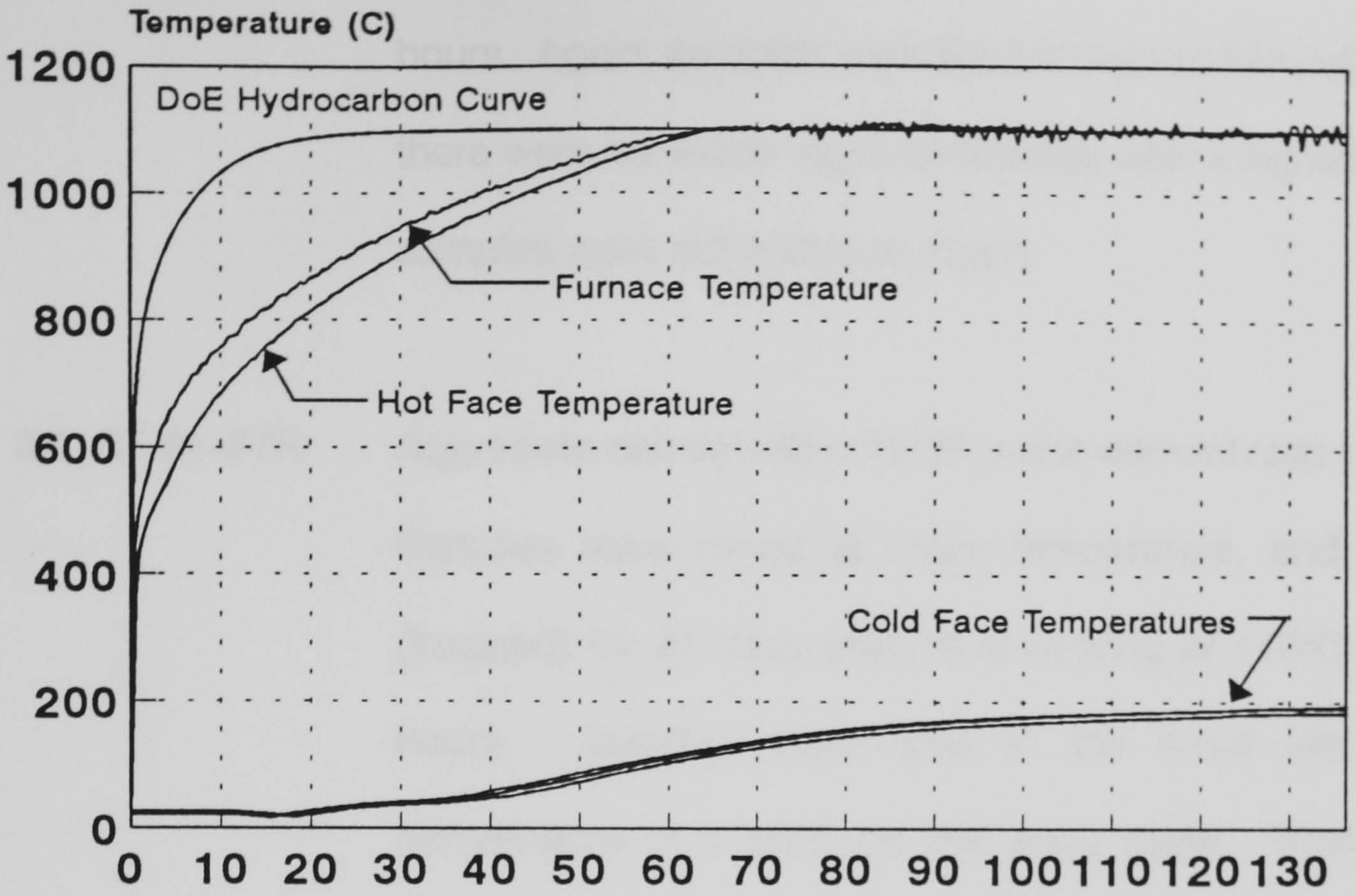

Figure A.4.8 Fire Testing of Samples #5-R
Small Furnace - Salford University 13-01-95
Sample Thickness ≈ 70mm

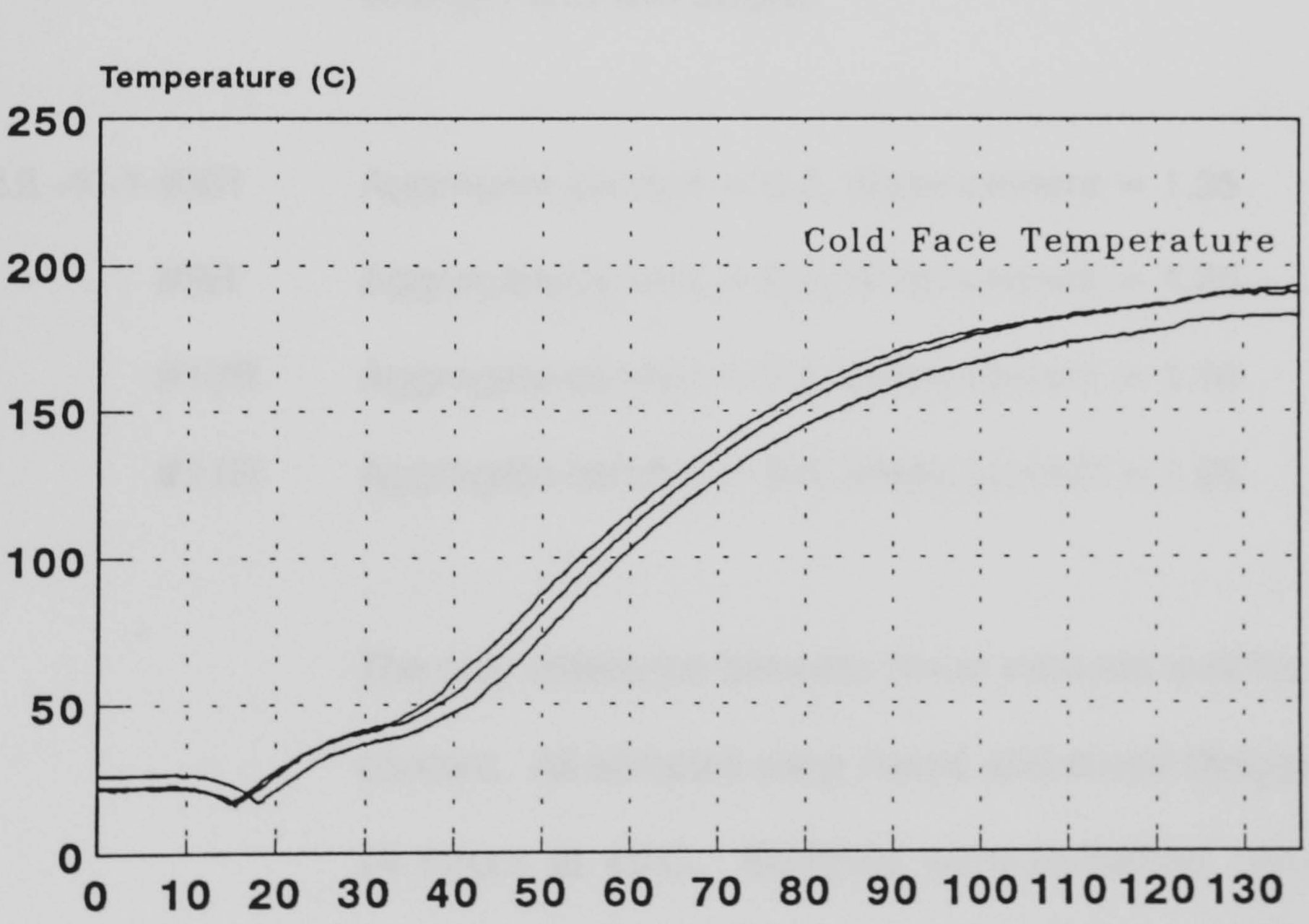

Figure A.4.9 Fire Testing of Samples #5-R
Small Furnace - Salford University 13-01-95
Sample Thickness ≈ 70mm

hours. Again, samples were fired to the fast kiln cycle and there were no visible signs of damage after firing although samples were still friable to touch.

2JL-RT-21-#7R Aggregate-cement ratio of 0.57, water-cement ratio of 1.07. Samples were mixed at room temperature, and cured (bagged) for 21 days prior to re-heating at 110°C for 24 hours. Samples were fired in the small kiln to a temperature of 1150°C on the short cycle. Post firing inspection found minor cracks where samples had been in contact with each other, otherwise samples had good strength and firm edges.

2JL-40-1-#8R Aggregate-cement = 0.8, Water-cement = 1.35

#9R Aggregate-cement = 0.8, Water-cement = 1.26

#10R Aggregate-cement = 0.8, Water-cement = 1.16

#11R Aggregate-cement = 0.8, Water-cement = 1.06

The only difference between these samples was the water content. All samples were mixed and cured (bagged) for 24 hours at 40°C. Samples were re-heated (when still warm from curing cabinet) in pre-heated oven at 110°C. Bricks were fired in the small kiln to the short firing cycle, post firing inspection gave the following results:

#8R	Samples had short, medium width (approx 0.5mm) cracks in the edges of the bricks, however otherwise the bricks were in good condition, firm corners and apparent good strength
#9/10/11R	Samples were uncracked after the firing cycle. Edges were firm and faces were in good condition. Bricks had apparent good strength. Some of the bricks had distorted during firing due to the stacking method used. Of all samples, #11R seemed to be in slightly better condition than the other samples.
2JL-#3R(300S)	Two fired samples of 2JL-RT-1-#3R were soaked in a mixture of 300ml of colloidal silica and 1100ml of additional water between them. The samples were then dried at 110°C for 24 hours and re-fired on the short firing sequence. Post firing inspection showed the samples still to have poor edges, but no cracking of the samples had occurred, and there appeared to have been an increase in strength of the samples (faces).

A.4.6 Maximum Temperature - Short Term Exposure.

As the bricks manufactured with secar-51 cement were fired at 1150°C it was obvious that they would survive this temperature during service. However the pyrometric cone equivalent suggested that the operating temperature my be far in excess of this (1440°C).

Several representative bricks of #11R were rapidly fired to 1300°C and held at that temperature for 5 hours. Complete melt down of the bricks occurred, and the bricks were hardly recognisable when inspected after cooling. A glassy surface to the melted surface was evident also. Figure A.4.10 following shows a photograph of the post-heated samples.

The test was repeated at 1200°C and the bricks survived satisfactarily with no noticeable damage. It should be noted that the samples were fully immersed within the furnace, and this is a much more severe condition than just one face exposed which applies to lining situations. The discrepancy between the pyrometric softening point of the cement, and the melting temperature of the tested samples was explained by the combination of the cement with perlite which acted as a flux to promote a lower melting point.

Three Secar-71 bricks (aggregate/cement ratio = 0.8, density = 370kg/m^3) were made following the normal procedure, however following the drying stage they were fired directly to 1300°C. The firing cycle was RT to 1150°C over five

hours, followed by 1150-1300°C in three hours with zero dwell at 1300°C. This was then followed by natural cooling to room temperature.

Following cooling of the samples inspection showed the typical length to be approximately 206mm, however there were some cracks in the bricks, in particular in one brick which had been arranged as a beam between two others. This length indicated similar shrinkage as would be expected for the Secar-51 samples fired to 1150°C. No development work was carried out on the Secar-71 bricks as a substantial amount of work would be required to find the necessary mix proportions and curing-drying-firing cycle to prevent cracking of the bricks. However, this brief investigation does show that similar compositions to those investigated fully could satisfy much more demanding temperature resistance requirements.

Figure A.4.10 - Condition of #11-R samples after heating to 1300°C

A.5 Full thickness panel testing.

For the purpose of evaluating the new furnace lining material at its proposed full thickness it was decided that a test panel should be manufactured which could be tested for extended periods. The long runs of the tests were to ensure that the cold face temperatures of the samples had stabilised, and hence steady state conditions achieved.

The test panel arrangement can be seen in **figure A.5.1** on the following page, and consisted of a Vermiculux surround which was lined with ceramic wool and contained the brick samples tightly packed in the centre. The test was performed on a programmable electric kiln as it was decided that a test running unsupervised on the gas fired furnace would not be safe. The manufacture of the test panel was such that it would fit into the aperture of the kiln and the thickness of the panel which extended into the kiln was similar to the wall thickness of the kiln. Hence the test panel formed an integral part of the kiln wall, and the ceramic wool surround provided an effective seal around the edges of the test panel. The ceramic wool and Vermiculux in the non-exposed area of the sample provided a good insulation against loss of heat from the panel edges.

The test panel was manufactured using a "dry fit" method (i.e. the was no mortar or sealant used in the joints between the bricks). Many of the bricks had slight distortions after the firing cycle due to the method of stacking within

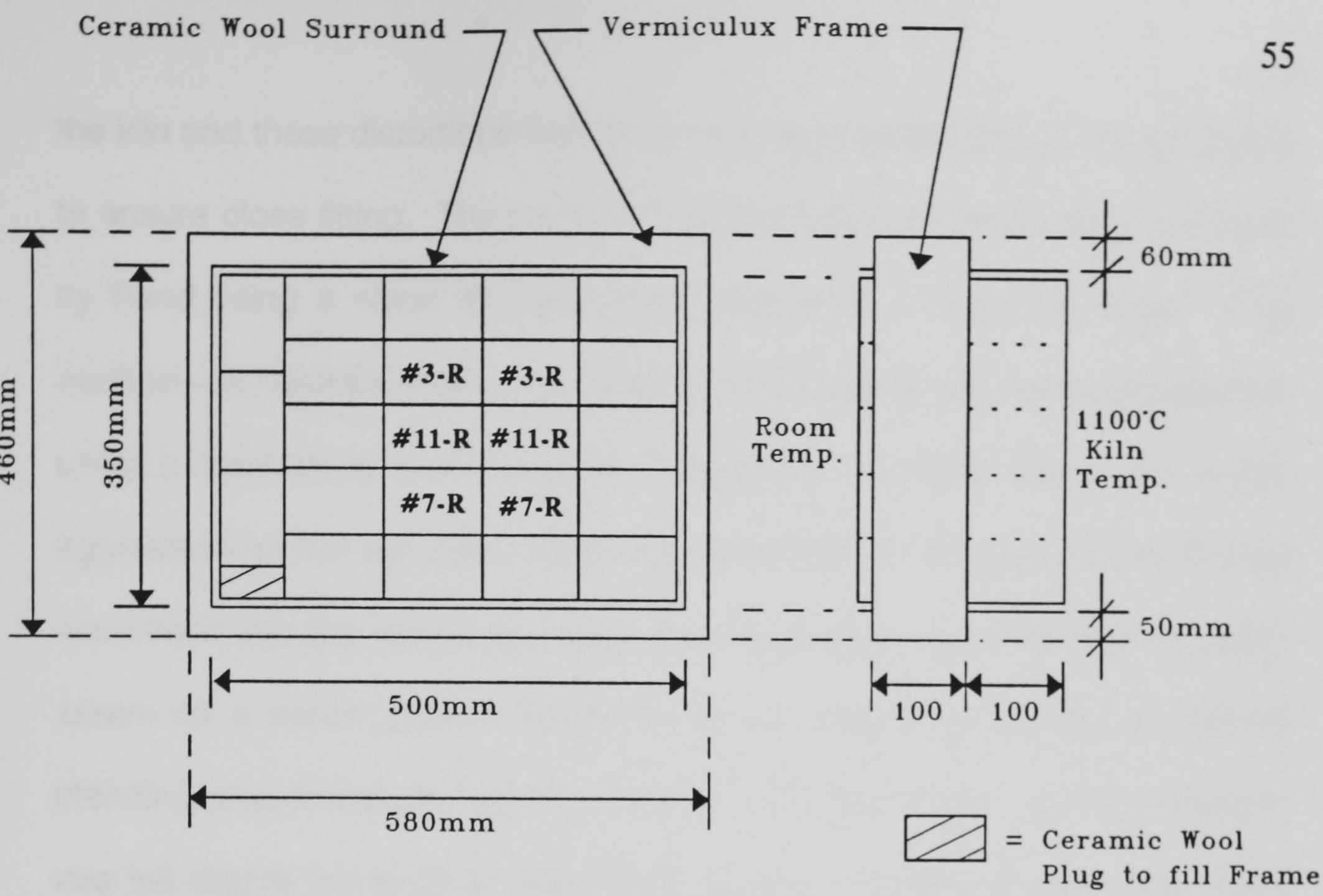

Figure A.5.1 General arrangement of Test Piece

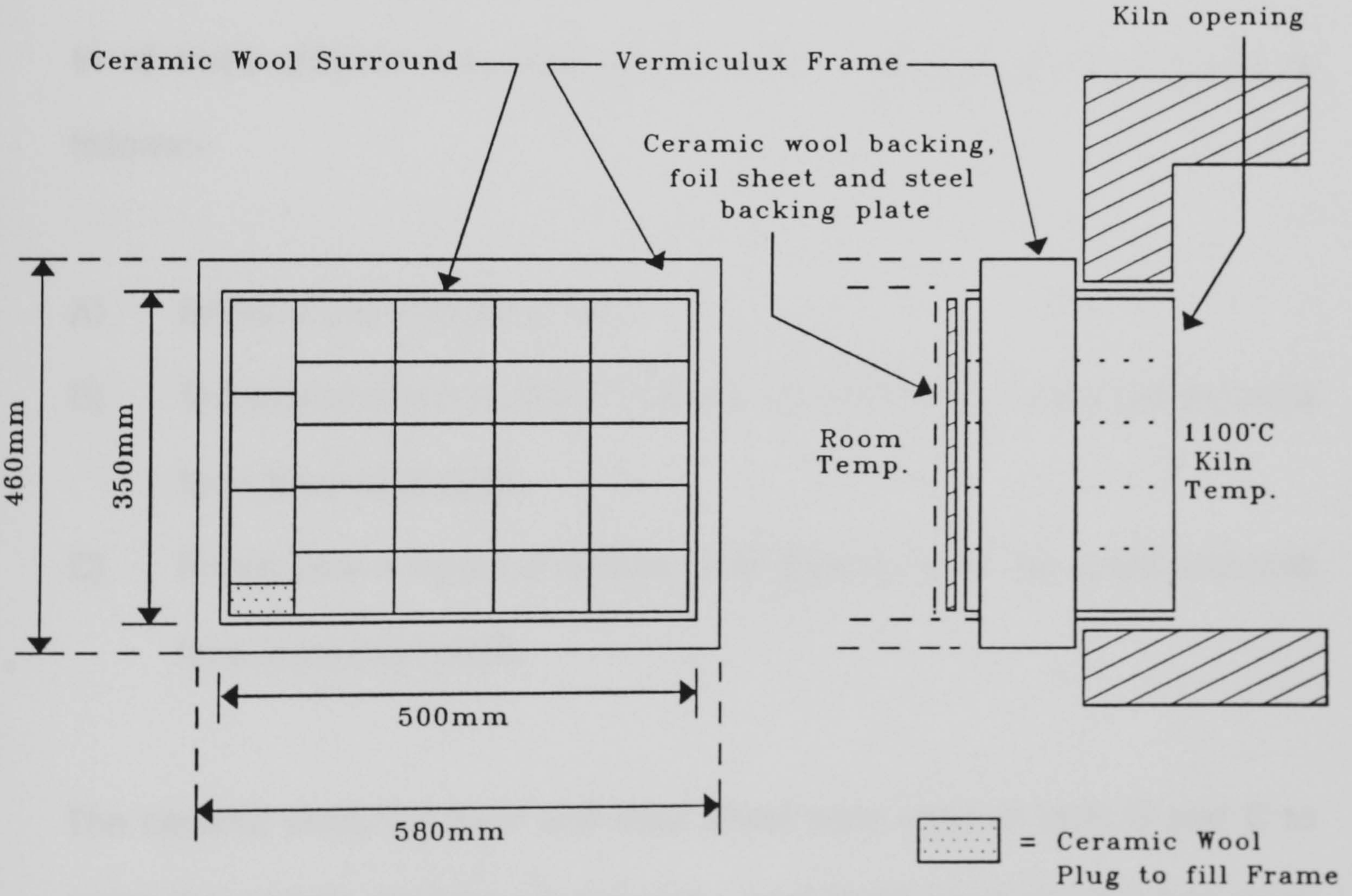

Figure A.5.2 Test Arrangement for Ceramic Wool Backing

the kiln and these distortions had to be removed before using in the test panel to ensure close fitting. The machining of the individual bricks was performed by hand using a sheet of glass paper stapled to a large flat board. This method was suitable due to the nature of the bricks and it was envisaged that using a mechanical machining (i.e. cutting with a circular saw) may be too aggressive for the samples. Once the samples had been sanded to fit they were fitted into the Vermiculux surround which was supported approximately 10mm off a bench (thus if frame is 100mm deep, there would be 100mm standing proud from the top of the frame). The final brick in a row or column was left slightly too large and fitted by forcing the sample between the others already mounted, in this way a very tight fit could be managed.

In all three different test arrangements were investigated, those being as follows:-

A) Bricks alone (210mm thick)

B) Bricks plus 25mm nominal thickness of ceramic wool, foil sheet and cold face 3mm steel plate.

C) Bricks plus 4 layers of 3.5mm thick ceramic wool, foil sheet and cold face 3mm steel plate.

The ceramic wool, foil layer and steel sheet were used in tests B and C to mimic the system used for a full ceramic wool lining used at present in many kilns. The ceramic wool used in test B was excess material taken from the

3mx3m ceramic wool lined test furnace under construction at the University and as such would be directly comparable to the ceramic wool systems, and their quoted figures for cold face steady state temperatures. The ceramic wool used in test C was a medium density blanket of approximately 190kg/m^3, and the foil sheet was the one which was removed from the ceramic lining used in test B. Cross section test arrangements for tests B and C (including kiln opening) can be seen in **figure A.5.2**.

The main samples being tested were located in the centre of the test panel and each had a thermocouple attached to monitor cold face temperature. Other thermocouples were located inside the kiln (mounted through the test panel) and in open air slightly above the test panel to measure ambient temperature. The samples to which the thermocouples were mounted are shown on **figure A.5.1**, and were the best bricks in terms of low density (#3-R), finished condition (#7-R) and (#11-R). Temperature measurement on the cold face of samples was via K type copper disc thermocouples as prescribed in BS476 with 30mm square by 1.5mm thick insulating cover pieces to restrict cold face thermal losses. Ambient temperature and kiln temperature were read with inconnel sheathed 1.5mm diameter K type thermocouples.

The three brick samples under test, and their dimensions etc were as follows:-

#3-R

Perlite	Cement	Water
695g	1069g	1439g

Aggregate:Cement Ratio = 0.65, Water:Cement ratio = 1.35

Average fired density of bricks = 328kg/m^3

Average heat path (hot-cold face) = 211mm

#11-R

Perlite	Cement	Water
829g	1035g	1100g

Aggregate:Cement Ratio = 0.80, Water:Cement ratio = 1.06

Average fired density of bricks = 367kg/m^3

Average heat path (hot-cold face) = 213mm

#7-R

Perlite	Cement	Water
800g	1400g	1500g

Aggregate:Cement Ratio = 0.57, Water:Cement ratio = 1.07

Average fired density of bricks = 380kg/m^3

Average heat path (hot-cold face) = 215mm

Figures A.5.3 and A.5.4 on the following page show the first two tests of the furnace lining material at full thickness with no backing. Problems were encountered where the furnace program crashed overnight, however from inspecting data files it can be seen that the cold face temperatures had reached steady state conditions.

Figures A.5.5 and A.5.6 show the test results for the test panel with backings of 25mm ceramic wool and 14mm ceramic wool respectively. In both cases it

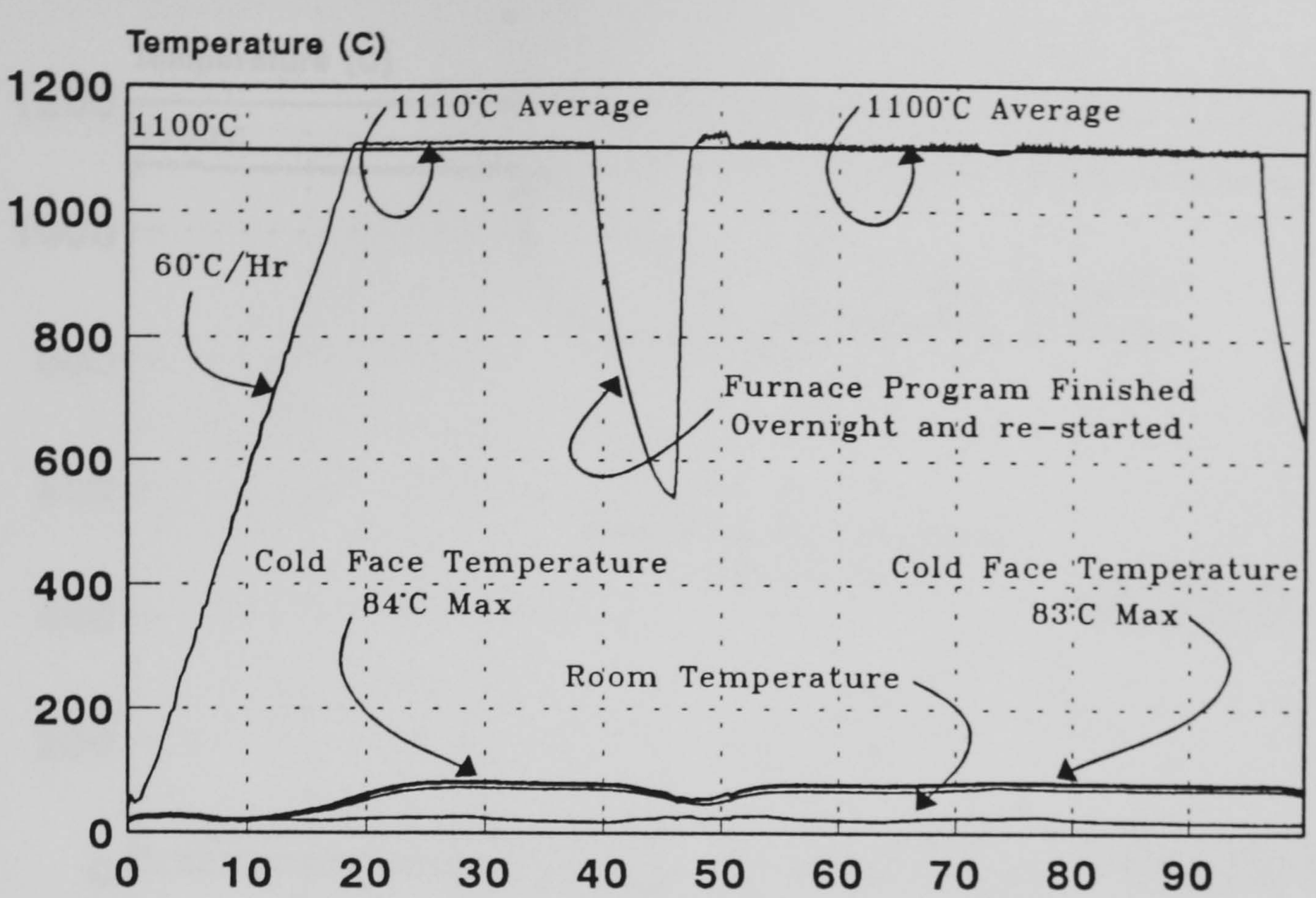

Figure A.5.3 - Kiln Fire Test of New Furnace Lining Material
Samples 210mm thick 24-27th January 1995
Mixes #3-R, #7-R and #11-R, No backing

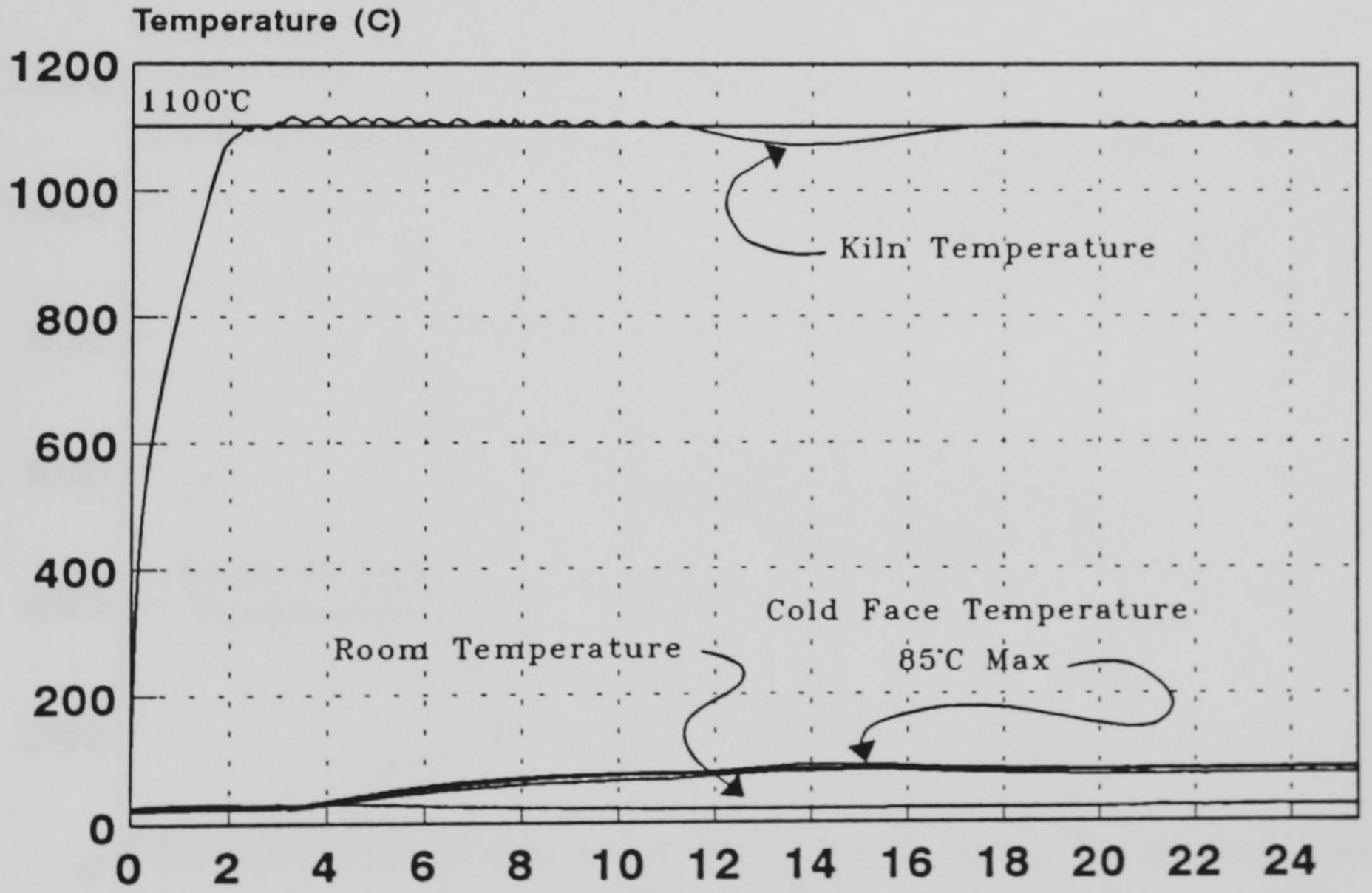

Figure A.5.4 - Second Test of Brick Samples. Carbolite Kiln.
No cold face insulation, 30/01/95-31/01/95
Mixes #3-R, #7-R and #11-R

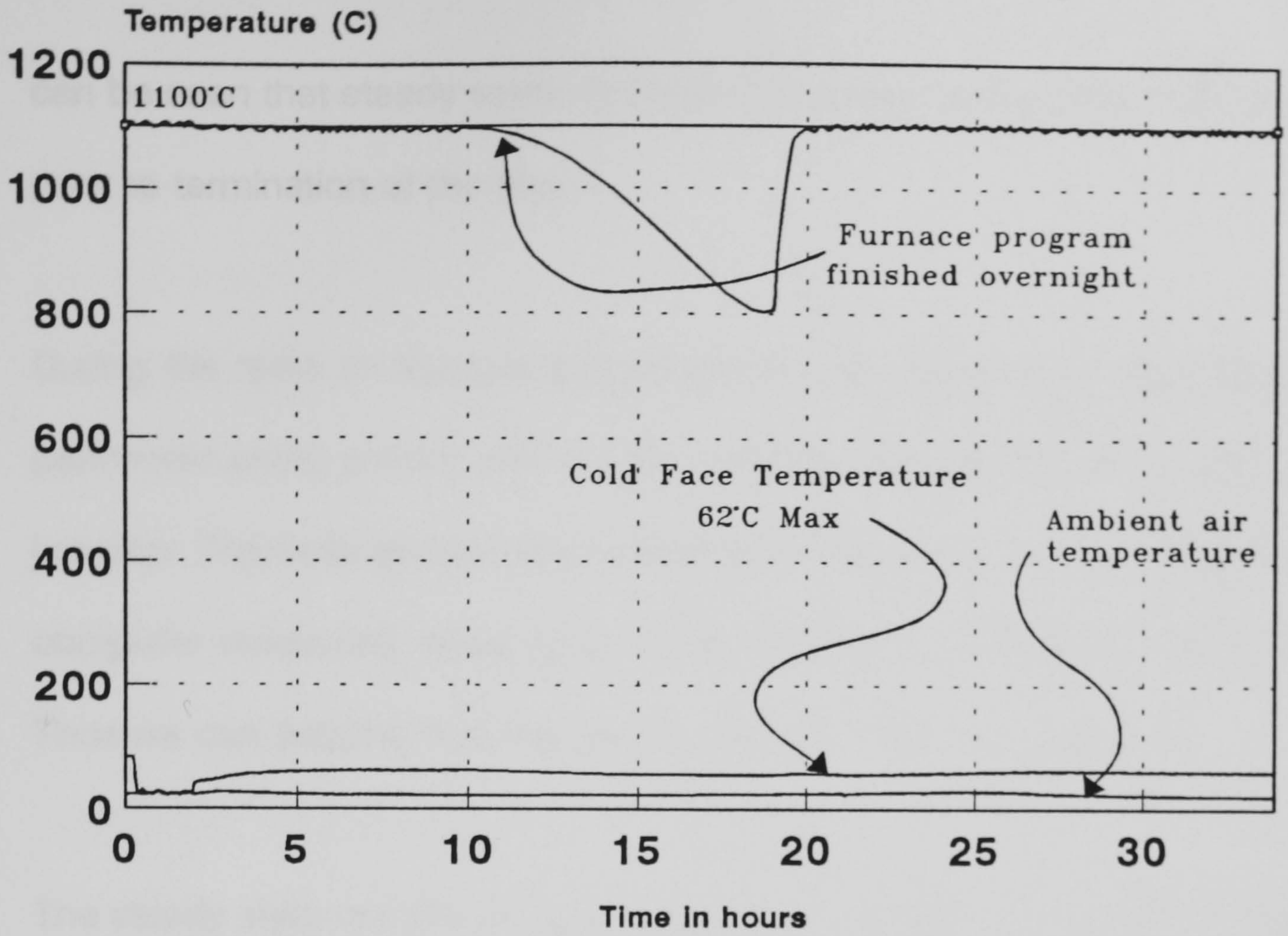

Figure A.5.5 - Test of New furnace Lining Material.
Backing of 25mm ceramic wool + foil layer + steel.
31/01/95-01/02/95.

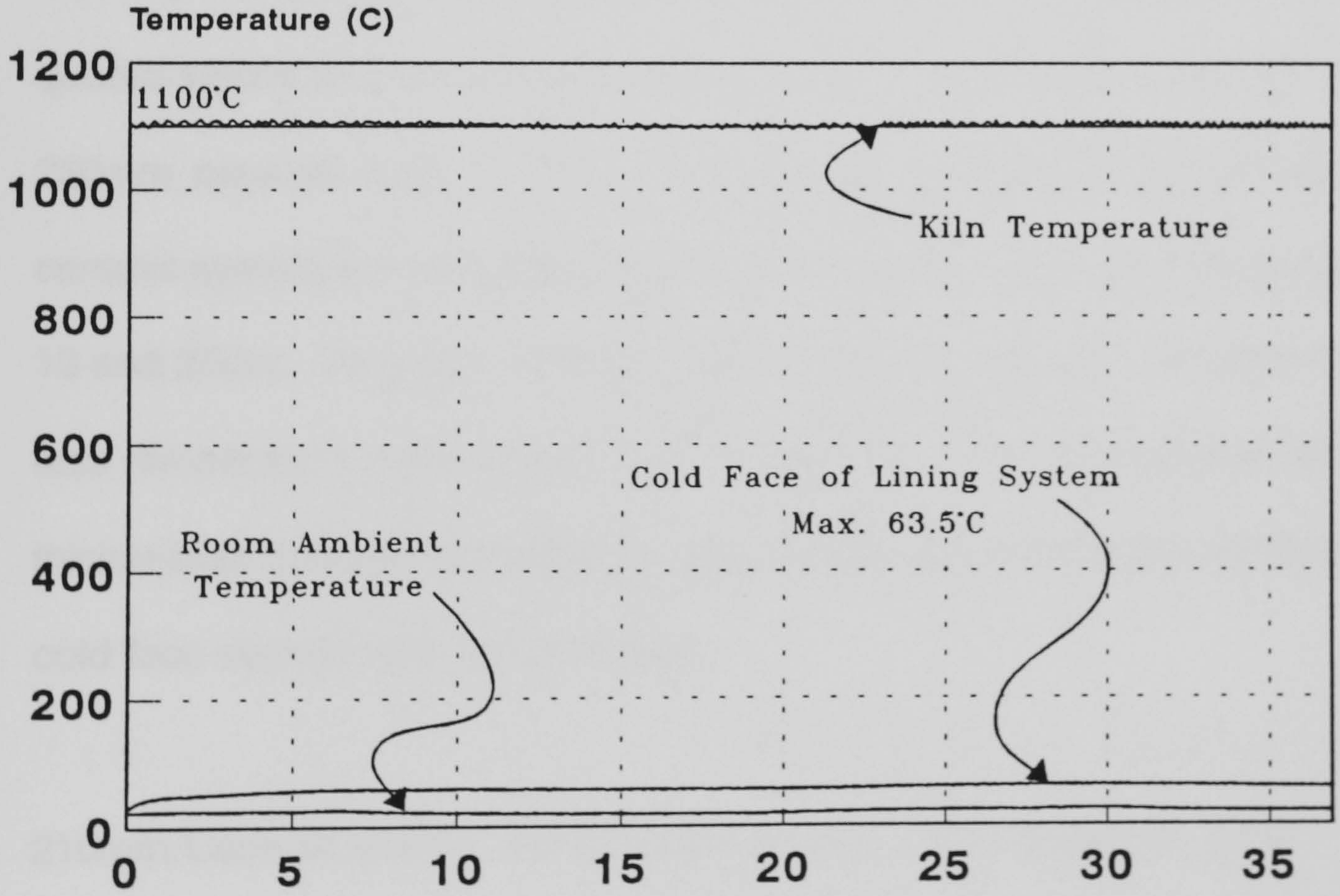

Figure A.5.6 - Test of New furnace Lining Material
4 Layers of 3.5mm thk ceramic wool cold face, plus foil.
02/02/95-04/02/95

can be seen that steady state conditions had been achieved on the cold face prior to termination of the test.

During the tests an independent thermocouple temperature verification was performed using a bare wire K type thermocouple with a well insulated cold junction. The independent measurement corresponded extremely well with the computer measured value (only 0.1°C difference between the two values). Thus we can assume that the results are both valid and accurate.

The steady state conditions on the cold face were 62°C for the 25mm ceramic wool backing and 63.5°C for the 14mm ceramic wool backing. These values are very favourable when compared to a full ceramic wool system where the quoted values from a manufacturer for 200mm ceramic wool is 81°C, and for 250mm ceramic wool of 71°C. The thickness of the backing lining of the ceramic system is not quoted but it is known that the type used varies between 13 and 25mm. Assuming that the 13mm backing was used, and that the cold face temperature measurements are reasonably linear between the two lining thicknesses quoted it is possible to draw a reasonable comparison between the cold face steady state temperatures:

210mm Ceramic wool + 13mm Backing wool + Foil Sheet = 79°C

210mm New Lining + 14mm Backing wool + Foil Sheet = 63.5°C

Thus it can be seen that an improvement of 15.5°C may be possible. It should be remembered that the test performed on the new furnace lining was in an electric heated kiln, and not in a gas fired one, which could possibly alter the results (this needs to be investigated further). However assuming these values to be correct the corresponding heat losses (W/m^2) for the two systems may be interpolated to give the following values:

Ceramic Wool 210mm system = $655W/m^2$

New Lining System 210mm = $450W/m^2$

On a following page a predictive calculation is given for the possible savings in terms of thermal insulation which may be obtained if the new lining material were to be used in the clay brick manufacturing industry. The new material however may have uses reaching much further than this, and other industries to which it may be applied could include the metal industry (smelting and section forming), the whole of the pottery industry and even down to insulating panels for industrial and domestic appliances such as cookers.

It can be seen from before that a possible saving of $200W/m^2$ could be achieved when using the new lining material as opposed to ceramic wool. If a typical brick tunnel kiln is 100m long, with the hottest zone being 30m long, the area of the hottest zone may be $30x(2+5+2)=270m^2$.

If a saving of 200W/m² can be achieved, the possible energy saving per year is area x time x saving:

Total Energy Saving ≈ 270 x (24 x 365) x 200 ÷ 1000 ≈ 473,040 kW hours/year.

Assuming the remaining 70m of the tunnel kiln may achieve a similar saving as for the hottest zone the full potential saving per kiln is 946,080 kW hours/year. This is approximately 32,000 therms. Gas firing is normal, and at the current cost of 25p/therm a saving of £8,000 per kiln per year may be possible.

The easiest way to assume a yearly potential saving for clay brick firing kilns is to assume an equivalent number of kilns. The normal annual brick production is in the order of 3×10^9 bricks and the annual output per tunnel kiln is typically 25×10^6 bricks. This gives 120 equivalent kilns which would result in a potential saving of almost £1m per year if all furnaces were to be re-lined with the new material.

Following the extremely encouraging results given in the full thickness test it was decided that two further tests should be performed, the first on mix #11-R which had a fired density of approximately 370kg/m^3 with aggregate-cement ratio of 0.8, water-cement ratio of 1.06, and the second additional test panel would consist of a new mix #12-R with a fired density of approximately 420kg/m^3, aggregate-cement ratio of 0.65, water-cement ratio of 1.07.

The following graph shown as **figure A.5.7** gives the full test data for the full thickness test panel using #11-R bricks alone with a 14mm ceramic wool foil backed lining and steel backing sheet. The constructed panel was of the same form as used for the multiple sample panel, and after testing for approximately two and a half days a cold face steady state temperature of 59°C was achieved. This cold face temperature corresponded to an ambient room temperature of 24°C. It was noticed however that room temperature had only a very slight effect on the panel cold face temperature. Using the steady state cold face data it is possible to calculate the yearly potential energy saving for clay brick firing kilns as £1.18m pa.

Figure A.5.8 shows the full test data for the full thickness test panel using #12-R bricks only. These denser bricks felt to be much stronger after the firing cycle, and once again a full thickness panel was constructed and tested mounted to the front of an electric kiln. The panel was again lined with a 14mm ceramic wool blanket, foil layer and steel backing sheet. The steady state temperature on the cold face of the panel was observed to be 59°C which would again correspond to a potential yearly energy saving of £1.18m pa for clay brick firing kilns when calculated as shown previously. This cold face temperature was again verified using the independent thermocouple arrangement with a heavily insulated cold junction.

Figures A.5.9 and A.5.10 show the post test condition of the full thickness test pieces for the assorted samples and for the #11-R bricks respectively.

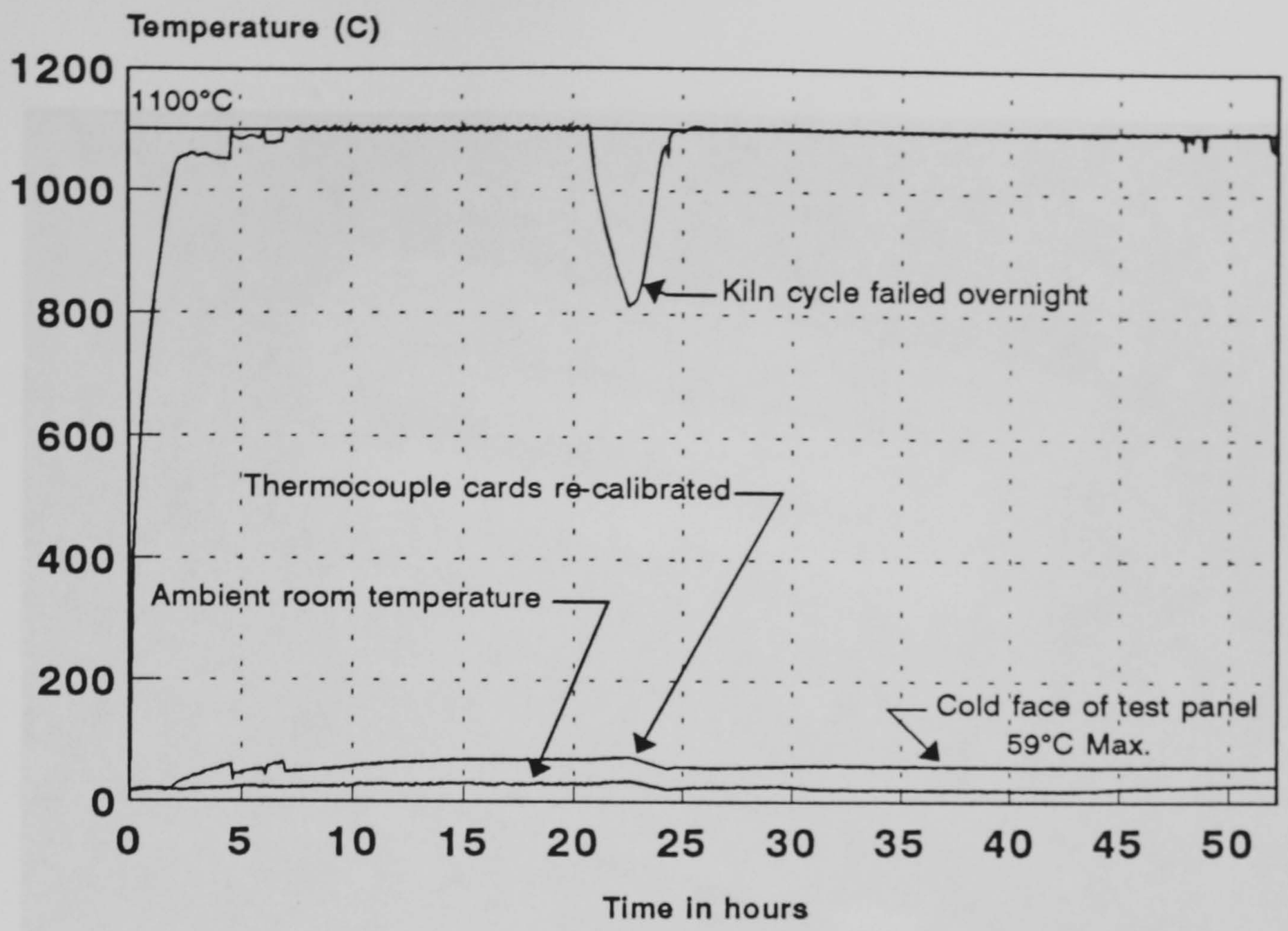

Figure A.5.7 - Full thickness test of #11-R bricks
New furnace lining material development
27-02-95 to 01-03-95

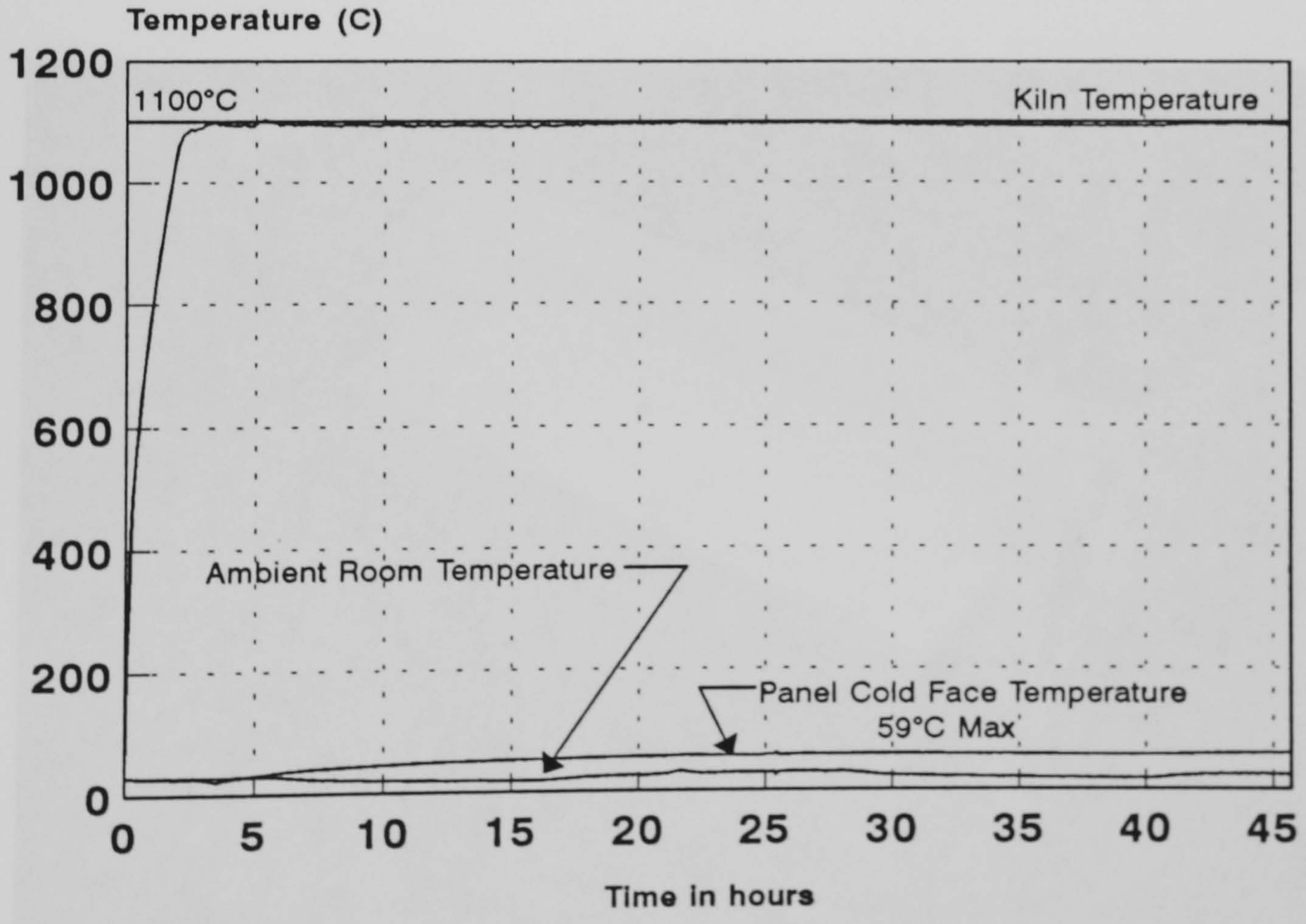

Figure A.5.8 - Full thickness test of #12-R bricks
New furnace lining material development
07-03-95 to 09-03-95

Figure A.5.9 Post test condition of assorted Insuline samples

Figure A.5.10 Post test condition of Insuline #11-R samples

A.5.1 Thermal Conductivity of Insuline

Following the encouraging results from the ad-hoc testing of Insuline bricks it was decided to send representative samples for high temperature thermal conductivity testing. This work was performed at Ceram Research, British Ceramic Research Limited, to BS 1902: 5.5: 1991 and is a NAMAS approved testing facility.

Table A.20 below gives comparisons of cold face temperatures between ceramic fibre anchored modules at 100mm thick with 20mm backing layer of ceramic wool plus foil sheet, and those results obtained in the thermal conductivity test of insuline (notionally 75mm thickness).

Ceramic Wool Anchored Modules @100mm thick + 20mm + foil		Insuline Mix #12R @75mm thick	
Hot Face °C	Cold Face °C	Hot Face °C	Cold Face °C
800	80	805	85
900	92	904	95
1000	104	1002	108

Table A.20 Comparison of Insuline #12R and Ceramic Wool Anchored Modules

Table A.21 overleaf gives the thermal conductivity test results obtained for samples of Mix #12-R tested at notionally 800, 900, 1000, and 1100°C and comparisons with trade figures for the thermal conductivity of ceramic fibre products at differing densities.

Sample	Density kg/m^3	Temperature °C	Thermal Conductivity W/mK
Insuline Mix #12R	431	805	0.172
		904	0.180
		1002	0.195
		1102	0.205
Ceramic Wool	96	800	0.22
		1000	0.30
		1200	0.41
	128	800	0.17
		1000	0.23
		1200	0.36
	160	800	0.16
		1000	0.21
		1200	0.32
Ceramic Fibre Board	290-310	800	0.15
		1000	0.21-0.24
		1200	0.36

Table A.21 High Temperature Thermal Conductivities of Insuline and Ceramic Wool

Figure A.5.11 gives a graphical representation of thermal conductivity as given in table A.21 above.

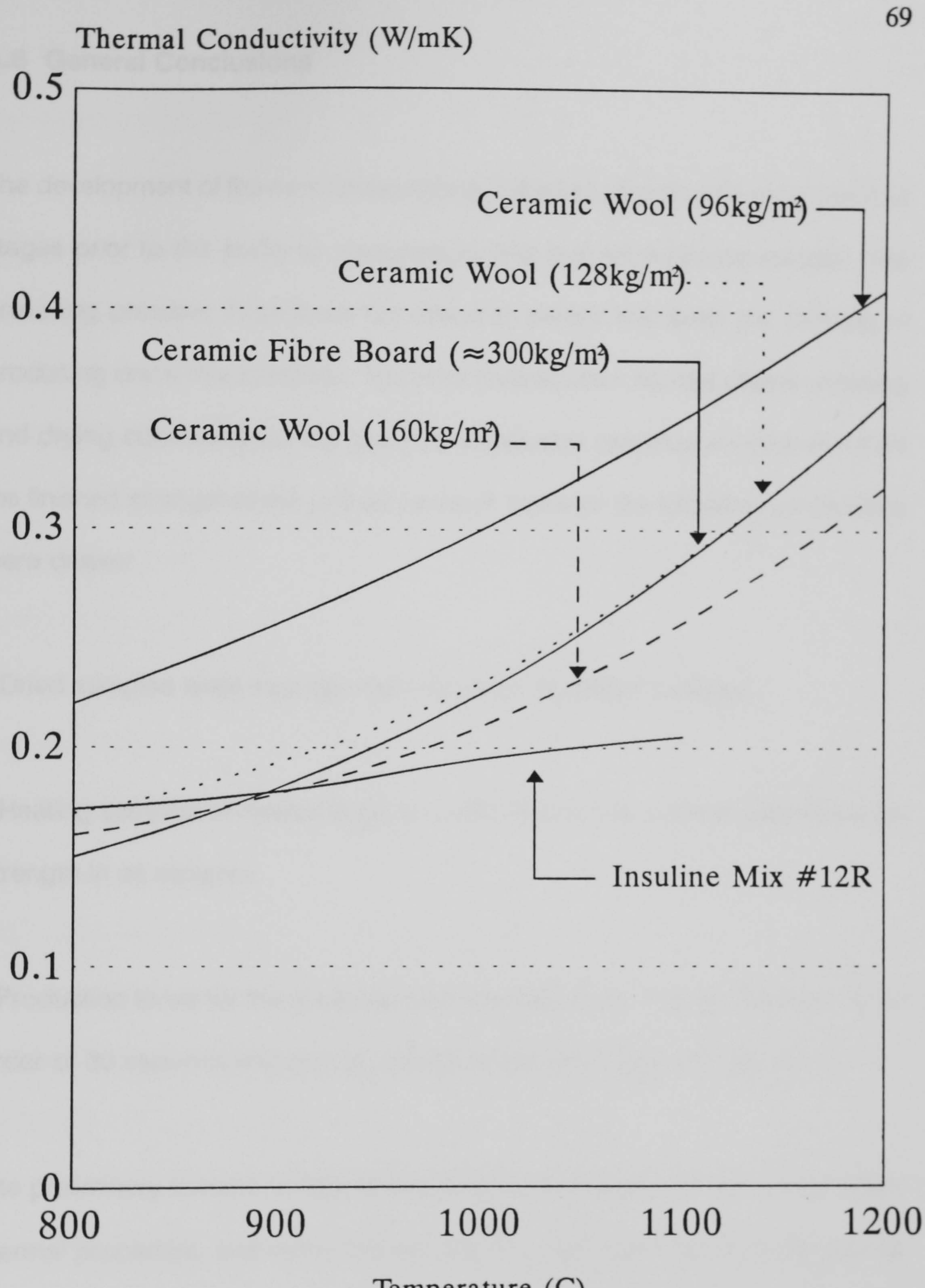

Figure A.5.11 Graphical Comparison of Insuline Mix #12R with Ceramic Fibre Products of Various Densities

A.6 General Conclusions

The development of the new furnace lining material has passed through several stages prior to the ability to manufacture and test full thickness panels. The prevailing problem throughout the research period has been the difficulty in producing crack free samples. The initial investigation into the effects of curing and drying conditions did not give fully conclusive evidence on their effect on the finished strength of the unfired product, however the following conclusions were drawn:

- Dried samples were stronger than damp or re-wetted samples.

- Heating samples in roaster bags to 110°C to dry had a detrimental effect on strength in all samples.

- Production times for the samples could be very short: mixing time was of the order of 30 seconds and curing periods could be of less than 24 hours.

The preliminary furnace testing of the samples showed them to have excellent thermal properties, and numerical analysis showed that if the material were to be developed fully it may be possible for the new furnace lining material to compete with ceramic wool in terms of high temperature performance. It would also have the inherent benefit of being non-fibrous and hence free from the danger of air-borne fibre inhalation and related disease.

The standard method of drying was observed to encourage crack and fault formation within the brick samples. Inspection with a crack microscope showed that these cracks tended to propagate via perlite-perlite boundaries within the sample, however using long careful hand mixing techniques did not solve this problem. The re-heat method of drying was observed to promote a weaker structure which is well known within the ceramics industry to provide a higher degree of thermal shock resistance.

Additions of different grades of perlite, fine grade exfoliated vermiculite, cellulose fibre or mica did not prevent the formation of cracks within the samples during normal drying. The additions were used in an attempt to reduce the shrinkage of the samples during the drying cycle by providing an aid to water loss from the sample. The additions were observed to reduce the severity of the cracks formed both in magnitude and occurrence, but cracks were still present both after the drying cycle and also after the firing cycle. The use of cellulose fibre was also observed to retard the set and cure of the cement and due to difficulty in dispersal of the fibres during mixing large localised shrinkage of samples was observed during the firing cycle.

Increasing the water-cement ratio (whilst maintaining aggregate-cement ratio and density) to ensure full wetting of the cement particles has been shown to have little if no effect on the prevention of crack formation during the drying cycle. Change of density was also found to have no significant effect in crack prevention, either by increasing the volume of mix used per brick, or by

increasing the water and cement content of the sample.

The use of programmed drying cycles (i.e. using slow rates of climb in temperature with or without plateaus during the cycle) was investigated. The effect of the ramped drying cycles was if anything to aggravate the drying cracking problem of the samples.

Bricks of very low density (and assumedly the best thermal performance) appeared to be extremely friable to the touch and had very poor edges after firing. These samples may not be suitable for an eroding or aggressive environment when used alone, however there is the possibility that they may well be ideal in a situation where a high density refractory facing layer is used.

Addition of colloidal silica prior to the first firing cycle has been shown to promote large shrinkage and severe cracking during firing. When the sample is pre-fired and then given a flat wash of diluted colloidal silica no cracking was promoted during the subsequent drying and firing cycle. The addition appeared to increase the overall compressive strength of the samples, but did not effect the friability and edge conditions significantly. Addition of colloidal silica to higher density samples has not been investigated, and may well prove beneficial in terms of sample integrity and strength however, it is more than likely to reduce the thermal resistance of the material, and may well reduce the thermal shock performance of the samples as well.

An increased cement content in fired samples does not appear to be as beneficial as general increase in density. It is thought that the cold condition of the fired higher density samples is mainly effected by the 'glazing' effect of the perlite after its melt temperature has been achieved. The best samples in terms of post-fired condition to date have been #11-R and #12-R with notional fired densities of 370kg/m^3 and 420kg/m^3 respectively.

Full thickness panel tests have been performed on a) assorted samples, b) #11-R samples alone and c) #12-R samples alone. The panels were mounted to the front of an electric kiln which was programmed to run at 1100°C for long periods. The initial test performed of assorted samples showed very good thermal performance with a steady state cold face temperature of 85°C max. This test panel was then modified to incorporate a cold face lining of 25mm ceramic wool, foil and steel backing sheet. The effect of this backing was to reduce the steady state cold face temperature to 62°C. When a similar test panel arrangement was constructed, this time using 14mm (4x3.5mm layers) ceramic wool, the cold face temperature measured at steady state was 63.5°C. This cold face temperature could indicate very large monetary savings in long firing duration kilns when compared to ceramic wool systems of a similar thickness.

Both full thickness test panels using #11-R and #12-R with the 14mm ceramic backing system showed a steady state cold face temperature of 59°C. This cold face temperature was verified using independent measuring equipment.

This would indicate that the density of the sample does not have a great effect on the insulation properties of the samples at these high temperatures. It was also noticed that the cold face temperature

was not particularly sensitive to fluctuations in room temperature.

Post firing testing of cut samples from a brick showed that the fired strength of #12-R was of the order of 0.27N/mm^2. This is very weak compared to the unfired strength, however, when considered fully, it would indicate that if the fired samples were to be stacked, a height of 65m may be reached before the bottom bricks would begin to fail in compression.

Preliminary investigations have shown that the new furnace lining material is capable of withstanding temperatures in excess of 1200°C when Secar 51 cement is used, and temperatures of 1300°C+ may be possible when using a higher grade cement (Secar 71). When the standard samples were heated to 1300°C they melted down, and when cooled they had formed a very strong ceramic. This ceramic had a glossy appearance, and this would tend to indicate that the cement does pass into a glassy phase upon reaching its melt temperature.

A.7 Mix proportions for samples.

Mix A) Perlite 729g, Cement 594g, Water 954g, 885g wet mix per brick for 220x110x70mm samples.

Mix 1) Perlite 667g, Cement 833g, Water 1125g for a 300x300x50mm slab sample.

Mix 1 proportion brick samples were made with perlite 2JS at varying density by changing the mass of wet mix used per brick. Wet mix per brick at differing densities were as follows:-

325kg/m^3 - 868g per brick.

350kg/m^3 - 935g

375kg/m^3 - 1000g

400kg/m^3 - 1068g

Perlite 3JS bricks were made at higher density by reducing the water content of the mix:

Perlite 1193g, Cement 1492g, Water 1333g and for following densities:

600kg/m^3 - 1250g wet mix per brick

700kg/m^3 - 1458g

Perlite 2JL was used to investigate the lower density end of the range and mix proportions were as follows:

Perlite 783g, Cement 979g, Water 1321g and for following densities:

275kg/m^3 - 688g wet mix per brick

300kg/m^3 - 750g

310kg/m^3 - 775g

325kg/m^3 - 813g

350kg/m^3 - 875g

Cellulose fibre and Mica additions were calculated as a percentage of dry mass of the aggregate and cement. The increase in wet mix used per brick was as follows:

310kg/m^3 density, 4% addition - 20g extra wet mix, 2% - 10g extra.

#2) Perlite 695g, Cement 1390g, Water 1872g, 1123g wet mix per 220x110x70mm brick sample.

#3) Perlite 695g, Cement 1069g, Water 1439g, 910g wet mix per 220x110x70mm brick sample.

#4) As #3, but left in mould with extra water added after pressing.

#5) Perlite 2JS 753g, Cement 941g, Water 1270g, 1200g wet mix per 220x110x70mm brick sample.

#6) Perlite 2JL 783g, Cement 1069g, Water 1439g, 940g wet mix per 220x110x70mm brick sample.

#7) Perlite 2JL 800g, Cement 1400g, Water 1500g, 1050g wet mix per 220x110x70mm brick sample.

#8) Perlite 2JL 829g, Cement 1035g, Water 1400g, 988g wet mix per 220x110x70mm brick sample.

#9) Perlite 2JL 829g, Cement 1035g, Water 1300g, 966g wet mix per 220x110x70mm brick sample.

#10) Perlite 2JL 829g, Cement 1035g, Water 1200g, 933g wet mix per 220x110x70mm brick sample.

#11) Perlite 2JL 829g, Cement 1035g, Water 1100g, 900g wet mix per 220x110x70mm brick sample.

#12) Perlite 2JL 884g, Cement 1360g, Water 1455g, 1150g wet mix per 220x110x70mm brick sample.

A.8 List of Main References

1) Baker, R: "Recent advances in ceramic fibre for high temperature applications", Metallurgia (ISSN 0141-8602), v[51 supplement], May 1984

2) Midgeley, H.G, Trans. J. Brit. Ceram. Soc. 66, 4, pp161+, 1967

3) Parker, K.M, Sharp, J.H, Trans. J. Brit. Ceram. Soc, 81, 2, pp35-42, 1982

4) Givan, G.Y, Hart, L.D, Helich, R.P, Maccura, G, Bull. Amer. Ceram. Soc, 54, pp710+, 1975

5) George, C.M, Trans. J. Brit. Ceram. Soc, 79, 82, 1980

6) Kula, T.M, Meiser, M.D, Tressler, R.E, Cem. Conc. Res, 10, p491, 1980

7) Davey, N, Bldg. Res. Tech. Paper 14, 1933, HMSO London

8) Bakker, W.T, Refractory Concrete, Amer. Conc. Inst. Pub, SP-57, 2, p11, 1978

9) Ciment Fondu Lafarge, Specialist Cements, Technical Data Sheets